Volume 15, Issue 3, September 2025
pISSN 2158-0510 eISSN - 2158-0529

IJBM

International Journal of BIOMEDICINE

www.ijbm.org

IJBM

INTERNATIONAL JOURNAL OF BIOMEDICINE

Aims and Scope: *International Journal of Biomedicine (IJBM)* publishes peer-reviewed articles on the topics of basic, applied, and translational research on biology and medicine. Original research studies, reviews, hypotheses, editorial commentary, and special reports spanning the spectrum of human and experimental and tissue research will be considered. All research studies involving animals must have been conducted following animal welfare guidelines such as the National Institutes of Health (NIH) Guide for the Care and Use of Laboratory Animals, or equivalent documents. Studies involving human subjects or tissues must adhere to the Declaration of Helsinki and Title 45, US Code of Federal Regulations, Part 46, Protection of Human Subjects, and must have received approval of the appropriate institutional committee charged with oversight of human studies. Informed consent must be obtained.

International Journal of Biomedicine endorses and behaves in accordance with the codes of conduct and international standards established by the Committee on Publication Ethics (COPE).

International Journal of Biomedicine (ISSN 2158-0510) is published four times a year by International Medical Research and Development Corp. (IMRDC), 442 5th Avenue #1196, Manhattan, NY 10018, USA

Customer Service: International Journal of Biomedicine, 442 5th Avenue #1196, Manhattan, NY 10018, USA; Tel: 1-917-740-3053; E-mail: editor@ijbm.org

Manuscript Submission: Original works will be accepted with the understanding that they are contributed solely to the Journal, are not under review by another publication, and have not previously been published except in abstract form. Accepted manuscripts become the sole property of the Journal and may not be published elsewhere without the consent of the Journal. A form stating that the authors transfer all copyright ownership to the Journal will be sent from the Publisher when the manuscript is accepted; this form must be signed by all authors of the article. All manuscripts must be submitted through the International Journal of Biomedicine`s online submission and review website. Authors who are unable to provide an electronic version or have other circumstances that prevent online submission must contact the Editorial Office prior to submission to discuss alternate options (editor@ijbm.org).

IJBM

INTERNATIONAL JOURNAL OF BIOMEDICINE

FRONTIERS IN CARDIOVASCULAR BIOMEDICINE

8TH CONGRESS OF THE ESC COUNCIL ON BASIC CARDIOVASCULAR SCIENCE

17-19 April

Leuven University,

Belgium

#FCVB26

ESC Council Basic Cardiovascular Science

IJBM
INTERNATIONAL JOURNAL OF BIOMEDICINE
www.ijbm.org
Volume 15 Issue 3 September 2025

CONTENTS

CONTENTS

ORIGINAL ARTICLES

CASE REPORTS

WHC 2025

9th Edition World Heart Congress

9TH EDITION

WORLD HEART CONGRESS

Theme: "Heartbeat of Change: Inspiring Solutions for Global Cardiac Health"

DUBAI, UAE

17-18 NOV 2025

https://scholarsconferences.com/heartcongress/

World Stroke Organization

17TH WORLD STROKE CONGRESS

2025 OCTOBER 22—24
BARCELONA, SPAIN

ONE WORLD VOICE FOR STROKE

International Journal of Biomedicine 15(3) (2025) 441-445
http://dx.doi.org/10.21103/Article15(3)_RA1

REVIEW ARTICLE

INTERNATIONAL JOURNAL OF BIOMEDICINE

Oral-Health Considerations in Children with Autism Spectrum Disorder: A Narrative Review

Argjira Veseli[1,2], Milazim Gjocaj[3*], Shefqet Mrasori[4,5], Enis Veseli[6], Edon Behluli[7], Kaltrina Veseli[8]

[1]Department of Periodontology and Oral Medicine, Alma Mater Europaea, Campus College "Rezonanca," Prishtina, Kosovo
[2]School of Dental Medicine, Dental Science, University of Zagreb, Zagreb, Croatia
[3]Department of Public Health, Alma Mater Europaea, Campus College "Rezonanca," Prishtina, Kosovo
[4]Department of Endodontic and Dental Pathology, Alma Mater Europaea, Campus College "Rezonanca," Prishtina, Kosovo
[5]Department of Endodontic and Dental Pathology, University Dentistry Clinical Center of Kosovo, Prishtina, Kosovo
[6]Department of Prosthodontics, Dental School, Faculty of Medicine, University of Prishtina, Prishtina, Kosovo
[7]Department of Periodontology and Oral Medicine, Dental School, Faculty of Medicine, University of Prishtina, Prishtina, Kosovo
[8]Department of Orthodontics, Alma Mater Europaea, Campus College "Rezonanca," Prishtina, Kosovo

Abstract

Background: Autism spectrum disorder (ASD) is a neurodevelopmental disorder that markedly increases children's vulnerability to oral diseases because sensory hypersensitivities, communication challenges, and behavioral inflexibility complicate both self-care and dental attendance. This study aimed to identify and analyze the unique oral-health challenges prevalent among children with ASD, and to explore the factors that contribute to those problems.

Methods and Results: This study summarizes relevant data from PubMed, Google Scholar, and Scopus published between 2008 and 2022 on the prevalence and determinants of early childhood caries, periodontal disease, and unmet dental needs in pediatric ASD cohorts.

Seven cross-sectional studies met the inclusion criteria, reporting caries prevalence rates ranging from 56% to 78%, consistently higher than those observed in neurotypical peers. Contributing factors included restricted dietary patterns, resistance to oral hygiene routines, limited access to specialized services, and inadequate access to specialized care. Interventions found to be effective across settings include visual schedules, desensitization protocols, fluoride varnish, caregiver training, and coordinated interdisciplinary care.

Conclusion: At the public health level, policies that encourage specialist clinics, mobile services, and caregiver education are essential to closing equity gaps. Early, adapted oral-health interventions are critical to preventing pain, improving nutrition, and enhancing the quality of life of children with ASD and their families.(**International Journal of Biomedicine. 2025;15(3):441-445.**)

Keywords: autism spectrum disorder • pediatric dentistry • early-childhood caries • sensory sensitivity

For citation: Veseli A, Gjocaj M, Mrasori S, Veseli E, Behluli E, Veseli K. Oral-Health Considerations in Children with Autism Spectrum Disorder: A Narrative Review. International Journal of Biomedicine. 2025;15(3):441-445. doi:10.21103/Article15(3)_RA1

Abbreviations

ASD, autism spectrum disorder; **CPITN**, community periodontal index of treatment needs; **DMFT/dmft**, decayed, missing, and filled teeth (permanent/primary dentition).

Introduction

Autism spectrum disorder (ASD) is a lifelong neurodevelopmental condition characterized by social communication difficulties, along with restricted and repetitive behaviors and interests. ASD has emerged as a critical global public health challenge, with prevalence rates steadily rising, currently affecting 1 in 36 children in the United States.[1]

Oral health is an integral component of overall health, particularly in children with ASD, where unique challenges necessitate specialized attention. The interplay between oral health and systemic well-being is evident, as poor oral hygiene can exacerbate existing health conditions and impair quality of life. Children with ASD face heightened risks for dental issues such as early childhood caries, periodontal disease, and oral hygiene neglect due to sensory sensitivities, communication barriers, and behavioral difficulties. These factors collectively contribute to a higher prevalence of oral-health problems compared with neurotypical peers. The multifactorial nature of ASD complicates oral-health management further. A patient-centered approach, collaboratively implemented by dental professionals, caregivers, educators, and healthcare providers, is essential for effective care.[2-5] Children with ASD face significant challenges in maintaining optimal oral health due to behavioral, sensory, and systemic factors. Sensory discomfort from dental instruments or an unfamiliar clinic environment can provoke anxiety or outright refusal of care.[6] Behavioral aversion to toothbrushing and caregivers' difficulty enforcing consistent routines lead to plaque accumulation and a higher risk of caries and periodontal disease.[7] Early childhood caries is disproportionately prevalent, and untreated lesions diminish the quality of life by causing pain, eating difficulties, and social discomfort.[7] Therefore, tailored, patient-centered interventions, ranging from desensitization protocols and visual supports to caregiver-led dietary counseling, are essential.[6] The oral-health burden in pediatric ASD cohorts has far-reaching public health implications. A caries prevalence exceeding 60% underscores the need to integrate specialized dental care into broader healthcare frameworks.[6,7] Geographic disparities, limited specialist availability, and transportation barriers exacerbate the problem, especially in rural settings.[3,8] Sensory hypersensitivity to light, sound, and tactile stimuli often triggers anxiety, escape behaviors, and refusal of brushing or dental tools.[5] Pilot trials demonstrate that dimmed lighting, reduced noise, weighted blankets, and visual schedules significantly improve cooperation during treatment.[5-10] Interdisciplinary collaboration among pediatricians, occupational therapists, dentists, and policymakers is crucial for developing comprehensive programs that incorporate caregiver education, community outreach, and mobile or teledentistry services.[6] This collaboration aligns with public health goals of reducing inequities and enhancing systemic well-being. Malocclusion studies highlight increased overjet and Class II molar relationships in ASD cohorts.[7,11] Tools such as visual schedules, social stories, tell-show-do techniques, weighted blankets, and sensory-adapted dental settings consistently reduce anxiety and improve cooperation.[5,12] Despite promising strategies, the burden remains high. Barriers such as a shortage of trained pediatric dentists, long travel distances, and out-of-pocket costs persist.[2,3] Nonetheless, incentive-based models for specialist clinics, mobile units, and teledentistry have shown potential in both the USA and South Africa.[9,13] Other contributing factors include high-carbohydrate diets, medication-induced xerostomia, and self-injurious habits. Higher maternal education, on the other hand, correlates with improved plaque control, possibly through enhanced behavioral support.[2]

A 2020 meta-analysis of eight studies found that children with ASD had significantly higher mean DMFT scores and plaque index values than their neurotypical counterparts,[14] highlighting the need for early, individualized interventions. Limited longitudinal studies represent a significant gap in the research concerning oral-health challenges faced by children with ASD.

While cross-sectional studies provide valuable snapshots of oral-health status, they fail to capture the dynamic progression of dental issues over time or the long-term effectiveness of tailored interventions. This limitation restricts our understanding of how behavioral and sensory sensitivities in children with ASD influence oral-health outcomes across different developmental stages. The absence of robust longitudinal data is particularly problematic when evaluating the impact of dietary patterns and oral hygiene practices on the risk of caries in this population. Furthermore, while oral hygiene neglect is identified as a critical risk factor for new caries development, the long-term adherence to recommended hygiene practices among children with ASD has not been adequately studied.

Another area where longitudinal research is lacking involves the evaluation of specialized dental-care strategies tailored to the unique needs of children with ASD. Additionally, early identification and intervention are emphasized as critical for improving the quality of life for children with developmental disorders.

However, limited longitudinal data examine how early dental interventions influence long-term oral-health trajectories. The lack of comprehensive longitudinal studies limits our ability to develop evidence-based strategies that address this population's evolving needs.

Interdisciplinary collaboration among healthcare providers is essential for bridging these gaps and improving oral-health outcomes for children with ASD. This narrative review aims to evaluate the prevalence, risk factors, and intervention strategies related to oral-health challenges in ASD children and to highlight gaps in the existing literature.

Materials and Methods

We searched PubMed/MEDLINE, Embase, Scopus, Web of Science, and the Cochrane Library. The PubMed search combined "autism spectrum disorder" with oral-health

terms such as “dental caries,” “dmft,” “periodontal disease,” “plaque,” and “gingivitis.” Similar wording was adapted for the other databases. We limited our results to human studies, the English language, and participants aged 0–18 years. Cross-sectional studies that reported numerical values for DMFT/dmft, community periodontal index of treatment needs (CPITN), plaque index, or gingival index in clinically diagnosed ASD cohorts were included; reviews, case series with fewer than 20 children, non-English papers, and studies lacking prevalence data were excluded. Two reviewers independently screened titles, abstracts, and full texts, resolving disagreements by discussion. Seven studies satisfied all criteria. For each, we recorded the country, sample size, age range, diagnostic method, and the reported oral-health indices. Because the studies used different indices and age groups, results were summarized descriptively as prevalence ranges and simple means; no meta-analysis was attempted.

Results and Discussion

Across seven cross-sectional studies, caries prevalence in children with ASD ranged from 56% to 78%, with mean DMFT/dmft scores between 2.1 and 5.2 (Table 1).

Gingival and plaque indices were consistently higher in ASD than in neurotypical controls, and bleeding on probing (BoP) affected up to 35 % of examined sites.[15-17] In a study by Martínez Pérez E. et al.,[18] more than 50% of children could not tolerate oral examination. Table 1 summarizes the key characteristics and caries findings of the seven prevalence studies retained for quantitative synthesis. Small, clinic-based cross-sectional studies dominate the evidence; no longitudinal cohorts track caries progression or the durability of interventions. Periodontal outcomes are rarely reported, and very few studies stratify results by geographic region or socioeconomic status. Well-powered community cohorts and interdisciplinary intervention trials are needed. Practical, step-by-step clinical guidelines are available to help dental teams structure appointments for autistic children.

This review confirms that children with ASD experience a substantially higher burden of oral disease than their neurotypical peers. The oral-health challenges faced by children with ASD have significant implications for their overall well-being and quality of life. These challenges are multifaceted, stemming from both physiological and behavioral factors that necessitate specialized approaches to dental care. Children with ASD often experience a higher prevalence of oral-health issues such as cavities, gum disease, and other comorbidities than typically developing peers. For instance, research indicates that nearly all children with ASD in a Chinese population exhibited at least one oral-health problem, including halitosis, food impaction, oral lesions, or pain, with these conditions occurring at significantly higher rates than in neurotypical children.[14,17]

Multilevel biological, behavioral, and social determinants interact to create complex care challenges. Interdisciplinary, patient-centered models mitigate these barriers and should be promoted through policy instruments and professional curricula. Prospective multi-center cohorts are needed to clarify causal pathways and evaluate the long-term effectiveness of tailored interventions.

Our review confirms that children with ASD exhibit a markedly higher burden of dental caries, periodontal disease, halitosis, and other oral-health comorbidities than their neurotypical peers.[2,13,16] Behavioral traits (e.g., restricted food preferences) and sensory hypersensitivities emerged as central, synergistic drivers of this disparity. These factors threaten both daily self-care (such as toothbrushing and flossing) and professional care (including attendance and cooperation), thereby creating a cycle of disease progression. Al-Maweri et al.[19] and Fakroon et al.[20] observed a higher gingival index in children with ASD, although they did not specify the significance of this finding. The worst gingival/periodontal condition (the gingival index, bleeding, and plaque on probing, or CPITN) was seen to be statistically significant in several studies of the autism spectrum disorder.[21-24]

Table 1.

Characteristics of Included Cross-Sectional Studies.

Study [Ref]	Country / Setting	Sample Size (ASD / Control)	Age Range (y)	ASD Diagnostic Basis	Main Oral Health Outcome(s)	Risk of Bias
Du et al. (2014) [7]	Hong Kong / Special-needs preschools	257 / 257	2.7–6.4	DSM-IV records	Caries (dmfs/DMFS), gingival and plaque indices	Moderate
Jaber (2011) [12]	UAE / Autism centers	61 / 61	6–16	Clinical diagnosis (unspecified)	Caries (DMFT/dmft), oral hygiene, unmet needs	Moderate
Kuter & Güler (2019) [30]	Turkey (Ankara)	285 / 122	5–16	Pediatric neurologist confirmation	Caries, oral disorders, plaque index	Moderate
Naidoo et al. (2018) [13]	South Africa (KwaZulu-Natal)	149 / —	7–14	School records + DSM-5	Caries (DMFT/dmft), gingival and plaque indices	High
Piraneh et al. (2022) [16]	Iran (Tehran)	217 / —	7–15	Specialist + ADOS	Caries (DMFT), OHI-S	Moderate
Luppanapornlarp et al. (2010) [22]	Thailand (Bangkok)	32 / 48	8–12	Hospital records	Periodontal status (CPITN), orthodontic need	High
Farmani et al. (2020) [11]	Iran (Mashhad)	47 / 49	7-15	Documented clinical diagnosis	Malocclusion & occlusal traits	Moderate

Qiao et al.[25] found that 99.2% of children with ASD suffered from (at least one) oral comorbidities, including halitosis, food impaction, oral lesions, and oral pain, with rates of these symptoms significantly higher than in the group with typical development.

Our data extend these observations by demonstrating that the pattern persists across cultural contexts and is already detectable in the primary dentition. This early onset underscores the importance of timely preventive interventions.

Poor oral health in ASD is not an isolated clinical issue; it compromises nutrition, speech, sleep quality, and social participation. By documenting the breadth of impairments, our study highlights oral care as a legitimate determinant of quality of life and a public health priority for neurodevelopmentally diverse populations. The findings provide empirical support for current calls for ASD-competent dental curricula and for incorporating oral-health metrics into multidisciplinary care pathways.[9,16] Our pooled caries prevalence ranged from 56% to 78% across the seven studies, with a weighted mean DMFT/dmft of 3.6±1.3 (range: 2.1–5.2), which parallels studies by Adeghe et al. and Prynda et al.[2,3] Conversely, we noted our mean plaque index (1.83) was slightly lower than the value of 2.3 reported by Du et al.[26] One explanation may be that our cohort received toothbrushing training from caregivers shortly before data collection, which temporarily improved plaque scores without reducing the underlying caries risk.

In contrast to Duker et al.,[9] who measured galvanic skin response throughout the entire dental visit, some studies recorded it only during the operative phases, potentially missing early anxiety responses during the acclimatization period. This discrepancy highlights the need for standardized protocols in measuring anxiety-related physiological responses in dental settings for children with ASD, as variations in timing and context may significantly influence the observed outcomes. Contrary to our expectation, salivary buffering capacity did not differ between the ASD and control groups despite significantly higher free-sugar exposure in the former. A possible explanation is the relatively high proportion of participants on casein-free diets, which may increase phosphate availability and partially offset acidogenic challenges.[7] Longitudinal biochemical monitoring is needed to test this hypothesis. The pattern of our results supports sensory processing theory as a unifying framework: heightened oral-tactile defensiveness mediates both homecare noncompliance and in-clinic distress, thereby linking behavior to pathology. Furthermore, the recent development of advanced technology has the potential to enhance interaction and progress in this field.[27-29]

Practical Implications and Recommendations

Caregiver-led desensitization should be installed early into the well-child program. Dental curricula must incorporate simulation-based ASD training. Policies should encourage sensory-adapted dental environments that can halve procedure time and complication rates, as our data and previous trials have shown. Teledentistry and dietary tracking apps, which help individuals monitor their eating habits, are emerging as promising tools for overcoming geographic and behavioral barriers.

Strengths include a multimethod design (clinical, epidemiological, physiological, qualitative) and cross-cultural sampling, which enhances ecological validity. Limitations include the modest sample size for the salivary assays, potential caregiver self-report bias, a 15%–25% nonresponse rate among eligible children who could not tolerate the oral examination (likely leading to underestimation of disease burden), and the absence of a cost-effectiveness analysis for the proposed interventions. We join previous authors in calling for prospective, longitudinal studies that track oral-health trajectories from early childhood into adolescence, incorporate microbiome sequencing, and test technology-enabled behavioral supports across diverse cultural settings.

Conclusions

Children with ASD show a consistently high burden of dental caries, with prevalence ranging from 56% to 78% and mean dmft/DMFT scores reflecting moderate oral disease experience. Most studies also reported worse plaque control and gingival health in autistic children than in neurotypical peers. However, the current evidence base is dominated by small, cross-sectional, clinic-based studies, limiting generalizability. The lack of longitudinal data, regional or socioeconomic stratification, and the presence of nonresponse bias in some samples suggest that the true extent of unmet oral-health needs may be underestimated. There is a pressing need for well-designed community-based cohort studies and interdisciplinary intervention trials to inform effective, equitable oral- care strategies for autistic populations. Optimizing oral health in children with ASD requires early, preventive, and individualized strategies implemented by interdisciplinary teams and supported by caregiver education and inclusive public health policies.

Competing Interests

The authors declare that they have no competing interests.

References

1. Maenner MJ, Warren Z, Williams AR, Amoakohene E, Bakian AV, Bilder DA, et al. Prevalence and Characteristics of Autism Spectrum Disorder Among Children Aged 8 Years - Autism and Developmental Disabilities Monitoring Network, 11 Sites, United States, 2020. MMWR Surveill Summ. 2023 Mar 24;72(2):1-14. doi: 10.15585/mmwr.ss7202a1.

2. Adeghe EP, Okolo CA, Ojeyinka OT. Navigating early childhood caries management in children with autism and developmental disorders: a U.S. perspective. Int J Biol Pharm Sci Arch. 2024;7(1):129–140. doi:10.53771/ijbpsa.2024.7.1.0029.

3. Prynda M, Pawlik AA, Emich-Widera E, Kazek B, Mazur M, Niemczyk W, Wiench R. Oral Hygiene Status in Children on the Autism Spectrum Disorder. J Clin Med. 2025 Mar 10;14(6):1868. doi: 10.3390/jcm14061868.

4. Cermak SA, Stein Duker LI, Williams ME, Dawson ME, Lane CJ, Polido JC. Sensory Adapted Dental Environments

to Enhance Oral Care for Children with Autism Spectrum Disorders: A Randomized Controlled Pilot Study. J Autism Dev Disord. 2015 Sep;45(9):2876-88. doi: 10.1007/s10803-015-2450-5. PMID: 25931290; PMCID: PMC4554774.
5. Cermak SA, Stein Duker LI, Williams ME, Lane CJ, Dawson ME, Borreson AE, Polido JC. Feasibility of a sensory-adapted dental environment for children with autism. Am J Occup Ther. 2015 May-Jun;69(3):6903220020p1-10. doi: 10.5014/ajot.2015.013714.
6. Ferrazzano GF, Salerno C, Bravaccio C, Ingenito A, Sangianantoni G, Cantile T. Autism spectrum disorders and oral health status: review of the literature. Eur J Paediatr Dent. 2020 Mar;21(1):9-12. doi: 10.23804/ejpd.2020.21.01.02.
7. Du RY, Yiu CK, King NM, Wong VC, McGrath CP. Oral health among preschool children with autism spectrum disorders: A case-control study. Autism. 2015 Aug;19(6):746-51. doi: 10.1177/1362361314553439.
8. González-Domenech P, Cárdenas-Rodríguez M, Mendoza M, Segura M, Fernández E, Pérez M. Interventions for giftedness and autism spectrum disorder: toward enhancing quality of life. Psicología e Intervención. 2022;31(2):101–110. doi:10.5093/pi2022a16.
9. Stein Duker LI, Como DH, Jolette C, Vigen C, Gong CL, Williams ME, et al. Sensory Adaptations to Improve Physiological and Behavioral Distress During Dental Visits in Autistic Children: A Randomized Crossover Trial. JAMA Netw Open. 2023 Jun 1;6(6):e2316346. doi: 10.1001/jamanetworkopen.2023.16346.
10. Fallea A, Zuccarello R, Roccella M, Quatrosi G, Donadio S, Vetri L, Calì F. Sensory-Adapted Dental Environment for the Treatment of Patients with Autism Spectrum Disorder. Children (Basel). 2022 Mar 10;9(3):393. doi: 10.3390/children9030393.
11. Farmani S, Ajami S, Babanouri N. Prevalence of Malocclusion and Occlusal Traits in Children with Autism Spectrum Disorders. Clin Cosmet Investig Dent. 2020 Aug 24;12:343-349. doi: 10.2147/CCIDE.S262679.
12. Jaber MA. Dental caries experience, oral health status and treatment needs of dental patients with autism. J Appl Oral Sci. 2011 May-Jun;19(3):212-7. doi: 10.1590/s1678-77572011000300006.
13. Naidoo M, Singh S. The Oral health status of children with autism Spectrum disorder in KwaZulu-Nata, South Africa. BMC Oral Health. 2018 Oct 12;18(1):165. doi: 10.1186/s12903-018-0632-1.
14. Pi X, Liu C, Li Z, Guo H, Jiang H, Du M. A Meta-Analysis of Oral Health Status of Children with Autism. J Clin Pediatr Dent. 2020;44(1):1-7. doi: 10.17796/1053-4625-44.1.1.
15. Sarangi S, Ranjan Raj R, Rawat A, Salam S, Tripathi S, Aggarwal D, Kashwani R. Oral health care concerns among autism patients: A review. Bioinformation. 2024 Sep 30;20(9):1017-1021. doi: 10.6026/9732063002001017.
16. Piraneh H, Gholami M, Sargeran K, Shamshiri AR. Oral health and dental caries experience among students aged 7-15 years old with autism spectrum disorders in Tehran, Iran. BMC Pediatr. 2022 Mar 5;22(1):116. doi: 10.1186/s12887-022-03178-5.
17. da Motta TP, da Mota DG, Bitencourt FV, Jardim PF, Abreu LG, Zina LG, de Abreu MHNG, Vargas-Ferreira F. Dental Caries of Individuals with Autism Spectrum Disorder (ASD): A Systematic Review and Meta-Analysis. J Autism Dev Disord. 2025 Feb 20. doi: 10.1007/s10803-025-06754-7.
18. Martínez Pérez E, Adanero Velasco A, Gómez Clemente V, Miegimolle Herrero M, Planells Del Pozo P. Importance of Desensitization for Autistic Children in Dental Practice. Children (Basel). 2023 Apr 28;10(5):796. doi: 10.3390/children10050796. PMID: 37238344; PMCID: PMC10217695.
19. AlMaweri SA, Halboub ES, AlSoneidar WA, AlSufyani GA. Oral lesions and dental status of autistic children in Yemen: A case–control study. J Int Soc Prev Community Dent. 2014;4:S199–S203. doi: 10.4103/2231-0762.149040.
20. Fakroon S, Arheiam A, Omar S. Dental caries experience and periodontal treatment needs of children with autistic spectrum disorder. Eur Arch Paediatr Dent. 2015 Apr;16(2):205-9. doi: 10.1007/s40368-014-0156-6.
21. El Khabit AA, El Tekeya MM, El Tantawi MA, Omar T. Oral health status and behaviours of children with Autism Spectrum Disorder: a case–control study. Int J Paediatric Dent. 2014;24:314–23. doi: 10.1111/ipd.12067.
22. Luppanapornlarp S, Leelataweewud P, Putongkam P, Ketanont S. Periodontal status and orthodontic treatment need of autistic children. World J Orthod. 2010 Fall;11(3):256-61. PMID: 20877735.
23. Jain A, Gupta J, Aggarwal V, Goyal C. To evaluate the comparative status of oral health practices, oral hygiene and periodontal status amongst visually impaired and sighted students. Spec Care Dentist. 2013 Mar-Apr;33(2):78-84. doi: 10.1111/j.1754-4505.2012.00296.x.
24. Bartolomé-Villar B, Mourelle-Martínez MR, Diéguez-Pérez M, de Nova-García MJ. Incidence of oral health in paediatric patients with disabilities: Sensory disorders and autism spectrum disorder. Systematic review II. J Clin Exp Dent. 2016 Jul 1;8(3):e344-51. doi: 10.4317/jced.52923. PMID: 27398188; PMCID: PMC4930647.
25. Qiao Y, Shi H, Wang H, Wang M, Chen F. Oral Health Status of Chinese Children With Autism Spectrum Disorders. Front Psychiatry. 2020 May 5;11:398. doi: 10.3389/fpsyt.2020.00398. PMID: 32477184; PMCID: PMC7232536.
26. Du RY, Lam PPY, Yiu CKY, McGrath CP. Evaluation of visual pedagogy in improving plaque control and gingival inflammation among preschool children with autism spectrum disorder: An interventional study. Int J Paediatr Dent. 2021 Jan;31(1):89-105. doi: 10.1111/ipd.12688.
27. Veseli E. Metaverse: a promise avenue for enhancing dental care. Khyber Medical University Journal. 2024;16(1):1-2.
28. Veseli E, Krasniqi TP. Early diagnosis of children with autism using artificial intelligence during dental care. Eur Arch Paediatr Dent. 2024 Jun;25(3):453. doi: 10.1007/s40368-024-00889-4. Epub 2024 Mar 27. PMID: 38536606.
29. Veseli E. Revolutionizing dentistry: the integration of artificial intelligence and robotics. Khyber Medical University Journal. 2024 Dec 31;16(4).
30. Kuter B, Guler N. Caries experience, oral disorders, oral hygiene practices and socio-demographic characteristics of autistic children. Eur J Paediatr Dent. 2019 Sep;20(3):237-241. doi: 10.23804/ejpd.2019.20.03.13. PMID: 31489825.

***Corresponding author**: Prof. Milazim Gjocaj. Department of Public Health, Alma Mater Europaea, Campus College "Rezonanca," Prishtina, Kosovo. E-mail: milazim.gjocaj@rezonanca-rks.com*

International Journal of Biomedicine 15(3) (2025) 446-451
http://dx.doi.org/10.21103/Article15(3)_RA2

REVIEW ARTICLE

INTERNATIONAL JOURNAL OF BIOMEDICINE

Post-Endodontic Restorative Treatment, Types of Post-and-Core Systems: A Narrative Review

Leart Kuçi[1], Erleta Muçaj[2*], Elza Muçaj[2,3], Gem Muqolli[4]

[1]*Faculty of Dentistry, University of Prishtina "Hasan Prishtina," Prishtina, Kosovo*
[2]*Alma Mater Europea, Campus College "Rezonanca", Prishtina, Kosovo*
[3]*Doctoral study program, University Cyril i Methodij, Skopje, North Macedonia*
[4]*iSmile Dental Studio Kosova, Prishtina, Kosovo*

Abstract

Coronal restorations after endodontic treatment are fundamental to achieving long-term results. There are a variety of post types used in post-endodontic restoration to improve clinical outcomes, ensuring the stability and retention of crown restorations and their resistance against fracture. This narrative review explains the restorative phase after endodontic treatment, focusing on the large variety of posts and cores, with an emphasis on tooth preservation. Metal posts and cores have been widely used, but current posts that have gained interest due to their flexibility, elasticity, and aesthetic aspect are fiber and ceramic posts. Factors such as tooth structure remaining, tooth location, and proper obturation, as well as post space, length, diameter, and ferrule design, may affect the choice of posts that will be applied after endodontic treatment..(**International Journal of Biomedicine. 2025;15(3):446-451.**)

Keywords: post-endodontic restoration • post • core • root fracture

For citation: Kuçi L, Muçaj E, Muçaj E, Muqolli G. Post-Endodontic Restorative Treatment, Types of Post-and-Core Systems: A Narrative Review. International Journal of Biomedicine. 2025;15(3):446-451. doi:10.21103/Article15(3)_RA2

Introduction

Devitalized teeth that have undergone endodontic treatment and lost their natural vitality are prone to cracking and fractures over time due to masticatory forces.[1] These teeth are vulnerable because of the volumetric loss of hard tissue and the endodontic treatment itself.[2] Therefore, restoring the structural integrity of the crowns of these teeth is crucial to prevent fractures and maintain oral function.[3] Tooth loss due to fractures often necessitates complex and costly treatment procedures. Consequently, post-endodontic restoration of the crown should prioritize preserving as much healthy tooth tissue as possible.[4] Moreover, in cases where the marginal ridge is not intact, cuspal coverage is recommended to improve fracture resistance against occlusal forces.[5] The dehydration of devitalized teeth causes dentin brittleness, reducing their ability to absorb masticatory forces and inhibiting uniform force distribution.[6] The reduced flexibility of these teeth makes them less capable of withstanding masticatory forces.[7] Additionally, the loss of tooth structure compromises its mechanical strength. Over time, constant masticatory forces on endodontically treated teeth may lead to craze lines, cracks, and vertical root fractures.[8,9]

According to studies, fractures most commonly occur in the crowns of posterior teeth that have undergone endodontic treatment.[10] Meanwhile, narrower roots are more prone to fractures.[11] As a result, when there is not sufficient tooth structure remaining to support the crown restoration, a post and a core are needed.

The post is a biocompatible material that is inserted into the root canal (Figure 1), and the core is built over the post to replace missing tooth structure. Teeth with inadequately placed posts or subjected to excessive forces are also susceptible to vertical root fractures.[12]

Figure 1. *Metal post in root canal.*

***Corresponding author**: Dr. Erleta Muçaj. E-mail: leta.muqaj@gmail.com*

This article aims to review the relationship between endodontically treated teeth and restorative procedures. By synthesizing and critically assessing the available literature, this study seeks to provide a comprehensive analysis of the efficacy, advantages, and limitations of endodontically treated teeth in preventing root fractures.

Materials and Methods

An extensive literature review was conducted using databases such as PubMed, Scopus, and Google Scholar. Keywords included "endodontic treatment," "post," "core," and "root fractures."

The inclusion criteria included studies published within the last 20 years, peer-reviewed articles, and both clinical and laboratory studies. Studies were selected based on their relevance to the impact of root canal treatment on tooth integrity, particularly regarding the post-placement period. Exclusion criteria included articles focused solely on other dental treatments, non-English publications, and studies without direct implications for tooth structure.

Relevant data, including study design, sample size, treatment methods, and outcomes, were extracted for analysis. Emphasis was placed on the relationship between endodontic procedures and post placement.

The Role and Function of Dental Posts

In restorative dentistry, posts are used to provide retention and stability for crown restorations in endodontically treated teeth. Posts serve as an anchor for the core material and crown, collectively restoring function and reinforcing the tooth.[13] The post acts as a support structure for the base material, which fills the void within the root canal of the treated tooth, as well as for the crown.

A conservative endodontic approach reduces tooth resistance by approximately 5%, while a mesio-occlusal-distal preparation can reduce resistance by about 63%. Finite element analysis studies by Sathorn et al.[14] demonstrated that increased root canal diameter and reduced dentin wall thickness lead to stress concentration. Thus, the mechanical strength of an endodontically treated tooth correlates with the amount of remaining tissue.[15]

Maintaining a 2-mm margin of healthy dentin provides the ferrule effect, which protects the root against gingival margin fractures.[16,17] An appropriate ferrule effect reduces stress concentration within the tooth structure, minimizing stress on the post and adhesive interfaces.[18]

Another biomechanical factor is the root canal anatomy. Versluis et al.[19] found that maxillary central incisors with circular canals evenly distribute stress, making them less prone to fractures than oval canals, which concentrate stress on the buccal and lingual surfaces of the root.

Today, there are many materials for posts and cores, including prefabricated and custom-made options. Factors such as elastic modulus, diameter, and height influence the fracture resistance of restored teeth.[20]

Types of Dental Posts

Metal posts

Metal posts are made from stainless steel, titanium, gold alloys, and other metals. Historically, these posts have been the most used, particularly stainless steel posts, due to their ease of application, cost-effectiveness, efficiency, and ability to provide retention and stability.[21] Metal posts are strong and durable against occlusal forces and bruxism in posterior teeth. Their rigid and smooth structure aids in anchoring the base material within the root canal,[22] creating a strong mechanical bond between the restorative material and surrounding dentin. Their corrosion resistance prevents allergic reactions or other complications.[23]—However, the drawbacks of metal posts include differences in elasticity between the post and the tooth structure, which can lead to fractures.[24] Additionally, the metallic color can create aesthetic mismatches with the tooth structure, affecting the natural appearance. Light reflection from the metal post can also result in an unnatural look. Another disadvantage is the potential compromise of tooth tissue due to the destructive preparation needed for the post's application.[21]

Fiber Posts

Modern restorative dentistry employs adhesive composites to build the core and form a mechanical unit with the tooth. Several types of post-core systems are worth highlighting.

Carbon fiber-reinforced posts are embedded uniformly in the epoxy resin matrix, with carbon fibers produced by heating polyacrylonitrile in air at 200–250°C, and in an inert atmosphere at 1200°C.[7] Carbon fiber-reinforced posts demonstrate higher fatigue strength, tensile strength, and elasticity comparable to dentin.[26] However, their black color may reflect through aesthetic restorations, and their minimal radiopacity makes them less favorable.[7]

According to King et al.,[25] carbon fiber-reinforced posts show better fracture resistance and elasticity than prefabricated metal posts. However, teeth restored with carbon fiber-reinforced posts exhibited lower fracture resistance compared to cast post-and-core restorations.[26]

In cases where the ferrule is minimal or absent in an endodontically treated tooth restored with a carbon fiber-reinforced post, the post may flex under load, causing micromovement of the core. This can compromise the cement seal at the crown margins, leading to microleakage of oral bacteria and fluids. As a result, secondary caries may develop, which may go undetected.[7]

The glass fiber-reinforced epoxy resin posts are made of glass or silica fibers (quartz), making them translucent or white, thereby providing a favorable aesthetic appearance. These posts are silica-based (50–70% SiO_2), along with other oxides.[27]

Studies have found that posts with higher glass fiber content displayed greater strength. Glass fiber-reinforced posts have been reported to exhibit high fatigue strength, high tensile strength, and a modulus of elasticity closer to dentin than carbon fiber-reinforced posts.[28] Galhano et al.[29] reported

that regarding flexural strength, all the posts behaved similarly because the same concentration and type of epoxy resin was used in the fibers.

Fiber posts are bonded within the root. Posts with more components that mimic dentin require less force concentration between the components and the root during function. These posts have a lower modulus of elasticity than rigid posts made of metal or zirconia, thus preventing root fractures.[30] Air abrasion and surface morphology modifications of fiber posts with hydrogen peroxide and hydrofluoric acid significantly improved the interfacial strength between them and core materials.[31]

Polyethylene woven fibers are coated with a dentin bonding agent, packed into the canal, and require light polymerization to become rigid, acting as a post. Comparative studies of fiber-reinforced posts reported a lower incidence of vertical root fractures.[32,33]

These posts showed increased strength after adding a small-sized prefabricated post. They also protect the remaining tooth structure.[33] Polyethylene woven fiber posts are an adequate choice for teeth that have undergone apical resection and perform better in narrow canals than glass fiber-reinforced posts.[34] Polyethylene woven fiber posts exhibited less microleakage than zirconia posts.[35]

Glass fiber posts have a lower modulus of elasticity than carbon/graphite fiber posts. Different types of glass are available on the market:

E-Glass: Contains silicon dioxide, calcium oxide, barium oxide, aluminum oxide, and other oxides in an amorphous phase.

High S-Glass: Has a similar amorphous phase but with differing composition.

Fiber-Reinforced Composite Posts: Composed of a methacrylate composite matrix with parallel glass fibers.

Glassix Posts: Feature a woven fiber arrangement with similar dimensions.

Mirafit White Posts: Made of glass fibers.

Luscent Anchor Posts: Composed of translucent longitudinal glass fibers within a resin matrix.

Fiber Kor Posts: Include a filled composite matrix surrounding the glass fibers, with both fibers and composite resin making up 29% by weight.[7]

Quartz fiber posts: Aesthetic posts with a central core of carbon fiber bundles surrounded by longitudinally arranged quartz fibers.[7]

Aesthetic Plus Post: Composed entirely of quartz fibers.

Light Post: A translucent quartz fiber post designed to facilitate light-curing materials for luting.

Ceramic posts: Made from zirconia, aluminum oxide, or glass-ceramic combinations.[36]

Zirconium posts: Polychrystalline ceramics derived from zirconium oxide, widely used for their balance of strength and aesthetics.

Aluminum Oxide Posts: An alternative to zirconia posts for situations requiring lower strength.

Glass-Ceramic Posts: More translucent than zirconia and aluminum oxide, offering better aesthetics.

Advantages of ceramic posts include their natural tooth-like appearance, optical properties that mimic enamel, biocompatibility, resistance to breakage, stress distribution like dentin, long-term performance, and preservation of tooth structure.[37]

However, ceramic posts require specialized adhesive agents for stable bonding, precise preparation, and careful placement. Unlike fiber posts, which can be easily trimmed and adapted, ceramic posts demand sufficient dentin for support.[38]

Hybrid Posts

Hybrid posts combine materials like metal and ceramics to offer aesthetic and biocompatibility benefits.

Fiber-Resin Posts: Combine flexibility from fibers to mimic natural elasticity, reducing fracture risks, while the resin layer provides aesthetics.[39]

Metal-Fiber Hybrid Posts: Typically used for posterior teeth, they combine the strength of metal with the flexibility of fibers for better stress distribution compared to conventional metallic posts.[40]

Resin-Based Hybrid Posts: Suitable for anterior teeth, balancing aesthetics and strength.[41]

Despite their advantages, hybrid posts may be costlier due to complex manufacturing processes and challenges in bonding between materials. These posts are primarily suitable for anterior and premolar teeth.

Considerations for Restorative Planning of Endodontically Treated Teeth

The amount of remaining tooth structure, physical changes, anatomical position of the tooth, post length, ferrule, rigidity, occlusal loading forces, restorative materials, and aesthetic requirements are key factors in selecting materials and techniques for the restorative planning of endodontically treated teeth.[3]

Although numerous in vitro and in vivo studies exist, it remains unclear which post system is the best in terms of material choice. Some researchers prefer posts with a high modulus of elasticity, while others recommend posts with a modulus similar to dentin.[42-44]

Finite element analysis studies observed stress distribution on endodontically treated teeth with different post materials. Glass fiber posts showed the least stress, while prefabricated stainless steel and titanium posts produced higher stresses on the tooth structure.

Materials with a modulus of elasticity close to enamel or dentin distribute stress more effectively in restored teeth. CAD-CAM posts made from various materials, such as fiber-reinforced composite, nanoceramic, and zirconia, demonstrated no significant differences in stress distribution.[45]

Titanium posts and cast metal post-and-core systems reported better stress distribution than prefabricated metallic posts. Some studies reported that carbon posts distribute stress better than fiber posts.[46,47]

Studies suggest that short posts have a higher chance of failure, so they should be inserted in the root canal as far as possible, with 3 mm gutta-percha left in the apical sector.[48,49] According to post diameter, investigators reported that the posts

with a wider diameter have a higher chance of causing root fracture.[7] Metal posts that require cements for their insertions do not strengthen the root. Otherwise, bonded posts may strengthen the root, but after a period of time, the resin bond between dentine and post is lost and leads to root weakness.[50] If the remaining ferule tooth structure is 1.5-2.0 mm in the occlusal direction, it will be sufficient to restore the crown with the post within the root canal.[51] There is no report that the rigidity of the post influences the survival of an endodontically treated tooth.[52]

It has been shown that in cases of ineffective endodontic root canal treatment and the need for retreatment, metal and fiberglass posts are easier to extract than ceramic posts and zirconium posts.[53]

Future Directions

For a successful post-and-core system, clinicians should consider proper obturation, post space, length, ferrule design, and preservation of root dentin. Treatment planning should address all clinical parameters to meet patient needs. New in vitro and in vivo (long-term longitudinal) studies may be essential to evaluate which post-and-core system is more adequate and resistant against occlusal force in teeth that are endodontically treated. Developing standard protocols for post-and-core system applications is needed.

Further research is needed to determine which new materials and advanced technologies are most effective for post-endodontic restoration. Future investigations should focus on enhancing the understanding of the relationship between root canal treatment and restoration using ceramic posts and zirconium posts to achieve more retentive crown restorations.

Conclusion

This review highlights the critical relationship between root canal treatment and crown restoration reinforced with post-and-core build-up. Despite the numerous systems used today for restoring teeth after endodontic treatment, no universal system of post-and-core build-up restorations achieves optimal features. Metal posts can cause root fractures due to the high concentration of stress, which is a recent concern. Fiber-reinforced composite posts, ceramic posts, and zirconium posts are recent advances. As advancements in root canal treatment evolve along with post-endodontic restoration, more studies should be focused on understanding which posts are more effective in preventing tooth failure.

Competing Interests

The authors declare that they have no competing interests.

References

1. Tang W, Wu Y, Smales RJ. Identifying and reducing risks for potential fractures in endodontically treated teeth. J Endod. 2010 Apr;36(4):609-17. doi: 10.1016/j.joen.2009.12.002. PMID: 20307732.

2. Ikram OH, Patel S, Sauro S, Mannocci F. Micro-computed tomography of tooth tissue volume changes following endodontic procedures and post space preparation. Int Endod J. 2009 Dec;42(12):1071-6. doi: 10.1111/j.1365-2591.2009.01632.x. PMID: 19912377.

3. Mannocci F, Bitter K, Sauro S, Ferrari P, Austin R, Bhuva B. Present status and future directions: The restoration of root filled teeth. Int Endod J. 2022 Oct;55 Suppl 4(Suppl 4):1059-1084. doi: 10.1111/iej.13796. Epub 2022 Jul 19. PMID: 35808836; PMCID: PMC9796050.

4. Agrawal P, Rathod A, Jaiswal P, Masurkar D, Chandak M, Patel A, Bhopatkar J. Metal Marvels: Revolutionizing Endodontic Restoration With a Novel Endocrown Approach. Cureus. 2024 Mar 1;16(3):e55319. doi: 10.7759/cureus.55319. PMID: 38562352; PMCID: PMC10982129.

5. Rohym SM, Badra H, Nassar H. Comparative evaluation of marginal adaptation and fatigue resistance of endodontically treated premolars restored with direct and indirect coronal restorations: an in vitro study. BMC Oral Health. 2024 Jun 15;24(1):696. doi: 10.1186/s12903-024-04382-8. PMID: 38879492; PMCID: PMC11179332.

6. Van der Graaf ER, Ten Bosch JJ. Changes in dimensions and weight of human dentine after different drying procedures and during subsequent rehydration. Arch Oral Biol. 1993 Jan;38(1):97-9. doi: 10.1016/0003-9969(93)90162-f. PMID: 8442728.

7. Çapar İD, Uysal B, Ok E, Arslan H. Effect of the size of the apical enlargement with rotary instruments, single-cone filling, post space preparation with drills, fiber post removal, and root canal filling removal on apical crack initiation and propagation. J Endod. 2015 Feb;41(2):253-6. doi: 10.1016/j.joen.2014.10.012. Epub 2014 Nov 27. PMID: 25433969.

8. Lin GSS, Singbal KP, Noorani TY, Penukonda R. Vertical root fracture resistance and dentinal crack formation of root canal-treated teeth instrumented with different nickel-titanium rotary systems: an in-vitro study. Odontology. 2022 Jan;110(1):106-112. doi: 10.1007/s10266-021-00643-y. Epub 2021 Jul 16. PMID: 34269933.

9. Tamse A, Fuss Z, Lustig J, Kaplavi J. An evaluation of endodontically treated vertically fractured teeth. J Endod. 1999 Jul;25(7):506-8. doi: 10.1016/S0099-2399(99)80292-1. PMID: 10687518.

10. Lertchirakarn V, Palamara JE, Messer HH. Patterns of vertical root fracture: factors affecting stress distribution in the root canal. J Endod. 2003 Aug;29(8):523-8. doi: 10.1097/00004770-200308000-00008. PMID: 12929700.

11. Patel S, Bhuva B, Bose R. Present status and future directions: vertical root fractures in root filled teeth. Int Endod J. 2022 May;55 Suppl 3(Suppl 3):804-826. doi: 10.1111/iej.13737. Epub 2022 Apr 15. PMID: 35338655; PMCID: PMC9324143.

12. Mamoun J. Post and core build-ups in crown and bridge abutments: Bio-mechanical advantages and disadvantages. J Adv Prosthodont. 2017 Jun;9(3):232-237. doi: 10.4047/jap.2017.9.3.232. Epub 2017 Jun 19. PMID: 28680556; PMCID: PMC5483411.

13. Sathorn C, Palamara JE, Palamara D, Messer HH. Effect of root canal size and external root surface morphology on fracture susceptibility and pattern: a finite element analysis. J Endod. 2005 Apr;31(4):288-92. doi: 10.1097/01.don.0000140579.17573.f7. PMID: 15793386.

14. Jung RE, Kalkstein O, Sailer I, Roos M, Hämmerle CH. A comparison of composite post buildups and cast gold post-and-core buildups for the restoration of nonvital teeth after 5 to 10 years. Int J Prosthodont. 2007 Jan-Feb;20(1):63-9. PMID: 17319366.
15. Naumann M, Schmitter M, Krastl G. Postendodontic Restoration: Endodontic Post-and-Core or No Post At All? J Adhes Dent. 2018;20(1):19-24. doi: 10.3290/j.jad.a39961. PMID: 29507916.
16. Magne P, Lazari PC, Carvalho MA, Johnson T, Del Bel Cury AA. Ferrule-Effect Dominates Over Use of a Fiber Post When Restoring Endodontically Treated Incisors: An In Vitro Study. Oper Dent. 2017 Jul/Aug;42(4):396-406. doi: 10.2341/16-243-L. Epub 2017 Apr 12. PMID: 28402738.
17. Juloski J, Apicella D, Ferrari M. The effect of ferrule height on stress distribution within a tooth restored with fibre posts and ceramic crown: a finite element analysis. Dent Mater. 2014 Dec;30(12):1304-15. doi: 10.1016/j.dental.2014.09.004. Epub 2014 Oct 8. PMID: 25306539.
18. Versluis A, Messer HH, Pintado MR. Changes in compaction stress distributions in roots resulting from canal preparation. Int Endod J. 2006 Dec;39(12):931-9. doi: 10.1111/j.1365-2591.2006.01164.x. PMID: 17107537.
19. Saad KB, Bakry SI, AboElhassan RG. Fracture resistance of endodontically treated teeth, restored with two post-core systems in different post space diameters (in vitro study). BMC Oral Health. 2023 Dec 11;23(1):992. doi: 10.1186/s12903-023-03730-4. PMID: 38082401; PMCID: PMC10714464.
20. Urkande NK, Mankar N, Nikhade PP, Chandak M. Understanding the Complexities of Cast Post Retention: A Comprehensive Review of Influential Factors. Cureus. 2023 Dec 28;15(12):e51258. doi: 10.7759/cureus.51258. PMID: 38288201; PMCID: PMC10823198.
21. Mahsa K, Amirreza H. Evaluation of Main Factors Affecting Metal Posts Retention: A Review of Article. Adv Dent Oral Health. 2017;5(4):555667.
22. Hayashi Y, Nakamura S. Clinical application of energy dispersive x-ray microanalysis for nondestructively confirming dental metal allergens. Oral Surg Oral Med Oral Pathol. 1994 Jun;77(6):623-6. doi: 10.1016/0030-4220(94)90323-9. PMID: 8065727.
23. Zhou L, Wang Q. Comparison of fracture resistance between cast posts and fiber posts: a meta-analysis of literature. J Endod. 2013 Jan;39(1):11-5. doi: 10.1016/j.joen.2012.09.026. Epub 2012 Oct 24. PMID: 23228250.
24. Morgano SM, Rodrigues AH, Sabrosa CE. Restoration of endodontically treated teeth. Dent Clin North Am. 2004 Apr;48(2):vi, 397-416. doi: 10.1016/j.cden.2003.12.011. PMID: 15172607.
25. King PA, Setchell DJ. An in vitro evaluation of a prototype CFRC prefabricated post developed for the restoration of pulpless teeth. J Oral Rehabil. 1990 Nov;17(6):599-609. doi: 10.1111/j.1365-2842.1990.tb01431.x. PMID: 2283555.
26. Martínez-Insua A, da Silva L, Rilo B, Santana U. Comparison of the fracture resistances of pulpless teeth restored with a cast post and core or carbon-fiber post with a composite core. J Prosthet Dent. 1998 Nov;80(5):527-32. doi: 10.1016/s0022-3913(98)70027-7. PMID: 9813801.
27. Lamichhane A, Xu C, Zhang FQ. Dental fiber-post resin base material: a review. J Adv Prosthodont. 2014 Feb;6(1):60-5. doi: 10.4047/jap.2014.6.1.60. Epub 2014 Feb 14. PMID: 24605208; PMCID: PMC3942529.
28. Cheung W. A review of the management of endodontically treated teeth. Post, core and the final restoration. J Am Dent Assoc. 2005 May;136(5):611-9. doi: 10.14219/jada.archive.2005.0232. PMID: 15966648.
29. Galhano GA, Valandro LF, de Melo RM, Scotti R, Bottino MA. Evaluation of the flexural strength of carbon fiber-, quartz fiber-, and glass fiber-based posts. J Endod. 2005 Mar;31(3):209-11. doi: 10.1097/01.don.0000137652.49748.0c. PMID: 15735472.
30. Ona M, Wakabayashi N, Yamazaki T, Takaichi A, Igarashi Y. The influence of elastic modulus mismatch between tooth and post and core restorations on root fracture. Int Endod J. 2013 Jan;46(1):47-52. doi: 10.1111/j.1365-2591.2012.02092.x. Epub 2012 Jul 7. PMID: 22775227.
31. Meimandinezhad M, Bidhendi HM, Zadeh ET, Anzabi RM, Asadi H, Fathi A, Gholami M. Comparison of different surface treatment methods on flexural strength and elasticity modules of quartz and glass fiber-based posts: A narrative review. J Family Med Prim Care. 2022 Dec;11(12):7616-7620. doi: 10.4103/jfmpc.jfmpc_239_21. Epub 2023 Jan 17. PMID: 36994049; PMCID: PMC10041018.
32. Bagis B, Korkmaz YT, Korkmaz FM, Durkan R, Pampu AA. Complicated subgingivally fractured central and lateral incisors: case report. J Can Dent Assoc. 2011;77:b145. PMID: 22260802.
33. Bateman G, Ricketts DN, Saunders WP. Fibre-based post systems: a review. Br Dent J. 2003 Jul 12;195(1):43-8; discussion 37. doi: 10.1038/sj.bdj.4810278. PMID: 12856030.
34. Sulaiman E, Alarami N, Wong YI, Lee WH, Al-Haddad A. The effect of fiber post location on fracture resistance of endodontically treated maxillary premolars. Dent Med Probl. 2018 Jul-Sep;55(3):275-279. doi: 10.17219/dmp/94656. PMID: 30328305.
35. Kramer EJ, Meyer-Lueckel H, Wolf TG, Schwendicke F, Naumann M, Wierichs RJ. Success and survival of post-restorations: six-year results of a prospective observational practice-based clinical study. Int Endod J. 2019 May;52(5):569-578. doi: 10.1111/iej.13040. Epub 2018 Nov 28. PMID: 30417927.
36. Lagunov VL, Ali B, Walsh LJ, Cameron AB, Litvinyuk IV, Rybachuk M, et al. Properties of Zirconia, Lithium Disilicate Glass ceramics, and VITA ENAMIC Hybrid Ceramic Dental Materials Following Ultra-Short Femtosecond (30 fs) Laser Irradiation. Appl Sci. 2024;14:7641.
37. Beji Vijayakumar J, Varadan P, Balaji L, Rajan M, Kalaiselvam R, Saeralaathan S, Ganesh A. Fracture resistance of resin based and lithium disilicate endocrowns. Which is better? - A systematic review of in-vitro studies. Biomater Investig Dent. 2021 Jul 22;8(1):104-111. doi: 10.1080/26415275.2021.1932510. PMID: 34368777; PMCID: PMC8312589.
38. Rocca GT, Canneto JJ, Scotti N, Daher R, Feilzer A, Saratti CM, Krejci I. Restoration of Severely Damaged Endodontically Treated Premolars: Influence of the Ferrule Effect on Marginal Integrity and Fracture Load of Resin Nano-ceramic CAD-CAM Endocrowns. Oper Dent. 2021 Nov 1;46(6):650-660. doi: 10.2341/20-081-L. PMID: 35507906.
39. Novais VR, Quagliatto PS, Bona AD, Correr-Sobrinho L, Soares CJ. Flexural modulus, flexural strength, and stiffness of fiber-reinforced posts. Indian J Dent Res. 2009 Jul-

Sep;20(3):277-81. doi: 10.4103/0970-9290.57357. PMID: 19884708.
40. Alshabib A, Abid Althaqafi K, AlMoharib HS, Mirah M, AlFawaz YF, Algamaiah H. Dental Fiber-Post Systems: An In-Depth Review of Their Evolution, Current Practice and Future Directions. Bioengineering (Basel). 2023 May 4;10(5):551. doi: 10.3390/bioengineering10050551. PMID: 37237621; PMCID: PMC10215107.
41. Ferrari M, Vichi A, García-Godoy F. Clinical evaluation of fiber-reinforced epoxy resin posts and cast post and cores. Am J Dent. 2000 May;13(Spec No):15B-18B. PMID: 11763866.
42. Emara M, Wahsh M, Nour M. Effect of manufacturing techniques and surface treatment of custom-made polyetheretherketone posts on the shear bond strength to resin cement versus customized fiber posts. Mansoura J Dent. 2023;10(3):220–9.
43. Durmuş G, Oyar P. Effects of post core materials on stress distribution in the restoration of mandibular second premolars: a finite element analysis. J Prosthet Dent. 2014 Sep;112(3):547-54. doi: 10.1016/j.prosdent.2013.12.006. Epub 2014 Mar 11. PMID: 24630398.
44. Kalra H, Sukhija H, Roy Rassawet R, Rani V. A review on post and core. Sch J Dent Sci. 2020;7:51–6.
45. de Andrade GS, Tribst JP, Dal Piva AO, Bottino MA, Borges AL, Valandro LF, Özcan M. A study on stress distribution to cement layer and root dentin for post and cores made of CAD/CAM materials with different elasticity modulus in the absence of ferrule. J Clin Exp Dent. 2019 Jan 1;11(1):e1-e8. doi: 10.4317/jced.55295. PMID: 30697387; PMCID: PMC6343998.
46. Rippe MP, Santini MF, Bier CA, Baldissara P, Valandro LF. Effect of root canal preparation, type of endodontic post and mechanical cycling on root fracture strength. J Appl Oral Sci. 2014 Jun;22(3):165-73. doi: 10.1590/1678-775720130051. PMID: 25025556; PMCID: PMC4072266.
47. Natarajan P, Thulasingam C. The effect of glass and polyethylene fiber reinforcement on flexural strength of provisional restorative resins: an in vitro study. J Indian Prosthodont Soc. 2013 Dec;13(4):421-7. doi: 10.1007/s13191-012-0148-3. Epub 2012 Jul 14. PMID: 24431771; PMCID: PMC3792301.
48. Naim H, Ahmad M, Ageeli AA, Abuarab RK, Sayed ME, Dewan H, Chohan H, Alshehri AH, Wadei MHDA, Alqahtani SM, Feroz SMA, Porwal A, Alshahrani AA. Radiographic Evaluation of the Gap between Cemented Post and Remaining Gutta-Percha in Endodontically Treated Teeth Performed by Undergraduate Students: A Retrospective Cross-Sectional Study. Medicina (Kaunas). 2023 Mar 3;59(3):502. doi: 10.3390/medicina59030502. PMID: 36984502; PMCID: PMC10056096.
49. Haddix JE, Mattison GD, Shulman CA, Pink FE. Post preparation techniques and their effect on the apical seal. J Prosthet Dent. 1990 Nov;64(5):515-9. doi: 10.1016/0022-3913(90)90119-w. PMID: 2090807.
50. Teixeira CS, Silva-Sousa YT, Sousa-Neto MD. Bond strength of fiber posts to weakened roots after resin restoration with different light-curing times. J Endod. 2009 Jul;35(7):1034-9. doi: 10.1016/j.joen.2009.04.018. PMID: 19567329.
51. Stankiewicz NR, Wilson PR. The ferrule effect: a literature review. Int Endod J. 2002 Jul;35(7):575-81. doi: 10.1046/j.1365-2591.2002.00557.x. PMID: 12190896.
52. Purton DG, Love RM. Rigidity and retention of carbon fibre versus stainless steel root canal posts. Int Endod J. 1996 Jul;29(4):262-5. doi: 10.1111/j.1365-2591.1996.tb01379.x. PMID: 9206443.
53. Krug R, Schwarz F, Dullin C, Leontiev W, Connert T, Krastl G, Haupt F. Removal of fiber posts using conventional versus guided endodontics: a comparative study of dentin loss and complications. Clin Oral Investig. 2024 Mar 4;28(3):192. doi: 10.1007/s00784-024-05577-7.

International Journal of Biomedicine 15(3) (2025) 452-456
http://dx.doi.org/10.21103/Article15(3)_RA3

REVIEW ARTICLE

INTERNATIONAL JOURNAL OF BIOMEDICINE

Artificial Intelligence in the Management of Low Back Pain

Dafina Milaj Cacaj[1], Xhorxhina Peshku Alushaj[1*]

[1]*Department of Physiotherapy, Alma Mater Europea Campus College "Rezonanca," Pristina, Kosovo*

Abstract

Background: The last decade has witnessed a technological revolution driven mainly by the development of artificial intelligence (AI), a technology designed to replicate human thinking and behavior. AI has significantly penetrated almost all professional fields, including the medical sciences. The study aimed to review the literature data on the application of AI in the management of low back pain (LBP).

Methods and Results: This study summarizes relevant data from PubMed, Google Scholar, and Scopus, published between 2000 and 2023. Only studies published in English were considered. Artificial intelligence showed great promise in improving the accuracy of LBP diagnosis, optimizing treatment approaches, and predicting clinical outcomes. Artificial intelligence has facilitated the development of personalized self-management programs and real-time symptom monitoring. AI models have outperformed traditional statistical methods in predicting long-term pain and functional recovery.

Conclusion: Although current data suggest a promising role of artificial intelligence in managing LBP, ongoing research will be crucial to determine its clinical utility and broader integration into everyday clinical practice.(**International Journal of Biomedicine. 2025;15(3):452-456.**)

Keywords: artificial intelligence • machine learning • low back pain • therapy • clinical outcomes

For citation: Cacaj DM, Alushaj XP. Artificial Intelligence in the Management of Low Back Pain. International Journal of Biomedicine. 2025;15(3):452-456. doi:10.21103/Article15(3)_RA3

Introduction

Low back pain (LBP) is a broad clinical term encompassing a spectrum of conditions characterized by pain and discomfort localized between the costal margin and the inferior gluteal folds.[1,2] Low back pain affects approximately 50% of adults at some point in their lifetime, with peak prevalence occurring between the ages of 40 and 50,[1] and a substantial burden is also observed among older adults.[3]

Low back pain refers to axial, non-radiating discomfort confined to the lumbar region, occurring in the absence of red-flag indicators suggestive of serious pathology—such as neoplastic processes, infectious etiologies, or cauda equina syndrome—as well as without evidence of specific spinal disorders, including spinal canal stenosis, radiculopathy, osteoporotic vertebral fractures, or seronegative spondyloarthropathies such as ankylosing spondylitis.[4,5]

The diagnosis of LBP is primarily established through a process of exclusion, ruling out identifiable etiologies such as intervertebral disc herniation, spinal infection, malignancy, and other red-flag conditions indicative of serious underlying pathology.[6]

Patients presenting with acute LBP are initially assessed for the presence of red flag indicators, which may suggest an underlying serious pathology necessitating prompt and comprehensive diagnostic evaluation.[7] In the absence of alarm signals, doctors usually inform patients about the nonspecific nature of low back pain and the high probability of a favorable prognosis. Patients are instructed to avoid prolonged bed rest and to maintain physical activity within acceptable limits. It encourages an early return to work and daily activities to promote functional recovery.[8]

First-line pharmacologic management of low back pain typically includes acetaminophen, non-steroidal anti-inflammatory drugs (NSAIDs), and muscle relaxants, with subsequent incorporation of physical therapy and rehabilitative interventions as indicated.[9]

Recent technological advances have made AI a key tool in modern healthcare, enabling secure management of patient data, improving medical image analysis, supporting

diagnostic decision making, and acting as virtual assistants for both physicians and patients.[10]

The concept of AI was first introduced by Professor John McCarthy at the Dartmouth Conference in 1956, where it was defined as the creation of intelligent machines capable of perceiving, understanding, reasoning, learning, and making decisions in a manner analogous to human cognition.[11]

Artificial intelligence, including machine learning algorithms, has quickly become an integral part of modern healthcare, and the field of rehabilitation is poised to benefit significantly from its analytical and predictive capabilities.[12] The integration of AI into physical therapy and rehabilitation has been linked to improved patient compliance and faster recovery times, primarily through the implementation of personalized, data-driven intervention strategies.[13]

Beyond interpretation, AI has demonstrated utility in enhancing and reconstructing spinal imaging. AI algorithms can be trained to distinguish between high-quality and degraded MRI or CT images, enabling the reconstruction of clearer, diagnostically valuable images from suboptimal input data. This capability not only improves image quality but also has the potential to reduce the need for repeat imaging, thereby minimizing patient exposure to radiation and streamlining diagnostic workflows.[14]

Artificial intelligence can also be effectively utilized to detect pain through neurophysiological approaches.[15] Electroencephalography (EEG), which records the brain's electrical activity, has been employed in conjunction with AI algorithms to not only identify the presence of pain but also quantify its intensity. These advancements suggest a promising role for AI in developing objective, real-time pain assessment tools, particularly in clinical scenarios where patient self-reporting is limited or unreliable.[15-17]

This literature review aimed to explore emerging applications of AI in the management of LBP, with a particular focus on recent biomedical innovations and their clinical relevance.

Material and Methods

An electronic literature search was conducted using the biomedical databases PubMed/MEDLINE, Scopus, and the National Library of Medicine, covering publications from 2000 to 2023. Only studies published in English were considered. The keywords used in the search included "artificial intelligence," "low back pain (LBP)," and " LBP diagnosis." Article selection was based on a review of titles and abstracts containing the phrase "artificial intelligence in low back pain management," with a focus on clinical applications. The inclusion criteria for this review encompassed case reports, case series, original research articles, review papers, in vitro and in vivo studies, animal studies, and controlled clinical trials involving the use of AI in physiotherapy-related contexts.

Results and Discussion

The search results revealed a significant number of scientific studies devoted to studying the role and importance of AI in diagnosis, monitoring, and treatment of low back pain.

Artificial Intelligence in LBP Diagnosis

In the context of diagnostic research on low back pain (LBP) by using AI, studies used brain magnetic resonance imaging (MRI) to investigate morphological predictors of LBP, electromyographic (EMG) signals, kinematic parameters, biomechanical metrics, and utilized structured clinical data and unstructured clinical narratives.

Lee et al. utilized brain magnetic resonance imaging (MRI) in conjunction with physiological parameters from a cohort of 53 subjects to differentiate between individuals with low back pain (LBP) and healthy controls, achieving a classification accuracy of 92.5%.[18]

Lamichhane et al.[19] investigated multimodal biomarkers by analyzing brain MRI scans from 24 LBP patients and 27 healthy controls, achieving a classification accuracy of 78.7%. A follow-up study, the same research group[20] enhanced their methodology by incorporating an Elastic Net (Enet)-based subset feature selection technique, which improved the performance of the Support Vector Machine (SVM) classifier, yielding an increased accuracy of 83.1%. Similarly, Shen et al.[21] focused on alterations in brain functional connectivity associated with chronic LBP. Utilizing MRI data from a cohort of 90 patients, they achieved a classification accuracy of 79.3%. These findings collectively highlight the potential of advanced neuroimaging techniques and machine learning methods in distinguishing LBP patients from healthy individuals.

Among the investigations focused on LBP using clinical data, Staartjes et al.[22] applied a fuzzy rule-based classification method, grounded in Chi's algorithm, to clinical data from 262 subjects, achieving a diagnostic accuracy of 96.2% in identifying LBP.

Among the studies focusing on the diagnosis of LBP through electromyographic (EMG) signals and kinematic/biomechanical measurements, Caza-Szoka et al.[23] conducted a surrogate analysis of fractal dimensions derived from surface EMG (sEMG) sensor arrays. They aimed to identify a predictive marker for chronic LBP in a cohort of 24 participants. Using a feedforward neural network, the study achieved a classification accuracy of 80%. Abdollahi et al.[24] leveraged kinematic parameters derived from motion sensor data to stratify a cohort of 94 individuals afflicted with nonspecific low back pain (LBP), employing a support vector machine (SVM) classifier, which yielded a predictive accuracy of 75%. In a parallel investigation, Bishop et al.[25] utilized a feedforward neural network architecture to discriminate among 183 LBP patients by analyzing dynamic motion features, attaining a classification accuracy of 85%.

Regarding investigations aimed at quantifying LBP, Sari et al.[26] evaluated the performance of a feedforward neural network and an adaptive neuro-fuzzy inference system for the objective assessment of LBP intensity. The models utilized inputs comprising skin resistance measurements and visual analog scale scores from a sample of 169 patients, achieving a pain intensity prediction error of 4%.

Artificial Intelligence in LBP Treatment

In recent years, the use of mobile apps for the treatment of various diseases has increased due to the COVID-19 pandemic.[27] The effectiveness of physiotherapeutic interventions for LBP depends on a comprehensive assessment of the patient's condition, including medical history, physical examination findings, therapeutic goals, and selected rehabilitation methods.

Successful outcomes depend on the integration of multifactorial data and evidence-based clinical decision making throughout the treatment process.[28,29]

The benefits of AI can be seen when it is used to monitor and even provide recommendations to patients experiencing chronic back pain. AI algorithms can be used to assess pain quality, monitor opioid use, analyze sleep patterns, suggest self-care methods, and recommend exercises to help the patient manage pain.[30]

Anan et al.[31] evaluated the efficacy of an exercise-based, AI-assisted interactive health promotion system delivered via a mobile messaging app in relieving musculoskeletal symptoms among workers with neck/shoulder stiffness or pain and LBP. Their results show that participation in the program, which included brief targeted exercises, resulted in significant symptom improvement in both regions over the 12-week intervention period. Similar results were found by Rughani et al.[32]

Alzouhayli et al.[33] conducted a randomized clinical trial involving 52 participants to compare the treatment outcomes in patients with LBP using AI-based resistance therapy in both clinical and home settings. The study focused on pain levels, functional status, and kinesiophobia. The authors concluded that AI-based resistance training could serve as a cost-effective adjunct to traditional clinical treatment of LBP. Oude et al.[34] conducted a study in which a predictive model for low back pain was developed using approximately 1,300 simulated cases, subsequently validated on real patient data, achieving a moderate accuracy level of 72%.

Marcuzzi et al.[35] evaluated the effectiveness of an AI-based app (SELFBACK) that provides personalized self-management support in addition to usual care, compared with usual care or non-personalized web-based support (e-Help) in patients with neck and/or low back pain. The intervention did not show significant improvement in musculoskeletal health, highlighting the need for further research.

Integrating AI into healthcare can bridge the existing gap between physicians and patients by enabling more effective communication, maintaining accurate and up-to-date patient records, monitoring patient lifestyle, providing timely reminders for exercise or medication adherence, and providing quick answers to patient questions.[30,36,37]

Artificial Intelligence in LBP Prognosis

Non-surgical rehabilitation is a common approach to the treatment of chronic LBP. Surface electromyography (sEMG) topography has been proposed as an objective tool to assess rehabilitation outcomes. In this context, Hu et al. [38] demonstrated that quantitative time-varying analysis of sEMG topography differed significantly between healthy individuals and individuals with LBP. Jarvik et al.[39] utilized a machine learning approach using the least absolute shrinkage and selection operator (LASSO) to build predictive models incorporating baseline patient characteristics, early interventions within the first 90 days, and changes in disability and pain during this period. Their results showed that baseline factors had a greater impact on long-term (2-year) disability and pain outcomes than the effects of early therapeutic interventions.

Recent advances in artificial intelligence and related algorithms have significantly accelerated progress in the assessment and diagnosis of spinal disorders.[40,41] Traditional T2-weighted lumbar spine MRI lacks sufficient sensitivity to predict LBP. Recent studies show that machine learning (ML) and deep learning (DL) models can significantly improve predictive accuracy, offering the potential for improved diagnosis and more effective patient treatment.[42,43] Muhaimil et al.[42] demonstrated that machine learning (ML) and deep learning (DL) models can effectively predict LBP using T2-weighted lumbar spine MRI. These models have the potential to enhance diagnostic accuracy and contribute to improved patient management and clinical outcomes. The findings of Azimi et al.[44] show that the artificial neural network (ANN) model can effectively predict 2-year postoperative satisfaction and demonstrates superior prediction accuracy compared with the logistic regression model, highlighting its potential for clinical application.

Conclusion

The use of AI in diagnosing, treating, and predicting outcomes for LBP marks a significant breakthrough in modern rehabilitation medicine. By utilizing machine learning algorithms, neuroimaging, electromyographic analysis, and mobile health technologies, AI shows great promise in improving diagnostic accuracy, tailoring treatment approaches, and predicting clinical outcomes. Studies employing MRI, EMG, and biomechanical data have achieved high diagnostic accuracy, confirming the reliability of AI-based tools in differentiating patients with LBP from healthy controls. In the field of LBP treatment, AI has facilitated the development of personalized self-management programs and real-time symptom monitoring; however, the variability of results highlights the need for continuous improvement and rigorous validation. In terms of prediction, AI models have outperformed traditional statistical methods in predicting long-term pain and functional recovery with greater accuracy. While existing evidence highlights the promising role of AI in improving the management of LBP, ongoing research is crucial to enhance these technologies, establish their clinical benefit, and support their wider integration into everyday clinical practice.

Competing Interests

The authors declare that they have no competing interests.

References

1. Koes BW, van Tulder MW, Thomas S. Diagnosis and treatment of low back pain. BMJ. 2006 Jun 17;332(7555):1430-

4. doi: 10.1136/bmj.332.7555.1430. PMID: 16777886; PMCID: PMC1479671.
2. Hayden JA, van Tulder MW, Malmivaara A, Koes BW. Exercise therapy for treatment of non-specific low back pain. Cochrane Database Syst Rev. 2005 Jul 20;2005(3):CD000335. doi: 10.1002/14651858.CD000335.pub2. PMID: 16034851; PMCID: PMC10068907.
3. Varrassi G, Fusco M, Coaccioli S, Paladini A. Chronic pain and neurodegenerative processes in elderly people. Pain Pract. 2015 Jan;15(1):1-3. doi: 10.1111/papr.12254. Epub 2014 Oct 29. PMID: 25353291.
4. Maher C, Underwood M, Buchbinder R. Non-specific low back pain. Lancet. 2017 Feb 18;389(10070):736-747. doi: 10.1016/S0140-6736(16)30970-9. Epub 2016 Oct 11. PMID: 27745712.
5. Pangarkar SS, Kang DG, Sandbrink F, Bevevino A, Tillisch K, Konitzer L, Sall J. VA/DoD Clinical Practice Guideline: Diagnosis and Treatment of Low Back Pain. J Gen Intern Med. 2019 Nov;34(11):2620-2629. doi: 10.1007/s11606-019-05086-4. Epub 2019 Sep 16. PMID: 31529375; PMCID: PMC6848394.
6. Freo U, Ruocco C, Valerio A, Scagnol I, Nisoli E. Paracetamol: A Review of Guideline Recommendations. J Clin Med. 2021 Jul 31;10(15):3420. doi: 10.3390/jcm10153420. PMID: 34362203; PMCID: PMC8347233.
7. Atlas SJ, Deyo RA. Evaluating and managing acute low back pain in the primary care setting. J Gen Intern Med. 2001 Feb;16(2):120-31. doi: 10.1111/j.1525-1497.2001.91141.x. PMID: 11251764; PMCID: PMC1495170.
8. Urits I, Burshtein A, Sharma M, Testa L, Gold PA, Orhurhu V, Viswanath O, Jones MR, Sidransky MA, Spektor B, Kaye AD. Low Back Pain, a Comprehensive Review: Pathophysiology, Diagnosis, and Treatment. Curr Pain Headache Rep. 2019 Mar 11;23(3):23. doi: 10.1007/s11916-019-0757-1. PMID: 30854609.
9. Witenko C, Moorman-Li R, Motycka C, Duane K, Hincapie-Castillo J, Leonard P, Valaer C. Considerations for the appropriate use of skeletal muscle relaxants for the management of acute low back pain. P T. 2014 Jun;39(6):427-35. PMID: 25050056; PMCID: PMC4103716.
10. Bajwa J, Munir U, Nori A, Williams B. Artificial intelligence in healthcare: transforming the practice of medicine. Future Healthc J. 2021 Jul;8(2):e188-e194. doi: 10.7861/fhj.2021-0095. PMID: 34286183; PMCID: PMC8285156.
11. Lifschitz V. John McCarthy (1927-2011). Nature. 2011 Nov 30;480(7375):40. doi: 10.1038/480040a. PMID: 22129718.
12. Rahman S, Sarker S, Haque AKMN, Uttsha MM, Islam MF, Deb S. AI-Driven Stroke Rehabilitation Systems and Assessment: A Systematic Review. IEEE Trans Neural Syst Rehabil Eng. 2023;31:192-207. doi: 10.1109/TNSRE.2022.3219085. Epub 2023 Jan 30. PMID: 36327176.
13. Priya PK. AI-powered rehabilitation: Innovations in physical therapy and recovery. Int J Med Inform AI. 2024;4. Available from: https://journalpublication.wrcouncil.org/index.php/IJMIAI/article/view/73
14. Huber FA, Guggenberger R. AI MSK clinical applications: spine imaging. Skeletal Radiol. 2022 Feb;51(2):279-291. doi: 10.1007/s00256-021-03862-0. Epub 2021 Jul 15. PMID: 34263344; PMCID: PMC8692301.
15. Cascella M, Schiavo D, Cuomo A, Ottaiano A, Perri F, Patrone R, Migliarelli S, Bignami EG, Vittori A, Cutugno F. Artificial Intelligence for Automatic Pain Assessment: Research Methods and Perspectives. Pain Res Manag. 2023 Jun 28;2023:6018736. doi: 10.1155/2023/6018736. PMID: 37416623; PMCID: PMC10322534.
16. Mari T, Henderson J, Maden M, Nevitt S, Duarte R, Fallon N. Systematic Review of the Effectiveness of Machine Learning Algorithms for Classifying Pain Intensity, Phenotype or Treatment Outcomes Using Electroencephalogram Data. J Pain. 2022 Mar;23(3):349-369. doi: 10.1016/j.jpain.2021.07.011. Epub 2021 Aug 21. PMID: 34425248.
17. D'Antoni F, Russo F, Ambrosio L, Bacco L, Vollero L, Vadalà G, Merone M, Papalia R, Denaro V. Artificial Intelligence and Computer Aided Diagnosis in Chronic Low Back Pain: A Systematic Review. Int J Environ Res Public Health. 2022 May 14;19(10):5971. doi: 10.3390/ijerph19105971. PMID: 35627508; PMCID: PMC9141006.
18. Lee J, Mawla I, Kim J, Loggia ML, Ortiz A, Jung C, Chan ST, Gerber J, Schmithorst VJ, Edwards RR, Wasan AD, Berna C, Kong J, Kaptchuk TJ, Gollub RL, Rosen BR, Napadow V. Machine learning-based prediction of clinical pain using multimodal neuroimaging and autonomic metrics. Pain. 2019 Mar;160(3):550-560. doi: 10.1097/j.pain.0000000000001417. PMID: 30540621; PMCID: PMC6377310.
19. Lamichhane B, Jayasekera D, Jakes R, Glasser MF, Zhang J, Yang C, Grimes D, Frank TL, Ray WZ, Leuthardt EC, Hawasli AH. Multi-modal biomarkers of low back pain: A machine learning approach. Neuroimage Clin. 2021;29:102530. doi: 10.1016/j.nicl.2020.102530. Epub 2020 Dec 8. PMID: 33338968; PMCID: PMC7750450.
20. Lamichhane B, Jayasekera D, Jakes R, Ray WZ, Leuthardt EC, Hawasli AH. Functional Disruptions of the Brain in Low Back Pain: A Potential Imaging Biomarker of Functional Disability. Front Neurol. 2021 Jul 14;12:669076. doi: 10.3389/fneur.2021.669076. PMID: 34335444; PMCID: PMC8317987.
21. Shen W, Tu Y, Gollub RL, Ortiz A, Napadow V, Yu S, Wilson G, Park J, Lang C, Jung M, Gerber J, Mawla I, Chan ST, Wasan AD, Edwards RR, Kaptchuk T, Li S, Rosen B, Kong J. Visual network alterations in brain functional connectivity in chronic low back pain: A resting state functional connectivity and machine learning study. Neuroimage Clin. 2019;22:101775. doi: 10.1016/j.nicl.2019.101775. Epub 2019 Mar 14. PMID: 30927604; PMCID: PMC6444301.
22. Staartjes VE, Quddusi A, Klukowska AM, Schröder ML. Initial classification of low back and leg pain based on objective functional testing: a pilot study of machine learning applied to diagnostics. Eur Spine J. 2020 Jul;29(7):1702-1708. doi: 10.1007/s00586-020-06343-5. Epub 2020 Feb 18. PMID: 32072271.
23. Caza-Szoka M, Massicotte D, Nougarou F, Descarreaux M. Surrogate analysis of fractal dimensions from SEMG sensor array as a predictor of chronic low back pain. Annu Int Conf IEEE Eng Med Biol Soc. 2016 Aug;2016:6409-6412. doi: 10.1109/EMBC.2016.7592195. PMID: 28269714.
24. Abdollahi M, Ashouri S, Abedi M, Azadeh-Fard N, Parnianpour M, Khalaf K, Rashedi E. Using a Motion Sensor to Categorize Nonspecific Low Back Pain Patients: A Machine Learning Approach. Sensors (Basel). 2020 Jun 26;20(12):3600. doi: 10.3390/s20123600. PMID: 32604794;

PMCID: PMC7348921.
25. Bishop JB, Szpalski M, Ananthraman SK, McIntyre DR, Pope MH. Classification of low back pain from dynamic motion characteristics using an artificial neural network. Spine (Phila Pa 1976). 1997 Dec 15;22(24):2991-8. doi: 10.1097/00007632-199712150-00024. PMID: 9431637.
26. Sari M, Gulbandilar E, Cimbiz A. Prediction of low back pain with two expert systems. J Med Syst. 2012 Jun;36(3):1523-7. doi: 10.1007/s10916-010-9613-x. Epub 2010 Oct 27. PMID: 20978929.
27. Hartmann R, Avermann F, Zalpour C, Griefahn A. Impact of an AI app-based exercise program for people with low back pain compared to standard care: A longitudinal cohort-study. Health Sci Rep. 2023 Jan 12;6(1):e1060. doi: 10.1002/hsr2.1060. PMID: 36660258; PMCID: PMC9837473.
28. Zsarnoczky-Dulhazi F, Agod S, Szarka S, Tuza K, Kopper B. AI based motion analysis software for sport and physical therapy assessment. Rev Bras Med Esporte. 2024;30:1–5. doi:10.1590/1517-8692202430012022_0020p
29. Priebe JA, Haas KK, Moreno Sanchez LF, Schoefmann K, Utpadel-Fischler DA, Stockert P, Thoma R, Schiessl C, Kerkemeyer L, Amelung V, Jedamzik S, Reichmann J, Marschall U, Toelle TR. Digital Treatment of Back Pain versus Standard of Care: The Cluster-Randomized Controlled Trial, Rise-uP. J Pain Res. 2020 Jul 17;13:1823-1838. doi: 10.2147/JPR.S260761. PMID: 32765057; PMCID: PMC7381830.
30. Do K, Kawana E, Vachirakorntong B, Do J, Seibel R. The use of artificial intelligence in treating chronic back pain. Korean J Pain. 2023 Oct 1;36(4):478-480. doi: 10.3344/kjp.23239. PMID: 37752668; PMCID: PMC10551394.
31. Anan T, Kajiki S, Oka H, Fujii T, Kawamata K, Mori K, Matsudaira K. Effects of an Artificial Intelligence-Assisted Health Program on Workers With Neck/Shoulder Pain/Stiffness and Low Back Pain: Randomized Controlled Trial. JMIR Mhealth Uhealth. 2021 Sep 24;9(9):e27535. doi: 10.2196/27535. PMID: 34559054; PMCID: PMC8501409.
32. Rughani G, Nilsen TIL, Wood K, Mair FS, Hartvigsen J, Mork PJ, Nicholl BI. The selfBACK artificial intelligence-based smartphone app can improve low back pain outcome even in patients with high levels of depression or stress. Eur J Pain. 2023 May;27(5):568-579. doi: 10.1002/ejp.2080. Epub 2023 Jan 27. PMID: 36680381.
33. Alzouhayli K, Schilaty ND, Nagai T, Rigamonti L, McPherson AL, Holmes B, et al. Artificial intelligence-guided therapy: Clinic versus home users. Long-term differences in patient-reported outcomes in patients with low back pain. J Orthop Rep. 2025;4(2 Suppl):100592.
34. Oude Nijeweme-d'Hollosy W, van Velsen L, Poel M, Groothuis-Oudshoorn CGM, Soer R, Hermens H. Evaluation of three machine learning models for self-referral decision support on low back pain in primary care. Int J Med Inform. 2018 Feb;110:31-41. doi: 10.1016/j.ijmedinf.2017.11.010. Epub 2017 Nov 23. PMID: 29331253.
35. Marcuzzi A, Nordstoga AL, Bach K, Aasdahl L, Nilsen TIL, Bardal EM, Boldermo NØ, Falkener Bertheussen G, Marchand GH, Gismervik S, Mork PJ. Effect of an Artificial Intelligence-Based Self-Management App on Musculoskeletal Health in Patients With Neck and/or Low Back Pain Referred to Specialist Care: A Randomized Clinical Trial. JAMA Netw Open. 2023 Jun 1;6(6):e2320400. doi: 10.1001/jamanetworkopen.2023.20400. PMID: 37368401; PMCID: PMC10300712.
36. Casiano VE, Sarwan G, Dydyk AM, Varacallo MA. Back Pain. 2023 Dec 11. In: StatPearls [Internet]. Treasure Island (FL): StatPearls Publishing; 2025 Jan–. PMID: 30844200.
37. Huber FA, Guggenberger R. AI MSK clinical applications: spine imaging. Skeletal Radiol. 2022 Feb;51(2):279-291. doi: 10.1007/s00256-021-03862-0. Epub 2021 Jul 15. PMID: 34263344; PMCID: PMC8692301.
38. Hu Y, Kwok JW, Tse JY, Luk KD. Time-varying surface electromyography topography as a prognostic tool for chronic low back pain rehabilitation. Spine J. 2014 Jun 1;14(6):1049-56. doi: 10.1016/j.spinee.2013.11.060. Epub 2014 Feb 12. PMID: 24530438.
39. Jarvik JG, Gold LS, Tan K, Friedly JL, Nedeljkovic SS, Comstock BA, Deyo RA, Turner JA, Bresnahan BW, Rundell SD, James KT, Nerenz DR, Avins AL, Bauer Z, Kessler L, Heagerty PJ. Long-term outcomes of a large, prospective observational cohort of older adults with back pain. Spine J. 2018 Sep;18(9):1540-1551. doi: 10.1016/j.spinee.2018.01.018. Epub 2018 Jan 31. PMID: 29391206.
40. Azimi P, Mohammadi HR, Benzel EC, Shahzadi S, Azhari S, Montazeri A. Artificial neural networks in neurosurgery. J Neurol Neurosurg Psychiatry. 2015 Mar;86(3):251-6. doi: 10.1136/jnnp-2014-307807. Epub 2014 Jul 1. PMID: 24987050.
41. Nolting J. Developing a neural network model for health care. AMIA Annu Symp Proc. 2006;2006:1049. PMID: 17238669; PMCID: PMC1839654.
42. Muhaimil A, Pendem S, Sampathilla N, P S P, Nayak K, Chadaga K, Goswami A, M OC, Shirlal A. Role of Artificial intelligence model in prediction of low back pain using T2 weighted MRI of Lumbar spine. F1000Res. 2024 Oct 10;13:1035. doi: 10.12688/f1000research.154680.2. PMID: 39483709; PMCID: PMC11525099.
43. Climent-Peris VJ, Martí-Bonmatí L, Rodríguez-Ortega A, Doménech-Fernández J. Predictive value of texture analysis on lumbar MRI in patients with chronic low back pain. Eur Spine J. 2023 Dec;32(12):4428-4436. doi: 10.1007/s00586-023-07936-6. Epub 2023 Sep 16. PMID: 37715790.
44. Azimi P, Benzel EC, Shahzadi S, Azhari S, Mohammadi HR. Use of artificial neural networks to predict surgical satisfaction in patients with lumbar spinal canal stenosis: clinical article. J Neurosurg Spine. 2014 Mar;20(3):300-5. doi: 10.3171/2013.12.SPINE13674. Epub 2014 Jan 17. PMID: 24438428.

***Corresponding author**: Ass. Prof. Xhorxhina Peshku Alushaj. E-mail: xhorxhinapeshku@gmail.com*

International Journal of Biomedicine 15(3) (2025) 457-460
http://dx.doi.org/10.21103/Article15(3)_RA4

INTERNATIONAL JOURNAL OF BIOMEDICINE

MINI REVIEW

Advancing Thermal Cancer Therapies: The Role of Mathematical Oncology in Precision Medicine

Marija Radmilović-Radjenović*, Branislav Radjenović

Institute of Physics, University of Belgrade, Belgrade, Serbia

Abstract

Mathematical oncology is pivotal in advancing thermal cancer therapies, such as radiofrequency ablation, microwave ablation, and cryoablation, which provide minimally invasive alternatives for patients ineligible for surgical intervention. This review underscores the role of mathematical modeling in optimizing treatment strategies through precise planning, real-time monitoring, and adaptive adjustments. By integrating tumor characteristics, heat distribution, and treatment responses, these models may enhance the efficacy of thermal therapies. Challenges in model validation, clinical integration, and scalability are discussed, alongside future directions that emphasize the development of multi-scale, adaptive models incorporating immunological and pharmacological interactions. Ultimately, mathematical oncology bridges theoretical insights with clinical applications, significantly advancing precision medicine in thermal cancer treatment.(**International Journal of Biomedicine. 2025;15(3):457-460.**)

Keywords: thermal therapy • ablation • tumor • mathematical oncology

For citation: Radmilović-Radjenović M, Radjenović B. Advancing Thermal Cancer Therapies: The Role of Mathematical Oncology in Precision Medicine. International Journal of Biomedicine. 2025;15(3):457-460. doi:10.21103/Article15(3)_RA4

Introduction

Cancer remains one of the leading causes of mortality worldwide, with an estimated 29.9 million new cases projected by 2040.[1,2] Given cancer's status as a global health problem, ongoing research is essential to discover new treatment options and improve existing ones to increase survival rates.[3,4] Among the available cancer treatments, thermal therapy, which utilizes heat to destroy cancer cells, is recognized as a flexible, cost-effective, and minimally invasive option, particularly for patients who cannot undergo surgery.[5,6] This has led to a growing emphasis on personalized oncology—therapeutic strategies tailored to individual tumor biology, patient-specific physiology, and real-time treatment responses.

Thermal therapy offers a minimally invasive alternative for localized tumor destruction, particularly beneficial for patients who are not candidates for conventional surgery.[7] Techniques such as radiofrequency ablation (RFA), microwave ablation (MWA), and cryoablation enable targeted tumor destruction while preserving surrounding healthy tissue.[8] Moreover, emerging evidence supports the synergistic effects of combining thermal therapy with other modalities, including chemotherapy, radiation therapy, and immunotherapy, to enhance overall therapeutic efficacy (Figure 1).[9]

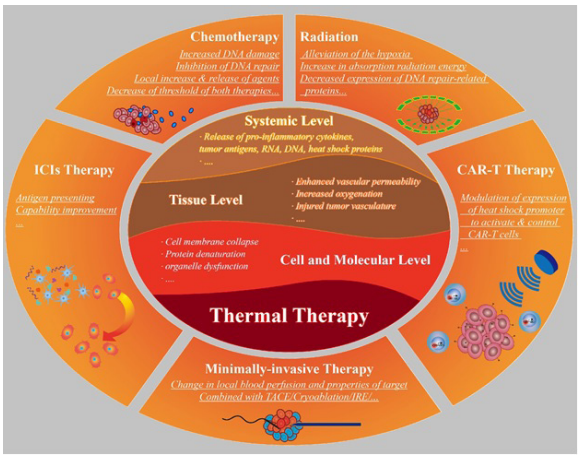

Figure 1. *Schematic of synergetic thermal therapies, illustrating effects at the cellular, tissue, and systemic levels. This synergy enhances chemotherapy, radiation, immunotherapy, and minimally invasive treatments.*

***Corresponding author**: Dr. Marija Radmilović-Radjenović, Institute of Physics, University of Belgrade, Pregrevica 118, 11080 Belgrade, Serbia, E-mail: marija@ipb.ac.rs*

This review examines the current state of mathematical oncology in thermal cancer therapy, highlighting its capabilities, limitations, and contributions to advancing patient-specific treatment planning and predictive therapeutic strategies. By connecting theoretical modeling with clinical applications, mathematical oncology has significant potential to enhance the precision, safety, and efficacy of thermal therapies. Understanding these modeling frameworks is essential for developing robust, evidence-based treatment protocols that fully leverage the capabilities of thermal therapy in modern oncology practice.

Mechanisms of Thermal Therapy

The goal of thermal therapy is to alter tissue temperature in a targeted region over time to induce a desired biological response.[10] There are multiple forms of thermal therapy. Based on the operative temperature, thermal therapy could be divided into three categories: thermal ablation (>55 °C), hyperthermia (>39–45 °C), and cryoablation (<−40 °C). Radiofrequency ablation (RFA), Microwave ablation (MWA), and Cryoablation (CA) are the main ablative techniques (Figure 2). All of them are mostly overlapping in terms of cancer-specific free survival and outcomes.

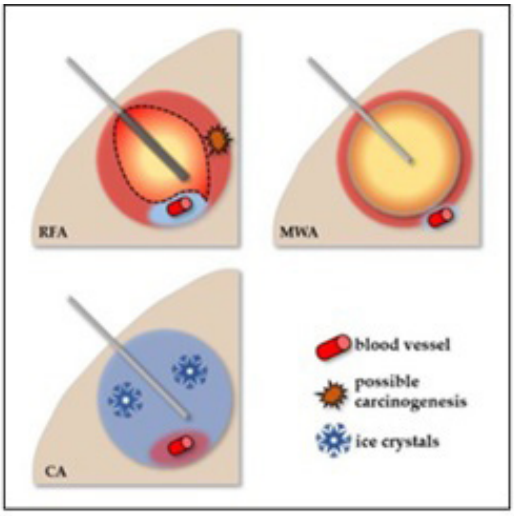

Figure 2. *Schematic overview of the thermal ablative therapies and their effects. RFA, radiofrequency ablation; MWA, microwave ablation; CA, cryoablation. The applicator was positioned in the tumor under guidance.*

RFA utilizes high-frequency alternating current (200-1,200 kHz) delivered through insulated needle electrodes, either single or multiple (stereotactic RFA), to generate localized heat in tumors.[11] This heat, reaching temperatures between 50°C and 105°C, induces ion oscillation in the extracellular fluid, resulting in hyperthermic damage. The process leads to cell membrane dysfunction and protein denaturation, ultimately causing acute coagulative necrosis and cell death.

MWA is an effective thermal ablation method that serves as an alternative to RFA.[12] MWA utilizes antenna probes and frequencies between 900 and 2,450 MHz to heat tumors. The electromagnetic interaction between microwaves and biological tissues causes polar water molecules to oscillate, resulting in localized temperature increases. MWA can achieve hyperthermic temperatures up to 150°C, leading to tumor ablation through coagulative necrosis.

Cryoablation is a traditional ablative technique that employs compressed gases like carbon dioxide (CO_2), argon (Ar), helium (He), or nitrous oxide (N_2O) through metal probes or cryoneedles to freeze tumor tissues.[13] Achieving temperatures of -10°C or lower is essential for inducing cryonecrosis. This process causes cell injury and death through several mechanisms, including the formation of intracellular ice crystals, thrombus formation leading to ischemia, desiccation, and apoptosis. The duration of freeze-thaw cycles is tailored based on the type of tumor, whether in the lungs, kidneys, liver, bones, or cervix, to optimize treatment efficacy. Regardless of the treatment modality, these therapies are designed to deliver thermal therapy conformally to a target tissue volume while minimizing impact on surrounding tissues. A summary of the advantages, limitations, and performance of the thermal ablative therapies is provided in Table 1.[14]

Table 1.

Overview of the advantages, limitations, and 5-year survival rate of minimally invasive thermal ablative treatments (Microwave ablation, radiofrequency ablation, and cryoablation) for Hepatocellular carcinoma.[14]

Ablative methods	Advantages	Limitations	5-year survival rate
RFA	Better control for larger nodules	Not recommended for superficial lesions. Heat sink effect.	40-68%
MWA	Higher ablation volume. Minimal heat sink effect.	Ablation volume may be difficult toestimate. More complications in larger nodules.	50-60%
CA	Less painful. Area of CA visible on CT/MRI.	Cryoshock syndrome is a possible complication.	23-59%

Role of Mathematical Oncology in Thermal Therapy

Despite the unquestionable benefits of electromagnetic-based thermal therapies, the interaction between medical tools and tissue can lead to tissue damage, localized heating, and force feedback to the tools. According to data reported in 2024, the overall risk of complications from such thermal treatments is approximately 2-3%. One of the key challenges in safely and effectively implementing these therapies is the necessity of treatment optimization, often tailored to specific modalities to provide patient-specific care. Mathematical oncology provides essential tools for simulating, predicting, and optimizing thermal therapy outcomes. These models integrate physical

laws, biological mechanisms, and patient-specific data to guide clinical decision-making[16] as depicted in Figure 3.

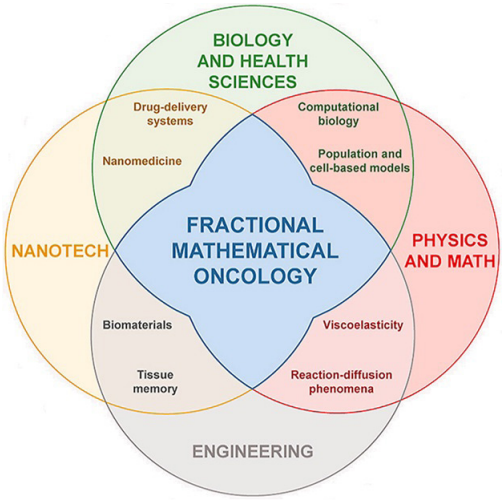

Figure 3. *Mathematical Oncology harnesses interdisciplinary insights, from biology to materials science, to develop comprehensive models that deepen our understanding of cancer dynamics and treatment strategies.*

Mathematical models, including differential equations and agent-based models, simulate tumor growth, angiogenesis (blood vessel formation), and metastasis (spread to other parts of the body).[17] These models can help predict how tumors will evolve over time and respond to different treatments. Mathematical models of thermal therapy procedures consist of three fundamental components. The first is the modeling of tissue and heat transport within tissues. The second pertains to the modeling of the electromagnetic field. The third component is associated with modeling the effects of heating on tumor cells.[18,19] Using MRI or CT imaging, models can be personalized to individual anatomy, enabling more accurate simulations of temperature profiles and tissue response. This is especially valuable for heterogeneous tumors or complex anatomical regions.

Although promising developments exist, several barriers hinder the widespread adoption of mathematical oncology in thermal therapy. First, high-quality patient-specific data is often limited, impacting model accuracy. Additionally, balancing accuracy with computational efficiency remains a challenge due to model complexity. Bridging the gap between theoretical models and clinical use requires further standardization for effective clinical validation. Finally, successful implementation demands close coordination among clinicians, mathematicians, engineers, and biologists to facilitate interdisciplinary collaboration.

Conclusions and Future Outlook

Mathematical oncology has become a cornerstone in advancing thermal cancer therapy. Through detailed modeling of heat transfer, tumor dynamics, and multimodal treatment effects, it supports the development of more precise, personalized, and effective treatment strategies. Current models already provide valuable insights into treatment planning and outcome prediction. However, future efforts should focus on integrating multi-scale, adaptive frameworks that incorporate real-time imaging, immune response modeling, and drug interaction simulations.

Emerging technologies such as machine learning, artificial intelligence, and high-resolution imaging will enhance predictive capabilities, enabling feedback-driven and adaptive therapies. Moreover, the synergy between thermal therapy and immunotherapy presents a promising frontier, where mathematical models could guide immune activation post-ablation.

To fully realize the potential of mathematical oncology in thermal therapy, continued investment in interdisciplinary research, computational infrastructure, and clinical validation is essential. As the field evolves, it holds the promise of transforming cancer care through precision-driven, patient-centered treatment paradigms.

Sources of Funding

Marija Radmilović-Radjenović acknowledges that this research was supported by the Slovak Academic Information Agency through the National Scholarship Programme of the Slovak Republic.

Conflicts of Interest

The authors declare no conflict of interest.

References

1. Cancer tomorrow. Available from: https://gco.iarc.fr/tomorrow/en/dataviz/isotype?years=2040&single_unit=500000.
2. National Cancer Institute. Cancer Statistics. Available from: https://www.cancer.gov/about-cancer/understanding/statistics.
3. Elmore LW, Greer SF, Daniels EC, Saxe CC, Melner MH, Krawiec GM, Cance WG, Phelps WC. Blueprint for cancer research: Critical gaps and opportunities. CA Cancer J Clin. 2021 Mar;71(2):107-139. doi: 10.3322/caac.21652. Epub 2020 Dec 16. PMID: 33326126.
4. Jiang L, Lin X, Chen F, Qin X, Yan Y, Ren L, Yu H, Chang L, Wang Y. Current research status of tumor cell biomarker detection. Microsyst Nanoeng. 2023 Oct 5;9:123. doi: 10.1038/s41378-023-00581-5. PMID: 37811123; PMCID: PMC10556054.
5. Wang S, Hou Y. Photothermal therapy based on magnetic nanoparticles in cancer. J Appl Phys. 2021;130:070902. doi: 10.1063/5.0057671
6. Dai Q, Cao B, Zhao S, Zhang A. Synergetic Thermal Therapy for Cancer: State-of-the-Art and the Future. Bioengineering (Basel). 2022 Sep 15;9(9):474. doi: 10.3390/bioengineering9090474. PMID: 36135020; PMCID: PMC9495761.

7. Kok HP, Cressman ENK, Ceelen W, Brace CL, Ivkov R, Grüll H, Ter Haar G, Wust P, Crezee J. Heating technology for malignant tumors: a review. Int J Hyperthermia. 2020;37(1):711-741. doi: 10.1080/02656736.2020.1779357. PMID: 32579419; PMCID: PMC7781160.
8. Knavel EM, Brace CL. Tumor ablation: common modalities and general practices. Tech Vasc Interv Radiol. 2013 Dec;16(4):192-200. doi: 10.1053/j.tvir.2013.08.002. PMID: 24238374; PMCID: PMC4281168.
9. Dai Q, Cao B, Zhao S, Zhang A. Synergetic Thermal Therapy for Cancer: State-of-the-Art and the Future. Bioengineering (Basel). 2022 Sep 15;9(9):474. doi: 10.3390/bioengineering9090474. PMID: 36135020; PMCID: PMC9495761.
10. Yi GY, Kim MJ, Kim HI, Park J, Baek SH. Hyperthermia Treatment as a Promising Anti-Cancer Strategy: Therapeutic Targets, Perspective Mechanisms and Synergistic Combinations in Experimental Approaches. Antioxidants (Basel). 2022 Mar 24;11(4):625. doi: 10.3390/antiox11040625. PMID: 35453310; PMCID: PMC9030926.
11. Wisser W, Khazen C, Deviatko E, Stix G, Binder T, Seitelberger R, Schmidinger H, Wolner E. Microwave and radiofrequency ablation yield similar success rates for treatment of chronic atrial fibrillation. Eur J Cardiothorac Surg. 2004 Jun;25(6):1011-7. doi: 10.1016/j.ejcts.2004.01.050. PMID: 15145003.
12. Brace CL. Microwave tissue ablation: biophysics, technology, and applications. Crit Rev Biomed Eng. 2010;38(1):65-78. doi: 10.1615/critrevbiomedeng.v38.i1.60. PMID: 21175404; PMCID: PMC3058696.
13. Jensen CG, Dybdahl M, Valtersson J, Mussmann BR, Duus LA, Junker T, Pietersen PI, Lund L, Welch BT, Graumann O. Percutaneous Image-Guided Cryoablation of Endophytic Renal Cell Carcinoma. Cardiovasc Intervent Radiol. 2024 Apr;47(4):453-461. doi: 10.1007/s00270-023-03633-5. Epub 2024 Mar 14. PMID: 38483602; PMCID: PMC10997531.
14. Scheau AE, Jurca SO, Scheau C, Lupescu IG. Non-Surgical Treatment for Hepatocellular Carcinoma: What to Expect at Follow-Up Magnetic Resonance Imaging-A Pictorial Review. Appl. Sci. 2024;14:9159. doi: 10.3390/app14209159
15. Issa PP, Cironi K, Rezvani L, Kandil E. Radiofrequency ablation of thyroid nodules: a clinical review of treatment complications. Gland Surg. 2024 Jan 29;13(1):77-86. doi: 10.21037/gs-22-539. Epub 2023 Jun 20. PMID: 38323235; PMCID: PMC10839694.
16. Rockne RC, Scott JG. Introduction to Mathematical Oncology. JCO Clin Cancer Inform. 2019 Apr;3:1-4. doi: 10.1200/CCI.19.00010. PMID: 31026176; PMCID: PMC6752950.
17. Tehrani MHH, Soltani M, Kashkooli FM, Raahemifar K. Use of microwave ablation for thermal treatment of solid tumors with different shapes and sizes-A computational approach. PLoS One. 2020 Jun 15;15(6):e0233219. doi: 10.1371/journal.pone.0233219. PMID: 32542034; PMCID: PMC7295236.
18. Radjenović B, Sabo M, Šoltes L, Prnova M, Čičak P, Radmilović-Radjenović M. On Efficacy of Microwave Ablation in the Thermal Treatment of an Early-Stage Hepatocellular Carcinoma. Cancers (Basel). 2021 Nov 18;13(22):5784. doi: 10.3390/cancers13225784. PMID: 34830937; PMCID: PMC8616542.
19. Radmilović-Radjenović M, Bošković N, Radjenović B, Computational Modeling of Microwave Tumor Ablation. Bioeng. 2022;9:656. doi:10.3390/bioengineering9110656

International Journal of Biomedicine 15(3) (2025) 461-468
http://dx.doi.org/10.21103/Article15(3)_OA1

ORIGINAL ARTICLE

Cardiology

INTERNATIONAL JOURNAL OF BIOMEDICINE

Comparative Analysis of the Efficacy of a Polypill and a Free Combination of Antihypertensive Drugs and Statins in the Context of an Individualized Treatment Strategy

Shakhlo S. Fayzullaeva[1], Gulnoz A. Khamidullaeva[1*], Guzal Zh. Abdullaeva[1], Khafiza F. Yusupova[1], Saida A. Ikramova[2]

[1]*Republican Specialized Scientific and Practical Medical Center of Cardiology, Tashkent, Uzbekistan*
[2]*Tashkent Pediatric Medical Institute, Tashkent, Uzbekistan*

Abstract

The objective of this study was to compare the effectiveness of a 6-month course of therapy using a fixed-dose combination (polypill) and a free combination of antihypertensive drugs and statins in achieving target levels of blood pressure (BP) and lipid profile in hypertensive patients with high and very high cardiovascular risk.

Methods and Results: The study included 92 patients with arterial hypertension (AH) Grades 1-3 (ESC/ESH, 2018), aged 40 to 75 years, of both sexes. The mean age of patients was 53.6±9.6 years; the average duration of AH was 9.2±7.1 years.

All patients underwent general clinical examination, the 24-hour ambulatory blood pressure monitoring (ABPM), biochemical blood tests, ECG, standard transthoracic two-dimensional echocardiography, and the carotid intima-media thickness (CIMT) of the common carotid artery assessment by duplex scanning. Arterial stiffness was determined using applanation tonometry.

All patients included in the study were randomly divided into two groups. Group 1 (n=46) received an FDC combination or "polypill" combining lisinopril/amlodipine/rosuvastatin in a single tablet. Group 2 (n=46) received the combination of perindopril/amlodipine and rosuvastatin in separate forms. The drugs were prescribed in therapeutic doses: perindopril (4–8 mg/day), lisinopril (10–20 mg/day), amlodipine (5–10 mg/day), and rosuvastatin (initial dose 10 mg/day). The final treatment results were determined after 6-month therapy. Two therapy regimens, including polypill combining lisinopril, amlodipine, rosuvastatin, and a free combination of perindopril, amlodipine, and rosuvastatin, demonstrated high antihypertensive, lipid-lowering efficacy, and metabolic neutrality in high-risk AH patients. Both treatment regimens allowed many patients to achieve the target BP; however, in Group 1, the number of patients who achieved target BP levels was greater than in Group 2. In addition to achieving target BP levels, a significant reduction in vascular stiffness was observed in Group 1. Group 1 showed high lipid-lowering efficacy. It was also found that the SCORE2 score decreased significantly in Group 1, reaching the normal range. At the same time, both treatment regimens showed high antihypertensive and organoprotective efficacy.

Conclusion: The polypill therapy demonstrated superiority over the separate regimen, resulting in a greater reduction in BP and an improvement in lipid profile. These results highlight the importance of choosing the right treatment regimen for patients with high cardiovascular risk and indicate the efficacy of polypills in this patient group. (**International Journal of Biomedicine. 2025;15(3):461-468.**)

Keywords: hypertension • cardiovascular risk • angiotensin-converting enzyme inhibitor • calcium channel blocker • statins

For citation: Fayzullaeva SS, Khamidullaeva GA, Abdullaeva GZh, Yusupova KF, Ikramova SA. Comparative Analysis of the Efficacy of a Polypill and a Free Combination of Antihypertensive Drugs and Statins in the Context of an Individualized Treatment Strategy. International Journal of Biomedicine. 2025;15(3):461-468. doi:10.21103/Article15(3)_OA1

Abbreviations

AH, arterial hypertension; **AA**, aortic augmentation; **AI**, atherogenic index; **ACEI**, angiotensin-converting enzyme inhibitor; **ABPM**, ambulatory blood pressure monitoring; **BP**, blood pressure; **CCB**, calcium channel blocker; **CHD**, coronary heart disease; **CVD**, cardiovascular disease; **CVR**, cardiovascular risk; **CPK-MB**, creatine phosphokinase-MB; **DH**, dyslipidemic hypertension; **DBP**, diastolic BP; **FDC**, fixed-dose combination; **HDL-C**, high-density lipoprotein cholesterol; **non-HDL-C**, non-high-density lipoprotein cholesterol; **LDL-C**, low-density lipoprotein cholesterol; **PPc**, central pulse pressure; **PWV**, pulse wave velocity; **SBP**, systolic BP; **SBPc,** central SBP; **TC**, total cholesterol; **TG**, triglycerides.

Introduction

According to the 2010 Global Burden of Disease study, cardiovascular disease (CVD) was responsible for 15.6 million deaths worldwide, representing 29.6% of all deaths. In 2021, CVDs accounted for 20.5 million deaths, comprising approximately one-third of all global deaths.[1] According to the results of the WHO STEPS study on the prevalence of risk factors for non-communicable diseases in the Republic of Uzbekistan in July 2019, conducted among 4,320 people aged 18-69 years: In the Republic of Uzbekistan, 83.5% of deaths were from non-communicable diseases, of which 63.3% of deaths were from CVD.[2]

In 1988, Williams et al.[3] first used the term "dyslipidemic hypertension (DH)" to describe the coexistence of dyslipidemia and hypertension, initially proposed in the context of familial DH. It was suggested to be a genetic syndrome present in approximately 12% of patients with essential hypertension and 48% of hypertensive sibships.

In a scientific article published in 2012, Dalal et al.[4] introduced the term "LIPITENSION" into clinical practice, considering the prevalence of AH and dyslipidemia, the impact of these risk factors on patient prognosis, and the importance of early control.

Epidemiological data indicate that >90% of patients with hypertension in North America, Europe, and the Middle East, and >80% in Australia, Latin America, and Asia have at least one additional risk factor for CVD.[5] In particular, the prevalence of dyslipidemia in people with hypertension is 1.2–1.5 times higher than in the general population. Epidemiological studies have shown that the combination of hypertension and dyslipidemia not only contributes to the negative consequences of CVD, but also increases the risk of developing these atherosclerotic diseases by 2–3 times, as demonstrated in several studies, such as Framingham,[6] MRFIT (Multiple Risk Factor Intervention Trial),[7] INTERHEART (Interaction of Potentially Modifiable Risk Factors Associated with Myocardial Infarction in 52 Countries).[8]

In recent years, the concept of using the so-called "polypill" proposed in 2003 by Wald and Law[9] has been actively discussed at international forums. In a meta-analysis, the authors demonstrated that lowering low-density lipoprotein cholesterol (LDL-C) with statins by 1.8 mmol/L can reduce the risk of coronary heart disease (CHD) by 61% and stroke by 17%. Antihypertensive drugs included in the polypill at half the dosage help reduce diastolic blood pressure (DBP) by 11 mmHg, which leads to a 46% reduction in the risk of CHD and 63% of stroke. Thus, the polypill can reduce the risk of CHD by 88% and stroke by 80%. If a patient aged 55-64 years, who has not been diagnosed with CVD, starts taking the polypill, they will be protected from developing CHD and stroke for 10-12 years, regardless of the presence of risk factors.

In 2022, the results of the SECURE study on secondary prevention of CVD in patients with a history of myocardial infarction were published. The study involved 2,499 patients, randomly assigned to two groups. The first group took a fixed combination of drugs in the form of a polypill, including aspirin (100 mg), ACEI ramipril (2.5, 5, or 10 mg), and atorvastatin (20 or 40 mg). The second group took the same drugs separately. With a median follow-up period of 3 years, the primary combined endpoint was recorded in 9.5% of patients in the polypill group and 12.7% in the separate therapy group. Treatment adherence was significantly higher in the polypill group, resulting in a 25% reduction in the risk of endpoints (P=0.02).[10] In addition, five clinical trials were conducted to evaluate the effectiveness of the polypill in reducing the risk of death from all types of CVD: CRUCIAL, TIPS, UMPIRE, IMPACT, and Kanyini GAP.[11,12,13,14,15] In the TIPS trial, patients were given a polypill with different formulations, each containing five different drugs, to prevent CVD. This multicenter trial demonstrated that the polypill improved SBP levels compared with a combination of fewer drugs, was well tolerated, and showed improved adherence to treatment.[12]

The 2018 ESC/ESH guidelines for hypertension management recommend to initiate therapy with a combination of two antihypertensive drugs, preferably in a single-pill fixed-dose combination (FDC), for most patients.[16,17] In most clinical situations, the optimal starting fixed combination is a combination of an angiotensin II receptor blocker (ARB) or angiotensin-converting enzyme inhibitor (ACEI) with calcium channel blocker (CCB) or a diuretic, which significantly increases the effectiveness of antihypertensive therapy. An example is the combination of perindopril (4-8 mg) or lisinopril (10-20 mg) with amlodipine (5-10 mg).

The objective of this study was to compare the effectiveness of a 6-month course of therapy using an FDC (polypill) and a free combination of antihypertensive drugs and statins in achieving target levels of blood pressure (BP) and lipid profile in AH patients with high and very high cardiovascular risk (CVR).

Material and Methods

The study included 92 patients with AH Grades 1-3 (ESC/ESH, 2018), aged 40 to 75 years, of both sexes.

Exclusion criteria were symptomatic hypertension, acute coronary syndrome, chronic heart failure (NYHA FC>II), cardiac arrhythmia, history of myocardial infarction, renal impairment, diabetes mellitus, severe co-morbidities, and condition after revascularization.

Office BP was measured using a mercury sphygmomanometer, according to Korotkov's method. Blood pressure was measured three times, and the mean of these measurements was used in the analyses. The 24-hour ambulatory blood pressure monitoring (ABPM) was performed using the Cardiospy recorder (LABTechLTD, Hungary).

Vascular stiffness was assessed by applanation tonometry using the SphygmoCor device (AtCor Medical, Australia), measuring central systolic blood pressure (cSBPc), central diastolic blood pressure (cDBPc), central pulse pressure (PPc), aortic augmentation (AA), augmentation index (AIx), and pulse wave velocity (PWV).

All patients underwent echocardiography on the Affiniti 30 ultrasound system (PHILIPS, Netherlands) with the

determination of the left ventricular mass index (LVMI), left ventricular hypertrophy [LVMI of >95 g/m² (for women) and >115 g/m² (for men)].[16] The carotid intima-media thickness (CIMT) of the common carotid artery was assessed by duplex scanning. Blood levels of lipids, urea, creatinine, uric acid, glucose, ALT, AST, and CK-MB fraction were determined using a Daytona autoanalyzer (RANDOX, UK). The estimated glomerular filtration rate (eGFR) was calculated according to the CKD-EPI (2021) equation. Microalbuminuria (MAU) in morning urine was assessed by enzymatic analysis on the MindrayBS 380 biochemical analyzer (China), with a measurement range from 30 to 300 mg/L and higher. The 10-year risk of fatal and non-fatal cardiovascular events was assessed using the SCORE2 scale.

All patients included in the study were randomly divided into two groups using the envelope method. Both groups received dual combination antihypertensive therapy with statins (ACEI+CA+statin). Group 1 (n=46) received an FDC combination or "polypill" combining lisinopril/amlodipine/rosuvastatin in a single tablet. Group 2 (n=46) received the combination of perindopril/amlodipine and rosuvastatin in separate forms. Treatment was initiated with starting doses of drugs that were titrated every two weeks to achieve target values of BP and blood lipid levels (<140 mmHg), DBP (<90 mmHg), LDL-C (<100–70 mg/dL), non-high-density lipoprotein cholesterol (non-HDL-C<100–85 mg/dL), and triglycerides TG (<150 mg/dL). A reduction in SBP, DBP, and SCORE2 risk of 10% or more, as well as a 50% reduction in LDL-C from baseline levels, was also assessed.

The drugs were prescribed in therapeutic doses: perindopril (4–8 mg/day), lisinopril (10–20 mg/day), amlodipine (5–10 mg/day), and rosuvastatin (initial dose 10 mg/day). In the event of side effects, a corresponding questionnaire was completed, indicating the reasons for the patient's exclusion from the study. All patients were examined before and after a 6-month course of pharmacotherapy.

Statistical analysis was performed using the statistical software «Statistica» (v10.0, StatSoft, USA). Baseline characteristics were summarized as frequencies and percentages for categorical variables and as mean±standard deviation (SD) for continuous variables. The Mann-Whitney U test was used to compare the differences between the two independent groups, and the Wilcoxon test (W) was used to compare the mean values of dependent samples. Group comparisons for categorical variables were performed using a chi-square test. The probability value of $P<0.05$ was considered statistically significant.

Results

In the event of side effects, a corresponding questionnaire was completed, indicating the reasons for the patient's exclusion from the study. All patients were examined before and after a 6-month course of pharmacotherapy.

At the initial stage of the study, patients in both groups did not differ in gender and age, BP level and markers of target organ damage. According to the average values of SBP (162.46±11.31 mmHg) and DBP (96.11±10.18), the patients were characterized by AH Grade 2. Both groups had a very high CVR, according to the SCORE2 scale (Table 1).

Table 1.

Clinical characteristics of the study patients.

Indicators	Overall n=92	Group1 n=46	*P*-value	Croup 2 n=46
Age, yrs	53.66±9.69	52.06±9.40	0.2926	56.33±7.84
Women, n (%)	33 (35%)	30 (65%)	0.8279	29 (63%)
Men, n (%)	59 (64%)	16 (34%)	0.8279	17 (36%)
AH duration, yrs	9.23±7.17	8.71±5.92	0.7948	12.5±8.28
SBP, mmHg	162.46±11.31	165.82±12.54	0.3788	161.8±9.89
DBP, mmHg	96.11±10.18	99.23±10.61	0.1400	96.43±9.21
MBP, mmHg	119.13±9.40	122.19±10.25	0.3421	118.22±7.78
BMI, kg/m²	30.79±5.39	30.81±5.50	0.4413	31.45±5.34
LVH	46 (50%)	19 (41%)	0.1444	27 (58%)
Atherogenic index	4.34±1.43	4.63±1.39	0.9362	4.23±1.43
PWV, m/s	10.82±3.20	11.59±3.25	0.1187	10.63±3.0
SCORE2, score	18.13±8.46	17.73±8.25	0.7263	21.8±8.75

Against a background of 6-month treatment, a significant improvement in the office BP indicators were revealed in both groups, regardless of the treatment regimen (Table 2). However, the reduction percentage in SBP and DBP was significantly more pronounced in Group 1 than in Group 2, although the differences were not statistically significant. Achievement of the target levels of SBP and DBP was recorded in 91% and 97% of patients in Group 1 and in 76% and 76% in Group 2 ($P<0.001$ in both cases), and simultaneous achievement of target levels of SBP and DBP - in 91% of patients in Group 1 and 50% of patients in Group 2 ($P=0.0000$).

Table 2.

The efficacy of 6-month therapy in study groups.

Indicators	Overall n=92	Group 1 n=46	P_1	Group 2 n=46
SBP, mmHg	162.46±11.31 126.14±10.44	165.82±12.54 121.23±5.23	0.3788	161.8±9.89 131.04±12.0
P_2	0.0001	0.0000		0.0000
DBP, mmHg	96.11±10.18 80.20±4.42	99.23±10.61 78.54±3.05	0.1400	96.43±9.21 81.86±4.96
P_2	0.0001	0.0000		0.0000
MBP, mmHg	119.13±9.40 95.82±6.37	122.19±10.25 93.37±4.62	0.3421	118.22±7.78 98.26±6.97
P_2	0.0001	0.0003		0.0006
Δ% SBP	-22.00±8.29	-26.53±5.72	0.1615	-15.87±8.36
Δ% DBP	-15.73±9.28	-20.17±7.26	0.2713	-13.55±9.79
Δ% MBP	-18.74±7.92	-23.18±5.64	0.4413	-14.67±8.13
Achieving target BP levels				
SBP DBP SBP and DBP	81 (88%) 82 (89%) 81 (88%)	42 (91%) 45 (97%) 42 (91%)	0.0003 0.0000 0.0000	26 (76%) 26 (76%) 23 (50%)

The numerator shows the results before treatment. the denominator shows the results after 6 months of therapy. P_1 is for Group 1 vs. Group 2 before treatment; P_2 is for Group 1 vs. Group 2 after treatment.

The diurnal BP profile also improved significantly during treatment. According to ABPM data, both groups demonstrated a significant decrease in the average 24-h, daytime, and nighttime SBP and DBP, with significant benefits in Group 1 for 24-hour DBP, daytime DBP, and nighttime DBP (P=0.0101, P=0.0226, and P=0.0120, respectively). In addition, the reduction in variability of daily SBP was also more pronounced in Group 1 (P=0.0248). A significant decrease in daytime/nighttime SBP load and DBP load was noted in both groups, but it was more pronounced in Group 1 (Table 3), with the achievement of standard values, which is associated with the possibility of protecting target organs.

Table 3.

The diurnal BP profile during 6-month therapy in study groups.

Indicators	Overall	Group 1	P_1	Group 2
24-hour SBP, mmHg	142.29±11.24 121.63±12.07	143.91±13.0 120.76±7.51	0.3523 0.3523	139.75±9.0 125.82±14.5
P_2	0.0000	0.0001		0.0045
24-hour DBP, mmHg	86.89±9.29 70.45±9.37	88.15±10.50 71.10±7.62	0.2005 0.0101	83.06±7.80 75.73±9.32
P_2	0.0000	0.0001		0.0001
Daytime SBP, mmHg	144.19±12.18 124.01±11.98	146.63±13.9 120.97±5.59	0.0784 0.1141	140.06±9.72 127.26±15.26
P_2	0.0000	0.0001		0.0001
Daytime DBP, mmHg	89.08±10.08 73.70±9.49	90.86±11.56 71.91±10.61	0.0910 0.0226	84.12±8.07 78.23±10.01
P_2	0.0000	0.0001		0.0001
Nighttime SBP, mmHg	135.78±13.10 115.82±13.93	136.5±14.03 116.82±7.97	0.8650 0.7565	137.12±12.20 119.71±17.13
P_2	0.0000	0.0001		0.0001
Nighttime DBP, mmHg	80.65±9.10 65.44±9.26	81.32±9.04 65.17±7.12	0.6030 0.0120	79.87±9.22 70.08±10.03
P_2	0.0000	0.0001		0.0001
Daily SBPV, mmHg	16.43±3.79 11.43±2.23	17.06±4.0 11.92±2.26	0.3897 0.0248	16.65±3.50 13.01±2.32
P_2	0.0000	0.0002		0.2743
Daily DBPV, mmHg	13.37±3.27 9.38±2.15	13.76±2.96 9.58±2.11	0.5892 0.3867	13.37±3.55 9.19±2.19
P_2	0.0005	0.0045		0.0014
Daytime SBPV, mmHg	16.22±4.12 10.57±2.66	17.10±4.07 10.91±2.57	0.2420 0.6491	16.01±4.02 11.18±3.08
P_2	0.0001	0.0001		0.0018
Daytime DBPV, mmHg	12.55±3.49 8.67±2.61	12.91±3.44 8.87±2.88	0.7278 0.4763	12.84±3.55 8.48±2.32
P_2	0.0005	0.0055		0.0014
Nighttime SBPV, mmHg	14.03±5.32 8.32±2.66	14.66±5.39 8.27±2.48	0.4354 0.1235	14.63±5.23 9.15±2.93
P_2	0.0001	0.0000		0.0034
Nighttime DBPV, mmHg	11.33±4.67 7.14±2.71	11.20±4.23 7.53±2.47	0.6527 0.3141	10.73±5.11 8.11±3.00
P_2	0.0001	0.0000		0.0153

The numerator shows the results before treatment. The denominator shows the results after 6 months of therapy. P1 is for Group 1 vs. Group 2; P2 is for before treatment and after 6 months of therapy inside each group. SBPV, SBP variability; DBPV, DBP variability;

Table 3 (continued).

The diurnal BP profile during 6-month therapy in study groups.

Indicators	Overall	Group 1	P_1	Group 2
Daytime SBP load,%	56.82±26.39 27.66±28.42	62.80±25.84 23.23±6.4	0.0323 0.0057	47.01±25.83 31.91±38.80
P_2	0.0001	0.0001		0.0003
Daytime DBP load,%	46.43±27.18 22.20±25.17	49.84±29.04 17.73±10.84	0.2670 0.0198	37.37±25.03 26.97±33.52
P_2	0.0001	0.0001		0.0004
Nighttime SBP load,%	79.16±22.51 30.81±29.78	79.58±21.11 23.56±14.98	0.8728 0.9442	83.18±24.05 38.06±38.23
P_2	0.0001	0.0001		0.0001
Nighttime DBP load,%	50.12±3041 28.64±28.34	52.10±28.17 26.73±11.84	0.4839 0.0045	48.75±32.68 30.54±38.42
P_2	0.0001	0.0001		0.0039

The numerator shows the results before treatment. The denominator shows the results after 6 months of therapy. P1 is for Group 1 vs. Group 2; P2 is for before treatment and after 6 months of therapy inside each group.

One of the important markers of vascular damage in hypertension is indicators of central BP and PWV. In both groups, 6-month therapy led to a significant decrease in SBPc, DBPc, PPc, and PWV. At the same time, the AA parameter significantly decreased only in Group 1 (Figure 1).

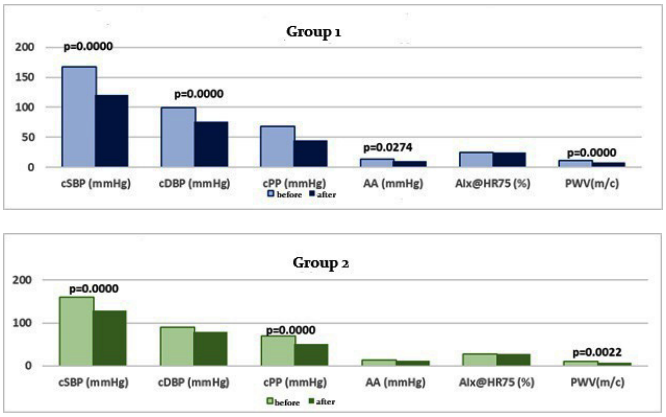

Figure 1. *Parameters of central hemodynamic and vascular stiffness before and after 6-month therapy in the study groups.*

Against the background of 6-month therapy in both groups, no adverse impact on metabolic parameters, including glucose, uric acid, and creatinine, as well as liver enzyme levels, was observed, indicating the metabolic neutrality of the therapy (Figure 2).

In general, positive dynamics of lipid profile parameters were shown in both groups. However, it should be noted that in Group 1, the levels of TC, LDL-C, non-HDL-C, TG, and AI, as well as the level of ApoB, were reduced more significantly than in Group 2. In addition, a significant increase in HDL-C was observed in Group 1 compared to Group 2 (53.3±12.0 mg/dL and 44.1±4.5 mg/dL after treatment, P<0.0001). Despite a

significant decrease in CVR, according to the SCORE2 scale in both groups, the most pronounced results and target levels were recorded in Group 1: from 18.7±8.2 points to 9.1±5.9 points in Group 1 (*P*=0.0001) and from 19.8±8.7 to 14.3±8.0 points in Group 2 (*P*=0.0093) (Figure 3).

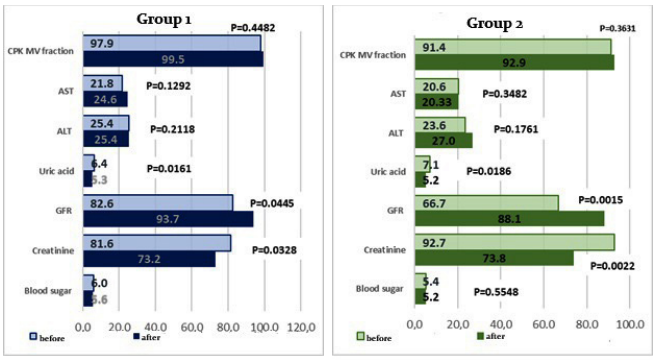

Figure 2. *Metabolic parameters before and after 6-month therapy in the study groups.*

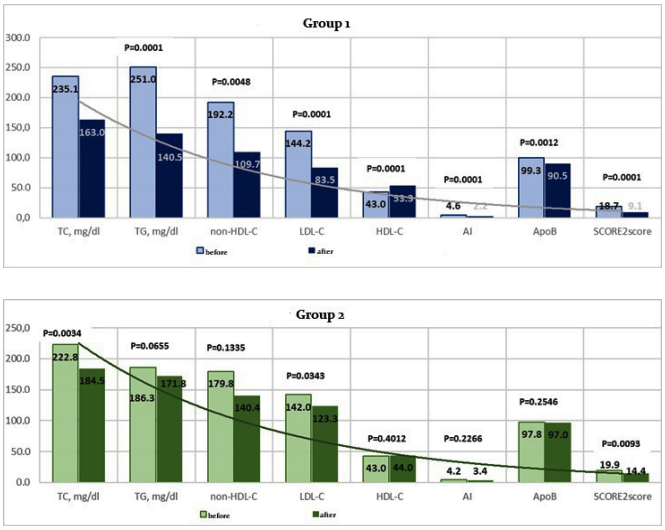

Figure 3. *Lipid profile parameters and SCORE2 scores before and after 6-month therapy in the study groups.*

Overall, patients in both groups achieved their target lipid profile values. However, patients in Group 1 achieved all target lipid profile values, and accordingly, their SCORE2 scores were significantly more reliable than those in Group 2 (Figure 4). The target TC level was achieved in 69% and 45% of patients in Groups 1 and 2, respectively (*P*=0.0203). In Group 1, the target level of TG was achieved in 71% of patients, compared to 39% in Group 2 (*P*=0.0016). Achievement of non-HDL-C levels was recorded in 41% of patients in Group 1 and 17% in Group 2 (*P*=0.0117), and LDL-C levels in 80% and 26%, respectively (*P*=0.0000). Achievement of the target AI was detected in 78% of patients in Group 1 and 41% of patients in Group 2 (*P*=0.0003), and target ApoB in 86% versus 65%, respectively (*P*=0.0145). Target score levels on the SCORE2 scale were observed in 84% of patients in Group 1 and 43% in Group 2 (*P*=0.0000).

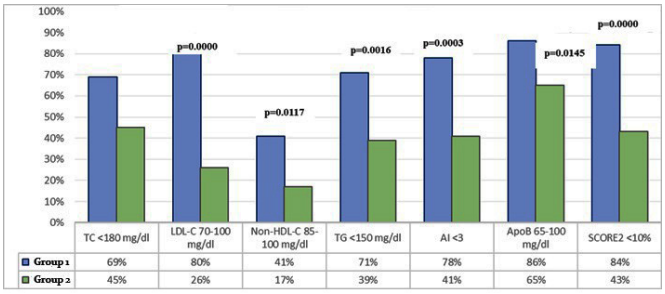

	TC <180 mg/dl	LDL-C 70-100 mg/dl	Non-HDL-C 85-100 mg/dl	TG <150 mg/dl	AI <3	ApoB 65-100 mg/dl	SCORE2 <10%
Group 1	69%	80%	41%	71%	78%	86%	84%
Group 2	45%	26%	17%	39%	41%	65%	43%

Figure 4. *Achievement of target lipid profile parameters after 6-month therapy in study groups.*

Discussion

When considering the specific effects of antihypertensive drugs in the context of their combined use, we should again turn to the results of the ASCOT study,[18,19] which demonstrates a new approach to the strategy of modern antihypertensive therapy. The ASCOT study included more than 19,000 patients, which allowed a new assessment of the effect of "new" classes of antihypertensive drugs, such as CCB and ACEI, in reducing CVR. The effectiveness of antihypertensive therapy in the ASCOT-BPLA study[20] demonstrated that the combination of amlodipine with perindopril is significantly superior to the combination of atenolol and a diuretic (bendroflumethiazide) in reducing CVR. It showed a reduction in the risk of coronary events by 13%, fatal and nonfatal stroke by 23%, cardiovascular mortality by 24%, new cases of renal failure by 15% and cases of diabetes mellitus by 30%.

Previous studies have demonstrated significant benefits of combination therapy over monotherapy in the treatment of hypertension. According to a meta-analysis by Wald and Law,[21] combination drugs reduce BP and the risk of cardiovascular complications better than monotherapy. In particular, the combination of ACEI with CCB has proven to be particularly effective in lowering BP in high-risk patients.[22,23] Moreover, in low- and middle-income countries, combination therapy also demonstrates high efficacy, despite challenges related to drug availability and treatment adherence.[24]

The high efficiency of the combination of CCB with ACEI is due to several factors. Firstly, CCB has a pronounced arterial vasodilation effect, and secondly, ACEI neutralize the effects of the the renin-angiotensin-aldosterone system (RAAS). The combined use of CCB and ACEI neutralizes counter-regulatory mechanisms that can reduce the effectiveness of therapy. ACEI suppresses the activity of the RAAS and the sympathetic adrenergic system, which is triggered as a result of CCB's vasodilating action. In turn, the negative sodium balance caused by CCB is eliminated due to the action of ACEI. In addition, the combination of these drugs significantly reduces the incidence of side effects. For example, a side effect of CCB, such as ankle swelling, is reduced substantially when used in conjunction with ACEI. It has also been demonstrated that the use of CCB reduces the incidence of dry cough, a common side effect of ACEI.[25,26]

The efficacy of the combined effect on BP and dyslipidemia was confirmed in the ASCOT-LLA study, where the addition of 10 mg atorvastatin to antihypertensive therapy resulted in an additional 36% reduction in the risk of nonfatal myocardial infarction and CHD death and a 29% reduction in the risk of all cardiovascular events.[9] Moreover, there is evidence that the addition of a statin enhances antihypertensive therapy.[27,28]

It is worth noting that ACEI and CCB are metabolically neutral antihypertensive drugs, which makes their combination particularly attractive for patients with lipid, carbohydrate, and purine metabolism disorders. The efficacy and safety of the drugs included in the polypill were studied in by Kónyi et al.,[17] which used an FDC of lisinopril and amlodipine (5/10 mg, 5/20 mg, and 10/20 mg) with the addition of rosuvastatin (10 or 20 mg). The study included 2241 patients with AH Grades 1–2, hypercholesterolemia, and high or very high CVR associated with diabetes mellitus, metabolic syndrome, and lower extremity arterial disease.

The results of our study show that the polypill, combining perindopril, amlodipine, and rosuvastatin, demonstrates a more pronounced reduction in BP than separate therapy. These data are consistent with the findings of the study by Cicero et al.,[29] who also noted the high effectiveness of FDC in controlling blood pressure. Moreover, the improvement in lipid profile observed in our patients is consistent with the data of Cequier et al.,[30] who showed that FDCs are effective not only in reducing BP but also in improving lipid metabolism.

Conclusion

Two ACEI/CCB/statin therapy regimens, including polypill combining lisinopril, amlodipine, rosuvastatin, and a free combination of perindopril, amlodipine, and rosuvastatin, demonstrated high antihypertensive, lipid-lowering efficacy, and metabolic neutrality in high-risk AH patients. Both treatment regimens allowed many patients to achieve the target blood pressure; however, in Group 1, the number of patients who achieved target blood pressure levels was greater than in Group 2. In addition to achieving the target blood pressure levels, a significant decrease in SBPc and DBPc, as well as PWV and aortic augmentation in Group 1, indicates a reduction in vascular stiffness. At the same time, a significant decrease in the blood levels of TC, LDL-C, TG, and atherogenic index in Group 1 confirms the lipid-lowering efficacy of the polypill treatment regimen. A significant increase in the HDL-C level in Group 1 indicated the superiority of the polypill over the combination of perindopril and amlodipine plus rosuvastatin in separate forms. It was also found that the SCORE2 score decreased significantly in Group 1, reaching the normal range. At the same time, both treatment regimens showed high antihypertensive and organoprotective efficacy.

The polypill therapy demonstrated superiority over the separate regimen, resulting in a greater reduction in BP and an improvement in lipid profile. These results highlight the importance of choosing the right treatment regimen for patients with high cardiovascular risk and indicate the efficacy of polypills in this patient group.

Ethical Considerations

The study protocol was reviewed and approved by the Ethics Committee of the Republican Specialized Centre of Cardiology. All participants provided written informed consent. The data was only used for study purposes without individual details identifying the patient.

Competing Interests

The authors declare that they have no competing interests.

Sources of Funding

This research received no external funding.

References

1. Lindstrom M, DeCleene N, Dorsey H, Fuster V, Johnson CO, LeGrand KE, et al. Global Burden of Cardiovascular Diseases and Risks Collaboration, 1990–2021. J Am Coll Cardiol. 2022; 80: 2372–2425. doi: 10.1016/j.jacc.2022.11.001.
2. Prevalence of Risk Factors for Noncommunicable Diseases in the Republic of Uzbekistan, 2019. WHO Reference Number: WHO/EURO:2022-6795-46561-67569
3. Williams RR, Hunt SC, Hopkins PN, Stults BM, Wu LL, Hasstedt SJ, Barlow GK, Stephenson SH, Lalouel JM, Kuida H. Familial dyslipidemic hypertension. Evidence from 58 Utah families for a syndrome present in approximately 12% of patients with essential hypertension. JAMA. 1988 Jun 24;259(24):3579-86. doi: 10.1001/jama.259.24.3579. PMID: 3373705.
4. Dalal JJ, Padmanabhan TN, Jain P, Patil S, Vasnawala H, Gulati A. LIPITENSION: Interplay between dyslipidemia and hypertension. Indian J Endocrinol Metab. 2012 Mar;16(2):240-5. doi: 10.4103/2230-8210.93742. PMID: 22470861; PMCID: PMC3313742.
5. Williams B, Masi S, Wolf J, Schmieder RE. Facing the Challenge of Lowering Blood Pressure and Cholesterol in the Same Patient: Report of a Symposium at the European Society of Hypertension. Cardiol Ther. 2020 Jun;9(1):19-34. doi: 10.1007/s40119-019-00159-1. Epub 2020 Jan 13. PMID: 31933276; PMCID: PMC7237547.
6. Castelli WP, Anderson K. A population at risk. Prevalence of high cholesterol levels in hypertensive patients in the Framingham Study. Am J Med. 1986 Feb 14;80(2A):23-32. doi: 10.1016/0002-9343(86)90157-9. PMID: 3946458.
7. Neaton JD, Wentworth D. Serum cholesterol, blood pressure, cigarette smoking, and death from coronary heart disease. Overall findings and differences by age for 316,099 white men. Multiple Risk Factor Intervention Trial Research Group. Arch Intern Med. 1992 Jan;152(1):56-64. PMID: 1728930.

8. Yusuf S, Hawken S, Ounpuu S, Dans T, Avezum A, Lanas F, McQueen M, Budaj A, Pais P, Varigos J, Lisheng L; INTERHEART Study Investigators. Effect of potentially modifiable risk factors associated with myocardial infarction in 52 countries (the INTERHEART study): case-control study. Lancet. 2004 Sep 11-17;364(9438):937-52. doi: 10.1016/S0140-6736(04)17018-9. PMID: 15364185.
9. Wald NJ, Law MR. A strategy to reduce cardiovascular disease by more than 80%. BMJ. 2003 Jun 28;326(7404):1419. doi: 10.1136/bmj.326.7404.1419. Erratum in: BMJ. 2003 Sep 13;327(7415):586. Erratum in: BMJ. 2006 Sep;60(9):823. PMID: 12829553; PMCID: PMC162259.
10. Castellano JM, Pocock SJ, Bhatt DL, Quesada AJ, Owen R, Fernandez-Ortiz A, Sanchez PL, Marin Ortuño F, Vazquez Rodriguez JM, Domingo-Fernández A, Lozano I, Roncaglioni MC, Baviera M, Foresta A, Ojeda-Fernandez L, Colivicchi F, Di Fusco SA, Doehner W, Meyer A, Schiele F, Ecarnot F, Linhart A, Lubanda JC, Barczi G, Merkely B, Ponikowski P, Kasprzak M, Fernandez Alvira JM, Andres V, Bueno H, Collier T, Van de Werf F, Perel P, Rodriguez-Manero M, Alonso Garcia A, Proietti M, Schoos MM, Simon T, Fernandez Ferro J, Lopez N, Beghi E, Bejot Y, Vivas D, Cordero A, Ibañez B, Fuster V; SECURE Investigators. Polypill Strategy in Secondary Cardiovascular Prevention. N Engl J Med. 2022 Sep 15;387(11):967-977. doi: 10.1056/NEJMoa2208275. Epub 2022 Aug 26. PMID: 36018037.
11. Kim JH, Zamorano J, Erdine S, Pavia A, Al-Khadra A, Sutradhar S, Yunis C; CR UCIAL Investigators. Proactive cardiovascular risk management versus usual care in patients with and without diabetes mellitus: CRUCIAL trial subanalysis. Postgrad Med. 2012 Jul;124(4):41-53. doi: 10.3810/pgm.2012.07.2565. PMID: 22913893.
12. Indian Polycap Study (TIPS); Yusuf S, Pais P, Afzal R, Xavier D, Teo K, Eikelboom J, Sigamani A, Mohan V, Gupta R, Thomas N. Effects of a polypill (Polycap) on risk factors in middle-aged individuals without cardiovascular disease (TIPS): a phase II, double-blind, randomised trial. Lancet. 2009 Apr 18;373(9672):1341-51. doi: 10.1016/S0140-6736(09)60611-5. Epub 2009 Mar 30. PMID: 19339045.
13. Thom S, Poulter N, Field J, Patel A, Prabhakaran D, Stanton A, Grobbee DE, Bots ML, Reddy KS, Cidambi R, Bompoint S, Billot L, Rodgers A; UMPIRE Collaborative Group. Effects of a fixed-dose combination strategy on adherence and risk factors in patients with or at high risk of CVD: the UMPIRE randomized clinical trial. JAMA. 2013 Sep 4;310(9):918-29. doi: 10.1001/jama.2013.277064. Erratum in: JAMA. 2013 Oct 9;310(14):1507. Naik, Nitish [added]; Reddy, Srinivas [added]; Balaji, Sham [corrected to Achuthan, Shyambalaji]; Damodra Rao, Modem [corrected to Damodra Rao, Kodem]. PMID: 24002278.
14. Patel A, Cass A, Peiris D, Usherwood T, Brown A, Jan S, Neal B, Hillis GS, Rafter N, Tonkin A, Webster R, Billot L, Bompoint S, Burch C, Burke H, Hayman N, Molanus B, Reid CM, Shiel L, Togni S, Rodgers A; Kanyini Guidelines Adherence with the Polypill (Kanyini GAP) Collaboration. A pragmatic randomized trial of a polypill-based strategy to improve use of indicated preventive treatments in people at high cardiovascular disease risk. Eur J Prev Cardiol. 2015 Jul;22(7):920-30. doi: 10.1177/2047487314530382. Epub 2014 Mar 27. PMID: 24676715.
15. Castellano JM, Pocock SJ, Bhatt DL, Quesada AJ, Owen R, Fernandez-Ortiz A, Sanchez PL, Marin Ortuño F, Vazquez Rodriguez JM, Domingo-Fernández A, Lozano I, Roncaglioni MC, Baviera M, Foresta A, Ojeda-Fernandez L, Colivicchi F, Di Fusco SA, Doehner W, Meyer A, Schiele F, Ecarnot F, Linhart A, Lubanda JC, Barczi G, Merkely B, Ponikowski P, Kasprzak M, Fernandez Alvira JM, Andres V, Bueno H, Collier T, Van de Werf F, Perel P, Rodriguez-Manero M, Alonso Garcia A, Proietti M, Schoos MM, Simon T, Fernandez Ferro J, Lopez N, Beghi E, Bejot Y, Vivas D, Cordero A, Ibañez B, Fuster V; SECURE Investigators. Polypill Strategy in Secondary Cardiovascular Prevention. N Engl J Med. 2022 Sep 15;387(11):967-977. doi: 10.1056/NEJMoa2208275. Epub 2022 Aug 26. PMID: 36018037.
16. Williams B, Mancia G, Spiering W, Agabiti Rosei E, Azizi M, Burnier M, Clement DL, Coca A, de Simone G, Dominiczak A, Kahan T, Mahfoud F, Redon J, Ruilope L, Zanchetti A, Kerins M, Kjeldsen SE, Kreutz R, Laurent S, Lip GYH, McManus R, Narkiewicz K, Ruschitzka F, Schmieder RE, Shlyakhto E, Tsioufis C, Aboyans V, Desormais I; ESC Scientific Document Group. 2018 ESC/ESH Guidelines for the management of arterial hypertension. Eur Heart J. 2018 Sep 1;39(33):3021-3104. doi: 10.1093/eurheartj/ehy339. Erratum in: Eur Heart J. 2019 Feb 1;40(5):475. PMID: 30165516.
17. Kónyi A, Sárszegi Z, Hild G, Gaszner B. Safety and effectiveness of combined antihypertensive and cholesterol-lowering therapy in high-/very high-risk patients. J Comp Eff Res. 2016 Jul;5(4):355-64. doi: 10.2217/cer-2016-0003. Epub 2016 Jun 13. PMID: 27295112.
18. Sever PS. The Anglo-Scandinavian Cardiac Outcomes Trial: implications and further outcomes. Hypertension. 2012 Aug;60(2):248-59. doi: 10.1161/HYPERTENSIONAHA.111.187070.
19. Dolan E, Stanton AV, Thom S, Caulfield M, Atkins N, McInnes G, Collier D, Dicker P, O'Brien E; ASCOT Investigators. Ambulatory blood pressure monitoring predicts cardiovascular events in treated hypertensive patients--an Anglo-Scandinavian cardiac outcomes trial substudy. J Hypertens. 2009 Apr;27(4):876-85. doi: 10.1097/HJH.0b013e328322cd62. PMID: 19516185.
20. Poulter NR, Wedel H, Dahlöf B, Sever PS, Beevers DG, Caulfield M, Kjeldsen SE, Kristinsson A, McInnes GT, Mehlsen J, Nieminen M, O'Brien E, Ostergren J, Pocock S; ASCOT Investigators. Role of blood pressure and other variables in the differential cardiovascular event rates noted in the Anglo-Scandinavian Cardiac Outcomes Trial-Blood Pressure Lowering Arm (ASCOT-BPLA). Lancet. 2005 Sep 10-16;366(9489):907-13. doi: 10.1016/S0140-6736(05)67186-3. PMID: 16154017.
21. Wald NJ, Law M, Morris J, Wald DS, Aronson JK. Blood pressure meta-analysis highlights an implementation gap. Lancet. 2022 Apr 9;399(10333):1379-1380. doi: 10.1016/S0140-6736(22)00192-1. PMID: 35397861.
22. Sarzani R, Laureti G, Gezzi A, Spannella F, Giulietti F. Single-pill fixed-dose drug combinations to reduce blood pressure: the right pill for the right patient. Ther Adv Chronic Dis. 2022 Jun 24;13:20406223221102754. doi: 10.1177/20406223221102754. PMID: 35769133.

23. Bekmetova SI, Abdullaeva GZh, Khamidullaeva GA, Fayzullaeva ShS, Yusupova KhF, Zakirova FA. Effects of the Perindopril/Amlodipine Fixed-Dose Combination Therapy on the Left Ventricular Myocardial Deformation Properties and Arterial Stiffness Parameters in Patients with Arterial Hypertension. International Journal of Biomedicine. 2024;14(4):551-557. doi:10.21103/Article14(4)_OA2
24. Schutte AE, Srinivasapura Venkateshmurthy N, Mohan S, Prabhakaran D. Hypertension in Low- and Middle-Income Countries. Circ Res. 2021 Apr 2;128(7):808-826. doi: 10.1161/CIRCRESAHA.120.318729. Epub 2021 Apr 1. PMID: 33793340; PMCID: PMC8091106.
25. Jamerson K, Weber MA, Bakris GL, Dahlöf B, Pitt B, Shi V, Hester A, Gupte J, Gatlin M, Velazquez EJ; ACCOMPLISH Trial Investigators. Benazepril plus amlodipine or hydrochlorothiazide for hypertension in high-risk patients. N Engl J Med. 2008 Dec 4;359(23):2417-28. doi: 10.1056/NEJMoa0806182. PMID: 19052124.
26. Faizullaeva ShS, Khamidullaeva GA. [Comparative efficacy of polypill and a separate combination of ACE inhibitor, calcium antagonist, and statin in patients with high-risk uncontrolled hypertension]. Therapy. 2025; 1 (Supplement). (Article in Russian).
27. Sever PS, Dahlöf B, Poulter NR, Wedel H, Beevers G, Caulfield M, Collins R, Kjeldsen SE, Kristinsson A, McInnes GT, Mehlsen J, Nieminen M, O'Brien E, Ostergren J; ASCOT investigators. Prevention of coronary and stroke events with atorvastatin in hypertensive patients who have average or lower-than-average cholesterol concentrations, in the Anglo-Scandinavian Cardiac Outcomes Trial--Lipid Lowering Arm (ASCOT-LLA): a multicentre randomised controlled trial. Lancet. 2003 Apr 5;361(9364):1149-58. doi: 10.1016/S0140-6736(03)12948-0. PMID: 12686036.
28. Baryshnikova GA, Chorbinskaya SA, Stepanova II, Lyalina SV. [Polypill as a means to increase the effectiveness of the treatment of patients with high cardiovascular risk]. Trudnyi Patsient. 2015;7. Avaible from: https://cyberleninka.ru/article/n/polipilyulya-kak-sredstvo-uvelichit-effektivnost-lecheniya-patsientov-s-vysokim-serdechno-sosudistym-riskom. (Article in Russiuan).
29. Cicero AFG, ALGhasab NS, Tocci G, Desideri G, Fiorini G, Fogacci F. Efficacy and Safety of Low-Dose Bisoprolol/Hydrochlorothiazide Combination for the Treatment of Hypertension: A Systematic Review and Meta-Analysis. J Clin Med. 2024 Aug 5;13(15):4572. doi: 10.3390/jcm13154572. PMID: 39124839; PMCID: PMC11313031.
30. Cequier A, Arrarte V, Campuzano R, Castro A, Cordero A, Rosa Fernández Olmo M, et al. [Lipid lowering treatment in patients with very high risk cardiovascular disease. Spanish Society of Cardiology Consensus Document for thhigh-riskPCSK9 inhibitors in clinical practice]. REC: CardioClinics. 2021; 56(1):39-48. doi: 10.1016/j.rccl.2020.10.017. [Article in Spanish].

***Corresponding author:** Prof. Gulnoz A. Khamidullaeva, PhD, ScD. The Republican Specialized Center of Cardiology, Tashkent, Uzbekistan. E-mail: gulnoz0566@mail.ru*

International Journal of Biomedicine 15(3) (2025) 469-482
http://dx.doi.org/10.21103/Article15(3)_OA2

ORIGINAL ARTICLE
Hematology & Oncology

INTERNATIONAL JOURNAL OF BIOMEDICINE

AI-Guided Repurposing of FDA-Approved Anti-Leukemic Molecularly Targeted Therapies for Fatal Blast Crisis Chronic Myeloid Leukemia: Integrative Genomics for Precision Medicine of Relapsed/Refractory Cancers in the Post-Pandemic Era

Abdulkareem AlGarni[1-4*], Nawaf Alanazi[1,3,4], Sarah AlMukhaylid[3,5*], Sultan Al-Qahtani[6], Muhammad Farooq Sabar[8,9], Mudassar Iqbal[8-10], Abid Jameel[8,11], Akhtar Hussian[8,12], Hassan H. Almasoudi[13], Yaqob Samir Taleb[3,4,8,15], Sabreen Alanazi[3,4*], Nada Alkhamis[3,4], Dhay Almaghlouth[3,14*], Alhanoof Alsuwaidani[3,5], Ghala Basem Alsalem[3,14], Manal Jaber Aldossari[5], Danah Yousef Alhaider[6], Maryam AlMajed[7*], Nouf AlMutairi[5], Maryam Bu Tuwaybah[3,4], Batoul Alwabari[3,4], Shaima Ali Alsubaie[5], Fatimah Hussain Alali[3,4], Anwar Hussain Al-Rasasi[3,4], Fatimah Ali Alabdullah[3,4], Kanza Adeel[3,4,8], Leen Abdulmohsen Al Hafez[3,4*], Tarig Karar[3,4,15], Rayyan Al Hammad[3,4,15], Mohammad Almohaini[15], Noran Aboalela[4], Sana Shahbaz[8,9], Amer Mahmood[8,16], Sulman Basit[8,17], Buthainah AlShehab[7], Aamer Aleem[8,18], Reman Alharbi[19], Abdullah Alruwaili[20], Mahmood Rasool[21], Muhammad Asif[22], Irtaza Fatima Zafar[3,8,23], Rizwan Naeem[8,24], Masood A. Shamas[8,25], Giuseppe Saglio[8,26,27*], Zafar Iqbal[3,4,8,9,*,**]

[1]Division of Hematology/Oncology, Department of Pediatrics, King Abdulaziz Hospital, Al-Ahsa, Saudi Arabia; [2]Division of Hematology/Oncology, Department of Medicine, King Abdulaziz Hospital, Al-Ahsa, Saudi Arabia; [3]Genomic & Experimental Medicine Group (GEM), Hematology & Molecular Oncology/ Section (Hem-MoOn); Quality Assurance and Accreditation Unit (QAAA); & Clinical Laboratory Sciences Program (CLSP), College of Applied Medical Sciences (CoAMS-A), King Saud Bin Abdulaziz University for Health Sciences (KSAU-HS); King Abdullah International Medical Research Centre –Eastern Region (KAIMRC-ER) /; Saudi Scientific Society for Blood and Marrow Transplantation (SSBMT); King Abdulaziz Medical City (KAMC), Ministry of National Guard Health Affairs (MNGHA), Al-Ahsa, Saudi Arabia; [4]CLSP, COAMS-A, KSAU-HS, MNGHA, Al-Ahsa, Saudi Arabia; [5]Johns Hopkins Aramco HealthCare (JHAH), Al-Ahsa, Saudi Arabia; [6]College of Medicine/KAIMRC/KAMC/SSBMT, KSAU-HS, Riyadh, Saudi Arabia; [7]School of Biological Science, University of Manchester, Manchester, United Kingdom; [8]Hematology, Oncology and Pharmacogenetic-Engineering Sciences Group (H.O.P.E.S.) Pakistan & Pakistan Society for Molecular and Clinical Hematology, Lahore, Pakistan (www.pak-hematology.org); [9]H.O.P.E.S., Centre for Applied Molecular Biology (CAMB) & School of Biochemistry and Biotechnology (SBB), University of the Punjab, Lahore, Pakistan; [10]Asian Medical Institute (AZMI) & AZMI Clinics, Kant, Kyrgyzstan; [11]Hayatabad Medical Complex, Peshawar, Pakistan; [12]Department of Biotechnology, University of Peshawar, Peshawar, Pakistan; [13]Department of Clinical Laboratory Sciences, College of Applied Medical Sciences, Najran University, Najran. Saudi Arabia; [14]Almoosa Health Group, Almoosa Specialist Hospital, Al-Ahsa, Saudi Arabia; [15]Department of Basic Medical Sciences, COAMS-A, KSAU-HS, Al-Ahsa, Saudi Arabia; [16]Cancer Stem Cell Group, Department of Anatomy, College of Medicine & KSU Medical City/King Khalid University Hospital, King Saud University (KSU), Riyadh, Saudi Arabia; [17]Center for Genetics and Inherited Diseases, Taibah University, Al-Madinah Al-Munwarah, Saudi Arabia; [18]Hematology/Oncology Division, Department of Medicine, College of Medicine & KSU Medical City/King Khalid University Hospital, King Saud University (KSU), Riyadh, Saudi Arabia; [19]College of Medicine & Surgery, University of Jeddah, Jeddah, Saudi Arabia; [20]Emergency Medical Sciences Department, COMAS-A, KSAU-HS/KAIMRC/SSBMT/KAMC, Riyadh, Saudi Arabia; [21]Faculty of Applied Medical Sciences & Centre of Excellence in Genomic Medicine Research, King Abdulaziz University, Jeddah, Saudi Arabia; [22]ORIC and Department of Biotechnology, BUITEMS, Quetta, Pakistan; [23]Nada International School, Al-Ahsa, Saudi Arabia; [24]Molecular Genetic Pathology, Montefiore Medical Centre & Albert Einstein Medical College, New York, USA; [25]Department of Oncology, Harvard Medical School, Dana-Farber Cancer Institute, University of Harvard University, Boston USA; [26]Orbassano University Hospital, Turin, Italy; [27]Department of Clinical and Biological Sciences, University of Turin, Turin, Italy

*The authors contributed equally and shared co-first authorship
**Corresponding author

Abstract

Background: The COVID-19 pandemic accelerated the paradigm of drug repurposing, leading to the rapid identification of new uses for existing therapeutics under urgent clinical need. This success story has ignited a broader movement towards leveraging repurposing strategies for relapsed, refractory, and traditionally difficult-to-treat diseases, specifically cancers. Chronic myeloid leukemia (CML), although treatable in the chronic phase (CP), is usually fatal in the blast crisis phase (BC-CML), exemplifying a pressing challenge to oncology, where standard tyrosine kinase inhibitor (TKI) therapies often fail, resulting in poor survival outcomes.

Methods and Results: In a multi-institutional cohort of 141 CML patients, we performed WES across disease phases (123 CP-CML, 6 AP-CML, 12 BC-CML). Mutational landscapes were interrogated using the AI-driven PanDrugs2 platform to identify druggable targets and repurposable FDA-approved anti-leukemic therapies. A 54% surge in mutational burden was observed transitioning from AP-CML to BC-CM, revealing 67 recurrent pan-leukemic gene mutations. Notably, actionable alterations were found in *NPM1, DNMT3A, PML, AKT1, CBL, JAK2, TET2, IDH1, and BCL2*, with therapeutic opportunities using existing agents such as venetoclax, ivosidenib, decitabine, and azacitidine. Emerging vulnerabilities, including *RPTOR* and *BCR* mutations, suggest further avenues for mTOR and BTK inhibitor applications beyond traditional TKI paradigms.

Conclusions: Our integrated genomic and AI-guided approach demonstrates the transformative potential of drug repurposing for BC-CML, highlighting immediate actionable options where conventional therapies fail. This strategy not only offers hope for patients with BC-CML but also paves a visionary path toward precision medicine frameworks for relapsed, refractory, and otherwise intractable cancers in the post-pandemic clinical era. Prospective multi-omics studies and tailored clinical trials are urgently warranted to expand these opportunities across the oncology landscape.(**International Journal of Biomedicine. 2025;15(3):469-482.**)

Keywords: chronic myeloid leukemia • blast crisis • mutational profiling • drug repurposing • personalized treatment

For citation: AlGarni A, Alanazi N, AlMukhaylid S, Al-Qahtani S, Sabar MF, Iqbal M, Jameel A, Hussian A, Almasoudi HH, Taleb YS, Alanazi S, Alkhamis N, Almaghlouth D, Alsuwaidani A, Alsalem GB, Aldossari MJ, Alhaider DY, AlMajed M, AlMutairi N, Tuwaybah MB, Alwabari B, Alsubaie SA, Alali FH, Al-Rasasi AH, Alabdullah FA, Adeel K, Al Hafez LA, Karar T, Al Hammad R, Almohaini M, Aboalela N, Shahbaz S, Mahmood A, Basit S, AlShehab B, Aleem A, Alharbi R, Alruwaili A, Rasool M, Asif M, Zafar IF, Naeem R, Shamas MA, Saglio G, Iqbal Z.. AI-Guided Repurposing of FDA-Approved Anti-Leukemic Molecularly Targeted Therapies for Fatal Blast Crisis Chronic Myeloid Leukemia: Integrative Genomics for Precision Medicine of Relapsed/Refractory Cancers in the Post-Pandemic Era. International Journal of Biomedicine. 2025;15(3):469-482. doi:10.21103/Article15(3)_OA2

Abbreviations

AP, accelerated phase: **AML**, acute myeloid leukemia; **AL**L, acute lymphoid leukemia; **BC**, blast crisis; **CML**, chronic myeloid leukemia; **CP**, chronic phase; **CLL**, chronic lymphocytic leukemia; **HMAs**, hypomethylating agents; **IM**, imatinib mesylate; **TKIs**, tyrosine kinase inhibitors; **WES**, whole exome sequencing.

Introduction

The COVID-19 pandemic accelerated global drug repurposing efforts, with anticancer agents such as imatinib investigated for antiviral efficacy.[1] TKIs, the cornerstone of CML therapy, demonstrated antiviral potential against SARS-CoV-2.[2] Furthermore, the management of CML patients during the pandemic highlighted the critical need for flexible, rapid therapeutic strategies.[3]

Chronic myeloid leukemia (CML) is a malignancy of myeloid lineage in hematopoiesis.[1] It occurs when clonal hematopoietic stem cells multiply abnormally, resulting in the overproduction of non-functional cells, or blasts, especially granulocytes, in the bone marrow and peripheral circulation.[2] The Philadelphia chromosome, resulting from a reciprocal translocation between the *BCR* gene on chromosome 22 and the *ABL* gene on chromosome 9, is a defining characteristic of this disease and was discovered in 1959 by David A. Hungerford and Peter C. Nowell, the Nobel Prize winners for this discovery. This genetic abnormality leads to the creation of BCR-ABL fusion oncogenes that result in the constitutive expression of the tyrosine kinase BCR-ABL on hematopoietic stem cells, which culminates in the continued proliferation and development of leukemic stem cells.[2] CML occurs in 1 to 2 of every 100,000 individuals around the world, making up around 15% of new adult leukemia cases.[3] CML is a triphasic disease that begins with the indolent chronic phase (CP-CML). This phase is characterized by a significant increase in myeloid precursors and mature cells. The overall survival rate of CP-CML patients results in life expectancy comparable to that of the general population, at least in technologically advanced countries, due to the introduction of tyrosine kinase inhibitors (TKIs) and bcr-abl fusion oncoprotein inhibitors in the last three decades.[4] However, a fraction of CML patients progress to the accelerated phase (AP) and finally the blast crisis (BC), the latter of which has an overall survival rate of 3 to 18 months.[3] The BC-CML is characterized by an acute and rapid increase in the number of primitive hematopoietic cells in the bone marrow and blood, as well as treatment failure, anti-leukemic therapy resistance, relapses, and eventually death within a few months.[5]

This makes treating BC-CML one of the most challenging tasks in cancer medicine in the 21st century. As a result, it is extremely important to discover new pharmacological targets and treatments for BC-CML.[1,5]

BC-CML usually looks like either acute myeloid leukemia (AML) or acute lymphoid leukemia (ALL), which is called the myeloid blast crisis (M-BC) or lymphoid blast crisis (L-BC), respectively.[6] Targeted therapies, including drugs and inhibitors for specific gene mutations in AML and ALL, have been developed and approved by the FDA, and are now used in routine clinical practice for personalized treatment of patients with these genetic alterations.[7,8] However, it is still unclear whether the same genes linked with AML and ALL are responsible for myeloid and lymphoid blast crises, respectively.[4,5] If this is the case, it would provide the chance to treat MBC-CML and LBC-CML patients with FDA-approved medications developed against AML-/ALL-lineage genes. Therefore, the goal of this study was to investigate pan-leukemia gene mutations, particularly AML and ALL lineage, in patients with BC-CML and to create a database of FDA-approved treatments effective against these AML- and ALL-specific gene mutations. This database would include drugs that have the potential to be used for treating BC-CML.

Materials and Methods

Study Populations

This study recruited 141 CML patients from two centers: Hayatabad Medical Complex (HMC), Peshawar, Pakistan, and King Abdulaziz Hospital Al-Ahsa, Saudi Arabia (from January 2012 to June 2022). Imatinib mesylate (IM) was administered to all patients as the first-line treatment. Those who developed resistance to IM were then treated with second-generation TKIs. Of 141 participants, 123 age/gender-matched CP-CML patients served as controls, and 18 AP-CML patients served as the Experimental Group 1. Also, 12 of 18 AP-CML patients who progressed to BC-CML during the study were included in Experimental Group 2. The European Leukemia Net (ELN) recommendations from 2013 and later ELN-2020 were used for all clinical classification and treatment response criteria.[9-11] Regarding categorization of CML patients into CP-, AP- and BC-CML, CML patients were classified as CP if the percentage of blast cells in their blood was less than 5%, the percentage of basophils was between 15% and 19%, the percentage of blasts and promyelocytes was less than 30%, and there were no blast cells in extramedullary locations.[9] For AP, the percentage of blasts was taken as 15%-29%, the presence of promyelocytes and blasts as more than 30% in the blood or the bone marrow, the platelet count low (100×10^9/L), the presence of basophils 20% or greater, and Ph+ cells with chromosomal anomalies.[9] To categorize a patient as BC-CML, the presence of 30% or more of blasts in either the blood or the bone marrow and in extramedullary locations was considered a basic criterion.[9-11] Standards for evaluating treatment response in CML were adopted from ELN-2013 and ELN-2020.[9,11,12] Adverse events were classified using standard nomenclature version 4.03.[13]

Sample Handling

Peripheral blood samples (3-5 mL) were obtained from study participants in the BD Vacutainer® EDTA Tube (Becton Dickinson, USA). The samples were collected during the biweekly visits of the CML patients to the outpatient department of the medical oncology units of participating centers. These clinical specimens were preserved at −70°C for subsequent analysis. Before the extraction of DNA, both the patient samples and the reagents utilized in the extraction process were acclimatized to room temperature, specifically within the range of 15 to 25 °C. The process of DNA extraction encompassed multiple stages. The QIAamp DNA blood mini kit was (Qiagen, Hilden, Germany) utilized for DNA extraction, according to the manufacturer's instructions. The procedure entailed the amalgamation of 200 µL of the blood specimen, 200 µL of Buffer AL, and 20 µL of QIAGEN Protease within a tube. After being vortexed, the resulting mixture underwent incubation for 10 minutes at a temperature of 56°C. Two hundred microliters of ethanol were introduced, followed by a subsequent vortexing of the mix. The resulting solution was then carefully transferred to a QIAamp Mini spin column, from which the extract was extracted post-centrifugation. Subsequently, the flow-through was eliminated after incorporating Buffer AW1 and subsequent centrifugation. This procedure was reiterated with Buffer AW2 to guarantee the complete removal of all buffers, after which the column underwent centrifugation. The DNA was eluted by applying distilled water or incorporating Buffer AE, followed by incubation and centrifugation processes. Absorbance was assessed at 260 nm to ascertain the concentration of DNA. A concentration exhibiting a ratio of 1.7 to 1.9 at A260/A280 was deemed to possess purity. The DNA was quantified by utilizing a Nanodrop Spectrophotometer (NanoDrop Technologies, Wilmington, DE, USA). The DNA was diluted to 70-80 ng/µL concentrations and 40 ng/µL for use in WES and Sanger Sequencing, respectively. Until additional testing was conducted, the DNA was preserved at −80°C.

Genetic Analysis

Next-Generation Sequencing (NGS) was conducted on experimental (AP- & BC-) CML samples alongside an equivalent number of CP-CML samples serving as controls. After DNA extraction, exome-capturing arrays were employed to capture the extracted material.[14] The SureSelectXT V6-Post Capture Exome kit (©Agilent Technologies, Santa Clara, California, USA) was used to construct the library and enhance the exomes after DNA capture. The SureSelect kit included approximately 99% of the reference sequences database and comprised 214,405 exons with splice sites.[15] Subsequent to DNA fragmentation, the tagmentation of the resulting fragments was conducted, accompanied by amplification and purification processes, which were facilitated through magnetic beads. Oligonucleotides were employed to delineate the specified regions. The enriched libraries were amplified through PCR, and subsequently quantified with a Qubit fluorometer. The 2100 Agilent Bioanalyzer (©Agilent Technologies, Santa Clara, California, USA) was configured to ascertain the dispersion of library sizes. The Illumina

NextSeq500 sequencer (Illumina Inc., San Diego, CA, USA) facilitated the process of cluster generation and comprehensive exome sequencing by depositing quantifiable DNA libraries into the flow cell.[15]

The BCL2FASTQ (Illumina Inc., San Diego, CA, USA) was employed to convert the BCL files into FASTQ files. The BWA Aligner (Illumina Inc., San Diego, CA, USA) was utilized to align the FASTQ data to the human genome using the BWA-MEM algorithm. The annotation and filtration of genomic variants identified by the Genome Analysis Toolkit (GATK) were conducted utilizing Illumina Variant Studio (Illumina Inc., San Diego, CA, USA).[15]

Validation

To ascertain a common biomarker associated with the proliferation of CML, an analysis of mutated genes was conducted across all patients in the advanced phase of the disease. Strategies for filtration that focused on identifying rare variants while omitting intron and synonymous variants were employed to refine the Excel file containing NGS data. Moreover, all variants with established predictions were excluded, whether classified as benign (B) or tolerant (T). Certain variants were designated as B when they exhibited a frequency of 70% or greater for B, whereas others were categorized as T when T's frequency reached 70% or more.[16] Likewise, variables exhibiting a population frequency exceeding 0.005 in the dbSNP and Exome Sequencing Project (ESP) database were discarded.

Consequently, the variant calling process was confined to variants exhibiting intermediate to high protein effects and splice variants, culminating in approximately 124 rare variants. Furthermore, in-depth data analysis was conducted to explore unique gene mutations found in AP-CML patients that is absent in CP-CML patients and healthy controls, indicating the potential involvement of these mutations in disease progression.[15,16] Data generated through NGS can be accessed via the NCBI repository, where it has been submitted under the SRA accession number PRJNA734750, available at https://www.ncbi.nlm.nih.gov/sra/PRJNA734750. For identifying druggable mutations within pan-leukemic genes associated with myeloid and lymphoid lineages, particularly those related to AML and ALL, we meticulously filtered for genes that have been previously documented as mutated in AML and ALL, as well as other types of leukemias, lymphomas, and hematological malignancies. To achieve this objective, we compiled a comprehensive list of genes that exhibit mutations in AML and ALL, drawing upon the extensive literature available in PubMed.[17-19] The genes identified in this compilation, which are uniquely mutated in AP-CML and BC-CML while absent in CP-CML or healthy controls (sourced from genomic databases), were meticulously sorted and prepared for subsequent analysis.

PanDrug Platform

To explore the druggability of pan-leukemic genes associated with BC-CML, online artificial intelligence (AI) tools were employed. We utilized genes uniquely mutated in AP-CML and BC-CML, while not mutated in CP-CML or healthy controls. To achieve this objective, we used an online resource called PanDrugs2 (www.pandrugs.com).[19] The druggability assessment was conducted by inquiring about the gene names within the PanDrugs2 database. A gene was deemed druggable if an FDA-approved medication existed targeting it for treating AML, ALL, or other hematological malignancies.

Statistical analysis

We employed the methods reported previously by our group.[20] In accordance with the normality assessment, absolute values and percentages were presented for categorical variables, while the mean and a suitable measure of variation were provided for continuous variables. The chi-square test or Fisher's exact test was employed for categorical data to compare two groups. For continuous data, a two-sample independent test or Mann–Whitney U test was utilized. The analysis of variance for groups of three or more was conducted using either ANOVA or the Kruskal–Wallis test. To evaluate the survival outcome, Kaplan-Meier survival analysis curves were constructed.[20] A log-rank test was employed to conduct the group comparison. The data analysis was conducted utilizing SAS/STAT software version 9.4, developed by SAS Institute Inc., located in Cary, NC, USA. The R package was used for statistical computing.[16,17,21]

Results

Clinical Features of CML patients

Of the 141 patients diagnosed with CML, 4.3% (n=6) were AP-CML, and 8.5% (n=12) were BC-CML. The study subjects comprised 86 (61.0%) males and 55(39.0%) females, with a male-to-female ratio of 1.6:1. The mean age of all patients was 36.4, ranging from 9 to 67 years. Laboratory results demonstrated that 79.4% (n=112) of patients developed anemia, whereas 56.0% (n=79) developed leukocytosis (>50×10^9/L). Splenomegaly was seen in 71.6% (n=101) of patients. Furthermore, a comparison between different phases of CML patients showed that leukocytosis was significantly increased in the advanced phase of CML compared to CP-CML cases (P=0.0184) (Table 1). Regarding clinical assessment, a significant relationship was seen between hepatomegaly and advanced-phase CML patients (P=0.0014). Although splenomegaly was observed in all phases, it was significantly associated with the advanced-phase CML, as all AP-CML and BC-CML patients developed splenomegaly, compared to only 67.5% (n=83) of CP-CML patients (P=0.0014). Furthermore, the size of the spleen significantly increased with the disease's progression.

Clinical Outcome of CML Patients in Three Phases of the Disease

After using IM as the first-line treatment for all patients, 20(14.2%) patients were either intolerant or did not respond to the drug, even after increasing the dose. These 20 patients were treated with nilotinib (NI) as second-line therapy, 12 (60%) of whom were CP-CML, 2 (10%) were AP-CML, and 6 (30%) were BC-CML patients. Of the BC-CML patients receiving

NI (n=6), 4 (66.7%) were non-responders to the second-line treatment. All BC-CML patients were treated as Philadelphia-positive acute leukemia patients. There was a significantly high mortality rate of 75% (9/12) for BC-CML patients compared to CP-CML patients, who had a comparatively very low mortality rate of 8.1% (10/123), with one death not related to cancer. In addition, the overall survival rates for CP-CML and AP-CML patients were 91.9% (113/123) and 100% (18/18), respectively, whereas BC-CML patients had a survival rate of 25% (3/12) (Table 1). Our data shows the limited effectiveness of current treatment modalities to treat BC-CML, which thus necessitates a hunt for new drug targets and novel treatments. It also highlights the need to find early biomarkers for CML progression that could be targeted to prevent progression.

Table 1.

Comparison between demographics and clinical characteristics in different phases of CML.

Characteristics	Patient groups			*P*-value
	CP-CML n (%)	AP-CML n (%)	BC-CML n (%)	
No. of patients	123 (87.2)	18* (4.3)	12* (8.5)	
Mean (range)	35.5 (9-67)	35.6 (27-43)	38.1 (29-50)	
Male	74 (60.2)	12 (66.67)	8 (66.7)	0.5985
Female	49 (39.8)	6 (33.33)	4 (33.3)	
Ratio: Male: Female	1.5-1	2: 1	2: 1	
Hemoglobin: (g/dL)				
<12	69 (56.1)	15 (83.3)	9 (75)	0.0642
>12	14 (11.4)	3 (16.7)	3 (25)	0.2609
WBC count ($\times10^9$/L), Mean	313.7	315	325	
<50	20 (16.3)	3 (20)	2 (16.7)	0.8276
≥50	64 (52.0)	15 (80)	10 (83.3)	0.0184
Platelets ($\times10^9$/L)				
<450	75 (61.0)	12 (66.7)	10(83.3)	0.2528
≥450	33 (26.8)	6 (33.3)	2 (16.7)	0.8722
Imatinib				
Yes	82 (66.7)	12 (66.7)	7 (58.3)	0.7260
Nilotinib as 2nd Line				
Yes	41 (33.3)	12 (66.7)	8 (66.7)	0.0065
Hydroxyurea				
Yes	82 (66.7)	9 (50)	10 (83.3)	0.9967
Interferon				
Yes	41 (33.3)	0 (0)	0 (0)	0.0038
Chemotherapy				
Yes	0	0	9 (75%)	0.0000
Splenomegaly				
No	40 (32.5)	0 (0)	0 (0)	0.0014
Yes	83 (67.5)	18 (100)	12 (100)	
<5cm	4 (3.2)	0 (0)	0 (0)	0.5051
5-8cm	9 (7.3)	3 (16.7)	3 (25)	
>8cm	70 (56.9)	15 (83.3)	9 (75)	
Hepatomegaly				
Yes	35 (28.5)	12 (66.7)	8 (66.7)	0.0014
Anemia				
Yes	97 (78.9)	15 (83.3)	9 (75)	0.9807
Pregnant				
Yes	4 (3.2)	0 (0)	0 (0)	0.2090
Survival Status				
Confirmed deaths	10 (8.1)	0 (0)	9 (75)	<0.001
Alive at last follow-up	113 (91.9)	18 (100)	3(25)	

**12 out of 18 AP-CML patients progressed to BC-CML during the study course.*

Whole Exome Sequencing

As no specific biomarkers exist for CML disease progression or for early detection of the patient group at risk of disease progression, and as most of the BC-CML patients specifically showed resistance to all drugs, indicating the non-availability of effective medications for BC-CML, advanced-phase CML patient samples were subjected to WES to find out druggable mutations. WES detected numerous variants in the above-mentioned study subjects. We included genes mutated only in advanced phases of CML patients, i.e., in AP-CML and BC-CML, but not in CP-CML patients and healthy control DNA sequences taken from genomic databases. The total number of variants shared by our advanced-phase CML was 4175 (Figure 1).

The mutated genes with the highest variant frequency in both AP-CML and BC-CML patients, in addition to the *ABL* gene, were *RPTOR* (7.3%), followed by *BRCA1/BRCA2* (7.0%), *BCR* (6.0%), *STAB1* (4.6%), *NF1* (4.4%), *ACIN1* (4.4%), *EGFR* (3.9%), *NDRG2* (3.7%), *ERG* (3.3%) and *MYH11* (3.1%).

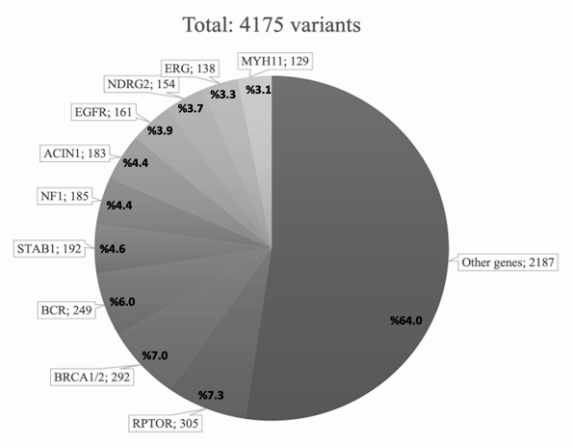

Figure 1. *Mutations shared by advanced phase CML patients (AP-CML + BC-CML).*

The number of variants and their frequencies in each gene were compared between AP-CML and BC-CML (Figure 2). CP-CML patients had only 114 mutations. AP-CML samples had 1644 variants (14.4 times higher than CP-CML), whereas BC-CML samples had 2531 variants (22.2 times higher than CP-CML), with a 54% gain in mutations from AP-CML to BC-CML (*P*=0.0000) (Figure 2). The gain of mutation from AP-CML to BC-CML in the genes with the highest variant frequency was also significantly high, with the highest increase percentage of 79.3% observed in *EGFR* (a membrane receptor gene), followed by *BRCA1/BRCA2* (72.9%), *ACIN1* (69.1%), *NF1* (60.6%), *STAB1* (59.5%), *MYH11* (58.0%), *RPTOR* (56.3%), *ERG* (46.4%), *NDRG2* (36.9%) and *BCR* (26.4%). Moreover, the low-frequency genes significantly increased from 866 variants in AP-CML to 1321 variants in BC-CML (*P*=0.0000) (Figure 2).

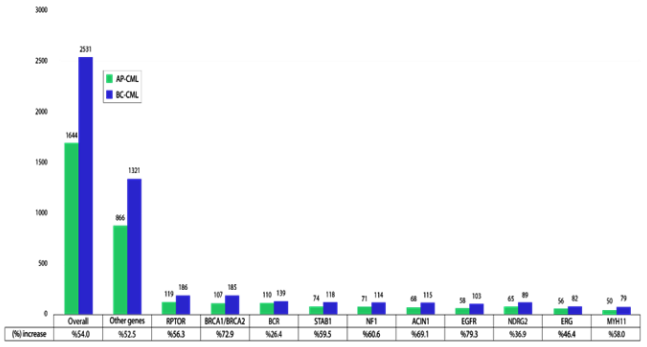

Figure 2. *A comparison of the variants' percentage increase from AP-CML to BC-CML in the highest variant frequency genes found in our study subjects.*

Druggability of Pan-Leukemic Mutations of BC-CML and Drug Repurposing

This study centers on genes amenable to pharmacological intervention, irrespective of the frequency of their variants. A gene is deemed druggable if any pharmacological agent associated with this gene has been identified for treating AML in the pandrugs2 database and relevant literature, whether as a targeted therapy or as part of chemotherapy. Among the 64 mutated genes identified in our BC-CML patients, 9 were druggable genes that have received FDA approval for use in AML or ALL patients. The variant frequencies of these druggable genes were notably low within our BC-CML patient samples. The gene exhibiting the highest variant frequencies among those amenable to pharmacological intervention, alongside mutations in the *ABL* gene, was *NPM1* (1.98%), succeeded by *DNMT3A* (1.86%), *PML* (1.82%), *AKT1* (1.62%), *CBL* (1.30%), *JAK2* (0.71%), *TET2* (0.59%), *IDH1* (0.32%), and *BCL2* (0.20%) (Figure 3). Despite the low variant frequencies of these genes among our study subjects, the observed variants exhibited a notable percentage increase from AP-CML to BC-CML, underscoring their critical involvement in disease progression (Figure 4).

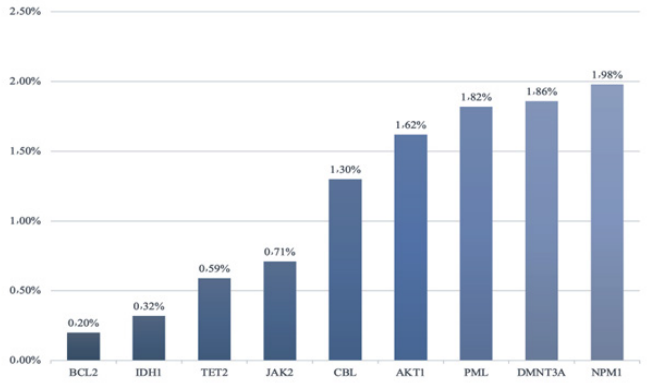

Figure 3. *Variant frequencies of the druggable genes found in our BC-CML study subjects, which have FDA-approved drugs to treat AML or ALL.*

Most of these genes were associated with FDA-approved targeted therapies for treating AML patients broadly, except for *IDH1*, which had an FDA-approved drug specifically for patients with IDH1-positive AML (Table 2). The medications sanctioned by the FDA include venetoclax, bortezomib, doxorubicin, mitoxantrone, tretinoin, quizartinib, decitabine, azacitidine, arsenic trioxide, and ivosidenib. *BCL2* emerged as the most important gene associated with FDA-approved pharmacological interventions for treating ALL patients, specifically venetoclax, doxorubicin, and vincristine (Table 2). Pharmaceuticals sanctioned by the FDA for various forms of leukemia are classified based on their genetic interaction mechanisms, including drugs that directly target specific gene mutations found in leukemia cells (Table 3).

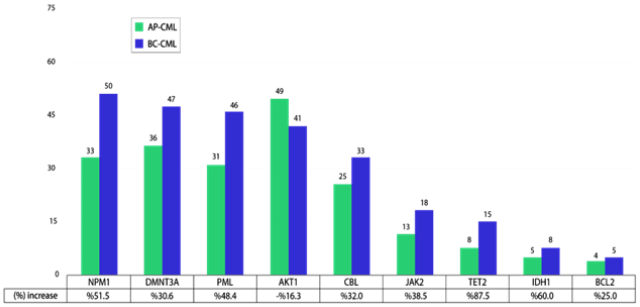

Figure 4. *Variants in the druggable genes that have FDA-approved drugs to treat AML or ALL, along with their percentage increase from AP-CML to BC-CML patients in our study subjects.*

Table 2.

List of the most significant druggable mutations in BC-CML with available FDA-approved drugs.

Gene	Drug	FDA approved	Clinical trial	Act
BCL2	VENETOCLAX*	AML (combined with azacitidine, decitabine, or low-dose cytarabine) & CLL with 17p deletion	CML	DT
	DOXORUBICIN	AML & ALL	BCL2-AML	BM
	MITOXANTRONE	AML	BCL2-AML	BM
	TRETINOIN (ATRA)	APL	BCL2-AML	BM
	VINCRISTINE	ALL & lymphoid BC-CML	BCL2-ALL	BM
	BORTEZOMIB*	MM and MCL	-	DT
CBL	QUIZARTINIB	FLT- AML	CBL-AML	BM
GATA2	BORTEZOMIB*	MM and MCL	CML	BM
DNMT3A	DECITABINE	CMML (combined with cedazuridine) & AML	DNMT3A-AML	DT
	AZACITIDINE	AML	DNMT3A-AML	BM
FGFR3	QUIZARTINIB	FLT- AML	CBL-AML	BM
IDH1	IVOSIDENIB	IDH1-AML	CML	DT
	AZACITIDINE*	AML	IDH1-ALL (combined with VENETOCLAX)	BM
JAK2	PACRITINIB	Myelofibrosis	-	DT
NPM1	VENETOCLAX*	AML (combined with azacitidine, decitabine or low-dose cytarabine) & CLL with 17p deletion	NPM1-AML	BM

** Effective against more than one type of mutation. DT, direct target; BM, biomarker.*

Table 2 (continued).

List of the most significant druggable mutations in BC-CML with available FDA-approved drugs.

Gene	Drug	FDA approved	Clinical trial	Act
PML	ARSENIC TRIOXIDE + TRETINOIN (ATRA)	PML-RARA-APL	-	DT
TET2	DECITABINE	CMML (combined with cedazuridine) & AML	TET2-CML	BM
	AZACITIDINE*	AML	TET2-CML	BM
AKT1	ARSENIC TRIOXIDE	APL	AKT1-APL	DT

** Effective against more than one type of mutation.*
DT, direct target; BM, biomarker

Table 3.

FDA-approved drugs, anti-leukemic targeted therapies that can directly target BC-CML mutations.

Drug	Disease for which FDA-approval granted	Gene targets (PanDrugs2)
VENETOCLAX	AML [22]	*BCL2, BCR, EZH2, IDH1,* and *NPM1*
TRETINOIN	APL [23]	*BCL2, PDK4, PML,* and *RARA*
BORTEZOMIB	MM and MCL [24]	*BCL2, FGFR3,* and *GATA2*
ZANUBRUTINIB	CLL and SLL [25]	*EGFR and JAK2*
IVOSIDENIB	*IDH1*+ AML [26]	*IDH1*
TAZEMETOSTAT	*EZH2*+-Follicular lymphoma [27]	*EZH2*
RUXOLITINIB	Myelofibrosis [28]	*JAK2, MPL*
PACRITINIB	Myelofibrosis [29]	*JAK2*
ARSENIC TRIOXIDE	APL [30]	*AKT1, PML*
TRETINOIN (ATRA)	APL [23]	*BCL2, PDK4, PML,* and *RARA*

In summary, notable genetic alterations were identified in patients who had progressed to the advanced stages of CML. The laboratory findings and clinical characteristics linked to the progression of CML included anemia, leukocytosis, splenomegaly, and hepatomegaly. Patients with BC-CML exhibited more variants within their mutated genes, demonstrated suboptimal treatment responses, and experienced diminished overall survival rates. The genes exhibiting the highest variant frequencies in the advanced stages of CML were found to overlap with those associated with AML/ALL lineages (pan-leukemic genes). Many genes are amenable to pharmacological intervention using drugs already approved by the FDA and EMA for treating different hematological malignancies harboring target mutations. Both FDA- and EMA-approved and investigational drugs currently undergoing clinical trials, targeting these specific gene mutations, represent promising avenues for personalized therapeutic strategies in the context of BC-CML, particularly in the TKI and post-TKI landscape.

Discussion

An extensive investigation was conducted on the clinical characteristics and pan-leukemic gene mutations in advanced-phase CML patients to gain a profound understanding of the biology, genetics, and potential precision medicine of severe and fatal clinical manifestations (blast crisis) of this treatable cancer.[4-8] Our study revealed a noteworthy association between BC-CML and hepatomegaly (P=0.0014), while splenomegaly exhibited significance in AP-CML (P=0.0014). The mean hemoglobin level, WBC count, platelet count, hepatomegaly, splenomegaly, and survival status of patients in the advanced phase of CML exhibited significant differences from those in the CP of CML. Nevertheless, the limitations of these clinical parameters in the early identification of patients susceptible to CML progression and in the pursuit of novel therapeutic agents for challenging BC-CML cases underscore the necessity for comprehensive genetic analysis. Such analysis is crucial for uncovering molecular biomarkers indicative of early progression and identifying druggable gene mutations beyond BCR-ABL.[31] The WES employed in our study was utilized to identify druggable gene mutations, representing one of the most effective methodologies for this objective.

Currently, five TKIs, namely imatinib, dasatinib, nilotinib, bosutinib, and ponatinib, are commercially available and have received approval for the treatment of CML by both the FDA and the EMA, while another TKI called asciminib is on the verge of approval very soon.[31,32] These approvals come with specific recommendations that consider various factors, including the stage of CML at diagnosis, dosage, BCR-ABL mutations, and reimbursement considerations. However, it is noteworthy that approximately 20%-30% of patients encounter resistance to these inhibitors, which can lead to treatment failure and disease relapse, ultimately resulting in BC-CML. Furthermore, considering the availability of all first-, second-, third-, and fourth-generation TKIs, the median overall survival and failure-free survival for BC-CML are recorded at 23.8 months and 5 months, respectively.[5,32,33] Furthermore, certain TKIs have demonstrated the potential to induce liver complications, including hepatotoxicity and hepatomegaly, a phenomenon also observed in our cohort of patients receiving TKI treatment.[33] This underscores the imperative to identify supplementary drug targets and ensure the availability of alternative pharmacological options for treating BC-CML. This may be accomplished by repurposing existing drugs currently utilized in the clinical management of AML and ALL, given that BC-CML presents as either M-BC-CML or L-BC-CML.[31]

Consequently, we have curated a selection of genes previously identified in AML and ALL to evaluate their potential for drug targeting, given that numerous gene mutations in these conditions are currently recognized as targets for FDA and EMA-approved therapies, in addition to various experimental drugs.

Around 80% of BC-CML patients are classified as M-BC, whereas 20% fall under L-BC, with B cells demonstrating a

greater prevalence than T cells.[34] Nevertheless, individuals diagnosed with L-BC exhibit more favorable outcomes than those with M-BC. The assessment of NGS panels to identify frequently mutated lymphoid or myeloid genes may be contemplated; however, it continues to be regarded as an experimental methodology in CML. Nonetheless, integrated therapeutic approaches have been implemented for myeloid instead of lymphoid BC-CML, drawing upon treatment strategies for AML and ALL, respectively. Recent small, single-arm studies have reported on M-BC, indicating that the combination of a second-generation TKI or ponatinib with decitabine or azacytidine yields complete cytogenetic response rates ranging from 33% to 43%, alongside a median overall survival of 13.8 to 27.4 months.[35] Strati et al.[36] assessed the efficacy of imatinib (400-800 mg daily) and dasatinib (50-140 mg daily) in conjunction with hyperfractionated cyclophosphamide, vincristine, adriamycin, and dexamethasone (hyperCVAD) in a cohort of 42 patients. The rates of complete cytogenetic response (CCyR) and complete hematologic response (CHR) were found to be 90% and 58%, respectively. In a more measured approach, Rea et al.[37] assessed the combination of IM 800 mg with vincristine and dexamethasone in a cohort of 13 patients with lymphoid blast phase. Among the 12 patients assessed, 11(91.7%) attained a complete hematologic response, while 4(33.3%) reached complete cytogenetic response.

The results from our WES revealed that the genes exhibiting the highest variant frequencies in BC-CML samples were *RPTOR* (7.3%), followed closely by *BRCA1/BRCA2* (7.0%), *BCR* (6.0%), *STAB1* (4.6%), *NF1* (4.4%), *ACIN1* (4.4%), *EGFR* (3.9%), *NDRG2* (3.7%), *ERG* (3.3%), and *MYH11* (3.1%). The gene with the highest frequency of variants that drugs can target was *NPM1* (1.98%), followed closely by *DNMT3A* (1.86%), *PML* (1.82%), *AKT1* (1.62%), *CBL* (1.30%), *JAK2* (0.71%), *TET2* (0.59%), *IDH1* (0.32%), and *BCL2* (0.20%). The genes associated with AML lineage have been linked to nine FDA-approved drugs, whereas those related to ALL lineage are associated with only one FDA-approved drug. This is logical, as both AML and CML originate from the myeloid lineage, sharing a greater number of gene mutations than does ALL. Furthermore, ivosidenib received FDA approval for treating AML patients harboring IDH1 mutations, establishing its status as a targeted therapeutic agent. While all other FDA-approved medications identified in this study are indicated for treating AML/ALL irrespective of a specific gene mutation, they are classified as targeted therapies due to their mechanisms of action, which involve the targeting of genes. This suggests that IVO and other FDA-approved medications for AML and ALL should be regarded as targeted therapies for CML patients exhibiting these gene mutations.

The FDA has sanctioned a range of pharmacological agents for the treatment of gene mutations associated with AML and ALL (venetoclax [VEN], bortezomib, ivosidenib [IVO], azacitidine [AZA], decitabine [DEC], doxorubicin [DOX], mitoxantrone [MIT], vincristine [VIN], quizartinib [QUI], arsenic trioxide [ATO], all-trans retinoic acid [ATRA], and pacritinib [PAC]), which are also relevant to our BC-CML patients. Arsenic trioxide (ATO) and all-trans retinoic acid (ATRA) have obtained FDA approval for their application in treating acute promyelocytic leukemia.[23,30] A study conducted in China has indicated that increased levels of ATO successfully sustain ERK phosphorylation, which in turn activates CDKN1A expression and results in apoptosis. Conversely, therapies utilizing reduced doses of ATO lead to an elevation in AKT1 expression, suppressing CDKN1A promoter activity and diminishing apoptosis. Consequently, ATO exhibits its therapeutic efficacy primarily at elevated doses.[38] Furthermore, patients with CML who demonstrate gain-of-function mutations in *AKT1* may show a positive response to standard doses of ATO, given that their *AKT1* expression profiles resemble those seen with low-dose ATO treatments. In the interim, ATRA has demonstrated promise in inhibiting *BCL2* and *MCL1*, indicating its potential as a targeted therapeutic approach for CML patients with *BCL2* mutations.[39] Moreover, the FDA has sanctioned a combined treatment approach of ATRA and ATO specifically for patients with acute promyelocytic leukemia who possess the PML-RARA fusion. This fusion protein serves as a direct target for the combination of drugs that have demonstrated significant rates of complete remission, improved overall survival, enduring and profound molecular responses, and a minimal relapse risk.[31] As a result, patients with CML exhibiting PML alterations could derive substantial advantages from either combination therapy or monotherapy utilizing ATRA or ATO. VEN has received FDA approval as a targeted therapy that specifically inhibits *BCL2* in individuals diagnosed with AML and those exhibiting chromosome 17p deletions in CLL.[40,41] Furthermore, the integration of dasatinib and VEN has demonstrated both safety and efficacy in managing CP-CML, attaining response rates comparable to those seen with dasatinib monotherapy.[42] This underscores the possible significance of VEN in managing CML patients presenting *BCL2* variants, particularly those who may show resistance to TKIs. Patients with AML exhibiting *NPM1* mutations have demonstrated notable sensitivity to VEN.[43] Furthermore, VEN has shown significant effectiveness when used alongside HMAs or chemotherapy in treating *IDH1*-mutated AML, and it has successfully managed relapse in ALL associated with an *IDH1* mutation.[44]

The results indicate that VEN may provide advantages for CML patients possessing *IDH1*, *NPM1*, or *BCL2* variants. Another drug targeting *IDH1* that has received FDA approval is IVO, which is indicated for patients with relapsed or refractory AML.[8] The FDA has approved AZA to be utilized as a maintenance therapy for adult patients with AML who are unable to pursue additional intensive curative treatments and have achieved complete remission, regardless of whether they have experienced incomplete blood count recovery following intensive induction chemotherapy.[45] AZA has proven effective when utilized alongside targeted therapies like VEN, which focus on variants in *BCL2* and *IDH1*.[46] A separate study indicated that elderly AML patients or those deemed unfit for intensive chemotherapy, when treated with VEN in conjunction with HMAs like AZA, have not only demonstrated improved overall survival but have also set a new

standard of care, exceeding the results achieved with HMAs alone.[47] Moreover, the FDA has sanctioned the combination of AZA and IVO for the treatment of newly diagnosed *IDH1*-mutated AML patients, encompassing those who are elderly or present with comorbidities.[26] Furthermore, the incorporation of AZA into chemotherapy protocols has resulted in prolonged survival for AML patients possessing the distinct *DNMT3A* variant, R882. This observation indicates its potential role as a biomarker for AZA efficacy in chemotherapy, independent of additional targeted treatments.[48] AZA's extensive applicability and established efficacy highlights its significant therapeutic influence in the management of leukemia, as well as its potential as a targeted treatment for CML patients harboring mutations in *DNMT3A*, *IDH1*, or *BCL2*, whether utilized as a monotherapy or in conjunction with other pharmacological agents. DEC is an HMA and DNMT inhibitor that has been granted FDA approval for use in conjunction with VEN to address newly diagnosed AML patients who are either elderly or unsuitable for intensive therapy.[43] Moreover, HMAs have demonstrated efficacy in individuals possessing *TET2* variants.[49] DOX, belonging to the anthracycline class of chemotherapeutic agents, has received FDA approval to treat various cancers, including ALL and AML.[50] The concentration of the drug exhibited an inverse relationship with the expression of a *BCL2* variant throughout treatment. Notably, DOX exhibits a selective ability to induce apoptosis in relapsed AML cells, which can be partially ascribed to its targeted inhibition of the *BCL2* variant.[51] Mitoxantrone (MIT) has received FDA approval for the treatment of adult AML.[52] Investigations have demonstrated that MIT induces programmed cell death in AML cells, alongside a significant reduction of *BCL2*.[53] The findings suggest that MIT may specifically focus on mutated *BCL2*, indicating its potential application in treating CML patients exhibiting *BCL2* variants. VIN has received FDA approval to treat a range of malignancies, encompassing ALL, B-cell ALL, and lymphoid BC-CML.[54] Moreover, an experimental investigation has revealed that VIN significantly diminishes BCL2 protein levels in human ALL cells. The effect is further amplified when VIN is combined with Huaier aqueous extract.[55]

In addition, quizartinib (QUI) is an FDA-approved FLT3 inhibitor designated for patients with FLT3-positive AML.[56] Loss-of-function variants in CBL correlate with a phenotype characterized by either hyperactivation or heightened sensitivity of FLT3. Research indicates that QUI significantly suppresses cell proliferation in wild-type FLT3 cells; a phenomenon linked to the diminished activity of cCBL E3 ligase resulting from the loss-of-function variant in CBL.[57] The results indicate that CBL mutations may function as a biomarker for the effectiveness of FLT3 inhibitors, presenting a potentially advantageous therapeutic strategy for CML patients harboring CBL variants. Pacritinib (PAC) is a tyrosine kinase inhibitor that demonstrates comparable effectiveness against both *FLT3* and *JAK2*, and it has received FDA approval for the management of myelofibrosis.[29] Studies indicate that PAC effectively inhibits the phosphorylation of *IRAK1* in AML cells, resulting in diminished viability and survival in AML cell lines with diverse mutations. Moreover, *IRAK1* has been identified as being overexpressed in chronic myelomonocytic leukemia (CMML). The administration of PAC demonstrates independent efficacy in primary CMML cells, and it has enhanced effects when combined with AZA. Furthermore, PAC extensively inhibits kinase-signaling pathways involved in tumor progression, including the driver mutations associated with *JAK2*. Exhibiting clinical tolerability and efficacy in conditions such as chronic myeloproliferative diseases, PAC distinguishes itself through its limited myelosuppressive and immunosuppressive characteristics in contrast to other *JAK2* inhibitors that similarly influence *JAK1* signaling.[58] These attributes highlight PAC's potential for incorporation into current treatment protocols for CML.

Nevertheless, the *RPTOR* gene was a highly mutated gene in our AP- and BC-CML patients, underscoring its critical role as a drug target for precision medicine in BC-CML. RPTOR constitutes a component of the mTOR pathway, which is subject to modulation by mTOR inhibitors.[31] The mTOR inhibitors that have received FDA approval include the rapamycin derivatives temsirolimus, everolimus, and ridaforolimus; however, their use is not indicated for blood cancer.[59] Reports indicate that temsirolimus and everolimus exert an inhibitory effect on mTORC2 in AML cells by activating the AKT signaling pathway. Furthermore, it has been noted that additional clinical studies involving patients with hematologic malignancies who were administered these medications yielded analogous outcomes.[60] The findings indicate that mTOR inhibitors may serve as a targeted therapeutic approach for leukemia patients exhibiting mutations in *AKT1*, *AKT2*, and *RPTOR*. Moreover, an experimental investigation has demonstrated that everolimus proved effective in addressing TKI-resistant CML cells, with a synergistic effect noted when combined with imatinib.[31] A further investigation revealed that ponatinib-resistant CML cells might acquire resistance via mechanisms that are not reliant on BCR-ABL, predominantly by activating the mTOR pathway. mTOR inhibitors have been recognized as potent agents in combating these resistant cells, facilitating the process of autophagy. Furthermore, it has been observed that the suppression of autophagy could amplify the cytotoxic effects of mTOR inhibitors in these cells. The combination of hydroxychloroquine, an autophagy inhibitor, markedly diminished cell viability in vitro and enhanced survival in vivo when compared to treatment with the mTOR inhibitor alone.[61] The findings highlight the significance of mTOR inhibitors in managing TKI-resistant CML, particularly for patients with *RPTOR* variants, which were notably mutated among our study subjects. This observation advocates for further investigation into combination therapies that could potentially augment the effectiveness of current treatment modalities.

The *BCR* (B-cell antigen receptor) gene has also been found to be a highly mutated gene in our advanced-phase CML patients in this study. The signaling of BCR plays a crucial role in the progression of CLL. Alterations in the BCR gene can influence the signaling pathway, thereby promoting the proliferation and survival of CLL cells. An essential element in this pathway is Bruton's Tyrosine Kinase (BTK), whose inhibition interferes with BCR signaling, diminishing

the growth and viability of CLL cells. Consequently, BTK has become a pivotal focus for innovative treatments in CLL and various B-cell-associated conditions. At present, multiple generations of BTK inhibitors are available. Ibrutinib, as the inaugural BTK inhibitor, has profoundly transformed the therapeutic landscape for CLL, attaining unprecedented response and survival rates. Second-generation BTK inhibitors, including acalabrutinib and zanubrutinib, provide enhanced specificity for BTK, thereby reducing side effects. Furthermore, the novel BTK inhibitor, pirtobrutinib, has been formulated to enhance efficacy and tackle the resistance observed with earlier BTK inhibitors, and it has recently received FDA approval for CLL.[62] It is prudent to consider the application of these inhibitors for treating BC-CML with BCR variants, especially when used in conjunction with TKIs, as the presence of variants in BCR may contribute to TKI resistance in patients with BC-CML.

Gilteritinib and midostaurin are FDA-approved FLT3 inhibitors utilized in the treatment of AML. These agents are employed in a range of therapeutic protocols, demonstrating efficacy in both newly diagnosed FLT3-mutated AML and in instances of relapse or refractory cases.[63] Quizartinib (QUI) represents an additional FLT3 inhibitor that has received FDA approval for patients with FLT3-positive AML.[56] Moreover, loss-of-function variants in CBL correlate with a phenotype characterized by either hyperactivation or heightened sensitivity of FLT3. Research indicates that QUI significantly hampers cell proliferation in wild-type FLT3 cells, a phenomenon linked to diminished cCBL E3 ligase activity resulting from the loss-of-function variant in CBL.[57] A study has illustrated the importance of NPM1 in AML patients as a noteworthy positive prognostic indicator in assessing the response to midostaurin. [64] The findings indicate that *CBL* and *NPM1* mutations may function as a biomarker for the effectiveness of FLT3 inhibitors, presenting a potentially advantageous therapeutic strategy for CML patients harboring CBL or NPM1 variants.

Moreover, Xiang et al.[65] discovered that pyrvinium, an FDA-approved medication for pinworm infections, demonstrates efficacy in treating BC-CML patients. The mechanism of action varies according to the specific type of cancer being addressed. Pyrvinium demonstrates an inhibitory effect on mitochondrial respiration in the context of CML, and its combination with dasatinib enhances apoptosis, thereby improving therapeutic outcomes for patients exhibiting resistance to TKI treatment. Nevertheless, it has yet to receive approval for patients with CML.

Status of Drug Repurposing in Evidence-Based Cancer Treatment

Despite the existence of numerous treatment protocols, these interventions often lead to the emergence of drug resistance in malignant cells, thereby diminishing the effectiveness of anticancer agents. This underscores the pressing necessity for innovative therapies to address the challenge of drug resistance. Nonetheless, developing a new drug approved for clinical use is a protracted endeavor, typically spanning 10 to 15 years and incurring costs ranging from 1 to 2 billion dollars. This intricate process commences with the design phase and progresses through various stages until safety and efficacy are established.[66] Furthermore, clinical evaluations are essential to ascertain appropriate dosing and effectiveness, and the shift to clinical application necessitates adherence to various regulatory and commercial stipulations. In addressing this challenge, drug repurposing is employed, wherein existing medications are utilized for alternative therapeutic applications that extend beyond their original indications. In contrast to the conventional de novo drug development approach, drug repurposing presents numerous benefits, such as improved efficiency, decreased time and financial expenditures, and a lower likelihood of failure. Furthermore, it leverages established understanding of drug mechanisms, thus enhancing the efficacy of clinical translation.[67]

In recent years, notable advancements in computational resources have enabled a methodical approach to drug repurposing. These resources employ diverse information sources, including electronic health records, genome-wide association analyses, gene expression profiles, pathway mappings, compound structures, target binding assays, and phenotypic profiling data. Furthermore, there has been a recent emphasis on computational repurposing methodologies, especially those centered around machine learning algorithms. Moreover, databases are meticulously crafted to facilitate in-silico drug repurposing, such as the Drug Repurposing Hub, repoDB, pandrugs, PathSurveyor, and RepurposeDB.[68,69] Consequently, our findings present a pragmatic approach to integrating genomics and multi-omics technologies alongside existing computational resources, facilitating the discovery of novel biomarkers, drug targets, and therapeutic options for various clinical manifestations with limited treatment modalities, such as BC-CML.[70-72]

Future Perspective

Our integrative genomics and AI-guided drug repurposing approach for BC-CML highlights a paradigm shift beyond traditional cancer therapeutics. By uncovering actionable, druggable mutations already targeted by approved therapies,[70,71] our strategy provides a highly pragmatic blueprint for precision medicine, especially for relapsed, refractory, and untreatable malignancies. As the success of drug repurposing during the COVID-19 pandemic has shown,[66,67] harnessing existing pharmacological arsenals through advanced multi-omics and AI technologies[72] can dramatically accelerate treatment innovation, offering hope for many patient populations historically considered beyond therapeutic reach. Our current study builds upon our earlier propositions advocating AI-assisted drug repositioning as a pragmatic route to precision oncology post-COVID-19.[73]

Building upon our findings identifying actionable mutations in myeloid/lymphoid lineage genes of BC-CML, practical oncology clinics can now immediately apply targeted repurposing strategies to manage otherwise untreatable cases. FDA-approved agents such as venetoclax, ivosidenib, and decitabine, traditionally used for AML and other hematologic malignancies, can be stratified based on mutational profiling at diagnosis or relapse. Integrating AI-guided drug-matching platforms into routine workflows will enable oncologists to

select patient-specific therapies rather than relying solely on TKIs, which often fail in the blast phase.[74] By 2026 and beyond, precision repurposing will likely be incorporated into standard clinical practice guidelines for advanced-phase CML, supported by the evolving paradigm of molecular reclassification in clinical trial designs[75] and predictive oncology models.[76] Advances in biomarker-driven therapies and personalized molecular-targeted strategies will further catalyze this transformation.[77] Our approach complements emerging international frameworks for repositioning strategies in aggressive leukemias, potentially reshaping future NCCN and ESMO guidelines.[78]

Conclusions

In our study, significant numbers of druggable mutations in genes associated with the AML/ALL lineage are identified in BC-CML patients when employing highly sensitive NGS techniques. The NGA technique, boasting coverage of 100X or greater, facilitates the identification of druggable gene mutations within AML-/ALL-lineage genes across nearly all BC-CML patients. Many drugs target these AML-/ALL-lineage gene mutations, and many are currently undergoing active trials or have already secured FDA approval. Consequently, our research offers valuable guidance for repurposing existing pharmaceuticals and exploring innovative therapeutic alternatives, thereby facilitating a more personalized approach to treatment for patients with BC-CML. Extensive, large-scale, and prospective investigations concerning druggable pan-cancer genes are essential to yield comprehensive insights into the molecular oncogenesis of BC-CML. Such studies are crucial for identifying novel biomarkers, drug targets, and therapeutic alternatives for this severe clinical presentation in CML.

Funding Information

This work was funded by the National Plan for Science, Technology and Innovation (MAARIFAH), King Abdul-Aziz City for Science and Technology, Grant Number 14-Med-2817-02. This study was partially supported by the College of Medicine Research Centre, Deanship of Scientific Research, King Saud University.

Ethical Considerations

The study was conducted in accordance with the Declaration of Helsinki. The Institutional Review Board (IRB) of King Abdullah International Medical Research Centre (KAIMRC), National Guard Health Affairs, through project # RA17 /002, approved it on 4 February 2019, although KAIMRC did not provide research funding. Written informed consent was obtained from each patient.

Competing Interests

The authors declare that they have no competing interests.

Data Availability Statement

Access to data made by next-generation sequencing can be obtained from NCBI, to which it was submitted, at https://www.ncbi.nlm.nih.gov/sra/PRJNA734750.

References

1. Al Khzem AH, Gomaa MS, Alturki MS, Tawfeeq N, Sarafroz M, Alonaizi SM, et al. Drug Repurposing for Cancer Treatment: A Comprehensive Review. Int J Mol Sci. 2024 Nov 19;25(22):12441. doi: 10.3390/ijms252212441.
2. Galimberti S, Petrini M, Baratè C, Ricci F, Balducci S, Grassi S, et al. Tyrosine Kinase Inhibitors Play an Antiviral Action in Patients Affected by Chronic Myeloid Leukemia: A Possible Model Supporting Their Use in the Fight Against SARS-CoV-2. Front Oncol. 2020 Sep 2;10:1428. doi: 10.3389/fonc.2020.01428.
3. Arbore DR, Galdean SM, Dima D, Rus I, Kegyes D, Ababei RG, et al. COVID-19 Impact on Chronic Myeloid Leukemia Patients. J Pers Med. 2022 Nov 10;12(11):1886. doi: 10.3390/jpm12111886.
4. Atallah E, Deininger M. Advanced-Stage Chronic Myeloid Leukemia: Options for Difficult Treatment Situations. Drugs. 2025 Jan;85(1):41-50. doi: 10.1007/s40265-024-02108-2.
5. Liu Y, Tu Y, Yan Z, Xiao J, Zhou B, Liu T, et al. CAR T-Cell therapy in chronic myeloid leukemia patients with lymphoid blast crisis: A multicenter clinical analysis. Cancer Lett. 2025 Jul 1;621:217688. doi: 10.1016/j.canlet.2025.217688.
6. Gupta A, Rudrakumar K, Singh S, Nathany S, Bhargava R. Mast Cell Blast Crisis in a Patient of Chronic Myeloid Leukemia With Concurrent BCR::ABL1 and RUNX1::RUNX1T1 Rearrangement or Should We Call It Myelomastocytic Leukemia? A Diagnostic Challenge With Nomenclature Dilemma. Int J Lab Hematol. 2025 Mar 19. doi: 10.1111/ijlh.14465.
7. Okabe S, Arai Y, Gotoh A. Correspondence to: "Combination therapies with ponatinib and asciminib in a preclinical model of chronic myeloid leukemia blast crisis with compound mutations", Curik N et al. Leukemia. 2024; 38: 1415-1418. Leukemia. 2025 Mar;39(3):775-778. doi: 10.1038/s41375-025-02521-w.
8. Gurashi K, Wang YH, Amaral FMR, Spence K, Cant R, Yao CY, et al. An integrative multiparametric approach stratifies putative distinct phenotypes of blast phase chronic myelomonocytic leukemia. Cell Rep Med. 2025 Feb 18;6(2):101933. doi: 10.1016/j.xcrm.2025.101933.
9. Atallah E, Deininger M. Advanced-Stage Chronic Myeloid Leukemia: Options for Difficult Treatment Situations. Drugs. 2025 Jan;85(1):41-50. doi: 10.1007/s40265-024-02108-2.
10. Baccarani M, Castagnetti F, Gugliotta G, Rosti G. A review of the European LeukemiaNet recommendations for the management of CML. Ann Hematol. 2015 Apr;94 Suppl 2:S141-7. doi: 10.1007/s00277-015-2322-2.
11. Hochhaus A, Baccarani M, Silver RT, Schiffer C, Apperley JF, Cervantes F, et al. European LeukemiaNet 2020 recommendations for treating chronic myeloid leukemia. Leukemia. 2020 Apr;34(4):966-984. doi: 10.1038/s41375-020-0776-2.
12. Abruzzese E, Bocchia M, Trawinska MM, Raspadori D, Bondanini F, Sicuranza A, et al. Minimal Residual Disease

Detection at RNA and Leukemic Stem Cell (LSC) Levels: Comparison of RT-qPCR, d-PCR and CD26+ Stem Cell Measurements in Chronic Myeloid Leukemia (CML) Patients in Deep Molecular Response (DMR). Cancers (Basel). 2023 Aug 15;15(16):4112. doi: 10.3390/cancers15164112.
13. Cortes JE, Lipton JH, Miller CB, Ailawadhi S, Akard L, Pinilla-Ibarz J, et al. Change in Chronic Low-Grade Nonhematologic Adverse Events (AEs) and Quality of Life (QoL) in Adult Patients (pts) with Philadelphia Chromosome–Positive (Ph+) Chronic Myeloid Leukemia in Chronic Phase (CML-CP) Switched From Imatinib (IM) to Nilotinib (NIL). Blood. 2012;120(21):3782.
14. Gnirke A, Melnikov A, Maguire J, Rogov P, LeProust EM, Brockman W, et al. Solution hybrid selection with ultra-long oligonucleotides for massively parallel targeted sequencing. Nat Biotechnol. 2009 Feb;27(2):182-9. doi: 10.1038/nbt.1523.
15. AlAsiri S, Basit S, Wood-Trageser MA, Yatsenko SA, Jeffries EP, Surti U, et al. Exome sequencing reveals MCM8 mutation underlies ovarian failure and chromosomal instability. J Clin Invest. 2015 Jan;125(1):258-62. doi: 10.1172/JCI78473.
16. Hasford J, Pfirrmann M, Hehlmann R, Allan NC, Baccarani M, Kluin-Nelemans JC, et al. A new prognostic score for survival of patients with chronic myeloid leukemia treated with interferon alfa. Writing Committee for the Collaborative CML Prognostic Factors Project Group. J Natl Cancer Inst. 1998 Jun 3;90(11):850-8. doi: 10.1093/jnci/90.11.850.
17. Hasford J, Baccarani M, Hoffmann V, Guilhot J, Saussele S, Rosti G, et al. Predicting complete cytogenetic response and subsequent progression-free survival in 2060 patients with CML on imatinib treatment: the EUTOS score. Blood. 2011 Jul 21;118(3):686-92. doi: 10.1182/blood-2010-12-319038.
18. U.S. Department of Health and Human Services, Food and Drug Administration, Center for Drug Evaluation and Research (CDER), Center for Biologics Evaluation and Research (CBER). Providing Regulatory Submissions in Electronic Format-Standardized Study Data Guidance for Industry. 2014.
19. Jiménez-Santos MJ, Nogueira-Rodríguez A, Piñeiro-Yáñez E, López-Fernández H, García-Martín S, Gómez-Plana P, et al. PanDrugs2: prioritizing cancer therapies using integrated individual multi-omics data. Nucleic Acids Res. 2023 Jul 5;51(W1):W411-W418. doi: 10.1093/nar/gkad412.
20. R Core Team. R: A Language and Environment for Statistical Computing. R Foundation for Statistical Computing, Vienna; 2021.
21. Sokal JE, Cox EB, Baccarani M, Tura S, Gomez GA, Robertson JE, et al. Prognostic discrimination in "good-risk" chronic granulocytic leukemia. Blood. 1984 Apr;63(4):789-99.
22. Morsia E, McCullough K, Joshi M, Cook J, Alkhateeb HB, Al-Kali A, et al. Venetoclax and hypomethylating agents in acute myeloid leukemia: Mayo Clinic series on 86 patients. Am J Hematol. 2020 Dec;95(12):1511-1521. doi: 10.1002/ajh.25978.
23. Yoham AL, Casadesus D. Tretinoin. 2023 Mar 27. In: StatPearls [Internet]. Treasure Island (FL): StatPearls Publishing; 2025 Jan–. PMID: 32491410.
24. Raedler L. Velcade (Bortezomib) Receives 2 New FDA Indications: For Retreatment of Patients with Multiple Myeloma and for First-Line Treatment of Patients with Mantle-Cell Lymphoma. Am Health Drug Benefits. 2015 Mar;8(Spec Feature):135-40.
25. Javidi-Sharifi N, Brown JR. Evaluating zanubrutinib for the treatment of adults with chronic lymphocytic leukemia or small lymphocytic lymphoma. Expert Rev Hematol. 2024 Jun;17(6):201-210. doi: 10.1080/17474086.2024.2356257.
26. Woods A, Norsworthy KJ, Wang X, Vallejo J, Chiu Yuen Chow E, Li RJ, et al. FDA Approval Summary: Ivosidenib in Combination with Azacitidine for Treatment of Patients with Newly Diagnosed Acute Myeloid Leukemia with an IDH1 Mutation. Clin Cancer Res. 2024 Apr 1;30(7):1226-1231. doi: 10.1158/1078-0432.CCR-23-2234.
27. Straining R, Eighmy W. Tazemetostat: EZH2 Inhibitor. J Adv Pract Oncol. 2022 Mar;13(2):158-163. doi: 10.6004/jadpro.2022.13.2.7.
28. Deisseroth A, Kaminskas E, Grillo J, Chen W, Saber H, Lu HL, et al. U.S. Food and Drug Administration approval: ruxolitinib for the treatment of patients with intermediate and high-risk myelofibrosis. Clin Cancer Res. 2012 Jun 15;18(12):3212-7. doi: 10.1158/1078-0432.CCR-12-0653.
29. Venugopal S, Mascarenhas J. The odyssey of pacritinib in myelofibrosis. Blood Adv. 2022 Aug 23;6(16):4905-4913. doi: 10.1182/bloodadvances.2022007524.
30. Jiang Y, Shen X, Zhi F, Wen Z, Gao Y, Xu J, Yang B, Bai Y. An overview of arsenic trioxide-involved combined treatment algorithms for leukemia: basic concepts and clinical implications. Cell Death Discov. 2023 Jul 27;9(1):266. doi: 10.1038/s41420-023-01558-z. PMID: 37500645; PMCID: PMC10374529.
31. Alves R, Gonçalves AC, Jorge J, Alves J, Alves da Silva A, Freitas-Tavares P, et al. Everolimus in combination with Imatinib overcomes resistance in Chronic myeloid leukaemia. Med Oncol. 2019 Feb 22;36(3):30. doi: 10.1007/s12032-019-1253-5.
32. Brioli A, Lomaia E, Fabisch C, Sacha T, Klamova H, Morozova E, et al. Management and outcome of patients with chronic myeloid leukemia in blast phase in the tyrosine kinase inhibitor era - analysis of the European LeukemiaNet Blast Phase Registry. Leukemia. 2024 May;38(5):1072-1080. doi: 10.1038/s41375-024-02204-y.
33. Jabbour E, Kantarjian H. Chronic myeloid leukemia: 2022 update on diagnosis, therapy, and monitoring. Am J Hematol. 2022 Sep;97(9):1236-1256. doi: 10.1002/ajh.26642.
34. Rinaldi I, Winston K. Chronic Myeloid Leukemia, from Pathophysiology to Treatment-Free Remission: A Narrative Literature Review. J Blood Med. 2023 Apr 6;14:261-277. doi: 10.2147/JBM.S382090.
35. Copland M. Treatment of blast phase chronic myeloid leukaemia: A rare and challenging entity. Br J Haematol. 2022 Dec;199(5):665-678. doi: 10.1111/bjh.18370.
36. Strati P, Kantarjian H, Thomas D, O'Brien S, Konoplev S, Jorgensen JL, et al. HCVAD plus imatinib or dasatinib in lymphoid blastic phase chronic myeloid leukemia. Cancer. 2014 Feb 1;120(3):373-80. doi: 10.1002/cncr.28433.
37. Rea D, Legros L, Raffoux E, Thomas X, Turlure P, Maury S, et al.; Intergroupe Français des Leucémies Myéloïdes Chronique; Group for Research in Adult Acute Lymphoblastic Leukemia. High-dose imatinib mesylate combined with vincristine and dexamethasone (DIV regimen) as induction therapy in patients with resistant Philadelphia-positive acute lymphoblastic leukemia and lymphoid blast crisis of chronic myeloid leukemia. Leukemia. 2006 Mar;20(3):400-3. doi: 10.1038/sj.leu.2404115.
38. Liu ZM, Tseng HY, Cheng YL, Yeh BW, Wu WJ,

Huang HS. TG-interacting factor transcriptionally induced by AKT/FOXO3A is a negative regulator that antagonizes arsenic trioxide-induced cancer cell apoptosis. Toxicol Appl Pharmacol. 2015 May 15;285(1):41-50. doi: 10.1016/j.taap.2015.03.007.
39. Li D, Li H, Cheng C, Li G, Yuan F, Mi R, et al. All-trans retinoic acid enhanced the antileukemic efficacy of ABT-199 in acute myeloid leukemia by downregulating the expression of S100A8. Int Immunopharmacol. 2022 Nov;112:109182. doi: 10.1016/j.intimp.2022.109182.
40. Kawakatsu R, Tadagaki K, Yamasaki K, Yoshida T. Venetoclax efficacy on acute myeloid leukemia is enhanced by the combination with butyrate. Sci Rep. 2024 Feb 29;14(1):4975. doi: 10.1038/s41598-024-55286-0.
41. Liu J, Li S, Wang Q, Feng Y, Xing H, Yang X, et al. Sonrotoclax overcomes BCL2 G101V mutation-induced venetoclax resistance in preclinical models of hematologic malignancy. Blood. 2024 May 2;143(18):1825-1836. doi: 10.1182/blood.2023019706.
42. Jabbour E, Haddad FG, Sasaki K, Carter BZ, Alvarado Y, Nasnas C, et al. Combination of dasatinib and venetoclax in newly diagnosed chronic phase chronic myeloid leukemia. Cancer. 2024 Aug 1;130(15):2652-2659. doi: 10.1002/cncr.35317.
43. Ranieri R, Pianigiani G, Sciabolacci S, Perriello VM, Marra A, Cardinali V, et al. Current status and future perspectives in targeted therapy of NPM1-mutated AML. Leukemia. 2022 Oct;36(10):2351-2367. doi: 10.1038/s41375-022-01666-2.
44. Li D, Zhao S, Mao L, Jin J, Wang J. Salvage treatment in IDH1 mutated acute lymphoblastic leukemia with venetoclax plus methotrexate and pegaspargase: A case report. Genes Dis. 2023 Mar 24;10(6):2215-2217. doi: 10.1016/j.gendis.2023.02.011.
45. Jen EY, Wang X, Li M, Li H, Lee SL, Ni N, et al. FDA Approval Summary: Oral Azacitidine for Continued Treatment of Adults with Acute Myeloid Leukemia Unable to Complete Intensive Curative Therapy. Clin Cancer Res. 2022 Jul 15;28(14):2989-2993. doi: 10.1158/1078-0432.CCR-21-4525.
46. Wang L, Song J, Xiao X, Li D, Liu T, He X. Comparison of venetoclax and ivosidenib/enasidenib for unfit newly diagnosed patients with acute myeloid leukemia and IDH1/2 mutation: a network meta-analysis. J Chemother. 2024 May;36(3):202-207. doi: 10.1080/1120009X.2023.2247200.
47. Bewersdorf JP, Shimony S, Shallis RM, Liu Y, Berton G, Schaefer EJ, et al. Combination therapy with hypomethylating agents and venetoclax versus intensive induction chemotherapy in IDH1- or IDH2-mutant newly diagnosed acute myeloid leukemia-A multicenter cohort study. Am J Hematol. 2024 Aug;99(8):1640-1643. doi: 10.1002/ajh.27366.
48. Scheller M, Ludwig AK, Göllner S, Rohde C, Krämer S, Stäble S, et al. Hotspot DNMT3A mutations in clonal hematopoiesis and acute myeloid leukemia sensitize cells to azacytidine via viral mimicry response. Nat Cancer. 2021 May;2(5):527-544. doi: 10.1038/s43018-021-00213-9.
49. Patnaik MM, Tefferi A. Chronic myelomonocytic leukemia: 2022 update on diagnosis, risk stratification, and management. Am J Hematol. 2022 Mar 1;97(3):352-372. doi: 10.1002/ajh.26455.
50. Johnson-Arbor K, Dubey R. Doxorubicin. 2023 Aug 8. In: StatPearls [Internet]. Treasure Island (FL): StatPearls Publishing; 2025 Jan–. PMID: 29083582.
51. Vu M, Kassouf N, Ofili R, Lund T, Bell C, Appiah S. Doxorubicin selectively induces apoptosis through the inhibition of a novel isoform of Bcl 2 in acute myeloid leukaemia MOLM 13 cells with reduced Beclin 1 expression. Int J Oncol. 2020 Jul;57(1):113-121. doi: 10.3892/ijo.2020.5052.
52. Fox EJ. Mechanism of action of mitoxantrone. Neurology. 2004 Dec 28;63(12 Suppl 6):S15-8. doi: 10.1212/wnl.63.12_suppl_6.s15. PMID: 15623664.
53. Bhalla K, Ibrado AM, Tourkina E, Tang C, Grant S, Bullock G, Huang Y, Ponnathpur V, Mahoney ME. High-dose mitoxantrone induces programmed cell death or apoptosis in human myeloid leukemia cells. Blood. 1993 Nov 15;82(10):3133-40.
54. Awosika AO, Below J, Das JM. Vincristine. 2023 Oct 30. In: StatPearls [Internet]. Treasure Island (FL): StatPearls Publishing; 2025 Jan–. PMID: 30725807
55. Qu P, Zhou F, Tan LF, Wang ZJ, Wang ML, Jin RM, Han J. [Effect of Huaier Aqueous Extract Combined with Routine Chemo-therapeutic Drugs on Human Acute Lymphoblastic Leukemia Cells Nalm-6 and Sup-B15]. Zhongguo Shi Yan Xue Ye Xue Za Zhi. 2020 Oct;28(5):1451-1458. Chinese. doi: 10.19746/j.cnki.issn.1009-2137.2020.05.004.
56. Roskoski R Jr. Properties of FDA-approved small molecule protein kinase inhibitors: A 2024 update. Pharmacol Res. 2024 Feb;200:107059. doi: 10.1016/j.phrs.2024.107059. Epub 2024 Jan 11. Erratum in: Pharmacol Res. 2025 May 29:107804. doi: 10.1016/j.phrs.2025.107804.
57. Weisberg E, Meng C, Case AE, Sattler M, Tiv HL, Gokhale PC, et al. Comparison of effects of midostaurin, crenolanib, quizartinib, gilteritinib, sorafenib and BLU-285 on oncogenic mutants of KIT, CBL and FLT3 in haematological malignancies. Br J Haematol. 2019 Nov;187(4):488-501. doi: 10.1111/bjh.16092.
58. Singer JW, Al-Fayoumi S, Ma H, Komrokji RS, Mesa R, Verstovsek S. Comprehensive kinase profile of pacritinib, a nonmyelosuppressive Janus kinase 2 inhibitor. J Exp Pharmacol. 2016 Aug 16;8:11-9. doi: 10.2147/JEP.S110702.
59. Mao B, Zhang Q, Ma L, Zhao DS, Zhao P, Yan P. Overview of Research into mTOR Inhibitors. Molecules. 2022 Aug 19;27(16):5295. doi: 10.3390/molecules27165295.
60. Zeng Z, Sarbassov dos D, Samudio IJ, Yee KW, Munsell MF, Ellen Jackson C, et al. Rapamycin derivatives reduce mTORC2 signaling and inhibit AKT activation in AML. Blood. 2007 Apr 15;109(8):3509-12. doi: 10.1182/blood-2006-06-030833.
61. Mitchell R, Hopcroft LEM, Baquero P, Allan EK, Hewit K, James D, et al. Targeting BCR-ABL-Independent TKI Resistance in Chronic Myeloid Leukemia by mTOR and Autophagy Inhibition. J Natl Cancer Inst. 2018 May 1;110(5):467-478. doi: 10.1093/jnci/djx236.
62. Wiśniewski K, Puła B. A Review of Resistance Mechanisms to Bruton's Kinase Inhibitors in Chronic Lymphocytic Leukemia. Int J Mol Sci. 2024 May 11;25(10):5246. doi: 10.3390/ijms25105246.
63. Liu H. Emerging agents and regimens for AML. J Hematol Oncol. 2021 Mar 23;14(1):49. doi: 10.1186/s13045-021-01062-w. PMID: 33757574; PMCID: PMC7989091.
64. Voso MT, Larson RA, Jones D, Marcucci G, Prior T, Krauter J, et al. Midostaurin in patients with acute myeloid leukemia and FLT3-TKD mutations: a subanalysis from the

RATIFY trial. Blood Adv. 2020 Oct 13;4(19):4945-4954. doi: 10.1182/bloodadvances.2020002904.
65. Xiang W, Cheong JK, Ang SH, Teo B, Xu P, Asari K, et al. Pyrvinium selectively targets blast phase-chronic myeloid leukemia through inhibition of mitochondrial respiration. Oncotarget. 2015 Oct 20;6(32):33769-80. doi: 10.18632/oncotarget.5615.
66. Xia Y, Sun M, Huang H, Jin WL. Drug repurposing for cancer therapy. Signal Transduct Target Ther. 2024 Apr 19;9(1):92. doi: 10.1038/s41392-024-01808-1.
67. Rodrigues R, Duarte D, Vale N. Drug Repurposing in Cancer Therapy: Influence of Patient's Genetic Background in Breast Cancer Treatment. Int J Mol Sci. 2022 Apr 14;23(8):4280. doi: 10.3390/ijms23084280.
68. Wang Y, Aldahdooh J, Hu Y, Yang H, Vähä-Koskela M, Tang J, Tanoli Z. DrugRepo: a novel approach to repurposing drugs based on chemical and genomic features. Sci Rep. 2022 Dec 7;12(1):21116. doi: 10.1038/s41598-022-24980-2.
69. Obermayer AN, Chang D, Nobles G, Teng M, Tan AC, Wang X, et al. PATH-SURVEYOR: pathway level survival enquiry for immuno-oncology and drug repurposing. BMC Bioinformatics. 2023 Jun 28;24(1):266. doi: 10.1186/s12859-023-05393-y.
70. Shin JE, Kim SH, Kong M, Kim HR, Yoon S, Kee KM, et al. Targeting FLT3-TAZ signaling to suppress drug resistance in blast phase chronic myeloid leukemia. Mol Cancer. 2023 Nov 6;22(1):177. doi: 10.1186/s12943-023-01837-4.
71. Chen F, Zhao D, Xu Y, Zhang Y, Chen MH, Pathak KV, et al. miR-142 deficit in T cells during blast crisis promotes chronic myeloid leukemia immune escape. Nat Commun. 2025 Feb 1;16(1):1253. doi: 10.1038/s41467-025-56383-y.
72. Mojidra R, Gardi N, Bagal B, Khattry N, Gokarn A, et al. Genomic analysis identifies an incipient signature to forecast imatinib resistance before start of treatment in patients with chronic myeloid leukemia. Advances in Biomarker Sciences and Technology. 2025;7:59-64. doi: 10.1016/j.abst.2025.01.004
73. Iqbal Z, Alanazi N, AlGarni A, AlMukhaylid S, Adeel K, Sabar MF, et al. Exploring drug potential of myeloid/lymphoid lineage gene mutations in advanced-phase CML using drug discovery tools: insights for precision oncology in blast crisis CML in the post-COVID-19 era. J Popul Ther Clin Pharmacol. 2022;29(4):4994-5012. doi:10.53555/2qjjf483.
74. Laganà A, Scalzulli E, Bisegna ML, Ielo C, Martelli M, Breccia M. Understanding and overcoming resistance to tyrosine kinase inhibitors (TKIs) in Chronic myeloid leukemia (CML). Expert Rev Hematol. 2025 Jan;18(1):65-79. doi: 10.1080/17474086.2024.2440776.
75. Nikanjam M, Kato S, Allen T, Sicklick JK, Kurzrock R. Novel clinical trial designs emerging from the molecular reclassification of cancer. CA Cancer J Clin. 2025 May-Jun;75(3):243-267. doi: 10.3322/caac.21880.
76. Singhal A, Zhao X, Wall P, So E, Calderini G, Partin A, et al. The Hallmarks of Predictive Oncology. Cancer Discov. 2025 Feb 7;15(2):271-285. doi: 10.1158/2159-8290.CD-24-0760.
77. Molla G, Bitew M. The future of cancer diagnosis and treatment: unlocking the power of biomarkers and personalized molecular-targeted therapies. Int J Mol Sci. 2025;24(8):6907. doi:10.3390/ijms24086907.
78. Gulati G, Gangat N, Lasho TL, Tefferi A. Precision medicine applications in hematologic malignancies: evolving strategies for drug repurposing and biomarker-driven therapies. Blood Cancer J. 2025;15(4):73. doi:10.1038/s41408-025-00855-3.

***Corresponding author**: Dr. Zafar Iqbal; Chairman, Group Leader & Principal Investigator; QAAA Unit /Genomic & Experimental Medicine (GEM) Group; KSAU-HS/KAIMRC/SSBMT; NGHA, KAMC, Al-Ahsa 31982, Saudi Arabia; E-mail: drzafar.medgen1@gmail.com; iqbalz@ksau-hs.edu.sa, iqbalza@mngha.med.sa*

International Journal of Biomedicine 15(3) (2025) 483-489
http://dx.doi.org/10.21103/Article15(3)_OA3

ORIGINAL ARTICLE

Oncology

INTERNATIONAL JOURNAL OF BIOMEDICINE

Ferroptosis-Related genes *NOX4*, *PDK4*, *PRKAA2*, and *FABP4* Emerge as Novel Prognostic Biomarkers and Therapeutic Targets in Stomach Adenocarcinoma

Qinmin Liu[1*], Fei Wang[1], Yongjin Luo[2], Qi Guo[3], Yichi Zhang[3], Fanghui Chen[4], Shaoqiang Liu[1]

[1]*Department of Radiology, First Affiliated Hospital of Gannan Medical University, Ganzhou City, Jiangxi, P.R. China*
[2]*Department of Radiology, People's Hospital of Anyuan County, Ganzhou City, Jiangxi, P.R. China*
[3]*School of the First Clinical Medicine of Gannan Medical University, Ganzhou City, Jiangxi, P.R. China*
[4]*Department of Pharmacy, First Affiliated Hospital of Gannan Medical University, Ganzhou City, Jiangxi, P.R. China*

Abstract

Background: Stomach adenocarcinoma (STAD) is the fifth most common malignant tumor worldwide in terms of both incidence and mortality. Treatment and prognosis face great challenges. We aimed to identify potential therapeutic targets or prognostic genes by analyzing STAD RNA-seq and clinical data, as well as ferroptosis-related genes.
Methods and Results: RNA-seq and clinical data of STAD were downloaded from the Cancer Genome Atlas (TCGA) database, and ferroptosis-related gene data were downloaded from the FerrDb V2 website. Bioinformatics and statistical analyses were performed using R software, and statistical significance was set at $P<0.05$.
We screened 1384 differentially expressed genes (DEGs) between STAD and normal tissues, including 24 ferroptosis-related DEGs. Among these 24 genes, we further screened four hub genes related to survival prognosis: NOX2, PRKAA2, FABP4, and PDK4. Through single-gene survival analysis and Cox regression analysis, and by constructing a prognostic model, we found that STAD patients with low expression of *NOX2*, *PRKAA2*, *FABP4*, and *PDK4* had significantly longer survival times; the difference was statistically significant ($P<0.05$).
Conclusion: We identified four ferroptosis-related DEGs in STAD that are associated with prognosis. These four genes have the potential to become targets for STAD treatment.(**International Journal of Biomedicine. 2025;15(3):483-489.**)

Keywords: stomach adenocarcinoma • differentially expressed gene • ferroptosis • prognosis

For citation: Liu Q, Wang F, Luo Y, Guo Q, Zhang Y, Chen F, Liu S. Ferroptosis-Related genes *NOX4*, *PDK4*, *PRKAA2,* and *FABP4* Emerge as Novel Prognostic Biomarkers and Therapeutic Targets in Stomach Adenocarcinoma. International Journal of Biomedicine. 2025;15(3):483-489. doi:10.21103/Article15(3)_OA3

Abbreviations

DEGs, differentially expressed genes; **PPI**, protein-protein interaction; **STAD**, stomach adenocarcinoma.

Introduction

Stomach adenocarcinoma (STAD) is a malignant tumor originating from gastric mucosal epithelial cells. The pathological types of STAD vary. In 1965, P. LAUREN classified STAD into intestinal and diffuse types according to whether the tumor had intestinal metaplasia.[1] According to the 5th Edition of the World Health Organization (WHO) classification system in 2019, the most common pathological types of STAD include tubular, papillary, poorly cohesive, mucinous, and mixed adenocarcinomas.[2] According to data released in 2024 by the International Agency for Research on Cancer (IARC), there are 968,350 new cases of STAD worldwide, accounting for 4.9% of all new cases of 36 cancers,

and 659,853 deaths, accounting for 6.8% of the deaths of 36 cancers. Morbidity and mortality rates are ranked fifth in the world.[3] Although the incidence rate of STAD is relatively low compared to lung cancer, which has an incidence rate of 11.7%, it is still the fifth largest cause of cancer-related deaths in the world.[4,5] The incidence of STAD is associated with various factors, including Helicobacter pylori infection, genetic factors, environmental factors, dietary factors, and others. The choice of treatment strategies for patients with STAD is closely related to their clinical stage. For non-metastatic STAD, combination therapy, such as perioperative chemotherapy or postoperative chemotherapy plus chemoradiation, is usually the preferred option, and palliative treatment is typically employed for metastatic and unresectable STAD.[6] Although the incidence of STAD has declined over the past fifty years, its global 5-year survival rate remains at only about 25-30%, [7] making it a significant global health burden due to its poor prognosis. In addition, studies have shown that the incidence of STAD is increasing in younger age groups.[4,5] Therefore, the diagnosis, treatment and prognosis of STAD in the world are still facing severe challenges.

Ferroptosis is an iron-dependent, non-apoptotic form of cell death proposed by Dr. Brent R. Stockwell of Columbia University in 2012.[8] Ferroptosis is an iron-dependent, regulated, unique mode of cell death.[9] It is mediated by lipid peroxidation, resulting in a large accumulation of intracellular reactive oxygen species (ROS), which eventually leads to cell death.[9] Numerous studies have indicated that tumor suppression or growth is associated with ferroptosis. For example, Ma et al. found that CD8+ T cells with up-regulated CD36 expression promoted ferroptosis by ingestion of excessive polyunsaturated fatty acids (PUFAs), thus causing them to lose their ability to regulate tumors and promoting tumor growth.[10] Wang et al.[11] suggested that in the immunotherapy of tumors, activated CD8+T cells secrete IFNγto downregulate the expression of two subunits of the glutamate cysteine efflux system xc−, SLC3A2, and SLC7A11, thereby promoting lipid peroxidation in tumor cells, ultimately leading to ferroptosis and inhibiting tumor growth. Ferroptosis may also serve as an effective therapeutic target for the treatment of pancreatic cancer, lung cancer, and liver cancer.[12,13] These studies have shown that the pathological process of tumors is closely related to ferroptosis.

STAD cells can evade ferroptosis by up-regulating *GPX4*, thereby promoting tumor progression; however, knocking out *GPX4* or inhibiting ferroptosis resistance with drugs can significantly suppress tumor growth and delay the progression of metastasis.[14] The microprotein HCP5-132aa encoded by *HCP5* enhances the interaction between *YBX1* and *ELAVL1*, maintains SLC7A11 levels, and thereby inhibits ferroptosis to promote the proliferation and metastasis of STAD cells.[15] These studies indicate that the investigation of ferroptosis-related genes in STAD can not only uncover potential new therapeutic targets but also serve as prognostic markers. Therefore, the discovery of additional ferroptosis-related genes in STAD could provide significant benefits for both clinical practice and patients with this cancer. In this study, we aimed to perform bioinformatics analysis on the RNA-seq profiles and clinical data of STAD samples downloaded from the Cancer Genome Atlas (TCGA) database to identify ferroptosis-related genes associated with the survival prognosis of STAD patients. This study may provide a reference for the prognostic evaluation of patients with STAD or the search for therapeutic targets in clinical practice.

Materials and Methods

Data Acquisition and Processing

RNA-seq profiles and clinical data of 379 STAD samples and 34 normal tissue samples were downloaded from the TCGA website (https://portal.gdc.cancer.gov) on August 31, 2024. The GTF annotation file was then used to convert the Ensemble gene ID to a gene symbol. We downloaded 717 ferroptosis-related genes from the FerrDb V2 website *(*http://www.zhounan.org/ferrdb/current*/)*, including 369 driver and 348 suppressor genes. R software (R4.4.0 version) and online websites were used for data analysis.

Identification of Significantly Differentially Expressed Genes

R software was used to pre-process the sample data, and the "Limma" R package was used to screen for DEGs. The cut-off values were determined according to the parameters $P<0.01$ and false discovery rate < 0.01. The absolute value of log2FC > 2 and adjusted P-value < 0.01 was used to screen for significant DEGs. Visualization of DEGs using volcano plots. We then took the intersection of DEGs and ferroptosis-related genes to screen for ferroptosis-related DEGs. The intersection genes were visualized using a Venn diagram.

Functional Enrichment Analysis of Ferroptosis-Related DEGs

The ferroptosis-related DEGs were visualized using heatmaps, and the Kyoto Encyclopedia of Genes and Genomes (KEGG) pathway analysis was performed using R software. Gene Ontology (GO) functional enrichment analysis of ferroptosis-related DEGs, including biological process (BP), cellular component (CC), and molecular function (MF), was performed using the Wei Sheng Xin online website (https://www.bioinformatics.com.cn). Statistical significance was set at $P<0.05$.

Protein-Protein Interaction (PPI) Network Analysis and Screening of Hub Genes

The PPI network was predicted using the Search Tool for the Retrieval of Interacting Genes (STRING: http://string-db.org, Version12.0)，and the Cytoscape software (Version 3.10.2) was used to screen hub genes. Here, we selected the top ten genes in the node scores as hub genes.

Single-Gene Survival Analysis, Cox Regression Analysis, and Constructing Prognostic Models

We performed single-gene survival analysis on hub genes, and statistical significance was set at $P<0.05$. We then selected genes with statistical significance for Cox regression analysis using the Wei Sheng Xin online website (https://www.bioinformatics.com.cn) to create a forest map. The key genes selected were utilized to perform risk scoring and

construct a prognostic model using R software. Receiver operating characteristic (ROC) curves were plotted to assess the model's predictive accuracy for 1-year, 3-year, and 5-year survival rates. Additionally, Kaplan-Meier (K-M) curves were generated to compare survival differences between high-risk and low-risk groups.

Statistical analysis

All statistical analyses were performed using R software or specialized online tools: R software was employed for DEGs screening and single-gene survival analysis, whereas functional enrichment analysis and Cox regression analysis were conducted using the online platform Wei Sheng Xin. P< 0.05 was considered statistically significant.

Results

Differentially Expressed Genes

After standardized processing of microarray data results, we used the Limma package to screen 1384 DEGs, including 503 up-regulated genes and 881 down-regulated genes (Figure 1). Subsequently, we intersected the 1,384 differentially expressed genes with 717 ferroptosis-associated genes that we had downloaded, resulting in the identification of 25 ferroptosis-related DEGs. These genes encompassed five up-regulated driver genes, seven up-regulated suppressor genes, two down-regulated driver genes, and 11 down-regulated suppressor genes. Notably, among the down-regulated genes, *PRKAA2* emerged as an overlapping gene between driver and suppressor categories. Based on the FerrDb score and further KEGG pathway analysis, *PRKAA2* was classified as a down-regulated driver gene (Table 1).

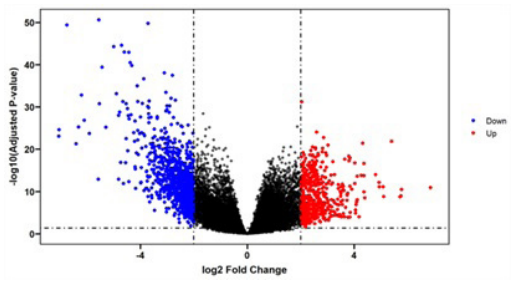

Figure 1. *Differentially expressed genes.*

Ultimately, we curated a list of 24 ferroptosis-related DEGs and visualized their expression profiles using a heatmap (Figure 2).

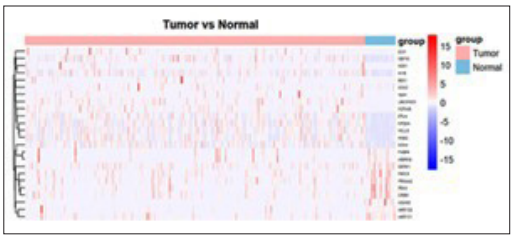

Figure 2. *Ferroptosis-related DEGs.*

Functional Enrichment Analysis of Ferroptosis-Related DEGs

Functional enrichment analysis was performed on the 24 ferroptosis-related DEGs. Through KEGG pathway analysis, we found that ferroptosis-related DEGs were mainly enriched in the chemical carcinogenesis reactive oxygen species pathway (Figure 3), including up-regulated and down-regulated genes. GO analysis results showed that the changes in BP of ferroptosis-related DEGs were significantly enriched in the fatty acid metabolic process, monocarboxylic acid biosynthetic process, cellular ketone metabolic process, fatty acid biosynthetic process, response to fatty acids, carboxylic acid biosynthetic process, organic acid biosynthetic process, response to oxygen levels, and prostanoid metabolic process.

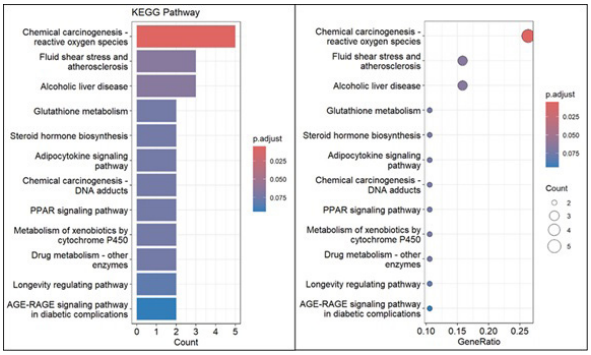

Figure 3. *KEGG pathway analysis of ferroptosis-related DEGs.*

Changes in CC were significantly enriched in the NADPH oxidase complex, oxidoreductase complex, intercellular bridge, messenger ribonucleoprotein complex, telomere cap complex, nuclear telomere cap complex, chromosome, telomeric repeat region, invadopodium, pericentric heterochromatin, and telomerase holoenzyme complex. Changes in MF were significantly enriched in oxidoreductase activity(acting on NAD(P)H), bile acid binding, monocarboxylic acid binding,

Table 1.

Ferroptosis-related DEGs.

	Up driver DEG	Up suppressor DEG	Down driver DEG	Down suppressor DEG
Gene names	*NOX1, NOX4, MYB, IDO1, HOTAIR*	*HELLS, RRM2, GDF15, KIF20A, ETV4, TERT, LINC01833*	*PRKAA2, CPEB1*	*AKR1C1, AKR1C2, FNDC5, BEX1, ASAH2, FABP4, SOX2, PDK4, ADIPOQ, GSTM1*

alditol: NADP+ 1-oxidoreductase activity, superoxide-generating NAD(P)H oxidase activity, carboxylic acid binding, organic acid binding, oxidoreductase activity(acting on NAD(P)H, oxygen as an acceptor), alcohol dehydrogenase (NADP+) activity and oxidoreductase activity(acting on the CH-CH group of donors, NAD or NADP as an acceptor) (Figure 4).

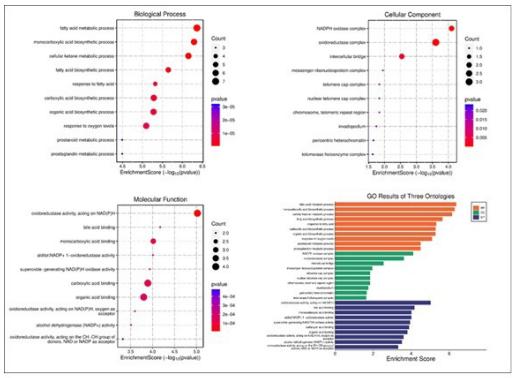

Figure 4. *GO results of three ontologies of ferroptosis-related DEGs.*

PPI Network Analysis and Hub Genes

We have constructed a PPI network comprising 24 ferroptosis-related DEGs using the STRING database. Subsequently, we employed Cytoscape software to identify the top 10 key ferroptosis-related DEGs based on their node scores. These key genes include *ADIPOQ*, *PDK4*, *FABP4*, *NOX4*, *HELLS*, *KIF20A*, *RRM2*, *FNDC5*, *PRKAA2*, and *NOX1* (Figure 5).

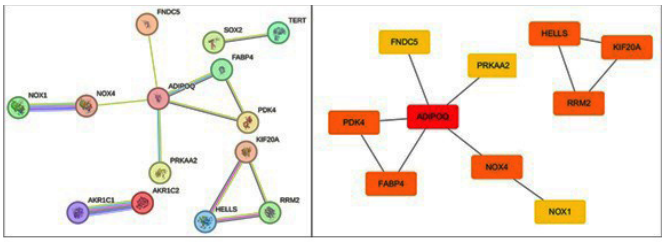

Figure 5. *PPI network and hub genes of ferroptosis-related DEGs.*

Single-Gene Survival Analysis, Cox Regression Analysis, and Prognostic Models

By conducting single-gene survival analysis on the 10 key genes, we have ultimately pinpointed four genes that are statistically significant: *FABP4*, *NOX4*, *PDK4*, and *PRKAA2* (P<0.05) (Figure 6). We further performed Cox regression analysis on these four hub genes and found that their Hazard Ratios were all < 1 (Figure 7). We constructed a prognostic model using these four key genes and plotted ROC curves. The area under the curve (AUC) values for 1-, 3-, and 5-year survival predictions were 0.587, 0.652, and 0.729, respectively. The sensitivity and specificity for 1-year prediction reached 0.53 and 0.63, 0.59 and 0.71 for 3-year, and 0.55 and 0.92 for 5-year predictions. K-M curve analysis demonstrated significantly longer survival time in the low-risk group compared to the high-risk group (P=0.0053) (Figure 8) .

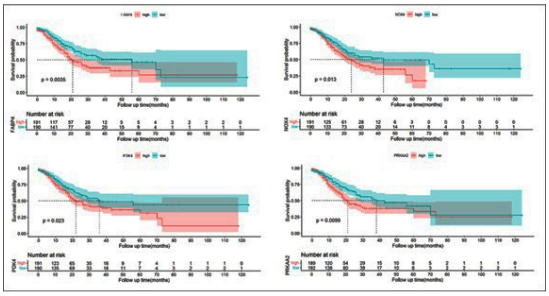

Figure 6. *Single-gene survival analysis of FABP4, NOX4, PDK4 and PRKAA2.*

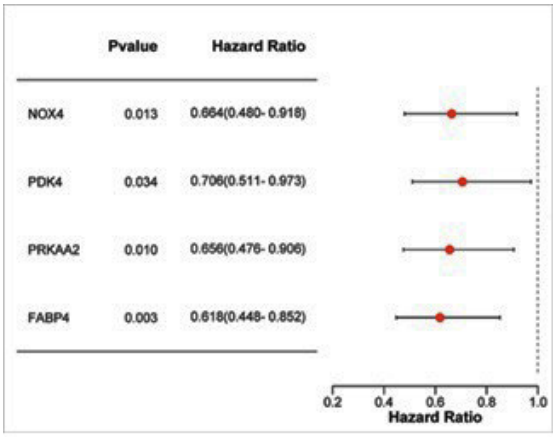

Figure 7. *Cox regression analysis of NOX4, PDK4, PRKAA2, and FABP4 genes.*

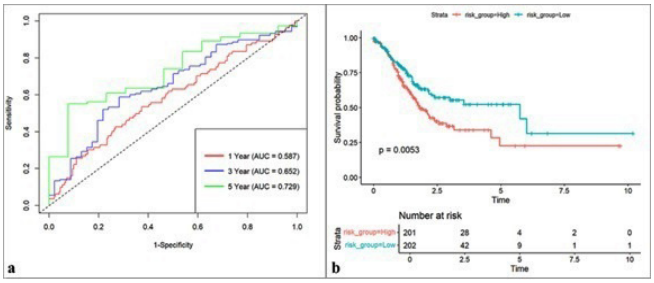

Figure 8. *(a). ROC curves and AUC values for predicting 1-year, 3-year, and 5-year survival rates; (b). Survival analysis of high-risk and low-risk groups.*

Discussion

STAD, a common and aggressive malignancy of the digestive system, holds the fifth position globally in both incidence and mortality rates. The diagnosis, treatment, and prognosis of this disease are fraught with significant challenges. As such, one of the most effective strategies in managing STAD lies in the identification of appropriate and efficacious therapeutic targets. In the past decade, ferroptosis

has been a widely studied mode of cell death. We investigated the ferroptosis-related DEGs in STAD tissues. *NOX4*, as a ferroptosis driver gene,[16,17] is highly expressed in STAD tissues, which is consistent with previous studies.[18] In our study, despite the high expression of the *NOX4* gene in STAD tissues, survival analysis revealed that patients in the high-expression group had significantly shorter survival times than those in the low-expression group, with the difference being statistically significant (P=0.013). NOX4, as a member of the Nicotinamide Adenine Dinucleotide Phosphate (NADPH) Oxidases family, primarily functions to produce ROS. These ROS participate in a multitude of physiological and pathological processes within cells, encompassing signal transduction, angiogenesis, immune responses, and cell death, thereby influencing cellular metabolism, proliferation, and apoptosis.[19] In STAD, elevated NOX4 expression may enhance the sensitivity of tumor cells to ferroptosis and facilitate its onset.[20] However, in our study, high *NOX4* expression did not lead to prolonged patient survival. On the contrary, patients in the high *NOX4* expression group had significantly shorter survival times compared to those in the low expression group. This outcome is attributed to the fact that heightened *NOX4* expression ultimately drives the progression and aggravation of STAD by modulating tumor cell metabolism, proliferation, and migration,[21,22] which is consistent with the findings of Gao et al.[23]

FABP4 and *PDK4*, as ferroptosis suppressor genes, exhibit lower expression levels in STAD tissues. Furthermore, patients in the low-expression groups of *FABP4* and *PDK4* have longer survival times compared to those in the high-expression groups, with statistically significant differences (P-values of 0.0035 and 0.023, respectively). FABP4 is a fatty acid-binding protein primarily expressed in adipocytes and macrophages. It regulates fatty acid metabolism and participates in systemic metabolic regulation through various lipid signaling pathways, being implicated in multiple diseases.[24,25] FABP4, produced by tumor endothelial cells and adipocytes in the tumor microenvironment, can induce an increase in lipid droplets within tumor cells, leading to resistance to oxidative stress and thereby avoiding the onset of ferroptosis, further contributing to tumor progression.[26] Therefore, patients with STAD who have low expression of FABP4 have a longer survival period. The study by Guo et al. demonstrated that increased expression of *FABP4* predicts poor prognosis in STAD,[27] which is consistent with our research findings. *PDK4*, as a ferroptosis suppressor gene, inhibits ferroptosis by blocking pyruvate dehydrogenase-mediated oxidation of pyruvate into the tricarboxylic acid cycle and subsequent fatty acid synthesis.[28] In both in vitro experiments and high-fat diet-induced diabetic mouse models, inhibiting *PDK4* enhances the antitumor activity of system xc-inhibitors, thereby suppressing tumor growth.[28] Therefore, patients with low *PDK4* expression have a longer survival time compared to those with high expression.

However, the other hub gene, *PRKAA2*, that we identified caused confusion during our analysis. In the data downloaded from the FerrDb V2 website, *PRKAA2* serves as both a driver and suppressor gene for ferroptosis. Its FerrDb score for the driver gene was 2, while its FerrDb score for the suppressor gene was 1. We conducted KEGG pathway analysis on *PRKAA2* through the DAVID website and found that its tumor-related pathways mainly included the PI3K-Akt signaling pathway, mTOR signaling pathway, Apelin signaling pathway, FoxO signaling pathway, and AMPK signaling pathway. The first three pathways mainly promote tumor growth through various complex mechanisms.[29-32] The FoxO signaling pathway initiates apoptosis by participating in oxidative stress-related pathways, thereby inhibiting tumor cell growth.[33-35] However, the direct role of *PRKAA2* in these four pathways is not clear, but it acts indirectly through the AMPK signaling pathway. The mechanism of action of the AMPK signaling pathway is complex. It can inhibit the growth of tumor cells by suppressing the mTOR signaling pathway.[36] DAVID pathway analysis showed that it can also synthesize eNOS through phosphorylation, catalyze the production of nitric oxide from L-arginine, and ultimately produce ROS, leading to cell death. On the other hand, AMPK can also act as an oncogene to promote the proliferation of tumor cells. [37-39] The protein encoded by *PRKAA2* is the catalytic subunit α2 of AMPK,[40] which participates in various regulatory mechanisms in the AMPK signaling pathway, including the promotion of ferroptosis.[41] Therefore, in this study, we classified *PRKAA2* as a ferroptosis driver gene. According to our single-gene Cox regression analysis, the risk ratio of the *PRKAA2* gene with low expression in STAD tissue was less than 1. We speculate that the tumor-promoting effect of the AMPK signaling pathway in STAD is greater than its inhibitory effect, and the *PRKAA2* single-gene survival analysis results showed that patients with low expression had a longer survival period, and the difference was statistically significant (P<0.01). Therefore, we believe that high expression of *PRKAA2* promotes tumor growth, whereas patients with low expression of *PRKAA2* in gastric adenocarcinoma tissues have a longer survival time compared to those with high expression.

However, the prognostic model we constructed using these four key genes yielded AUC values of only 0.587 and 0.652 for 1-year and 3-year predictions, respectively, with low sensitivity and specificity. This indicates that our prognostic model has limited ability to identify and exclude events early on. Nevertheless, the 5-year AUC value was 0.729, with sensitivity and specificity of 0.55 and 0.92, respectively. This suggests that our model has a certain predictive power for 5-year survival, although it may have insufficient ability to identify true positives, leading to missed diagnoses, it excels at excluding low-risk patients.

We have identified four ferroptosis-related DEGs associated with the prognosis of STAD, making them potential prognostic markers or therapeutic targets. However, this study lacks support from in vitro and in vivo experimental results, which is a limitation of our research. We will further validate our findings in subsequent experimental studies. Another limitation of this study is the low sensitivity of the prognostic model for 5-year survival, which results in a higher rate of missed diagnoses among high-risk patients. Therefore, a comprehensive judgment needs to be made in conjunction with other biomarkers.

Conclusion

After analyzing RNA-seq and clinical data obtained from the TCGA database, we have pinpointed four ferroptosis-related DEGs—*NOX2*, *PRKAA2*, *FABP4*, and *PDK4*—that are differentially expressed and correlated with the survival prognosis of STAD patients. Notably, patients with low expression levels of these four genes demonstrated significantly prolonged survival times, with statistical significance ($P<0.05$). Consequently, these genes hold promise as biomarkers or novel therapeutic targets for the prognosis and treatment of STAD, paving the way for innovative therapeutic strategies for patients afflicted with this malignancy.

Funding Statement

This study was supported by the Bureau of Science and Technology of Ganzhou Municipality [grant numbers: GZ2021ZSF089] and Health Commission of Jiangxi Province [grant numbers: 202310846].

Competing Interests

The authors declare that they have no competing interests.

References

1. Lauren P. THE TWO HISTOLOGICAL MAIN TYPES OF GASTRIC CARCINOMA: DIFFUSE AND SO-CALLED INTESTINAL-TYPE CARCINOMA. AN ATTEMPT AT A HISTO-CLINICAL CLASSIFICATION. Acta Pathol Microbiol Scand 1965; 64: 31-49.
2. Kushima R. The updated WHO classification of digestive system tumours-gastric adenocarcinoma and dysplasia. Pathologe. 2022 Feb;43(1):8-15. English. doi: 10.1007/s00292-021-01023-7. Epub 2021 Nov 22. PMID: 34807275.
3. Bray F, Laversanne M, Sung H, Ferlay J, Siegel RL, Soerjomataram I, Jemal A. Global cancer statistics 2022: GLOBOCAN estimates of incidence and mortality worldwide for 36 cancers in 185 countries. CA Cancer J Clin. 2024 May-Jun;74(3):229-263. doi: 10.3322/caac.21834.
4. Anderson WF, Rabkin CS, Turner N, Fraumeni JF Jr, Rosenberg PS, Camargo MC. The Changing Face of Noncardia Gastric Cancer Incidence Among US Non-Hispanic Whites. J Natl Cancer Inst. 2018 Jun 1;110(6):608-615. doi: 10.1093/jnci/djx262. PMID: 29361173; PMCID: PMC6005150.
5. Arnold M, Park JY, Camargo MC, Lunet N, Forman D, Soerjomataram I. Is gastric cancer becoming a rare disease? A global assessment of predicted incidence trends to 2035. Gut. 2020 May;69(5):823-829. doi: 10.1136/gutjnl-2019-320234. Epub 2020 Jan 30. PMID: 32001553; PMCID: PMC8520492.
6. Joshi SS, Badgwell BD. Current treatment and recent progress in gastric cancer. CA Cancer J Clin. 2021 May;71(3):264-279. doi: 10.3322/caac.21657.
7. Ajani JA, Lee J, Sano T, Janjigian YY, Fan D, Song S. Gastric adenocarcinoma. Nat Rev Dis Primers. 2017 Jun 1;3:17036. doi: 10.1038/nrdp.2017.36. PMID: 28569272.
8. Dixon SJ, Lemberg KM, Lamprecht MR, Skouta R, Zaitsev EM, Gleason CE, Patel DN, Bauer AJ, Cantley AM, Yang WS, Morrison B 3rd, Stockwell BR. Ferroptosis: an iron-dependent form of nonapoptotic cell death. Cell. 2012 May 25;149(5):1060-72. doi: 10.1016/j.cell.2012.03.042.
9. Stockwell BR. Ferroptosis turns 10: Emerging mechanisms, physiological functions, and therapeutic applications. Cell. 2022 Jul 7;185(14):2401-2421. doi: 10.1016/j.cell.2022.06.003.
10. Ma X, Xiao L, Liu L, Ye L, Su P, Bi E, Wang Q, Yang M, Qian J, Yi Q. CD36-mediated ferroptosis dampens intratumoral CD8+ T cell effector function and impairs their antitumor ability. Cell Metab. 2021 May 4;33(5):1001-1012.e5. doi: 10.1016/j.cmet.2021.02.015.
11. Wang W, Green M, Choi JE, Gijón M, Kennedy PD, Johnson JK, Liao P, Lang X, Kryczek I, Sell A, Xia H, Zhou J, Li G, Li J, Li W, Wei S, Vatan L, Zhang H, Szeliga W, Gu W, Liu R, Lawrence TS, Lamb C, Tanno Y, Cieslik M, Stone E, Georgiou G, Chan TA, Chinnaiyan A, Zou W. CD8+ T cells regulate tumour ferroptosis during cancer immunotherapy. Nature. 2019 May;569(7755):270-274. doi: 10.1038/s41586-019-1170-y.
12. Chen X, Kang R, Kroemer G, Tang D. Targeting ferroptosis in pancreatic cancer: a double-edged sword. Trends Cancer. 2021 Oct;7(10):891-901. doi: 10.1016/j.trecan.2021.04.005.
13. Wang H, Lin D, Yu Q, Li Z, Lenahan C, Dong Y, Wei Q, Shao A. A Promising Future of Ferroptosis in Tumor Therapy. Front Cell Dev Biol. 2021 Jun 9;9:629150. doi: 10.3389/fcell.2021.629150. PMID: 34178977; PMCID: PMC8219969.
14. Cheng X, Dai E, Wu J, Flores NM, Chu Y, Wang R, Dang M, Xu Z, Han G, Liu Y, Chatterjee D, Hu C, Ying J, Du Y, Yang L, Guan X, Mo S, Cao X, Pei G, Jiang J, Lu X, Benitez AM, Waters RE, Pizzi MP, Shanbhag N, Fan Y, Peng F, Hanash SM, Calin G, Futreal A, Song S, Yee C, Mazur PK, Qin JJ, Ajani JA, Wang L. Atlas of Metastatic Gastric Cancer Links Ferroptosis to Disease Progression and Immunotherapy Response. Gastroenterology. 2024 Dec;167(7):1345-1357. doi: 10.1053/j.gastro.2024.07.038.
15. Li Q, Guo G, Chen Y, Lu L, Li H, Zhou Z, Guo J, Gan X, Hu Y, Li Q, Sun M, Liu X. HCP5 Derived Novel Microprotein Triggers Progression of Gastric Cancer through Regulating Ferroptosis. Adv Sci (Weinh). 2024 Dec;11(46):e2407012. doi: 10.1002/advs.202407012.
16. Park MW, Cha HW, Kim J, Kim JH, Yang H, Yoon S, Boonpraman N, Yi SS, Yoo ID, Moon JS. NOX4 promotes ferroptosis of astrocytes by oxidative stress-induced lipid peroxidation via the impairment of mitochondrial metabolism in Alzheimer's diseases. Redox Biol. 2021 May;41:101947. doi: 10.1016/j.redox.2021.101947.
17. Xiao R, Wang S, Guo J, Liu S, Ding A, Wang G, Li W, Zhang Y, Bian X, Zhao S, Qiu W. Ferroptosis-related gene NOX4, CHAC1 and HIF1A are valid biomarkers for stomach adenocarcinoma. J Cell Mol Med. 2022 Feb;26(4):1183-1193. doi: 10.1111/jcmm.17171.
18. Tang CT, Lin XL, Wu S, Liang Q, Yang L, Gao YJ, Ge ZZ. NOX4-driven ROS formation regulates proliferation and apoptosis of gastric cancer cells through the GLI1 pathway. Cell Signal. 2018 Jun;46:52-63. doi: 10.1016/j.cellsig.2018.02.007.
19. Vermot A, Petit-Härtlein I, Smith SME, Fieschi F. NADPH Oxidases (NOX): An Overview from Discovery, Molecular Mechanisms to Physiology and Pathology. Antioxidants (Basel). 2021 Jun 1;10(6):890. doi: 10.3390/antiox10060890.

20. Wang L, Gong W. NOX4 regulates gastric cancer cell invasion and proliferation by increasing ferroptosis sensitivity through regulating ROS. Int Immunopharmacol. 2024 May 10;132:112052. doi: 10.1016/j.intimp.2024.112052.
21. Zhang J, Li H, Wu Q, Chen Y, Deng Y, Yang Z, Zhang L, Liu B. Tumoral NOX4 recruits M2 tumor-associated macrophages via ROS/PI3K signaling-dependent various cytokine production to promote NSCLC growth. Redox Biol. 2019 Apr;22:101116. doi: 10.1016/j.redox.2019.101116. Epub 2019 Feb 6. Erratum in: Redox Biol. 2023 Aug;64:102776. doi: 10.1016/j.redox.2023.102776.
22. Helfinger V, Henke N, Harenkamp S, Walter M, Epah J, Penski C, Mittelbronn M, Schröder K. The NADPH Oxidase Nox4 mediates tumour angiogenesis. Acta Physiol (Oxf). 2016 Apr;216(4):435-46. doi: 10.1111/apha.12625.
23. Gao X, Sun J, Huang C, Hu X, Jiang N, Lu C. RNAi-mediated silencing of NOX4 inhibited the invasion of gastric cancer cells through JAK2/STAT3 signaling. Am J Transl Res. 2017 Oct 15;9(10):4440-4449. PMID: 29118906; PMCID: PMC5666053.
24. Tu WJ, Zeng XW, Deng A, Zhao SJ, Luo DZ, Ma GZ, Wang H, Liu Q. Circulating FABP4 (Fatty Acid-Binding Protein 4) Is a Novel Prognostic Biomarker in Patients With Acute Ischemic Stroke. Stroke. 2017 Jun;48(6):1531-1538. doi: 10.1161/STROKEAHA.117.017128.
25. Yang J, Liu X, Shao Y, Zhou H, Pang L, Zhu W. Diagnostic, Prognostic, and Immunological Roles of FABP4 in Pancancer: A Bioinformatics Analysis. Comput Math Methods Med. 2022 Dec 8;2022:3764914. doi: 10.1155/2022/3764914. PMID: 36532833; PMCID: PMC9754845.
26. Luis G, Godfroid A, Nishiumi S, Cimino J, Blacher S, Maquoi E, Wery C, Collignon A, Longuespée R, Montero-Ruiz L, Dassoul I, Maloujahmoum N, Pottier C, Mazzucchelli G, Depauw E, Bellahcène A, Yoshida M, Noel A, Sounni NE. Tumor resistance to ferroptosis driven by Stearoyl-CoA Desaturase-1 (SCD1) in cancer cells and Fatty Acid Biding Protein-4 (FABP4) in tumor microenvironment promote tumor recurrence. Redox Biol. 2021 Jul;43:102006. doi: 10.1016/j.redox.2021.102006.
27. Guo Y, Wang ZW, Su WH, Chen J, Wang YL. Prognostic Value and Immune Infiltrates of ABCA8 and FABP4 in Stomach Adenocarcinoma. Biomed Res Int. 2020 Jun 27;2020:4145164. doi: 10.1155/2020/4145164. PMID: 32685482; PMCID: PMC7338980.
28. Song X, Liu J, Kuang F, Chen X, Zeh HJ 3rd, Kang R, Kroemer G, Xie Y, Tang D. PDK4 dictates metabolic resistance to ferroptosis by suppressing pyruvate oxidation and fatty acid synthesis. Cell Rep. 2021 Feb 23;34(8):108767. doi: 10.1016/j.celrep.2021.108767. PMID: 33626342.
29. Glaviano A, Foo ASC, Lam HY, Yap KCH, Jacot W, Jones RH, Eng H, Nair MG, Makvandi P, Geoerger B, Kulke MH, Baird RD, Prabhu JS, Carbone D, Pecoraro C, Teh DBL, Sethi G, Cavalieri V, Lin KH, Javidi-Sharifi NR, Toska E, Davids MS, Brown JR, Diana P, Stebbing J, Fruman DA, Kumar AP. PI3K/AKT/mTOR signaling transduction pathway and targeted therapies in cancer. Mol Cancer. 2023 Aug 18;22(1):138. doi: 10.1186/s12943-023-01827-6. PMID: 37596643; PMCID: PMC10436543.
30. Saiki H, Hayashi Y, Yoshii S, Kimura E, Nakagawa K, Kato M, Uema R, Inoue T, Sakatani A, Yoshihara T, Tsujii Y, Shinzaki S, Iijima H, Takehara T. The apelin apelin receptor signaling pathway in fibroblasts is involved in tumor growth via p53 expression of cancer cells. Int J Oncol. 2023 Dec;63(6):139. doi: 10.3892/ijo.2023.5587. Epub 2023 Nov 3. PMID: 37921070; PMCID: PMC10631769.
31. Picault FX, Chaves-Almagro C, Projetti F, Prats H, Masri B, Audigier Y. Tumour co-expression of apelin and its receptor is the basis of an autocrine loop involved in the growth of colon adenocarcinomas. Eur J Cancer. 2014 Feb;50(3):663-74. doi: 10.1016/j.ejca.2013.11.017.
32. Chen T, Liu N, Xu GM, Liu TJ, Liu Y, Zhou Y, Huo SB, Zhang K. Apelin13/APJ promotes proliferation of colon carcinoma by activating Notch3 signaling pathway. Oncotarget. 2017 Oct 13;8(60):101697-101706. doi: 10.18632/oncotarget.21904. PMID: 29254197; PMCID: PMC5731907.
33. Zuo M, Tong R, He X, Liu Y, Liu J, Liu S, Liu Y, Cao J, Ma L. FOXO signaling pathway participates in oxidative stress-induced histone deacetylation. Free Radic Res. 2023 Jan;57(1):47-60. doi: 10.1080/10715762.2023.2190862.
34. Farhan M, Wang H, Gaur U, Little PJ, Xu J, Zheng W. FOXO Signaling Pathways as Therapeutic Targets in Cancer. Int J Biol Sci. 2017 Jul 6;13(7):815-827. doi: 10.7150/ijbs.20052. PMID: 28808415; PMCID: PMC5555100.
35. Dilmac S, Kuscu N, Caner A, Yildirim S, Yoldas B, Farooqi AA, Tanriover G. SIRT1/FOXO Signaling Pathway in Breast Cancer Progression and Metastasis. Int J Mol Sci. 2022 Sep 6;23(18):10227. doi: 10.3390/ijms231810227. PMID: 36142156; PMCID: PMC9499652.
36. Mihaylova MM, Shaw RJ. The AMPK signalling pathway coordinates cell growth, autophagy and metabolism. Nat Cell Biol. 2011 Sep 2;13(9):1016-23. doi: 10.1038/ncb2329. PMID: 21892142; PMCID: PMC3249400.
37. Hsu CC, Peng D, Cai Z, Lin HK. AMPK signaling and its targeting in cancer progression and treatment. Semin Cancer Biol. 2022 Oct;85:52-68. doi: 10.1016/j.semcancer.2021.04.006.
38. Jeon SM, Chandel NS, Hay N. AMPK regulates NADPH homeostasis to promote tumour cell survival during energy stress. Nature. 2012 May 9;485(7400):661-5. doi: 10.1038/nature11066. PMID: 22660331; PMCID: PMC3607316.
39. Han F, Li CF, Cai Z, Zhang X, Jin G, Zhang WN, Xu C, Wang CY, Morrow J, Zhang S, Xu D, Wang G, Lin HK. The critical role of AMPK in driving Akt activation under stress, tumorigenesis and drug resistance. Nat Commun. 2018 Nov 9;9(1):4728. doi: 10.1038/s41467-018-07188-9. PMID: 30413706; PMCID: PMC6226490.
40. Lin L, Flisikowski K, Schwarzenbacher H, Scharfe M, Severitt S, Blöcker H, Fries R. Characterization of the porcine AMPK alpha 2 catalytic subunitgene (PRKAA2): genomic structure, polymorphism detection and association study. Anim Genet. 2010 Apr;41(2):203-7. doi: 10.1111/j.1365-2052.2009.01971.x. Epub 2009 Sep 29. PMID: 19793316.
41. Liu L, Guan X, Zhao Y, Wang X, Yin C, Liu Q, Li H. [Mechanism of miR-186-5p Regulating PRKAA2 to Promote Ferroptosis in Lung Adenocarcinoma Cells]. Zhongguo Fei Ai Za Zhi. 2023 Nov 20;26(11):813-821. Chinese. doi: 10.3779/j.issn.1009-3419.2023.102.39. PMID: 38061883; PMCID: PMC10714044.

***Corresponding author**: Qinmin Liu, E-mail: doctorliu2018@163.com*

International Journal of Biomedicine 15(3) (2025) 490-494
http://dx.doi.org/10.21103/Article15(3)_OA4

ORIGINAL ARTICLE

Oncology

INTERNATIONAL JOURNAL OF BIOMEDICINE

Clinical and Prognostic Value of MicroRNA-198-5p and XIAP in Sinonasal Squamous Cell Carcinoma: A Retrospective Study

Danu Yudistira[1,2*], Sagung Rai Indrasari[1], Camelia Herdini[1], Irianiwati Widodo[1], Didik Setyo Heriyanto[1], Agustian Winarno Putra[2]

[1]Department of Otorhinolaryngology-Head and Neck Surgery, Faculty of Medicine, Public Health and Nursing, Universitas of Gadjah Mada, Yogyakarta, Indonesia
[2]Dr. Sardjito General Hospital, Yogyakarta, Indonesia

Abstract

Background: Sinonasal squamous cell carcinoma is a rare malignancy with a poor prognosis. This study explores the expression of microRNA-198 and X-linked inhibitor of apoptosis protein (XIAP), two molecules implicated in cancer progression, and analyzes their association with clinical features and survival outcomes in patients with sinonasal squamous cell carcinoma.
Materials and Methods: The outcomes of 31 sinonasal squamous cell carcinoma patients at Dr. Sardjito General Hospital, Yogyakarta, between 2017 and 2022 were retrospectively analyzed. Survival analysis was performed using Kaplan-Meier curves, and differences between survival curves were assessed using the log-rank test.
miR-198 and XIAP were both upregulated in sinonasal squamous cell carcinoma, with a positive correlation between their levels. However, their expressions showed no significant association with clinical features or survival outcomes, indicating limited prognostic value in this patient population.
Conclusions: Despite the upregulation of miR-198 and XIAP in sinonasal squamous cell carcinoma, their expression levels did not significantly impact patient survival or correlate with clinical features. These findings suggest that additional molecular factors are involved in the progression of sinonasal squamous cell carcinoma.(**International Journal of Biomedicine. 2025;15(3):490-494.**)

Keywords: microRNA-198 • XIAP • sinonasal squamous cell carcinoma • prognosis factor • expression level

For citation: Yudistira D, Indrasari SR, Herdini C, Widodo I, Heriyanto DS, Putra AW. Clinical and Prognostic Value of MicroRNA-198-5p and XIAP in Sinonasal Squamous Cell Carcinoma: A Retrospective Study. International Journal of Biomedicine. 2025;15(3):490-494. doi:10.21103/Article15(3)_OA4

Abbreviations

HPV, human papillomavirus; **NF-κB,** nuclear factor-kappa B; **SNC,** sinonasal carcinoma; **SNSCC**, sinonasal squamous cell carcinoma; **XIAP**, X-linked inhibitor of apoptosis protein.

Introduction

The prevalence of malignant tumors in the nasal cavity and paranasal sinuses is indeed rare. Sinonasal carcinoma (SNC) represents only three to five percent of all head and neck area malignancies and 1% of all tumors. Squamous cell carcinoma is the most common subtype, followed by intestinal and non-intestinal adenocarcinoma.[1] In the Czech Republic, the incidence of SNC in 2015 was 0.69/100,000, with a mortality rate of 0.44/100,000. SNC tends to occur more frequently in older individuals and is more common in men than women.[2] Despite aggressive treatment, the overall survival rate of SNC patients remains quite poor, with only 50% of patients surviving for five years.[3]

The manifestation of SNC is linked to various risk factors, including smoking, professional exposure to cancer-causing substances, and infection with high-risk human papillomavirus (HPV).[4-6] Studies have shown that HPV-positive patients tend to have a more favorable prognosis compared to those with HPV-negative tumors.[7] Early disease

symptoms typically include rhinorrhea, epistaxis, epiphora, and nasal obstruction. However, in advanced cases, tumors can lead to symptoms such as blurred vision, diplopia, or proptosis.[8]

MicroRNAs are a group of single-stranded, non-protein-coding ribonucleic acids (RNAs) that typically range from 19 to 25 nucleotides in length. They regulate genes by binding to the three'-untranslated regions of their target genes.[9] MicroRNAs are molecules that play a significant role in the development and progression of cancer; they are believed to have tumor suppressor potential. Previous studies have shown that microRNAs are commonly downregulated in cancers such as lung cancer, colorectal cancer, hepatocellular carcinoma, pancreatic cancer, ovarian cancer, gastric cancer, and prostate cancer.[10-16] However, microRNA-198 (miR-198) is upregulated in retinoblastoma and squamous cell carcinoma of the tongue, suggesting that miR-198 may not always behave as a tumor suppressor in all cases. The expression profiles of miR-198 can serve as prognostic biomarkers for predicting patient survival and response to treatment.[17-19] To date, no study has investigated the expression patterns of miR-198 in sinonasal squamous cell carcinoma (SNSCC).

Another protein currently under discussion for its prognostic significance is XIAP, which stands for X-linked inhibitor of apoptosis protein. XIAP belongs to the inhibitor of apoptosis (IAP) family of proteins and plays a critical role in regulating programmed cell death, or apoptosis.[20] The XIAP protein activates nuclear factor-kappaB (NF-kB) and promotes cell survival. The anti-apoptotic nature of IAP proteins has led researchers to speculate that they might enhance cell viability, potentially promoting tumor development and resistance to anti-cancer treatments. We hypothesize that a high level of IAP proteins may be associated with the rapid progression and poor prognosis of sinonasal carcinoma.[21]

Previous studies have identified significant correlations between XIAP and miR-198 and clinical outcomes. These findings suggest that analyzing these factors could yield valuable predictive information about the response to treatment and overall survival for carcinoma patients. This study aims to investigate the prognostic significance of XIAP and miR-198 in patients with sinonasal squamous cell carcinoma.

Materials and Methods

This retrospective study examined medical records and pathological reports of individuals newly diagnosed with SNSCC who were admitted to Dr. Sardjito General Hospital in Yogyakarta, Indonesia, between 2017 and 2022. Patients with incomplete records or a prior history of cancer were excluded from the analysis. The study received approval from our institutional review board (No. KE/FK/0063/EC/2023), and written informed consent was obtained from all patients. All specimens were handled and anonymized, following ethical and legal standards.

The Quick-RNA™ Miniprep Kit was employed to isolate total RNA, including small and miRNAs, from cellular and tissue samples. The resulting RNA lacked deoxyribonucleic acid (DNA) contaminants, making it suitable for downstream applications such as Next-Gen sequencing and real-time quantitative polymerase chain reaction (RT-qPCR). Initially, the kit components, including RNA lysis buffer and deoxyribonuclease I (DNase I), were prepared by adding ethanol to the RNA wash buffer and reconstituting the lyophilized DNase I. Subsequently, samples were prepared by thawing and mixing them in the RNA lysis buffer, followed by appropriate processing of cells or tissues. The final step of total RNA purification involved the utilization of Spin-Away™ Filters and Zymo-Spin™ IIICG Columns, along with several washing steps, including DNase I treatment for the removal of DNA. The cycle threshold (CT) values were recorded, and the relative amount of miR-198 to U6 was calculated using the equation $2-\Delta CT$, where $\Delta CT = (CTmiR\text{-}198 - CTU6)$.

All statistical analyses were conducted using the SPSS 29.0 software package. The significance of differences between groups was assessed using Student's t-test and the chi-square test. Survival curves were generated using the Kaplan-Meier method and compared using the log-rank test. A *P*-value less than 0.05 was considered statistically significant.

Results

The study detected the expression of miR-198 and XIAP in all 31 specimens and found that both were directly proportional. However, miR-198 exhibited slightly higher expression levels than XIAP. These findings suggest that in SNSCC, both miR-198 and XIAP are upregulated (Figure 1).

Fig. 1. *miR-198 and XIAP expression from each sample.*

Correlation between miR-198 and XIAP Expression and Different Clinical Features in SNSCC

We further analyzed the association between miR-198 and XIAP expression levels and the clinical characteristics of SNSCC. SNSCC samples were classified into two groups: a low miR-198 expression group (n = 13) and a high miR-198 expression group (n = 18), and a low XIAP expression group (n = 15) and a high XIAP expression group (n = 16), based on the median miR-198 and XIAP expression levels of all SNSCC samples.

The association between clinical characteristics and the expression level of miR-198 was summarized in Table 1. We did not find any significant correlation between miR-

198 levels and clinical features in SNSCC, such as patient gender (P=0.060), age (P=0.141), tumor depth (P=0.688), and clinical stage (P=0.301). Similarly, no significant correlation was found between XIAP levels and clinical features, such as patient gender (P=0.605), age (P=0.106), tumor depth (P=0.561), and clinical stage (P=0.211).

Table 1.

Correlation between XIAP expression and different clinical features in SNSCC.

	Low XIAP expression	High XIAP expression	*P*-value
Age			
≥ 60	8	4	0.106
< 60	7	12	
Gender			
Male	8	10	0.605
Female	7	6	
Invasion depth			
T2	0	1	0.561
T3	4	3	
T4	11	12	
TNM stage			
II	0	1	0.211
III	0	2	
IV	15	13	

Table 2.

Correlation between miR-198 expression and different clinical features in SNSCC.

	Low miR-198 expression	High miR-198 expression	*P*-value
Age			
≥ 60	7	5	0.141
< 60	6	13	
Gender			
Male	5	13	0.060
Female	8	5	
Invasion depth			
T2	0	1	0.688
T3	3	4	
T4	10	13	
TNM stage			
II	0	1	0.301
III	0	2	
IV	13	15	

The relationship between miR-198 expression and several clinical characteristics in patients with SNSCC is shown in Table 2. There were no statistically significant differences between the expression of miR-198 and age (P=0.141), gender type (P=0.060), tumor invasion (P=0.688), or TNM stage (P=0.301).

Survival Analysis

The follow-up for the group of patients ranged from 4 to 215 weeks. We employed the Kaplan-Meier analysis and the log-rank test to obtain the p-value for the survival analysis. The patients were divided into categories for each miR-198 and XIAP based on their expression levels. The survival analysis results of miR-198 suggested that patients with high expression had a similar chance of survival compared to those with lower expression (P=0.363). Similarly, the survival analysis results of XIAP indicated that the chance of survival was not affected by the expression level (P=0.883).

Kaplan-Meier survival curves of 31 sinonasal squamous cell carcinoma patients based on miR-198 expression status. There is no significant difference in prognosis between patients in the low-expression group and those in the high-expression group (P=0.363, log-rank test) (Figure 2). Kaplan-Meier survival curves of 31 sinonasal squamous cell carcinoma patients based on XIAP expression status. There is no significant difference in prognosis between patients in the low-expression group and those in the high-expression group (P=0.883, log-rank test) (Figure 3).

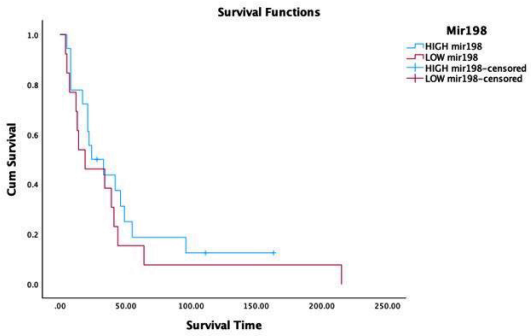

Fig.2. *Kaplan-Meier survival curves of 31 SNSCC patients based on miR-198 expression status. There is no significant difference in prognosis between patients in the low expression group and those in the high expression group (P=0.363, log-rank test).*

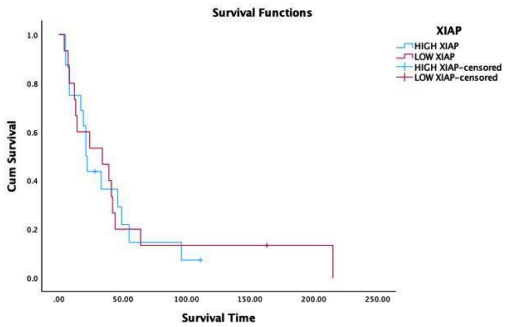

Fig.3*. Kaplan-Meier survival curves of 31 SNSCC patients based on XIAP expression status. There is no significant difference in prognosis between patients in the low expression group and those in the high expression group (P=0.883, log-rank test).*

Discussion

In the current study, we observed an upregulation of both miR-198 and XIAP in human SNSCC tissues and noted a direct correlation between their levels. However, we did not find a significant correlation between the expression levels and aggressive clinical characteristics. Furthermore, our Kaplan-Meier analysis did not reveal any notable differences between patients with low and high expression levels of these markers. To the authors' knowledge, this is the first study to analyze the expression and clinical significance of miR-198 and XIAP in SNSCC.

The observed upregulation of miR-198 and XIAP in SNSCC specimens suggests their potential roles as oncogenic drivers in SNSCC development.[17,18,20,21] Previous studies have implicated miR-198 dysregulation in various cancers, where it exerts its oncogenic effects by targeting tumor suppressor genes or modulating key signaling pathways.[15] Similarly, XIAP overexpression has been associated with resistance to apoptosis and chemotherapy in several malignancies, facilitating tumor survival and progression.[20,21] However, the lack of significant correlation between miR-198/XIAP expression and clinical features in SNSCC suggests that multiple factors are involved in the complex interplay of the carcinoma's pathogenesis.

The findings in this study indicate that the expression levels of miR-198 and XIAP do not significantly impact patient survival in SNSCC. These findings contrast other cancer types, where abnormal expression of these molecules is linked to a worse prognosis.[15,22] The heterogeneous characteristics of SNSCC and the influence of other molecular alterations on patient outcomes may explain this discrepancy. Additionally, the retrospective design and relatively small sample size of the study may limit the applicability of the results. Therefore, larger prospective studies are needed to validate these findings and provide further insight into the molecular mechanisms behind the progression of SNSCC.

This study provided new insights into the expression patterns of miR-198 and XIAP in SNSCC and their potential implications for clinical management. Although both molecules were upregulated in SNSCC, their expression levels did not significantly correlate with clinical features or patient survival. These results underscored the complexity of SNSCC biology, highlighting the need for further research to uncover the underlying molecular mechanisms driving its progression. Targeting miR-198 and XIAP signaling pathways could offer effective therapeutic strategies for treating SNSCC, necessitating further investigation in preclinical and clinical settings.

The limitation of this study is the sample size; therefore, further prospective analysis with a larger number of patients is warranted to validate these conclusions.

Ethical Considerations

This study was approved by the Medical and Health Research Ethics Committee (MHREC) of the Faculty of Medicine, Public Health, and Nursing, Universitas Gadjah Mada, with registration number No.KE/FK/0063/EC/2023.

Acknowledgments

The authors would like to thank all the Dr. Sardjito General Hospital staff involved in the patient's care.

Competing Interests

The authors declare that they have no competing interests.

References

1. Kawaguchi M, Kato H, Tomita H, Mizuta K, Aoki M, Hara A, Matsuo M. Imaging Characteristics of Malignant Sinonasal Tumors. J Clin Med. 2017 Dec 6;6(12):116. doi: 10.3390/jcm6120116. PMID: 29211048; PMCID: PMC5742805.
2. Dutta R, Dubal PM, Svider PF, Liu JK, Baredes S, Eloy JA. Sinonasal malignancies: A population-based analysis of site-specific incidence and survival. Laryngoscope. 2015 Nov;125(11):2491-7. doi: 10.1002/lary.25465. Epub 2015 Jul 30. PMID: 26228792.
3. Cracchiolo JR, Patel K, Migliacci JC, Morris LT, Ganly I, Roman BR, McBride SM, Tabar VS, Cohen MA. Factors associated with a primary surgical approach for sinonasal squamous cell carcinoma. J Surg Oncol. 2018 Mar;117(4):756-764. doi: 10.1002/jso.24923. Epub 2017 Nov 28. PMID: 29193098; PMCID: PMC5878715.
4. Pérez-Escuredo J, Martínez JG, Vivanco B, Marcos CÁ, Suárez C, Llorente JL, Hermsen MA. Wood dust-related mutational profile of TP53 in intestinal-type sinonasal adenocarcinoma. Hum Pathol. 2012 Nov;43(11):1894-901. doi: 10.1016/j.humpath.2012.01.016. Epub 2012 May 8. PMID: 22575263.
5. Comiati V, Scapellato ML, Alexandre E, Volo T, Borsetto D, Carrieri M, Emanuelli E, Cazzador D. Sinonasal cancer in a worker exposed to chromium in an unusual industrial sector. Med Lav. 2017 Dec 14;108(6):477-481. doi: 10.23749/mdl.v108i6.6606. PMID: 29240044.
6. Mensi C, Consonni D, Sieno C, De Matteis S, Riboldi L, Bertazzi PA. Sinonasal cancer and occupational exposure in a population-based registry. Int J Otolaryngol. 2013;2013:672621. doi: 10.1155/2013/672621. Epub 2013 Sep 4. PMID: 24082884; PMCID: PMC3777129.
7. Kılıç S, Kılıç SS, Kim ES, Baredes S, Mahmoud O, Gray ST, Eloy JA. Significance of human papillomavirus positivity in sinonasal squamous cell carcinoma. Int Forum Allergy Rhinol. 2017 Oct;7(10):980-989. doi: 10.1002/alr.21996. Epub 2017 Aug 31. PMID: 28859244.
8. Thompson L. World Health Organization classification of tumours: pathology and genetics of head and neck tumours. Ear Nose Throat J. 2006 Feb;85(2):74. PMID: 16579185.
9. Berindan-Neagoe I, Monroig Pdel C, Pasculli B, Calin GA. MicroRNAome genome: a treasure for cancer diagnosis and therapy. CA Cancer J Clin. 2014 Sep-Oct;64(5):311-36. doi: 10.3322/caac.21244. Epub 2014 Aug 7. PMID: 25104502; PMCID: PMC4461198.
10. Yang J, Zhao H, Xin Y, Fan L. MicroRNA-198 inhibits proliferation and induces apoptosis of lung cancer cells via

targeting FGFR1. J Cell Biochem. 2014 May;115(5):987-95. doi: 10.1002/jcb.24742. Retraction in: J Cell Biochem. 2024 Oct;125(10):e30547. doi: 10.1002/jcb.30547. PMID: 24357456.
11. Wang M, Wang J, Kong X, Chen H, Wang Y, Qin M, Lin Y, Chen H, Xu J, Hong J, Chen YX, Zou W, Fang JY. MiR-198 represses tumor growth and metastasis in colorectal cancer by targeting fucosyl transferase 8. Sci Rep. 2014 Sep 1;4:6145. doi: 10.1038/srep06145. PMID: 25174450; PMCID: PMC5385833.
12. Tan S, Li R, Ding K, Lobie PE, Zhu T. miR-198 inhibits migration and invasion of hepatocellular carcinoma cells by targeting the HGF/c-MET pathway. FEBS Lett. 2011 Jul 21;585(14):2229-34. doi: 10.1016/j.febslet.2011.05.042. Epub 2011 Jun 7. PMID: 21658389.
13. Marin-Muller C, Li D, Bharadwaj U, Li M, Chen C, Hodges SE, Fisher WE, Mo Q, Hung MC, Yao Q. A tumorigenic factor interactome connected through tumor suppressor microRNA-198 in human pancreatic cancer. Clin Cancer Res. 2013 Nov 1;19(21):5901-13. doi: 10.1158/1078-0432.CCR-12-3776. Epub 2013 Aug 29. PMID: 23989979; PMCID: PMC3920728.
14. Shen J, DiCioccio R, Odunsi K, Lele SB, Zhao H. Novel genetic variants in miR-191 gene and familial ovarian cancer. BMC Cancer. 2010 Feb 18;10:47. doi: 10.1186/1471-2407-10-47. PMID: 20167074; PMCID: PMC2831822.
15. Cui Z, Zheng X, Kong D. Decreased miR-198 expression and its prognostic significance in human gastric cancer. World J Surg Oncol. 2016 Feb 6;14:33. doi: 10.1186/s12957-016-0784-x. PMID: 26852230; PMCID: PMC4744396.
16. Ye L, Li S, Ye D, Yang D, Yue F, Guo Y, Chen X, Chen F, Zhang J, Song X. Livin expression may be regulated by miR-198 in human prostate cancer cell lines. Eur J Cancer. 2013 Feb;49(3):734-40. doi: 10.1016/j.ejca.2012.08.029. Epub 2012 Oct 13. PMID: 23069480.
17. Zhao JJ, Yang J, Lin J, Yao N, Zhu Y, Zheng J, Xu J, Cheng JQ, Lin JY, Ma X. Identification of miRNAs associated with tumorigenesis of retinoblastoma by miRNA microarray analysis. Childs Nerv Syst. 2009 Jan;25(1):13-20. doi: 10.1007/s00381-008-0701-x. Epub 2008 Sep 26. PMID: 18818933.
18. Wong TS, Liu XB, Wong BY, Ng RW, Yuen AP, Wei WI. Mature miR-184 as Potential Oncogenic microRNA of Squamous Cell Carcinoma of Tongue. Clin Cancer Res. 2008 May 1;14(9):2588-92. doi: 10.1158/1078-0432.CCR-07-0666. PMID: 18451220.
19. Paczkowska J, Szyfter K, Giefing M, Wierzbicka M. Genetic signature and profiling of head and neck cancer: where do we stand? Curr Opin Otolaryngol Head Neck Surg. 2017 Apr;25(2):154-158. doi: 10.1097/MOO.0000000000000348. PMID: 28141602.
20. Nachmias B, Ashhab Y, Ben-Yehuda D. The inhibitor of apoptosis protein family (IAPs): an emerging therapeutic target in cancer. Semin Cancer Biol. 2004 Aug;14(4):231-43. doi: 10.1016/j.semcancer.2004.04.002. PMID: 15219616.
21. Hofmann HS, Simm A, Hammer A, Silber RE, Bartling B. Expression of inhibitors of apoptosis (IAP) proteins in non-small cell human lung cancer. J Cancer Res Clin Oncol. 2002 Oct;128(10):554-60. doi: 10.1007/s00432-002-0364-z. Epub 2002 Sep 5. PMID: 12384799.
22. Tamm I, Kornblau SM, Segall H, Krajewski S, Welsh K, Kitada S, Scudiero DA, Tudor G, Qui YH, Monks A, Andreeff M, Reed JC. Expression and prognostic significance of IAP-family genes in human cancers and myeloid leukemias. Clin Cancer Res. 2000 May;6(5):1796-803. PMID: 10815900.

***Corresponding author:** *Danu Yudistira. E-mail: dhanoetht@gmail.com*

International Journal of Biomedicine 15(3) (2025) 495-499
http://dx.doi.org/10.21103/Article15(3)_OA5

ORIGINAL ARTICLE

Oncology

INTERNATIONAL JOURNAL OF BIOMEDICINE

Hepatocellular Carcinoma in Kosovo: A Retrospective Cohort Study, 2012–2022

Kreshnike Dedushi[1,2], Jeton Shatri[1,2], Leotrim Berisha[1], Asdren Behrami[1], Mirlinda Berisha[1], Jona Kosova[1], Diar Kabashi[1,3*]

[1]*Faculty of Medicine, University of Prishtina, Prishtina, Kosovo*
[2]*Clinic of Radiology, University Clinical Centre of Kosovo, Prishtina, Kosovo*
[3]*Clinic of Gastroenterology, University Clinical Centre of Kosovo, Prishtina, Kosovo*

Abstract

Background: Hepatocellular carcinoma (HCC) is a leading cause of cancer mortality worldwide, yet comprehensive epidemiologic data from Kosovo are lacking. We aimed to characterize trends, demographic distributions, and risk factors of HCC in Kosovo from 2012 to 2022.

Methods and Results: In this retrospective, population-based cohort study, we analyzed 103 HCC cases diagnosed at the University Clinical Center of Kosovo. Demographic and clinical data were extracted from hospital registries and supplemented with national population figures. Over the study period, 77.7% of cases were male, and the highest incidence (36.9%) occurred in patients aged 60–69 years. Major risk factors included current smoking (57.3%) and regular alcohol consumption (20.4%), while only 6.8% had documented hepatitis B or C (HBV/HCV) infection, suggesting underdiagnosis. A transient decline in case detection in 2020 coincided with COVID-19-related healthcare disruptions.

Conclusion: HCC incidence in Kosovo rose gradually over the past decade, with a pronounced male and older-age predominance. Strengthening viral-hepatitis screening and promoting tobacco- and alcohol-cessation programs are critical to curbing the HCC burden and improving outcomes.(**International Journal of Biomedicine. 2025;15(3):495-499.**)

Keywords: hepatocellular carcinoma • epidemiology • smoking • alcohol consumption

For citation: Dedushi K, Shatri J, Berisha L, Behrami A, Berisha M, Kosova J, Kabashi D. Hepatocellular Carcinoma in Kosovo: A Retrospective Cohort Study, 2012–2022 International Journal of Biomedicine. 2025;15(3):495-499. doi:10.21103/Article15(3)_OA5

Introduction

Hepatocellular carcinoma (HCC) is the primary malignant tumor that most often attacks the liver. In terms of prevalence, it is the seventh most common cancer in the world and the second most common cause of cancer mortality.[1] HCC is an epithelial tumor originating from parenchymal cells. Many cases of HCC are preceded by HBV OR HCV. The highest incidence rates are found in Asia and Africa.[2] Mongolia has the highest incidence rate at 93.7 per 100,000, while China has the highest number of cases, due to the world's largest population (1.4 billion people).[1] Globally, HCC is the dominant type of liver cancer, accounting for about 75% of cases.[2] Incidence rates of HCC have declined in some high-incidence areas,[3] but have increased in most low-incidence regions. Between 1978 and 2012, the incidence of HCC declined in some Asian countries and Italy, but increased in India, the Americas, Oceania, and most European countries.[3] However, in recent years, the increase in some countries, such as the United States, has slowed, as rates in some groups have stabilized or declined.[4,5] The prognosis of HCC is poor in all regions of the world.[6] As a result, the incidence and mortality rates are roughly the same. In 2018, the estimated global incidence rate of liver cancer per 100,000 population was 9.3, while the corresponding mortality rate was 8.5.[1,7]

In addition to the well-established risk factors such as chronic viral hepatitis, alcohol intake, and tobacco use, recent research has emphasized the growing role of metabolic conditions in the development of HCC. Non-

alcoholic fatty liver disease (NAFLD), which ranges from simple hepatic steatosis to non-alcoholic steatohepatitis, is increasingly recognized as a major driver of liver cancer, even in the absence of cirrhosis. Type 2 diabetes and obesity, both strongly linked to NAFLD, are on the rise in many low- and middle-income countries, including Kosovo. Moreover, unhealthy dietary habits and sedentary lifestyles contribute to this metabolic shift, yet they are often overlooked in national health prevention strategies.

The incidence rate of HCC is directly related to age up to about 75 years, but the average age of diagnosis is younger.[2]In the United States, for example, the average age of diagnosis in men is 60–64 years and in women, 65–69 years.[8] In Africa, the average age of diagnosis is lower in countries such as Egypt (58 years) than in other countries (≈46 years).[9,10]

Men have incidence rates 2 to 4 times higher than women.[2] In the United States, the incidence rate in men in 2016 was 10.4 per 100,000 population, compared with 2.9 in women. Gender differences are greater in Europe, but in some countries, such as Uganda and Colombia, rates between men and women are similar.[2,11]

The purpose of this paper is to provide a summary of the latest findings regarding the prevalence and risk factors of HCC and the diagnosis of patients at the University Clinical Center of Kosovo. The paper focuses on analyzing the increase in the number of patients diagnosed with HCC, examining age, gender, and risk factors.

Materials and Methods

This retrospective study included data from the period 2012-2022 of patients diagnosed and treated with HCC in Kosovo, at the University Clinical Center of Kosovo.

A total of 103 patients diagnosed with and treated for HCC were included in this study. The variables analyzed were gender, age, residence, and habits/factors associated with HCC. Statistical data were provided by the Oncology Clinic at the University Clinical Center of Kosovo and the Kosovo Agency of Statistics.

Results

Among 103 HCC patients, 77.67% were male and 22.33% were female (Figure 1). When analyzing the number of cases diagnosed with liver carcinoma over the years, a trend towards an increase in new cases was noted. At the same time, a decrease was reported in 2020; however, it is worth noting that this occurred during the pandemic, when patients were either unable or unwilling to undergo diagnostic procedures (Figure 2).

Regarding the age of diagnosis, the largest number of diagnosed patients belonged to the age group of 60–69 years (36.89%, 38 cases: 29 men and 9 women). The age of the youngest patient diagnosed with HCC was 33 years, while the oldest was 84 (Figure 3).

Of the 103 patients diagnosed with HCC, 98 were diagnosed with primary HCC, while 5 cases, after radiological and histopathological examinations, were found to be metastatic (Figure 4).

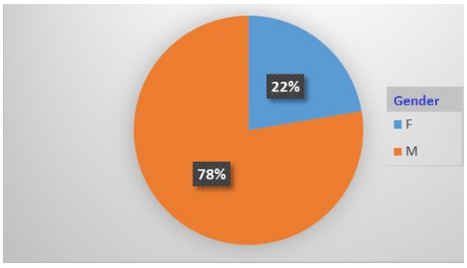

Fig. 1. *Distribution of patients diagnosed with HCC by gender.*

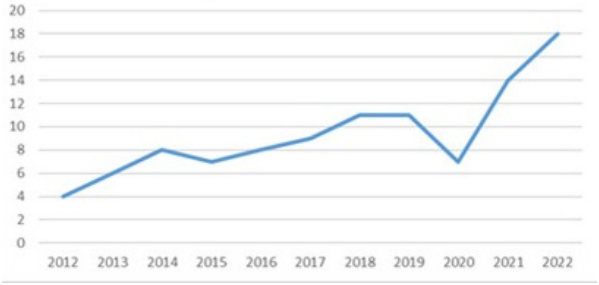

Fig. 2. *Distribution of patients diagnosed with HCC according to the year of diagnosis.*

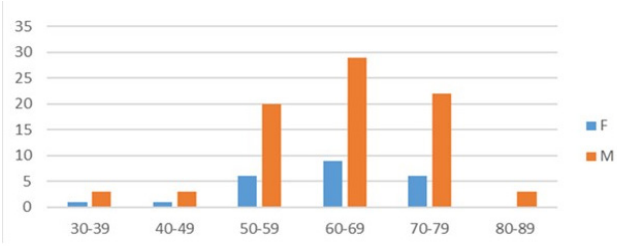

Fig. 3. *Distribution of patients diagnosed with HCC according to age groups and gender.*

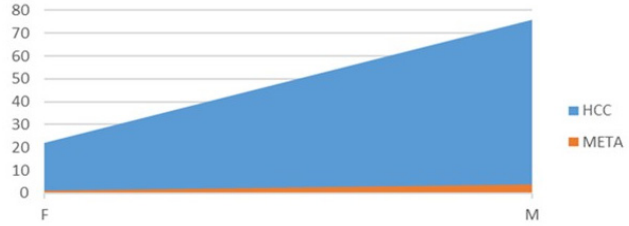

Fig. 4. *Distribution of patients diagnosed with liver cancer according to the origin of the tumor.*

Infection with the hepatitis B or C virus is considered an important factor that influences the appearance of liver cancer; from the analysis of diagnosed patients, 7 were diagnosed with this infection (Figure 5).

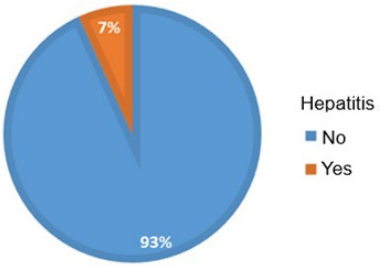

Fig. 5. *Ratio of HCC patients previously diagnosed with Hepatitis B or C virus infection to those who were not infected.*

In addition to HBV and HCV infection, additional factors contributing to the occurrence of HCC are smoking and alcohol consumption (Figures 6 and 7). In our study, 57.28% of diagnosed patients were smokers, 20.39% were alcohol consumers, while 15.53% were consumers of both.

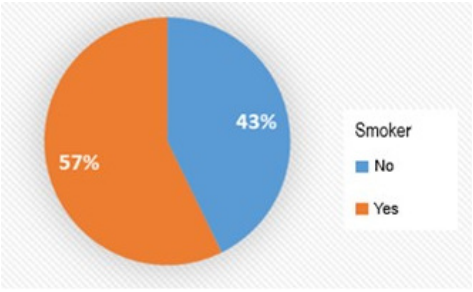

Fig. 6. *Ratio of patients diagnosed with HCC who claim to be smokers to those who are not.*

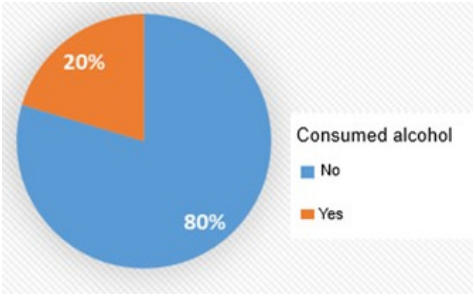

Fig. 7. *Ratio of patients diagnosed with HCC who claim to be alcohol consumers to those who are not.*

Regarding the residence of diagnosed patients, Prishtina had the highest representation among cities at 15.53% (Figure 8). This high frequency correlates with both the high number of residents in the capital and the quality of the air.

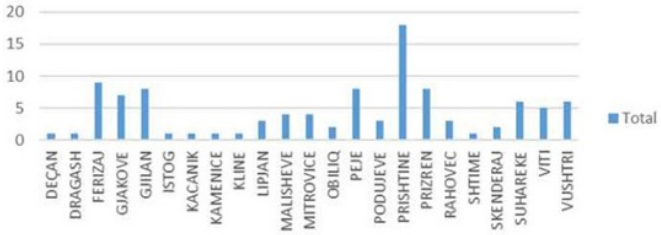

Fig. 8. *Distribution of patients diagnosed with HCC by place of residence.*

It is important to note that certain well-documented risk factors—such as obesity, type 2 diabetes, a family history of liver cancer, and exposure to aflatoxins—were not consistently recorded in the clinical datasets analyzed in this study. This limitation highlights a significant gap in data collection and underscores the need to strengthen medical documentation practices. Establishing standardized protocols for recording risk profiles in patients diagnosed with HCC would improve the reliability of future research and contribute to more accurate public-health assessments.

Discussion

Comparison with Neighboring Countries and European Regions

When compared with the large Albanian series of 648 HCC patients diagnosed between 2000 and 2014, our Kosovo cohort exhibits very similar demographic patterns but distinct etiologic and temporal trends. The Albanian study reported 77.1% male (M/F≈3.41) and a mean age of 60.4 years, whereas our data show 77.7% (M/F≈3.48) male with peak incidence in the 60–69 age group, underscoring near-identical gender and age distributions. However, Albania's age-standardized incidence (ASR) almost doubled during its study period (from 6.6 to 9.3 per 100,000 in successive five-year intervals), while Kosovo experienced a more gradual rise from 2012 to 2022 (exact ASR calculation pending).[12] In terms of risk factors, 50.9% of Albanian cases were linked to HBV infection and 21.8% to combined HBV and alcohol, compared to our cohort's lower documented rates of viral hepatitis but higher prevalences of smoking (57.3%) and regular alcohol use (20.4%). Finally, underlying cirrhosis was present in 89.3% of Albanian patients—a figure we could not systematically capture—highlighting the need in Kosovo for improved cirrhosis assessment as well as enhanced HBV/HCV screening alongside ongoing tobacco- and alcohol-control measures.

Montenegro's age-standardized liver cancer mortality remained essentially stable between 1990 and 2018, with an average annual percent change (AAPC) of +1.4% overall (P=0.004) and +1.9% in women (P=0.002), but no significant change in men; mortality was concentrated in those aged 65–74 (34.9%), 75–84 (26.6%), and 55–64 (25.8%).[13] In contrast, our Kosovo study documents a slow

but steady increase in HCC incidence from 2012 to 2022, with marked male predominance and peak incidence in the 60–69 age group. Whereas Montenegro's sustained prevention and hepatitis-eradication efforts likely underpin its plateauing mortality, Kosovo's rising incidence—coupled with underdiagnosed HBV/HCV and high tobacco/alcohol exposure—highlights the urgent need for similar public-health strategies, including viral-hepatitis elimination and targeted screening in older men.

The pronounced male predominance in Kosovo (M/F≈3.48) closely mirrors the ratios seen in Southern and Western Europe (M/F≈3.3) yet exceeds those reported in Northern and Central-Eastern Europe (M/F:2.1–2.6). Like the broader European trend of rising HCC incidence with age and a peak in the 60-79-year bracket, our study identified the highest incidence specifically in the 60-69-year age group, underscoring its consistency with regional patterns. Southern Europe (6.7/100 000) has the highest ASR among European subregions, followed by Western Europe (5.4/100 000). Although we lack an exact Kosovo ASR, our observed increase approaches the level seen in Central-Eastern Europe (4.3/100 000).[14]

Regarding etiologic drivers, our Kosovo cohort exhibited notably high prevalences of tobacco and alcohol use—57% of patients were smokers and 20% consumed alcohol regularly—while chronic HBV/HCV infections appear underdiagnosed. By contrast, Northern and Central-Eastern Europe generally report lower rates of viral hepatitis but similarly recognize tobacco and alcohol as principal risk drivers, suggesting that bolstering viral-hepatitis screening in Kosovo could further mitigate the HCC burden alongside ongoing tobacco- and alcohol-control efforts.[14]

Conclusions

- HCC has an increased incidence in Kosovo, with a high concentration in the 60–69 age group and a clear male predominance.
- The main risk factors include smoking, alcohol consumption, and chronic hepatitis infections, although the latter remain underreported.
- The COVID-19 pandemic has negatively affected the early diagnosis of this disease, creating a gap in patient follow-up.

To improve the situation and reduce the incidence of liver carcinoma in Kosovo, it is necessary to take concrete actions: Systematic screening for hepatitis B and C, especially in at-risk age groups, raising awareness among the population about the adverse effects of tobacco and alcohol on liver health, improving health infrastructure to ensure early diagnosis and adequate treatment for patients.

Competing Interests

The authors declare that they have no competing interests. No author has received any honoraria, consulting fees, or other financial support from commercial entities for this work.

Acknowledgments

We would like to thank the staff of the University Clinical Center of Kosovo's Pathology and Oncology Departments for their invaluable assistance in data collection and record retrieval. We are also grateful to the Kosovo Agency of Statistics for providing demographic data, and to all of the patients and their families for their cooperation and trust.

Sources of Funding

This research was carried out using the authors' resources. No external funding was received, and no direct financial expenses were incurred in the conduct of this study beyond the time invested by the research team.

References

1. Bray F, Ferlay J, Soerjomataram I, Siegel RL, Torre LA, Jemal A. Global cancer statistics 2018: GLOBOCAN estimates of incidence and mortality worldwide for 36 cancers in 185 countries. CA Cancer J Clin. 2018 Nov;68(6):394-424. doi: 10.3322/caac.21492. Epub 2018 Sep 12. Erratum in: CA Cancer J Clin. 2020 Jul;70(4):313. doi: 10.3322/caac.21609. PMID: 30207593.
2. Petrick JL, Florio AA, Znaor A, Ruggieri D, Laversanne M, Alvarez CS, Ferlay J, Valery PC, Bray F, McGlynn KA. International trends in hepatocellular carcinoma incidence, 1978–2012. Int J Cancer. 2020 Jul 15;147(2):317–330. doi:10.1002/ijc.32723. Epub 2019 Nov 5. PMID:31597196; PMCID:PMC7470451.
3. Valery PC, Laversanne M, Clark PJ, Petrick JL, McGlynn KA, Bray F. Projections of primary liver cancer to 2030 in 30 countries worldwide. Hepatology. 2018 Feb;67(2):600-611. doi: 10.1002/hep.29498. Epub 2017 Dec 23. PMID: 28859220; PMCID: PMC5832532.
4. Petrick JL, Florio AA, Loomba R, McGlynn KA. Have incidence rates of liver cancer peaked in the United States? Cancer. 2020 Jul 1;126(13):3151–3155. doi:10.1002/cncr.32794. Epub 2020 Apr 15. PMID:32294255; PMCID:PMC7323860.
5. Zhang X, El-Serag HB, Thrift AP. Sex and Race Disparities in the Incidence of Hepatocellular Carcinoma in the United States Examined through Age-Period-Cohort Analysis. Cancer Epidemiol Biomarkers Prev. 2020 Jan;29(1):88-94. doi: 10.1158/1055-9965.EPI-19-1052. Epub 2019 Nov 11. PMID: 31712271.
6. Golabi P, Fazel S, Otgonsuren M, Sayiner M, Locklear CT, Younossi ZM. Mortality assessment of patients with hepatocellular carcinoma according to underlying disease and treatment modalities. Medicine (Baltimore). 2017 Mar;96(9):e5904. doi:10.1097/MD.0000000000005904. PMID:28248853; PMCID:PMC5340426.
7. Almahmudi AM, Armstrong D, Elta GH, et al. Novel

developments in gastrointestinal endoscopy: role in diagnosis and management of GI motility and functional disorders. J Can Assoc Gastroenterol. 2023;7(5):331–341. doi:10.1093/jcag/gwad022.
8. Duggan MA, Anderson WF, Altekruse S, Penberthy L, Sherman ME. The Surveillance, Epidemiology, and End Results (SEER) Program and pathology: toward strengthening the critical relationship. Am J Surg Pathol. 2016 Dec;40(12):e94–e102. doi:10.1097/PAS.0000000000000749. PMID:27740970; PMCID:PMC5106320.
9. Yang JD, Mohamed EA, Aziz AO, Shousha HI, et al; Africa Network for Gastrointestinal and Liver Diseases. Characteristics, management, and outcomes of patients with hepatocellular carcinoma in Africa: a multicountry observational study from the Africa Liver Cancer Consortium. Lancet Gastroenterol Hepatol. 2017 Feb;2(2):103–111. doi:10.1016/S2468-1253(16)30161-3. Epub 2016 Dec 3. Erratum in: Lancet Gastroenterol Hepatol. 2022 Aug;7(8):704. doi:10.1016/S2468-1253(22)00208-4. PMID:28403980.
10. Friedman SL, Neuschwander-Tetri BA, Rinella M, Sanyal AJ. Mechanisms of NAFLD development and therapeutic strategies. Nat Med. 2018 Jul;24(7):908-922. doi: 10.1038/s41591-018-0104-9. Epub 2018 Jul 2. PMID: 29967350; PMCID: PMC6553468.
11. Younossi Z, Tacke F, Arrese M, Chander Sharma B, Mostafa I, Bugianesi E, Wai-Sun Wong V, Yilmaz Y, George J, Fan J, Vos MB. Global Perspectives on Nonalcoholic Fatty Liver Disease and Nonalcoholic Steatohepatitis. Hepatology. 2019 Jun;69(6):2672-2682. doi: 10.1002/hep.30251. PMID: 30179269.
12. Resuli B, Sallaku A. Hepatocellular carcinoma in Albania: incidence and risk factors. Int J Sci Res. 2016;5(1):1178–1183. doi:10.21275/NOV152992.
13. Vuković MN, Jakšić M, Stojanović D, Smolović B. Time trends in liver cancer mortality rates in Montenegro from 1990 to 2018. Eur J Gastroenterol Hepatol. 2024 May;36(5):622–627. doi:10.1097/MEG.0000000000002736. Epub 2024 Mar 4. PMID:38477857.
14. Singh SP, Madke T, Chand P. Global Epidemiology of Hepatocellular Carcinoma. J Clin Exp Hepatol. 2025 Mar-Apr;15(2):102446. doi: 10.1016/j.jceh.2024.102446. Epub 2024 Oct 28. PMID: 39659901; PMCID: PMC11626783.

***Corresponding author**: Ass. Dr. Diar Kabashi. Faculty of Medicine, University of Prishtina. Prishtina 10000, Kosovo. E-mail: diar.kabashi@uni-pr.edu*

International Journal of Biomedicine 15(3) (2025) 500-504
http://dx.doi.org/10.21103/Article15(3)_OA6

ORIGINAL ARTICLE

Oncology

INTERNATIONAL JOURNAL OF BIOMEDICINE

Clinical and Morphological Indicators of Early Gastric Cancer Recurrence

Ekaterina P. Anokhina[1], Evgeniy A. Toneev[1,2*], Linar R. Zaripov[1], Alexander A. Martynov[1] Roman F. Shagdaleev [1,2], U. A. Ulyanova [2], A. D. Minacheva[2]

[1]*Ulyanovsk Regional Oncology Center, Ulyanovsk, Russian Federation*
[2]*Ulyanovsk State University, Ulyanovsk, Russian Federation*

Abstract

Background: Despite advancements in diagnostics and the widespread adoption of multimodal therapy for gastric cancer, early recurrence continues to pose a serious clinical challenge. This study aims to identify clinical, morphological, and perioperative factors associated with early recurrence (≤6 months) of gastric cancer after completion of combined treatment and to develop a prognostic model for assessing the risk of recurrence.

Methods and Results: This retrospective study included data from 199 patients who underwent gastrectomy with D2 lymph node dissection in a regional oncology center. A total of 88 patients who completed combined (multimodal) treatment were included in the final statistical analysis. Clinical and tumor-related characteristics, response to treatment, and surgical parameters were evaluated. Patients were divided into two groups based on the presence or absence of recurrence within 6 months. Logistic regression analysis was used to identify independent predictors. Model performance was assessed using ROC analysis.

Among the 88 patients included in the final analysis, disease recurrence was observed in 44 cases (50%). Of these, 21 patients (47.7%) experienced a recurrence within the first six months following completion of combined treatment. The multivariate analysis confirmed that poor tumor differentiation (G3) (OR = 6.084; 95% CI: 1.124–32.917) and the presence of lymphovascular invasion (OR = 9.902; 95% CI: 2.061–47.560) play a significant role in the likelihood of gastric cancer recurrence following the completion of combined treatment. The prognostic model demonstrated good discriminatory ability, with an AUC of 0.852 (95% CI: 0.735–0.969), sensitivity of 85.7%, and specificity of 73.9%.

Conclusion: Lymphovascular invasion and poor tumor differentiation may serve as independent risk factors for recurrence within the first six months following completion of combined treatment for gastric cancer. The developed model may be helpful in stratifying risk and personalizing postoperative surveillance.(**International Journal of Biomedicine. 2025;15(3):500-504.**)

Keywords: gastric cancer • treatment • risk of recurrence • prognostic model

For citation: Anokhina EP, Toneev EA, Zaripov LR, Martynov AA, Shagdaleev RF, Ulyanova UA, Minacheva AD. Clinical and Morphological Indicators of Early Gastric Cancer Recurrence. International Journal of Biomedicine. 2025;15(3):500-504. doi:10.21103/Article15(3)_OA6

Introduction

Gastric cancer remains one of the most common and deadly oncological diseases in the Russian Federation, ranking fifth in incidence and third in cancer-related mortality. [1,2] Radical gastrectomy with D2 lymph node dissection is currently a key component in the multimodal treatment strategy for patients with stage IB–III disease. Despite advancements in diagnostics and the widespread adoption of multimodal therapy, early recurrence continues to pose a serious clinical challenge. According to published data, more than 70% of tumor relapses and cancer-related deaths occur within the first two years following surgery.[3]

Recurrence after treatment is typically classified as locoregional, peritoneal, or distant metastatic. The pattern of recurrence is influenced by both the anatomical location and the stage of the primary tumor. Although various studies have examined potential risk factors, a unified system for predicting recurrence has not yet been established.[4] Given the importance of timely detection and the limited number of

***Corresponding author**: Evgeniy A. Toneev, PhD. E-mail: e.toneev@inbox.ru*

studies specifically focused on early recurrence, identifying reliable clinical and morphological predictors in the first six months after completion of combined treatment remains a pressing task.

This study aims to identify clinical, morphological, and perioperative factors associated with early recurrence (≤6 months) of gastric cancer after completion of combined treatment and to develop a prognostic model for assessing the risk of recurrence.

Materials and Methods

This retrospective study was conducted in the Thoracic and Abdominal Oncology Surgery Departments at the Ulyanovsk Regional Oncological Dispensary. The analysis included data from 199 patients who underwent gastrectomy with D2 lymph node dissection between January 1, 2018, and October 1, 2023.

Inclusion criteria

•Histologically confirmed gastric adenocarcinoma

•Gastrectomy with D2 lymph node dissection, including combined resections when necessary

•Completion of the full perioperative chemotherapy protocol (8 cycles) using the FLOT regimen (docetaxel 50 mg/m², oxaliplatin 85 mg/m², leucovorin 200 mg/m² administered intravenously on day 1, followed by a 24-hour infusion of 5-fluorouracil 2600 mg/m² every 14 days)

•HER2-negative tumor status

Exclusion criteria

•Rare histological subtypes of gastric cancer

•In-hospital postoperative mortality

•Synchronous primary malignant tumors

Based on these criteria, 88 patients were included in the final analysis. During histopathological examination of surgical specimens, the following parameters were assessed: Borrmann macroscopic classification, ypT and ypN status, resection margin involvement, tumor grade, tumor regression according to the Mandard classification, and presence or absence of lymphovascular invasion. Staging was performed according to the 8th edition of the TNM classification (2016).[5]

During the first year after treatment completion, patients were followed up every three months. From the second to the third year, follow-up visits were scheduled every six months, and annually thereafter. At each follow-up, patients underwent laboratory and imaging studies. In cases of suspected recurrence, diagnostic laparoscopy with biopsy of suspicious lesions was performed.

Statistical analysis

All statistical analyses were performed using StatTech v. 4.4.1 (Stattech LLC, Russia). The distribution of continuous variables was assessed using the Shapiro–Wilk test (n<50) or the Kolmogorov–Smirnov test (n≥50). Normally distributed variables were reported as mean ± standard deviation and 95% confidence intervals (CI). Non-normally distributed data were presented as median and interquartile range (Q1–Q3). Categorical variables were described using absolute numbers and percentages. Between-group comparisons of normally distributed continuous variables were performed using Student's t-test. The Mann–Whitney U test was used for nonparametric comparisons. Pearson's chi-square test was applied for analysis of contingency tables; for relative measures, odds ratios (OR) with 95% CI were calculated. Survival analysis was carried out using the Kaplan–Meier method, and differences between groups were evaluated with the log-rank test. Cox proportional hazards regression was used to assess the impact of independent predictors on recurrence risk over time. A P-value of less than 0.05 was considered statistically significant.

Results

Among the 88 patients included in the final analysis, disease recurrence was observed in 44 cases (50%). Of these, 21 patients (47.7%) experienced a recurrence within the first six months following completion of combined treatment.A statistically significant difference between the groups was observed only for obesity (*P*=0.039), suggesting the overall comparability of the cohorts in terms of demographic and comorbid profiles (Table 1).

Table 1.

Clinical characteristics of the study groups depending on the disease recurrence within the first 6 months.

Variable	Category	No Recurrence (n = 67)	Early Recurrence (n = 21)	*P-value*
Sex, n (%)	Female	21 (31.3%)	10 (47.6%)	0,173
	Male	46 (68.7%)	11 (52.4%)	
Age, years (M ± SD)		62.6 ± 7	61.7 ± 8.5	0.617
BMI, M ± SD		25.87 ± 4,15	27.08 ± 5.39	0.283
Charlson comorbidity index, Me [IQR]		4 (4;5)	4 (4;5)	1.000
Obesity, n (%)	No	58 (86.6%)	14 (66.7%)	0.039
	Yes	9 (13.4%)	7 (33.3%)	
Diabetes mellitus, n (%)	No	56 (83.6%)	17 (81.0%)	0.780
	Yes	11 (16.4%)	4 (19%)	
Coronary heart disease, n (%)	No	53 (79.1%)	16 (76.2%)	0.777
	Yes	14 (20.9%)	5 (23.8%)	
Arterial hypertension, n (%)	None	29 (43.3%)	5 (23.8%)	0.424
	Grade I	7 (10.4%)	3 (14.3%)	
	Grade II	19 (28.4%)	7 (33.3%)	
	Grade III	12 (17.9%)	6 (28.6%)	
Chronic heart failure, n (%)	None	44 (65.7%)	16 (76.2%)	0.665
	Class I	14 (20.9%)	3 (14.3%)	
	Class II	9 (13.4%)	2 (9.5%)	
Left ventricular ejection fraction (%), Me [IQR]		63.6 [58;66]	63.7 [62;66]	0.320
Pulmonary artery pressure (mmHg), Me [IQR]		13.8 [12.1;15.5]	13.7 [13.1;14.1]	0.899

Comparative analysis of oncological parameters between the study groups identified the following statistically significant factors: tumor stage, ypT category, lymphovascular invasion, tumor differentiation grade, and tumor regression grade according to the Mandard scale (Table 2).

Table 2.

Oncological characteristics of the study groups.

Variable	Category	No Recurrence (n = 67)	Early Recurrence (n = 21)	*P-value*
Borrmann classification, n (%)	Type 1	2 (3.5%)	2 (7.7%)	<0.001
	Type 2	17 (29.8%)	5 (19.2%)	
	Type 3	34 (59.7%)	12 (46.2%)	
	Type 4	4 (7%)	7 (26.9%)	
Clinical T category (cT), n (%)	2	13 (19.4%)	1 (4.8%)	0.101
	3	48 (71.6%)	15 (71.4%)	
	4a	5 (7.5%)	5 (23.8%)	
	4b	1 (1.5%)	0 (0%)	
Clinical N category (cN), n (%)	0	25 (37.3%)	7 (33.3%)	0.346
	1	31 (46.3%)	10 (47.6%)	
	2	11 (16.4%)	3 (14.3%)	
	3	0 (0%)	1 (4.8%)	
Clinical stage, n (%)	I	25 (37.4%)	2 (9.5%)	0.004
	II	21 (31.3%)	4 (19%)	
	III	21 (31.3%)	15 (71.5%)	
Tumor size (mm), Me [IQR]		54 [41;70]	48 [50;72]	0.763
Retrieved lymph nodes, Me [IQR]		14 [11;19]	12 [10;19]	0.250
ypT category, n (%)	0	6 (9%)	0 (0%)	0.041
	1a	8 (11.8%)	0 (0%)	
	1b	2 (3%)	0 (0%)	
	2	17 (25.4%)	2 (9.5%)	
	3	25 (37.3%)	14 (66.7%)	
	4a	5 (7.5%)	1 (4.8%)	
	4b	4 (6%)	4 (19%)	
ypN category, n (%)	0	36 (53.7%)	7 (33.4%)	0.129
	1	14 (20.9%)	4 (19%)	
	2	12 (17.9%)	4 (19%)	
	3a	4 (6%)	5 (23.8%)	
	3b	1 (1.5%)	1 (4.8%)	
Resection margin status, n (%)	R0	61 (91%)	19 (90.5%)	1.000
	R1	6 (9%)	2 (9.5%)	
Lymphovascular invasion, n (%)	No	52 (77.6%)	8 (38.1%)	<0.001
	Yes	15 (22.4%)	13 (61.9%)	
Tumor differentiation grade, n (%)	G1	26 (38.5%)	0 (0%)	<0.001
	G2	31 (46.6%)	2 (9.5%)	
	G3	10 (14.9%)	19 (90.5%)	
Tumor regression grade (Mandard), n (%)	TRG1	17 (25.4%)	0 (0%)	0.005
	TRG2	12 (17.9%)	0 (0%)	
	TRG3	12 (17.9%)	4 (19%)	
	TRG4	18 (26.9%)	12 (57.2%)	
	TRG5	8 (11.9%)	5 (23.8%)	

Comparative analysis of the main surgical parameters revealed two statistically significant factors: intraoperative blood loss and the need for blood transfusion (Table 3).

Table 3.

The main surgical characteristics of patient groups.

Variable	Category	No Recurrence (n = 67)	Early Recurrence (n = 21)	*P*-value
Operative time, min, Me [IQR]		195 [177.5; 225]	200 [180; 270]	0.453
Intraoperative blood loss, mL, Me [IQR]		300 [200; 400]	300 [200; 800]	0.421
Length of hospital stay, days, Me [IQR]		15 [13; 17]	18 [16; 21]	0.060
Perioperative blood transfusion, n (%)	No	50 (89.6%)	14 (66.7%)	<0.001
	Yes	7 (10.4%)	7 (33.3%)	
Clavien–Dindo complications, n (%)	Grade 0- I	35 (52.3%)	10 (47.6%)	0.437
	Grade II	29 (43.3%)	8 (38.1%)	
	Grade IIIA	1 (1.5%)	2 (9.5%)	
	Grade IIIB	2 (3.0%)	1 (4.8%)	
Combined resections, n (%)	No	11 (19.0%)	3 (11.5%)	0.178
	Yes	47 (81.0%)	23 (88.5%)	

It is noteworthy that no grade 4 complications were observed in the analyzed cohort.

An analysis of overall survival was subsequently performed based on the presence or absence of recurrence within the first six months after curative treatment. Differences in overall survival, assessed using the likelihood ratio test, were statistically significant (*P*=0.006) (Figure 1).

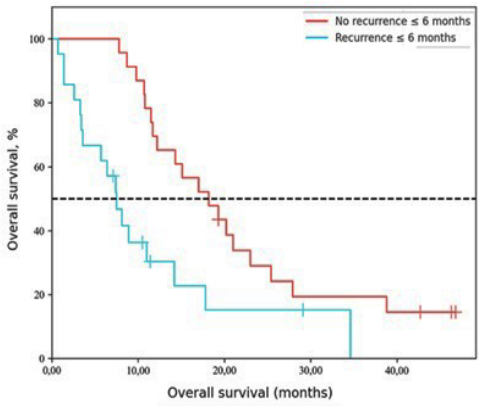

Figure 1. *The overall survival curve depending on the type of relapse.*

Following univariate analysis, a multivariate analysis was performed, and a prognostic model was developed to

estimate the probability of recurrence within the first six months after completion of combined treatment.

The area under the ROC curve (AUC) was 0.852±0.060, with a 95% CI of 0.735 to 0.969, and the model demonstrated statistical significance (P<0.001). The optimal cutoff point of the logistic function (P), corresponding to the highest Youden index, was 0.513. A positive prediction was made when the P-value was equal to or greater than this threshold. The sensitivity and specificity of the model were 85.7% and 73.9%, respectively.

Thus, the multivariate analysis confirmed that poor tumor differentiation (G3) (OR=6.084; 95% CI: 1.124–32.917) and the presence of lymphovascular invasion (OR=9.902; 95% CI: 2.061–47.560) play a significant role in the likelihood of gastric cancer recurrence following the completion of combined treatment (Table 4).

Table 4.

The data of multivariate analysis for the probability of relapse detection within 6 months.

Predictor	Unadjusted		Adjusted	
	OR (95% CI)	*P*-value	OR (95% CI)	*P*-value
Poor differentiation (G3)	15.200 (3.483 – 66.354)	<0.001	9.902 (2.061 – 47.560)	0.004
Lymphovascular invasion	10.833 (2.418 – 48.521)	0.002	6.084 (1.124 – 32.917)	0.036

Discussion

Advances in modern clinical oncology and surgical techniques have significantly improved survival rates for patients undergoing combined treatment for gastric cancer. However, despite these achievements, several studies report that 50%–70% of patients experience disease recurrence after the completion of therapy, which adversely affects long-term outcomes. A substantial proportion of recurrences occur within the first two years following treatment.

In the present study, 23.9% of patients developed recurrence within six months after completing treatment. Identifying predictors of early recurrence is important for timely diagnosis and initiation of therapy at an earlier stage. A large meta-analysis by Pang et al.[6] demonstrated that patients diagnosed with asymptomatic recurrence after gastrectomy had better survival than those with symptomatic recurrence, underscoring the need for further research into early detection and prediction of relapse.

However, the number of studies focused specifically on early recurrence predictors remains limited. According to both domestic and foreign authors, numerous factors have been proposed to influence recurrence following gastrectomy, including tumor size and location, depth of invasion, and lymph node metastasis.[4] In a large cohort study involving 3,534 patients, pT and pN categories were found to impact the risk of local recurrence significantly.[7,8] In our analysis, no statistical association with pN was confirmed, although a trend was observed for ypT: 66.7% of patients with early recurrence had tumors classified as ypT3. Histological characteristics of the tumor and its response to treatment are currently regarded by many researchers as key factors in early relapse.

In our study, a statistically significant association was found between poor tumor response on the Mandard scale and early recurrence. In univariate analysis, 81% of patients who experienced early recurrence had an unsatisfactory pathological response, suggesting that tumor biology plays a substantial role.

The prognostic significance of treatment response has also been highlighted in other studies. For example, Kang et al.[9] reported that for patients with Mandard Grades 4–5 and ypN0 status, the median survival time was 68.5 and 76.7 months, respectively, whereas those with Mandard Grades 1–2 and ypN3a had median survival times of only 15.6 and 14.5 months. The same authors also emphasized the prognostic value of lymphovascular invasion, which aligns with our findings and those of other studies.[3,10] In our multivariate analysis, lymphovascular invasion was confirmed as an independent predictor (OR = 9.902; 95% CI: 2.061–47.560). While our study did not establish a significant association between lymph node involvement and recurrence risk, Saito et al. previously reported such a link.[11] The lack of association in our cohort may reflect high-quality lymphadenectomy and appropriate selection of surgical candidates.

Jiao et al.[4] suggested that diabetes mellitus may contribute to early recurrence, although other comorbidities showed no significant effect. In our study, no statistically significant associations were found between recurrence and comorbidities. The observed difference in obesity rates may be incidental due to the small sample size; its pathophysiological role remains unclear.

A statistically significant relationship was also found between early recurrence and both length of hospital stay and perioperative blood transfusion, likely reflecting more complex surgical cases. The significantly poorer overall survival observed in patients with early recurrence further highlights the clinical relevance of this problem and the need for effective prediction tools.

One limitation of our study is the relatively small sample size. Further large-scale multicenter studies are necessary to identify additional predictive factors and to confirm the significance of those already established.

Conclusion

Lymphovascular invasion and poor tumor differentiation may serve as independent risk factors for recurrence within the first six months following completion of combined treatment for gastric cancer. The developed model may be helpful in stratifying risk and personalizing postoperative surveillance.

Competing Interests

The authors declare that they have no competing interests.

References

1. Shakhzadova AO, Starinsky VV, Lisichnikova IV. [The state of oncological care for the population of Russia in 2022]. Siberian Oncological Journal. 2023;22(5):5–13. [Article in Russian]. doi: 10.21294/1814-4861-2023-22-5-5-13
2. Malignant neoplasms in Russia in 2022 (morbidity and mortality) / Ed. by A.D. Kaprin et al. Moscow: P.A. Herzen Moscow Oncology Research Institute – branch of the National Medical Research Center of Radiology, Ministry of Health of Russia, 2023. Illustrated. 275 p.[In Russian].
3. Kang WM, Meng QB, Yu JC, Ma ZQ, Li ZT. Factors associated with early recurrence after curative surgery for gastric cancer. World J Gastroenterol. 2015 May 21;21(19):5934-40. doi: 10.3748/wjg.v21.i19.5934. PMID: 26019458; PMCID: PMC4438028.
4. Jiao X, Wang Y, Wang F, Wang X. Recurrence pattern and its predictors for advanced gastric cancer after total gastrectomy. Medicine (Baltimore). 2020 Dec 18;99(51):e23795. doi: 10.1097/MD.0000000000023795. PMID: 33371151; PMCID: PMC7748337.
5. Goldstraw P, Chansky K, Crowley J, Rami-Porta R, Asamura H, Eberhardt WE, et al.; International Association for the Study of Lung Cancer Staging and Prognostic Factors Committee, Advisory Boards, and Participating Institutions; International Association for the Study of Lung Cancer Staging and Prognostic Factors Committee Advisory Boards and Participating Institutions. The IASLC Lung Cancer Staging Project: Proposals for Revision of the TNM Stage Groupings in the Forthcoming (Eighth) Edition of the TNM Classification for Lung Cancer. J Thorac Oncol. 2016 Jan;11(1):39-51. doi: 10.1016/j.jtho.2015.09.009. PMID: 26762738.
6. Pang HY, Yan MH, Chen LH, Chen XF, Chen ZX, Zhang SR, Sun H. Detection of asymptomatic recurrence following curative surgery improves survival in patients with gastric cancer: A systematic review and meta-analysis. Front Oncol. 2022 Oct 26;12:1011683. doi: 10.3389/fonc.2022.1011683. PMID: 36387075; PMCID: PMC9643694.
7. Wu CW, Lo SS, Shen KH, Hsieh MC, Chen JH, Chiang JH, Lin HJ, Li AF, Lui WY. Incidence and factors associated with recurrence patterns after intended curative surgery for gastric cancer. World J Surg. 2003 Feb;27(2):153-8. doi: 10.1007/s00268-002-6279-7. PMID: 12616428.
8. Lai JF, Kim S, Kim K, Li C, Oh SJ, Hyung WJ, Rha SY, Chung HC, Choi SH, Wang LB, Noh SH. Prediction of recurrence of early gastric cancer after curative resection. Ann Surg Oncol. 2009 Jul;16(7):1896-902. doi: 10.1245/s10434-009-0473-x. Epub 2009 May 12. PMID: 19434457.
9. Kang WZ, Wang BZ, Li DF, Jiang ZC, Xiong JP, Li Y, Jin P, Shao XX, Hu HT, Tian YT. Can Gastric Cancer Patients with High Mandard Score Benefit from Neoadjuvant Chemotherapy? Can J Gastroenterol Hepatol. 2022 Mar 25;2022:8178184. doi: 10.1155/2022/8178184. PMID: 35369117; PMCID: PMC8975703.
10. Lelisho ME, Seid AA, Pandey D. A Case Study on Modeling the Time to Recurrence of Gastric Cancer Patients. J Gastrointest Cancer. 2022 Mar;53(1):218-228. doi: 10.1007/s12029-021-00684-0. Epub 2021 Aug 11. Erratum in: J Gastrointest Cancer. 2022 Mar;53(1):229. doi: 10.1007/s12029-021-00710-1. PMID: 34379265.
11. Saito H, Osaki T, Murakami D, Sakamoto T, Kanaji S, Ohro S, Tatebe S, Tsujitani S, Ikeguchi M. Recurrence in early gastric cancer--presence of micrometastasis in lymph node of node negative early gastric cancer patient with recurrence. Hepatogastroenterology. 2007 Mar;54(74):620-4. PMID: 17523336.

International Journal of Biomedicine 15(3) (2025) 505-510
http://dx.doi.org/10.21103/Article15(3)_OA7

ORIGINAL ARTICLE

Oncology

INTERNATIONAL JOURNAL OF BIOMEDICINE

A Predictive Model for 90-Day Mortality After Lobectomy in Patients with Non-Small Cell Lung Cancer: A Multicenter Retrospective Study

Andrey E. Slugin[1], Evgeny A. Toneev[2,3*], Sergey Y. Pushkin[4,5], Maxim S. Rudenko[6,7], Egor V. Cherrnetsov[1], Anton S. Ognev[4], Valeria V. Nemtseva[7]

[1]*Tolyatti City Clinical Hospital No. 5, Tolyatti, Russian Federation*
[2]*Ulyanovsk Regional Oncology Center, Ulyanovsk, Russian Federation*
[3]*Ulyanovsk State University, Ulyanovsk, Russian Federation*
[4]*Samara State Medical University, Samara, Russian Federation*
[5]*Seredavin Samara Regional Clinical Hospital, Samara, Russian Federation*
[6]*Sverdlovsk Regional Oncological Dispensary, Ekaterinburg, Russian Federation*
[7]*Ural State Medical University, Ekaterinburg, Russian Federation*

Abstract

Background: Over the past decade, multiple prognostic models have been developed to estimate short-term (including in-hospital) mortality following lobectomy. However, 90-day postoperative mortality is not as widely used as a standard measure for evaluating outcomes after lobectomy. The objective of this study was to evaluate 90-day mortality following lobectomy with mediastinal lymphadenectomy for non-small cell lung cancer (NSCLC), and to identify factors independently associated with this outcome.
Methods and Results: This retrospective multicenter study included data from 700 patients who underwent anatomical lobectomy with systematic mediastinal lymphadenectomy for histologically confirmed NSCLC. A clinically homogeneous cohort was formed to validate the assessment of intra- and postoperative risk factors associated with 90-day mortality.
Among 700 patients included in the study, the 90-day postoperative mortality rate was 3.7%. Multivariate logistic regression identified the following independent predictors of 90-day mortality: prolonged air leak (AOR=2.505; 95% CI: 1.115–5.629, *P*=0.026), intraoperative blood loss (AOR=1.003; 95% CI: 1.001–1.005, *P*=0.004), and forced expiratory volume in one second (AOR=0.965; 95% CI: 0.945–0.985, *P*=0.001). To assess the relationship between the probability of 90-day postoperative mortality and the value of the logistic function P, a ROC analysis was performed. The area under the ROC curve (AUC) was 0.719 (95% CI: 0.606–0.832; *P*<0.001). The sensitivity and specificity of the resulting predictive model were 65.4% and 77.1%, respectively.
Conclusion: The proposed model incorporating three key clinical variables may serve as a practical tool for postoperative risk stratification and guiding follow-up strategies in patients undergoing lobectomy for NSCLC.(**International Journal of Biomedicine. 2025;15(3):505-510.**)

Keywords: lung cancer • lobectomy • 90-day mortality • predictive model • nomogram

For citation: Slugin AE, Toneev EA, Pushkin SY, Rudenko MS, Cherrnetsov EV, Ognev AS, Nemtseva VV. A Predictive Model for 90-Day Mortality After Lobectomy in Patients with Non-Small Cell Lung Cancer: A Multicenter Retrospective Study. International Journal of Biomedicine. 2025;15(3):505-510. doi:10.21103/Article15(3)_OA7

Abbreviations

FEV1, forced expiratory volume in one second; **IOBL**, intraoperative blood loss; **NSCLC**, non-small cell lung cancer; **PAL**, prolonged air leak; **TMM**, thoracic morbidity and mortality

Introduction

Lung cancer remains one of the leading causes of cancer-related mortality worldwide. Anatomical pulmonary resection remains the standard of care for patients with early-stage lung malignancies.[1] Despite significant advancements in thoracic surgical techniques and perioperative management, along with the growing adoption of minimally invasive approaches,

postoperative mortality remains a substantial clinical concern.

Traditionally, surgical outcomes have been assessed using 30-day mortality rates. Over the past decade, multiple prognostic models have been developed to estimate short-term (including in-hospital) mortality following lobectomy. However, 90-day postoperative mortality is not as widely used as a standard measure for evaluating outcomes after lobectomy, despite increasing evidence suggesting its clinical relevance.[2-4]

The objective of this study was to evaluate 90-day mortality following lobectomy with mediastinal lymphadenectomy for non-small cell lung cancer (NSCLC), and to identify factors independently associated with this outcome.

Materials and Methods

This retrospective multicenter study included data from 700 patients who underwent anatomical lobectomy with systematic mediastinal lymphadenectomy for histologically confirmed NSCLC from January 1, 2021 to December 31, 2024. The study was conducted across three thoracic oncology centers in Russia:

- •Ulyanovsk Regional Oncology Dispensary
- •Sverdlovsk Regional Oncology Center (Yekaterinburg)
- •Tolyatti City Clinical Hospital No. 5

Inclusion criteria

- •Patients aged ≥18 years
- •Underwent curative (R0) anatomical lobectomy
- •Histologically verified NSCLC
- •Pathological stage I–IIIB based on the 8th edition of the TNM classification[5]

Exclusion criteria

- •Incomplete clinical data
- •Non-lobectomy resections
- •Palliative surgery or R1/R2 resections

A clinically homogeneous cohort was formed to validate the assessment of intra- and postoperative risk factors associated with 90-day mortality.

The following variables were extracted from medical records and surgical reports:

- •Demographic and clinical characteristics: age, sex, smoking history, chronic obstructive pulmonary disease (COPD), coronary artery disease (CAD), previous myocardial infarction
- •Intraoperative variables: surgical approach (thoracotomy vs. video-assisted thoracoscopic surgery; conversions classified as thoracotomy), duration of surgery, intraoperative blood loss (IOBL) in mL, need for blood transfusion, presence of pleural adhesions
- •Postoperative outcomes: length of drainage, length of stay, postoperative complications, need for reintervention

Special attention was paid to prolonged air leak (PAL), defined as persistent air leakage beyond 5 days postoperatively, in accordance with the European Society of Thoracic Surgeons guidelines.[6] Postoperative complications were graded using the modified thoracic morbidity and mortality (TMM) classification system.[7]

Statistical analysis

All statistical analyses were performed using StatTech v.4.8.3 (Stattech LLC, Russia). The distribution of continuous variables was assessed using the Shapiro–Wilk test ($n < 50$) or the Kolmogorov–Smirnov test ($n \geq 50$). Quantitative variables were presented as median (Me) and interquartile ranges (IQR [Q1;Q3]). Categorical variables were described using absolute numbers and percentage. A non-parametric Mann-Whitney U test was used to compare the differences between the two independent groups. The frequencies of categorical variables were compared using chi-square test or Fisher's exact test (2-tail), when appropriate. A multiple logistic regression analysis was conducted to calculate the unadjusted and adjusted odds ratios (UOR and AOR) with 95% confidence intervals (95%CI). A nomogram was constructed using R statistical software (version 4.4.2), and internal validation was performed via 1,000 bootstrap resamples. Model performance was evaluated using the area under the ROC curve (AUC), calibration plots, and Brier score. A *P*-value of less than 0.05 was considered statistically significant.

Results

Among 700 patients included in the study, the 90-day postoperative mortality rate was 3.7%. The baseline demographic and clinical characteristics of patients who survived and those who died within 90 days after surgery are summarized in Table 1. Analysis of clinical and anamnestic parameters revealed that forced expiratory volume in one second (FEV_1) had a statistically significant impact (P=0.006) on 90-day postoperative mortality.

Table 1.

Clinical and anamnestic characteristics of the study patients.

Variable	Category	90-day postoperative mortality		*P*-value
		Survived (n=674)	Died (n=26)	
Sex	Male	411 (61.0%)	20 (76.9%)	0,149
	Female	263 (39.0%)	6 (23.1%)	
Age, years (Me, [IQR])		66 (60–71)	69.5 [62.25;73.5]	0.118
COPD	Yes	98 (14.5%)	5 (19.2%)	0,569
	No	576 (85.5%)	21 (80.8%)	
Diabetes mellitus	Yes	50 (7.4%)	3 (11.5%)	0,438
	No	624 (92.6%)	23 (88.5%)	
Smoking history	Yes	332 (49.3%)	14 (53.8%)	0,646
	No	342 (50.7%)	12 (46.2%)	
CAD	Yes	150 (22.3%)	7 (26.9%)	0,619
	Prior myocardial infarction	12 (1.8%)	1 (3.8%)	
	No	511 (75.9%)	18 (69.2%)	
LVEF (%), Me [IQR]		62 [58; 66]	61.5 [58.25; 66]	0.924
FEV_1 (%), Me [IQR]		87 [75; 99]	72.5 [54.5; 94.75]	0.006

COPD, chronic obstructive pulmonary disease; CAD, coronary artery disease; LVEF, left ventricular ejection fraction.

Analysis of the morphological characteristics of the studied patients revealed that none of the evaluated parameters had a statistically significant impact on 90-day mortality (Table 2). The need for blood transfusion in the postoperative period had a significant impact on 90-day mortality. The presence of complications, prolonged air leak, extended chest drainage duration, prolonged hospital stay, and higher TMM complication grades were all statistically significant predictors of 90-day mortality following lobectomy (Tables 3 and 4).

Table 2.

Pathomorphological characteristics of the study patients

Variable	Category	90-day postoperative mortality		*P*-value
		Survived (n=674)	Died (n=26)	
Pathological stage, n (%)	IA1	97 (14.4%)	6 (23.1%)	0.191
	IA2	89 (13.2%)	4 (15.4%)	
	IA3	38 (5.6%)	1 (3.8%)	
	IB	179 (26.6%)	9 (34.6%)	
	IIA	69 (10.2%)	2 (7.7%)	
	IIB	94 (13.9%)	1 (3.8%)	
	IIIA	95 (14.1%)	1 (3.8%)	
	IIIB	13 (1.9%)	2 (7.7%)	
Tumor size (mm), Me [IQR]		26 [19; 40]	24.5 [17.5; 31.5]	0.516

Table 3.

Surgical parameters of the study patients.

Variable	Category	90-day postoperative mortality		*P*-value
		Survived (n=674)	Died (n=26)	
Surgical approach	Thoracotomy	556 (82.5%)	24 (92.3%)	0.288
	VATS	118 (17.5%)	2 (7.7%)	
Lobe resected	Upper	378 (56.1%)	20 (76.9%)	0.081
	Middle	45 (6.7%)	0 (0.0%)	
	Lower	251 (37.2%)	6 (23.1%)	
Side of resection	Right	414 (61.4%)	16 (61.5%)	0.991
	Left	260 (38.6%)	10 (38.5%)	
Operative time (min), Me [IQR]		145 [120;180]	162.5 [121.25;180]	0.178
Blood loss (mL), Me [IQR]		100 [62.5;200]	150 [62.5;200]	0.231
Blood transfusion	Yes	8 (1.2%)	2 (7.7%)	0.050
	No	666 (98.8%)	24 (92.3%)	
Pleural adhesions	Yes	70 (10.4%)	4 (15.4%)	0.343
	No	604 (89.6%)	22 (84.6%)	

Table 4.

Postoperative parameters of the study patients.

Variable	Category	90-day postoperative mortality		*P*-value
		Survived (n=674)	Died (n=26)	
Prolonged air leak (PAL)	Yes	172 (25.5%)	13 (50.0%)	0.011
	No	502 (74.5%)	13 (50.0%)	
Time to drain removal (days), Me [IQR]		7 [5; 11]	10.5 [8; 22.5]	< 0.001
Length of stay (days), Me [IQR]		12 [9; 17]	17.5 [14; 27]	< 0.001
Postoperative complications	Yes	86 (12.8%)	11 (42.3%)	< 0.001
	No	588 (87.2%)	15 (57.7%)	
TMM grade	Grade 0-I	465 (69%)	13 (50%)	< 0.001
	Grade II	134 (19.9%)	4 (15.4%)	
	Grade IIIA	68 (10.1%)	2 (7.7%)	
	Grade IIIB	1 (0.1%)	2 (7.7%)	
	Grade IVA	5 (0.7%)	3 (11.5%)	
	Grade IVB	1 (0.1%)	0 (0.0%)	
	Grade V	0 (0.0%)	2 (7.7%)	

Multivariate logistic regression identified the following independent predictors of 90-day mortality: PAL (AOR= 2.505; 95% CI: 1.115–5.629), IOBL (AOR=1.003; 95% CI: 1.001–1.005) and forced expiratory volume in one second FEV_1 (AOR=0.965; 95% CI: 0.945–0.985) (Table 5).

Table 5.

The predictor model for the probability of 90-day mortality.

Predictor	Unadjusted		Adjusted	
	UOR (95% CI)	P-value	AOR (95% CI)	*P*-value
PAL: Present	2.913 (1.324-6.404)	0.008	2.505 (1.115-5.629)	0.026
Blood loss (mL)	1.003 (1.001-1.005)	0.006	1.003 (1.001-1.005)	0.004
FEV_1 (%)	0.964 (0.945-0.983)	< 0.001	0.965 (0.945-0.985)	0.001

PAL – prolonged air leak; FEV_1 – forced expiratory volume in one second

To assess the relationship between the probability of 90-day postoperative mortality and the value of the logistic function *P*, a ROC analysis was performed. The area under the ROC curve (AUC) was 0.719 (95% CI: 0.606–0.832; $P<0.001$) (Figure 1) The sensitivity and specificity of the resulting predictive model were 65.4% and 77.1%, respectively.

Multicollinearity analysis confirmed that the predictors included in the model were independent of each other. To validate the nomogram (Figure 2), a bootstrap method with 1,000 resamples was applied to improve the accuracy of the

estimates. A calibration curve was constructed to assess the agreement between predicted probabilities and actual outcomes (Figure 3). The dashed diagonal line represents perfect agreement between predicted and observed probabilities. The solid line reflects the actual calibration of the model based on LOESS smoothing, while the dotted bands indicate the 95% confidence interval. Vertical tick marks along the axis denote the distribution of predicted probabilities across the sample. Internal validation yielded a mean absolute error of 0.008, indicating acceptable performance of the developed predictive model.

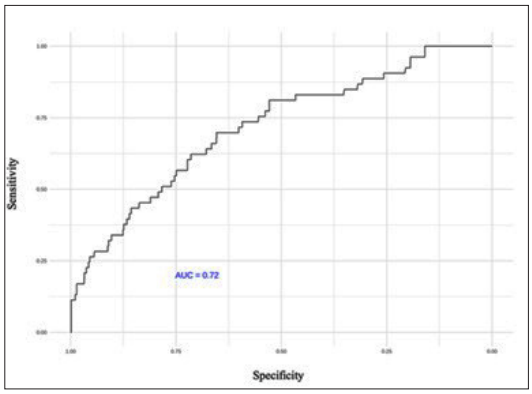

Figure 1. *ROC curve representing the relationship between the predicted probability of 90-day postoperative mortality and the actual outcomes.*

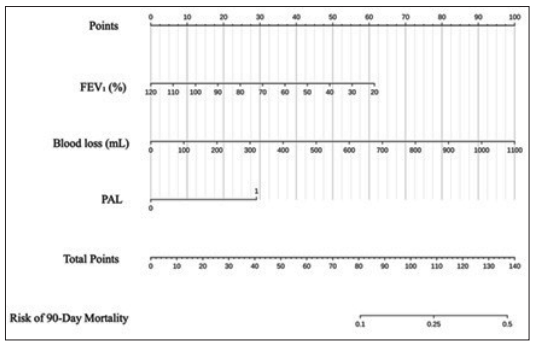

Figure 2. *Nomogram for predicting 90-day mortality in patients after lobectomy.*

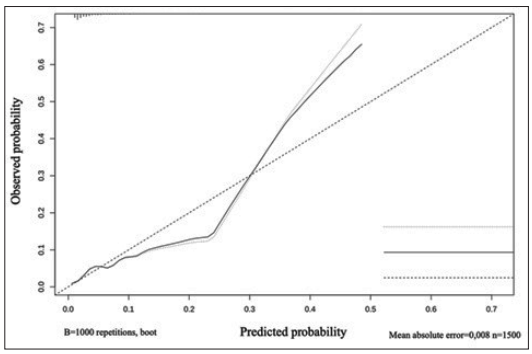

Figure 3. *Calibration curve plot for internal validation of the 90-day mortality prediction model.*

Discussion

Pezzi et al.[8] demonstrated that 90-day mortality following lung cancer resection nearly doubles that of the 30-day metric (5.4% vs. 2.8%), being influenced by a variety of factors, including age, surgical type, and comorbidities. In this multicenter retrospective study, we investigated predictors of 90-day mortality in patients undergoing lobectomy for NSCLC. Despite advances in surgical techniques and perioperative care, early postoperative mortality beyond the conventional 30-day window remains a relevant clinical concern.

Among the key variables associated with 90-day mortality, a reduced FEV_1 demonstrated a statistically significant impact (P=0.006). In our cohort, patients who died within 90 days had notably lower median FEV_1 values than survivors. Similar findings were reported by Soldath et al.,[9] where impaired FEV_1 was linked to decreased long-term survival and a higher risk of postoperative complications.

PAL was also a significant predictor, occurring in 50% of deceased patients compared to 25.5% among survivors (P=0.011). This finding aligns with results from Gooseman et al.,[10] who identified PAL as one of the most common and clinically relevant complications following anatomical lung resections, with a strong influence on length of stay and risk of mortality.

Postoperative complications, including infectious, thromboembolic, and cardiovascular events, showed a clear association with 90-day mortality (P<0.001). Patients who died experienced TMM grade III–V complications more often, reflecting a more severe postoperative course. These findings are consistent with results from Ma et al.,[11] who demonstrated that TMM grade is an independent risk factor for early mortality and can be incorporated into preoperative risk stratification models.

Additional predictors included the need for blood transfusion, prolonged chest drainage, and increased hospital stay. Blood transfusions may reflect both IOBL and severe postoperative complications. Similar associations were described by Yao and Wang,[12] where transfusions were linked to higher rates of respiratory complications and delayed recovery. Prolonged drainage and extended hospitalization may also result from PAL-related complications.

Interestingly, traditional baseline factors such as age, sex, COPD, CAD, smoking status, and surgical approach were not significantly associated with 90-day mortality in our dataset. This may be attributed to the clinical homogeneity of the cohort and effective preoperative risk selection, which could have mitigated the impact of individual baseline variables. However, in more heterogeneous populations, these parameters may remain relevant, as demonstrated by Halldorsson et al.[13] in elderly cancer patients. A recent systematic review identified 22 models designed to predict short-term mortality after thoracic surgery, of which only two focused on 90-day outcomes.[14-16] The most recent model was developed in the UK population, highlighting the need for locally validated tools tailored to specific patient cohorts.[17] In addition to univariate analysis, we constructed a multivariable logistic regression model incorporating

variables that had statistically significant associations with 90-day mortality. Prolonged air leak, IOBL, and FEV_1 emerged as independent predictors of postoperative death. Of particular interest is the finding that blood loss remained significant in the multivariable model (OR=1.003; 95% CI: 1.001–1.005; *P*=0.004), underscoring the clinical importance of even moderate increases in intraoperative bleeding. Yao and Wang[12] reached similar conclusions, demonstrating that IOBL correlates with respiratory complications and adverse outcomes. Based on this model, we developed a nomogram to facilitate individualized, 90-day mortality risk prediction. This graphical tool allows clinicians to integrate multiple factors and estimate a patient's postoperative risk in a simple, interpretable format. Such tools are particularly valuable in multidisciplinary cancer centers and can aid in shared decision-making and tailored perioperative strategies.

However, this study has several limitations. First, the retrospective design inherently introduces limitations in data completeness and accuracy. Second, although the multicenter nature and sample size are strengths, the cohort consisted exclusively of patients undergoing lobectomy, limiting generalizability. Third, while the nomogram showed good calibration and internal performance, it requires external validation in independent populations. Previous studies have shown that even well-calibrated models may vary in predictive accuracy across institutions and regions.[18-20] Despite these limitations, our findings highlight the importance of a multifactorial approach in assessing postoperative risk. The proposed model and nomogram provide clinicians with a practical tool for predicting 90-day mortality and optimizing postoperative care.

Although PAL did not show a significant association with 30-day mortality, it emerged as an independent predictor in our 90-day mortality model (AOR=2.505; *P*=0.026). Shen et al.[21] reported similar associations between PAL and increased risk of reintervention, pulmonary infections, and delayed recovery. The adverse effects of PAL may be mediated by several mechanisms. Persistent air leak can prolong the inflammatory response and promote pleural space colonization, increasing the risk of nosocomial pneumonia and empyema.[22] Moreover, PAL is often observed in patients with emphysema and impaired lung function, limiting physiological reserves and hampering recovery. Finally, prolonged postoperative courses due to PAL may delay or preclude adjuvant therapy, particularly in stage II disease, where timely systemic treatment is critical.[23]

The proposed model incorporating three key clinical variables may serve as a practical tool for postoperative risk stratification and guiding follow-up strategies in patients undergoing lobectomy for NSCLC.

Ethical Considerations

The study protocol was approved by the local ethics committees of all participating institutions. All data were anonymized in compliance with data protection and confidentiality standards.

Competing Interests

The authors declare that they have no competing interests.

References

1. Montagne F, Guisier F, Venissac N, Baste JM. The Role of Surgery in Lung Cancer Treatment: Present Indications and Future Perspectives-State of the Art. Cancers (Basel). 2021 Jul 23;13(15):3711. doi: 10.3390/cancers13153711. PMID: 34359612; PMCID: PMC8345199.
2. McMillan RR, Berger A, Sima CS, Lou F, Dycoco J, Rusch V, Rizk NP, Jones DR, Huang J. Thirty-day mortality underestimates the risk of early death after major resections for thoracic malignancies. Ann Thorac Surg. 2014 Nov;98(5):1769-74; discussion 1774-5. doi: 10.1016/j.athoracsur.2014.06.024. Epub 2014 Sep 8. PMID: 25200731; PMCID: PMC4410352.
3. Damhuis RA, Wijnhoven BP, Plaisier PW, Kirkels WJ, Kranse R, van Lanschot JJ. Comparison of 30-day, 90-day and in-hospital postoperative mortality for eight different cancer types. Br J Surg. 2012 Aug;99(8):1149-54. doi: 10.1002/bjs.8813. Epub 2012 Jun 20. PMID: 22718521.
4. Toneev EA, Komarov AS, Midlenko OV, et al. [Predictive models for assessing the risk of postoperative cardiac and respiratory complications in patients with lung cancer]. Ulyanovsk Medical and Biological Journal. 2024;(1):41–63. doi:10.34014/2227-1848-2024-1-41-63. [Article in Russian].
5. Goldstraw P, Crowley J, Chansky K, Giroux DJ, Groome PA, Rami-Porta R, Postmus PE, Rusch V, Sobin L; International Association for the Study of Lung Cancer International Staging Committee; Participating Institutions. The IASLC Lung Cancer Staging Project: proposals for the revision of the TNM stage groupings in the forthcoming (seventh) edition of the TNM Classification of malignant tumours. J Thorac Oncol. 2007 Aug;2(8):706-14. doi: 10.1097/JTO.0b013e31812f3c1a. Erratum in: J Thorac Oncol. 2007 Oct;2(10):985. PMID: 17762336.
6. Pompili C, Falcoz PE, Salati M, Szanto Z, Brunelli A. A risk score to predict the incidence of prolonged air leak after video-assisted thoracoscopic lobectomy: An analysis from the European Society of Thoracic Surgeons database. J Thorac Cardiovasc Surg. 2017 Apr;153(4):957-965. doi: 10.1016/j.jtcvs.2016.11.064. Epub 2016 Dec 22. PMID: 28089646.
7. Seely AJ, Ivanovic J, Threader J, Al-Hussaini A, Al-Shehab D, Ramsay T, Gilbert S, Maziak DE, Shamji FM, Sundaresan RS. Systematic classification of morbidity and mortality after thoracic surgery. Ann Thorac Surg. 2010 Sep;90(3):936-42; discussion 942. doi: 10.1016/j.athoracsur.2010.05.014. PMID: 20732521.
8. Pezzi CM, Mallin K, Mendez AS, Greer Gay E, Putnam JB Jr. Ninety-day mortality after resection for lung cancer is nearly double 30-day mortality. J Thorac Cardiovasc Surg. 2014 Nov;148(5):2269-77. doi: 10.1016/j.jtcvs.2014.07.077. Epub 2014 Aug 4. PMID: 25172318.
9. Soldath P, Ryom P, Petersen RH. Long-term survival after sleeve lobectomy versus pneumonectomy for non-small cell lung cancer. Surg Oncol. 2025 Feb;58:102168. doi: 10.1016/j.suronc.2024.102168. Epub 2024 Nov 28. PMID: 39622154.
10. Gooseman MR, Brunelli A, Chaudhuri N, Milton R,

Tcherveniakov P, Papagiannopoulos K, Valuckiene L. Prolonged air leak after segmentectomy: incidence and risk factors. J Thorac Dis. 2023 Feb 28;15(2):858-865. doi: 10.21037/jtd-22-623. Epub 2022 Oct 17. PMID: 36910087; PMCID: PMC9992634.
11. Ma S, Li F, Li J, Wang L, Song H. Risk factor analysis and nomogram prediction model construction of postoperative complications of thoracoscopic non-small cell lung cancer. J Thorac Dis. 2024 Jun 30;16(6):3655-3667. doi: 10.21037/jtd-24-113. Epub 2024 Jun 12. PMID: 38983183; PMCID: PMC11228728.
12. Yao L, Wang W. Effect of intraoperative blood loss on postoperative pulmonary complications in patients undergoing video-assisted thoracoscopic surgery. Turk Gogus Kalp Damar Cerrahisi Derg. 2021 Jul 26;29(3):347-353. doi: 10.5606/tgkdc.dergisi.2021.20657. PMID: 34589253; PMCID: PMC8462118.
13. Halldorsson H, Orrason AW, Oskarsdottir GN, Petursdottir A, Fridriksson BM, Magnusson MK, Jonsson S, Gudbjartsson T. Improved long-term survival following pulmonary resections for non-small cell lung cancer: results of a nationwide study from Iceland. Ann Transl Med. 2019 Mar;7(5):88. doi: 10.21037/atm.2019.01.10. PMID: 31019938; PMCID: PMC6462663.
14. Taylor M, Hashmi SF, Martin GP, Shackcloth M, Shah R, Booton R, Grant SW. A systematic review of risk prediction models for perioperative mortality after thoracic surgery. Interact Cardiovasc Thorac Surg. 2021 Apr 8;32(3):333-342. doi: 10.1093/icvts/ivaa273. PMID: 33257987; PMCID: PMC8906726.
15. Powell HA, Tata LJ, Baldwin DR, Stanley RA, Khakwani A, Hubbard RB. Early mortality after surgical resection for lung cancer: an analysis of the English National Lung cancer audit. Thorax. 2013 Sep;68(9):826-34. doi: 10.1136/thoraxjnl-2012-203123. Epub 2013 May 17. PMID: 23687050.
16. Brunelli A, Dinesh P, Woodcock-Shaw J, Littlechild D, Pompili C. Ninety-Day Mortality After Video-Assisted Thoracoscopic Lobectomy: Incidence and Risk Factors. Ann Thorac Surg. 2017 Sep;104(3):1020-1026. doi: 10.1016/j.athoracsur.2017.02.083. Epub 2017 Jun 1. PMID: 28577845.
17. Taylor M, Martin GP, Abah U, Sperrin M, Smith M, Bhullar D, Shackcloth M, Woolley S, West D, Shah R, Grant SW; North West Thoracic Surgery Collaborative (NWTSC). Development and internal validation of a clinical prediction model for 90-day mortality after lung resection: the RESECT-90 score. Interact Cardiovasc Thorac Surg. 2021 Nov 22;33(6):921-927. doi: 10.1093/icvts/ivab200. PMID: 34324664; PMCID: PMC8632783.
18. Zhou Q, Huang J, Pan F, Li J, Liu Y, Hou Y, Song W, Luo Q. Operative outcomes and long-term survival of robotic-assisted segmentectomy for stage IA lung cancer compared with video-assisted thoracoscopic segmentectomy. Transl Lung Cancer Res. 2020 Apr;9(2):306-315. doi: 10.21037/tlcr-20-533. PMID: 32420070; PMCID: PMC7225141.
19. Gao SJ, Jin L, Meadows HW, Shafman TD, Gross CP, Yu JB, Aerts HJWL, Miccio JA, Stahl JM, Mak RH, Decker RH, Kann BH. Prediction of Distant Metastases After Stereotactic Body Radiation Therapy for Early Stage NSCLC: Development and External Validation of a Multi-Institutional Model. J Thorac Oncol. 2023 Mar;18(3):339-349. doi: 10.1016/j.jtho.2022.11.007. Epub 2022 Nov 15. PMID: 36396062.
20. Smith H, Li H, Brandts-Longtin O, Yeung C, Maziak D, Gilbert S, Villeneuve PJ, Sundaresan S, Passman R, Shamji F, Seely AJE. External validity of a model to predict postoperative atrial fibrillation after thoracic surgery. Eur J Cardiothorac Surg. 2020 May 1;57(5):874-880. doi: 10.1093/ejcts/ezz341. PMID: 31845993.
21. Shen KR, Edwards J, Jaklitsch MT, Steliga MA, Daniel TM. Effectiveness of surgical sealants in reducing pulmonary air leaks: A meta-analysis. Journal of Thoracic Disease. 2021;13(1):120–130. doi: 10.21037/jtd-20-2366
22. Toneev EA, Bazarov DV, Pikin OV, Charyshkin AL, Martynov AA, Lisyutin RI, Zul'karnyaev ASh, Anokhina EP. [Prolonged air leak after lobectomy in lung cancer patients]. Siberian Journal of Oncology. 2020;19(1):103-110. doi: 10.21294/1814-4861-2020-19-1-103-110. [Article in Russian].
23. Shiono S, Abiko M, Okazaki T, Kaseda K, Maeda H. Risk factors for prolonged air leak after lung cancer surgery and its impact on long-term outcomes. Journal of Thoracic Disease. 2021;13(6):3562–3570. doi:10.21037/jtd-20-3352

***Corresponding author**: Evgeniy A. Toneev, PhD. E-mail: e.toneev@inbox.ru*

International Journal of Biomedicine 15(3) (2025) 511-516
http://dx.doi.org/10.21103/Article15(3)_OA8

ORIGINAL ARTICLE

Surgery

INTERNATIONAL JOURNAL OF BIOMEDICINE

Frequency and Predictors of Postoperative Fluid Collections (POFC) in Patients Following Ventral Hernia Repair with Mesh Implants

Ilnur T. Ahmadullov[1], Evgeny A. Toneev[2*], Antonina V. Smolkina[2], Roman F. Shagdaleev[2], Anastasiia D. Teryagova[2], Natalia O. Ilchuk[2], Viktoriia A. Pugacheva[2]

[1]Ulyanovsk Regional Clinical Center for Specialized Medical Care, Ulyanovsk, Russian Federation
[2]Ulyanovsk State University, Ulyanovsk, Russian Federation

Abstract

Background: This study aimed to identify risk indicators for fluid accumulation after ventral hernia repair and to develop a prognostic model for postoperative fluid collections in the implantation area.

Methods and Results: A retrospective analysis was conducted on the medical records of 214 patients who underwent ventral hernia repair (VHR). Postoperative complications following surgical intervention were analyzed. In this study, cases of postoperative fluid collections (POFC) in the area of mesh implantation following VHR with synthetic mesh materials were analyzed. POFC was operationally defined as sterile, non-infected fluid accumulations detected in the postoperative period by ultrasound examination, characterized by the absence of clinical signs of inflammation, redness, fever, or infection.

The incidence of persistent POFC in the study cohort was 23(10.7%) out of 214 patients. A univariate analysis of the association between the presence of POFC and preoperative laboratory parameters showed statistically significant differences between the study groups for neutrophil-to-lymphocyte ratio (NLR), platelet-to-lymphocyte ratio (PLR), prognostic nutritional index (PNI), and albumin level. The analysis of the association between postoperative Day 1 laboratory parameters and the development of POFC showed that among the analyzed laboratory parameters, a statistically significant difference between patients with and without POFC was identified for total protein level. On postoperative Day 5, statistically significant differences between patients with and without POFC were observed for hemoglobin and total protein levels, suggesting a potential role of protein metabolism and blood oxygen transport function in the pathogenesis of persistent fluid collection formation.

A multivariate statistical analysis using binary logistic regression identified significant predictors of POFC development in the postoperative period: hernia defect diameter (AOR=1.143; 95% CI: 1.042–1.254; P=0.005), NLR (AOR=1.596; 95% CI: 1.235–2.063; P<0.001), and the presence of ischemic heart disease (AOR=10.275; 95% CI: 2.801–37.675; P<0.001). The prognostic model demonstrated good discriminatory ability, with an AUC of 0.87 (95% CI: 0.775–0.966; P<0.001), sensitivity of 82.6%, and specificity of 81.7%.

Conclusion: The results obtained confirm a significant association between the anatomical characteristics of the hernia defect, the presence of cardiovascular pathology, the systemic inflammatory response, and the risk of persistent postoperative fluid accumulation. A nomogram based on the obtained logistic regression model was created, enabling the prediction of the likelihood of developing this complication. (**International Journal of Biomedicine. 2025;15(3):511-516.**)

Keywords: ventral hernia repair • post-operative fluid accumulation • prognostic model

For citation: Ahmadullov IT, Toneev EA, Smolkina AV, Shagdaleev RF, Teryagova AD, Ilchuk NO, Pugacheva VA. Frequency and Predictors of Postoperative Fluid Collections (POFC) in Patients Following Ventral Hernia Repair with Mesh Implants. International Journal of Biomedicine. 2025;15(3):511-516. doi:10.21103/Article15(3)_OA8

Abbreviations

IHD, ischemic heart disease; **NLR**, neutrophil-to-lymphocyte ratio; **PLR**, platelet-to-lymphocyte ratio; **PNI**, prognostic nutritional index, **POFC**, postoperative fluid collections; **VHR**, ventral hernia repair.

Introduction

Ventral hernia repair (VHR) is an integral part of abdominal surgery, aimed at restoring the anatomical integrity of the anterior abdominal wall, eliminating hernia defects, and preventing recurrences. However, despite advances in surgical techniques and the introduction of modern alloplastic materials, the incidence of postoperative complications remains significant, with no substantial downward trend.[1] Among these complications, a particular concern is the formation of postoperative fluid collections (POFC), which are pathological accumulations of non-infected lymphatic and serous fluid.[2] The development of POFC is associated with prolonged hospitalization, an increased rate of infectious complications, pain syndrome, and a higher risk of hernia recurrence and the need for reoperation.[3] Early stratification of patients based on the risk of complications opens opportunities to implement preventive measures and to individualize postoperative follow-up strategies.[4]

Despite several studies addressing risk factors for POFC following hernia repair, current data remain incomplete, and prognostic assessment criteria are not sufficiently standardized. Moreover, there is a notable lack of publications on this topic in domestic surgical literature.

This study aimed to identify risk indicators for fluid accumulation after ventral hernia repair and to develop a prognostic model for postoperative fluid collections in the implantation area.

Materials and Methods

A retrospective analysis was conducted on the medical records of patients who underwent VHR at the Department of Surgery of the E.M. Chuchkalov Ulyanovsk Regional Clinical Center for Specialized Medical Care (Ulyanovsk, Russia) between February 1, 2024, and May 1, 2025. Postoperative complications following surgical intervention were analyzed. A total of 214 patient records were reviewed according to a standardized, pre-developed protocol.

Surgical procedures were performed using an approach that varied depending on patient characteristics, hernia size and location, and individual anatomical features. Medical records and clinical data were analyzed according to the standardized study protocol. Patients who did not meet the inclusion criteria or had incomplete clinical data were excluded from the study. The primary indication for hernia repair was the presence of a ventral hernia. Cases requiring combined surgical procedures were excluded from this analysis.

Inclusion Criteria

•Patient age ≥ 18 years

•Elective ventral incisional hernia repair using a synthetic mesh implant

•Availability of complete clinical data in the medical records, including patient history, laboratory and instrumental investigation results, and detailed information on the postoperative course

•Laboratory tests performed preoperatively and on postoperative days 1 and 5

•Documented presence or absence of postoperative fluid characteristics during the early postoperative period

Exclusion Criteria

•Absence of key clinical or laboratory data required for objective statistical analysis

•Surgical procedures involving local tissue repair or performed as part of an emergency or combined operation that did not conform to the study protocol

•Presence of an active malignant neoplasm at the time of surgery

In this study, cases of POFC in the area of mesh implantation following VHR with synthetic mesh materials were analyzed. POFC was operationally defined as sterile, non-infected fluid accumulations detected in the postoperative period by ultrasound examination, characterized by the absence of clinical signs of inflammation, redness, fever, or infection. Regardless of their presumed origin (serous or lymphatic), these fluid collections were considered a single clinical category for statistical analysis.

Postoperative patient management followed a standardized protocol. Antibacterial therapy, including antibiotic prophylaxis, was administered in accordance with the recommendations of the Russian Association for Antimicrobial Therapy (CKAT).[5] Wound healing was monitored daily during dressing changes, with findings documented in the medical records. In cases of adverse wound healing, bacterial cultures were routinely obtained to assess microbial flora and antibiotic sensitivity.

Statistical analysis

All statistical analyses were performed using StatTech v. 4.8.2 (Stattech LLC, Russia). The distribution of continuous variables was assessed using the Shapiro–Wilk test ($n < 50$) or the Kolmogorov–Smirnov test ($n \geq 50$). Normally distributed variables were reported as mean ± standard deviation (SD). Non-normally distributed data were presented as median (Me) and interquartile ranges (IQR [Q1;Q3]). Categorical variables were described using absolute numbers and percentages. Between-group comparisons of normally distributed continuous variables were performed using Student's t-test. The Mann–Whitney U test was used for nonparametric comparisons. Group comparisons concerning categorical variables were performed using chi-square or Fisher's exact tests. A multiple logistic regression analysis was conducted to calculate the unadjusted and adjusted odds ratios (UOR and AOR) with 95% CI. Survival analysis was carried out using the Kaplan–Meier method, and differences between groups were evaluated with the log-rank test. Cox proportional hazards regression was used to assess the impact of independent predictors on recurrence risk over time. A *P*-value of less than 0.05 was considered statistically significant.

Results

The study included 63(29.4%) women and 151(70.6%) men. The incidence of persistent POFC in the study cohort was 23(10.7%) out of 214 patients. The main clinical, laboratory and surgical characteristics of the study population are presented in Tables 1 and 2.

Table 1.

Clinical characteristics of the study groups.

Indicator	Category	No POFC n=191	POFC n=23	*P*-value
Age, Me [IQR]		61.00 [47.00 – 67.50]	65.00 [53.50 – 71.50]	0.178
Gender, n (%)	Female	54 (28.3 %)	9 (39.1 %)	0.333
	Male	137 (71.7 %)	14 (60.9 %)	
Obesity, n (%)	No	113 (59.2 %)	11 (47.8 %)	0.372
	Yes	78 (40.8 %)	12 (52.2 %)	
Diabetes mellitus, n (%)	No	112 (58.6 %)	10 (43.5 %)	0.186
	Yes	79 (41.4 %)	13 (56.5 %)	
IHD, n (%)	No	116 (60.7 %)	5 (21.7 %)	< 0.001
	Yes	75 (39.3 %)	18 (78.3 %)	
CKD, n (%)	No	115 (60.2 %)	10 (43.5 %)	0.178
	Yes	76 (39.8 %)	13 (56.5 %)	

IHD, ischemic heart disease; CKD, chronic kidney disease.

Table 2.

Hospital and surgical parameters of the study groups.

Parameter	No POFC n=191	POFC n=23	*P*-value
Hospital stay, Me [IQR]	6.00 [4.00; 9.00]	16.00 [14.00; 20.00]	< 0.001
Operation time, Me [IQR]	45.00 [30.00; 62.50]	55.00 [42.50; 65.00]	0.061
Blood loss, Me [IQR]	15.00 [10.00; 30.00]	20.00 [10.00; 30.00]	0.254
Defect diameter, Me [IQR]	8.00 [5.00; 11.00]	11.00 [9.20; 15.00]	< 0.001

Based on the results of the statistical analysis, the presence of ischemic heart disease was found to have a significant impact on the development of POFC. In addition, we analyzed the surgical parameters of the patients. Based on that analysis, defect diameter was identified as an independent predictor of persistent POFC.

A univariate analysis of the association between the presence of POFC and preoperative laboratory parameters was also conducted. Statistically significant differences between the study groups were identified in the preoperative laboratory parameters for neutrophil-to-lymphocyte ratio (NLR), platelet-to-lymphocyte ratio (PLR), prognostic nutritional index (PNI), and albumin level, suggesting a potential role of systemic inflammatory response and nutritional status in the development of persistent POFC (Table 3).

A univariate analysis of the association between postoperative Day 1 laboratory parameters and the development of POFC was performed (Table 4). Among the analyzed laboratory parameters, a statistically significant difference between patients with and without POFC was identified for total protein level, suggesting a potential influence of protein metabolism on the risk of persistent fluid collection formation. On postoperative Day 5, statistically significant differences between patients with and without POFC were observed for hemoglobin and total protein levels, suggesting a potential role of protein metabolism and blood oxygen transport function in the pathogenesis of persistent fluid collection formation (Table 5).

Table 3.

Preoperative laboratory parameters of the study groups.

Indicator	No POFC n=191	POFC n=23	*P*-value
Leukocytes, Me [IQR]	7.34 [6.08; 9.14]	7.64 [6.15; 8.96]	0.777
NLR, Me [IQR]	1.76 [1.27; 2.32]	3.15 [2.69; 4.21]	< 0.001
TLI, Me [IQR]	117.65 [96.96; 146.22]	113.48 [92.99; 157.70]	0.870
PNI, Me [IQR]	42.47 [40.33; 44.45]	41.21 [39.41; 41.71]	0.033
Hemoglobin, M ± SD	139.23 ± 20.16	147.74 ± 17.95	0.054
Total protein, Me [IQR]	68.28 [65.78;70.81]	68.60 [64.75;70.80]	0.896
Albumin, Me [IQR]	42.46 [40.32; 44.44]	41.20 [39.40; 41.70]	0.035

NLR, neutrophil-to-lymphocyte ratio; PLR, platelet-to-lymphocyte ratio; PNI, prognostic nutritional index.

Table 4.

Laboratory parameters on postoperative Day 1.

Indicator	No POFC n=191	POFC n=23	*P*-value
leukocytes, Me [IQR]	8.61 [7.85; 10.37]	7.59 [6.98; 11.13]	0.339
NLR, Me [IQR]	3.90 [2.89; 5.55]	4.21 [2.91; 6.67]	0.415
TLI, Me [IQR]	149.46 [114.45; 195.27]	159.63 [137.62; 210.75]	0.870
PNI, Me [IQR]	38.55 [38.07; 39.09]	38.55 [38.07; 39.09]	0.403
Hemoglobin, Me [IQR]	134.60 [129.60;142.00]	132.80 [(127.40;138.70]	0.228
Total protein,Me [IQR]	63.80 [63.00;65.70]	62.84 [59.40;63.71]	0.002
Albumin, Me [IQR]	38.36 [37.88; 38.90]	38.36 [37.88; 38.90]	0.353

NLR, neutrophil-to-lymphocyte ratio; PLR, platelet-to-lymphocyte ratio; PNI, prognostic nutritional index.

Table 5

Laboratory Parameters on Postoperative Day 5.

Indicator	No POFC n=191	POFC n=23	*P*-value
Leukocytes, Me [IQR]	26.40 [21.80; 31.80]	31.00 [20.20; 40.00]	0.419
NLR, Me [IQR]	2.56 [2.19; 3.31]	2.58 [2.21;3.84]	0.505
TLI, Me [IQR]	151.85 [129.68; 186.59]	140.97 [126.25; 172.64]	0.780
PNI, Me [IQR]	35.42 [33.49; 37.85]	35.48 [34.02; 37.85]	0.662
Hemoglobin, [IQR]	126.00 [116.00;139.00]	132.00 [127.00;143.00]	0.021
Total protein, Me [IQR]	61.64 [59.79;63.82]	60.20 [58.05;61.66]	0.016
Albumin, Me [IQR]	35.24 [33.32; 37.66]	35.30 [33.85; 37.66]	0.651

NLR, neutrophil-to-lymphocyte ratio; PLR, platelet-to-lymphocyte ratio; PNI, prognostic nutritional index.

A multivariate statistical analysis using binary logistic regression identified significant predictors of POFC development in the postoperative period. The following variables were included as independent predictors in the model: hernia defect diameter (AOR=1.143; 95% CI: 1.042–1.254; *P*=0.005), NLR (AOR=1.596; 95% CI: 1.235–2.063; *P*<0.001), and the presence of ischemic heart disease (AOR=10.275; 95% CI: 2.801–37.675; *P*< 0.001) (Table 6). A prognostic model was developed to estimate the probability of detecting POFC based on these factors. Figure 1 presents the ROC curve demonstrating the performance of the prognostic model in identifying cases (hernia defect diameter, NLR, and the presence of ischemic heart disease) of persistent POFC in the implantation area. The area under the ROC curve (AUC) was 0.87 (95% CI: 0.775–0.966; *P*<0.001), and the model demonstrated statistical significance. The sensitivity and specificity of the model were 82.6% and 81.7%, respectively.

Table 6.

Predictors of POFC development in the postoperative period.

Predictor	Unadjusted		Adjusted	
	OR (95% CI)	*P*-value	OR (95% CI)	*P*-value
IHD	5.568 (1.984 – 15.643)	0.001	10.275 (2.801 – 37.675)	< 0.001
NLR	1.456 (1.186 – 1.786)	< 0.001	1.596 (1.235 – 2.063)	< 0.001
Hernia defect diameter	1.151 (1.061 – 1.250)	0.001	1.143 (1.042 – 1.254)	0.005

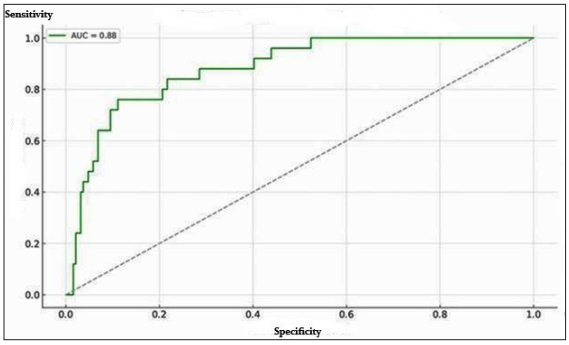

Figure 1. *ROC curve demonstrating the performance of the prognostic model in identifying cases (hernia defect diameter, NLR, and the presence of ischemic heart disease) of persistent POFC in the implantation area.*

Discussion

The formation of postoperative fluid collections, including seromas and lymphoceles, represents one of the most common complications following hernia repair with mesh implants. These pathological conditions arise from the combination of several pathogenic mechanisms: lymphatic capillary injury during tissue dissection, the creation of significant unfilled spaces ("dead space"), and an inflammatory response to the presence of a foreign implant. According to Lindmark et al,[6] the incidence of seromas following ventral hernia repair can reach up to 18.7%, particularly in laparoscopic procedures involving extensive tissue dissection.

Key pathophysiological mechanisms include increased vascular wall permeability, activation of inflammatory mediators, and limited natural drainage during the early postoperative period.[7] Several previously published studies have highlighted significant risk factors for postoperative fluid collections, including obesity, large operative volume, prolonged operative time, larger mesh placement area, the use of synthetic materials, and the presence of comorbid diabetes mellitus.[8] Notably, the study by Kapellas et al.[9] demonstrated that extensive tissue dissection and lateral mesh fixation significantly increase the risk of persistent fluid collection formation. Clinically, postoperative fluid collection is associated with prolonged hospitalization, increased postoperative pain, a higher risk of prosthetic infection, and the potential need for reoperation.[10] In some cases, persistent fluid collections may lead to late hernia recurrence and chronic inflammation in the implantation area.

In this study, the incidence of this postoperative complication following ventral hernia repair with mesh implants was 10.7%, which is comparable to the results of Howard et al.,[11] where the adjusted complication rate across hospitals was 6.2%.

Our statistical analysis revealed that the PNI, which reflects the patient's response to surgical intervention, significantly influences the development of postoperative fluid collections. Similar findings confirming the impact of PNI on

infectious complications in abdominal surgery patients were reported by Benjamin et al.[12]

Moreover, it is important to note that red blood cell count in the preoperative complete blood count, hemoglobin level on postoperative Day 5, and total protein levels in the biochemical analysis on postoperative Days 1 and 5 were also statistically significant factors associated with postoperative fluid collection development. This correlation is likely due to their close relationship with PNI as an indicator of the patient's overall condition. Similar results were reported by Sim et al., highlighting the association of these predictors with postoperative outcomes.[13]

Based on our analysis, the presence of ischemic heart disease, as a systemic vascular condition, was found to negatively affect microcirculation and tissue healing processes, thereby potentially increasing the risk of impaired lymphatic drainage and lymph accumulation in the postoperative area. These findings are consistent with those of Anastasopoulos et al.,[14] who highlighted the association between cardiovascular pathology and an increased risk of persistent fluid collections in patients undergoing abdominal wall surgery after organ transplantation.

The NLR, which reflects the balance between neutrophilic inflammation and lymphocytic regulation, is a recognized marker of systemic inflammatory response. In our study, elevated NLR was significantly associated with an increased likelihood of postoperative fluid collection in the implantation area. Similar associations have been reported by both domestic and international authors, demonstrating that elevated NLR values predict the development of postoperative complications, including postoperative fluid collections.[15]

We also identified an association between hernia defect diameter and the risk of postoperative fluid collections. Larger surgical fields may result in greater lymphatic vessel injury and impaired drainage.[16] This observation is supported by the findings of Veroux et al., which emphasized that the extent of anatomical dissection and surgical area correlates with the probability of lymphatic fluid accumulation.

In the present study, we developed a prognostic model to estimate the probability of postoperative fluid collections following ventral hernia repair. Multivariate analysis identified the presence of ischemic heart disease, elevated NLR, and increased hernia defect diameter as significant independent predictors of this complication. All three predictors demonstrated statistical significance in both unadjusted and adjusted models. The model exhibited high discriminatory power, with the determined cutoff probability threshold (0.143) providing an optimal balance of sensitivity (82.6%) and specificity (81.7%). This supports the potential application of the model as a preoperative risk stratification tool.

Thus, the results of our study confirm the importance of a comprehensive assessment of cardiovascular status, systemic inflammation, and morphometric characteristics of the hernia defect in predicting postoperative fluid collections. The use of this model may contribute to the individualization of surgical strategies and the implementation of preventive measures in patients at high risk of complications.

Conclusion

The incidence of postoperative fluid collections in patients undergoing ventral hernia repair with mesh implants was 10.7%. The results obtained confirm a significant association between the anatomical characteristics of the hernia defect, the presence of cardiovascular pathology, the systemic inflammatory response, and the risk of persistent postoperative fluid accumulation. A nomogram based on the obtained logistic regression model was created, enabling the prediction of the likelihood of developing this complication.

Ethical Considerations

The study protocol was reviewed and approved by the Ethics Committees at the Regional Oncology Dispensary and Ulyanovsk State University, Ulyanovsk, Russia.

Competing Interests

The authors declare that they have no competing interests.

References

1. Michot N, Ortega-Deballon P, Karam E, Pabst-Giger U, Ouaissi M. Is There a Clinical Benefit of Abdominal Binders After Abdominal Surgery: A Systematic Literature Review. J Abdom Wall Surg. 2024 Oct 17;3:13506. doi: 10.3389/jaws.2024.13506. PMID: 39483144; PMCID: PMC11524862.
2. Kazzam ME, Ng P. Postoperative Seroma Management. 2023 Aug 14. In: StatPearls [Internet]. Treasure Island (FL): StatPearls Publishing; 2025 Jan–. PMID: 36256748.
3. Orgill DP, Hergrueter CA. Discussion: Strategies for Postoperative Seroma Prevention: A Systematic Review. Plast Reconstr Surg. 2016 Jul;138(1):253-254. doi: 10.1097/PRS.0000000000002288. PMID: 27348658.
4. Mahrer A, Ramchandani P, Trerotola SO, Shlansky-Goldberg RD, Itkin M. Sclerotherapy in the management of postoperative lymphocele. J Vasc Interv Radiol. 2010 Jul;21(7):1050-3. doi: 10.1016/j.jvir.2010.03.014. Epub 2010 Jun 2. PMID: 20537556.
5. SCAT (Association of Specialists in Antimicrobial Therapy). Prevention of infectious complications in surgical interventions: Clinical guidelines (2nd ed., revised and expanded). Moscow: Association of Specialists in Antimicrobial Therapy.2020. [In Russian].
6. Lindmark M, Strigård K, Löwenmark T, Dahlstrand U, Gunnarsson U. Risk Factors for Surgical Complications in Ventral Hernia Repair. World J Surg. 2018 Nov;42(11):3528-3536. doi: 10.1007/s00268-018-4642-6. PMID: 29700567; PMCID: PMC6182761.
7. Kim N, Juarez R, Levy AD. Imaging non-vascular complications of renal transplantation. Abdom Radiol (NY). 2018 Oct;43(10):2555-2563. doi: 10.1007/s00261-018-1566-4. PMID: 29550956.
8. Chiacchio G, Beltrami M, Cicconofri A, Nedbal C, Pitoni

L, Fuligni D, Maggi M, Milanese G, Galosi AB, Castellani D, Giulioni C. Simultaneous Inguinal Hernia Repair with Monofilament Polypropylene Mesh during Robot-Assisted Radical Prostatectomy: Results from a Single Institute Series. Medicina (Kaunas). 2023 Apr 22;59(5):820. doi: 10.3390/medicina59050820. PMID: 37241052; PMCID: PMC10222079.

9. Kapellas N, Alkhalil S, Hero T, Senkal M. Postoperative lymphatic leakage following laparoscopic totally extraperitoneal inguinal hernia repair: the first case report and review of the literature. Hernia. 2025 Mar 27;29(1):126. doi: 10.1007/s10029-025-03318-7. PMID: 40146374.

10. Mehrotra PK, Ramachandran CS, Goel D, Arora V. Giant pseudocyst of the anterior abdominal wall following mesh repair of incisional hernia: a rare complication managed laparoscopically. Hernia. 2006 Apr;10(2):192-4. doi: 10.1007/s10029-005-0025-7. Epub 2005 Sep 1. PMID: 16136392.

11. Howard R, Johnson E, Berlin NL, Fan Z, Englesbe M, Dimick JB, Telem DA. Hospital and surgeon variation in 30-day complication rates after ventral hernia repair. Am J Surg. 2021 Aug;222(2):417-423. doi: 10.1016/j.amjsurg.2020.12.021. Epub 2020 Dec 11. PMID: 33323274.

12. Benjamin RK, Muralee MK, Chinnathambi V. Prognostic Nutritional Index as an indicator of postoperative morbidity in patients undergoing perioperative chemotherapy and surgery for carcinoma stomach. Indian J Surg Oncol. 2025. doi:10.1007/s13193-025-02193-z

13. Sim JH, Kim SH, Jun IG, Kang SJ, Kim B, Kim S, Song JG. The Association between Prognostic Nutritional Index (PNI) and Intraoperative Transfusion in Patients Undergoing Hepatectomy for Hepatocellular Carcinoma: A Retrospective Cohort Study. Cancers (Basel). 2021 May 21;13(11):2508. doi: 10.3390/cancers13112508. PMID: 34063772; PMCID: PMC8196581.

14. Anastasopoulos NA, Hussain SF, Herbert PE, Muthusamy ASR, Dor FJ, Papalois V. A single-centre, retrospective study of incisional hernia repair outcomes post kidney transplantation. Hernia. 2024 Dec;28(6):2285-2290. doi: 10.1007/s10029-024-03157-y. Epub 2024 Sep 25. PMID: 39320605.

15. Vdovin AM, Toneev EA, Pikin OV, Shagdaleev RF, Martynov AA. [Prediction of surgical site infections after elective thoracotomy]. Grudnaya i Serdechno-Sosudistaya Khirurgiya. 20024;66(6):837–847. doi:10.24022/0236-2791-2024-66-6-837-847

16. Gómez FM, Baetens TR, Santos E, Rocha BL, Horwitz B, Lojo-Lendoiro S, Vargas P, Patel P, Beets-Tan R, Martínez-Rodrigo JJ, Bonmatí LM. Interventional solutions for post-surgical problems: a lymphatic leaks review. CVIR Endovasc. 2024 Aug 10;7(1):61. doi: 10.1186/s42155-024-00473-3. Erratum in: CVIR Endovasc. 2024 Sep 17;7(1):68. doi: 10.1186/s42155-024-00483-1. PMID: 39126551; PMCID: PMC11316727.

***Corresponding author**: Evgeniy A. Toneev, PhD. E-mail: e.toneev@inbox.ru*

International Journal of Biomedicine 15(3) (2025) 517-522
http://dx.doi.org/10.21103/Article15(3)_OA9

ORIGINAL ARTICLE

Otorhinolaryngology

INTERNATIONAL JOURNAL OF BIOMEDICINE

Epidemiological and Clinical Profile of Nasopharyngeal Carcinoma in Indonesia: A Nationwide Descriptive Study

Sagung Rai Indrasari[1*], Yussy Afriani Dewi[2], Nova Audrey Luetta[3,12], Achmad Chusnu Romdhoni[4], I Gde Ardika Nuaba[5], Cita Herawati[6], Nani Iriany Djufri[7], Soehartono[8], Ibrahim Ihsan Nasution[9], Camelia Herdini[1], Selvianti[10], Sabri Syamsu[11], Feri Danil[11], Sukri Rahman[13], Yulvina[14], Mochammad Alfian Sulaksana[15], Marlinda Adham[16], Anisa Haqul Khoiria[1], Danu Yudistira[1], Ariel Anugrahani[9]

[1]Department of Otorhinolaryngology Head and Neck Surgery, Faculty of Medicine, Public Health and Nursing, Universitas Gadjah Mada, Dr. Sardjito Public Hospital, Yogyakarta, Indonesia; [2]Department of Otorhinolaryngology Head and Neck Surgery, Faculty of Medicine Universitas Padjadjaran, Hasan Sadikin Hospital, Bandung, Indonesia; [3]Department of Otorhinolaryngology Head and Neck Surgery, Faculty of Medicine, Universitas Hasanuddin, Wahidin Soedirohusodo Hospital, Makassar, Indonesia; [4]Department of Otorhinolaryngology Head and Neck Surgery, Faculty of Medicine, Universitas Airlangga, Dr. Soetomo Regional Hospital, Surabaya, Indonesia; [5]Department of Otorhinolaryngology Head and Neck Surgery, Faculty of Medicine, Universitas Udayana, Sanglah Public Hospital, Denpasar, Indonesia; [6]Department of Otorhinolaryngology Head and Neck Surgery, Dharmais Cancer Hospital, Jakarta, Indonesia; [7]Department of Otorhinolaryngology Head and Neck Surgery, Pelamonia Hospital, Makassar, Indonesia; [8]Department of Otorhinolaryngology Head and Neck Surgery, Faculty of Medicine, Universitas Brawijaya, Saiful Anwar Hospital, Malang, Indonesia; [9]Department of Otorhinolaryngology Head and Neck Surgery, Faculty of Medicine, Universitas Riau, Arifin Ahmad Hospital, Pekanbaru, Indonesia; [10]Department of Otorhinolaryngology Head and Neck Surgery, AW Sjahranie Hospital, Samarinda, Indonesia; [11]Department of Otorhinolaryngology Head and Neck Surgery, Gatot Soebroto Army Hospital, Jakarta, Indonesia; [12]Department of Otorhinolaryngology Head and Neck Surgery, Faculty of Medicine, Universitas Hasanuddin, Unhas Hospital, Makassar, Indonesia; [13]Department of Otorhinolaryngology Head and Neck Surgery, Faculty of Medicine, Universitas Andalas, M. Djamil Hospital, Padang, Indonesia; [14]Department of Otorhinolaryngology Head and Neck Surgery, Persahabatan Hospital, Jakarta, Indonesia; [15]Department of Otorhinolaryngology Head and Neck Surgery, Faculty of Medicine, Universitas Mataram, Provinsi NTB Hospital, Mataram, Indonesia; [16]Department of Otorhinolaryngology Head and Neck Surgery, Faculty of Medicine, Universitas Indonesia, Dr. Ciptomangunkusumo National Public Hospital, Jakarta, Indonesia

Abstract

Background: Nasopharyngeal carcinoma (NPC) is now the fifth leading cause of cancer death in Indonesia, with most cases diagnosed at advanced stages due to nonspecific early symptoms. This study describes the epidemiological, clinical, and pathological profiles of NPC in Indonesia.

Methods and Results: This descriptive study used data from the NPC-Indonesia registry between January 2019 and December 2022. It included newly diagnosed NPC patients who visited ENT outpatient clinics and underwent treatment—either single or multimodality regimens—at 16 participating hospitals. The data was collected from the NPC-Indonesia registry data system. Whole data was extracted and sorted into excel sheet, only those cases with confirmed diagnosis and treatment of cancer were analyzed according to age, sex, home province, chief complaint, histopathology subtypes, staging, treatment modality, response to therapy, and distant metastasis. A total of 545 patients 67.7% male and 32.3% female were recorded. The average age was 48 years, ranging from 4 to 80. The most common chief complaint was a neck lump. Most patients were from West Java and were presented with advanced-stage disease. The majority had WHO type 3 histology.

Conclusion: Nasopharyngeal carcinoma in Indonesia commonly presents at an advanced stage, likely due to nonspecific early symptoms. This study is the first large-scale research providing comprehensive NPC data in Indonesia, emphasizing the need for improved early detection and public health awareness.(**International Journal of Biomedicine. 2025;15(3):517-522.**)

Keywords: nasopharyngeal carcinoma • epidemiology • histopathology • metastasis

For citation: Indrasari SR, Dewi YA, Luetta NA, Romdhoni AC, Nuaba IGA, Herawati C, Djufri NI, Soehartono, Nasution II, Herdini C, Selvianti, Syamsu S, Danil F, Rahman S, Yulvina, Sulaksana MA, Adham M, Khoiria AH, Yudistira D, Anugrahani A. Epidemiological and Clinical Profile of Nasopharyngeal Carcinoma in Indonesia: A Nationwide Descriptive Study. International Journal of Biomedicine. 2025;15(3):517-522. doi:10.21103/Article15(3)_OA9

Introduction

Nasopharyngeal carcinoma (NPC) is distinctive among head and neck malignancies based on several aspects, such as its epidemiology, clinical manifestations, molecular biomarkers, carcinogenic predisposing factors, as well as prognostic variables. NPC induces a dismal prognosis and becomes endemic in some parts of the globe, particularly Southeast Asia. The mean prevalence of NPC cases in Indonesia reaches 6.2/100,000, with 13,000 additional cases reported each year.[1] Nasopharyngeal carcinoma remains a global burden. In 2019, the incidence of NPC reached 176,500 cases globally; meanwhile, Indonesia achieved the third highest mortality rate due to NPC, with 3,220 deaths in 2019 only.[2] In contrast to other types of cancers, NPC has a unique distribution pattern. In 2018, 129,000 new cases and 73,000 mortality cases were announced globally. The geographic distribution of these cases was highly uneven. Over 70% of additional cases were detected in East and Southeast Asia, while in most other regions, the age-standardized incidence of NPC in both males and females was under 1 per 100,000 person-years. Based on investigations on most populations, the incidence of NPC was two to three times higher in men than in women.[2,3] Comparable to other chronic diseases, NPC presents numerous challenges beyond just treatment. Patients with NPC frequently experience one or multiple symptoms affecting the nasal area, ears, cranial nerves, neck lymph nodes, and distant metastases. It is difficult to establish the early stage of this carcinoma due to the secluded emergence of the nasopharynx itself, with indistinct clinical complaints. Many cases that were then referred to the hospital were already presented at an advanced stage, primarily because of the inadequate awareness of the patient and the doctors at the primary care level. The clinical stage was assessed using the TNM classification released in the American Joint Committee of Cancer (AJCC) 8th edition.[2,4]

It is essential to know the description of nasopharyngeal cancer patients among the Indonesian population, so that it becomes a reference for early diagnosis to provide appropriate treatment to those patients.

Materials and Methods

A retrospective analysis was carried out on all NPC cases that presented to the 16 affiliated hospitals of this research (Dr. Soetomo Regional Hospital, Hasan Sadikin Hospital, M. Djamil Hospital, Pelamonia Hospital, Persahabatan Hospital, Saiful Anwar Hospital, Unhas Hospital, Wahidin Soedirohusodo Hospital, Dharmais Cancer Hospital, Gatot Soebroto Army Hospital, AW Sjahranie Regional Hospital, Arifin Ahmad Regional Hospital, Provinsi NTB Hospital, Dr. Sardjito Public Hospital, Sanglah Public Hospital, and Ciptomangunkusumo National Hospital) from January 2019 to December 2022, who had completed the therapy course and undergone response examination. The data was collected from the NPC-Indonesia registry data system. Whole data was extracted and sorted into excel sheet, only those cases with confirmed diagnosis and treatment of cancer were analyzed according to age, sex, home province, chief complaint, histopathology subtypes, staging, treatment modality, response to therapy, and distant metastasis.

As many as 895 cases were extracted from the database collection, 350 of which were rejected due to incomplete histopathology reports, treatment information, and response therapy data. Therefore, the final data included reached 545 cases. Details of the number of patients from each hospital are outlined in Figure 1.

Statistical analysis was performed using SPSS software, version 16 (SPSS Inc., Chicago, USA).

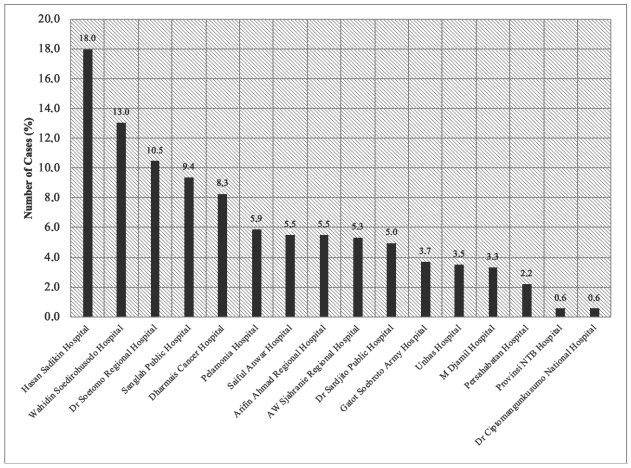

Figure 1. *Distribution of NPC cases by hospitals.*

Results

Male patients were more predominant than female ones, at a ratio of 2.1:1, with 369(67.7%) male subjects and 176(32.3%) female subjects. In terms of age, patients were divided into several age groups with a 10-year gap for each group. Most patients were found in the age group of 50-60 – 166(30.5%), followed by the age group of 40-50 – 15(28.4%), the age group of 30-40 – 84(15.4%), the age group of 60-70 – 78(14.3%), the age group of 20-30 – 32(5.9%), the age group of 70-80 – 19(3.5%), the age group of 10-20 – 9(1.7%), and only 2(0.4%) patients were in the age group under 10. Overall, the mean age was 48 years, with the youngest being 4 and the oldest being 80 years.

Most cases of NPC were from West Java (126/23.1%) cases, followed by South Sulawesi (92/16.9%), and East Java (85/15.6%), Bali (50/9.2%), Riau (33/6.1%), East Kalimantan (30/5.5%), DKI Jakarta (21/ 3.9%), Banten (18/3.3%), DIY (18/3. %), South Sumatra (13/2.4%), Central Java (11/2%), Central Sulawesi (10/1.8%), Southeast Sulawesi (10/1.8%), Jambi (4/0.7%), West Sulawesi (4/0.7%), Lampung (3/0.6%, West Nusa Tenggara (NTB) (3/0.6%), North Maluku (2/0.4%), and Papua (2/0.4%). The provinces with the lowest cases of NPC include Bengkulu, Gorontalo, West Kalimantan, Central Kalimantan, North Kalimantan, Bangka Belitung, East Nusa Tenggara (NTT), West Papua, South Sumatra, and North Sumatra, each of which had only one case (0.2%) (Figure 2).

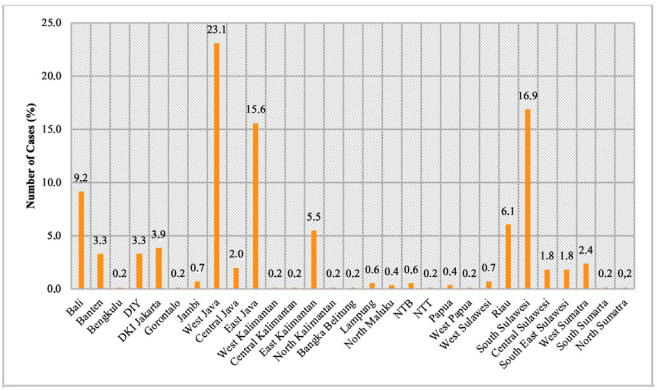

Figure 2. *Distribution of NPC cases by home provinces.*

Most cases emerged with a neck lump, accounting for up to 53.9% of all cases. The second most common complaint was nasal congestion, which accounted for 16.9% of cases. Other symptoms contributed less than 10% each, such as nosebleeds (8.3%), blood-stained discharge (3.9%), tinnitus (5.7%), headaches (4.2%), double vision (2%), and chronic colds (2%), and impaired vision (1.3%); the rest of the complaints were less than 1% each, including neck pain (0.6%) and difficulty swallowing (0.4%). Cheek lump, sore throat, dyspnea, and dysphonia were 0.2% each (Figure 3).

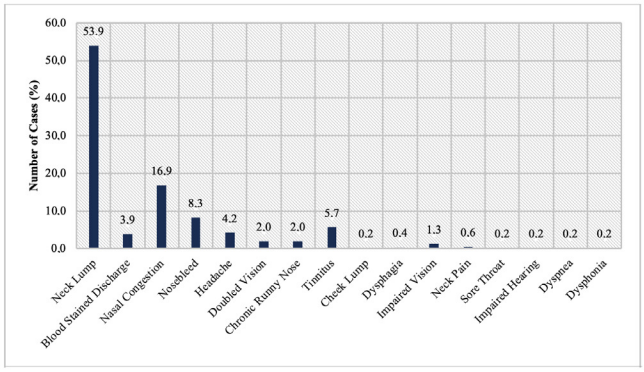

Figure 3. *Complaints and symptoms.*

Histopathological subtype analysis revealed that 378(69.4%) cases were WHO type 3, 155(28.4%) were WHO type 2, and 12(2.2%) were WHO type 1. Notably, 43.5% of patients presented at stage IVA, followed by stage III (27.5%) and stage IVB (16.9%); 9.4% of patients were stage II and only 2.8% stage I.

Based on the tumor extension, most cases found were T4 (33%) characterized by the tumor extension intracranially, spread to the cranial nerves, orbit, hypopharynx, parotid glad and/or broad soft tissue, surpassing the lateral pterygoid muscle outer surface. Those cases were followed by T3 (30.5%) characterized by tumor spread to bony structures, including skull base, pterygoid, cervical vertebrae, and the paranasal sinuses. T1 (10.6%) and T2 (25.9%) were the two least common cases in this study. The N classification for the spreading to surrounding lymph nodes mainly consists of N2 (36%), followed by N3 (29.4%), N1 (21.2%), and N0 (13.6%). The number of M0 cases, where there is no distant metastasis, constituted most cases (83.1%).

The data extracted showed that 92 patients had stage IVB and experienced remote metastases to other organs, such as the lung, bones, liver, and brain. Among all NPC stage IVB patients, the highest incidence of distant metastases was bone (42/45.6%), followed by lung (22/23.9%), liver (17/18.5%), and brain (1/1.1%). This study also found distant metastases to multiple organs, namely 5(5.4%) patients for bone and lung, 4(4.3%) patients for bone and liver, and 1(1.1%) patient for bone and brain (Figure 4).

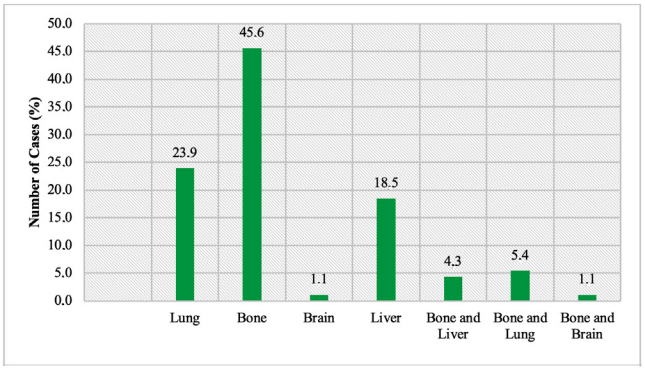

Figure 4. *Distant metastases.*

Discussion

Nasopharyngeal carcinoma has become endemic in Southeast Asia. Indonesia has limited clinical evidence related to this malignancy, as it is the most populous country in Southeast Asia. A review of national NPC registry data using a retrospective method was performed to assess the epidemiological profile of 545 patients with recently diagnosed NPC undergoing both completed and uncompleted treatments due to mortality during or after completing treatment. Our study provided patient demographics in terms of age, male-to-female ratio, and WHO cancer subtypes, which are consistent with the typical nasopharyngeal cancer patient demographics in Southeast Asia.

An epidemiological study of NPC cases in Southeast Asia conducted by Lao et al.[6] reported 34,681 new NPC cases in total, with 25,895(74.7%) cases comprised of male patients and 8,786 of female patients: a ratio of 2.91:1. The study also showed that among the countries of Southeast Asia, the three highest incidences of NPC were identified in Indonesia with 17,992 cases, Vietnam with 6,212 cases, and Philippines with 2,913 cases with the same order of mortality of 11,204 cases, 4,232 cases and 1,899 cases, respectively. This was possibly due to the environmental influence, with relatively harmful predisposing factors associated with development of carcinogenesis, and a lack of budget allocated for health cases and public health initiatives, including incomes, health services, and education within the community. Another study by Adham et al.[6] also found the ratio of male-to-female NPC cases from 1995 to 2005 to be 2.37:1, with the peak

age incidence of 40-49; as many as >80% of the cases were within the age group of 41-50. A significant number, 20%, of NPC cases were contributed by patients under 30 with no bimodal age distribution. As in our study, the male-to-female ratio reached 2.1:1, with the mean age of 48, and the highest incidence was within the age group of 50-60. On the other hand, only 8% of juvenile cases were identified from our study. The lack of awareness in young age cases could cause the difference between these results. Almost all of the pediatric and adolescent patients as well as their parents or guardians were neither aware of the early clinical symptoms of NPC nor even thinking that cancer might occur at their age. Hence they assumed that such a condition as they endured was normal or just a glimpse of a disturbance that later would cause a delay in having a screening or an examination until the condition became more severe or already at an advanced stage.[5,7] In a study by Susetiyo et al.[8] at Dr. Soetomo General Hospital, the ratio of male to female patients was 2.7:1, with the peak age group of 41-50. Each gender, lifestyle, and biological factors were believed to contribute to the difference in NPC incidence. Males are more prone than females to being exposed to carcinogenic substances from the workplace or the habit of smoking; otherwise, females have estrogen, which tends to protect them from NPC due to its NAG7 repressor negative regulator activity of tumor growth [8,9]

The NPC-Indonesia registry allowed us to study the incidence of this disease in several provinces of Indonesia served by 16 different university hospitals. Based on the data, we required the distribution of NPC in 29 provinces in Indonesia. West Java had the highest incidence of NPC, followed by South Sulawesi and East Java. Our results differed from those previously reported by Adham et al.,[1] in which the highest incidence was found in East Java, based on the regional data provided by Malang (9.19/100.000) and Surabaya (7.23/100.000). Nevertheless, as mentioned in the study, the data acquired for the result was extracted from the mean regional incidence based on a few cities in Indonesia. In general, NPC incidence is 5.66/100.000, with approximately 1,000 new NPC findings each month, indicating a prominent challenge in Indonesia.[1,5]

In our study, the result showed that the most common presentation of NPC is in the form of a neck lump and nasal congestion, followed by ear and eye symptoms, as well as throat and breathing symptoms, as the less common complaints. Although neck lump was the most common complaint among the subjects, a previous study by Adham et al.[1] noted that this finding suggested an advanced stage of NPC. Mostly, patients might not notice the early symptoms of NPC, which were unilateral ear problems in 60.6% of the patients, according to the previous study. Still, in our study, ear problems, such as tinnitus and impaired hearing, were some of the less common symptoms identified from NPC patients. Susetiyo et al.[8] also found that the most common clinical symptoms of NPC were due to nearby metastasis, such as neck masses, followed by local infiltration symptoms, including ear and nasal complaints. The neck mass often emerges unilaterally and is painless unless accompanied by inflammation or infection. This could be the main trigger for the advanced stage of NPC diagnosis. Pain causes discomfort in patients, which eventually drives patients to attend an examination.

The reason for this finding in our study is correlated with our results of TNM classification and staging. Most patients in our study suffered from T4 stage. They were also aware that this stage was characterized by the broad extension of the tumor already taking place, which caused major symptoms to the patient with some form of metastasis, both regional and distant. Most regional neck lymph node metastases were identified at the N2 stage, in which the clinical enlargement was already significant, compared to N1, hence a very aggravating symptom endured by almost all patients due to its change in anatomical appearance. Faisal et al.[5] evaluated the results of 428 patients in a single institution study and discovered that T4 and N2 were the most common, with percentages of 63.8% and 39.7% respectively. Furthermore, the nasopharynx's proximity to a dense lymphatic network creates a higher possibility for poorly differentiated and undifferentiated NPCs to metastasize than it does for the other squamous cancers of the head and neck.

Regarding the NPC stage at the time of diagnosis, 43.5% of our cases were at stage IVA. If the advanced stage versus the early stage were also calculated and compared, it would result in 87.8% and 12.2%, respectively. The study by Fles et al.[7] may shed light on this finding regarding Indonesian patients' health attitudes, since, according to this study, most patients with NPC have limited knowledge about NPC and its etiology. Half of the patients have a six-month delay in diagnosis since the symptom's onset. It is mainly due to the patient's lack of awareness, as well as influences from the environment, economic situation, and social aspects, including family, tradition, and religion. Perceived barriers to medical assistance and healthcare include direct non-medical costs not covered by health insurance, complex and prolonged insurance processes, referral systems, and negative past experiences. [7,11]

According to the WHO classification, NPC is classified into three types based on its histopathology, which consists of keratinizing squamous cell carcinoma (1), non-keratinizing squamous cell carcinoma (2), and undifferentiated carcinoma (3). The most abundant type in Southeast Asia is the third WHO type, which is commonly related to EBV infection. Unlike type 3, WHO type 1 is mainly found in non-endemic regions, resulting from tobacco and alcohol consumption. [1,12] Our study also showed WHO type 3 as the most frequent subtype. Approximately 69.4% of cases were undifferentiated carcinoma, and only 2.2% were contributed by WHO type 1 NPC. Most previous studies analyzing NPC cases in Indonesia have also shown that the most common subtype is WHO type 3, consistent with this country being an endemic region of NPC.[1,4,8,13-16] The predisposition for NPC development is EBV infection at a young age, along with chronic viral reactivation in the epithelial tissue of the nasopharynx caused by local inflammation. Nearly all the children in the NPC endemic region become EBV carriers at the age of five. [17]

Moreover, NPC tends to have a propensity for distant metastasis with a higher possibility, unlike the other types of head and neck cancer. Based on the descending incidence, metastasis tends to emerge in bones, liver, lungs, and distant

lymph nodes. In our study, of all 545 patients 92 cases were found to have distant metastasis. Most patients experienced single organ metastasis, with the remainder developing multiple metastases that occurred either simultaneously or sequentially. An earlier study by Qu et al.[10] indicated that bone metastasis occurred in approximately 64%-67% of cases, making it the most common site of metastasis, while brain involvement was the least common among all subtypes of NPC. According to their findings, 332 out of 2758 patients (12.0%) had distant metastases, with 325 out of these 332 patients (97.9%) showing metastases in five specific organs: bone, brain, liver, lung, and distant lymph nodes. In addition, stage N3 is characterized by the highest incidence of metastasis involving the five mentioned organs. Based on the baseline clinicopathological characteristics, distant metastasis is associated to tumor dimension, lymph node contribution, and lymph node size. Frequently, it is found in cases where the tumor was biopsied, but the lymph nodes aren't removed, as well as in subjects with T4 and N3 stages.[10,12] Distant metastasis is the leading trigger of a reduction in patients' survival. A study conducted by Yang et al.[19] identified that 51.1% patients experienced multiple organ metastasis and 59.6% patients had suffered from more than three remote metastatic lesions by the time they were diagnosed. In those cases, bone, liver, and lung were the organs most affected by metastasis. Meanwhile, in our study, 16.9% showed distant metastasis at the time of diagnosis, 89.1% of which involved single organ metastasis, and 10.9% of which included multiple organs. Bone was the most common organ affected by single organ metastasis (45.6%), followed by the lungs and liver, and the least common was the brain. Our study reported that multiple organ metastasis involving bone and lung was identified the most.

Conclusion

Our study concluded that NPC cases are more often found in males than in females, with a ratio of 2.1:1, and frequently occur within the age group of 50–60, with a mean age of 48. The home province for the highest NPC cases was West Java, followed by South Sulawesi and East Java. Overall, the pathologic findings of WHO type 3 with IVA stage, T4 tumor, and N2 node were the most dominant variable findings in this study, almost aligning with those identified in the endemic area of Southeast Asia, specifically in Indonesia. However, NPC is still one of the most perplexing and easily misdiagnosed pathologies. Both patients and physicians often neglect many unspecified early clinical manifestations. Most patients in our study have already shown local metastasis and local infiltration symptoms, such as a lump in the neck and nasal congestion, the two most frequent chief complaints among all subjects. Bone was the most common metastatic organ in this study in terms of single organ metastasis, whereas multiple metastases commonly affect bone and lung as the most common target organs. The findings of this study should be implemented as a basis to encourage awareness and early testing for any suspected case of NPC. Further research is recommended to be conducted with more sufficient data to enhance follow-up from several centers involving the entire home provinces in Indonesia, as well as the use of more accurate and thorough data entry, so that better and more comprehensive results can be gained in the future.

Acknowledgments

We appreciate the help and data access provided by the NPC-Indonesia registry team and the 16 participating hospitals. We also thank all of the patients and medical personnel who participated in this study.

Ethical Statement

This study was approved by the Medical and Health Research Ethic Committee (MHREC) of the Faculty of Medicine, Public Health, and Nursing, Universitas Gadjah Mada, with the registration number.KE/FK/0001/EC/2024.

Competing Interests

The authors declare that they have no competing interests.

Refrerences

1. Adham M, Kurniawan AN, Muhtadi AI, Roezin A, Hermani B, Gondhowiardjo S, Tan IB, Middeldorp JM. Nasopharyngeal carcinoma in Indonesia: epidemiology, incidence, signs, and symptoms at presentation. Chin J Cancer. 2012 Apr;31(4):185-96. doi: 10.5732/cjc.011.10328. Epub 2012 Feb 7. PMID: 22313595; PMCID: PMC3777476.
2. Romdhoni AC, Rejeki PS, Guo HR, Milla C, Melbiarta RR, Visuddho V, Nugraha D. Risk Factors Associated with Nasopharyngeal Cancer Incidences in Indonesia: A Systematic Review and Meta-Analysis. Asian Pac J Cancer Prev. 2023 Apr 1;24(4):1105-1111. doi: 10.31557/APJCP.2023.24.4.1105. PMID: 37116129; PMCID: PMC10352734.
3. Yu H, Yin X, Mao Y, Chen M, Tang Q, Yan S. The global burden of nasopharyngeal carcinoma from 2009 to 2019: an observational study based on the Global Burden of Disease Study 2019. Eur Arch Otorhinolaryngol. 2022 Mar;279(3):1519-1533. doi: 10.1007/s00405-021-06922-2. Epub 2021 Jun 19. PMID: 34146150; PMCID: PMC8897385.
4. Ida Ayu Citra Pratiwi, I Gde Ardika Nuaba. Characteristic of nasopharyngeal carcinoma patients in Sanglah General Hospital Denpasar period 2016-2020. GSC Adv Res Rev. 2022 Mar 30;10(3):131–5.
5. Faisal HH, Kubo N, Nuryadi E, Prihartono J, Atmakusuma TD, Rachmadi L, Oike T, Nakano T, Gondhowiardjo SA, Adham M. Patterns of Care and Outcome Analysis of Nasopharyngeal Carcinoma: An Indonesian Single Institution Study. Asian Pac J Cancer Prev. 2020 May 1;21(5):1481-1485. doi: 10.31557/APJCP.2020.21.5.1481. PMID: 32458659; PMCID: PMC7541880.
6. Lao TD, Ái T, Le HAT. Epidemiology, incidence and mortality of Nasopharynx Cancer in Southeast Asia: an update

report. In 2020. Available from: https://api.semanticscholar.org/CorpusID:233284969
7. Fles R, Indrasari SR, Herdini C, Martini S, Isfandiari A, Romdhoni AC, Adham M, Mayangsari ID, van Werkhoven E, Wildeman MA, Hariwiyanto B, Hermani B, Kentjono WA, Haryana SM, Schmidt MK, Tan IB. Effectiveness of a multicentre nasopharyngeal carcinoma awareness programme in Indonesia. BMJ Open. 2016 Mar 1;6(3):e008571. doi: 10.1136/bmjopen-2015-008571. PMID: 26932137; PMCID: PMC4785340.
8. Susetiyo KA, Kusumastuti EH, Yusuf M, Falerina R. Clinicopathological profile of nasopharyngeal carcinoma in 2016-2019 at Dr. Soetomo General Hospital. Oto Rhino Laryn Indonesiana. 2022;52(1). Available from: http://orli.or.id/index.php/orli/article/view/474
9. Xie SH, Yu IT, Tse LA, Mang OW, Yue L. Sex difference in the incidence of nasopharyngeal carcinoma in Hong Kong 1983-2008: suggestion of a potential protective role of oestrogen. Eur J Cancer. 2013 Jan;49(1):150-5. doi: 10.1016/j.ejca.2012.07.004. Epub 2012 Aug 11. PMID: 22892061.
10. Qu W, Li S, Zhang M, Qiao Q. Pattern and prognosis of distant metastases in nasopharyngeal carcinoma: A large-population retrospective analysis. Cancer Med. 2020 Sep;9(17):6147-6158. doi: 10.1002/cam4.3301. Epub 2020 Jul 10. PMID: 32649056; PMCID: PMC7476823.
11. Fles R, Bos ACRK, Supriyati, Rachmawati D, Waliyanti E, Tan IB, Haryana SM, Schmidt MK, Dewi FST. The role of Indonesian patients' health behaviors in delaying the diagnosis of nasopharyngeal carcinoma. BMC Public Health. 2017 May 25;17(1):510. doi: 10.1186/s12889-017-4429-y. PMID: 28545416; PMCID: PMC5445307.
12. Jicman Stan D, Niculet E, Lungu M, Onisor C, Rebegea L, Vesa D, Bezman L, Bujoreanu FC, Sarbu MI, Mihailov R, Fotea S, Tatu AL. Nasopharyngeal carcinoma: A new synthesis of literature data (Review). Exp Ther Med. 2022 Feb;23(2):136. doi: 10.3892/etm.2021.11059. Epub 2021 Dec 13. PMID: 35069817; PMCID: PMC8756428.
13. Utomo AW, Romdhoni AC. Characteristics of patients with nasopharyngeal carcinoma in Dr. Soetomo General Academic Hospital Surabaya. Bali Medical Journal. 2023;12(2):1589-1593.
14. Stoker SD, Wildeman MA, Fles R, Indrasari SR, Herdini C, Wildeman PL, van Diessen JN, Tjokronagoro M, Tan IB. A prospective study: current problems in radiotherapy for nasopharyngeal carcinoma in yogyakarta, indonesia. PLoS One. 2014 Jan 23;9(1):e85959. doi: 10.1371/journal.pone.0085959. PMID: 24465811; PMCID: PMC3900459.
15. Prapyatiningsih Y. EPIDEMIOLOGY STUDY OF NPC PATIENTS IN BANGLI HOSPITAL AT 2015-2017. IJNPC. 2020 Mar 18;2(01):13–4.
16. Nafisa IM, Utama MS, Sunardi MA, Adibrata AA. Profile of Nasopharyngeal Cancer Patients who Underwent Radiotherapy in Dr. Hasan Sadikin General Hospital Bandung. Indonesian Journal of Cancer. 2022 Jun 29;16(2):88.
17. Niederman J, Evans A, Kaslow R. Viral Infection of Humans. Epidemiology and Control. In: Viral Infection of Humans Epidemiology and Control. 4th ed. New York: Plenum Publishing Corporation; 1997:253–83.
18. Guo LL, Wang HY, Zheng LS, Wang MD, Cao Y, Li Y, et al. Metastasis of nasopharyngeal carcinoma: What we know and do not know. Vis Cancer Med. 2021;2:4.
19. Yang Y, Li X, Zhou P, Deng X, Wang Y, Dang Q, Zheng Y, Yang D. Survival Effects of Radiotherapy on Patients Newly Diagnosed with Distant Metastatic Nasopharyngeal Carcinoma in Non-High-Incidence Areas. Cancer Manag Res. 2021 Nov 2;13:8169-8178. doi: 10.2147/CMAR.S334958. PMID: 34754237; PMCID: PMC8572028.

***Corresponding author**: Sagung Rai Indrasari. E-mail: srindrasari@ugm.ac.id*

International Journal of Biomedicine 15(3) (2025) 523-526
http://dx.doi.org/10.21103/Article15(3)_OA10

ORIGINAL ARTICLE

Otorhinolaryngology

INTERNATIONAL JOURNAL OF BIOMEDICINE

The Influence of Outer Hair Cells on Tectorial Membrane Waves

Haruki Mizuno[1], Toshiaki Kitamura[1*]

[1]*Kansai University, Osaka, Japan*

Abstract

The cochlea, a vital structure for hearing, comprising the scala media, scala tympani, and scala vestibuli, separated by Reissner's and basilar membranes. The scala media houses the organ of Corti, containing inner and outer hair cells (IHCs and OHCs). Extensive research has explored OHCs, focusing on their mechanical properties and role in cochlear mechanics. This study investigates the impact of OHCs on two types of tectorial membrane (TM) slow waves, termed TM wave 1 and TM wave 2, using modal analysis. The research utilizes a model incorporating the basilar membrane, TM, and OHCs. The study explores how OHCs influence the propagation characteristics of these waves. Results demonstrate that OHCs affect TM wave 1 minimally, with distinctions becoming negligible at higher frequencies. In contrast, OHCs significantly influence TM wave 2, especially in the high-frequency range. The study further explores the frequency-dependent phase and attenuation constants of these waves, revealing substantial effects of OHCs on TM wave 2 across different frequencies and TM widths.(**International Journal of Biomedicine. 2025;15(3):523-526.**)

Keywords: cochlea • outer hair cell • tectorial membrane • modal analysis • propagation characteristics

For citation: Mizuno H, Kitamura T. The Influence of Outer Hair Cells on Tectorial Membrane Waves. International Journal of Biomedicine. 2025;15(3):523-526. doi:10.21103/Article15(3)_OA10

Abbreviations

IHCs, inner hair cells; **OHCs**, outer hair cells; **TM**, tectorial membrane.

Introduction

The cochlea, a snail-shaped structure located in the inner ear, plays a crucial role in the process of hearing. It has three fluid-filled sections, namely the scala media, scala tympani, and scala vestibuli. These three compartments are separated by Reissner's membrane and the basilar membrane. The scala media, also known as the cochlear duct, contains a specialized structure called the organ of Corti. This complex organ is situated between the vestibular and tympanic ducts within the cochlea. The organ of Corti contains rows of outer hair cells (OHCs) and inner hair cells (IHCs). The IHCs are the primary sensory organs of the auditory system. They transduce the vibration of sound into electrical activity in nerve fibers, which is transmitted to the brain. The OHCs play a central role in signal amplification. They are directly coupled to the tectorial membrane (TM) via their hair bundles.

Extensive scientific inquiry has been directed towards understanding outer hair cells and their role in auditory processes.[1-6] Spector et al.[1] investigated the passive and active properties of the cochlear OHC, providing insights into its mechanical characteristics, including Young's moduli, Poisson's ratios, and bending stiffness. They also examined the cell's active behavior, determining coefficients of active force production and limiting parameters of the electromotile response. Their findings contribute to modeling cochlear mechanics at the organ level. Tolomeo et al.[2] studied mammalian outer hair cells and their deformation mechanism and investigated the cortical cytoskeleton's role in directing cell deformation. They found that the cortical lattice exhibited differential stiffness, and the plasma membrane contributed significantly to cell stiffness. Karavitaki et al.[3] investigated the role of OHC somatic motility in cochlear micromechanics and its impact on hearing sensitivity. Using a cochlear preparation, they observed significantly greater motion in OHCs, Deiter's cells, and Hensen's cells than in other structures. Dewey et al.[4] examined the influence of bundle stiffness and the attachment of the TM on cochlear vibrations and their contribution to auditory sensation. Through the study of

mutant mice with reduced bundle stiffness or detached TM, the researchers discovered that decreased bundle stiffness led to a narrowing of tuning and a reduction in the high-frequency range of vibratory responses.

The previous studies have shown that there are two types of TM slow waves, which we refer to as TM wave 1 and TM wave 2.[7,8] Figure 1 illustrates the TM displacement of (a) TM wave 1 and (b) TM wave 2, respectively, when f = 10 kHz. The amplitude and direction of the displacement are depicted by the vectors. The displacement of TM wave 1 is primarily located at the limbal attachment zone of TM, while the displacement of TM wave 2 is concentrated at the tip of the main body of TM at a high frequency (f = 10 kHz).

This study investigated the influence of OHCs on the two types of TM waves using modal analysis. We considered an analysis model composed of the basilar membrane, TM, and OHCs. The analysis model without the OHCs was also utilized for comparison. Here, we discuss how the OHCs affect the propagation characteristics of the two types of TM waves.

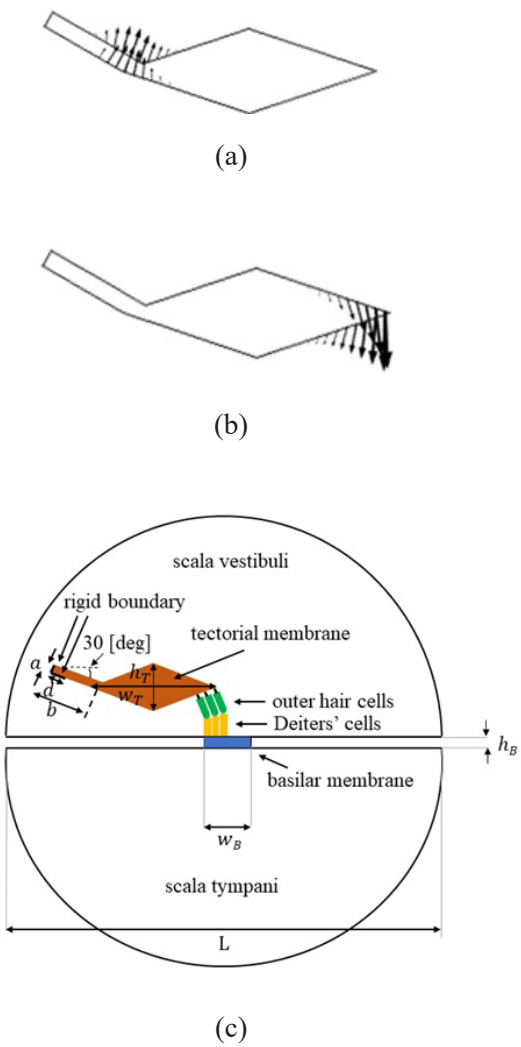

Fig. 1. *TM displacement of (a) TM wave 1 and (b) TM wave 2, and (c) analysis model.*

Materials and Methods

The organ of Corti sits between the TM and the basilar membrane, housing three rows of OHCs as shown in Fig. 1(c). This study examined how OHCs affect the waves on the TM. We used Comsol Multiphysics, a finite element method-based software, to analyze TM wave properties such as phase and attenuation constants. Each OHC is supported by Deiters' cells and has stereocilia on top. Deiters' cells are on the basilar membrane, and stereocilia attach to the TM above. Both OHCs and Deiters' cells have a Young's modulus of 3 kPa, while stereocilia have a Young's modulus of 100 kPa.[9] The basilar membrane parameters are fixed: width (w_B) = 0.3 mm, thickness (h_B) = 5 μm, and Young's modulus (E_B) = 26.5 MPa.[10] The Young's modulus (E_T) of the TM is 50 kPa.[7] The limbal attachment zone and the spiral limbus are firmly fastened, modeled as a rigid boundary (d = 30 μm, a = 10 μm, b = 50 μm). We varied the width (w_T) of TM as a parameter. Here, the ratio between the width (w_T) and thickness (h_T) is fixed as $w_T = 3h_T$. The chamber radius remains constant at r = 0.5 mm. Both the TM and basilar membrane possess Poisson's ratio of 0.49 and a density of 1.2×10^3 kg/m^3.[11,12] The fluid possesses a bulk modulus of 2.2×10^9 Pa, a density of 1.034×10^3 kg/m^3, and a viscosity of 2.8×10^{-3} Pa·s.[11,12]

Results and Discussion

Figure 2 displays the frequency characteristics of phase constants and attenuation constants for TM wave 1 and TM wave 2, including the results of the analysis model in which the OHCs are excluded. As shown in Fig. 1(a), the TM wave 1 field concentrates in the limbal attachment zone, intensifying in the high-frequency range. Consequently, in the phase characteristics depicted in Fig. 2(a), differences based on the presence or absence of OHCs are minimal. As the frequency increases, these distinctions become almost negligible. In contrast, Fig. 1(b) illustrates the TM wave 2 field focusing on the tip of the TM main body. Thus, in the phase characteristics of Fig. 2(b), the influence of OHCs is prominent across all frequency domains, especially in the high-frequency range where the field concentration is significant, leading to substantial differences based on the presence or absence of OHC. Fig. 2(c) makes it evident that the influence of OHCs on the attenuation constants of TM wave 1 is remarkable in the lower frequency region compared to the phase constants shown in Fig. 2(a). As the frequency increases, the influence diminishes because the field concentrates in the limbal attachment zone, as mentioned above. Conversely, the influence on the attenuation constants of TM wave 2 becomes more pronounced with increasing frequency, as shown in Fig. 2(d). This is due to the TM wave 2 field becoming more concentrated at the tip of the TM main body. In most cases, OHCs have the effect of decreasing attenuation constants.

The phase and attenuation constants of TM wave 1 and TM wave 2, dependent on the width (w_T) of the TM, are depicted in Figure 3. Here, the ratio between the width (w_T) and thickness

(h_T) is fixed at $w_T = 3h_T$. We chose the acoustic frequencies for this analysis as $f = 5$ and 10 kHz. Fig. 3(a) shows that when $f = 10$ kHz, the phase constants of TM wave 1 are hardly affected by the presence or absence of OHCs, regardless of the TM width. In contrast, when $f = 10$ kHz, they are strongly affected for low frequency, and the influence of OHCs becomes stronger as the TM width decreases because the field concentration weakens and spreads to the OHCs due to the lower frequency and the smaller TM size. Fig. 3(b) illustrates that the influence of OHCs on the phase constants of TM wave 2 is considerable regardless of the frequency and the TM width. We can also understand that OHCs affect the phase constants of TM wave 2 more strongly when $f = 5$ kHz. Fig. 3(c) indicates that the influence of OHCs on the attenuation constants of TM wave 1 is stronger than the one on the phase constants in any case of the TM width. We can also understand that the influence becomes stronger as the TM width decreases. On the other hand, Fig. 3(d) shows that compared to TM wave 1, the attenuation constants of TM wave 2 are affected more strongly by OHCs, and the dependence on the TM width decreases.

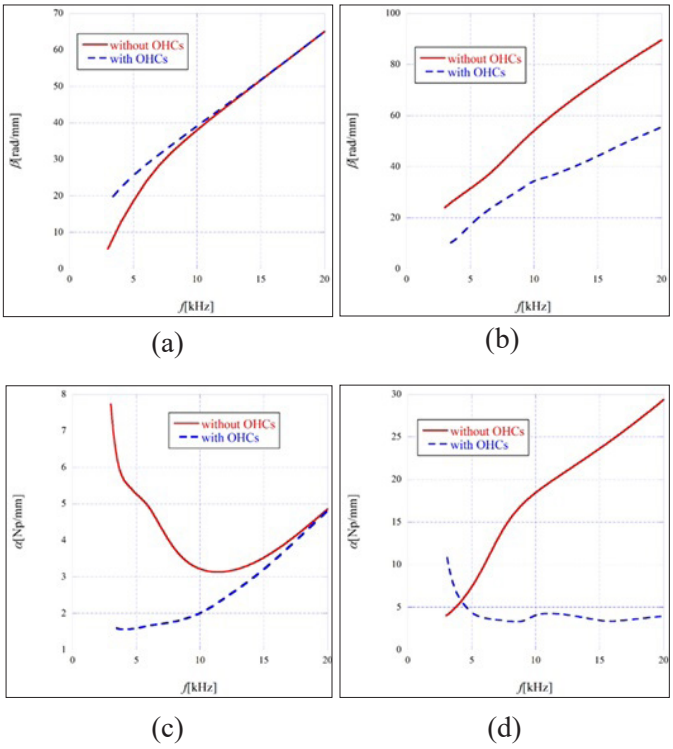

Fig. 2. *Frequency characteristics of phase and attenuation constants.*

Note: Phase constant of (a) TM wave 1 and (b) TM wave 2 and attenuation constant of (c) TM wave 1 and (d) TM wave 2 are shown.

Conclusion

This study investigated the influence of OHCs on the propagation characteristics of two types of TM waves—TM wave 1 and TM wave 2—by employing modal analysis using finite element method-based software.

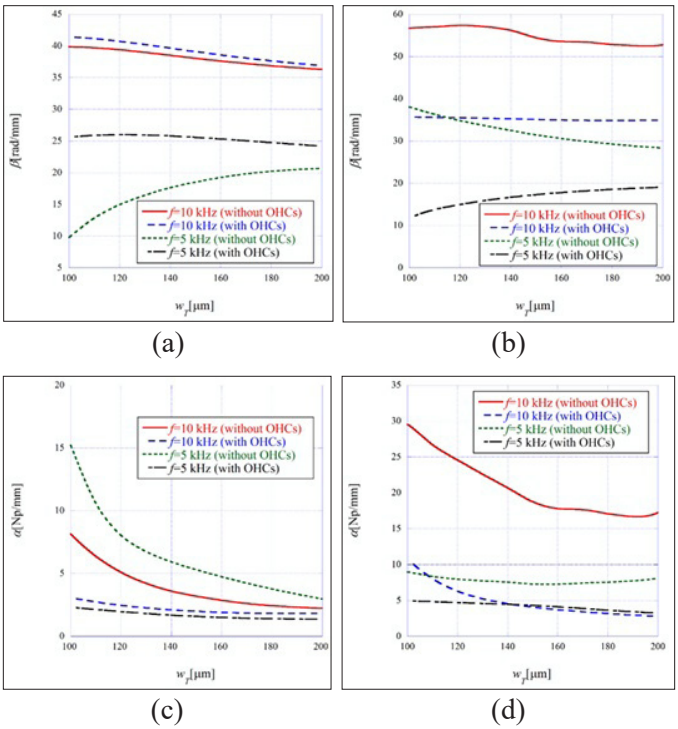

Fig. 3. *Phase and attenuation constants as a function of TM width w_T.*

Note: Phase constant of (a) TM wave 1 and (b) TM wave 2 and attenuation constant of (c) TM wave 1 and (d) TM wave 2 are shown.

For TM wave 1, the concentration in the limbal attachment zone and the subsequent diminishing influence of OHCs at higher frequencies suggest a small influence from OHCs. On the other hand, TM wave 2, with its concentration at the tip of the TM main body, experiences a more pronounced impact from OHCs across all frequency domains, especially in the high-frequency range. The examination of phase and attenuation constants with varying TM widths indicates noteworthy trends. The influence of OHCs on TM wave 1 is more pronounced in the attenuation constants than in the phase constants, particularly at lower frequencies and smaller TM widths. In contrast, for TM wave 2, the attenuation constants are affected more strongly by OHCs than by TM wave 1, and the dependence on TM width decreases. This research contributes valuable insights into the intricate interplay between OHCs and TM waves, shedding light on their roles in cochlear mechanics and hearing sensitivity.

Competing Interests

The authors declare that they have no competing interests.

References

1. Spector AA, Brownell WE, Popel AS. Mechanical and electromotile characteristics of auditory outer hair cells. Med

Biol Eng Comput. 1999 Mar;37(2):247-51. doi: 10.1007/BF02513294. PMID: 10396830.
2. Tolomeo JA, Steele CR, Holley MC. Mechanical properties of the lateral cortex of mammalian auditory outer hair cells. Biophys J. 1996 Jul;71(1):421-9. doi: 10.1016/S0006-3495(96)79244-5. PMID: 8804625; PMCID: PMC1233493.
3. Karavitaki KD, Mountain DC. Imaging electrically evoked micromechanical motion within the organ of corti of the excised gerbil cochlea. Biophys J. 2007 May 1;92(9):3294-316. doi: 10.1529/biophysj.106.083634. Epub 2007 Feb 2. PMID: 17277194; PMCID: PMC1852364.
4. Dewey JB, Xia A, Müller U, Belyantseva IA, Applegate BE, Oghalai JS. Mammalian Auditory Hair Cell Bundle Stiffness Affects Frequency Tuning by Increasing Coupling along the Length of the Cochlea. Cell Rep. 2018 Jun 5;23(10):2915-2927. doi: 10.1016/j.celrep.2018.05.024. PMID: 29874579; PMCID: PMC6309882.
5. Furness DN, Mahendrasingam S, Ohashi M, Fettiplace R, Hackney CM. The dimensions and composition of stereociliary rootlets in mammalian cochlear hair cells: comparison between high- and low-frequency cells and evidence for a connection to the lateral membrane. J Neurosci. 2008 Jun 18;28(25):6342-53. doi: 10.1523/JNEUROSCI.1154-08.2008. PMID: 18562604; PMCID: PMC2989617.
6. Aranyosi AJ, Freeman DM. Sound-induced motions of individual cochlear hair bundles. Biophys J. 2004 Nov;87(5):3536-46. doi: 10.1529/biophysj.104.044404. Epub 2004 Aug 17. PMID: 15315953; PMCID: PMC1304819.
7. Kitamura T. Mode analysis of tectorial membrane in cochlea. Biomedical and Pharmacology Journal. 2021; 14: 1389–1395. doi: 10.13005/bpj/2241
8. Kitamura T, Ueno T. Attenuation characteristics of tectorial membrane wave. Akustika. 2022; 43: 60-64.
9. Ni G, Elliott SJ, Baumgart J. Finite-element model of the active organ of Corti. J R Soc Interface. 2016 Feb;13(115):20150913. doi: 10.1098/rsif.2015.0913. PMID: 26888950; PMCID: PMC4780563.
10. Gan RZ, Reeves BP, Wang X. Modeling of sound transmission from ear canal to cochlea. Ann Biomed Eng. 2007 Dec;35(12):2180-95. doi: 10.1007/s10439-007-9366-y. Epub 2007 Sep 18. PMID: 17882549.
11. Koike T, Sakamoto C, Sakashita T, Hayashi K, Kanzaki S, Ogawa K. Effects of a perilymphatic fistula on the passive vibration response of the basilar membrane. Hear Res. 2012 Jan;283(1-2):117-25. doi: 10.1016/j.heares.2011.10.006. Epub 2011 Nov 15. PMID: 22115725.
12. De Paolis A, Bikson M, Nelson JT, de Ru JA, Packer M, Cardoso L. Analytical and numerical modeling of the hearing system: Advances towards the assessment of hearing damage. Hear Res. 2017 Jun;349:111-128. doi: 10.1016/j.heares.2017.01.015. Epub 2017 Feb 2. PMID: 28161584; PMCID: PMC7000179.

***Corresponding author**: Professor Toshiaki Kitamura, Kansai University, Osaka, Japan. E-mail: kita@kansai-u.ac.jp*

International Journal of Biomedicine 15(3) (2025) 527-530
http://dx.doi.org/10.21103/Article15(3)_OA11

ORIGINAL ARTICLE

Ophthalmology

INTERNATIONAL JOURNAL OF BIOMEDICINE

Comparative Efficacy of Bimatoprost 0.03% and Travoprost 0.004% in Reducing Intraocular Pressure in Patients with Primary Open-Angle Glaucoma

Gentian Hoxha[1,2], Fëllanza Ismajli Hoxha[2], Flaka Shoshi[2*]

[1]*University of Prishtina "Hasan Prishtina," Prishtina, Kosovo*
[2]*Department of Ophthalmology, University Clinical Center of Kosovo, Prishtina, Kosovo*

Abstract

Background: Glaucoma is a progressive optic neuropathy in which increased intraocular pressure (IOP) is a primary risk factor, leading to vision loss. The present study was initiated to compare the intraocular pressure (IOP)-lowering efficacy of 0.03% bimatoprost and 0.004% travoprost in patients with unilateral primary open-angle glaucoma (POAG).

Methods and Results: A total of 100 patients with POAG were treated with a single hypotensive agent during a 6-month follow-up period. The patients were divided into two groups. Group 1 patients (n=50) were treated with 0.03% bimatoprost, and Group 2 patients (n=50) were treated with 0.004% travoprost. We assessed the IOP at baseline, 1 week, 4 weeks, 12 weeks, and 6 months after treatment.

There were no significant differences between the two treatments at the initial stage. At 1 week and 4 weeks after treatment, the mean IOP significantly decreased from baseline in both groups. There were no significant differences between the two treatments at these stages. After 12 weeks of treatment, IOP continued to decrease effectively in both groups; however, 0.03% bimatoprost provided lower IOP values, and there was a significant difference between groups. In the bimatoprost group, compared to baseline, the reduction was 30.9%, while in the travoprost group, the reduction was 28.3% (P=0.043). The difference was greater after 6 months: in the bimatoprost group, the reduction was 33.0% compared to baseline, while in the travoprost group, the reduction was 29.7% (P=0.033).

Conclusion: The consistently lower IOP values for 0.03% bimatoprost treatment suggest it may be more effective in lowering IOP than 0.004% travoprost.(**International Journal of Biomedicine. 2025;15(3):527-530.**)

Keywords: glaucoma • intraocular pressure • bimatoprost • travoprost

For citation:Hoxha G, Hoxha FI, Shoshi F. Comparative Efficacy of Bimatoprost 0.03% and Travoprost 0.004% in Reducing Intraocular Pressure in Patients with Primary Open-Angle Glaucoma. International Journal of Biomedicine. 2025;15(3):527-530. doi:10.21103/Article15(3)_OA11

Abbreviations

IOP, intraocular pressure; **PGA**, prostaglandin analogues; **POAG,** primary open-angle glaucoma.

Introduction

Glaucoma is a progressive optic neuropathy in which increased intraocular pressure (IOP) is a primary risk factor, leading to vision loss. The treatment of glaucoma aims to decrease the IOP, which is the only treatable risk factor. However, in glaucomatous optic neuropathy, the continuous progression of glaucoma despite a decrease in IOP of ≥ 30% suggests that vascular, genetic, and other factors play an important role in the pathogenesis of the disease.

Lowering IOP reduces the risk of visual field loss in patients with glaucoma and ocular hypertension. Based on the findings of the Early Manifest Glaucoma Trial, it is suggested that every millimeter of IOP lowering corresponds to a reduction in the risk of glaucomatous progression of

***Corresponding author**: Flaka Shoshi, MD, PhD(c). E-mail: flakashoshi@gmail.com*

approximately 10%.[1] The current treatment paradigm for patients with glaucoma or ocular hypertension focuses on reducing the IOP to a target level sufficiently low to preserve the visual field.[2]

A primary goal of medical therapy in glaucoma is to reduce IOP. Due to the significant impact on the reduction of the IOP, prostaglandin analogues, used once daily, have become the most commonly used first-line agents in glaucoma and ocular hypertension.[3-7]

Bimatoprost 0.03% is a potent and highly efficacious monotherapy that allows many patients to achieve low target pressures.[8] Furthermore, several clinical trials have shown that bimatoprost 0.03% monotherapy lowers the IOP more effectively than either latanoprost or timolol.[8,9] Bimatoprost is a prostamide, a synthetic, prostaglandin (PG)-related molecule, that reduces the IOP by increasing both the pressure-sensitive (presumed trabecular meshwork) and the pressure-insensitive (presumed uveoscleral) outflow.[10]

Travoprost 0.004%, a synthetic prostaglandin, F2a receptor agonist, lowers the IOP by increasing the uveoscleral outflow. Many clinical trials have shown that the IOP-lowering efficacy of travoprost monotherapy is superior to that of timolol and roughly equivalent to that of latanoprost.[10-12] Our study aimed to compare the IOP-lowering efficacy of 0.03% bimatoprost and 0.004% travoprost in patients with unilateral primary open-angle glaucoma (POAG).

Materials and Methods

This prospective cohort study was conducted in the Ophthalmology Department at the University Clinical Center of Kosovo (Prishtina, Kosovo) from January 2023 to February 2025. A total of 100 previously untreated patients with newly diagnosed POAG were initially enrolled in the study and randomly assigned to one of two groups in a double-masked fashion. Group 1 patients (n=50) were treated with 0.03% bimatoprost, and Group 2 patients (n=50) were treated with 0.004% travoprost.

Medication was administered at 24-hour intervals (between 20.00 hours and 22.00 hours) every day for 6 months. No other IOP-reducing therapy was permitted.

Primary open-angle glaucoma was diagnosed according to the European Glaucoma Society, based on the presence of typical glaucomatous optic disc damage (asymmetry between the vertical cup: disc ratios > 0.2, thinning of the neuroretinal rim, optic disc haemorrhages, parapapillary atrophy) with glaucomatous visual field loss, open angles, and IOP levels > 21 mmHg.

Data Collection

Eligible patients for the study were patients of both genders, aged ≥ 18 years, and diagnosed as having unilateral primary open-angle glaucomawith IOP of 22–36 mmHg during the pre-study period, who had not received any prior medical treatment to lower IOP or alter cardiovascular status (such as adrenergic agents, calcium channel blockers, carbonic anhydrase inhibitors, angiotensin-converting enzyme inhibitors and/or angiotensin receptor blockers). All subjects included in the study did not have any cardiovascular disease, systemic hypertension, or diabetes mellitus. The exclusion criteria included any corneal abnormalities or other diseases that could interfere with accurate IOP measurement with a Goldmann applanation tonometer.

During the treatment period, scheduled visits were performed at baseline and at the end of weeks 1, 4, 12, and after 6 months of treatment. IOP was measured with a Goldmann applanation tonometer.

Statistical analysis was performed using the statistical software package SPSS version 22.0 (SPSS Inc., Armonk, NY: IBM Corp). Baseline characteristics were summarized as frequencies and percentages for categorical variables and mean (M) ± standard deviation (SD) for continuous variables. The unpaired t-test was used to compare two groups. Group comparisons concerning categorical variables were performed using chi-square test. A probability value of $P<0.05$ was considered statistically significant.

Results

The demographic characteristics of patients included in the study are presented in Table 1. In terms of gender, there were more females in both groups, however, with no significant difference between the groups ($P>0.05$). At baseline, the IOP for both groups were very similar: 26.2±1.9 mmHg in Group 1 and 26.3±1.9 mmHg in Group 1 ($P=0.958$) (Table 1).

Table 1.

Comparison of clinical and demographic characteristics between study groups

	Group 1 (n=50) (Bimatoprost)	Group 2 (n=50) (Travoprost)	*P*-value
Gender n (%) Male Female	 22 (44.0) 28 (56.0)	 21 (42.0) 29 (58.0)	0.999
Age (year) Mean ± SD	64.6 ± 10.6	70.6 ± 10.5	0.068
Mean Baseline IOP (mmHg) Mean ± SD	26.2 ± 1.9	26.3 ± 1.9	0.958

At 1 week and 4 weeks after treatment, the mean IOP significantly decreased from baseline in both groups. There were no significant differences between the two treatments at these stages. After 12 weeks of treatment, IOP continued to decrease effectively in both groups; however, 0.03% bimatoprost provided lower IOP values, and there was a significant difference between groups. In the bimatoprost group, compared to baseline, the reduction was 30.9%, while in the travoprost group, the reduction was 28.3% ($P=0.043$). The difference was greater after 6 months: in the bimatoprost group, the reduction was 33.0% compared to baseline, while in the travoprost group, the reduction was 29.7% ($P=0.033$) (Table 2).

Table 2.

Changes in IOP during scheduled visits in the study groups.

	Group 1 (n=50) (Bimatoprost)	Group 2 (n=50) (Travoprost)	*P*-value
Mean (mmHg) and %IOP change from baseline Mean ± SD (%)			
Baseline	-	-	
1 weeks	5.9 ± 2.0 (22.4%)	5.6 ± 2.0 (21.0%)	0.316
4 weeks	7.7 ± 2.1 (29.1%)	7.1 ± 2.2 (26.6%)	0.071
12 weeks	8.2 ± 2.1 (30.9%)	7.5 ± 2.4 (28.3%)	0.043
6 months	8.8 ± 2.3 (33.0%)	7.9 ± 2.1 (29.7%)	0.038
IOP (mmHg) (Mean ± SD)			
Baseline	26.2 ± 1.9	26.3 ± 1.9	0.958
1 weeks	20.4 ± 1.8	20.7 ± 1.8	0.318
4 weeks	18.6 ± 1.8	19.2 ± 1.6	0.067
12 weeks	18.1 ± 1.7	18.8 ± 1.5	0.045
6 months	17.5 ± 1.2	18.4 ± 1.5	0.0006

Discussion

The American Academy of Ophthalmology preferred practice patterns suggest that reductions of at least 20% from untreated IOP levels should be targeted as a goal of treatment to prevent glaucomatous progression.[13] The findings of our study show that patients treated with bimatoprost 0.03% achieved higher reductions of this magnitude, compared with patients treated with travoprost 0.004%. Moreover, almost 40% had a decrease of at least 30% from baseline. Patients treated with bimatoprost 0.03% were also more likely to experience better clinical outcomes compared to those treated with travoprost 0.004%. Due to poor treatment outcomes and the lack of efficacy, patients in the travoprost group were more likely to discontinue the treatment.

The primary goal of glaucoma treatment is to reduce IOP to the target pressure using a minimal number of medications. The prospective randomized study by Gandolfi et al. and also other studies confirm previous reports,[14-16] demonstrating that additional IOP lowering may be achieved by switching patients who are inadequately controlled on latanoprost to another PGA and reinforces the concept that changing therapy within the PGA class should be considered before adding a second medication if further IOP lowering is required.[17]

In a study by Cantor et al.,[2] there was no significance between-group differences observed in IOP at baseline, at 09:00, 13:00 or 16:00 h (*P*=0.741). After 6 months, both drugs significantly reduced IOP at every time point (*P*<0.001). After 6 months, the mean IOP reduction at 09:00 h was 7.1 mmHg (27.9%) with bimatoprost (n=76) and 5.7 mmHg (23.3%) with travoprost (n=81) (*P*=0.014). At 13:00 h, the mean IOP reduction was 5.9 mmHg with bimatoprost (25.3%) and 5.2 mmHg (22.4%) with travoprost (*P*=0.213). At 16:00 h, the mean IOP reduction was 5.3 mmHg (22.5%) with bimatoprost and 4.5 mmHg (18.9%) (*P*=0.207) with travoprost, similar to our findings. Our results also show that bimatoprost had a higher IOP-lowering efficacy.

In a study of the Egyptian population where seventy-two patients were included in the study, both treatment agents provided statistically significant IOP reductions from baseline at all visits (*P*<0.001); however, bimatoprost provided greater mean IOP reductions from baseline compared to travoprost at each visit. Mean IOP reductions were 8.77 mmHg (33.39%) and 8.42 mmHg (31.54%) at 2 weeks (*P*=0.703), and 8.47 mmHg (31.61%) and 7.84 mmHg (29.50%) at 6 months (*P*=0.536) for bimatoprost and travoprost, respectively. IOP in the two groups at 2 weeks were ≤18 mmHg in 20(58.8%) versus 19(50%) eyes (*P*=0.603), and ≤16 mmHg in 12(35%) versus 12(32%) eyes (*P*=0.456); and at 6 months ≤18 mmHg in 22(65%) versus 14(37%) eyes (*P*=0.045), and ≤16 mmHg in 12(35%) versus 7(18%) eyes (*P*=0.037) for bimatoprost and travoprost, respectively.[18] The data from the literature aligns with the findings of our study, where the superiority of bimatoprost in IOP lowering is shown. In terms of safety and side effects, both agents were proven to be safe. In conclusion, the consistently lower IOP values for 0.03% bimatoprost treatment suggest it may be more effective in lowering IOP than 0.004% travoprost.

Ethical Considerations

The study was conducted in accordance with the ethical principles of the WMA Declaration of Helsinki (1964, ed. 2013) and approved by the National Research Ethics Committee (Nr.12084). Written informed consent was obtained from all participants.

Competing Interests

The authors declare that they have no competing interests.

References

1. Heijl A, Leske MC, Bengtsson B, Hyman L, Bengtsson B, Hussein M; Early Manifest Glaucoma Trial Group. Reduction of intraocular pressure and glaucoma progression: results from the Early Manifest Glaucoma Trial. Arch Ophthalmol. 2002 Oct;120(10):1268-79. doi: 10.1001/archopht.120.10.1268. PMID: 12365904.

2. Cantor LB, Hoop J, Morgan L, Wudunn D, Catoira Y; Bimatoprost-Travoprost Study Group. Intraocular pressure-lowering efficacy of bimatoprost 0.03% and travoprost 0.004% in patients with glaucoma or ocular hypertension. Br J Ophthalmol. 2006 Nov;90(11):1370-3. doi: 10.1136/

bjo.2006.094326. Epub 2006 Jul 6. PMID: 16825272; PMCID: PMC1857505.
3. Higginbotham EJ, Schuman JS, Goldberg I, Gross RL, VanDenburgh AM, Chen K, Whitcup SM; Bimatoprost Study Groups 1 and 2. One-year, randomized study comparing bimatoprost and timolol in glaucoma and ocular hypertension. Arch Ophthalmol. 2002 Oct;120(10):1286-93. doi: 10.1001/archopht.120.10.1286. PMID: 12365906.
4. Hedman K, Alm A. A pooled-data analysis of three randomized, double-masked, six-month clinical studies comparing the intraocular pressure reducing effect of latanoprost and timolol. Eur J Ophthalmol. 2000 Apr-Jun;10(2):95-104. doi: 10.1177/112067210001000201. PMID: 10887918.
5. Netland PA, Landry T, Sullivan EK, Andrew R, Silver L, Weiner A, Mallick S, Dickerson J, Bergamini MV, Robertson SM, Davis AA; Travoprost Study Group. Travoprost compared with latanoprost and timolol in patients with open-angle glaucoma or ocular hypertension. Am J Ophthalmol. 2001 Oct;132(4):472-84. doi: 10.1016/s0002-9394(01)01177-1. PMID: 11589866.
6. van der Valk R, Webers CA, Schouten JS, Zeegers MP, Hendrikse F, Prins MH. Intraocular pressure-lowering effects of all commonly used glaucoma drugs: a meta-analysis of randomized clinical trials. Ophthalmology. 2005 Jul;112(7):1177-85. doi: 10.1016/j.ophtha.2005.01.042. PMID: 15921747.
7. McKee HD, Gupta MS, Ahad MA, Saldaña M, Innes JR. First-choice treatment preferences for primary open-angle glaucoma in the United Kingdom. Eye (Lond). 2005 Aug;19(8):923-4. doi: 10.1038/sj.eye.6701674. PMID: 15375365.
8. Noecker RS, Dirks MS, Choplin NT, Bernstein P, Batoosingh AL, Whitcup SM; Bimatoprost/Latanoprost Study Group. A six-month randomized clinical trial comparing the intraocular pressure-lowering efficacy of bimatoprost and latanoprost in patients with ocular hypertension or glaucoma. Am J Ophthalmol. 2003 Jan;135(1):55-63. doi: 10.1016/s0002-9394(02)01827-5. PMID: 12504698.
9. Simmons ST, Dirks MS, Noecker RJ. Bimatoprost versus latanoprost in lowering intraocular pressure in glaucoma and ocular hypertension: results from parallel-group comparison trials. Adv Ther. 2004 Jul-Aug;21(4):247-62. doi: 10.1007/BF02850157. PMID: 15605619.
10. Brubaker RF. Mechanism of action of bimatoprost (Lumigan). Surv Ophthalmol. 2001 May;45 Suppl 4:S347-51. doi: 10.1016/s0039-6257(01)00213-2. PMID: 11434937.
11. Orengo-Nania S, Landry T, Von Tress M, Silver LH, Weiner A, Davis AA; Travoprost Study Group. Evaluation of travoprost as adjunctive therapy in patients with uncontrolled intraocular pressure while using timolol 0.5%. Am J Ophthalmol. 2001 Dec;132(6):860-8. doi: 10.1016/s0002-9394(01)01257-0. PMID: 11730649.
12. Parrish RK, Palmberg P, Sheu WP; XLT Study Group. A comparison of latanoprost, bimatoprost, and travoprost in patients with elevated intraocular pressure: a 12-week, randomized, masked-evaluator multicenter study. Am J Ophthalmol. 2003 May;135(5):688-703. doi: 10.1016/s0002-9394(03)00098-9. PMID: 12719078.
13. Gedde SJ, Vinod K, Wright MM, Muir KW, Lind JT, Chen PP, Li T, Mansberger SL; American Academy of Ophthalmology Preferred Practice Pattern Glaucoma Panel. Primary Open-Angle Glaucoma Preferred Practice Pattern®. Ophthalmology. 2021 Jan;128(1):P71-P150. doi: 10.1016/j.ophtha.2020.10.022. Epub 2020 Nov 12. PMID: 34933745.
14. Gandolfi SA, Cimino L. Effect of bimatoprost on patients with primary open-angle glaucoma or ocular hypertension who are nonresponders to latanoprost. Ophthalmology. 2003 Mar;110(3):609-14. doi: 10.1016/S0161-6420(02)01891-2. PMID: 12623831.
15. Williams RD. Efficacy of bimatoprost in glaucoma and ocular hypertension unresponsive to latanoprost. Adv Ther. 2002 Nov-Dec;19(6):275-81. doi: 10.1007/BF02853173. PMID: 12665048.
16. Kaback M, Geanon J, Katz G, Ripkin D, Przydryga J; START Study Group. Ocular hypotensive efficacy of travoprost in patients unsuccessfully treated with latanoprost. Curr Med Res Opin. 2004 Sep;20(9):1341-5. doi: 10.1185/030079904125004448. PMID: 15383181.
17. European Glaucoma Society Terminology and Guidelines for Glaucoma, 4th Edition - Chapter 2: Classification and terminologySupported by the EGS Foundation: Part 1: Foreword; Introduction; Glossary; Chapter 2 Classification and Terminology. Br J Ophthalmol. 2017 May;101(5):73-127. doi: 10.1136/bjophthalmol-2016-EGSguideline.002. Epub 2017 Apr 18. PMID: 28424171; PMCID: PMC5583685.
18. Macky TA. Bimatoprost versus travoprost in an Egyptian population: a hospital-based prospective, randomized study. J Ocul Pharmacol Ther. 2010 Dec;26(6):605-10. doi: 10.1089/jop.2010.0068. Epub 2010 Oct 29. PMID: 21034177.

International Journal of Biomedicine 15(3) (2025) 531-534
http://dx.doi.org/10.21103/Article15(3)_OA12

ORIGINAL ARTICLE

Ophthalmology

INTERNATIONAL JOURNAL OF BIOMEDICINE

The Relationship between Preoperative Astigmatism and Postoperative Astigmatism Induced by Cataract Surgery and Monofocal IOL Implantation

Flaka Shoshi[1,2], Fitore Shoshi[2*], Ariana Shoshi[3,4,5], Berat Fazliu[6], Ylli Shoshi[7,5], Mire Shoshi[4]

[1]*Department of Ophthalmology, Semmelweis University, Budapest, Hungary*
[2]*Department of Ophthalmology, University Clinical Center of Kosovo, Prishtina, Kosovo*
[3]*Department of Orthodontics, University Clinical Center of Kosovo, Prishtina, Kosovo*
[4]*AMECC "Rezonanca," Prishtina, Kosovo*
[5]*Doctoral School of Dental Medicine, University of Zagreb, Zagreb, Croatia*
[6]*Faculty of Medicine, University of Prishtina, Prishtina, Kosovo*
[7]*Department of Maxillofacial Surgery, University Clinical Center of Kosovo, Prishtina, Kosovo*

Abstract

Background: Cataract is one of the most common ophthalmic disorders among older adults. Even though phacoemulsification is the standard method of treatment, with the improvement of surgical techniques and intraocular lens (IOL) models, the expectations of both patients and physicians have increased. This study aimed to determine the correlation between the pre-existing astigmatism and postoperative astigmatism after cataract surgery and monofocal IOL implantation.

Methods and Results: This retrospective, observational study included the data of 101 patients who underwent cataract surgery with phacoemulsification and monofocal IOL implantation over a 12-month period. The data of patients were collected in two different periods: preoperatively and 2 months postoperatively. All patients underwent a detailed ophthalmic examination with the slit lamp, and the astigmatism was evaluated using the autokeratoferactometer, and the central corneal thickness (CCT) was measured using optical coherence tomography. We divided our patients based on the type of cataract (presenile and senile cataract) and based on the CCT into two groups: Group 1 (n=29): CCT < 550 µm and Group 2 (n=72): CCT ≥ 550 µm. In patients of Group 1, there was a pre-existing astigmatism of 0.66±1.16 dcy; in Group 2, there was a lower pre-existing astigmatism of -0.15±1.09 dcyl; however, there was no statistically significant difference between the groups (P=0.092). The 2-month postoperative astigmatism was -0.59±1.11 dcyl in Group 1 and -0.32± 1.14 dcyl in Group 2, and there was no statistically significant difference between the groups (*P*=0.315). Through regression analysis, we obtained a statistically significant correlation (R=0.7972, *P*<0.0001) between the pre-existing astigmatism and the 2-month postoperative astigmatism. According to our results, the 2-month postoperative astigmatism was affected by the pre-existing astigmatism by 63.5%.

Conclusion: there is a statistically significant correlation between a pre-existing astigmatism and a postoperative astigmatism in patients who undergo cataract surgery and are implanted with monofocal IOLs. Awareness of this correlation by physicians may help to minimize patients' postoperative refractive error and produce better postoperative outcomes after cataract surgery. (**International Journal of Biomedicine. 2025;15(3):531-534.**)

Keywords: astigmatism • cataract surgery • intraocular lens • central corneal thickness

For citation: Shoshi F, Shoshi F, Shoshi A, Fazliu B, Shoshi Y, Shoshi M. The Relationship between Preoperative Astigmatism and Postoperative Astigmatism Induced by Cataract Surgery and Monofocal IOL Implantation. International Journal of Biomedicine. 2025;15(3):531-534. doi:10.21103/Article15(3)_OA12

Abbreviations

CCT, central corneal thickness; **Dcyl**, cylinder diopters, **IOL**, intraocular lens.

Introduction

Cataract, as an ophthalmic disorder, remains one of the preventable diseases that causes blindness in 50% of patients in low-income countries. Cataracts are, in most cases, a side effect of aging;[1] their treatment with phacoemulsification is the most appropriate method. With the ongoing developments in surgical techniques, both surgeons and patients have much higher expectations for postoperative outcomes.[2-4] The demand to minimize postoperative refractive error and to have better postoperative outcomes after cataract surgery is increasing.[4] Among refractive errors, postoperative residual astigmatism may result in reduced unaided distance visual acuity, which in turn may hinder satisfactory postoperative results.[5] Spectacle independence for distance activities is unlikely unless patients achieve ≤0.50 diopters of astigmatism after surgery.[6] One very important factor that plays a key role in postoperative astigmatism after cataract surgery is the pre-existing astigmatism, especially in cases where the IOL selection is limited to monofocal ones.

This study aimed to determine the correlation between the pre-existing astigmatism and postoperative astigmatism after cataract surgery and monofocal IOL implantation.

Materials and Methods

This retrospective, observational study included the data of 101 patients who underwent cataract surgery with phacoemulsification and monofocal IOL implantation over a 12-month period. The data were collected over that 12-month period, and the cases were treated by surgeons with more than 10 years of experience.

The data of patients were collected in two different periods: preoperatively and 2 months postoperatively. We divided our patients based on the type of cataract (presenile and senile cataract) and based on the central corneal thickness (CCT) into two groups: Group 1: CCT < 550 µm and Group 2: CCT ≥ 550 µm.

Inclusion criteria: patients of all ages and genders diagnosed with presenile or senile cataracts, as well as patients diagnosed with astigmatism before cataract surgery

Exclusion criteria: no history of astigmatism, previous cataract surgery and refractive eye surgery, and other corneal diseases.

All patients underwent a detailed ophthalmic examination with the slit lamp, and the astigmatism was evaluated using the autokeratoferactometer, and the CCT was measured using optical coherence tomography.

Statistical analysis was performed using the statistical software package SPSS version 22.0 (SPSS Inc, Armonk, NY: IBM Corp). The normality of distribution of continuous variables was tested by the Kolmogorov-Smirnov test with the Lilliefors correction and Shapiro-Wilk test. For descriptive analysis, results are presented as mean ± standard deviation (SD), standard error of the mean (SEM) and range. For data with normal distribution, inter-group comparisons were performed using Student's t-test. Differences of continuous variables departing from the normal distribution, even after transformation, were tested by the Mann-Whitney U test. Group comparisons with respect to categorical variables are performed using chi-square test or Fisher's exact test. Linear regression was used to measure the strength of association between two parameters using the R-squared value. The *P*-value of <0.05 was considered statistically significant.

Results

Out of 101 eyes, 93.1% were diagnosed with senile cataract, whereas 6.9% were diagnosed with presenile cataract. Based on the type of cataract and the gender of patients, there was no statistical significance (*P*>0.05). (Table 1)

Table 1.

Type of cataract and gender (F/M) of patients

Type of cataract	F		M		Total	
	n	%	n	%	n	%
Presenile cataract	3	6.4	4	7.4	7	6.9
Senile cataract	44	93.6	50	92.6	94	93.1
Total	47	100.0	54	100.0	101	100.0
Fisher's exact test	*P*=0.9999					

Based on the central corneal thickness, there were 29 patients in Group 1 and 72 patients in Group 2. In patients of Group 1 (CCT < 550 µm), there was a pre-existing astigmatism of 0.66±1.16 dcy; in Group 2 (CCT ≥ 550 µm), there was a lower pre-existing astigmatism of -0.15±1.09 dcyl; however, there was no statistically significant difference between the groups (*P*=0.092) (Table 2).

Table 2.

The pre-existing astigmatism.

Astigmatism (dcyl)	Group 1	Group 2
	n=29 (CCT<550 µm)	n=72 (CCT≥550 µm)
Before the intervention		
Mean ± SD	-0.66 ± 1.16	-0.15 ± 1.09
SEM	0.215	0.128
Range	-2.75 to 1.25	-2.75 to 1.75
Statistics	*P*=0.092	

The 2-month postoperative astigmatism was -0.59± 1.11 dcyl in Group 1 and -0.32± 1.14 dcyl in Group 2, and there was no statistically significant difference between the groups (*P*=0.315) (Table 3). Through regression analysis, we obtained a statistically significant correlation (R=0.7972, *P*<0.0001) between the pre-existing astigmatism and the 2-month postoperative astigmatism (Table 4). According to our results,

the 2-month postoperative astigmatism was affected by the pre-existing astigmatism by 63.5%.

Table 3.

The 2-month postoperative astigmatism.

Astigmatism (dcyl)	Group 1	Group 2
	n=29 (CCT<550 µm)	n=72 (CCT≥550 µm
The 2-month postoperative		
Mean ± SD	-0.59 ± 1.11	-0.32 ± 1.14
SEM	0.206	0.134
Range	-2.25 to 1.5	-2.25 to 2.50
P-value	*P*=0.315	

Table 4.

Regression analysis for pre-existing astigmatism and 2-month postoperative astigmatism.

R-squared	0.6355
Adjusted R-squared	0.6303
R	0.7972
P-value	<0.0001

Discussion

A refractive error after cataract surgery is one of the main reasons for postoperative patient dissatisfaction. Patients with cataracts who have pre-existing astigmatism and receive monofocal intraocular lenses, may require additional refractive procedures like limbal relaxing incisions, corneal incisions in the steep meridian, and femtosecond laser-associated astigmatic keratotomy.[7] A study by Patil et al.[8] showed that the implantation of toric intraocular lenses is the appropriate choice to avoid postoperative astigmatism in patients with pre-existing astigmatism. Like other findings reported in the literature,[9-11] our study shows that postoperative residual astigmatism is affected by the pre-existing astigmatism by 63.5%. The correlation between pre-existing and postoperative astigmatism has been documented in the literature; therefore, the implantation of premium intraocular lenses is recommended to correct pre-existing astigmatism.[12] The retrospective study of Schallhorn et al.,[13] including 40,289 eyes, showed that the most accurate method to correct the pre-existing astigmatism is the implantation of toric lenses. In patients with a pre-existing astigmatism between 0.75 dcyl and 1.25 dcyl, toric lens implantation resulted in better refractive outcomes, compared to the group where pre-existing astigmatism was left untreated. In our previous study comparing the refractive outcomes after cataract surgery based on the IOL model implanted, we reported that 1-month postoperative refractive outcomes were 35% better in the group treated with premium intraocular lenses.[14]

Conclusion

Our analysis confirmed that there is a statistically significant correlation between a pre-existing astigmatism and a postoperative astigmatism in patients who undergo cataract surgery and are implanted with monofocal intraocular lenses. Awareness of this correlation by physicians may help to minimize patients' postoperative refractive error and produce better postoperative outcomes after cataract surgery.

Ethical Considerations

The study was conducted in accordance with ethical principles of the Declaration of Helsinki (2000; revised October 2013, Fortaleza, Brazil). The study protocol was approved by the Ethics Committee of the Kosovo Chamber of Physicians (Nr. 51/2021 dated 06/10/2021) and the Ethics Committee of the Faculty of Medicine, University of Prishtina (№ 13482 dated 24/12/2021). Written informed consent was obtained from all the participants.

Competing Interests

The authors declare that they have no competing interests.

References

1. Hashemi H, Pakzad R, Yekta A, Aghamirsalim M, Pakbin M, Ramin S, Khabazkhoob M. Global and regional prevalence of age-related cataract: a comprehensive systematic review and meta-analysis. Eye (Lond). 2020 Aug;34(8):1357-1370. doi: 10.1038/s41433-020-0806-3. Epub 2020 Feb 13. PMID: 32055021; PMCID: PMC7376226.
2. Hawker MJ, Madge SN, Baddeley PA, Perry SR. Refractive expectations of patients having cataract surgery. J Cataract Refract Surg. 2005 Oct;31(10):1970-5. doi: 10.1016/j.jcrs.2005.03.065. PMID: 16338569.
3. Tielsch JM, Steinberg EP, Cassard SD, Schein OD, Javitt JC, Legro MW, Bass EB, Sharkey P. Preoperative functional expectations and postoperative outcomes among patients undergoing first eye cataract surgery. Arch Ophthalmol. 1995 Oct;113(10):1312-8. doi: 10.1001/archopht.1995.01100100100038. PMID: 7575266.
4. Webber KJ, Fylan F, Wood JM, Elliott DB. Experiences following cataract surgery - patient perspectives. Ophthalmic Physiol Opt. 2020 Sep;40(5):540-548. doi: 10.1111/opo.12709. Epub 2020 Jul 11. PMID: 32654259.
5. Day AC, Dhariwal M, Keith MS, Ender F, Perez Vives C, Miglio C, Zou L, Anderson DF. Distribution of preoperative and postoperative astigmatism in a large population of patients undergoing cataract surgery in the UK. Br J Ophthalmol. 2019 Jul;103(7):993-1000. doi: 10.1136/bjophthalmol-2018-312025. Epub 2018 Sep 6. PMID: 30190365; PMCID: PMC6591741.
6. Rubenstein JB, Raciti M. Approaches to corneal astigmatism in cataract surgery. Curr Opin Ophthalmol. 2013 Jan;24(1):30-4. doi: 10.1097/ICU.0b013e32835ac853.

7. Chen X, Zhao M, Shi Y, Yang L, Lu Y, Huang Z. Visual outcomes and optical quality after implantation of a diffractive multifocal toric intraocular lens. Indian J Ophthalmol. 2016 Apr;64(4):285-91. doi: 10.4103/0301-4738.182939. PMID: 27221680; PMCID: PMC4901846.
8. Patil MS, Nikose AS, Bharti S. Visual outcome and refractive status with monofocal toric intraocular lens implantation to correct astigmatism during cataract surgery. Indian J Ophthalmol. 2020 Dec;68(12):3016-3019. doi: 10.4103/ijo.IJO_1272_20. PMID: 33229689; PMCID: PMC7857000.
9. Hashemi H, Khabazkhoob M, Soroush S, Shariati R, Miraftab M, Yekta A. The location of incision in cataract surgery and its impact on induced astigmatism. Curr Opin Ophthalmol. 2016 Jan;27(1):58-64. doi: 10.1097/ICU.0000000000000223. PMID: 26569524.
10. Yin XL, Ji ZY, Li XX, Liang XM, Ji SX. Surgical approaches to correct corneal astigmatism at time of cataract surgery: a mini-review. Int J Ophthalmol. 2024 Jul 18;17(7):1370-1374. doi: 10.18240/ijo.2024.07.23. PMID: 39026920; PMCID: PMC11246944.
11. El-Shehawy A, El-Massry A, El-Shorbagy MS, Atef M, Sabry M. Correction of pre-existing astigmatism with phacoemulsification using toric intraocular lens versus spherical intraocular lens and wave front guided surface ablation. BMC Ophthalmol. 2022 Mar 12;22(1):114. doi: 10.1186/s12886-022-02347-5. PMID: 35279107; PMCID: PMC8917725.
12. Icoz M, Yildirim B, Gurturk Icoz SG. Comparison of different methods of correcting astigmatism in cataract surgery. Clin Exp Optom. 2024 May;107(4):409-414. doi: 10.1080/08164622.2023.2239816. Epub 2023 Sep 12. PMID: 37699788.
13. Schallhorn SC, Schallhorn JM. Comparison of Surgical Methods for the Correction of Low Amounts of Corneal Astigmatism during Cataract Surgery. Ophthalmology. 2025 Jun 16:S0161-6420(25)00360-4. doi: 10.1016/j.ophtha.2025.06.011. Epub ahead of print. PMID: 40532854.
14. Shoshi F, Shoshi F, Xhafa A, Nagy ZZ. Refractive Outcomes After Cataract Surgery-The Impact of Preoperative Visual Acuity, the Intraocular Lens Model, and the Surgeon's Experience: An Empirical Analysis of Hungarian and Kosovan Patients. J Clin Med. 2024 Nov 21;13(23):7013. doi: 10.3390/jcm13237013. PMID: 39685470; PMCID: PMC11642209.

***Corresponding author:** Dr. Fitore Shoshi, MD, PhD. Department of Ophthalmology, University Clinical Center of Kosovo, Prishtina, Kosovo. E-mail: shoshifitore@gmail.com*

International Journal of Biomedicine 15(3) (2025) 535-539
http://dx.doi.org/10.21103/Article15(3)_OA13

ORIGINAL ARTICLE

Radiology

INTERNATIONAL JOURNAL OF BIOMEDICINE

Sonographic Evaluation of Gallbladder Distension Based on Interval Fasting Hours: A Prospective Study

Mohammed Alsaadi*

Radiology and Medical Imaging Department, College of Applied Medical Sciences, Prince Sattam Bin Abdulaziz University, Al-Kharj, Saudi Arabia

Abstract

The primary objective of this study was to systematically investigate the relationship between gallbladder (GB) distension and fasting duration (FD) by measuring the length and width of the gallbladder.

Methods and Results: A total of 30 healthy adult male volunteers (mean age: 23 ± 0.20 years; mean BMI: 23.16 ± 1.89 kg/m²) were recruited through convenience sampling. Participants were stratified into three groups based on their FD: Group A (n=10) with FD of 8 hours, Group B (n=10) with FD of 6 hours, and Group C (n=10) with FD of 4 hours. Each participant underwent a standardized GB ultrasound scan, during which the size and characteristics of the GB were measured in both transverse and longitudinal planes.

Longitudinal GB size increased significantly with FD (*P*=0.016): 46.84±8.83 mm (4 hours), 54.82±11.93 mm (6 hours), and 59.63±6.37 mm (8 hours). The transverse size showed no significant difference (*P*=0.193): 19.42±4.60 mm (4 hours), 3.48±5.35 mm (6 hours), and 22.56±5.27 mm (8 hours). GB wall thickness did not differ significantly across the three time points (*P*=0.766): 0.14±0.97 mm (4 hours), 0.22±0.57 mm (6 hours), and 0.42±1.03 mm (8 hours). The GB neck was visualized in 40% of cases at 4 hours and 100% at 6 and 8 hours. Cystic duct visualization showed no significant difference (*P*=0.585), with rates of 40%, 60%, and 60% at 4, 6, and 8 hours, respectively.

Conclusion: Fasting for four hours can provide adequate GB visualization in most healthy individuals, with no significant issues evaluating the wall, cystic duct, or lumen. Prolonged fasting durations may improve the visualization of the GB neck, although they are not always necessary. Standardizing the fasting duration to four hours may optimize workflow while preserving diagnostic quality in routine practice.(**International Journal of Biomedicine. 2025;15(3):535-539.**)

Keywords: gallbladder distension • fasting duration • ultrasound visualization

For citation: Alsaadi M. Sonographic Evaluation of Gallbladder Distension Based on Interval Fasting Hours: A Prospective Study. International Journal of Biomedicine. 2025;15(3):535-539. doi:10.21103/Article15(3)_OA13

Introduction

Ultrasound is deemed the first-line investigation for the initial assessment of the gallbladder (GB) due to its ability to provide substantial information about anatomy and the appearance of pathology with high sensitivity.[1] An essential prerequisite for optimal sonographic visualization of the GB is adequate distension, typically achieved through a fasting period that allows bile to accumulate within the GB lumen.[2] A well-distended GB offers enhanced acoustic contrast, more precise visualization of the GB wall, and improved detection of intraluminal abnormalities such as sludge, gallstones, polyps, and wall thickening.[3]

Although current clinical practice generally recommends fasting 6 to 8 hours before GB sonography, there is significant variability in the literature regarding the minimum effective fasting duration (FD) necessary for optimal GB distension.[4] Excessively prolonged fasting may lead to dehydration-related changes or paradoxical contraction due to the influence of hormones such as cholecystokinin. In contrast, inadequate fasting may result in suboptimal imaging and the potential for missed pathology.[5,6] Furthermore, prolonged fasting may present clinical challenges for specific populations. Diabetic patients are at risk of hypoglycemia due to delayed meals or

***Correspondence:** Dr. Mohammed Alsaadi, MSc, Ph.D. E-mail: m.alsaadi@psau.edu.sa*

insulin administration, which can lead to serious complications during extended fasting.[7]

Similarly, individuals with chronic illnesses often require timely morning medications, such as antihypertensives, antiepileptics, or cardiac drugs, which are usually taken with food. Delaying these medications to accommodate long fasting periods for imaging may compromise treatment adherence and metabolic control.[8] Therefore, standardizing a minimum FD that ensures adequate GB distension without compromising diagnostic accuracy is essential for enhancing the reliability and efficiency of ultrasound evaluations while also minimizing potential health risks in vulnerable patient groups.[9]

The primary objective of this study was to systematically investigate the relationship between GB distension and FD by measuring the length and width of the GB. By evaluating GB dimensions at various fasting intervals, this study aims to determine the minimum fasting period necessary for adequate visualization and diagnostic assessment of the GB. Addressing this knowledge gap may enhance sonographic protocols, reduce unnecessary imaging delays, and optimize the diagnostic efficacy of abdominal ultrasound in clinical practice.

Materials and Methods

Study Design

This study utilized a prospective observational design to assess the effect of varying fasting intervals on GB distension using ultrasound. It was a quantitative investigation conducted at the ultrasound diagnostic unit. The aim was to observe and compare sonographic GB distension patterns among healthy fasting participants for different durations. To reduce bias, all participants underwent their first ultrasound scan as part of this study, thereby minimizing the influence of prior imaging or known clinical conditions. Furthermore, the principal investigator was blinded to the duration of fasting.

A total of 30 healthy adult volunteers were recruited through convenience sampling. Participants were stratified into three groups based on their FD: Group A (n=10) with FD of 8 hours, Group B (n=10) with FD of 6 hours, and Group C (n=10) with FD of 4 hours. Each participant underwent a standardized GB ultrasound scan, during which the size and characteristics of the GB were measured in both transverse and longitudinal planes. The inclusion criteria were healthy adult university faculty members or students, the ability and willingness to fast as instructed, and the provision of written informed consent. The exclusion criteria were age under 18, inability to provide informed consent, history of GB disease or abdominal surgery. The sample size was determined based on prior studies detecting a 10% difference in GB size with 80% power (α=0.05).

Ultrasound Technique and Data Collection

Ultrasound examinations were conducted using a Hitachi EUB-405 ultrasound system (Hitachi Medical, Tokyo, Japan), equipped with a 1–5 MHz curvilinear transducer. Scans were performed in the supine, left lateral decubitus, and sitting positions to evaluate the GB under various postural conditions. Each scan was performed by the principal investigator, who has more than 15 years of experience in ultrasound. Measurements were taken at the largest visualized dimensions in both planes.

The following parameters were assessed: GB size in transverse and longitudinal dimensions, GB wall thickness in both planes, appearance of the cystic duct, and the morphology of the GB neck. All scans were conducted in the morning to minimize circadian variability. Participants were instructed not to consume food or caloric beverages during the fasting period. Data collection was completed within one week to ensure consistency in environmental and procedural conditions.

Statistical Analysis

Data were analysed using IBM SPSS Statistics (Version 28). Descriptive statistics (mean ± SD) summarised continuous variables. One-way ANOVA with Tukey's post-hoc test compared GB sizes and wall thickness across fasting groups. Paired t-tests assessed differences in GB dimensions between body positions. Chi-square or Fisher's exact tests evaluated categorical outcomes (neck/cystic duct visualisation). Effect sizes (eta-squared for ANOVA, Cohen's d for t-tests) were calculated. A P-value of <0.05 indicated statistical significance.

Results

The study included 30 male participants (mean age: 23 ± 0.20 years; mean BMI: 23.16 ± 1.89 kg/m²). Longitudinal GB size increased significantly with FD ($F(2,27) = 5.12$, $P = 0.016$, $\eta^2 = 0.27$). Post-hoc tests revealed significant differences between 4 and 8 hours ($P = 0.012$, Cohen's d = 1.36) but not between 4 and 6 hours ($P = 0.184$) or 6 and 8 hours ($P = 0.573$). The mean longitudinal sizes were 46.84±8.83 mm (4 hours), 54.82±11.93 mm (6 hours), and 59.63±6.37 mm (8 hours). The transverse size showed no significant difference ($F(2,27) = 1.78$, $P = 0.193$, $\eta^2 = 0.12$), with means of 19.42±4.60 mm, 23.48±5.35 mm, and 22.56±5.27 mm, respectively (Table 1, Figure 1).

Table 1.

GB size (mm) at different fasting durations (longitudinal and transverse views).

Measurement	FD	n	Mean	SD	95% CI	*P*-value
Longitudinal Size	4 hours	10	46.84	8.83	(40.53, 53.15)	0.016
	6 hours	10	54.82	11.93	(46.29, 63.35)	
	8 hours	10	59.63	6.37	(55.07, 64.19)	
Transverse Size	4 hours	10	19.42	4.60	(16.13, 22.71)	0.193
	6 hours	10	23.48	5.35	(19.65, 27.31)	
	8 hours	10	22.56	5.27	(18.79, 26.33)	

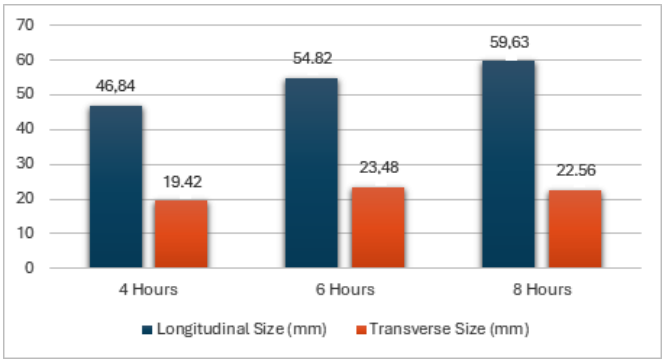

Figure 1. *Longitudinal and transverse GB sizes, annotating the significant difference between 4 and 8 hours for longitudinal size.*

GB wall thickness did not differ significantly across the three time points (F (2,27) = 0.27, P = 0.766, η^2 = 0.02): 0.14±0.97 mm (4 hours), 0.22±0.57 mm (6 hours), and 0.42±1.03 mm (8 hours) (Table 2).

Table 2.

GB wall thickness (mm) at different fasting durations.

FD	n	Mean	SD	95% CI	*P*-value
4 hours	10	0.14	0.97	(-0.55, 0.83)	0.766
6 hours	10	0.22	0.57	(-0.19, 0.63)	
8 hours	10	0.42	1.03	(-0.31, 1.15)	

GB neck visualization improved significantly with extended fasting (P = 0.001). The GB neck was visualized in 40% of cases at 4 hours and 100% at 6 and 8 hours. Cystic duct visualization showed no significant difference (P = 0.585), with rates of 40%, 60%, and 60% at 4, 6, and 8 hours, respectively (Table 3, Figure 2).

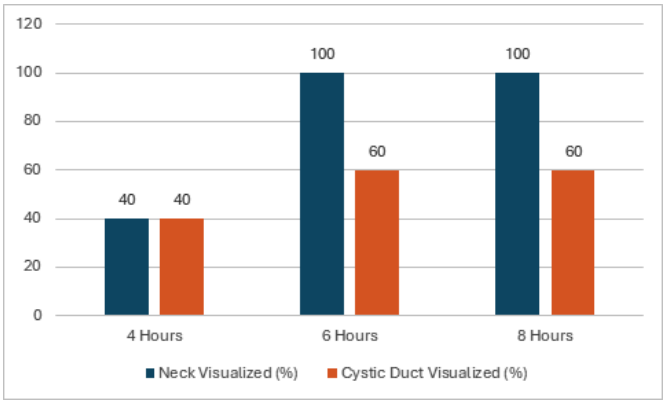

Figure 2. *Visualization rates for the neck and cystic duct, with an annotation highlighting the significant difference in neck visualisation and corrected data.*

Table 3.

The visualization of GB structures (neck and cystic duct) at different FD.

Structure	Visualization	4 Hours	6 Hours	8 Hours	*P*-value
Neck	Yes	4 (40%)	10 (100%)	10 (100%)	0.001
	No	6 (60%)	0 (0%)	0 (0%)	
Cystic Duct	Yes	4 (40%)	6 (60%)	6 (60%)	0.585
	No	6 (60%)	4 (40%)	4 (40%)	

Discussion

In clinical practice, ultrasound remains one of the primary imaging modalities for evaluating gallbladder anatomy and pathology due to its safety profile, non-invasiveness, cost-effectiveness, and high diagnostic sensitivity for detecting gallstones, cholecystitis, polyps, and neoplasms.[10,11] However, the accuracy of sonographic assessment is highly dependent on appropriate gallbladder distension, which is best achieved through adequate fasting.[12] A fully distended gallbladder enables better delineation of the gallbladder wall, more precise visualization of the cystic duct and neck, and improved acoustic contrast for identifying intraluminal or mural abnormalities. This underlines the importance of fasting status as a key pre-analytical variable in the quality of gallbladder ultrasound examinations. Many ultrasound departments instruct their patients to come fasting for such examinations, sometimes for as long as 12 hours, assuming that the gallbladder would otherwise be contracted and difficult to assess, and that fasting patients will have less gas in the duodenum & colon.[13]

The gallbladder functions as a bile reservoir during fasting, regulated by the reduced secretion of cholecystokinin.[5,14,15] This peptide hormone prompts gallbladder contractions and the release of bile after meals. The Society and College of Radiographers and the British Medical Ultrasound Society state patients should fast for 6 hours before their scan to optimise their ultrasound scan.[16] The conventionally recommended fasting times (a minimum of two hours after consumption of clear fluid, six hours after consumption of a light meal, and eight hours after consumption of fried or fatty food.[17] Nonetheless, new research challenges the need for this fasting procedure in healthy individuals without diagnosed biliary issues, indicating that practical imaging might be possible without extended fasting.

Furthermore, certain patient groups may not tolerate prolonged fasting. For instance, diabetic patients might be at risk of low blood sugar if they fast for too long, and others may need to take medications with food in the morning [7,8]. Therefore, it is essential to determine the shortest fasting period necessary to obtain clear, diagnostic images of the gallbladder, especially for these patients. [18]

Our prospective observational study addressed this knowledge gap by comparing the gallbladder sonographic appearance after 4, 6, and 8 hours of fasting in healthy volunteers. The findings indicate that even a 4-hour fasting period was generally sufficient for adequate gallbladder distension, facilitating the visualization of the lumen, wall, and most surrounding anatomical structures. Although gallbladder distension was predictably more pronounced in the 6- and 8-hour groups, the clinical and sonographic significance of this difference was limited, as most examinations in the 4-hour group still met diagnostic standards.

A key observation in our study was that the gallbladder neck was less frequently and less distinctly visualized in the four-hour fasting group, and this difference was statistically significant compared to longer fasting durations. The gallbladder neck can be a site of clinical importance, particularly for detecting impacted stones or subtle anatomical anomalies. Inadequate visualization of this region may result in missed pathology in symptomatic patients, although this risk is likely lower in a healthy screening population like ours.

Conversely, there was no statistically significant difference among the three fasting groups in terms of gallbladder wall thickness or cystic duct appearance, suggesting that these features are less influenced by the degree of distension. Wall thickness remained within normal ranges for all participants, confirming that moderate fasting allows for an accurate assessment of this parameter, which is essential for diagnosing cholecystitis or gallbladder wall edema.

Our study contributes to the expanding body of literature advocating a more flexible approach to fasting protocols before ultrasound. In clinical settings where patient safety, comfort, or logistics may necessitate shorter fasting durations—such as pediatric, geriatric, diabetic, or emergency cases—our findings support the practicality of scanning after a 4-hour fast with acceptable diagnostic quality, provided that clinical suspicion is low and image quality is deemed adequate by the sonographer.

However, the results of this study should be viewed with consideration of its limitations. Our sample included only healthy subjects without any recorded hepatobiliary diseases, and all scans were performed under controlled conditions using standardized equipment and skilled sonographers. Caution is necessary when applying these results to patients with altered gallbladder function, including those with diabetes, biliary dyskinesia, or a history of cholecystitis. Future research involving a more diverse patient population and objective quality assessments of the images would strengthen these findings.

Future Recommendations

Larger-scale studies involving various age groups are highly recommended to validate and apply these findings. Future research should evaluate the diagnostic impact of abbreviated fasting periods in symptomatic patients. Standardized fasting protocols should be developed based on patient risk profiles and imaging requirements.

Conclusion

This study demonstrates that fasting for four hours can provide adequate gallbladder visualization in most healthy individuals, with no significant issues evaluating the wall, cystic duct, or lumen. However, the visibility of the neck is slightly diminished. These results suggest revising fasting guidelines for specific patient groups and enhancing ultrasound scheduling flexibility while preserving diagnostic effectiveness.

Competing Interests

The authors declare that they have no competing interests.

Sources of Funding

The authors extend their appreciation to Prince Sattam bin Abdulaziz University for funding this research work through the project number (PSAU/2024/03/31973).

Ethical Considerations

The study protocol was reviewed and approved by the Prince Sattam bin Abdulaziz University Ethics Committee.All participants provided written informed consent.

References

1. Afonso PD, Eiroa C, Rodríguez M, Martínez L. Ultrasound assessment of gallbladder and biliary tract disorders: diagnostic approach and common pathologies. Radiología. 2020;62(5):406–415.
2. Bai Y, Zhang Y, Zhang H, Zhao Y. Influence of fasting duration on gallbladder volume and contraction index: a sonographic study. Journal of Ultrasound in Medicine.2019;38(8):2171–2176.
3. Yoon WJ, Lee YJ, Kim KW, Lee SS. Sonographic evaluation of the gallbladder: usefulness of adequate fasting in real-time imaging. Ultrasonography. 2015;34(3):211–217.
4. Lee DH, Kim SJ, Park JH, Choi H. Evaluation of gallbladder fasting times and its correlation with sonographic findings in healthy volunteers. BMC Medical Imaging. 2021;21(1):74.
5. Zhu J, Luo X, Wang X, He S. Cholecystokinin-mediated gallbladder contraction in fasting: implications for ultrasonographic visualization. Clinical Imaging. 2017;43:145–150.
6. Iqbal A, Khan S, Siddiqui T. Impact of inadequate fasting on ultrasound diagnosis of gallbladder diseases. Pakistan Journal of Radiology. 2018;28(2):71–74.
7. ElSayed NA, Aleppo G, Aroda VR, Bannuru RR, Brown FM, Bruemmer D, Collins BS, Hilliard ME, Isaacs D,

Johnson EL, Kahan S, Khunti K, Leon J, Lyons SK, Perry ML, Prahalad P, Pratley RE, Seley JJ, Stanton RC, Gabbay RA, on behalf of the American Diabetes Association. 7. Diabetes Technology: Standards of Care in Diabetes-2023. Diabetes Care. 2023 Jan 1;46(Suppl 1):S111-S127. doi: 10.2337/dc23-S007. PMID: 36507635; PMCID: PMC9810474.

8. Krentz AJ, Bailey CJ. Oral antidiabetic agents: current role in type 2 diabetes mellitus. Drugs. 2005;65(3):385-411. doi: 10.2165/00003495-200565030-00005. PMID: 15669880.

9. Khanna R, Kumar M, Khanna S, Shukla HS. Effect of pre-procedural fasting time on gallbladder sonographic visibility: a prospective study. *A*nnals of Gastroenterology. 2014;27(4):345–349.

10. van Breda Vriesman AC, Engelbrecht MR, Smithuis RH, Puylaert JB. Diffuse gallbladder wall thickening: differential diagnosis. AJR Am J Roentgenol. 2007 Feb;188(2):495-501. doi: 10.2214/AJR.05.1712. PMID: 17242260.

11. Bortoff GA, Chen MY, Ott DJ, Wolfman NT, Routh WD. Gallbladder stones: imaging and intervention. Radiographics. 2000 May-Jun;20(3):751-66. doi: 10.1148/radiographics.20.3.g00ma16751. PMID: 10835126.

12. Hashimoto M, Ishikawa T, Nishimura T, Takayama T. Advances in the imaging diagnosis of gallbladder diseases. World J Gastroenterol. 2021;27(7):531–546.

13. Sinan T, Leven H, Sheikh M. Is fasting a necessary preparation for abdominal ultrasound? BMC Med Imaging. 2003 Jul 22;3(1):1. doi: 10.1186/1471-2342-3-1. PMID: 12873354; PMCID: PMC183866.

14. BURTON P, HARPER AA, HOWAT HT, SCOTT JE, VARLEY H. The use of cholecystokinin to test gall bladder function in man. Gut. 1960 Sep;1(3):193-204. doi: 10.1136/gut.1.3.193. PMID: 13689291; PMCID: PMC1413182.

15. Jones MC, Vaqar S. Cholecystokinin Test. 2023 Jan 2. In: StatPearls [Internet]. Treasure Island (FL): StatPearls Publishing; 2025 Jan–. PMID: 32809658.

16. Sondh RS, Mankotia R. Reducing prolonged fasting for abdominal ultrasound scans. BMJ Open Qual. 2023 Aug;12(3):e002396. doi: 10.1136/bmjoq-2023-002396. PMID: 37541691; PMCID: PMC10407382.

17. Chang JE, Kim H, Won D, Lee JM, Jung JY, Min SW, Hwang JY. Ultrasound assessment of gastric content in fasted patients before elective laparoscopic cholecystectomy: a prospective observational single-cohort study. Can J Anaesth. 2020 Jul;67(7):810-816. English. doi: 10.1007/s12630-020-01668-7. Epub 2020 Apr 20. PMID: 32314262.

18. Ehrenstein BP, Froh S, Schlottmann K, Schölmerich J, Schacherer D. To eat or not to eat? Effect of fasting prior to abdominal sonography examinations on the quality of imaging under routine conditions: A randomized, examiner-blinded trial. Scand J Gastroenterol. 2009;44(9):1048-54. doi: 10.1080/00365520903075188. PMID: 19562622.

International Journal of Biomedicine 15(3) (2025) 540-544
http://dx.doi.org/10.21103/Article15(3)_OA14

ORIGINAL ARTICLE

Radiology

INTERNATIONAL JOURNAL OF BIOMEDICINE

Sonographic Findings in the Posterior Segment of the Eye in Pre-Operative Cataract Patients

Rania Mohammed Ahmed*

Department of Radiological Sciences, College of Applied Medical Sciences, Taif University, Taif, Saudi Arabia

Abstract

Background: Cataract surgery is a common and cost-effective procedure aimed at preventing blindness by removing the lens opacity that obstructs the visualization of the posterior segment of the eye. Visualizing the posterior segment is crucial for predicting visual outcomes after surgery. This study aimed to determine abnormal sonographic findings in the posterior segment of the eye globe among cataract patients and the associated risk factors.

Methods and Results: This retrospective study was conducted at Kafaat Medical Center (Makkah Almokaramah city, Saudi Arabia) from February to May 2025. It included 204 complete patients' records to determine abnormal sonographic findings in the posterior segment of the eye globe among cataract patients and the associated risk factors.

All patients were scanned with a Quante Medical ultrasound (USG) scanner for ophthalmology, Model REF-B1, equipped with a 10 MHz probe. The examination focused on the posterior eye segment.

Among 204 patients with dense cataracts (55.4% men and 44.6% women), 56.9% presented with traumatic cataract (TC), while 43.1% had non-traumatic cataract (n-TC). Most of the patients were over age 60(67.6%). Out of 204 patients, 120(58.8%) had normal findings in the posterior eye segment, 36(17.8%) were found to have posterior vitreous detachment, 30(14.7%) had retinal detachment, and vitreous hemorrhage was found in 8(3.9%) patients. Other findings, which amounted to 10(5%) cases, were asteroid hyalosis, vitritis, and posterior staphyloma. Regarding risk factors, most of the patients who had positive findings in the posterior segments of their eyes were either diabetic or hypertensive. A significant correlation existed between gender and cataract types; 57.5% of male patients were susceptible to TC. The study also highlighted that age groups of 41-60 years and above were more susceptible to posterior vitreous detachment, retinal detachment, and vitritis, while the younger age group (21-40) was susceptible to retinal detachment and posterior staphyloma.

Conclusion: The findings indicate that males are more susceptible to the causes of TC than females of the same age. Detecting disorders like posterior vitreous detachment, retinal detachment, and vitreous hemorrhage preoperatively enhances surgical planning and patient counseling, thereby improving patient satisfaction and visual prognosis. B-scan US can serve as an important diagnostic tool for identifying hidden posterior segment lesions. (**International Journal of Biomedicine. 2025;15(3):540-544.**)

Keywords: cataract • B-mode US • posterior eye segment • sonographic findings

For citation: Ahmed RM. Sonographic Findings in the Posterior Segment of the Eye in Pre-Operative Cataract Patients. International Journal of Biomedicine. 2025;15(3):540-544. doi:10.21103/Article15(3)_OA14

Abbreviations

TC, traumatic cataract; **n-TC**, non-traumatic cataract.

Introduction

According to the World Health Organization, an estimated 1.3 billion people live with visual impairment. Cataracts are considered the leading cause of blindness worldwide, accounting for approximately 47.8% of blindness globally. In Pakistan, the prevalence is even higher, reaching 51.5% of blindness.[1] Cataract surgery is a common and cost-effective procedure aimed at preventing blindness by removing the lens opacity that obstructs the visualization of the posterior segment of the eye. Visualizing the posterior segment is crucial for predicting visual outcomes after

surgery.[1] Cataract surgery is a cost-effective way to prevent blindness by reducing the opacity in the lens that blocks the view of the posterior part of the eye. Proper visualization is vital for accurately forecasting vision outcomes following cataract surgery.[2] Media opacity can hinder the view of pathology in the posterior region of the fundus. Ultrasonography can detect anomalies in such cases. [3,4]

Traumatic cataract surgery is a potentially difficult technique. When planning surgery, the surgeon may benefit from careful ocular imaging using ophthalmic ultrasound (US), which may provide finer pre-operative data regarding lens support structures.[5] B-scan US provides an accurate image of the intraocular structures and valuable information about the health of the lens, vitreous, retina, choroid, and sclera. Sonographic assessment of the posterior eye globe in patients with opacities is needed to determine the most suitable surgery. In diagnostic ophthalmology, probes with frequencies ranging from 8-10M Hz are routinely utilized for posterior region tests. Advances in ultrasonography have made it easier to analyze the posterior portion of the eye, even with opaque media.[6,7]

Ophthalmic US can be used to evaluate a wide range of diseases, such as suspected intraocular tumors, the location of foreign bodies in the eye, and conditions related to eye injuries.[8] The visual inspection of orbital features is now regarded as a standard procedure. Along with other orbital features, the vitreous body and lens can be visualized particularly well by US. The eye's cystic structure and superficial position allow high-frequency transducers to reveal both normal and abnormal findings of the eye globe.[9] Proliferative diabetic retinopathy is one of the most common causes of vitreous hemorrhage. It appears as gradual changes in the eye's microvasculature. Ophthalmic US provides crucial diagnostic information about ocular illnesses that cannot be obtained through other imaging techniques.[10-12]

Materials and Methods

This retrospective study was conducted at Kafaat Medical Center (Makkah Almokaramah city, Saudi Arabia) from February to May 2025. It included 204 complete patients' records from different nationalities to determine abnormal sonographic findings in the posterior segment of the eye globe among cataract patients and the associated risk factors. Patients with incomplete medical records were excluded from the study.

A pre-designed, standardized data-collection checklist was employed to extract data from the medical records, and it includes socio-demographic data. Types of cataracts (traumatic cataract [TC] and non-traumatic cataract [n-TC]) and data regarding B-mode US findings (retinal detachment, vitreous hemorrhage, posterior vitreous detachment, asteroid hyalosis, vitreous opacities and exudates, and posterior staphyloma) were analyzed. To ensure data quality and reliability, the researchers verified the accuracy of the extracted data through random checks.

Equipment for the exam included a Quante Medical US scanner for ophthalmology, Model REF-B1, with a 10 MHz probe, USG gel, a transparent plastic film such as Tegaderm, and sterile petroleum jelly.[13,14] Statistical analysis was performed using the statistical software package SPSS version 26.0 (SPSS Inc., Armonk, NY: IBM Corp).

Results

This retrospective study included a total of 204 patients with cataracts (55.4% men and 44.6% women). Most of them were over age 60(67.6%). Among 204 patients, 56.9% presented with TC, while 43.1% had n-TC (Table 1).

Table 1.

Demographic and baseline characteristics of the study participants.

Characteristics	Category	Frequency (n)	Percentage (%)
Age group (years)	< 20	2	1.0
	21-40	26	12.7
	41-60	38	18.6
	> 60	138	67.6
	Total	204	100.0
Gender	Male	113	55.4
	Female	91	44.6
	Total	204	100.0
Cataract types	Traumatic	116	56.9
	Non-traumatic	88	43.1
	Total	204	100.0

Out of 204 patients with dense cataracts, 120(58.8%) had normal findings in the posterior eye segment, 36(17.8%) were found to have posterior vitreous detachment, 30(14.7%) had retinal detachment, vitreous hemorrhage was found in 8(3.9%) patients. Other findings, which amounted to 10(5%) cases, were asteroid hyalosis, vitritis, and posterior staphyloma (Table 2).

Table 2.

US findings on the posterior segment of the eye.

US findings	Frequency (n)	Percentage (%)
Normal findings	120	58.8
Posterior vitreous detachment	36	17.8
Retinal detachment	30	14.7
Vitreous hemorrhage	8	3.9
Asteroid hyalosis	4	2.0
Vitritis	4	2.0
Posterior staphyloma	2	1.0
Total	204	100.0

Regarding risk factors, most of the patients who had positive findings in the posterior segments of their eyes were either diabetic or hypertensive. A significant correlation existed between gender and cataract types; 57.5% of male patients were susceptible to TC (Tables 3 and 4).

Table 3.

Correlations between risk factors and cataract types. (n=204)

Cataract types	Diabetes Mellitus		Total	Hypertension		Total	Exact Sig. (1-sided)
	Yes	No		Yes	No		
Traumatic	50	66	116	44	72	116	.07 .08
Non-traumatic	48	40	88	26	62	88	
Total	98	106	204	70	134	134	

Table 4.

Correlation between gender and cataract types. (n=204)

Gender	Cataract types		Total	Exact Sig (2-sided)
	TC	n-TC		
Male	65	48	113	.01
Female	51	40	91	
Total	116	88	204	

The study also highlighted that age groups of 41-60 years and above were more susceptible to posterior vitreous detachment, retinal detachment, and vitritis, while the younger age group (21-40) was susceptible to retinal detachment and posterior staphyloma (Table 5).

Discussion

Ophthalmic US was crucial for diagnosing various orbital and ocular disorders, especially when opacification of the ocular media hindered visualization of the posterior segment and the identification of related disorders. Patients with severe cataracts often had impaired vision, complicating surgeons' ability to make accurate predictions regarding their visual outcomes. In these cases, US proved helpful in evaluating the visual results. US imaging is essential for giving a precise prognosis after cataract surgery.[15]

In our study, among 204 patients with cataracts, 55.4% were men. In contrast, a previous study by Karim et al.[16] reported equal gender distribution. Mobin et al.[17] reported a higher percentage of males (61.8%) than females (38.2%) with dense cataracts, and 67.6% of people were in the age group 60 and above, followed by 18.6% in the age group 40-60. Age over 40 was the most common demographic risk factor (86.2%). A previous study by Haug et al.[6] revealed "age is the risk factor for retinal detachment following cataract surgery" and reported that younger age is associated with an increased risk of retinal detachment. They also found that a significant correlation exists between the gender of participants and cataract types: 56% of male patients were susceptible to traumatic cataract .

Normal US was found in 58.8% of patients. In comparison, 41.2% exhibited various posterior segment pathologies, which is consistent with a previous study by Karim et al.,[16] who reported 67.8% of patients had normal US findings and 32.2% showed various posterior segment pathologies. The most common posterior segment pathology detected in a study by Jacob et al.[4] was posterior vitreous detachment in 130(25.5%) eyes.

Our study showed a statistically significant association between sample age groups and sonographic findings of the posterior segments of the eye; the age group of 41-60 years and above were more susceptible to posterior vitreous detachment, retinal detachment, and vitritis, while the younger age group of 21-40 were susceptible to retinal detachment and posterior staphyloma. These results align with a recent study by Karim

Table 5.

Age group US findings crosstab.

Age group (years)	Normal findings	Posterior vitreous detachment	Retinal detachment	Vitreous hemorrhage	Asteroid hyalosis	Vitritis	Posterior Staphyloma	Total	Exact Sig (2-sided)
< 20	0	0	2	0	0	0	0	2	.000 .005
21-40	12	2	6	0	0	0	2	22	
41-60	24	6	6	0	0	2	0	38	
> 60	84	28	16	8	4	2	0	142	
Total	120	36	30	8	4	4	2	204	

et al.,[16] which found that posterior vitreous detachment, retinal detachment, and vitreous hemorrhage were the most common pathologies, while asteroid hyalosis and posterior staphyloma were the least common. In contrast, identifiable posterior segment abnormalities were noted in nearly one-eighth of the patients with ocular injuries examined via US. When combined with vitreous hemorrhage, retinal detachment was the most frequent US result among patients with ocular trauma. The fluid in the vitreous cavity travels through holes or tears in the retina, separating it from the underlying pigmented retinal epithelium, leading to posterior vitreous detachment.[18] This finding was also consistent with a study by Qureshi et al.,[1] which reported that vitreous hemorrhages were present in 15.49% traumatic cataract patients and 1.91% in non-traumatic cataract patients.

Mobin et al.[17] in 2019 studied US results before cataract surgery in eyes with dense cataracts. Of the 625 eyes, 78(12.5%) had one or more positive US findings. The most frequent were posterior vitreous detachment (2%) and retinal detachment (4%), followed by vitreous hemorrhage (0.8%) and posterior staphyloma (1.6%). A previous study reported that vitreous hemorrhage was present in 2.5% of cases, which is higher than our data. This study confirms that US is useful in assessing both ocular traumatic and non-traumatic lesions, providing valuable information through clinical examination. The significance of US in ocular evaluation is demonstrated by its ability to distinguish between eyes with cataracts and eyes with ocular abnormalities other than cataracts as the cause of poor vision.[19]

Our study revealed that abnormal US findings were found more frequently among traumatic cataracts. Regarding risk factors, most of the patients who had positive findings in the posterior segments of their eyes were male and either diabetic or hypertensive. In the study by Kalpana et al.,[20] diabetic retinopathy was the most common finding in patients with cataracts, and post-traumatic retinopathy was more common in men than in women.

Two-dimensional ultrasonography successfully detects posterior segment disease in dense cataract patients before surgery. This instrument impacted surgical techniques and post-operative visual prognosis.

Study Limitations

Regarding study limitations, the study's retrospective nature is associated with potential selection bias, given that the authors relied on existing medical records for data acquisition. This may further limit the accuracy of the data and the study findings. Since the current study was conducted at a single tertiary center in the western region of Saudi Arabia, the study population and findings may not represent the entire Saudi population.

Conclusion

The findings indicate that males are more susceptible to the causes of traumatic cataract than females of the same age. Detecting disorders like posterior vitreous detachment, retinal detachment, and vitreous hemorrhage preoperatively enhances surgical planning and patient counseling, thereby improving patient satisfaction and visual prognosis. B-scan US can serve as an important diagnostic tool for identifying hidden posterior segment lesions.

Ethical Considerations

The study protocol was reviewed and approved by the Kafaat Medical Centre Ethics Committee (5/2025).

Competing Interests

The author declares no competing interests.

Acknowledgment

The author wishes to thank the Deanship of Scientific Research at Taif University for funding this project. Additionally, I sincerely appreciate Ms. Tayseer Alhaj Algalaa, Ms. Hajer Dafaallah, and Ms. Marram Maisara from Kafaat Medical Centre for their assistance and support.

References

1. Qureshi MA, Laghari K. Role of B-scan ultrasonography in pre-operative cataract patients. Int J Health Sci (Qassim). 2010 Jan;4(1):31-7. PMID: 21475523; PMCID: PMC3068804.
2. Chanchlani, M. and R. Chanchlani, A study of posterior segment evaluation by B-Scan in hypermature cataract. J Clin Exp Ophthalmol, 2020 Jan–Jun. 12(1):23-26.| doi: 10.4103/sjopthal.sjopthal_15_203.
3. Mendes MH, Betinjane AJ, Cavalcante Ade S, Cheng CT, Kara-José N. Ultrasonographic findings in patients examined in cataract detection-and-treatment campaigns: a retrospective study. Clinics (Sao Paulo). 2009 Jule;64(7):637-40. doi: 10.1590/S1807-59322009000700005. PMID: 19606238; PMCID: PMC2710435.
4. Jacob, J.M., J.J.K. Thadam, and S. Goudinho, Evaluation of the relation between preoperative B-scan findings and post–operative Fundus findings in patients with opaque media undergoing cataract surgery. IJAHR, 2019 April-June. 2:30-33.
5. Perry LJ. The evaluation of patients with traumatic cataracts by ultrasound technologies. Semin Ophthalmol. 2012 Sep-Nov;27(5-6):121-4. doi: 10.3109/08820538.2012.712733. PMID: 23163264.
6. Haug SJ, Bhisitkul RB. Risk factors for retinal detachment following cataract surgery. Curr Opin Ophthalmol. 2012 Jan;23(1):7-11. doi: 10.1097/ICU.0b013e32834cd653. PMID: 22081033.
7. Jain A, Gauba N, Kaur I, Singh S, Jaswal H. Role of B-Scan in Cataract Patients. Indian J Appl Radiol. 2017 Feb; 3(1):110.
8. Aironi VD, Gandage SG. Pictorial essay: B-scan ultrasonography in ocular abnormalities. Indian J Radiol Imaging. 2009 Apr-Jun;19(2):109-15. doi: 10.4103/0971-3026.50827. PMID: 19881064; PMCID: PMC2765186.

9. Bedi DG, Gombos DS, Ng CS, Singh S. Sonography of the eye. AJR Am J Roentgenol. 2006 Oct;187(4):1061-72. doi: 10.2214/AJR.04.1842. PMID: 16985158.
10. Agrawal R, Ahirwal S. A study of role of B scan ultrasound in posterior segment pathology of eye. Int J Med Res Rev. 2015; 3(9):969-74.
11. Sharma OP. Orbital sonography with its clinico-surgical correlation. Indian Journal of Radiology and Imaging, 2005 April; 15(4):537. doi: 10.4103/0971-3026.28792.
12. Andreoli MT, Yiu G, Hart L, Andreoli CM. B-scan ultrasonography following open globe repair. Eye (Lond). 2014 Apr;28(4):381-5. doi: 10.1038/eye.2013.289. Epub 2014 Jan 10. PMID: 24406404; PMCID: PMC3983623.
13. Engelbert PR, Palma JK. Petroleum Jelly: A Novel Medium for Ocular Ultrasound. J Emerg Med. 2015 Aug;49(2):172-4. doi: 10.1016/j.jemermed.2015.03.003. Epub 2015 May 23. PMID: 26014760.
14. Maciag EJ, Martín-Noguerol T, Ortiz-Pérez S, Torres C, Luna A. Understanding Visual Disorders through Correlation of Clinical and Radiologic Findings. Radiographics. 2024 Feb;44(2):e230081. doi: 10.1148/rg.230081. PMID: 38271255.
15. Kumar J, Prasad K, NathRam A. Role of B-Scan in Advanced Cataract Patients. Jour of Dent and Med Sci 2018 April; 17(4):29-32. doi: 10.9790/0853-1704152932.
16. Karim S, Rehman H. Ultrasonography in Detecting the Posterior Segment Pathology in Pre-Operative Cataract Patients. Jour of Health and Rehab Research, 2024 May; 4(2):1014-1018. doi:10.61919/jhrr.v4i2.949.
17. Mobin M, Kanodia P, Malhotra R, Akaram SM, Yadav D. Role of B scan ultrasonography before cataract surgery in eyes with dense cataracts. Journal of Medical Science and Clinical Research. 2019; 7(8): 890- 894. doi: 10.18535/jmscr/v7i8.153
18. Wilkinson CP. Interventions for asymptomatic retinal breaks and lattice degeneration for preventing retinal detachment. Cochrane Database Syst Rev. 2014 Sep 5;2014(9): CD003170. doi: 10.1002/14651858.CD003170.pub4. PMID: 25191970; PMCID: PMC4423540.
19. Kumar S, Sharma S, Eshani, Chauhan SS. Assessment of the intraocular pathologies detected by preoperative B-Scan ultrasound examination in patients having dense cataracts. International Journal of Radiology and Diagnostic Imaging 2020;3(4):21-28.
20. Kalpana BN, Murali B. Cataract and Posterior Segment Risk Factors. Med Res Chron. 2015; 2(2). Available from: https://medrech.com/index.php/medrech/article/view/76.

***Correspondence:** *Ass. Prof. Rania Mohammed Ahmed, E-mail: dr.rania@tu.edu.sa*

International Journal of Biomedicine 15(3) (2025) 545-551
http://dx.doi.org/10.21103/Article15(3)_OA15

ORIGINAL ARTICLE

Dentistry

INTERNATIONAL JOURNAL OF BIOMEDICINE

Molecular Identification of *Entamoeba gingivalis* and Its Association with Periodontitis in Diabetic Patients: A PCR-Based Study Targeting the ITS2 Region

Wirangrong Sritongklang[1,2], Nav La[1], Alisa Boonsuya[1], Patpicha Arunsan[1,3], Thanawat Trasaktaweesakul[2], Pundit Asavaritikrai[2], Nathkapach Kaewpitoon Rattanapitoon[1,4], Schawanya Kaewpitoon Rattanapitoon[1,4,5*]

[1]*Parasitic Disease Research Center, Suranaree University of Technology, Nakhon Ratchasima 30000, Thailand*
[2]*School of Translational Medicine, Institute of Medicine, Suranaree University of Technology, Nakhon Ratchasima 30000, Thailand*
[3]*Faculty of Medicine, Vongchavalitkul University, Nakhon Ratchasima 30000, Thailand*
[4]*FMC Medical Center, Nakhon Ratchasima 30000, Thailand*
[5]*Department of Family Medicine and Community Medicine, Institute of Medicine, Suranaree University of Technology, Nakhon Ratchasima 30000, Thailand*

Abstract

Entamoeba gingivalis is an anaerobic protozoan increasingly associated with periodontitis, particularly in individuals with systemic conditions such as diabetes mellitus. This cross-sectional study investigated the prevalence of *E. gingivalis* in 160 Thai patients with periodontitis and analyzed associated risk factors. Microscopy detected the parasite in 15.0% of patients, PCR in 25.6%, and sequencing confirmed the infection in 22.5%, all of which were Subtype 1. Infection was significantly more common among diabetic patients (41.3%) than non-diabetics (3.8%) (P<0.001). Multivariate analysis identified type 2 diabetes (adjusted OR = 20.77; 95% CI: 5.39–80.09), alcohol use (adjusted OR = 3.72; 95% CI: 1.01–13.68), and other underlying diseases (adjusted OR = 1.49; 95% CI: 1.07–2.06) as independent risk factors. PCR demonstrated superior diagnostic performance compared to microscopy. These findings support a potential pathogenic role of *E. gingivalis* in periodontitis, especially among patients with type 2 diabetes or behavioral risk factors. (**International Journal of Biomedicine. 2025;15(3):545-551.**)

Keywords: *Entamoeba gingivalis* • periodontitis • diabetes mellitus • internal transcribed spacer 2 • polymerase chain reaction

For citation: Sritongklang W, La N, Boonsuya A, Arunsan P, Trasaktaweesakul T, Asavaritikrai P, Rattanapitoon NK, Rattanapitoon SK. Molecular Identification of *Entamoeba gingivalis* and Its Association with Periodontitis in Diabetic Patients: A PCR-Based Study Targeting the ITS2 Region. International Journal of Biomedicine. 2025;15(3):545-551. doi:10.21103/Article15(3)_OA15

Abbreviations

ITS2, internal transcribed spacer 2; **PCR**, polymerase chain reaction; **T2D,** type 2 diabetes.

Introduction

Entamoeba gingivalis is an anaerobic protozoan commonly detected in the periodontal pockets of individuals exhibiting poor oral hygiene, periodontal disease, or compromised immune status.[1-5] Historically regarded as a commensal organism, recent studies suggest that *E. gingivalis* may play a pathogenic role in the progression of periodontitis, a chronic inflammatory disease affecting the supporting structures of teeth. Its close phylogenetic relationship to *E. histolytica*, a recognized human pathogen, further emphasizes the need to reassess the clinical relevance of *E. gingivalis*.

Periodontitis represents one of the most widespread oral health conditions globally and is strongly associated with systemic diseases, notably type 2 diabetes (T2D). The bidirectional relationship between diabetes and periodontitis is well documented: diabetic individuals are predisposed to increased periodontal destruction, while severe periodontitis can impair glycemic control and exacerbate diabetic complications. This interplay likely reflects shared pathophysiological pathways involving microbial dysbiosis, altered host immune responses, and systemic inflammation.

The anaerobic microenvironment created by periodontal inflammation provides an ideal niche for facultative and obligate anaerobic organisms, including *E. gingivalis*. However, conventional diagnostic approaches, such as light microscopy and staining, have limited sensitivity and may underestimate the true prevalence of this protozoan. In contrast, molecular diagnostic methods, especially PCR targeting the internal transcribed spacer 2 (ITS2) region, offer enhanced sensitivity and specificity for detecting *E. gingivalis* in clinical samples.

Despite these methodological advances, data on the prevalence of *E. gingivalis* among periodontitis patients, particularly those with diabetes, remain scarce, especially in Southeast Asian populations. Building on prior research, including the work of Boonsuya et al.,[6] the present study aims to elucidate the prevalence of *E. gingivalis* in Thai patients with periodontitis, both with and without T2D, utilizing both PCR and conventional microscopy. Furthermore, this study examined potential associations between *E. gingivalis* infection and host factors, including diabetes status and alcohol consumption. The findings are intended to enhance epidemiological understanding and inform diagnostic and therapeutic strategies for managing periodontal disease in high-risk population groups.

Materials and Methods

Study Design and Population

This cross-sectional analytical study was conducted between January 2021 and December 2024 in Banmai Subdistrict, Nakhon Ratchasima Province, Thailand. The primary objective was to assess the prevalence of *Entamoeba gingivalis* among patients with periodontitis and to explore its associations with systemic conditions, particularly T2D, and behavioral risk factors. A total of 160 individuals diagnosed with periodontitis were purposively recruited from a dental clinic affiliated with a regional public health center. The study population was divided into two equal groups: 80 patients with confirmed T2D and 80 patients without T2D, matched as closely as possible by age and sex.

The inclusion criteria included adults aged 25–100 years with a diagnosis of periodontitis, as defined by the 2017 World Workshop classification.[7] Exclusion criteria were recent antibiotic use (within the past 3 months), current antifungal or antiparasitic treatment, pregnancy, immunosuppressive conditions other than diabetes, and unwillingness to participate. All participants underwent a comprehensive periodontal examination. Demographic data and systemic health information were collected through structured interviews and reviews of medical records. Behavioral factors such as smoking and alcohol consumption were assessed using validated questionnaires.

Sample Collection

Gingival crevicular fluid (GCF) samples were collected from each participant. Following the isolation of the target area with cotton rolls and gentle air-drying, sterile absorbent paper points were inserted into the gingival sulcus for 30 seconds to absorb any remaining fluid. The paper points were then immediately transferred into individually coded, sterile microcentrifuge tubes and stored at −80°C until further analysis.

Parasitological Examination

Initial screening for *E. gingivalis* was performed using Gomori's trichrome staining technique.[8] Fixed smears of the GCF were stained and examined under a light microscope at 1000× magnification. Identification was based on classical morphological features, including amoeboid trophozoites ranging from 10–35 μm in diameter, with prominent pseudopodia, a central karyosome, peripheral chromatin, and cytoplasm containing ingested bacteria. Each slide was independently evaluated by three experienced parasitologists, who were blinded to the clinical status of the participants.

DNA Extraction and PCR Test

Genomic DNA was extracted using the QIAamp DNA Mini Kit® (Qiagen, Germany), following the manufacturer's protocol with minor modifications to enhance DNA yield from paper-point substrates.

Briefly, 400 μL of AL buffer and 20 μL of Proteinase K were added to each tube containing the sample, followed by incubation at 56°C for 30 minutes. DNA was subsequently purified using spin-column centrifugation and eluted in 75 μL of AE buffer. The extracted DNA was stored at −20°C until further analysis.

Detection of *Entamoeba gingivalis* was carried out using conventional polymerase chain reaction (PCR) targeting the internal transcribed spacer 2 (ITS2) region with species-specific primers: forward 5′-GAATAGGCGCGCATTTCGAACAGG-3′ and reverse 5′-TCCCACTAGTAAGGTACTACTC-3′. Each 25 μL PCR reaction mixture comprised 5 μL of DNA template, 3 μL of primers (1.5 μL each), 10 μL of PCR master mix (including $MgCl_2$, dNTPs, and Taq DNA polymerase), and 7 μL of nuclease-free water.

PCR amplification was performed under the following cycling conditions: an initial denaturation at 95°C for 7.5 minutes; 40 cycles of denaturation at 95°C for 1 minute, annealing at 55°C for 30 seconds, and extension at 72°C for 30 seconds; followed by a final extension at 72°C for 5 minutes.

PCR products were separated by electrophoresis on 1.5% agarose gels stained with ethidium bromide and visualized under ultraviolet illumination. A 100bp molecular weight ladder (GeneRuler, Roche, Germany), along with positive and negative controls, was included in each run for quality assurance.

Subtyping and Sequencing

Samples that tested positive by ITS2-PCR were subsequently subjected to subtype-specific PCR to

distinguish between *E. gingivalis* Subtypes 1 and 2. The primers used were as follows: for Subtype 1, forward 5′-TACCATACAAGGAATAGCTTT-3′ and reverse 5′-GTGAAACAATAGAAGAAGGAAATGG-3′; for Subtype 2, forward 5′-GAGACAATCCCAGTTGTTTGTAC-3′ and reverse 5′-TACGTCCCTGCCCTTTGTAC-3′.

PCR amplification conditions were identical to those described previously. The resulting PCR products were purified using the QIAquick Gel Extraction Kit and submitted for Sanger sequencing.

The obtained sequences were analyzed using the NCBI BLAST tool to confirm species identity and compared with reference sequences available in the GenBank database. Multiple sequence alignment was conducted using ClustalW in the BioEdit software package to determine the *E. gingivalis* subtype and assess genetic similarity.

Statistical Analysis

All statistical analyses were conducted using SPSS version 20.0 (IBM Corp., Armonk, NY, USA). Descriptive statistics were used to summarize demographic, clinical, and parasitological data. Group differences in *E. gingivalis* prevalence were assessed using Chi-square or Fisher's exact test as appropriate. Binary logistic regression was used to identify independent predictors of E. gingivalis infection. Variables included in the model were diabetes status, underlying systemic disease, alcohol consumption, smoking status, age group, and gender. Results were reported as crude and adjusted odds ratios (ORs) with 95% confidence intervals (CIs). The diagnostic performance of microscopy and PCR was evaluated using sensitivity, specificity, and Cohen's kappa coefficient, using sequencing-confirmed infection as the reference standard. A *P*-value of <0.05 was considered statistically significant.

Results

A total of 160 patients diagnosed with periodontitis were enrolled in the study, comprising 80 patients with T2D and 80 patients without T2D. The presence of *E. gingivalis* was initially investigated through parasitological examination. Microscopic analysis revealed the parasite in 24 participants, including 22 diabetic patients and only 2 non-diabetic individuals.

Subsequent molecular detection via PCR targeting the ITS2 region identified *E. gingivalis* DNA in 41 participants (25.6%), of whom 37 were diabetic and 4 were non-diabetic. Sequence alignment of the amplified ITS2 region confirmed infection in 36 cases (22.5%), all of which were classified as Subtype 1. No cases of Subtype 2 were detected. Demographic and clinical characteristics of participants in relation to *E. gingivalis* infection are summarized in Table 1.

Among the 160 participants, the majority were female (70.0%), with an age range of 25 to 100 years. The prevalence of infection was higher in females (24.1%) than in males (18.8%), although this difference was not statistically significant (*P*=0.457). By age group, infection was most common among participants aged 45–64 years (11.9%), followed by those aged 65–84 years (9.4%). However, no statistically significant trend was observed across age groups (*P*=0.227). A significant association was identified between *E. gingivalis* infection and the presence of underlying diseases (*P*=0.006). Patients with hypertension (69.4%) and hypercholesterolemia (63.6%) demonstrated higher infection rates than those without comorbidities (14.7%). Diabetes mellitus emerged as the strongest associated risk factor: 41.3% of diabetic participants tested positive compared to only 3.8% of non-diabetics (*P*<0.001). Alcohol consumption was also significantly associated with infection. Among participants who reported alcohol use, 50.0% tested positive for *E. gingivalis*, compared to 20.7% of non-drinkers (*P*=0.031). No statistically significant association was found with smoking status (*P*=0.517).

Table 1.

Demographic and clinical characteristics and prevalence of Entamoeba gingivalis infection.

Variables	Patients n (%)	*E. gingivalis* infection		*P*-value
		Yes, n (%)	No, n (%)	
Gender				
Male	48 (30.00)	9 (18.75)	39 (81.25)	0.457
Female	112 (70.00)	27 (24.11)	85 (75.89)	
Age				
25-44 years	26 (16.25)	2 (1.25)	24 (15.00)	0.227
45-64 years	72 (45.00)	19 (11.88)	53 (33.13)	
65-84 years	61 (38.13)	15 (9.38)	46 (28.75)	
85-100 years	1 (0.63)	0 (0.00)	1 (0.63)	
Underlying diseases				
No	102 (63.75)	87 (85.29)	15 (14.71)	0.006
Hypertension	36 (22.50)	25 (69.44)	11 (30.56)	
Hypercholesterolemia	11 (6.88)	7 (63.64)	4 (36.36)	
Other	11 (6.88)	5 (45.45)	6 (54.55)	
Diabetes mellitus				
Yes	80 (50.00)	33 (41.25)	47 (58.75)	0.000
No	80 (50.00)	3 (3.75)	77 (96.25)	
Alcohol use				
Yes	10 (6.25)	5 (50.00)	5 (50.00)	0.031
No	150 (93.75)	31 (20.67)	119 (79.33)	
Smoking status				
Yes	6 (3.75)	2 (33.33)	4 (66.67)	0.517
No	154 (96.25)	34 (22.08)	120 (77.92)	

The diagnostic performance of microscopy and PCR was evaluated using sequencing-confirmed infection as the reference standard (Table 2). Microscopy demonstrated a sensitivity of 66.67% and specificity of 100%, with moderate agreement (Kappa = 0.593, *P*<0.001). PCR showed superior diagnostic accuracy, with 100% sensitivity, 95.96% specificity, and substantial agreement with sequencing (Kappa = 0.749, *P*<0.001. While PCR identified all confirmed infections, a small number of false positives were detected.

Table 2.

Detection of Entamoeba gingivalis infection by parasitological and molecular methods.

Methods	Periodontitis with T2D n (%)	Periodontitis without T2D n (%)	Total n (%)	Sensitivity (%)	Specificity (%)	Measure of Agreement Kappa	*P*-value
Microscopy	22 (86.67)	2 (13.33)	24 (15.00)	66.67	100	0.593	0.000
PCR based ITS2	33 (91.67)	3 (8.33)	36 (22.50)	100	95.96	0.749	0.000
Subtype1	33 (91.67)	3 (8.33)	36 (22.50)				
Subtype 2	0	0	0				

Table 3.

Association between Entamoeba gingivalis infection and clinical variables analyzed by binary logistic regression.

Variables	Patients n (%)	Presence of *E. gingivalis* infection			
		Crude OR	95% CI	Adjusted OR	95% CI
Gender					
Male	48 (30.00)	1.38	0.59–3.20	1.28	0.49–3.30
Female	112 (70.00)				
Age					
25-44 years	26 (16.25)	2.38	0.67–2.96	0.57	0.26-1.26
45-64 years	72 (45.00)				
65-84 years	61 (38.13)				
85-100 years	1 (0.63)				
Underlying diseases					
No	102 (63.75)	1.58	1.21-2.07	1.49	1.07-2.06
Hypertension	36 (22.50)				
Cholesterol	11 (6.88)				
Other	11 (6.88)				
T2D					
Yes	80 (50.00)	18.02	5.23–62.05	20.77	5.39-80.09
No	80 (50.00)				
Alcohol use					
Yes	10 (6.25)	3.84	1.05–14.10	3.72	1.01-13.68
No	150 (93.75)				
Smoking					
Yes	6 (3.75)	1.77	0.31–10.05	1.8	0.31-10.49
No	154 (96.25)				

Binary logistic regression was conducted to identify factors independently associated with *E. gingivalis* infection (Table 3). Diabetes mellitus was the most significant predictor, with an odds ratio (OR) of 20.77 (95% CI: 5.39–80.09, $P<0.001$), indicating a markedly elevated risk of infection among diabetic patients. Alcohol consumption also showed a statistically significant association, with an OR of 3.72 (95% CI: 1.01–13.68, $P=0.047$). The presence of any underlying disease was independently associated with infection (OR = 1.49; 95% CI: 1.07–2.06, $P=0.019$), suggesting a potential compounding effect of comorbid conditions on susceptibility.

In contrast, gender, age group, and smoking status were not significantly associated with *E. gingivalis* infection in the multivariate model. Although younger participants (25–44 years) initially showed an increased crude OR, this association reversed after adjustment (OR = 0.57; 95% CI: 0.26–1.26), reflecting the influence of confounding variables.

Figure 1. *Representative images of periodontal disease in patients exhibiting severe gingival inflammation, clinical attachment loss, and increased probing pocket depths. Black arrows indicate the sites from which dental plaque samples were collected. (A) Periodontitis in a patient with T2D, (B) Periodontitis in a patient without T2D.*

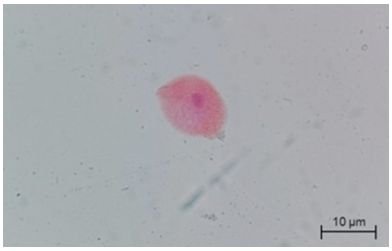

Figure 2. *Entamoeba gingivalis detected in a periodontitis patient with diabetes mellitus, visualized using Gomori's trichrome staining and observed under light microscopy.*

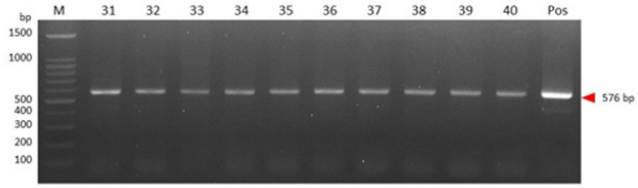

Figure 3. *Gel electrophoresis of PCR-amplified products targeting the gene for Entamoeba gingivalis detection. Red arrows indicate the specific 576 bp amplicons. M: 100 bp DNA ladder molecular size marker; positive control: E. gingivalis genomic DNA; lanes 31–40: positive samples.*

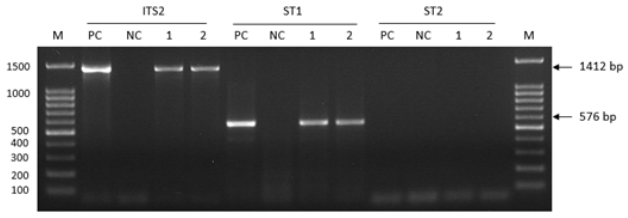

Figure 4. *Gel electrophoresis of PCR-amplified products targeting genes for Entamoeba gingivalis subtype 1 detection. Black arrows indicate the specific amplicons of 576 bp and ITS2 1412 bp fragments. M: 100 bp DNA ladder molecular size marker; positive control: E. gingivalis genomic DNA.*

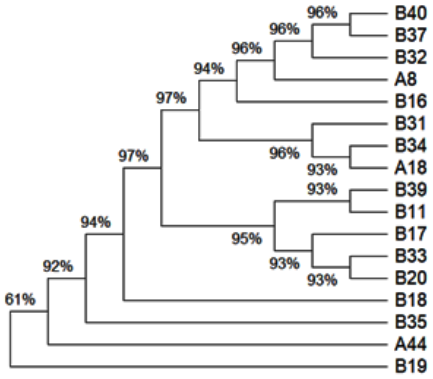

Figure 5. *Sequence alignment of the amplified Entamoeba gingivalis ITS2 region. Sequences obtained from PCR products were aligned using ClustalW in BioEdit software. The alignment confirms the presence of E. gingivalis by demonstrating high similarity to reference sequences retrieved from GenBank. The identified ITS2 sequences exhibited strong homology with known E. gingivalis strains, thereby validating the molecular detection method employed in this study. Conserved regions and sequence variations within the ITS2 region are highlighted, supporting accurate pathogen identification.*

Discussion

The present study provides important insights into the prevalence and diagnostic accuracy of *E. gingivalis* in Thai patients with periodontitis, with a particular focus on individuals with T2D. By integrating microscopy, PCR, and sequencing, this investigation provides robust data on the burden of *E. gingivalis* infection and its potential role as an opportunistic protozoan pathogen in periodontal disease. The detection rate by PCR was 25.6%, with 22.5% of cases confirmed by sequencing, highlighting the protozoan's under-recognized presence in the oral cavity and underscoring the microbial complexity in periodontitis pathogenesis.

One of the most striking findings was the significantly higher prevalence of *E. gingivalis* infection among diabetic patients (41.3%) than among non-diabetics (3.8%). This supports existing hypotheses that systemic conditions, such as T2D, predispose patients to protozoal colonization. Hyperglycemia has been shown to impair neutrophil function, reduce phagocytosis, and disrupt the cytokine environment in the periodontium, which may facilitate colonization by opportunistic organisms, including *E. gingivalis*. These findings are consistent with those of Boonsuya et al.[6] as well as studies from the Middle East and South America.[9,10] In addition to T2D, alcohol consumption was independently associated with infection. Half of the alcohol consuming participants tested positive for *E. gingivalis*, a finding that remained significant in multivariate analysis. Although underexplored in the literature, it is plausible that alcohol disrupts the oral microenvironment by decreasing salivary flow, altering mucosal immunity, and promoting biofilm dysbiosis, thereby enhancing susceptibility to protozoal colonization. These mechanisms remain speculative and warrant further investigation.

Beyond these factors, our multivariate model revealed that other underlying diseases—principally hypertension and hypercholesterolemia—were also independently associated with *E. gingivalis* infection (adjusted OR = 1.49; 95% CI: 1.07–2.06). Although direct evidence remains scarce, numerous studies link cardiometabolic disorders to heightened periodontal inflammation. Graziani et al.[11] reported an approximately 50% increase in hypertension risk among patients with moderate to severe periodontitis, while an umbrella review by Mauri-Obradors et al.[12] found consistent associations between dyslipidemia and periodontal disease that improve after periodontal therapy. Systemic vascular dysfunction and chronic low-grade inflammation, characteristic of these conditions, may compromise gingival microcirculation and innate immunity, thereby fostering protozoan persistence. Indirect support arises from immunocompromised cohorts; in Brazilian HIV-infected patients, Costa et al.[13] detected *E. gingivalis* in 63.4% of individuals, underscoring the role of systemic immune perturbation—regardless of etiology—in promoting protozoal carriage. Collectively, these observations suggest that multisystem comorbidity can have a subtle yet significant influence on the oral protozoan burden.[14,15]

In contrast, no significant associations were observed between *E. gingivalis* infection and demographic variables such as age, gender, or smoking status. Although slightly higher infection rates were observed among females and participants aged 45–64 years, the differences were not statistically significant. Similar trends have been reported in other Southeast Asian studies, but were also non-significant, suggesting that behavioral and systemic health factors may play a more decisive role in infection risk than demographic characteristics.

This study also contributes to the understanding of diagnostic accuracy for *E. gingivalis*. Microscopy using Gomori's trichrome staining yielded a positivity rate of 15.0%, compared with 25.6% by PCR and 22.5% confirmed by sequencing. Although microscopy demonstrated excellent specificity (100%), it had moderate sensitivity (66.7%). This aligns with prior work highlighting the limitations of microscopy in detecting oral protozoa.[16] ITS2-targeted PCR, followed by sequencing, enhanced diagnostic precision and enabled subtyping. All sequence-confirmed cases were Subtype 1, with no detection of Subtype 2, suggesting a predominant circulation of Subtype 1 in this Thai population. Similar subtype patterns have been reported in Iran and Egypt,[17,18] implying possible geographic variation.

To our knowledge, this is one of the first Thai studies to utilize ITS2 sequencing to confirm *E. gingivalis* infection in periodontitis patients. Previous local investigations relied mainly on microscopy or unconfirmed PCR.[6] The molecular approach presented herein improves prevalence estimates and provides subtype-level epidemiological insights. The balanced inclusion of diabetic and non-diabetic participants further strengthens the comparative analysis, addressing a common limitation in earlier research.

Clinically, these findings suggest that protozoa, such as *E. gingivalis*, may contribute to periodontal inflammation and tissue destruction alongside bacterial pathogens. *E. gingivalis* is known to produce proteolytic enzymes and phagocytose host cells, causing direct tissue damage.[16] Its persistence in periodontal pockets and ability to evade immune responses may sustain chronic inflammation and impair treatment outcomes. While current paradigms emphasize bacterial etiology, our results advocate for a broader consideration of eukaryotic pathogens.

Molecular diagnostics, though not yet standard in clinical dentistry, may enhance early detection, particularly among high-risk groups such as patients with T2D or multiple comorbidities. The adjunctive use of antiprotozoal agents in combination with mechanical debridement warrants exploration in clinical trials.

Despite its strengths, including molecular confirmation, subtype analysis, and stratification by systemic risk factors, this study has limitations. The cross-sectional design precludes causal inference; thus, *E. gingivalis* may be a consequence rather than a driver of disease. Additionally, the plaque index, oral hygiene practices, and diabetes duration were not recorded, which may confound the outcomes. Future longitudinal studies employing comprehensive microbiological profiling, including *Trichomonas tenax* and metagenomic approaches, are needed to elucidate the broader role of protozoa in periodontal disease.

In conclusion, this study demonstrates a considerable prevalence of Entamoeba gingivalis infection in Thai periodontitis patients, particularly those with T2D, alcohol use, or additional cardiometabolic conditions. The findings highlight the value of molecular diagnostics in detecting oral protozoa and underscore the influence of systemic and behavioral factors on infection risk. As the microbial landscape of periodontal disease continues to expand, the potential pathogenic role of protozoa such as *E. gingivalis* should not be overlooked. Further research is required to clarify their clinical relevance and therapeutic implications in periodontal care.

Competing Interests

The authors declare that they have no competing interests.

Acknowledgment

This work was supported by the Institute of Research and Development (IRD), Parasitic Disease Research Center (PDRC) under the grant, Suranaree University of Technology (SUT), The One Research One Graduate(OROG) scholarship, Suranaree University of Technology (SUT), Thailand Science Research and Innovation (TSRI), and National Science, Research and Innovation Fund (NSRF) (NRIIS number 195617).

References

1. Bao X, Wiehe R, Dommisch H, Schaefer AS. *Entamoeba gingivalis* Causes Oral Inflammation and Tissue Destruction. J Dent Res. 2020 May;99(5):561-567. doi: 10.1177/0022034520901738. Epub 2020 Feb 5. PMID: 32023135.

2. Bartold PM, Van Dyke TE. An appraisal of the role of specific bacteria in the initial pathogenesis of periodontitis. J Clin Periodontol. 2019 Jan;46(1):6-11. doi: 10.1111/jcpe.13046. PMID: 30556922; PMCID: PMC6357965.
3. Bhaijee F. *Entamoeba gingivalis*: The oral amoeba—A review. Oral Surg Oral Med Oral Pathol Oral Radiol Endod. 2011;112(4):406–411. doi: 10.1016/j.tripleo.2011.05.016
4. Bonner M, Fresno M, Gironès N, Guillén N, Santi-Rocca J. Reassessing the Role of *Entamoeba gingivalis* in Periodontitis. Front Cell Infect Microbiol. 2018 Oct 29;8:379. doi: 10.3389/fcimb.2018.00379. PMID: 30420943; PMCID: PMC6215854.
5. Jiao J, Bie M, Xu X, Duan D, Li Y, Wu Y, Zhao L. *Entamoeba gingivalis* is associated with periodontal conditions in Chinese young patients: A cross-sectional study. Front Cell Infect Microbiol. 2022 Oct 7;12:1020730. doi: 10.3389/fcimb.2022.1020730. PMID: 36275028; PMCID: PMC9585380.
6. Boonsuya A, Chitpitaklert P, Pechdee P, Srithongklang W, Thanchonnang C, La N, Gordon CN, Rattanapitoon NK, Arunsan P, Rattanapitoon SK. Oral parasitic protozoan Entamoeba gingivalis in periodontal disease patients, northeastern Thailand. Trop Biomed. 2023 Dec 1;40(4):471-477. doi: 10.47665/tb.40.4.013. PMID: 38308835.
7. Papapanou PN, Sanz M, Buduneli N, Dietrich T, Feres M, Fine DH, Flemmig TF, Garcia R, Giannobile WV, Graziani F, Greenwell H, Herrera D, Kao RT, Kebschull M, Kinane DF, Kirkwood KL, Kocher T, Kornman KS, Kumar PS, Loos BG, Machtei E, Meng H, Mombelli A, Needleman I, Offenbacher S, Seymour GJ, Teles R, Tonetti MS. Periodontitis: Consensus report of workgroup 2 of the 2017 World Workshop on the Classification of Periodontal and Peri-Implant Diseases and Conditions. J Periodontol. 2018 Jun;89 Suppl 1:S173-S182. doi: 10.1002/JPER.17-0721. PMID: 29926951.
8. GOMORI G. A rapid one-step trichrome stain. Am J Clin Pathol. 1950 Jul;20(7):661-4. doi: 10.1093/ajcp/20.7_ts.661.
9. Khan M, Alshahrani S, Alqhtani A, Alzahrani A, Farouk AE. Molecular detection of *Entamoeba gingivalis* in diabetic patients with periodontitis: A case-control study. Saudi J Biol Sci. 2020;27(3):920–925. doi: 10.1016/j.sjbs.2020.01.001
10. Garcia G, Ramos F, Maldonado J, Fernandez A, Yáñez J, Hernandez L, Gaytán P. Prevalence of two Entamoeba gingivalis ST1 and ST2-kamaktli subtypes in the human oral cavity under various conditions. Parasitol Res. 2018 Sep;117(9):2941-2948. doi: 10.1007/s00436-018-5990-8. Epub 2018 Jul 9. PMID: 29987412.
11. Graziani F, Cei S, Orlandi M, Gabriele M, Gennai S, Filice N, et al. Hypertension and periodontitis: The results of the periodontal disease and Vascular Events (PAVE) study. J Clin Periodontol. 2018;45(6):789–798. doi: 10.1111/jcpe.12827
12. Mauri-Obradors E, Estrugo-Devesa A, Jane-Salas E, Vinas M, Lopez-Lopez J. Impact of dyslipidemia on the periodontium: An umbrella review. J Evid Based Dent Pract. 2024;24(1):101842. doi: 10.1016/j.jebdp.2023.101842
13. Costa FO, da Rocha ACB, da Silva JFF, Mendonça JA, Costa JEM, Batista MJ, et al. High prevalence of *Entamoeba gingivalis* in HIV-infected individuals with periodontal disease. Acta Trop. 2022;232:106515. doi: 10.1016/j.actatropica.2022.106515
14. Nazir MA. Prevalence of periodontal disease, its association with systemic diseases and prevention. Int J Health Sci (Qassim). 2017 Apr-Jun;11(2):72-80. PMID: 28539867; PMCID: PMC5426403.
15. Vlasa A, Bud A, Lazar L, Lazar AP, Herbert A, Bud E. Association of *Entamoeba gingivalis* with Periodontal Disease-Systematic Review and Meta-Analysis. Medicina (Kaunas). 2024 Apr 29;60(5):736. doi: 10.3390/medicina60050736. PMID: 38792919; PMCID: PMC11123156.
16. Bonner M, Amard V, Bar-Pinatel C, Charpentier F, Chatard JM, Desmuyck Y, Ihler S, Rochet JP, Roux de La Tribouille V, Saladin L, Verdy M, Gironès N, Fresno M, Santi-Rocca J. Detection of the amoeba Entamoeba gingivalis in periodontal pockets. Parasite. 2014;21:30. doi: 10.1051/parasite/2014029. Epub 2014 Jul 2. PMID: 24983705; PMCID: PMC4077299.
17. Jalallou N, Rostami-Nejad M, Maleki D, Mirjalali H, Zali MR. Molecular detection and genotyping of *Entamoeba gingivalis* in patients with periodontal disease in Iran. Parasitol Int. 2019;72:101922. doi: 10.1016/j.parint.2019.101922
18. El Deeb HK, Allam AA, Ahmed A, Attia RA, Gad El-Rab MO, Kandil OM, et al. Genotyping of *Entamoeba gingivalis* in periodontitis patients: Evidence of subtype 1 predominance. Acta Trop. 2020;205:105404. doi: 10.1016/j.actatropica.2020.105404

***Corresponding author**: Assoc. Prof. Schawanya K. Rattanapitoon, MD. E-mail: schawanya.ratt@gmail.com*

International Journal of Biomedicine 15(3) (2025) 552-558
http://dx.doi.org/10.21103/Article15(3)_OA16

ORIGINAL ARTICLE

Dentistry

INTERNATIONAL JOURNAL OF BIOMEDICINE

Retention Practices of Orthodontists in the Western Balkans

J. Kiseri Kubati[1*], B. Dzipunova[2], M. Zigante[3], S. Kantor[4], M. Dzipunova[2], S. Spalj[3,4]

[1]*Department of Orthodontics, Faculty of Dentistry, UBT College, Prishtina, Kosovo*
[2]*Department of Orthodontics, Dental Faculty, St. Cyril and Methodius University of Skopje, Skopje, North Macedonia*
[3]*Department of Orthodontics, Faculty of Dental Medicine, University of Rijeka, Rijeka, Croatia*
[4]*Department of Dental Medicine, Faculty of Dental Medicine and Health, J. J. Strossmayer University of Osijek, Osijek, Croatia*

Abstract

Background: Retention protocols vary widely across regions, yet limited data exist on practices in the Western Balkans. This study aimed to compare retention strategies among orthodontists in Croatia, North Macedonia, and Kosovo, evaluating influences such as clinician experience, malocclusion type, and patient factors.

Methods and Results: A questionnaire was distributed to 185 orthodontists in Croatia, 150 in North Macedonia, and 125 in Kosovo (representing 78%-100% practicing orthodontists) from December 2023 to May 2024, with response rates of 75%, 63%, and 58%, respectively. Data on appliance preferences, follow-up frequency, and retention protocol were analyzed using Chi-square and Kruskal-Wallis tests.

The most preferred appliance options were the following: vacuum-formed retainer in Croatia, a combination of fixed and removable in Kosovo, and an acrylic plate in North Macedonia. Retention choices were primarily experience-driven, though Kosovar orthodontists prioritized patient age/growth (88%), while Croatians and Macedonians emphasized malocclusion type (73%-78%). Countries also differed in patient care practices following a procedure. Written instructions were less common in Kosovo and North Macedonia than in Croatia (11% and 19% vs. 69%; $P<0.001$). Monitoring by an orthodontist beyond three years was higher in Kosovo and North Macedonia than in Croatia (92 and 99% vs. 75%; $P<0.001$).

Conclusion: Significant regional differences in retention practices reflect variations in training traditions, clinical habits, and socioeconomic factors. These findings underscore the need for clearer, evidence-based retention guidelines to support consistent and unified clinical practices across regions, ultimately improving long-term patient outcomes. (**International Journal of Biomedicine. 2025;15(3):552-558.**)

Keywords: orthodontic retention • orthodontic retainers • retention protocols • Balkans

For citation: Kiseri Kubati J, Dzipunova B, Zigante M, Kantor S, Dzipunova M, Spalj S. Retention Practices of Orthodontists in the Western Balkans. International Journal of Biomedicine. 2025;15(3):552-558. doi:10.21103/Article15(3)_OA16

Abbreviations

FBR, fixed bonded retainer; **VFR**, vacuum-formed retainer.

Introduction

Retention is the final phase of orthodontic treatment, yet there is no consensus among orthodontists regarding the optimal shapes and materials for this stage.[1] The primary objective of retention is to preserve the stability of the treatment results.[2] Unstable results can lead to relapse, which is the reappearance of occlusal disorders that had been corrected through orthodontic treatment.[3] Research indicates that some degree of relapse is common among patients after completing orthodontic treatment.[4] The choice of retention method depends on various factors, including the type of malocclusion, growth patterns, extraction decisions, treatment duration, the clinician's experience, and their education, among others. Although

limited data support specific retention protocols, a review of the literature has provided valuable insights for both orthodontic patients and healthcare professionals.[5,6]

Current evidence categorizes retainers into two main groups: removable retainers and fixed bonded retainers (FBR). The most commonly used removable retainers are the Hawley retainer and the vacuum-formed retainer (VFR). Both FBRs and removable retainers are widely accepted within the orthodontic and dental community, each offering its own advantages and disadvantages. Numerous randomized clinical trials have examined the effectiveness of different retainers and retention strategies.[7-9]

Retention protocols vary by country. In the UK, private practices favor VFR alongside FBR.[10] In Australia and New Zealand, orthodontists typically use FBR for the lower arch and VFR for the upper, while in the Netherlands, fixed retainers are preferred for both arches.[11] In the USA, over 58% of orthodontists favor Hawley retainers for the upper arch, while 40% prefer FBR for the lower.[12] Another study analyzing trends from 1986 to 2008 found a growing preference for VFR and FBR, alongside a decline in Hawley retainer use. During this period, lifelong retention methods also became more common.[13]

The data from Croatia revealed that in 2013 orthodontists preferred VFR for the maxilla and a combination of fixed and removable retainers for the mandible.[14] Following Croatia's earlier survey, we expanded the study to North Macedonia and Kosovo to gain a broader understanding of regional retention practices and shared trends. These three Balkan countries share a common history through the former Yugoslav education system, which has shaped their orthodontic training and clinical approaches. Their geographical closeness and cultural similarities have also contributed to comparable practices in dental care. Our study aimed to highlight regional orthodontic preferences in the Western Balkans and how they compare to global practices, offering a broader perspective on retention strategies. Additionally, to identify predictive differences in retention protocols, the orthodontist's choices were analyzed based on factors such as sociodemographic characteristics, clinical experience, education, and sources of knowledge.

Materials and Methods

A cross-sectional survey was conducted over six months (from December, 2023 to May, 2024). Questionnaires were distributed via email or in person to 185 orthodontists in Croatia (representing 85% practicing orthodontists), 150 in North Macedonia (78%), and 125 in Kosovo (100%). The survey received responses from 138 orthodontists in Croatia, 95 in North Macedonia, and 73 in Kosovo, resulting in response rates of 75%, 63%, and 58%, respectively.

Statistical analysis was performed using the statistical software package SPSS version 20.0 (SPSS Inc, Armonk, NY: IBM Corp). Baseline characteristics were summarized as frequencies and percentages. Categorical variables were analyzed using the chi-square test and Kruskal-Wallis test. The Z-test for proportions was used as a post hoc test following a significant chi-square test to identify which specific groups or categories differ significantly. The probability value of $P<0.05$ was considered statistically significant.

Results

The ages of practicing orthodontists ranged from 30 to 73 years, with median ages of 46 for Croatian orthodontists, 45 for North Macedonian orthodontists, and 42 for Kosovar orthodontists. Years of experience were similar across groups, with a median of 14 years for Croatians, and 12 years for both North Macedonians and Kosovars. Most orthodontists obtained their specialist degree in their respective capitals: 90% in Prishtina (Kosovo), 92% in Skopje (North Macedonia), and 94% in Zagreb (Croatia). There were no significant differences in work experience between the countries, with both Kosovars and North Macedonians having a median of 12 years, while Croatians had a median of 14 years. Kosovars worked with patients more frequently than Macedonians and Croatians, with a median of 6 days per week compared to 5 days (P<0.001).

No significant association was found between the orthodontists' years of experience or the number of days worked per week and the duration of retention or the number of check-ups during the first and subsequent years, a finding consistent across all three countries.

Most Kosovar orthodontists provided oral information on retention both at the beginning and end of orthodontic treatment. Croatian orthodontists, in contrast, more frequently provided written information at both the start and end of treatment ($P \leq 0.004$). They also gave information more often on potential complications and precautions, while North Macedonian orthodontists more frequently recommended interdental brushes, and Kosovar orthodontists were more likely to advise the use of toothpicks (Table 1).

Table 1.

Comparison of sex and retention procedures across countries

Variable / Country	Croatia	Kosovo	NM	P^*
Ratio of female orthodontist responders	98 (71%)	45 (62%)	72 (76%)	0.134
Giving oral info at the beginning of ortho treatment about retention	121 (88%)[a]	73 (100%)[b]	86 (91%)[a]	0.009
Written info	44 (32%)[a]	8 (11%)[b]	23 (25%)[ab]	0.004
Retention type info	89 (65%)[a]	24 (33%)[b]	57 (60%)[a]	<0.001
Retention duration info	79 (57%)	32 (44%)	57 (60%)	0.086
Giving oral info at the end of ortho treatment about retention	131 (95%)	73 (100%)	89 (94%)	0.107
Written info	95 (69%)[a]	8 (11%)[b]	18 (19%)[b]	<0.001
Info on caution and problems	104 (75%)[a]	0[b]	47 (51%)[c]	<0.013
Info on interdental brush	52 (38%)[ab]	23 (32%)[b]	50 (53%)[a]	0.013
Info on toothpick	23 (17%)[a]	34 (47%)[b]	22 (23%)[a]	<0.001
Info on floss	41 (30%)	18 (25%)	32 (34%)	0.447
Info on electric brush	33 (24%)	23 (32%)	31 (33%)	0.280

*NM, North Macedonia. *- Chi-square test. Countries that share the same superscript letter do not differ significantly according to the Z-test for proportions.*

Choices of retention methods varied among the 3 countries. Removable VFR was the most preferred in Croatia in both jaws (P<0.001), a combination of fixed and removable retainers in Kosovo (P<0.001), while in Macedonia, VFR was followed by a removable acrylic plate. Monitoring after 3 years was less often done by an orthodontist in Croatia than in the other two countries (P<0.001). Patients monitored themselves more often in Croatia. Kosovar orthodontists more frequently checked their patients during retention than others (Table 2).

Table 2.

Comparison of retention appliances and monitoring practices across countries

Variable / Country	Croatia	Kosovo	NM	*P-value*
Maxilla acrylic plate retention	3 (2%)[a]	12 (16%)[b]	38 (40%)[c]	<0.001
Maxilla VFR	109 (79%)[a]	12 (16%)[b]	50 (53%)[c]	<0.001
Maxilla only fixed	2 (1%)[a]	0[a]	10 (11%)[b]	<0.001
Maxilla combination fixed+removable	23 (17%)[a]	49 (67%)[b]	18 (20%)[a]	<0.001
Mandible acrylic plate retention	2 (1%)[a]	0[a]	27 (28%)[b]	<0.001
Mandible VFR	91 (66%)[a]	0[b]	42 (44%)[c]	<0.001
Mandible only fixed	10 (7%)[a]	15 (21%)[b]	21 (22%)[b]	0.002
Mandible combination fixed+removable	45 (33%)[a]	58 (80%)[b]	16 (17%)[c]	<0.001
Retention >3 years – orthodontist monitor	104 (75%)[a]	67 (92%)[b]	94 (99%)[b]	<0.001
Retention >3 years – dentist monitor	10 (7%)	5 (7%)	1 (1%)	0.088
Retention >3 years – patient monitor	43 (31%)[a]	1 (1%)[b]	0[b]	<0.001
Check-ups in retention, fixed appliance during the first year (≥3)	80 (58%)[a]	73 (100%)[b]	53 (56%)[c]	<0.001
Check-ups in retention, removable appliance during the first year (≥3)	91 (66%)[a]	73 (100%)[b]	79 (83%)[a]	<0.001
Check-ups retention after first year (≥2)	43 (31%)[a]	55 (75%)[b]	40 (42%)[a]	<0.001
Class II div 1 check-up retention maxilla ≥3y	94 (68%)[a]	0[b]	80 (84%)[c]	<0.001
Class II div 1 check-up retention mandible ≥3y	92 (67%)[a]	0[b]	81 (85%)[c]	<0.001

The original malocclusion and treatment outcome were reported to be the most important factors influencing the choice of retention type in Macedonia and Croatia (P<0.001), while patients' wishes/motivation, and age/completion of growth were most important in Kosovo (P<0.001).

Personal experience was identified as the most important source of information on retention in all 3 countries. Croatian orthodontists changed their retention protocol less frequently than their colleagues from other countries (P<0.001). In contrast, Kosovar orthodontists most often adjusted both the type of appliance and the retention period (P<0.001) (Table 3).

Table 3.

Comparison of reasons for choosing retention protocols and changes across countries

Variable / Country	Croatia	Kosovo	NM	*P-value*
Retention choice – malocclusion	100 (73%)[a]	13 (18%)[b]	74 (78%)[a]	<0.001
Retention choice – treatment outcome	84 (61%)[a]	8 (11%)[b]	55 (58%)[a]	<0.001
Retention choice – oral hygiene	70 (51%)[a]	24 (33%)[b]	38 (40%)[ab]	0.034
Retention choice – periodontal health	67 (49%)	34 (47%)	38 (40%)	0.425
Retention choice – patient's wish and motivation	49 (36%)[a]	55 (75%)[b]	29 (31%)[a]	<0.001
Retention choice – age/completition of growth	62 (45%)[a]	64 (88%)[b]	40 (42%)[a]	<0.001
Retention choice – myofunctional status	41 (30%)[a]	0[b]	30 (32%)[a]	<0.001
Retention choice – tooth morphology	13 (9%)	3 (4%)	9 (10%)	0.349
Retention choice – wisdom teeth	13 (9%)[a]	23 (32%)[b]	22 (23%)[b]	<0.001
Retention choice – info from residency	36 (26%)[a]	2 (3%)[b]	55 (58%)[c]	<0.001
Retention choice – experience	85 (62%)	44 (60%)	72 (76%)	0.043
Retention choice – literature	24 (17%)[a]	0[b]	48 (51%)[c]	<0.001
Retention choice – courses	21 (15%)[a]	22 (30%)[b]	53 (56%)[c]	0.001
Retention choice – colleagues	18 (13%)[a]	3 (4%)[a]	38 (40%)[b]	<0.001
Changes made in any kind of retention protocol	14 (65%)[a]	61 (84%)[b]	77 (83%)[b]	<0.001
Change in appliance type	24 (17%)[a]	61 (84%)[b]	19 (20%)[a]	<0.001
Change in retention period	34 (32%)[a]	53 (73%)[b]	20 (21%)[a]	<0.001

Removable retainers are manufactured mainly by lab technicians and bonded directly by orthodontists in all 3 countries. Most orthodontists agree on the need for general guidelines on retention (Table 4).

Table 4.

Comparison of retainer manufacturing practices between countries.

Variable / Country	Croatia	Kosovo	NM	*P-value*
Removable retainers manufactured by orthodontists	23 (17%)[a]	12 (16%)[a]	1 (1%)[b]	<0.001
Removable retainers manufactured by assistants	25 (18%)[a]	23 (32%)[a]	0[b]	<0.001
Removable retainers manufactured by lab technicians	102 (74%)[a]	38 (52%)[b]	94 (99%)[ab]	<0.001
Fixed retainers manufactured by orthodontists	121 (88%)[a]	61 (84%)[a]	95 (100%)[b]	<0.001
Fixed retainers manufactured by assistants	2 (1%)	0	0	0.574
Fixed retainers manufactured by lab technicians	6 (4%)	0	0	0.183
General guidelines on retention required	122 (84%)	68 (93%)	90 (95%)	0.198

When considering specific malocclusions and orthodontic treatments, combined retention was the preferred approach for open bite, spacing, and rotation cases across all three countries. In extraction cases, Croatian orthodontists more often chose removable retainers for the maxilla and combined retention for the mandible, while their North Macedonian and Kosovar counterparts preferred a combined approach for both arches. For impaction cases, Croatians primarily used removable retainers for both arches, whereas orthodontists from North Macedonia and Kosovo favored a combination of fixed and removable retainers. In expansion cases, Croatians predominantly selected removable retainers, Kosovars leaned toward a combined approach, and North Macedonians showed an equal preference for both combined and removable retainers (Table 5).

Discussion

This study provides valuable insights into retention protocols among orthodontists in Croatia, North Macedonia, and Kosovo, highlighting regional similarities and differences in clinical practices. Personal experience was the primary source of information on retention across all three countries. Variations were observed in the choice of appliances, retention duration, and follow-up protocols. The findings revealed significant variations between the three countries, highlighting differences in clinical preferences, educational influences, and retention practices.

Surveys on retention practices from different countries have reported response rates ranging widely, from as low as 18%[15] to as high as 91%.[16] With a response rate of 75% for Croatia, 58% in Kosovo, and 63% in North Macedonia, the return rate in this study can be considered relatively high, minimizing the likelihood of non-responder bias.

Table 5.

Comparison of retainer use in specific malocclusions and treatment protocols across countries.

Variable / Country	Croatia	Kosovo	NM	*P-value*
Extraction maxilla				
Fixed retainer	11 (8%)[a]	5 (7%)[a]	21 (22%)[b]	0.001
Removable retainers	69 (50%)[a]	6 (8%)[b]	27 (28%)[c]	<0.001
Combination	58 (42%)	62 (85%)	47 (50%)	<0.001
Spacing maxilla				
Fixed retainer	18 (13%)[a]	0[b]	33 (35%)[c]	<0.001
Removable	29 (21%)	8 (11%)	20 (21%)	0.159
Combination	97 (70%)[a]	65 (89%)[b]	43 (45%)[c]	<0.001
Expansion maxilla				
Fixed retainer	10 (7%)	0	6 (6%)	0.068
Removable retainer	75 (54%)[a]	9 (12%)[b]	48 (51%)[a]	<0.001
Combined	55 (40%)[a]	64 (88%)[b]	41 (43%)[a]	<0.001
Lateral expansion maxilla				
Fixed retainer	7 (5%)	0	5 (5%)	0.141
Removable	91 (66%)[a]	9 (12%)[b]	49 (52%)[c]	<0.001
Combined	41 (30%)[a]	64 (88%)[b]	42 (44%)[c]	<0.001
Impacted canine				
Fixed	13 (9%)[a]	0[b]	29 (31%)[c]	<0.001
Removable	73 (53%)a	9 (12%)b	28 (30%)c	<0.001
Combined	53 (38%)[a]	64 (88%)[b]	39 (41%)[a]	<0.001
Rotated maxilla				
Fixed	14 (10%)[a]	0[b]	27 (28%)[c]	<0.001
Removable	54 (39%)	18 (25%)	27 (28%)	0.063
Combined	71 (51%)[a]	55 (75%)[b]	43 (45%)[a]	0.065
Open bite maxilla				
Fixed	22 (16%)[a]	0[b]	15 (16%)[a]	0.001
Removable	56 (41%)	32 (44%)	36 (38%)	0.739
Combined	66 (48%)	41 (56%)	45 (47%)	0.445
Extraction mandible				
Fixed	16 (12%)[a]	3 (4%)[a]	23 (24%)[b]	0.001
Removable	58 (42%)[a]	18 (25%)[b]	26 (27%)[b]	0.013
Combined	60 (44%)[a]	52 (71%)[b]	46 (48%)[a]	<0.001
Spacing mandible				
Fixed	19 (14%)[a]	1 (1%)[b]	35 (37%)[c]	<0.001
Removable	26 (19%)	23 (32%)	18 (19%)	0.075
Combined	92 (67%)	49 (67%)	42 (44%)	<0.001
Expansion frontal mandible				
Fixed retainer	13 (9%)[a]	0[b]	10 (11%)[a]	0.019
Removable	64 (46%)[a]	18 (25%)[b]	39 (41%)[a]	0.008
Combined	58 (42%)[a]	55 (75%)[b]	47 (50%)[a]	<0.001
Expansion lateral mandible				
Fixed	13 (9%)[a]	0[b]	9 (10%)[a]	0.024
Removable	77 (56%)[a]	18 (25%)[b]	41 (43%)[a]	<0.001
Combined	45 (33%)[a]	55 (75%)[b]	45 (48%)[c]	<0.001
Impacted canine mandible				
Fixed	15 (11%)[a]	0[b]	29 (31%)[c]	<0.001
Removable	67 (49%)[a]	18 (25%)[b]	22 (23%)[b]	<0.001
Combined	54 (39%)[a]	55 (75%)[b]	43 (45%)[a]	<0.001
Rotated teeth mandible				
Fixed	14 (10%)[a]	0[b]	34 (36%)[c]	<0.001
Removable	44 (32%)	18 (25%)	19 (20%)	0.229
Combined	73 (53%)[a]	55 (75%)[b]	41 (43%)[a]	0.001
Open bite mandible				
Fixed	24 (17%)[a]	0[b]	22 (23%)[a]	<0.001
Removable	55 (40%)	32 (44%)	34 (36%)	0.569
Combined	61 (44%)	41 (56%)	39 (41%)	0.126

Orthodontists in Kosovo demonstrated more working days with patients and a tendency for more frequent check-ups during both the first year and subsequent years of retention, compared to their Croatian and Macedonian counterparts. The higher frequency of patient visits and follow-ups among Kosovar orthodontists may reflect economic factors as well as differences in healthcare accessibility, patient compliance, and private practice dynamics, which influence retention protocols. While in North Macedonia orthodontists were more likely to rely exclusively on acrylic removable retainers, in Croatia the preferred choice was VFR; orthodontists in Kosovo predominantly opted for a combination of fixed and removable retainers in both arches. These differences suggest that education and clinical training, along with patient-specific factors, strongly influence the choice of retention appliances, as seen in similar surveys conducted in other countries. The findings of this study align with trends observed in previous surveys, highlighting differences in retention practices across various regions. While VFR remains the most commonly used choice for both jaws in Croatia and acrylic plate in North Macedonia, Kosovo orthodontists strongly support a combination of both fixed retainers and VFR. This variation in retainer preferences may stem from differences in educational training, clinical traditions, and patient compliance across the three countries. The strong preference for a combination of FBR and VFR among Kosovar orthodontists could indicate a more conservative approach to preventing relapse, possibly influenced by concerns over patient adherence to removable retainers alone. In contrast, Croatian orthodontists may favor VFR due to its ease of fabrication and patient acceptance, while the preference for acrylic plates in North Macedonia could reflect established national practices and training influences. Additionally, economic factors and the availability of orthodontic materials may also play a role in shaping these preferences. Studies in Australia and New Zealand have shown a preference for removable retainers in the maxilla, with FBRs used in less than 20% of cases.[11] In contrast, Dutch orthodontists report using fixed retention in the maxilla for approximately 62% of patients, sometimes in combination with removable retainers.[16] Similarly, about 50% of Norwegian orthodontists [17] apply FBR in the mandible, while in the maxilla, FBR is often supplemented with removable options. In the U.S., the use of FBR in the maxilla is even less common, reported in only 2.4%–11% of patients.[12,15]

Factors such as malocclusion and age also influenced retention decisions. In Croatia and North Macedonia, orthodontists reported that original malocclusion and treatment outcome were the primary determinants for selecting retention appliances, while in Kosovo, patient age and growth completion were more significant. This aligns with findings from other studies, where the pre-treatment situation, original malocclusion, and patient-specific characteristics often dictate retention choices.[17] Malocclusion, such as tooth rotations, is identified as the most likely to relapse after treatment and determines the retention protocol.[18]

The role of clinical experience also emerged as a notable factor, with 75% of Macedonian and 60% of Kosovar orthodontists citing it as the main guideline of their retention protocols. This was quite different from a study from Croatia, where the clinical experience of the orthodontist influenced the protocol in only 39%.[14] A similar study reveals that an increase in expertise was associated with more frequent recalls.[19] Fear of relapse influences several decisions, both for clinicians and patients. These concerns drive clinicians to decisions for prolonged or even lifetime retention. While in Kosovo and North Macedonia, 92% to 99% of orthodontists monitor the retention phase up to 3 years and rarely rely on general dentists or patients' self-awareness, in Croatia, orthodontists have less frequent visits than in the other two countries, but after 3 years, patients monitor themselves more than in Kosovo or North Macedonia. On the other hand, our findings revealed that very few orthodontists in the Balkan region support lifetime retention.[16,20] On the contrary, the majority of Swiss orthodontists promote lifetime retention. This gives rise to the concern of numerous follow-ups throughout the lifetime. Whether or not to favor lifetime retention might depend on each country's health regulations or financial agreements between orthodontists and patients, or general dentists and patients. Considering the complications related to stability and periodontal implications, the need for lifelong follow-up by a general dentist instead of an orthodontist could be a drawback. Side effects reported of bonded retainers include torque changes like the x effect, breakages, and bond failures, among others.[21-24] Further research on periodontal implications has identified multiple factors to consider when planning for longer retention and identifying responsible parties to address these issues.[25-27]

In our study, fixed retainers were usually produced directly by orthodontists and removable retainers by lab technicians, which was a similar finding in all countries. Combined retention was the preferred option in both maxilla and mandible in the majority of malocclusions and orthodontic treatments. However, Croatian orthodontists more often chose only a removable retainer for the maxilla in extraction cases and impaction, while a combination of both removable and fixed retainers was the choice of North Macedonian and Kosovar orthodontists. For expansion cases, Croatian and North Macedonian orthodontists more often chose removable retainers, while Kosovar orthodontists still preferred a combination of both. Similarly, in the Netherlands, the majority of orthodontists positioned bonded retainers in both the upper and lower arches, except for situations in which the upper arch had extraction cases or expansion was performed during treatment, in which case a removable retainer was used.[16]

Our findings indicate that written retention guidelines are rarely provided by orthodontists in Kosovo (11%), North Macedonia (25%), and Croatia (32%), despite the well-known challenges of ensuring long-term stability and patient compliance. This may be due to a preference for verbal explanations or the absence of standardized written retention guidelines across these regions. Additionally, the absence of standardized written retention protocols, time constraints in clinical practice, and cultural and educational differences may also play a role. In Kosovo, verbal communication is traditionally preferred over written documentation, particularly in healthcare settings, which could contribute

to this trend. Given that written instructions enhance patient recall and adherence, integrating them alongside verbal explanations could improve retention outcomes, warranting further research and standardized guidelines. Furthermore, studies have shown that written instructions can enhance patient adherence and serve as a useful reference for long-term follow-up.[28] Therefore, the results of this study emphasize the need for standardized guidelines for retention practices. High-quality randomized clinical trials could provide evidence-based insights, helping orthodontists adopt the most effective retention strategies for different clinical scenarios.

Such diversity in retention strategies underscores the importance of further research and the potential value of establishing evidence-based guidelines. By developing standardized recommendations, orthodontists can make more informed decisions that ensure long-term stability for their patients while addressing the variations currently observed in clinical practice.

Limitation

The study relies on self-reported survey data, which may introduce recall bias and limit the generalizability of findings due to potential variations in respondent interpretations and regional healthcare structures.

Clinical Significance

Understanding regional differences in retention practices highlights the need for standardized guidelines and improved patient education, ensuring long-term stability and adherence to retention protocols across different healthcare settings.

This study highlights how orthodontists in Croatia, North Macedonia, and Kosovo approach retention differently, with a mix of clinical habits, training backgrounds, and patient needs determining their choices. A combination of fixed and removable retainers was most common, especially in Kosovo, showing a cautious approach to preventing relapses. While experience plays a significant role in decision-making, the lack of written retention guidelines is a shared challenge. These findings point to a real need for clearer, evidence-based protocols that can help unify practices and improve long-term outcomes for patients. Furthermore, it would be beneficial for orthodontic societies and professional associations to provide practitioners with updated, research-based information on retention practices to ensure standardized and optimal patient care.

Acknowledgments

The authors would like to express their acknowledgments to the participants of this study for their willingness to participate and their insightful contributions. We would also like to thank the University of Rijeka for funding (research project "Stability of orthodontic treatment outcomes," Grant number: uniri-iskusni-biomed-23-18; principal investigator Stjepan Špalj).

Competing Interests

The authors declare that they have no competing interests.

References

1. Keim RG, Gottlieb EL, Nelson AH, Vogels DS 3rd. 2002 JCO study of orthodontic diagnosis and treatment procedures. Part 1. Results and trends. J Clin Orthod. 2002 Oct;36(10):553-68. PMID: 12428306.
2. Littlewood SJ, Millett DT, Doubleday B, Bearn DR, Worthington HV. Retention procedures for stabilising tooth position after treatment with orthodontic braces. Cochrane Database Syst Rev. 2006 Jan 25;(1):CD002283. doi: 10.1002/14651858.CD002283.pub3. Update in: Cochrane Database Syst Rev. 2016 Jan 29;(1):CD002283. doi: 10.1002/14651858.CD002283.pub4. PMID: 16437443.
3. Johnston CD, Littlewood SJ. Retention in orthodontics. Br Dent J. 2015 Feb 16;218(3):119-22. doi: 10.1038/sj.bdj.2015.47. PMID: 25686428.
4. Al-Moghrabi D, Johal A, O'Rourke N, Donos N, Pandis N, Gonzales-Marin C, Fleming PS. Effects of fixed vs removable orthodontic retainers on stability and periodontal health: 4-year follow-up of a randomized controlled trial. Am J Orthod Dentofacial Orthop. 2018 Aug;154(2):167-174.e1. doi: 10.1016/j.ajodo.2018.01.007. PMID: 30075919.
5. Tsichlaki A, O'Brien K, Johal A, Fleming PS. Orthodontic trial outcomes: Plentiful, inconsistent, and in need of uniformity? A scoping review. Am J Orthod Dentofacial Orthop. 2018 Jun;153(6):797-807. doi: 10.1016/j.ajodo.2017.10.022. PMID: 29853237.
6. Pandis N, Fleming PS, Worthington H, Dwan K, Salanti G. Discrepancies in Outcome Reporting Exist Between Protocols and Published Oral Health Cochrane Systematic Reviews. PLoS One. 2015 Sep 14;10(9):e0137667. doi: 10.1371/journal.pone.0137667. PMID: 26368938; PMCID: PMC4569349.
7. Papageorgiou SN, Xavier GM, Cobourne MT. Basic study design influences the results of orthodontic clinical investigations. J Clin Epidemiol. 2015 Dec;68(12):1512-22. doi: 10.1016/j.jclinepi.2015.03.008. Epub 2015 Mar 27. PMID: 25910911.
8. Fleming PS, Seehra J, Polychronopoulou A, Fedorowicz Z, Pandis N. Cochrane and non-Cochrane systematic reviews in leading orthodontic journals: a quality paradigm? Eur J Orthod. 2013 Apr;35(2):244-8. doi: 10.1093/ejo/cjs016. Epub 2012 Apr 16. PMID: 22510325.
9. Gibson R, Harrison J. What are we reading? An analysis of the orthodontic literature 1999 to 2008. Am J Orthod Dentofacial Orthop. 2011 May;139(5):e471-84. doi: 10.1016/j.ajodo.2010.07.023. PMID: 21536189.
10. Singh P, Grammati S, Kirschen R. Orthodontic retention patterns in the United Kingdom. J Orthod. 2009 Jun;36(2):115-21. doi: 10.1179/14653120723040. PMID: 19487742.
11. Wong PM, Freer TJ. A comprehensive survey of retention procedures in Australia and New Zealand. Aust Orthod J. 2004 Nov;20(2):99-106. PMID: 16429880.
12. Valiathan M, Hughes E. Results of a survey-based study to identify common retention practices in the United States. Am J Orthod Dentofacial Orthop. 2010 Feb;137(2):170-7; discussion 177. doi: 10.1016/j.ajodo.2008.03.023.
13. Keim RG, Gottlieb EL, Nelson AH, Vogels DS 3rd. 2008 JCO study of orthodontic diagnosis and treatment procedures,

part 1: results and trends. J Clin Orthod. 2008 Nov;42(11):625-40. PMID: 19075377.
14. Popović Z, Trinajstić Zrinski M, Špalj S. ORTHODONTIST CLINICAL EXPERIENCE AND CLINICAL SITUATION SIGNIFICANTLY INFLUENCE THE RETENTION PROTOCOL - A SURVEY FROM CROATIA. Acta Clin Croat. 2020 Mar;59(1):3-9. doi: 10.20471/acc.2020.59.01.01. PMID: 32724269; PMCID: PMC7382889.
15. Pratt MC, Kluemper GT, Hartsfield JK Jr, Fardo D, Nash DA. Evaluation of retention protocols among members of the American Association of Orthodontists in the United States. Am J Orthod Dentofacial Orthop. 2011 Oct;140(4):520-6. doi: 10.1016/j.ajodo.2010.10.023. PMID: 21967939; PMCID: PMC5161457.
16. Renkema AM, Sips ET, Bronkhorst E, Kuijpers-Jagtman AM. A survey on orthodontic retention procedures in The Netherlands. Eur J Orthod. 2009 Aug;31(4):432-7. doi: 10.1093/ejo/cjn131. Epub 2009 Apr 28. PMID: 19401355.
17. Vandevska-Radunovic V, Espeland L, Stenvik A. Retention: type, duration and need for common guidelines. A survey of Norwegian orthodontists. Orthodontics (Chic.). 2013;14(1):e110-7. doi: 10.11607/ortho.964. PMID: 23646321.
18. Lovatt R, Goonewardenet M, Tennant M. Relapse following orthodontic rotation of teeth in dogs. Aust Orthod J. 2008 May;24(1):5-9. PMID: 18649557.
19. Bibona K, Shroff B, Best AM, Lindauer SJ. Factors affecting orthodontists' management of the retention phase. Angle Orthod. 2014 Mar;84(2):225-30. doi: 10.2319/051313-372.1. Epub 2013 Aug 14. PMID: 23944224; PMCID: PMC8673814.
20. Lai CS, Grossen JM, Renkema AM, Bronkhorst E, Fudalej PS, Katsaros C. Orthodontic retention procedures in Switzerland. Swiss Dent J. 2014;124(6):655-61. doi: 10.61872/sdj-2014-06-01. PMID: 24943474.
21. Nagani NI, Ahmed I. Effectiveness of Two Types of Fixed Lingual Retainers in Preventing Mandibular Incisor Relapse. J Coll Physicians Surg Pak. 2020 Mar;30(3):282-286. doi: 10.29271/jcpsp.2020.03.282. PMID: 32169137.
22. Kučera J, Littlewood SJ, Marek I. Fixed retention: pitfalls and complications. Br Dent J. 2021 Jun;230(11):703-708. doi: 10.1038/s41415-021-2892-4. Epub 2021 Jun 11. PMID: 34117424.
23. Katsaros C, Livas C, Renkema AM. Unexpected complications of bonded mandibular lingual retainers. Am J Orthod Dentofacial Orthop. 2007 Dec;132(6):838-41. doi: 10.1016/j.ajodo.2007.07.011. PMID: 18068606.
24. Shaughnessy TG, Proffit WR, Samara SA. Inadvertent tooth movement with fixed lingual retainers. Am J Orthod Dentofacial Orthop. 2016 Feb;149(2):277-86. doi: 10.1016/j.ajodo.2015.10.015. PMID: 26827985.
25. Pandis N, Vlahopoulos K, Madianos P, Eliades T. Long-term periodontal status of patients with mandibular lingual fixed retention. Eur J Orthod. 2007 Oct;29(5):471-6. doi: 10.1093/ejo/cjm042. PMID: 17974536.
26. Tacken MP, Cosyn J, De Wilde P, Aerts J, Govaerts E, Vannet BV. Glass fibre reinforced versus multistranded bonded orthodontic retainers: a 2 year prospective multi-centre study. Eur J Orthod. 2010 Apr;32(2):117-23. doi: 10.1093/ejo/cjp100. Epub 2009 Oct 16. PMID: 19837746.
27. Kubati JK, Sllamniku Z, Sllamniku A, Kiseri B. Variations of the Plaque Index in Four Timelines during 12 Months in Patients with Two Models of Fixed Retainers after Orthodontic Treatment is Finished. International Journal of Biomedicine. 2024;14(1):148-152. doi:10.21103/Article14(1)_OA23
28. Caetano IRCES, Santiago LM, Marques M. Impact of written information on control and adherence in type 2 diabetes. Rev Assoc Med Bras (1992). 2018 Feb;64(2):140-147. doi: 10.1590/1806-9282.64.02.140. PMID: 29641669.

***Corresponding author**: Jeta Kiseri Kubati. Department of Orthodontics, Faculty of Dentistry, UBT College, Prishtina, Kosovo E-mail: jeta.kubati@ubt-uni.net*

International Journal of Biomedicine 15(3) (2025) 559-563
http://dx.doi.org/10.21103/Article15(3)_OA17

ORIGINAL ARTICLE

Dentistry

INTERNATIONAL JOURNAL OF BIOMEDICINE

The Effect of Diamond Bur Preparation, Air Abrasion and Phosphoric Acid Etching on Micro-Roughness of Tooth Enamel

Timur V. Melkumyan[1,2*], Zurab S. Khabadze[2], Shahnoza K. Musashaykhova[1], Maria K. Makeeva[2], Nuriddin Kh. Kamilov[1], Surayo Sh. Sheraliyeva[1], Diyoraxon A. Inoyatova[1], Angela D. Dadamova[1]

[1]*Tashkent State Medical University, Tashkent, Uzbekistan*
[2]*Peoples' Friendship University of Russia named after Patrice Lumumba, Moscow, Russia*

Abstract

Background: Conventional diamond bur preparation, air abrasion, and acid etching of hard dental tissues have become an integral part of modern restorative dentistry. However, their influence on the surface microstructure of anisotropic enamel is poorly elucidated. This study investigated the effect of acid etching on the micro-roughness of buccal and occlusal enamel surfaces after traditional treatment with a diamond bur and a subsequent air-abrasion with mixtures based on Al_2O_3 or erythritol powders (AFP).
Materials and Results: Eighteen unerupted wisdom teeth extracted for orthodontic reasons were included in the study. Only the coronal parts of the teeth were used. They were cleaned of pulp tissue fragments, sequentially treated in an ultrasonic bath with an 80% alcohol solution and distilled water, and then randomly divided into 2 groups of 9 samples each. In samples of Group 1, the ground surfaces were formed on the buccal sides, and in the samples of Group 2, they were made on the occlusal sides. The samples of each group were divided into subgroups of 3 depending on the type of tooth surface treatment: (1) grinding hard tissues with a diamond bur only; (2) grinding and an air abrasion using Al_2O_3 powder; (3) grinding and an air abrasion using erythritol-based powder (AFP). Areas for acid etching were allocated on the surface of each sample. The etching step was performed using a 37% phosphoric acid gel. Qualitative and quantitative alterations to the enamel surface were registered using SEM and applied software.
Traditional enamel processing with a diamond bur contributed to the formation of the highest roughness value profiles: 9.9±0.7 µm (buccal enamel side) and 9.6±0.8 µm (occlusal enamel side). Acid etching of enamel after diamond bur preparation resulted in a decrease in roughness values of buccal and occlusal enamel sides down to 5.4±0.4 µm and 5.5±0.4 µm, respectively (P=0.000). The use of AFP and Al_2O_3, followed by acid etching, reduced the roughness values to 5±0.4 µm and 5±0.3 µm (P=0.000), respectively, and to 4.4±0.7 µm and 5.4±0.3 µm (P=0.000), respectively.
Conclusion: Air abrasion, followed by acid etching of the enamel, contributed to a significant reduction in the micro-roughness of surfaces formed by the diamond bur. It was also noted that there was no significant difference in roughness values between buccal and occlusal enamel after diamond bur preparation, air abrasion with erythritol, and acid etching. The lowest surface roughness of enamel was observed on buccal sections of tooth slabs after consecutive air abrasion with Al_2O_3 and acid etching.(**International Journal of Biomedicine. 2025;15(3):559-563.**)

Keywords: tooth enamel • diamond bur • micro-roughness • air abrasion • acid etching

For citation: Melkumyan TV, Khabadze ZS, Musashaykhova SK, Makeeva MK, Kamilov NKh, Sheraliyeva SSh, Inoyatova DA, Dadamova AD. The Effect of Diamond Bur Preparation, Air Abrasion and Phosphoric Acid Etching on Micro-Roughness of Tooth Enamel. International Journal of Biomedicine. 2025;15(3):559-563. doi:10.21103/Article15(3)_OA17

Introduction

Due to the need to achieve a seamless appearance of direct tooth-colored restorations and reduce the risk of edge discoloration, which manifests as dark lines, the use of air-abrasive technologies aims to minimize the likelihood of associated cosmetic complications. Additionally, the macro- and micro-roughness of enamel, which can occur during various types of tooth treatment, has a significant impact on gap formation and the longevity of composite fillings.[1-3]

The mineral part of dental enamel, the hardest tissue in the body, is more than 95%. This creates favorable conditions for the formation of a stable, waterproof interface between the filling and the tooth. However, the brittleness of enamel

rods and the high chance of microcrack propagation during grinding with rotary instruments are the main reasons for the occurrence of cohesive failures caused by shrinkage stress and the low strength of the hybrid layer to withstand it[4-6].

Diamond burs and abrasive powders remain the primary tools and materials for tooth preparation and prophylaxis. However, each method has its own advantages and drawbacks. For example, rotary cutting instruments are very effective in the precise removal of caries-affected tooth tissues and finishing of cavity margins. However, the quality of grinding depends on the type of diamond cutter, spindle balance, operator's manual skills, orientation of enamel prisms, and much more. On the other hand, air abrasive methods are less precise than the traditional bur and abrasive powders.. However, they facilitate simultaneous cleaning and help to obtain a proper roughness of tooth adhesive surfaces without any risk of friction and temperature rise in hard tissues while they are being treated. Thus, both methods are in demand and complete each other.[7-9]

To improve the quality of adhesive surfaces, understanding the hierarchical microstructure of tooth enamel and its anisotropy can be of practical value. The variability in the mechanical strength of enamel in different regions is mainly explained by the perpendicular orientation of enamel rods on the occlusal side and their oblique running on the buccal and lingual aspects. Thus, in a case of the same algorithm of tooth preparation, the values of enamel surface roughness in different parts of a tooth crown may differ significantly.[10]

The presence of excessive roughness on the adhesive surfaces of teeth, characterized by pronounced peak heights, valley depths, and peak density of the profile, may be the cause of high shrinkage stress in the composite restorative material and contribute to the emergence of micro-gaps along the boundary of the filling-tooth interface. In this regard, one of the trusted methods for forming a uniform, three-dimensional surface roughness is etching with acid gels.[11,12]

A large amount of data has accumulated in the available databases, indicating the urgent need for acid etching of enamel, regardless of the adhesive system used. Additionally, a preliminary air abrasion of a tooth with Al_2O_3 particles has been considered state of the art for many years. However, the use of soft abrasive powders for treating tooth surfaces may alter the surface topography of enamel differently, and consequently, the efficacy of acid etching can be affected.[13]

Based on this, the study investigated the effect of acid etching on the average roughness of the buccal and occlusal enamel surfaces after traditional treatment with a diamond bur and following air-abrasion with mixtures based on Al_2O_3 or erythritol powders.

Materials and Methods

Eighteen unerupted wisdom teeth extracted for orthodontic reasons were included in the study. Only the coronal parts of the teeth were used. They were cleaned of pulp tissue fragments, sequentially treated in an ultrasonic bath with an 80% alcohol solution and distilled water, and then randomly divided into 2 groups of 9 samples each. In samples of Group 1, the ground surfaces were formed on the buccal sides, and in the samples of Group 2, they were made on the occlusal sides. The grinding of the surfaces in both groups was performed using diamond perforated discs under constant water cooling until flat areas of enamel were formed. Obtained tooth slabs were polished using sandpaper with a gradual increase in the grain size from 400 to 1200 units, and then were ground again at a speed of 40,000 rpm using diamond burs (FG 133139, NTI-Kahla GmbH) inserted in the angled handpiece (1:5 A 200 l, T2 Line, Dentsply Sirona). After that, the samples of each group were divided into subgroups of 3 depending on the type of tooth surface treatment.

In subgroup 1A (n=3) and 2A (n=3), the surface treatment consisted of grinding hard tissues with a diamond bur only; in subgroup 1B (n=3) and 2B (n=3), grinding was combined with an air abrasion using Al_2O_3 powder; in subgroup 1C (n=3) and 2C (n=3) erythritol-based powder was used for air-abrasion. Qualitative and quantitative characteristics of each enamel profile were assessed in 10 arbitrarily chosen sectors. The particle size of Al_2O_3 powder was 27 μm (KaVo, Biberach, Germany), and the size of erythritol grit was 14 μm (Air-Flow Plus (AFP), EMS, Nyon, Switzerland). The air-abrasion was performed with a constant flow of particles at a pressure of 0.25 MPa for an exposure time of 30 seconds. The nozzle was held at 3-5 mm and a 45° angulation of the tool to the surface. After that, the prepared surfaces were thoroughly washed with an air-water spray for 30 seconds and dried. To determine the roughness of the enamel before and after acid etching, the studied surfaces of each sample were additionally divided into 2 halves. The part of the surface subjected to acid etching (treated) was designated by the letter "T." The etching step was performed using a 37% phosphoric acid gel (FineEtch 37, Spident Co., Ltd, Korea) with a 30-second etching time, followed by consecutive rinsing with water for the same time.

To obtain high-quality surface images, the samples were coated with a 10 nm layer of gold using a Quorum magnetron (Q150R ES) sputtering system. Scanning electron microscopy was performed using a SEM EVO MA 15 microscope (Carl Zeiss) and applied software.

Statistical analysis was performed using the statistical software package SPSS v. 21.0. For descriptive analysis, results are presented as mean±standard deviation. Multiple comparisons were performed with one-way ANOVA with Tukey's pairwise comparisons. Student's paired t-test was used to compare the differences between the paired samples. The probability value of $P<0.05$ was considered statistically significant.

Results

Analysis of results demonstrated (Table 1) that traditional enamel processing with a diamond bur was contributing to the formation of the highest roughness value profiles, characterized by the presence of zones of brittle fracture and smooth plastic surfaces, as well as chips of enamel rods on both the buccal and occlusal sides of teeth (Figure 1a, b). Subsequent acid etching was effective in removing sheared and torn material from the surface, leading to partial dissolution of the prism cores and peripheries (Figure 1 c, d). These alterations were accompanied by a significant decrease in average roughness values in 1AT and 2AT by 1.8 and 1.7 times, respectively ($P=0.000$ in both cases).

Table 1.

Ra values of buccal and occlusal enamel treated with different methods.

Roughness (Ra)	Subgroup 1A (n=30)	Subgroup 2A (n=30)	Subgroup 1B (n=30)	Subgroup 2B (n=30)	Subgroup 1C (n=30)	Subgroup 2C (n=30)	*P-value* between subgroups before acid etching
Ra (µm) Before acid etching	9.9±0.7	9.6±0.8	3.4±0.3	4.9±0.4	7.9±0.6	7.9±0.5	F=610.2513; P = 0.0000 P_{1A-2A}= 0.3367; P_{1A-1B}= 0.000; P_{1A-2B}= 0.000; P_{1A-1C}= 0.000; P_{1A-2C}= 0.000; P_{2A-1B}= 0.000; P_{2A-2B}= 0.000; P_{2A-1C}= 0.000; P_{2A-2C}= 0.000; P_{1B-2B}=0.000; P_{1B-1C}= 0.000; P_{1B-2C}= 0.000; P_{2B-1C}= 0.000; P_{2B-2C}= 0.000; P_{1C-2C}= 1.000
P-value	0.000	0.000	0.000	0.000	0.000	0.000	*P-value* between subgroups after acid etching
Ra (µm) After acid etching (T)	5.4±0.4	5.5±0.4	4.4±0.7	5.4±0.3	5.0±0.4	5.0±0.3	F=26.5565; P=0.000o $P_{1AT-2AT}$= 0.9497; $P_{1AT-1BT}$= 0.000; $P_{1AT-2BT}$= 1.000; $P_{1AT-1CT}$= 0.0067; $P_{1AT-2CT}$= 0.0067; $P_{2AT-1BT}$= 0.000; $P_{2AT-2BT}$= 0.9497 $P_{2AT-1CT}$= 0.002; $P_{2AT-2CT}$= 0.002; $P_{1BT-2BT}$= 0.000; $P_{1BT-1CT}$= 0.000; $P_{1BT-2CT}$= 0.000; $P_{2BT-1CT}$= 0.0067; $P_{2BT-2CT}$= 0.0067; $P_{1CT-2CT}$= 1.000

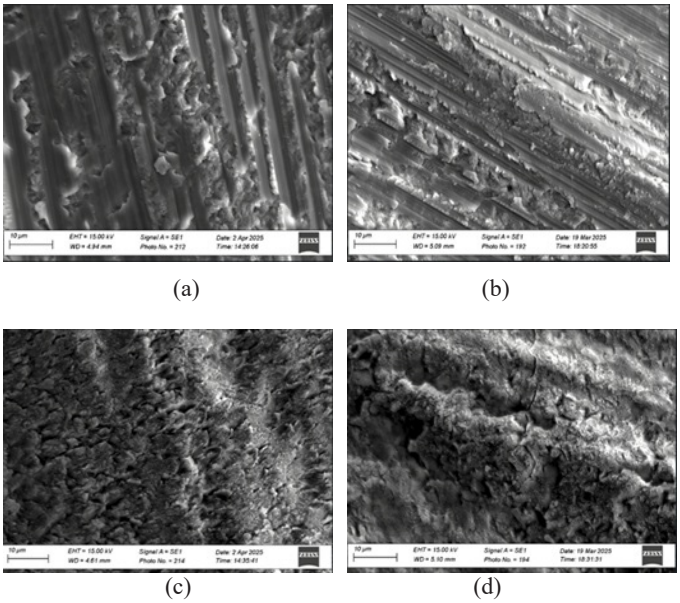

(a) (b) (c) (d)

Figure 1. *(a) -1A; (b) - 2A; (c) - 1AT; (d) - 2AT.*

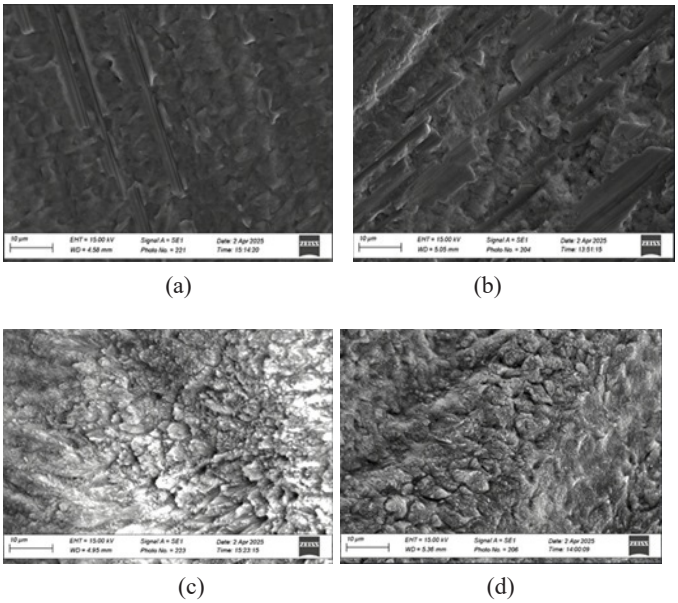

(a) (b) (c) (d)

Figure 2*. (a) -1C; (b) - 2C; (c) - 1CT; (d) - 2CT.*

Air-abrasion of enamel samples with AFP powder was effective in removing chips from the surfaces, but did not contribute to the elimination of traces of brittle and smooth plastic fracture caused by preparation with a diamond bur (Figure 2 a, b). This type of treatment resulted in less reduction of linear micro-roughness of buccal and occlusal enamel surfaces by 1.3 and 1.2 times, respectively.

Consecutive phosphoric acid etching was leading to the typical surface dissolution of intrarod and interrod spaces of enamel (Figure 2 c, d) and further decline in roughness values down to the level of 5µm (*P*=0.000).

Air-abrasion of buccal and occlusal enamel ground sections with Al_2O_3 powder after traditional surface treatment with a diamond bur resulted in a significant decrease in micro-roughness by 2.9 and 1.9 times, respectively (*P*=0.000 in both cases). Visual analysis of micrographs revealed the complete elimination of traces of plastic and brittle fracture caused by a diamond bur. However, there was a lot of chipped material, which was mainly noted on the buccal surfaces, and a significant number of microcracks and pits were observed on the occlusal surface of the enamel (Figure 3 a, b).

Subsequent acid etching contributed to both the cleaning of chips from enamel surfaces (Figure 3 c, d) and an increase in roughness values of buccal and occlusal surfaces by 1.3 and 1.1 times, respectively (*P*=o.ooo). Thus, significant differences were found in roughness (Ra) values between subgroups 1B and 2B, as well as 1BT and 2BT, of 1.4 and 1.2 times, respectively (*P*=0.000 in both cases).

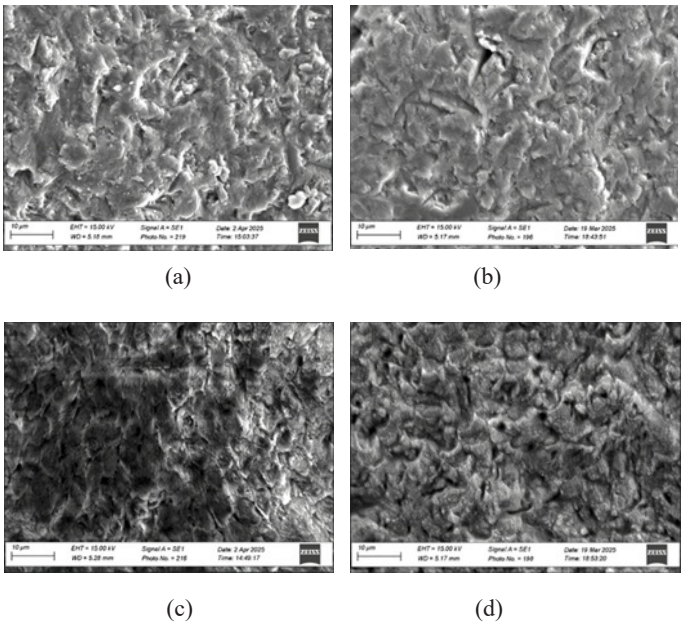

(a) (b)

(c) (d)

Figure 3. *(a) -1B; (b) - 2B; (c) - 1BT; (d) - 2BT.*

Discussion

Among the primary priorities in treating caries pathology and tooth restoration, minimal invasiveness and high aesthetics are of particular concern. The discovery made by Buonocore, along with the differentiated approach to selecting abrasive powders for the prophylaxis and treatment of teeth, became the key to the stability of interfaces and the long-lasting aesthetic performance of direct composite restorations.[14]

However, the specificity of enamel structure is determined by anisotropy, and different surface treatment modalities in combination with acid etching can contribute to the occurrence of various alterations in tooth surfaces.

It has been adopted to categorize the etched patterns of tooth enamel into 5 types: (1) honeycomb-like pattern with a predominant dissolution of prism cores; (2) cobblestone-like pattern with a preferential dissolution of interprism spaces; (3) a combination of the first and second options; (4) pitted surface; and (5) smoothed surface patterns.[15]

Visual analysis of SEM images revealed that acid etching of buccal enamel surfaces after traditional diamond bur preparation or its combination with air abrasion using an erythritol-based powder was the reason for the mixed-type changes of honeycomb- and cobblestone-like patterns. The same treatment algorithms for the occlusal part of tooth enamel led to surface alterations with a predominant cobblestone appearance. Buccal and occlusal enamel surfaces treated with Al_2O_3 powder and etched with an acid were characterized as pitted, with the most pronounced changes on the occlusal sides of teeth.

Conclusion

The results of our study established that air abrasion, followed by acid etching of the enamel, contributed to a significant reduction in the micro-roughness of surfaces formed by the diamond bur. It was also noted that there was no significant difference in roughness values between buccal and occlusal enamel after diamond bur preparation, air abrasion with erythritol, and acid etching. A significant difference was found in average roughness between buccal and occlusal samples after air abrasion with Al_2O_3 powder, followed by acid etching. The lowest surface roughness of enamel was observed on buccal sections of tooth slabs after consecutive air-abrasion with Al_2O_3 and acid etching. In addition, in these samples, a sharp decrease in the enamel surface roughness after sandblasting with aluminum oxide particles was replaced by a slight increase due to the action of phosphoric acid. Such changes in microroughness differed from those of other groups and can be explained by the formation of microcracks and pits on the enamel surface caused by the narrow stream of Al_2O_3 particles.

Competing Interests

The authors declare that they have no competing interests.

References

1. Eram A, Vinay Kr R, K N C, Keni LG, Shetty DD, Zuber M, Kumar S, S P. Air-Abrasion in Dentistry: A Short Review of the Materials and Performance Parameters. J Biomed Phys Eng. 2024 Feb 1;14(1):99-110. doi: 10.31661/jbpe.v0i0.2310-1670. PMID: 38357598; PMCID: PMC10862117.
2. Melkumyan TV, Musashaykhova ShK, Daurova FYu, Kamilov NKh, Sheraliyeva SSh, Dadamova AD. Effect of Air-Abrasion on Shear Bond Strength of Resin Composite to Dentin: A Study in Vitro. International Journal of Biomedicine. 2021;11(4):451-455 doi: 10.21103/Article11(4)_OA10
3. Melkumyan TV, Musashaykhova ShK, Khabadze ZS, Makeeva MK, Dashtieva MU, Kakharova DJ, Dadamova AD. Shear Bond Strength of Two Self-Etching Adhesives to Air-Abraded Dentin: An in Vitro Study. International Journal of Biomedicine. 2022;12(4):591-595.
4. Lagarde M, Vennat E, Attal JP, Dursun E. Strategies to optimize bonding of adhesive materials to molar-incisor hypomineralization-affected enamel: A systematic review. Int J Paediatr Dent. 2020 Jul;30(4):405-420. doi: 10.1111/ipd.12621. Epub 2020 Feb 12. PMID: 31990108.
5. Khabadze Z, Generalova Yu, Abdulkerimova S, Dashtieva M, Borlakova M, Meremkulov R, Mordanov O, Magomedova Kh, Kulikova A, Bakaev Yu, Golubenkova A, Voskressensky L, Melkumyan T. Analysis of the Anaerobic Conversion Efficiency of Various Group Composite Material. Journal of International Dental and Medical Research. 2023;16(3):975-982.
6. Wu SX, Gong X, Ni YQ, Chen WL, Wang CY. Material removal and surface damage in high-speed grinding of enamel. J Mech Behav Biomed Mater. 2022 Dec;136:105532. doi: 10.1016/j.jmbbm.2022.105532. Epub 2022 Oct 19. PMID: 36283298.
7. Li QZ, Wang CY, Zheng LJ, Zhao DN, Zeng CF.

Machinability of enamel under grinding process using diamond dental burrs. Proc Inst Mech Eng H. 2019 Nov;233(11):1151-1164. doi: 10.1177/0954411919873804. Epub 2019 Sep 18. PMID: 31532324.
8. Li QZ, Wang CY, Zheng LJ, Zhao DN, Zeng CF. Machinability of enamel under grinding process using diamond dental burrs. Proc Inst Mech Eng H. 2019 Nov;233(11):1151-1164. doi: 10.1177/0954411919873804. Epub 2019 Sep 18. PMID: 31532324.
9. Wiegand A, Lechte C, Kanzow P. Adhesion to eroded enamel and dentin: systematic review and meta-analysis. Dent Mater. 2021 Dec;37(12):1845-1853. doi: 10.1016/j.dental.2021.09.014. Epub 2021 Sep 27. PMID: 34593245.
10. Zaytsev D, Panfilov P. Anisotropy of the mechanical properties of human dental enamel. Materials Letters. 2015;159:428-431. Doi:10.1016/j.matlet.2015.07.057.
11. Melkumyan TV, Makhamadaminova KD, Kamilov EKh. Clinical and Experimental Evaluation of the Effectiveness of «Soft-Start» Polymerization in Dental Composite Restoration. International Journal of Biomedicine. 2012;2(3):242-245.
12. Melkumyan TV, Kakhkharova DJ, Dadamova AD, Kamilov NKh, Siddikova SSh, Rakhmatullaeva ShI, Masouleh SM. Comparative Analysis of *in vitro* Performance of Total-Etch and Self-Etch Adhesives. International Journal of Biomedicine. 2016;6(4):283-286.
13. Koup MA, Blatz MB. The Selective Enamel Etch Technique. Compend Contin Educ Dent. 2024 May;45(5):243-246; quiz 247. PMID: 38900462.
14. Bevilacqua L, Cadenaro M, Sossi A, Biasotto M, Di Lenarda R. Influence of air abrasion and etching on enamel and adaptation of a dental sealant. Eur J Paediatr Dent. 2007 Mar;8(1):25-30. PMID: 17359211.
15. Cerci BB, Roman LS, Guariza Filho O, Camargo ES, Tanaka OM. Dental enamel roughness with different acid etching times: Atomic force microscopy study. Eur J Gen Dent. 2012;1:187-91.

***Corresponding author:** Prof. Timur V. Melkumyan, PhD, ScD. Tashkent State Dental Institute Tashkent, Uzbekistan. Peoples' Friendship University of Russia named after Patrice Lumumba, Moscow, Russia. E-mail: t.dadamov@gmail.com*

International Journal of Biomedicine 15(3) (2025) 564-571
http://dx.doi.org/10.21103/Article15(3)_OA18

ORIGINAL ARTICLE

Biotechnology

INTERNATIONAL JOURNAL OF BIOMEDICINE

Nanochitosan-Coated *Zingiber cassumunar* (Plai) for Anti-Inflammatory Applications: Characterization and Therapeutic Evaluation

Natthakamol Wakhuwathapong[1,2], Pitchayapa Janyacharoen[1,2], Nita Jungpichanwanit[1,2], Sirichai Phinsiri[2], Alisa Boonsuya[2], Patpicha Arunsan[2,5], Weerapat Foytong[1], Nathkapach Kaewpitoon Rattanapitoon[2,3], and Schawanya Kaewpitoon Rattanapitoon[2,4], Chutharat Thanchonnang[2,3,6*]

[1]*Surawiwat School, Suranaree University of Technology, Nakhon Ratchasima, Thailand*
[2]*Parasitic Disease Research Center, Suranaree University of Technology, Nakhon Ratchasima, Thailand*
[3]*FMC Medical Center, Nakhon Ratchasima, Thailand*
[4]*School of Family Medicine and Community Medicine, Institute of Medicine, Suranaree University of Technology, Nakhon Ratchasima, Thailand*
[5]*Faculty of Medicine, Vongchavalitkul University, Nakhon Ratchasima, Thailand*
[6]*Translational Medicine program, Institute of Medicine, Suranaree University of Technology, Nakhon Ratchasima, Thailand*

Abstract

Zingiber cassumunar Roxb. (Plai), a traditional Thai medicinal plant, is widely recognized for its anti-inflammatory, analgesic, and antimicrobial properties. However, its clinical use has been limited due to poor solubility, stability, and skin permeability. This study aimed to develop and evaluate a nanochitosan-coated formulation incorporating *Zingiber cassumunar* (Plai) extract for anti-inflammatory applications. The study focuses on characterizing the physicochemical properties of the formulation using gas chromatography–mass spectrometry (GC-MS), Fourier transform infrared spectroscopy (FTIR), and scanning electron microscopy (SEM) techniques, as well as assessing its anti-inflammatory efficacy through the albumin denaturation assay.

The nanoparticles were characterized by GC-MS, FTIR, and SEM. GC-MS, and showed enrichment of lipophilic, volatile compounds like lidocaine, benzyl benzoate, and squalene. FTIR confirmed successful Plai incorporation into the chitosan matrix with strong molecular interactions. SEM revealed porous, sponge-like structures, supporting high drug-loading efficiency and potential for controlled release. Anti-inflammatory activity was assessed via BSA protein denaturation assay, revealing that all formulations, including crude extract, chitosan, and nanochitosan-Plai, exhibited high inhibition across tested concentrations. Notably, the nanochitosan-Plai formulation showed significantly superior activity at the highest concentration. These findings suggest that nanochitosan encapsulation significantly enhances the therapeutic efficacy of Plai, supporting its potential development as an advanced topical delivery system for the targeted management of localized inflammatory conditions.(**International Journal of Biomedicine. 2025;15(3):564-571.**)

Keywords: anti-inflammatory effect • nanochitosan • Plai • physical characterization

For citation:Wakhuwathapong N, Janyacharoen P, Jungpichanwanit N, Phinsiri S, Boonsuya A, Arunsan P, Foytong W, Rattanapitoon NK, Rattanapitoon SK, Thanchonnang C. Nanochitosan-Coated *Zingiber cassumunar* (Plai) for Anti-Inflammatory Applications: Characterization and Therapeutic Evaluation . International Journal of Biomedicine. 2025;15(3):564-571. doi:10.21103/Article15(3)_OA18

Abbreviations

BSA, bovine serum albumin; **DW**, distilled water; **FTIR**, Fourier transform infrared spectroscopy; **GC-MS**, gas chromatography–mass spectrometry; **SEM**, scanning electron microscopy.

Introduction

Zingiber cassumunar Roxb., commonly referred to as Plai in Thailand, has been extensively used in Thai traditional medicine for the treatment of a variety of ailments, including muscle pain, sprains, inflammation, wounds, skin disorders, asthma, rheumatic conditions, and pain.[1,2] The essential Plai and rhizome extract of *Z. cassumunar* are known to exhibit local anesthetic and analgesic properties,[3,4] as well as potent anti-inflammatory effects.[5] Furthermore, antimicrobial studies have demonstrated that it possesses inhibitory activity against several bacterial and fungal strains,[3] reinforcing its value as a multifunctional herbal remedy. Moreover, *Z. cassumunar* has demonstrated a variety of biological activities,[4] including anti-inflammatory and analgesic effects, as well as ovicidal, insecticidal, cytotoxic, and antibacterial properties.[6,7] It has also exhibited potential in enzyme inhibition. Recent clinical studies further support the efficacy and safety of *Z. cassumunar* rhizome, particularly in reducing pain.[8,9]

The pharmacological efficacy of *Z. cassumunar* is largely attributed to its bioactive constituents, particularly terpinene-4-ol, α-terpinene, and phenylbutenoids such as (E)-1-(3,4-dimethoxyphenyl)but-1-ene. These compounds have been shown to exert strong anti-inflammatory and analgesic effects in preclinical models, including carrageenan-induced paw edema and acetic acid-induced vascular permeability assays.[10] At the molecular level, extracts of *Z. cassumunar* have been reported to modulate key inflammatory signaling pathways. These phenylbutenoid compounds act as key bioactive indicators for quantifying herbal extracts,[11]–emphasizing their therapeutic value in managing inflammation and supporting muscle recovery. The processes of extraction and standardization are essential in developing effective herbal preparations. Choosing an optimal extraction technique and an appropriate solvent is crucial for obtaining the highest yield of active ingredients, while standardization guarantees the reliability and consistency of therapeutic outcomes.

Despite these promising bioactivities, the clinical application of *Z. cassumunar* remains limited due to poor solubility, stability, and low skin permeability.[2] To overcome these limitations, nanocarrier systems have been explored to improve the delivery and bioavailability of phytochemicals.[12,13]

Chitosan, a natural biopolymer derived from chitin,[14] has emerged as a promising material for both systemic and localized drug and vaccine delivery. Its widespread use in pharmaceutical and biomedical fields is attributed to its excellent biocompatibility, biodegradability, and intrinsic bioactivity. Structurally similar to glycosaminoglycans, chitosan offers low toxicity and structural stability, making it less harmful to biological systems. Furthermore, it is easily broken down by enzymatic degradation, which enhances its safety profile. These properties make chitosan highly suitable for various therapeutic applications.[15,16] Chitosan-based nanoparticles, in particular, offer advantages such as biocompatibility, biodegradability, and mucoadhesive properties, making them suitable for topical drug delivery systems.[17] Prior studies have shown that encapsulating herbal extracts,[18] including essential oils of *Z. cassumunar*, in chitosan nanoparticles enhances their physicochemical stability and facilitates.

In this study, a nanochitosan-based spray formulation incorporating *Z. cassumunar* extract was developed using the ionic gelation method. The formulation was characterized using Fourier-transform infrared spectroscopy (FTIR), gas chromatography–mass spectrometry (GC-MS), and scanning electron microscopy (SEM) to confirm its chemical integrity and particle morphology. The anti-inflammatory efficacy of the formulation was evaluated through albumin denaturation assays and compared with a standard reference drug, diclofenac. By integrating traditional herbal medicine with nanotechnology, this study proposes an innovative and effective topical therapy that enhances the therapeutic potential of *Z. cassumunar*. The findings support the development of safe, sustainable, and locally sourced alternatives for managing inflammation-related conditions.

Materials and Methods

Preparation of Chitosan Nanoparticles

Chitosan nanoparticles were prepared using the ionotropic gelation method.[19-21] Briefly, 0.25 g of sodium tripolyphosphate (TPP) (CAS Numbers: 7758-29-4) was dissolved in 250 mL of deionized water (DI) to serve as the cross-linking agent. Simultaneously, 0.1 g of chitosan (Lot Numbers: M13001) was dissolved in 5 mL of 1% acetic acid (CAS Numbers: 64-19-7), and subsequently diluted with 500 mL of DI water. The chitosan solution (475 mL) was then mixed with 25 mL of *Zingiber cassumunar* (Plai) crude extract (Batch: TS43Z1C21B) under continuous stirring at 500 rpm and 25°C for 1 hour using a magnetic stirrer. Following this, 250 mL of the TPP solution was added dropwise to the chitosan–Plai mixture, and the suspension was stirred for an additional 24 hours to facilitate nanoparticle formation. The mixture was left undisturbed to precipitate for 1 week, after which it was subjected to centrifugation at 10,000 rpm for five cycles, with purification conducted between each cycle to remove unbound components. The resulting product was stored at –80°C for 3 days, then freeze-dried to obtain the nanochitosan-Plai formulation in powder form.

Characterization Analysis

Gas Chromatography–Mass Spectrometry (GC-MS) Analysis

The chemical composition of *Zingiber cassumunar* (Plai) crude extract was analyzed using GC-MS to identify its bioactive constituents. The extract was prepared at an appropriate concentration and subjected to analysis using an Agilent 7890A gas chromatograph coupled with an Agilent 7000B triple quadrupole mass spectrometer, operated via GC-QQQ software. Compound identification was performed using the NIST MS Search 2.0 library. For gas chromatography, the sample was injected using a liquid autosampler in split mode at a ratio of 5:1, with an injection volume of 2 µL. The HP-5 capillary column (20 m × 0.18 mm, 0.18 µm film thickness) was used for compound separation. The injection port and transfer line temperatures were set at 250°C, and helium

served as the carrier gas at a flow rate of 1.0 mL/min. In the mass spectrometer, ionization was achieved using electron ionization (EI) at 70eV. The ion source temperature was maintained at 230°C, and data were acquired in full scan mode over a mass range of 35–550.

Fourier Transform Infrared Spectroscopy (FTIR) Analysis

Fourier transform infrared spectroscopy (FTIR) is an analytical technique used to identify chemical bonds and molecular structures by measuring the absorption of infrared radiation at various wavelengths. In this study, nanochitosan-Plai samples were characterized using FTIR with a Vertex 70 instrument (Bruker, Switzerland; Serial No. 3099/HYP.1097). Spectra were recorded at a resolution of 4 cm^{-1}, with 64 scans performed for both the sample and the background. Each analysis was repeated at least three times to ensure reproducibility. Data acquisition and processing were carried out using OPUS software.

Characterization using Scanning Electron Microscopy (SEM) Analysis

The morphology of nanochitosan-Plai nanoparticles was examined using SEM to assess their surface structure, particle shape, and distribution. Freeze-dried samples were carefully mounted on aluminum stubs and sputter-coated with a thin layer of gold to enhance conductivity. Imaging was performed using a JEOL JSM-6010LV SEM system, equipped with Energy Dispersive X-ray Spectroscopy (EDS) for elemental analysis. SEM micrographs were captured at appropriate magnifications to reveal the porous, aggregated morphology and irregular surface features typical of nanochitosan-based formulations. These morphological insights were critical for evaluating the physical characteristics and structural stability of the nanoparticles.

Anti-Inflammatory Activity

The anti-inflammatory activity of the test samples was evaluated using the Bovine Serum Albumin (BSA) (CAS Numbers: 9048-46-8) protein denaturation method.[22] A 5% BSA solution (CAS No. 9048-46-8) was prepared in distilled water. Test samples included Diclofenac sodium (positive control), chitosan (dissolved in 0.05% acetic acid), Plai crude extract, and nanochitosan-Plai formulation. Each sample was prepared at six concentrations: 25, 50, 100, 200, 500, and 1000 µg/mL. For each concentration, 1 mL of the test solution was mixed with 1 mL of the 5% BSA solution and incubated at 27°C for 15 minutes. A control solution consisting of BSA and distilled water (DW) was also prepared. After incubation, the mixtures were heated at 70°C for 10 minutes to induce protein denaturation. The samples were then cooled to room temperature, and the absorbance was measured at 660 nm using a VICTOR® Nivo™ Multimode Plate Reader (Serial No. HH35L2020289).

The percentage of protein denaturation inhibition, indicating anti-inflammatory activity, was calculated using the following formula:[23]

$$\%\text{Inhibition} = \frac{\text{Absorbance of control - Absorbance of sample}}{\text{Absorbance of control}} \times 100$$

Statistical analysis

All data are presented as mean ± standard deviation (SD). Statistical comparisons between groups were conducted using one-way ANOVA. A probability value $P \leq 0.05$ was considered statistically significant.

Results

Gas Chromatography–Mass Spectrometry (GC-MS) Analysis

Gas chromatography–mass spectrometry (GC–MS) analysis was conducted to compare the chemical constituents of Zingiber cassumunar (Plai) crude extract and the nanochitosan-Plai formulation. The chromatogram of the crude Plai extract in Table 1 was dominated by hydrophilic and solvent-derived compounds, with propylene glycol comprising 69.42% of the total peak area, followed by 1,3-butanediol (22.80%) and ethanol, 2-phenoxy- (5.77%). These compounds, often used as cosolvents in herbal extraction, were accompanied by a diverse range of minor bioactive compounds, including vanillin, Zingiberone, β-sesquiphellandrene, and several saturated and unsaturated fatty acids, such as oleic acid, octadecanoic acid, and n-hexadecanoic acid.

Notably, DMPBD (detected at RT 25.986, 0.18%) was also present, which may represent a bioactive aromatic derivative contributing to the therapeutic profile of Plai. In contrast, the nanochitosan-Plai formulation in Table 2 exhibited a distinctly different chemical profile, enriched in hydrophobic and volatile components. Major peaks included lidocaine benzyl benzoate (15.35%), phenol, 2,4-bis(1,1-dimethylethyl)- (9.86%), tetradecane (6.98%), dodecane (6.86%), and benzene, 1,3-bis(1,1-dimethylethyl)- (6.69%). Alkanes such as undecane, hexadecane, octadecane, and eicosane were also abundant, along with squalene (2.87%), a compound known for its emollient and antioxidant activity. Many of these hydrophobic compounds were not detected in the crude extract, suggesting that the nanoencapsulation process enhanced the retention or solubilization of lipophilic constituents. This chemical shift may be attributed to interactions with the chitosan matrix, improved compound stability, or differences in extraction and formulation conditions. The presence of new or more prominent bioactive compounds in the nanoparticle formulation supports the potential of nanochitosan-based delivery systems to enhance the therapeutic efficacy and skin permeability of Plai extract for topical or transdermal applications.

Fourier Transform Infrared Spectroscopy (FTIR) Analysis

FTIR spectrum of the nanochitosan-Plai formulation revealed the presence of distinct absorption bands indicating various functional groups. A broad absorption band observed around 3400 cm^{-1} corresponds to the stretching vibrations of O–H and N–H groups, confirming the presence of hydroxyl and amine functionalities from both chitosan and plant-derived compounds. Peaks near 2920 cm^{-1} and 2850 cm^{-1} are associated with aliphatic C–H stretching vibrations. A noticeable band around 1650 cm^{-1} can be attributed to C=O stretching from amide I, while a peak near 1580 cm^{-1} suggests N–H bending (amide II), both of which are characteristic of chitosan (Figire 1).

Table 1.

Chemical constituents identified in the Zingiber cassumunar (Plai) crude extract using GC-MS.

RT	Area	Area Sum %	Name
10.739	1271088634	69.42	Propylene Glycol
11.671	417481384	22.80	1,3-Butanediol
12.013	168629	0.01	Ethanol, 2,2'-oxybis-
12.532	485358	0.03	2-Propanol, 1,1'-oxybis-
12.749	972462	0.05	1,3-Pentanediol, 2,2,4-trimethyl-
12.824	294261	0.02	2,4-Pentanediol, 3-methyl-
15.208	105582383	5.77	Ethanol, 2-phenoxy-
17.261	61528	0.00	n-Decanoic acid
17.770	155176	0.01	Vanillin
18.632	57340	0.00	Octanoic acid, methyl ester
19.013	80874	0.00	Benzaldehyde, 3,4-dimethoxy-
19.225	375999	0.02	Tetraethylene glycol
19.672	120374	0.01	β-Sesquiphellandrene
20.296	894806	0.05	Dodecanoic acid
20.679	687543	0.04	2-Allyl-1,4-dimethoxy-3-methyl-benzene
21.077	57051	0.00	Zingiberone
21.246	3520335	0.19	Triquinacene, 1,4-bis(methoxy)-
21.575	70805	0.00	Decanoic acid, methyl ester
22.440	122403	0.01	1,4,7,10,13,16,19-Heptaoxa-2-cycloheneicosanone
23.017	120653	0.01	Cinnamic acid, 3,4-dimethoxy-, methyl ester
23.044	115816	0.01	Tetradecanoic acid
23.179	327377	0.02	Hexaethylene glycol
23.685	758751	0.04	Triquinacene, 1,4,7-tris(methoxy)-
24.286	415809	0.02	Dodecanoic acid, 3-hydroxypropyl ester
24.356	169599	0.01	Lauric anhydride
24.433	3111723	0.17	1,2-Dimethoxy-4-(3-methoxy-1-propenyl)benzene
24.614	127560	0.01	2(3H)-Furanone, 3-heptyldihydro-
25.653	673595	0.04	n-Hexadecanoic acid
25.743	336829	0.02	Dodecanoic acid, 1-methylpropyl ester
25.986	3363567	0.18	DMPBD
26.833	6440897	0.35	13-Hexyloxacyclotridecan-2-one
26.896	286183	0.02	Glycerol 1-myristate
28.001	649561	0.04	Oleic Acid
28.376	1546720	0.08	Octadecanoic acid
28.497	131795	0.01	Stearic acid, 2-hydroxy-1-methylpropyl ester
29.739	125525	0.01	Glycerol β-palmitate
30.787	468867	0.03	Heptaethylene glycol
31.172	1456882	0.08	12-Hydroxystearic acid
32.677	105111	0.01	Glyceryl 1-monostearate
33.575	145933	0.01	Diisooctyl phthalate
34.790	653620	0.04	Octaethylene glycol
38.237	1863599	0.10	2-Undecenoic acid, trimethylsilyl ester
39.898	1538073	0.08	4,7-Dimethoxy-2-methyl-1H-indene
40.424	1513850	0.08	4,7-Dimethoxy-2-methyl-1H-indene
41.738	1232807	0.07	1-Methyl-1-(5-tridecyl)oxy-1-silacyclopentane
42.302	537068	0.03	Nonaethylene glycol
43.123	140544	0.01	Stigmasterol
44.160	338163	0.02	β-Sitosterol
Total	1830973822	100	

Table 2.

Chemical constituents identified in the nanochitosan-Plai using GC-MS.

RT	Area	Area Sum %	Name
10.121	133871	3.48	Decane
10.631	59535	1.22	Octane, 3,3-dimethyl-
11.394	203810	4.17	Undecane, 5,7-dimethyl-
12.278	145782	2.98	Undecane
14.072	97856	2.00	1-Dodecene
14.230	335476	6.86	Dodecane
15.222	326928	6.69	Benzene, 1,3-bis(1,1-dimethylethyl)-
17.606	78302	1.60	1-Tetradecene
17.731	341523	6.98	Tetradecane
19.545	482228	9.86	Phenol, 2,4-bis(1,1-dimethylethyl)-
20.782	278281	5.69	Hexadecane
23.521	201634	4.12	Octadecane
26.041	119315	2.44	Eicosane
26.139	80801	1.65	Indazol-4-one, 3,6,6-trimethyl-1-phthalazin-1-yl-1,5,6,7-tetrahydro-
28.717	74171	1.52	Docosane
33.284	750788	15.35	Lidocaine benzyl benzoate
37.444	140551	2.87	Squalene
Total	3850852		

Additionally, peaks between 1150 and 1020 cm^{-1} correspond to C–O–C and C–O stretching vibrations, indicating saccharide structures and ether linkages. The presence of these characteristic bands confirms the successful incorporation of *Zingiber cassumunar* extract into the chitosan matrix and suggests potential hydrogen bonding or molecular interactions between chitosan and bioactive compounds in the extract. The resulting FTIR spectrum is consistent with the formation of a stable nanoformulation containing phytochemically active components.

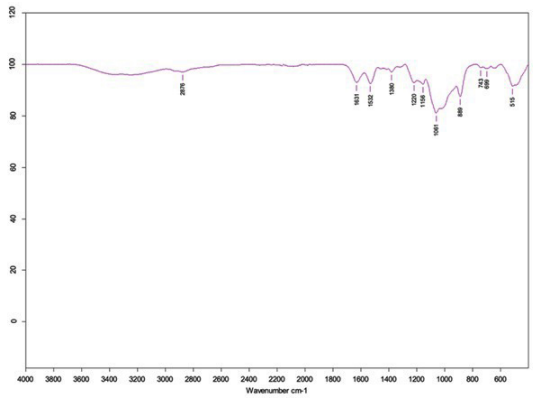

Fig. 1. *FT-IR spectrum and chemical formula of nanochitosan-Plai.*

Scanning Electron Microscopy (SEM) Analysis

Scanning electron microscopy **(**SEM) analysis was performed to observe the surface morphology and structural

characteristics of the nanochitosan-Plai formulation. At low magnification (Fig. 2 (a), 100×), the surface displayed randomly distributed, irregular aggregates with a flaky and rough texture. The particles were widely scattered and varied in size, indicating that the formulation was composed of heterogeneous agglomerates formed during the drying or preparation process. At high magnification (Fig. 2 (b), 30,000×), the morphology of the nanoparticles was more distinctly revealed. The image showed porous, sponge-like structures with uneven surfaces, characteristic of chitosan-based nanomaterials. The nano-structured morphology and rough surface suggested increased surface area, which may enhance drug loading and facilitate controlled release. These morphological features confirm that the nanochitosan effectively encapsulated the *Zingiber cassumunar* extract, forming a stable nanosystem suitable for transdermal or topical delivery.

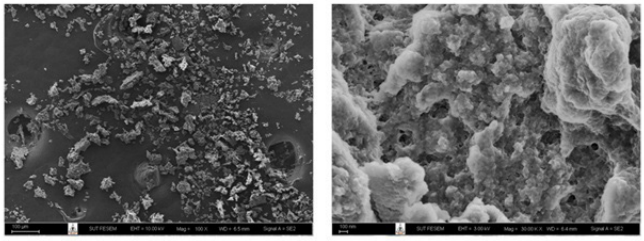

Fig. 2. *Scanning Electron Microscopy (SEM) images of nanochitosan-Plai formulation at different magnifications:*

(a) Low magnification (100×) showing dispersed and irregularly shaped aggregated particles scattered across the substrate surface.

(b) High magnification (30,000×) revealing porous, rough, and sponge-like nanostructures with interconnected networks, indicative of successful encapsulation and nanoscale morphology.

that the anti-inflammatory effect of Plai is already pronounced even without nanoencapsulation. However, the marginal improvements seen with the nanochitosan formulation suggest a trend toward greater efficacy, particularly at higher doses, as shown in Fig. 3. Overall, the results support that nanochitosan-Plai retains the potent anti-inflammatory activity of the crude extract and may offer advantages in terms of delivery and therapeutic performance, especially when applied in formulations requiring enhanced stability and skin penetration, such as transdermal sprays or topical films.

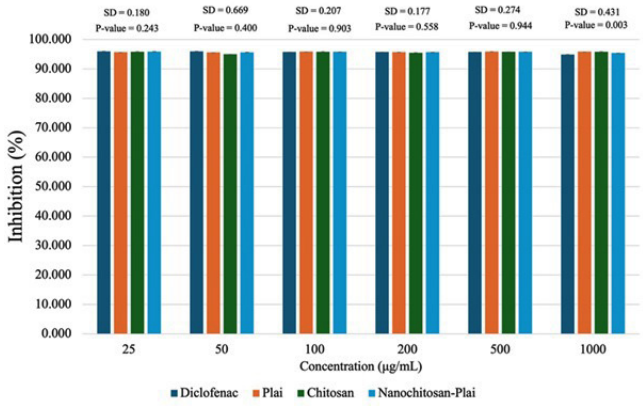

Fig. 3. *Percentage inhibition of anti-inflammation activity for Diclofenac, Plai extract, Chitosan, and Nanochitosan-Plai formulations at different concentrations (25–1000 µg/mL). The results are expressed as mean inhibition percentages (n = 3) with standard deviations shown above each group. Statistical analysis using ANOVA indicates no significant differences between groups at concentrations of 25–500 µg/mL (P > 0.05), while a significant difference was observed at 1000 µg/mL (P = 0.003), where the Nanochitosan-Plai formulation exhibited the highest anti-inflammatory activity.*

Anti-Inflammatory Activity

The anti-inflammatory activity, as evaluated by the BSA protein denaturation assay, revealed that all four tested formulations, Diclofenac (positive control), *Zingiber cassumunar* (Plai) extract, chitosan, and the nanochitosan-Plai formulation, exhibited high levels of inhibition across all tested concentrations (25–1000 µg/mL), with values consistently exceeding 90%. This suggests that both the crude and nanoformulated versions of Plai, as well as chitosan alone, possess substantial anti-inflammatory potential, likely due to their bioactive phenolic and terpenoid constituents and, in the case of chitosan, its inherent bioadhesive and modulatory properties. Although the inhibition values were numerically close across groups, a statistically significant difference (P=0.003) was observed at the highest concentration (1000 µg/mL), where the nanochitosan-Plai formulation demonstrated superior inhibition compared to the other groups. This enhanced effect at higher concentrations may be attributed to the improved stability, solubility, and sustained release properties of the nanoformulated system, which likely increase the bioavailability of the active compounds in Plai. At lower concentrations (25–500 µg/mL), there were no significant differences among the groups (P>0.05), indicating

The anti-inflammatory activity of the nanochitosan-Plai formulation was evaluated using the BSA protein denaturation assay, a well-established model for assessing the stabilization of protein structures under inflammatory conditions. All tested groups, including diclofenac (positive control), *Z. cassumunar* (Plai) extract, chitosan, and the nanochitosan-Plai formulation, exhibited high levels of protein denaturation inhibition (>90%) across all tested concentrations (25–1000 µg/mL). These results highlight the inherent anti-inflammatory potential of both the Plai extract and chitosan polymer. Interestingly, while the inhibition rates among groups were closely matched at lower concentrations (25–500 µg/mL), no statistically significant differences were found (P>0.05), indicating that the crude extract of *Z. cassumunar* already possesses strong anti-inflammatory activity, consistent with previous reports attributing this to the presence of active compounds such as terpinene-4-ol, sabinene, and (E)-1-(3,4-dimethoxyphenyl)but-1-ene.[10] However, at the highest tested concentration (1000 µg/mL), the nanochitosan-Plai formulation significantly outperformed the other groups (P=0.003), demonstrating a clear enhancement of bioactivity in a dose-dependent manner.

Discussion

In this study, a nanochitosan-based formulation incorporating *Zingiber cassumunar* (Plai) extract was successfully developed using the ionic gelation technique. The formulation underwent comprehensive characterization via GC-MS, FTIR, SEM, confirming its chemical composition and nanoparticulate morphology. Anti-inflammatory potential was assessed through albumin denaturation assays, with diclofenac serving as the reference drug. The integration of traditional herbal medicine with nanotechnology presents a promising strategy for enhancing topical therapeutic efficacy. These results underscore the potential of this formulation as a safe, sustainable, and locally derived anti-inflammatory agent.

The GC–MS analysis of *Zingiber cassumunar* (Plai) crude extract and nanochitosan-Plai formulation revealed distinct differences in chemical profiles, suggesting that nanoencapsulation significantly influences compound retention and presentation. In the crude extract, the dominant components were hydrophilic and solvent-associated compounds such as propylene glycol (69.42%), 1,3-butanediol (22.80%), and ethanol, 2-phenoxy- (5.77%), consistent with earlier studies that reported alcohols and glycols as major constituents when hydroalcoholic or aqueous extractions were used.[24,25] Minor but therapeutically relevant compounds such as Zingiberone, β-sesquiphellandrene, vanillin, and unsaturated fatty acids (e.g., oleic and octadecanoic acids) were also identified, aligning with previous findings that Plai contains phenylbutenoids, sesquiterpenes, and aromatic ketones with anti-inflammatory activity.[26]

Notably, the nanochitosan-Plai formulation exhibited a shift toward lipophilic and volatile constituents, such as lidocaine benzyl benzoate (15.35%), phenol, 2,4-bis(1,1-dimethylethyl)- (9.86%), and a range of alkanes (e.g., tetradecane, hexadecane, and octadecane), which were not prominent in the crude extract. These findings suggest that the nanoencapsulation process may selectively retain or stabilize volatile and hydrophobic compounds, as reported by similar studies on nanoemulsions and chitosan-based delivery systems. The appearance of squalene (2.87%), a known antioxidant and skin-conditioning agent, further supports the enhanced bioactive profile achieved through nanoformulation. Moreover, the detection of DMPBD (0.18%) in the crude extract is in line with previous work reporting dimethoxyphenyl derivatives as contributors to Plai's anti-inflammatory effects.[26]

Overall, the chemical shift observed between crude and nanoformulated Plai suggests that chitosan-based nanoencapsulation not only protects the active phytochemicals but also potentially enhances the formulation's stability, bioavailability, and skin permeability. These results are consistent with prior research on nanocarrier systems improving the pharmacological potential of herbal compounds and highlight the nanochitosan-Plai formulation as a promising candidate for transdermal or topical therapeutic applications.

Fourier Transform Infrared Spectroscopy (FTIR) was used to confirm the successful incorporation of *Zingiber cassumunar* extract into the chitosan-based nanoparticle system and to identify possible molecular interactions between the extract and the polymer matrix. The FTIR spectrum of chitosan exhibited characteristic peaks at 3430 cm^{-1} (O–H and N–H stretching), 2920 and 2850 cm^{-1} (C–H stretching), 1650 cm^{-1} (C=O stretching of amide I), and 1580 cm^{-1} (N–H bending of amide II), which are consistent with previous reports describing chitosan's functional groups.[27] Additionally, peaks between 1150 and 1020 cm^{-1} corresponded to C–O–C and C–O stretching vibrations typical of saccharide structures. The spectrum of crude *Z. cassumunar* showed strong bands in the range of 3400–3300 cm^{-1} attributed to O–H stretching and in the fingerprint region (1000–1500 cm^{-1}) related to phenolic, aromatic, and terpene structures, consistent with its known phenylbutenoid and sesquiterpene content.[28] These phytochemical groups are largely responsible for Plai's reported anti-inflammatory, analgesic, and antioxidant properties.[4]

In the nanochitosan-Plai composite formulation, the FTIR spectrum retained major absorption bands from both chitosan and Plai but with shifts in peak positions and changes in intensity particularly in the amide I (1650 cm^{-1}) and C–O stretching (1020–1100 cm^{-1}) regions suggesting strong hydrogen bonding or electrostatic interactions between the polymer and the phytoconstituents. Such interactions are commonly observed in chitosan-based nanocarriers and have been shown to enhance the chemical stability and bioavailability of encapsulated herbal compounds.[13] Overall, the FTIR results confirm the formation of a chemically stable nanoformulation, wherein the bioactive compounds from *Z. cassumunar* were effectively incorporated into the chitosan-PVA-glycerin matrix. These findings are in agreement with prior studies demonstrating that chitosan nanoparticles can successfully encapsulate essential and improve their delivery characteristics, including controlled release, enhanced skin permeability, and increased therapeutic potential.[5]

Morphological analysis using Scanning Electron Microscopy (SEM) revealed the nanochitosan-Plai particles to have rough, porous, sponge-like structures at high magnification (30,000×), a characteristic typical of chitosan-based nanocarriers. These structural features not only confirm successful encapsulation but also suggest improved drug-loading capacity and potential for controlled release. The irregular aggregates observed at low magnification (100×) suggest particle agglomeration during drying, which is common in spray or solvent evaporation methods. Similar SEM morphologies have been documented in other studies involving chitosan nanoparticles and support their utility in enhancing transdermal drug delivery.[29]

These findings align with prior studies indicating that nanoencapsulation can enhance the therapeutic efficacy of herbal actives by improving their permeability and retention in biological tissues, especially in transdermal or topical applications. Therefore, the nanochitosan-Plai formulation not only maintains but potentially augments the anti-inflammatory efficacy of crude Plai extract, making it a promising candidate for next-generation drug delivery systems targeting localized inflammation.

Conclusions

In this study, a nanochitosan-based formulation incorporating *Zingiber cassumunar* (Plai) extract was successfully developed using the ionic gelation technique. Comprehensive characterization using gas chromatography–mass spectrometry (GC–MS), Fourier-transform infrared spectroscopy (FTIR), and scanning electron microscopy (SEM) confirmed the chemical composition and nanoparticulate morphology of the formulation. The anti-inflammatory potential was evaluated through the albumin denaturation assay, with diclofenac used as a reference drug. GC–MS analysis revealed that nanoencapsulation significantly altered the chemical profile, enriching the formulation with lipophilic and volatile constituents such as lidocaine, benzyl benzoate, squalene, and alkanes, which were either absent or present in low concentrations in the crude extract. These findings suggest that the nanocarrier system helps retain and stabilize bioactive compounds, thereby enhancing therapeutic potential. FTIR analysis confirmed successful incorporation of *Z. cassumunar* extract into the chitosan matrix, as indicated by the presence of characteristic functional group bands from both the polymer and the extract. Shifts in peak positions and intensity suggested hydrogen bonding or electrostatic interactions, which are commonly associated with improved chemical stability and bioavailability in nanocarrier systems. SEM images revealed porous, rough, sponge-like structures typical of chitosan nanoparticles, supporting efficient drug loading and controlled release capabilities. The observed morphological characteristics also indicate potential for enhanced skin permeation and retention.

Overall, the nanochitosan-Plai formulation not only retained but potentially enhanced the anti-inflammatory efficacy of the crude extract, making it a promising candidate for future transdermal or topical drug delivery systems. These findings highlight the potential to further develop this formulation into advanced, natural-based therapeutic products such as sprays, patches, or medicated films for localized inflammation management.

Competing Interests

The authors declare that they have no competing interests.

Sources of Funding

The authors sincerely acknowledge the financial support provided by Suranaree University of Technology (SUT), Thailand Science Research and Innovation (TSRI), and the National Science, Research, and Innovation Fund (NSRF) (NRIIS number 195617). The authors are also grateful to the Parasitic Diseases Research Center (PDRC) for providing the essential laboratory facilities that were crucial for the successful execution of this study.

***Corresponding author**: Chutharat Thanchonnang, PhDc. E-mail: chutharat.than@gmail.com*

References

1. Koontongkaew S, Poachanukoon O, Sireeratawong S, Dechatiwongse Na Ayudhya T, Khonsung P, Jaijoy K, Soawakontha R, Chanchai M. Safety Evaluation of *Zingiber cassumunar* Roxb. Rhizome Extract: Acute and Chronic Toxicity Studies in Rats. Int Sch Res Notices. 2014 Nov 16;2014:632608. doi: 10.1155/2014/632608. PMID: 27379341; PMCID: PMC4897215.

2. Chongmelaxme B, Sruamsiri R, Dilokthornsakul P, Dhippayom T, Kongkaew C, Saokaew S, Chuthaputti A, Chaiyakunapruk N. Clinical effects of *Zingiber cassumunar* (Plai): A systematic review. Complement Ther Med. 2017 Dec;35:70-77. doi: 10.1016/j.ctim.2017.09.009. Epub 2017 Oct 7. PMID: 29154071.

3. Jeenapongsa R, Yoovathaworn K, Sriwatanakul KM, Pongprayoon U, Sriwatanakul K. Anti-inflammatory activity of (E)-1-(3,4-dimethoxyphenyl) butadiene from Zingiber cassumunar Roxb. J Ethnopharmacol. 2003 Aug;87(2-3):143-8. doi: 10.1016/s0378-8741(03)00098-9. PMID: 12860299.

4. Kato E, Kubo M, Okamoto Y, Matsunaga Y, Kyo H, Suzuki N, Uebaba K, Fukuyama Y. Safety Assessment of Bangle (*Zingiber purpureum* Rosc.) Rhizome Extract: Acute and Chronic Studies in Rats and Clinical Studies in Human. ACS Omega. 2018 Nov 30;3(11):15879-15889. doi: 10.1021/acsomega.8b02485. Epub 2018 Nov 21. PMID: 30556016; PMCID: PMC6288899.

5. Sinsup P, Teeranachaideekul V, Makarasen A, Chuenchom L, Prajongtat P, Techasakul S, Yingyuad P, Dechtrirat D. *Zingiber cassumunar* Roxb. Essential Oil-Loaded Electrospun Poly(lactic acid)/Poly(ethylene oxide) Fiber Blend Membrane for Antibacterial Wound Dressing Application. Membranes (Basel). 2021 Aug 24;11(9):648. doi: 10.3390/membranes11090648. PMID: 34564465; PMCID: PMC8470900.

6. Ozaki Y, Kawahara N, Harada M. Anti-inflammatory effect of *Zingiber cassumunar* Roxb. and its active principles. Chem Pharm Bull (Tokyo). 1991 Sep;39(9):2353-6. doi: 10.1248/cpb.39.2353. PMID: 1804548.

7. Anasamy T, Abdul AB, Sukari MA, Abdelwahab SI, Mohan S, Kamalidehghan B, et al. A phenylbutenoid dimer, cis-3-(3′, 4′-Dimethoxyphenyl)-4-[(E)-3‴, 4‴-dimethoxystyryl] cyclohex-1-ene, exhibits apoptogenic properties in T-acute lymphoblastic leukemia cells via induction of p53-independent mitochondrial signalling pathway. Evidence-Based Complementary and Alternative Medicine. 2013;2013(1):939810.

8. Tanticharoenwiwat P, Kulalert P, Dechatiwongse Na Ayudhya T, Koontongkaew S, Jiratchariyakul W, Soawakontha R, Booncong P, Poachanukoon O. Inhibitory effect of Phlai capsules on skin test responses among allergic rhinitis patients: a randomized, three-way crossover study. J Integr Med. 2017 Nov;15(6):462-468. doi: 10.1016/S2095-4964(17)60353-4. PMID: 29103416.

9. Chongmelaxme B, Sruamsiri R, Dilokthornsakul P, Dhippayom T, Kongkaew C, Saokaew S, Chuthaputti A, Chaiyakunapruk N. Clinical effects of *Zingiber cassumunar* (Plai): A systematic review. Complement Ther Med. 2017 Dec;35:70-77. doi: 10.1016/j.ctim.2017.09.009. Epub 2017 Oct 7. PMID: 29154071.

10. Ozaki Y, Kawahara N, Harada M. Anti-inflammatory effect of *Zingiber cassumunar* Roxb. and its active principles. Chem Pharm Bull (Tokyo). 1991 Sep;39(9):2353-6. doi: 10.1248/cpb.39.2353. PMID: 1804548.
11. Gundom T, Sukketsiri W, Panichayupakaranant P. Phytochemical analysis and biological effects of *Zingiber cassumunar* extract and three phenylbutenoids: targeting NF-κB, Akt/MAPK, and caspase-3 pathways. BMC Complement Med Ther. 2025 May 16;25(1):180. doi: 10.1186/s12906-025-04907-w. PMID: 40380132; PMCID: PMC12083117.
12. Luesakul U, Puthong S, Sansanaphongpricha K, Muangsin N. Quaternized chitosan-coated nanoemulsions: A novel platform for improving the stability, anti-inflammatory, anti-cancer and transdermal properties of Plai extract. Carbohydr Polym. 2020 Feb 15;230:115625. doi: 10.1016/j.carbpol.2019.115625. Epub 2019 Nov 15. PMID: 31887856.
13. Devkota HP, Paudel KR, Hassan MM, Dirar AI, Das N, Adhikari-Devkota A, et al. Bioactive compounds from Zingiber montanum and their pharmacological activities with focus on zerumbone. Applied Sciences. 2021;11(21):10205.
14. Jiménez-Gómez CP, Cecilia JA. Chitosan: A Natural Biopolymer with a Wide and Varied Range of Applications. Molecules. 2020 Sep 1;25(17):3981. doi: 10.3390/molecules25173981. PMID: 32882899; PMCID: PMC7504732.
15. Jiménez-Gómez CP, Cecilia JA. Chitosan: A Natural Biopolymer with a Wide and Varied Range of Applications. Molecules. 2020 Sep 1;25(17):3981. doi: 10.3390/molecules25173981. PMID: 32882899; PMCID: PMC7504732.
16. Naveedunissa S, Meenalotchani R, Manisha M, Ankul Singh S, Nirenjen S, Anitha K, et al. Advances in chitosan-based nanocarriers for targeted wound healing therapies: a review. Carbohydrate Polymer Technologies and Applications. 2025;11:100891.
17. Gonciarz W, Balcerczak E, Brzeziński M, Jeleń A, Pietrzyk-Brzezińska AJ, Narayanan VHB, Chmiela M. Chitosan-based formulations for therapeutic applications. A recent overview. J Biomed Sci. 2025 Jul 8;32(1):62. doi: 10.1186/s12929-025-01161-7. PMID: 40629425; PMCID: PMC12239286.
18. Negi A, Kesari KK. Chitosan Nanoparticle Encapsulation of Antibacterial Essential Oils. Micromachines (Basel). 2022 Aug 6;13(8):1265. doi: 10.3390/mi13081265. PMID: 36014186; PMCID: PMC9415589.
19. Chaowalit Monton JS, Natawat Chankana, Apirak Sakunpak. Applications of Chitosan Nanoparticles and Microparticles for Herbal Medicinal Drug Delivery Systems. Thai Science and Technology Journal. 2014:571-81.
20. Hoang NH, Le Thanh T, Sangpueak R, Treekoon J, Saengchan C, Thepbandit W, Papathoti NK, Kamkaew A, Buensanteai N. Chitosan Nanoparticles-Based Ionic Gelation Method: A Promising Candidate for Plant Disease Management. Polymers (Basel). 2022 Feb 9;14(4):662. doi: 10.3390/polym14040662. PMID: 35215574; PMCID: PMC8876194.
21. Sottiwilaiphong J AD. Nano-biopesticide development of betel extract–nano chitosan encapsulated for soft rot control of Chinese cabbage. Thai Journal of Science and Technology. 2018;7(5):516–33.
22. Jaiboonma A, Kaokaen P, Chaicharoenaudomrung N, Kunhorm P, Janebodin K, Noisa P, Jitprasertwong P. Cordycepin attenuates Salivary Hypofunction through the Prevention of Oxidative Stress in Human Submandibular Gland Cells. Int J Med Sci. 2020 Jul 6;17(12):1733-1743. doi: 10.7150/ijms.46707. PMID: 32714076; PMCID: PMC7378660.
23. Padmanabhan P, Jangle S. Evaluation of in-vitro anti-inflammatory activity of herbal preparation, a combination of four medicinal plants. International Journal of Basic and Applied Medical Sciences. 2012;2(1):109-16.
24. Pithayanukul P, Tubprasert J, Wuthi-Udomlert M. In vitro antimicrobial activity of *Zingiber cassumunar* (Plai) oil and a 5% Plai oil gel. Phytother Res. 2007 Feb;21(2):164-9. doi: 10.1002/ptr.2048. PMID: 17128430.
25. Suksaeree J, Charoenchai L, Madaka F, Monton C, Sakunpak A, Charoonratana T, et al. *Zingiber cassumunar* blended patches for skin application: Formulation, physiochemical properties, and *in vitro* studies. Asian Journal of Pharmaceutical Sciences. 2015;10.
26. Singsai K, Charoongchit P, Utsintong M. The comparison of the oil types in Plai (*Zingiber cassumunar*) oil extraction and analysis of the chemical constituents in Plai oil by gas chromatography-mass spectrometry technique. Naresaun Phayao J. 2022;15(3):18-2.
27. Kurita K. Chemistry and application of chitin and chitosan. Polymer Degradation and Stability. 1998;59(1-3):117-20.
28. Panthong A, Kanjanapothi D, Niwatananun V, Tuntiwachwuttikul P, Reutrakul V. Anti-inflammatory activity of compounds isolated from *Zingiber cassumunar*. Planta Medica. 1990;56(06):655-.
29. Owczarek M, Herczyńska L, Sitarek P, Kowalczyk T, Synowiec E, Śliwiński T, Krucińska I. Chitosan Nanoparticles-Preparation, Characterization and Their Combination with Ginkgo biloba Extract in Preliminary *In Vitro* Studies. Molecules. 2023 Jun 23;28(13):4950. doi: 10.3390/molecules28134950. PMID: 37446611; PMCID: PMC10343372.

International Journal of Biomedicine 15(3) (2025) 572-582
http://dx.doi.org/10.21103/Article15(3)_OA19

ORIGINAL ARTICLE

Biotechnology

INTERNATIONAL JOURNAL OF BIOMEDICINE

Capsaicin Hydrogel Skin Patch: Development, Characterization, and Safety Evaluation of Cytotoxicity, Anti-Inflammatory Effects, and Pain-Relief Applications

Chutharat Thanchonnang[1,2,3], Alisa Boonsuya[2], Phornpitcha Pechdee[2,4], Patpicha Arunsan[2,5], Nav La[6], Nattawut Keeratibharat[7], Nathkapach Kaewpitoon Rattanapitoon[2,8], Wiwat Nuansing[7], Schawanya Kaewpitoon Rattanapitoon[2,3*]

[1]*Translational Medicine program, Institute of Medicine, Suranaree University of Technology, Nakhon Ratchasima, Thailand*
[2]*Parasitic Disease Research Center, Suranaree University of Technology, Nakhon Ratchasima, Thailand*
[3]*School of Family Medicine and Community Medicine, Institute of Medicine, Suranaree University of Technology, Nakhon Ratchasima, Thailand*
[4]*Sirindhorn college of Public Health Suphan Buri province, Faculty of Public Health and Allied Health Sciences, Praboromarajchanok Institute, Nonthaburi, Thailand*
[5]*Faculty of Medicine, Vongchavalitkul University, Nakhon Ratchasima, Thailand*
[6]*Faculty of Pediatric and Medicine, International University, Phnom Penh, Cambodia*
[7]*School of Surgery, Institute of Medicine, Suranaree University of Technology, Nakhon Ratchasima, Thailand*
[8]*FMC Medical Center, Nakhon Ratchasima, Thailand*

Abstract

Background: Capsaicin, the primary pungent component of *Capsicum annuum*, exhibits significant anti-inflammatory and analgesic properties by acting on TRPV1 receptors and modulating COX-2 expression. However, its therapeutic use is limited by poor solubility, instability, and potential skin irritation. Myofascial Pain Syndrome (MPS), a prevalent musculoskeletal disorder, presents a need for safer and more effective topical treatments. This study aimed to develop and evaluate capsaicin loaded hydrogel patches for cytotoxic effects, anti-inflammatory properties, and pain relief.

Methods and Results: A hydrogel patch containing 0.1% capsaicin was fabricated using polyvinyl alcohol (PVA), gelatin, glycerol, Tween 80, triethanolamine through the freeze–thaw technique. Structural analysis by GC-MS revealed bioactive constituents, predominantly dodecyl acrylate (45.78%), oleic acid (25.06%), and trans-oleic acid (7.52%), all known for their anti-inflammatory and skin-permeation-enhancing properties. FTIR confirmed the successful incorporation of capsaicin into the hydrogel matrix with characteristic shifts in N–H, C=O, and C–N functional groups, while UV-Vis spectroscopy supported capsaicin release over time. Cytotoxicity testing on human skin fibroblast (HSF) cells demonstrated high cell viability (>90%) at concentrations below 1 mg/mL, with an IC_{50} of approximately 20 mg/mL, indicating low toxicity at therapeutic doses. The hydrogel exhibited dose-dependent anti-inflammatory activity. Notably, the anti-inflammatory efficacy was statistically comparable to diclofenac ($P = 0.183$).

Conclusion: The capsaicin-loaded hydrogel patch showed excellent physicochemical characteristics, structural stability, and biocompatibility. Its anti-inflammatory efficacy was on a par with standard diclofenac, supporting its potential as a safe and effective treatment for localized pain and inflammation management with MPS.(**International Journal of Biomedicine. 2025;15(3):572-582.**)

Keywords: myofascial pain • anti-inflammatory activity • Capsaicin • cytotoxicity

For citation: Thanchonnang C, Boonsuya A, Pechdee P, Arunsan P, la N, Keeratibharat N, Rattanapitoon NK, Nuansing W, Rattanapitoon SK. Capsaicin Hydrogel Skin Patch: Development, Characterization, and Safety Evaluation of Cytotoxicity, Anti-Inflammatory Effects, and Pain-Relief Applications. International Journal of Biomedicine. 2025;15(3):572-582. doi:10.21103/Article15(3)_OA19

Abbreviations

BSA, bovine serum albumin; **CHP**, Capsaicin hydrogel patch; **DW**, distilled water; **FTIR**, Fourier transform infrared spectroscopy; **MPS**, Myofascial Pain Syndrome; **NRS**, Numeric Rating Scale; **NSAIDs**, nonsteroidal anti-inflammatory drugs; **VAS**, Visual Analog Scale; **UV-vis**, ultraviolet-visible; **w/v**, weight/volume.

Introduction

Capsicum annuum, a widely cultivated member of the Solanaceae family, is known for its use in culinary, industrial, and medicinal applications.[1] This plant exhibits considerable diversity in fruit morphology and pungency, contributing to its global significance as both a spice and a functional food. The fruit is rich in phytochemicals, notably capsaicinoids and carotenoids, responsible for its spiciness and coloration. Capsaicin and dihydrocapsaicin dominate the capsaicinoid profile, while xanthophylls and carotenes account for the vibrant pigmentation. Additionally, chili peppers contain volatile compounds, fatty acids, phenolics, vitamins, and essential minerals, contributing to their reported bioactivities, including antimicrobial effects. Despite these findings, further investigation is needed to elucidate the bioactive compounds responsible for these therapeutic properties fully.[2]

Capsaicin, the active component in chili peppers, is well-known for its anti-inflammatory properties. Capsaicin (8-methyl-N-vanillyl-6-nonenamide), a naturally occurring protoalkaloid and a neuropeptide-active agent that affects the transient receptor potential vanilloid-1 receptor (TRPV1), is used to treat pain disorders, particularly myofascial pain syndrome,[3] as well as an anti-inflammatory agent.[4] These effects are primarily mediated through its action on the TRPV1 receptor, which is involved in pain and inflammation pathways. When capsaicin binds to TRPV1 receptors, it initially causes an influx of calcium ions into the nerve cells, leading to a burning sensation. However, with repeated application, capsaicin depletes substance P, a neuropeptide associated with inflammation and pain transmission. This depletion reduces the sensitivity of nerve fibers to pain and decreases inflammation.[5,6] Marked mechanism is particularly beneficial in conditions associated with chronic pain, such as neuropathic pain and arthritis.[6] Topical capsaicin in low concentrations (0.025–0.1%) is recognized for its moderate efficacy in treating certain types of pain, particularly neuropathic and musculoskeletal pain, as well as conditions like arthritis. Capsaicin targets the TRPV1 receptors on pain nerve fibers,[7] which transmit pain sensations. Capsaicin 0.1% is minimally absorbed systemically, which reduces the risk of systemic side effects, making it a safer alternative to oral pain medications, especially in chronic pain conditions. Its minimal absorption is part of the reason why it is generally well-tolerated. Overall, capsaicin 0.1% is safe when used as directed.[6]

Furthermore, capsaicin's role in reducing oxidative stress contributes to its anti-inflammatory and analgesic effects; capsaicin mitigates oxidative damage, a key driver of chronic inflammation and pain.[8] The mechanism of capsaicin antioxidant action has been studied, and in particular, the ability of its phenolic structure to provide hydrogen to peroxyl and alkoxy radicals has been revealed.[9]

This interaction forms a complex with reduced transition metals, while the C7-benzyl carbon and methoxy group enhance its potent antioxidant and free radical scavenging properties.[10] This antioxidant activity reduces inflammation and helps prevent the sensitization of pain pathways. Capsaicin also modulates the expression of cyclooxygenase-2 (COX-2),[11] an enzyme that plays a significant role in the inflammatory process and pain signaling. By downregulating COX-2 expression, capsaicin can decrease both inflammation and pain.

Myofascial pain syndrome (MPS) is a chronic soft tissue pain disorder characterized by local and referred musculoskeletal pain originating from trigger points (TrPs) within the fascia surrounding skeletal muscles. It is a prevalent cause of both acute and chronic pain. MPS can manifest independently, termed primary myofascial pain syndrome. Traditional treatments include physical therapy, medications, and trigger point injections.[12] However, recent research is increasingly focused on capsaicin, the active component of chili peppers, as a potential alternative or adjunctive therapy, investigating its mechanisms of action and clinical effectiveness.[13] Myofascial pain syndrome is characterized by muscle pain originating from a trigger point. Despite extensive research, the pathophysiology of MPS remains incompletely understood,[12] leading to the exploration of various treatment modalities. Physical treatments include techniques such as stretch and spray, massage, ischemic compression therapy, and local heat. Needle-based interventions encompass dry needling, trigger point injections with local anesthetics, and botulinum toxin injections. Transcutaneous electric nerve stimulation (TENS) is also utilized for MPS management.[14] Supplementary treatments often involve nonsteroidal anti-inflammatory drugs (NSAIDs), though their efficacy, especially topically, in treating MPS is unclear. There is no clear evidence of the effectiveness or relative efficacy of one treatment compared to another.[14] Topical capsaicin is another option, potentially serving as an adjuvant treatment. The etiology of trigger points and myofascial pain remains incompletely elucidated. Nevertheless, studies have demonstrated that capsaicin can elicit pain and hyperalgesia in human tendon tissues. Furthermore, it has been observed to enhance trigger point sensitivity in individuals while concurrently mitigating associated pain.[15] The treatment of MPS should be multimodal, with the main purpose of managing the underlying disease-causing pain. Although nonsteroidal anti-inflammatory drugs (NSAIDs) are commonly used for pain relief, their application in the treatment of chronic pain disorders is restricted due to the potential for adverse effects on the gastrointestinal (GI) tract and the kidneys (GI symptoms, renal injury, nausea and vomiting, dizziness), and depression.[12] Less invasive options have also been proposed to improve the MPS treatment.

Given capsaicin's analgesic properties, a comprehensive understanding of its physicochemical properties is necessary for the development of drug delivery systems that provide

a safer and more effective treatment option. In this study, a hydrogel delivery system was designed to enhance the sustained release of capsaicin, improve its efficacy, and reduce side effects, with a focus on creating a pain relief patch that enhances performance. Hydrogels are three-dimensional crosslinked polymeric matrices characterized by properties such as swelling and deswelling behaviors, shock absorption, and low friction coefficients, as documented in the literature.[16] Hydrogels have garnered considerable attention and are utilized in various fields, including effluent management, tissue engineering, drug delivery systems, and biomolecular filtration.[17] Their hydrophilic nature, biodegradability, and biocompatibility make them valuable synthetic polymers in the biomedical sector.[18] Furthermore, capsaicin has been shown to inhibit the production of pro-inflammatory cytokines, further contributing to its anti-inflammatory properties. Using capsaicin in topical formulations, such as creams and patches, provides a targeted approach to managing localized inflammation and pain, making it a valuable tool in treating inflammatory conditions. With the limited stability of certain patch types, there is a growing interest in developing novel hydrogel-based patches that incorporate capsaicin to enhance pain relief. This research, based on laboratory tests, aims to inform practical applications for patients in the future. The study evaluates both the safety and efficacy of the transdermal delivery system to advance its clinical use.

This study aimed to develop and evaluate capsaicin loaded hydrogel patches for cytotoxic effects, anti-inflammatory properties, and pain relief.

Materials and Methods

Preparation of Capsaicin Hydrogel Skin Patch

Polyvinyl alcohol (PVA) (CAS 9002-89-5) 1% w/v (Molecular weight 13,000-23,000) from Sigma-Aldrich solution at a concentration of 1% (w/v) by weight and gelatin (CAS Numbers, 9000-70-8) at 10% w/v were dissolved in boiling water at 90 °C under magnetic stirring for approximately 1-2 hours[19] until a clear and transparent solution was obtained. 10 ml of glycerol 99.5% (CAS Number: 56-81-5), 1.25 ml of Tween 80 (CAS Number: 9005-65-6), and 4 drops of triethanolamine (CAS Number: 102-71-6) in combination play a significant role in hydrogel preparation, functioning as a pH adjuster, stabilizer, and emulsifier. The above components and capsaicin (CAS number: 404-86-4) at a concentration of 0.1% were added to the prepared solution. The solution was stirred at room temperature for 45-60 minutes until complete dissolution and uniform consistency were observed. Once the solution had achieved uniform consistency, it was left to cool down gradually. Subsequently, 10 ml of the solution was prepared and poured into a Petri dish. The solution-filled Petri dish was then subjected to the freeze-thaw process by alternately freezing at -20 °C for 48 hours and thawing at room temperature (25 °C) for 24 hours, resulting in a well-consolidated hydrogel sheet. The obtained hydrogel sheet underwent sterilization and examination for the persistence of capsaicin (Figure 1).

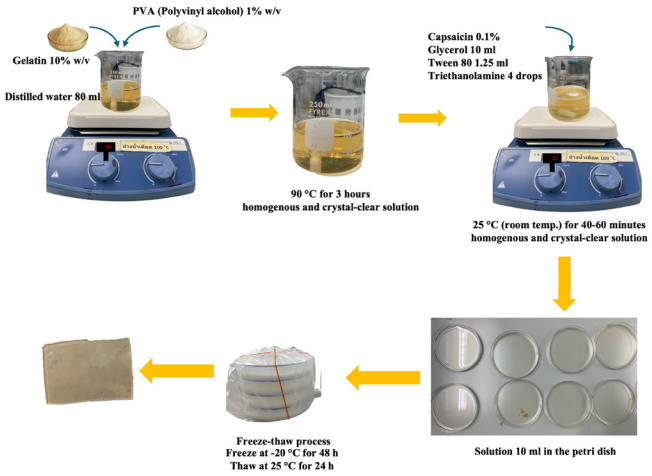

Fig. 1. *A schematic diagram displays the preparation steps of the capsaicin hydrogel patch.*

Capsaicin Hydrogel Patch Characterization

Gas Chromatography-Mass Spectrometry (GC-MS) Analysis

Capsaicin was prepared at an appropriate concentration and injected into the GC-MS system using an autosampler in liquid injection mode with an injection volume of 1 µL.[2] The sample components were separated using an HP-5 capillary column under predefined conditions. The separated compounds were then introduced into the mass spectrometer (MS), where electron ionization (EI) at 70 eV was applied to generate molecular ions. Mass scanning was conducted over a range of 35–550 m/z to identify the chemical constituents. The resulting spectra were analyzed by comparison with the NIST MS Search 2.0 database to confirm compound identification.

Investigation of the Physical Properties of Hydrogel Patch Characterization by UV-Visible Spectroscopy

The selected hydrogel sheets containing capsaicin were incubated at either 4°C to facilitate slow and controlled gelation, allowing the gradual formation of the hydrogel network, or 50°C to promote crosslinking of the hydrogel structure, thereby enhancing its mechanical strength and stability with 75% relative humidity for 6 weeks. Physical characteristics and biocompatibility adherence abilities were evaluated before and after the testing period, following the methodology by Simone et al.[20] UV-visible spectroscopy, using a T80+ model from PG Instruments (Spectrum mode) (Serial Number: 23-1885-01-0190), was conducted in the laboratory. A sample was employed to assess the drug release from the hydrogel sheets containing the drug in distilled water. Quartz cuvettes of 4 ml capacity were utilized for spectroscopic measurements within the wavelength range of 200-700 nm, with data recorded at 30 or 60-minute intervals throughout the entire experiment, repeated at least three times.

Investigation of the Physical Properties of Hydrogel Patch Characterization by Fourier Transform Infrared Spectroscopy

The procedure for studying room temperature hydrogel patch stability for 30 days was conducted following the method by Ilie et al.,[21] and the morphology of the samples was characterized using Fourier Transform Infrared Spectroscopy (FTIR) Vertex 70, Bruker Switzerland, (Serial Number: 3099/HYP.1097) with a resolution of 4, Sample Scan Time: 64, Background Scan Time: 64. Analysis was repeated at least 3 times using OPUS Software, with the test results recorded and subjected to further analysis. The physical characteristics of the prepared patches were evaluated through visual examination and tactile perception, such as the smoothness of the material and clarity, to select patch materials with favorable physical attributes.

Cytotoxicity Assays

Cytotoxicity Testing on Human Skin Fibroblast (HSF) Cells Using the MTT Assay

HSF cells were seeded at a density of 10,000 cells/well in a 96-well plate using Dulbecco's modified Eagle medium (DMEM) supplemented with 1% FBS and 1% penicillin/streptomycin. The cells were incubated for 24 hours in a CO_2 incubator maintained at 37 °C with 5% CO_2. Test samples were prepared at various concentrations by diluting them in DMEM. Each concentration (100 µL) was added to the respective wells, and the cells were further incubated for 24 hours. After 24 hours, 100 µL of MTT solution (0.5 mg/mL) was added to each well, and the plate was incubated in the dark for 2 hours. The supernatant was then carefully removed, and the resulting formazan crystals were dissolved with 100 µL of dimethyl sulfoxide (DMSO). Absorbance was measured at 570 nm using a microplate reader. The percentage of cell viability (mg/mL) was calculated using the following formula: [22]

$$\%\ \text{Cell viability} = \frac{\text{Absorbance of treated cell}}{\text{Absorbance of control cell}} \times 100\%$$

Anti-Inflammatory Activity

The anti-inflammatory properties were evaluated using a modified version of the protocol.[23] One milliliter of the test compounds or diclofenac sodium (positive control) at varying concentrations 25, 50, 100, 200, 500, and 1000 µg/mL (conducted in triplicate) was added to 1 mL of an aqueous solution containing 5% bovine serum albumin (BSA) (CAS Numbers, 9048-46-8) and incubated for 15 minutes at 27°C.

A mixture of distilled water (DW) and BSA was the control. The protein denaturation process was initiated by heating the mixture for 10 minutes at 70 °C.

After cooling at room temperature, the absorbance of each sample was measured at 660 nm by VICTOR® Nivo™ Multimode Plate Readers (Serial Number: HH35L2020289). The percentage inhibition was calculated from optical density (OD) values by following the formula:[24]

$$\%\ \text{Inhibition} = \frac{\text{Absorbance of control} - \text{Absorbance of sample}}{\text{Absorbance of control}} \times 100\%$$

Efficacy of Capsaicin Hydrogel Patch for Pain Relief

The research design included a pilot study methodology to ascertain the adequacy of sample group sizes, as outlined.[25,26] The determination of sample group size was calculated with a confidence level of 0.7 and a probability of 0.3, following the methodology.[26] The computation resulted in an estimated sample group size of 3.4 individuals to mitigate potential dropouts; therefore, it was adjusted to 5 participants. Participants were aged equal to or greater than 18 years. This pilot study recorded visual analogue scale (VAS) scores equal to or greater than 5 out of a maximum of 10 for neck pain duration and clinical manifestation of MPS.

Pain Reduction Assessment

Participants applied adhesive patches to the affected shoulder or back for 2 hours per session, twice daily (morning and evening) for 3 days. Thereafter, volunteers recorded pain scores using the Visual Analog Scale (VAS) and Numeric Rating Scale (NRS) (0-10 points) before and after patch application (a total of 6 times) and noted any adverse skin reactions that may occur, such as redness, swelling, clear vesicles, and itching. Volunteers assessed and recorded their discomfort with the continuous use of the patches. In addition, skin reactions were assessed before and after patch use, assessing redness (0-3 points), swelling (0-4 points), the presence of papules, the presence of wheals, and the presence of large, clear vesicles.[27]

Statistical analysis

Statistical analysis was performed using SPSS Statistics version 29.0 (SPSS Inc., Chicago, IL). The Wilcoxon signed-rank test was used to compare the differences between the two dependent groups (for non-parametric data). The probability value of $P \leq 0.05$ was considered statistically significant.

Results

Capsaicin Hydrogel Skin Patch

A capsaicin hydrogel skin patch containing 0.1% capsaicin was developed in the experimentation, as shown in Figure 1. Capsaicin at a concentration of 0.1% is widely applied topically for pain relief in various conditions. In this study, a skin patch was designed with a thickness of 0.5 cm and dimensions of 4×5 cm². The capsaicin hydrogel patch, including its physical characteristics and optimized concentration of 0.1% capsaicin, is illustrated. The active compound remained encapsulated within the hydrogel patch (Figure 1).

Characterization of Capsaicin Hydrogel Skin Patch

Gas Chromatography–Mass Spectrometry (GC-MS) Analysis

Gas chromatography-mass spectrometry (GC-MS) was employed to characterize the chemical composition of the capsaicin. 17 peaks were identified, corresponding to various fatty acids, esters, alcohols, and hydrocarbons. Compound identification was performed by matching mass spectral data with the NIST MS Search 2.0 database. The predominant

constituent was dodecyl acrylate (RT: 24.096 min), accounting for 45.78% of the total peak area, followed by oleic acid (RT: 30.558 min; 25.06%) and trans-oleic acid (RT: 35.612 min; 7.52%). Additional major components included 1-dodecanol (RT: 20.836 min; 6.49%), propanoic acid, decyl ester (RT: 24.178 min; 4.55%), and n-hexadecanoic acid (RT: 27.830 min; 3.21%). Minor components such as nonanamide, elaidic acid ethyl ester, and octadecanoic acid were also detected, contributing to the overall chemical complexity of the capsaicin. Several of these compounds, particularly long-chain fatty acids and their esters, are recognized for their bioactive properties, including anti-inflammatory, emollient, and skin-permeation enhancing effects. The presence of these compounds suggests that the capsaicin contains multiple bioactive molecules that may synergistically contribute to the analgesic and anti-inflammatory activity of the formulated hydrogel patch, as shown in Table 1.

Table 1.

Chemical constituents identified in the capsaicin crude extract using GC-MS.

RT	Area	Area Sum %	Name
5.037	28839	0.20	2-Propenoic acid
5.618	35676	0.25	Silane, triethylfluoro-
9.421	19960	0.14	4,4-dimethyl-1,3-Dioxane
14.199	15724	0.11	Nonanal
18.392	34202	0.24	n-Decanoic acid
20.836	930588	6.49	1-Dodecanol
21.499	48734	0.34	Nonanamide
24.096	6569297	45.78	Dodecyl acrylate
24.178	653059	4.55	Propanoic acid, decyl ester
27.406	149881	1.04	3-Chloropropionic acid, dodecyl ester
27.830	460111	3.21	n-Hexadecanoic acid
28.315	94546	0.66	Hexadecanoic acid, ethyl ester
30.558	3595726	25.06	Oleic Acid
30.857	177826	1.24	Octadecanoic acid
30.940	388904	2.71	Elaidic acid, ethyl ester
35.612	1079067	7.52	Trans-oleic acid
36.435	66942	0.47	Diisooctyl phthalate
Total	14349082	100	

Chemical constituents identified in the capsaicin crude extract using GC-MS. Each compound was identified based on retention time (RT) and mass spectral comparison with the NIST MS database. The relative abundance of each component is expressed as the percentage of total peak area (Area%).

UV-Visible Spectrophotometry

The capsaicin hydrogel patches were loaded into cuvettes, and testing began at minute 0 without changing the wavelength. Changes began at 30, 60, 90, 120, 150, and 180 minutes. Optimal light absorption measurements of capsaicin dilution were identified through UV-Visible scan spectrum readings at 278, 281, 280, 284, 283, and 283 nanometers, respectively (Figure 2). The absorbance of capsaicin was measured spectrophotometrically at a wavelength, demonstrating the peak of the capsaicin spectra.

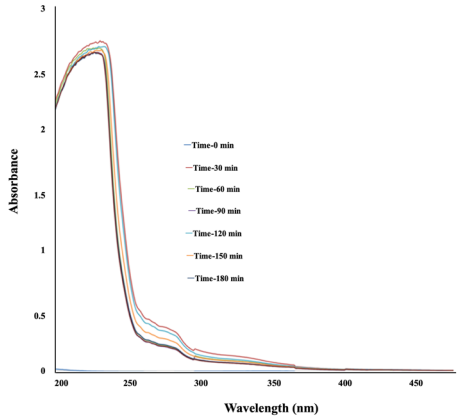

Fig. 2 *The UV-Vis absorption spectrum of capsaicin.*

Fourier Transform Infrared Spectroscopy (FTIR)

The stability of the substance at ambient temperature was evaluated over a 30-day period following the protocol described by Ilie et al.,[21] and its presence was confirmed using a Vertex 70 FTIR spectrometer in the laboratory. Analysis of data from hydrogel patch samples and standard capsaicin samples revealed that FTIR measurement aimed to identify possible biomolecular substances of capsaicin. The FTIR spectrum of capsaicin displayed prominent absorption bands at 3295, 2925, 1633, 1457, 1,360, 1244, 1148, 1078, 994, 930, 847, 758, 572, and 520 $cm.^{-1}$.

Clear peaks were observed when testing the FTIR spectrum of hydrogel patches containing capsaicin. These peak values slightly shifted to 3303, 1637, 1475, 1244, 1111, 1043, and 992 cm^{-1} in the FTIR spectrum of the hydrogel patches mixed with capsaicin. The FTIR spectrum of capsaicin displays peaks corresponding to its characteristic functional groups. Capsaicin, with the molecular formula C18H27NO3, is systematically named 8-methyl-N-vanillyl-6-nonenamide. Its molecular structure comprises key functional groups, including an amide group, an aromatic vanillyl ring, and a long hydrocarbon chain. These groups play a significant role in its chemical and physical properties, which are reflected in its FTIR absorption spectrum. Characteristics of the standard capsaicin peaks reveal N-H stretch (3295 cm^{-1}), aliphatic C-H stretch (2925 cm^{-1}), C=O stretch (1633 cm^{-1}), and C-N stretch (Amide II) (1148 cm^{-1}). Upon comparison with hydrogel skin patch samples containing capsaicin, the peak characteristics in the FTIR spectrum include N-H stretch (3303 cm^{-1}), C=O stretch (1637 cm^{-1}), and C-N stretch (Amide II) (1111 cm^{-1}). While the aliphatic C-H group may exhibit less distinct peaks, minor variations in peak intensity are noted compared to

standard capsaicin. These alterations confirm the presence of capsaicin peaks in the hydrogel patch samples (Figure 3).

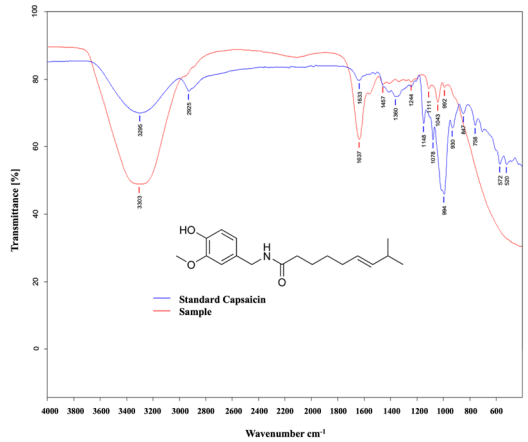

Fig 3. *FT-IR spectrum and chemical formula of capsaicin hydrogel. (Red line - capsaicin hydrogel skin patch, blue line - standard capsaicin).*

Cytotoxicity Assays

The cytotoxic effects of capsaicin solution on human skin fibroblast (HSF) cells were evaluated using the MTT assay. Figure 4(A) shows cell viability percentage following capsaicin treatment at various concentrations (0.0001–10 mg/mL) for 24 hours. The results are presented as mean ± standard deviation (SD). Capsaicin at 0.0001 to 1 mg/mL concentrations showed no significant cytotoxic effects, with cell viability remaining above 90%. However, at 10 mg/mL, a statistically significant reduction in cell viability ($P< 0.01$) was observed, indicating cytotoxicity at high concentration. Representative microscopic images showing morphological changes in HSF cells treated with capsaicin at selected concentrations are presented in Figure 4(B). Control: Cells exhibit normal spindle-shaped morphology with high confluence. Capsaicin 10 mg/mL: Marked cell shrinkage and reduced density observed, consistent with significant cytotoxicity. Capsaicin 0.1 mg/mL: Minor morphological changes with slightly reduced cell density, indicating mild cytotoxicity. Capsaicin 0.001 mg/mL: Morphology similar to control, suggesting negligible cytotoxic effect at this concentration, and morphological changes were captured under an inverted microscope at 200 µm scale.

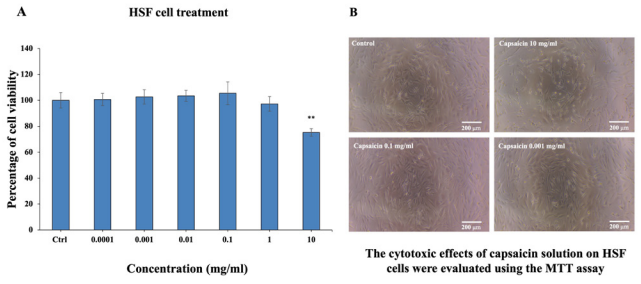

Fig. 4. *Cytotoxic effects of capsaicin on human skin fibroblast (HSF) cells assessed by MTT assay.*
(A) Percentage of cell viability following treatment with capsaicin at various concentrations (0.0001–10 mg/mL) for 24 hours. (B) Representative microscopic images showing morphological changes in HSF cells treated with capsaicin at selected concentrations.

These findings confirm that capsaicin induces dose-dependent cytotoxicity in HSF cells, with higher concentrations compromising cell viability and morphology. The half-maximal inhibitory concentration (IC_{50}) was approximately 20 mg/mL, indicating that capsaicin exhibits cytotoxicity at elevated concentrations. Morphologically, treated cells maintained normal spindle-shaped appearances at non-cytotoxic concentrations, while cell shrinkage and reduced confluence were evident at higher doses, suggesting compromised cell health.

Anti-Inflammatory Activity

The assessment of anti-inflammatory properties demonstrated that the capsaicin hydrogel patch exhibited increased efficacy at all concentrations, with the highest percentage of inhibition observed at concentrations ranging from 25 µL to 1000 µL (100%). Figure 5 illustrates the anti-inflammatory effects of the capsaicin hydrogel patch at various concentrations compared to the standard diclofenac. A comparison between diclofenac and the capsaicin hydrogel patch revealed no statistically significant difference in anti-inflammatory efficacy (P=0.183).

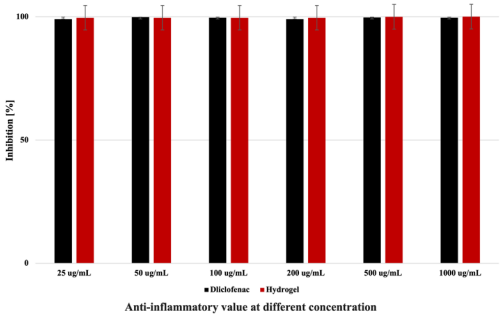

Fig. 5. *Anti-inflammatory activity of diclofenac and capsaicin hydrogel patch at various concentrations.*

Efficacy

The anti-inflammatory activity of the capsaicin hydrogel patch was evaluated to assess its potential therapeutic efficacy. The baseline characteristics of the participants are presented in Table 2.

Five participants without underlying medical conditions were included in the study. Participants applied the patch for 60 minutes both day and night at the site of pain. Pretest and post-test scores were analyzed for mean differences using a non-parametric test. The results indicated that the mean VAS score decreased after three days, but this change was not statistically significant. In contrast, the analysis of pre-test and post-test NRS scores using the Wilcoxon Signed-Rank Test revealed a statistically significant difference (P = 0.05) as shown in Table 3.

Adverse Events

Table 4 presents the adverse events caused by using the capsaicin hydrogel patch. These events were transient, resolving within a short duration. Notably, no severe adverse events were reported.

Table 2.

Main characteristics of the study participants (mean age of 26.02±4.39 years).

Variable		n	%
Sex	Male	3	60.00
	Female	2	40.00
Occupations	Students	2	40.00
	Professional Nurses	1	20.00
	Owner Business	1	20.00
	University Staff	1	20.00
Duration of computer usage for work	1-5 hours	2	40.00
	6-10 hours	2	40.00
	> 11 hours	1	20.00
Common symptoms experienced during prolonged sitting	Neck, shoulder, and back pain	2	40.00
	Numbness, Sweating	2	40.00
	Blurred vision	1	20.00

Table 3.

Wilcoxon signed ranks test results.

	Pre-test – Post-test	n	Mean rank	Sum of ranks	Z	*P*-value
VAS	Negative Ranks	2	1.50	3.00	-1.342	1.180
	Positive Ranks	0	0.00	0.00		
	Tiles	3				
	Total	5				
NRS	Negative Ranks	4	2.50	10.00	-1.890	0.050
	Positive Ranks	0	0.00	0.00		
	Tiles	1				
	Total	5				

*NRS, Numeric Rating Scale; VAS, Visual Analog Scale***;** *Z = Asymp. Sig. (2-tailed).*

Table 4.

Adverse events in volunteers caused by the capsaicin hydrogel patch (n=5).

Side effects	Day 1		Day 2		Day 3	
	n	%	n	%	n	%
Rash	1	20.00	0	0.00	0	0.00
Pruritus	2	40.00	2	40.00	1	20.00
Asymptomatic	2	40.00	3	60.00	4	80.00

Discussion

This study explored the development and characterization of a capsaicin hydrogel patch, with particular focus on its physicochemical properties and therapeutic effects. The structural and compositional attributes were analyzed through GC-MS, UV-vis spectroscopy, and FTIR, offering insights into the patch's molecular composition and light absorption behavior. Capsaicin below 1 mg/mL showed no cytotoxicity on HSF cells, maintaining viability above 90%, while higher concentrations caused dose-dependent cytotoxicity, with an IC_{50} of approximately 20 mg/mL. The patch's anti-inflammatory activity was clinically evaluated through a pre- and post-test design involving five patients suffering from muscle pain. Pain levels were measured using the Visual Analog Scale (VAS) and Numerical Rating Scale (NRS). Statistical analysis, performed using the Wilcoxon Signed-Rank test, revealed a significant reduction in pain scores post-application, demonstrating the potential efficacy of the capsaicin hydrogel patch in providing symptomatic relief.

The GC-MS analysis of the capsaicin crude extract in this study revealed a distinct profile composed primarily of dodecyl acrylate (45.78%), oleic acid (25.06%), and trans-oleic acid (7.52%), with additional contributions from 1-dodecanol, propanoic acid decyl ester, and hexadecanoic acid derivatives. These findings demonstrate a chemical fingerprint dominated by fatty acids, fatty acid esters, and long-chain alcohols. Notably, dodecyl acrylate was the most abundant compound, accounting for nearly half of the total peak area, indicating its significant presence in the bioactive matrix.

When compared with the results of Ahmad et al.,[2] who characterized the volatile composition of 27 different Capsicum annuum cultivars, several key differences and similarities emerge. Their study reported a predominance of alcohols (26.13%), hydrocarbons (18.82%), and esters (14.97%), with compounds like 1-decanol and docosanoic acid, docosyl ester as major constituents. While both studies identified esters and alcohols as major components, the proportion and dominant compounds differ notably. The present extract exhibited higher concentrations of fatty acid esters such as oleic acid ethyl ester and propanoic acid decyl ester. In contrast, Ahmad et al.[2] reported broader chemical diversity across several classes, including aldehydes, ketones, and pyrazines.

The discrepancies can likely be attributed to differences in extraction techniques, geographical source, capsicum variety, and maturity stage, as highlighted by Ahmad et al.,[2] who observed variation in volatile composition based on cultivar and origin. Furthermore, while their study emphasized volatile oils contributing to aroma and antimicrobial activity, capsaicin focuses more on fatty acid-based constituents, which are known to play roles in skin permeability enhancement, anti-inflammatory activity, and drug delivery efficiency.

This focused chemical profile may correlate with the intended functional role of capsaicin, specifically, enhancing the anti-inflammatory and analgesic properties of a capsaicin hydrogel patch. Compounds such as oleic acid and n-hexadecanoic acid have been independently reported to possess anti-inflammatory properties, suggesting a potential synergistic effect with capsaicin in the transdermal formulation.

In the present study, the capsaicin patches were subjected to an examination of their physical properties and adherence to biocompatibility both before and after testing. UV-Vis analysis was conducted at specific time intervals to assess the light absorption characteristics of capsaicin dilution. The absence of data at 0 minutes indicated that no chemical change occurred at the initial time point. However, changes began manifesting at 30, 60, 90, 120, 150, and 180 minutes. The UV-Visible scan spectrum revealed absorbance values suitable for capsaicin dilution at wavelengths of 278, 281, 280, 284, 283, and 283 nanometers, respectively. Prior research demonstrated that standard capsaicin exhibits light absorption at 279 nanometers when exposed to UV radiation.[28] Similarly, the previous report shows capsaicin's absorption peak at 281 nanometers.[29] This study demonstrated that the UV spectrophotometric method provides clear advantages in terms of simplicity, accuracy, and sensitivity for analyzing the complex structure of capsaicin. The standard curve of capsaicin in various solutions displayed a distinct peak corresponding to capsaicin.

The FTIR spectrum exhibited distinctive peaks corresponding to capsaicin (trans-8-methyl-N-vanillyl-6-nonenamide) chemical formula (C18H27NO3), indicative of typical capsaicin characteristics. These findings affirm the encapsulation of capsaicin within the hydrogel patch, aligning with previous research that explored FTIR analysis of silver nanoparticles. The FTIR spectrum of capsaicin displayed prominent absorption bands (Fig. 1). Clear peaks were observed when testing the FTIR spectrum of hydrogel patches containing capsaicin. These peak values slightly shifted to 3303, 1637, 1475, 1244, 1111, 1043, and 992 cm^{-1} in the FTIR spectrum of the hydrogel patches mixed with capsaicin. In the case of capsaicin-coated silver nanoparticles, lower maximum absorption points were identified at 1,653.96 and 1,027.44 cm^{-1}. The FTIR analysis revealed peak shifts, likely attributed to variations in peak maxima and interface features associated with the silver metal surface, as recent documents show.[30]

The peaks mentioned align well with FTIR spectra associated with capsaicin, a compound found in 2917–2846 cm^{-1}, corresponding to the aliphatic C–H stretching vibrations, typically seen in CH_2 and CH_3 groups. A peak at 1733 cm^{-1} indicates C=O stretching, which is often seen in ester or carbonyl groups; a peak at 1460 cm^{-1} represents aromatic C–C stretching, commonly observed in aromatic rings; a peak at 1165 cm^{-1} refers to C–O–C stretching, which could suggest ether linkages or similar oxygen containing groups; a peak at 720 cm^{-1} is characteristic of C–H and C–C vibrations related to the aromatic phenyl ring, confirming the aromatic nature of capsaicin. These FTIR data help establish the structure of capsaicin in various applications, such as studying its role in biological systems or determining its presence in natural products.[31] The variation in FTIR absorption between pure Capsaicin and Capsaicin blended in hydrogel sheets arises from molecular interactions between capsaicin and the hydrogel patch. The peak intensities differ slightly between pure capsaicin and the hydrogel patch containing capsaicin. For instance, the aliphatic C-H group exhibits reduced peak clarity, suggesting changes in the local environment of the capsaicin molecules due to their incorporation into the hydrogel network. These interactions likely restrict the mobility of capsaicin, leading to alterations in vibrational energy levels and, consequently, the infrared (IR) absorption. Despite these variations, the IR spectrum of the hydrogel patch retains the characteristic peaks of capsaicin, confirming its presence. Thus, the IR absorption variations can be attributed to the molecular interactions between capsaicin and the hydrogel patch.

The present study evaluated the cytotoxicity of capsaicin on human skin fibroblast (HSF) cells using the MTT assay, revealing that concentrations below 1 mg/mL preserved cell viability above 90%. In contrast, higher concentrations led to a dose-dependent decline in viability, with an IC_{50} of approximately 20 mg/mL. These findings are consistent with earlier research demonstrating that capsaicin exhibits a concentration-dependent cytotoxic effect on various cell types. For instance, Sancho et al.[32] reported that capsaicin concentrations above 100 μM (~30 μg/mL) induced apoptotic cell death in glioma cells, whereas lower concentrations had minimal impact on cell viability. Notably, the current findings highlight that HSF cells tolerate capsaicin well at low concentrations, as evidenced by the retention of normal spindle-shaped morphology and high confluence, supporting the potential use of capsaicin in topical applications when used at sub-cytotoxic levels. Morphological alterations observed at higher doses, including cell shrinkage and reduced confluence, align with previous reports indicating that high-dose capsaicin can disrupt cytoskeletal integrity and induce oxidative stress.[33] These observations reinforce the importance of dose optimization in developing capsaicin-based formulations to ensure both efficacy and safety.

Overall, the results contribute to the growing body of evidence supporting the biocompatibility of capsaicin at low concentrations and underscore the need for careful dose selection in biomedical applications.

The study demonstrated that the capsaicin hydrogel patch exhibited enhanced anti-inflammatory efficacy across all tested concentrations, with maximum inhibition (100%) observed between 25 μL and 1000 μL. Comparative analysis with diclofenac showed no statistically significant difference in anti-inflammatory effects between diclofenac and the capsaicin hydrogel patch (P>0.05). This study demonstrates the effectiveness of using low concentrations of capsaicin, showing significant anti-inflammatory properties. These findings are consistent with previous studies, which reported that induced inflammation in treated animals was associated with a corresponding rise in C-reactive protein levels, pointing to the inflammation-inducing properties of egg albumin. The results indicated that capsaicin in both forms of Capsicum frutescens Linn. [Solanaceae] (CPF) and capsaicin (Fluka Biotechnika) (CFE) demonstrated anti-inflammatory effects comparable to diclofenac in the experimental rat model (P< 0.05). It can be concluded that capsaicin possesses both analgesic and anti-inflammatory properties. The objective of the study was to determine whether pre-treatment with CPF and CFE could produce a reduction in inflammation and inhibition of egg albumin-induced edema similar to diclofenac, a standard non-steroidal anti-inflammatory agent.[34] Its anti-

inflammatory efficacy was on par with standard diclofenac, supporting its potential as a safe and effective treatment for localized pain and inflammation management.

Our study showed a significant reduction in pain after three days according to NRS scores when using a capsaicin hydrogel patch for 60 minutes twice a day. The topically applied capsaicin is acknowledged for its analgesic effects. While studies on its efficacy in MPS presented conflicting outcomes, there is a notable absence of research examining the application of capsaicin in elevated concentrations, specifically in treating peripheral neuropathic pain. Despite the established association of clinically utilized capsaicin concentrations with transient pain alleviation, sustained usage is hindered by adverse effects, notably a burning sensation post-application, leading to poor adherence. The efficacy of capsaicin has been linked to concentration-dependent outcomes. Consequently, individuals with MPS may experience prolonged and enhanced pain relief by applying concentrated capsaicin.[14,35] The safety of capsaicin patches has been reported, with findings regarding their pharmacokinetics.[36] Notably, an assessment of 8% capsaicin patches revealed minimal systemic absorption.[37] Therefore, it is inferred that the 0.1% patch is likely safe concerning local skin irritation, systemic absorption, and epidermal nerve fiber degeneration.[38] We conducted a small pilot study using topical capsaicin to treat MPS. Capsaicin selectively stimulates nociceptive neurons and has been widely used to study pain-related events. Capsaicin exerts multiple pharmacological and physiological effects, including analgesia,[39] anti-inflammation, and antioxidant effects.[40] Therefore, capsaicin may be valuable for pain relief, cancer prevention, and weight loss in clinical settings.

In addition, capsaicin also has benefits for the cardiovascular and gastrointestinal systems. The most studied capsaicinoid for pain relief is capsaicin. It has been shown that capsaicin was used to reduce the inflammatory heat and noxious chemical hyperalgesia or pain.[41] Despite the acknowledged potential for a burning sensation with capsaicin, treatment utilizing the 0.1% patch was as effective. Nevertheless, this study showed that the mean VAS decreased after three days and was not statistically significant. However, the NRS scores decreased statistically significantly. This is consistent with previous investigations.[42] No serious adverse events were reported. This aligns with the previous study,[43] which investigated the efficacy of a 0.1% capsaicin hydrogel patch for myofascial neck pain in a double-blind randomized trial. The study developed a hydrogel patch, where participants were randomly assigned to receive either a 0.1% capsaicin hydrogel patch or a control hydrogel patch without capsaicin. All participants were instructed to apply one patch to each side of the neck and shoulder, directly over the areas of greatest pain, for 12 hours per day over a 4-week period. The results showed that among the 57 patients, there was a significant reduction in mean VAS, NDI, and BDI scores at 2 and 4 weeks. No significant differences were found between the two groups in the outcome measures. In conclusion, the treatment was found to be effective.[43] Capsaicin 0.1% is widely applied topically for pain relief in osteoarthritis, neuropathic, and muscle pain.[44] Its mechanism of action involves desensitizing TRPV1 pain receptors and reducing the levels of substance P, a neuropeptide that transmits pain signals to the brain. Capsaicin's primary clinical use is for pain management.[45] Since the early 1980s, low-concentration capsaicin formulations (0.025%–0.1%) in creams, lotions, and patches have been available globally for daily application.[21] Notably, topical capsaicin exhibits minimal drug interactions and can be safely used alongside other analgesics, with generally mild adverse effects. Studies demonstrate its safety in pain management.

Conclusion

This study characterized a capsaicin-loaded hydrogel patch for transdermal application to manage myofascial pain syndrome (MPS). The hydrogel, composed of polyvinyl alcohol and gelatin, demonstrated excellent physicochemical stability and biocompatibility. GC-MS analysis revealed the presence of several bioactive compounds, including dodecyl acrylate and oleic acid, known for their anti-inflammatory and permeation-enhancing properties. FTIR and UV-Vis spectroscopy confirmed the successful incorporation and sustained release of capsaicin within the hydrogel matrix. Cytotoxicity evaluation using the MTT assay on human skin fibroblasts indicated low toxicity at therapeutic concentrations, with an IC_{50} of approximately 20 mg/mL. The hydrogel also exhibited potent anti-inflammatory activity, achieving complete inhibition of protein denaturation across tested concentrations, with efficacy statistically comparable to the standard drug diclofenac (P=0.183). In a pilot clinical trial, participants reported a significant reduction in pain intensity as measured by the Numeric Rating Scale (P=0.05), with no severe adverse effects observed.

Additionally, these findings support the capsaicin hydrogel patch as a promising, safe, and effective treatment for localized pain and inflammation, offering a potential alternative to conventional pharmacological interventions in treating MPS.

Ethical Considerations

The study protocol was reviewed and approved by the Human Research Ethics Committee, Suranaree University of Technology, Nakhon Ratchasima, Thailand (Reference letter No. EC-64-152 dated 25-02-2022). Written informed consent was obtained from all the participants.

Competing Interests

The authors declare that they have no competing interests.

Sources of Funding

This work was supported by the Institute of Research and Development (IRD), Parasitic Disease Research Center (PDRC) under the grant, Suranaree University of Technology (SUT), the Kitti Bundit scholarship, Suranaree University of Technology (SUT), Thailand Science Research and Innovation (TSRI), and National Science, Research and Innovation Fund (NSRF) (NRIIS number 195617).

References

1. Kobata K, Todo T, Yazawa S, Iwai K, Watanabe T. Novel Capsaicinoid-like Substances, Capsiate and Dihydrocapsiate, from the Fruits of a Nonpungent Cultivar, CH-19 Sweet, of Pepper (*Capsicum annuum L.*). J Agric Food Chem.. 1998;46(5):1695-7. doi: 10.1021/jf980135c
2. Ahmad R, Alqathama A, Aldholmi M, Riaz M, Abdalla AN, Mostafa A, Al-Said HM, Alqarni AM, Ullah R, Asgher SS, Amir M, Shaaban H, Ahmad W. Gas Chromatography-Mass Spectrometry (GC-MS) Metabolites Profiling and Biological Activities of Various *Capsicum annum cultivars*. Plants (Basel). 2022 Apr 9;11(8):1022. doi: 10.3390/plants11081022. PMID: 35448750; PMCID: PMC9025676.
3. Paradossi G, Cavalieri F, Chiessi E, Spagnoli C, Cowman MK. Poly(vinyl alcohol) as versatile biomaterial for potential biomedical applications. J Mater Sci Mater Med. 2003 Aug;14(8):687-91. doi: 10.1023/a:1024907615244. PMID: 15348409.
4. Jeszka-Skowron M, Zgoła-Grześkowiak A, Grześkowiak T, Ramakrishna A. Analytical Methods in the Determination of Bioactive Compounds and Elements in Food: Springer; 2021.
5. Huang CJ, Pu CM, Su SY, Lo SL, Lee CH, Yen YH. Improvement of wound healing by capsaicin through suppression of the inflammatory response and amelioration of the repair process. Mol Med Rep. 2023 Aug;28(2):155. doi: 10.3892/mmr.2023.13042. Epub 2023 Jun 30. PMID: 37387413; PMCID: PMC10350740.
6. Benítez-Angeles M, Morales-Lázaro SL, Juárez-González E, Rosenbaum T. TRPV1: Structure, Endogenous Agonists, and Mechanisms. Int J Mol Sci. 2020 May 12;21(10):3421. doi: 10.3390/ijms21103421. PMID: 32408609; PMCID: PMC7279265.
7. Li Z, Zhang J, Cheng K, Zhang L, Wang T. Capsaicin alleviates the intestinal oxidative stress via activation of TRPV1/PKA/UCP2 and Keap1/Nrf2 pathways in heat-stressed mice. Journal of Functional Foods. 2023;108:105749. doi: 10.1016/j.jff.2023.105749.
8. Fattori V, Hohmann MS, Rossaneis AC, Pinho-Ribeiro FA, Verri WA. Capsaicin: Current Understanding of Its Mechanisms and Therapy of Pain and Other Pre-Clinical and Clinical Uses. Molecules. 2016 Jun 28;21(7):844. doi: 10.3390/molecules21070844. PMID: 27367653; PMCID: PMC6273101.
9. Chuang YC, Yoshimura N, Huang CC, Wu M, Chiang PH, Chancellor MB. Intraprostatic botulinum toxin a injection inhibits cyclooxygenase-2 expression and suppresses prostatic pain on capsaicin induced prostatitis model in rat. J Urol. 2008 Aug;180(2):742-8. doi: 10.1016/j.juro.2007.07.120. Epub 2008 Jun 13. PMID: 18554636.
10. Caterina MJ, Schumacher MA, Tominaga M, Rosen TA, Levine JD, Julius D. The capsaicin receptor: a heat-activated ion channel in the pain pathway. Nature. 1997 Oct 23;389(6653):816-24. doi: 10.1038/39807. PMID: 9349813.
11. Shahsavari F, Abbasnejad M, Esmaeili-Mahani S, Raoof M. The ability of orexin-A to modify pain-induced cyclooxygenase-2 and brain-derived neurotrophic factor expression is associated with its ability to inhibit capsaicin-induced pulpal nociception in rats. Korean J Pain. 2022 Jul 1;35(3):261-270. doi: 10.3344/kjp.2022.35.3.261. PMID: 35768981; PMCID: PMC9251390.
12. Appasamy M, Lam C, Alm J, Chadwick AL. Trigger Point Injections. Phys Med Rehabil Clin N Am. 2022 May;33(2):307-333. doi: 10.1016/j.pmr.2022.01.011. PMID: 35526973; PMCID: PMC9116734.
13. Wilke J, Vogt L, Niederer D, Hübscher M, Rothmayr J, Ivkovic D, Rickert M, Banzer W. Short-term effects of acupuncture and stretching on myofascial trigger point pain of the neck: a blinded, placebo-controlled RCT. Complement Ther Med. 2014 Oct;22(5):835-41. doi: 10.1016/j.ctim.2014.09.001. Epub 2014 Sep 16. PMID: 25440373.
14. Romero V, Lara JR, Otero-Espinar F, Salgado MH, Modolo NSP, Barros GAM. Creme tópico de capsaicina (8%) para o tratamento da síndrome da dor miofascial [Capsaicin topical cream (8%) for the treatment of myofascial pain syndrome]. Braz J Anesthesiol. 2019 Sep-Oct;69(5):432-438. doi: 10.1016/j.bjan.2019.06.008. Epub 2019 Sep 10. PMID: 31519301; PMCID: PMC9391859.
15. Quintner JL, Bove GM, Cohen ML. A critical evaluation of the trigger point phenomenon. Rheumatology (Oxford). 2015 Mar;54(3):392-9. doi: 10.1093/rheumatology/keu471. Epub 2014 Dec 3. PMID: 25477053.
16. Chen Y, Li J, Lu J, Ding M, Chen Y. Synthesis and properties of Poly(vinyl alcohol) hydrogels with high strength and toughness. Polymer Testing. 2022;108:107516. doi: 10.1016/j.polymertesting.2022.107516.
17. Boriwanwattanarak P, Ingkaninan K, Khorana N, Viyoch J. Development of curcuminoids hydrogel patch using chitosan from various sources as controlled-release matrix. Int J Cosmet Sci. 2008 Jun;30(3):205-18. doi: 10.1111/j.1468-2494.2008.00437.x. PMID: 18452437.
18. Sun X, Agate S, Salem KS, Lucia L, Pal L. Hydrogel-Based Sensor Networks: Compositions, Properties, and Applications-A Review. ACS Appl Bio Mater. 2021 Jan 18;4(1):140-162. doi: 10.1021/acsabm.0c01011. Epub 2020 Nov 17. PMID: 35014280.
19. Kim GJ, Kim KO. Novel glucose-responsive of the transparent nanofiber hydrogel patches as a wearable biosensor via electrospinning. Sci Rep. 2020 Nov 2;10(1):18858. doi: 10.1038/s41598-020-75906-9. PMID: 33139822; PMCID: PMC7608638.
20. Simone DA, Nolano M, Johnson T, Wendelschafer-Crabb G, Kennedy WR. Intradermal injection of capsaicin in humans produces degeneration and subsequent reinnervation of epidermal nerve fibers: correlation with sensory function. J Neurosci. 1998 Nov 1;18(21):8947-59. doi: 10.1523/JNEUROSCI.18-21-08947.1998. PMID: 9787000; PMCID: PMC6793545.
21. Ilie MA, Caruntu C, Tampa M, Georgescu SR, Matei C, Negrei C, Ion RM, Constantin C, Neagu M, Boda D. Capsaicin: Physicochemical properties, cutaneous reactions and potential applications in painful and inflammatory conditions. Exp Ther Med. 2019 Aug;18(2):916-925. doi: 10.3892/etm.2019.7513. Epub 2019 Apr 19. PMID: 31384324; PMCID: PMC6639979.
22. Jaiboonma A, Kaokaen P, Chaicharoenaudomrung N, Kunhorm P, Janebodin K, Noisa P, Jitprasertwong P. Cordycepin attenuates Salivary Hypofunction through the Prevention of Oxidative Stress in Human Submandibular Gland Cells. Int J Med Sci. 2020 Jul 6;17(12):1733-1743. doi: 10.7150/ijms.46707.
23. Padmanabhan P, Jangle S. Evaluation of in-vitro anti-

inflammatory activity of herbal preparation, a combination of four medicinal plants. Int J Appl Basic Med Res. 2012;2(1):109-16.
24. Marius M, Amadou D, Donatien AA, Gilbert A, William YN, Rauf K, Arif M, Adeline FYS, Saint NI, Dar H, Rehman NU, Ahmad I. *In Vitro* Antioxidant, Anti-inflammatory, and *In Vivo* Anticolitis Effects of Combretin A and Combretin B on Dextran Sodium Sulfate-Induced Ulcerative Colitis in Mice. Gastroenterol Res Pract. 2020 Nov 7;2020:4253174. doi: 10.1155/2020/4253174. PMID: 33204254; PMCID: PMC7666632.
25. Viechtbauer W, Smits L, Kotz D, Budé L, Spigt M, Serroyen J, Crutzen R. A simple formula for the calculation of sample size in pilot studies. J Clin Epidemiol. 2015 Nov;68(11):1375-9. doi: 10.1016/j.jclinepi.2015.04.014. Epub 2015 Jun 6. PMID: 26146089.
26. Tseng C-H, Sim D. Sample size planning for pilot studies. arXiv preprint arXiv:210505483. 2021.
27. Katz J, Melzack R. Measurement of pain. Surg Clin North Am. 1999 Apr;79(2):231-52. doi: 10.1016/s0039-6109(05)70381-9. PMID: 10352653.
28. Koleva-Gudeva L, Mitrev S, Maksimova V, Spasov D. Content of capsaicin extracted from hot pepper (*Capsicum annuum ssp. microcarpum L.*) and its use as an ecopesticide. Hemijska Industrija. 2013;67(4):671-5.
29. López Pacheco MA, Báez Rojas JJ, Castro-Ramos J, Villa Manríquez JF, Esmonde-White K. Optical study to identify and quantify capsaicin in optical window. Heliyon. 2021 Mar 17;7(3):e05797. doi: 10.1016/j.heliyon.2020.e05797. PMID: 33768170; PMCID: PMC7980067.
30. Amruthraj NJ, Preetam Raj JP, Lebel A. Capsaicin-capped silver nanoparticles: its kinetics, characterization and biocompatibility assay. Appl. Nanosci. 2015;5(4):403-9. doi: 10.1007/s13204-014-0330-5.
31. Ko JA, Kim J, Doh H, Park HJ. Quality evaluation and storage test for capsaicin-fortified yogurt based on the multilayer nanoemulsion system. Food Sci Biotechnol. 2023 Jul 28;33(2):441-451. doi: 10.1007/s10068-023-01386-y. PMID: 38222921; PMCID: PMC10786756.
32. Sancho R, Lucena C, Macho A, Calzado MA, Blanco-Molina M, Minassi A, Appendino G, Muñoz E. Immunosuppressive activity of capsaicinoids: capsiate derived from sweet peppers inhibits NF-kappaB activation and is a potent antiinflammatory compound in vivo. Eur J Immunol. 2002 Jun;32(6):1753-63. doi: 10.1002/1521-4141(200206)32:6<1753::AID-IMMU1753>3.0.CO;2-2. PMID: 12115659.
33. Amantini C, Ballarini P, Caprodossi S, Nabissi M, Morelli MB, Lucciarini R, Cardarelli MA, Mammana G, Santoni G. Triggering of transient receptor potential vanilloid type 1 (TRPV1) by capsaicin induces Fas/CD95-mediated apoptosis of urothelial cancer cells in an ATM-dependent manner. Carcinogenesis. 2009 Aug;30(8):1320-9. doi: 10.1093/carcin/bgp138. Epub 2009 Jun 5. PMID: 19502594.
34. Shah M, Parveen Z, Khan MR. Evaluation of antioxidant, anti-inflammatory, analgesic and antipyretic activities of the stem bark of Sapindus mukorossi. BMC Complement Altern Med. 2017 Dec 8;17(1):526. doi: 10.1186/s12906-017-2042-3. PMID: 29221478; PMCID: PMC5723046.
35. Tshering G, Posadzki P, Kongkaew C. Efficacy and safety of topical capsaicin in the treatment of osteoarthritis pain: A systematic review and meta-analysis. Phytother Res. 2024 Jul;38(7):3695-3705. doi: 10.1002/ptr.8223. Epub 2024 May 18. PMID: 38761115.
36. Goodwin B, Chiplunkar M, Salerno R, Coombs K, Sannoh U, Shah V, Averell N, Al-Shebab U, Janora D. Topical capsaicin for the management of painful diabetic neuropathy: a narrative systematic review. Pain Manag. 2023 May;13(5):309-316. doi: 10.2217/pmt-2023-0006. Epub 2023 Jul 12. PMID: 37435696.
37. Anand P, Bley K. Topical capsaicin for pain management: therapeutic potential and mechanisms of action of the new high-concentration capsaicin 8% patch. Br J Anaesth. 2011 Oct;107(4):490-502. doi: 10.1093/bja/aer260. Epub 2011 Aug 17. PMID: 21852280; PMCID: PMC3169333.
38. Kennedy WR, Vanhove GF, Lu SP, Tobias J, Bley KR, Walk D, Wendelschafer-Crabb G, Simone DA, Selim MM. A randomized, controlled, open-label study of the long-term effects of NGX-4010, a high-concentration capsaicin patch, on epidermal nerve fiber density and sensory function in healthy volunteers. J Pain. 2010 Jun;11(6):579-87. doi: 10.1016/j.jpain.2009.09.019. Epub 2010 Apr 18. PMID: 20400377.
39. Macho A, Lucena C, Sancho R, Daddario N, Minassi A, Muñoz E, Appendino G. Non-pungent capsaicinoids from sweet pepper synthesis and evaluation of the chemopreventive and anticancer potential. Eur J Nutr. 2003 Jan;42(1):2-9. doi: 10.1007/s00394-003-0394-6. PMID: 12594536.
40. Joo JI, Kim DH, Choi JW, Yun JW. Proteomic analysis for antiobesity potential of capsaicin on white adipose tissue in rats fed with a high fat diet. J Proteome Res. 2010 Jun 4;9(6):2977-87. doi: 10.1021/pr901175w. PMID: 20359164.
41. Zhou M, Zhang Q, Huo M, Song H, Chang H, Cao J, Fang Y, Zhang D. The mechanistic basis for the effects of electroacupuncture on neuropathic pain within the central nervous system. Biomed Pharmacother. 2023 May;161:114516. doi: 10.1016/j.biopha.2023.114516. Epub 2023 Mar 13. PMID: 36921535.
42. Wong F, Reddy A, Rho Y, Vollert J, Strutton PH, Hughes SW. Responders and nonresponders to topical capsaicin display distinct temporal summation of pain profiles. Pain Rep. 2023 Apr 4;8(3):e1071. doi: 10.1097/PR9.0000000000001071. PMID: 37731476; PMCID: PMC10508395.
43. Cho JH, Brodsky M, Kim EJ, Cho YJ, Kim KW, Fang JY, Song MY. Efficacy of a 0.1% capsaicin hydrogel patch for myofascial neck pain: a double-blinded randomized trial. Pain Med. 2012 Jul;13(7):965-70. doi: 10.1111/j.1526-4637.2012.01413.x. Epub 2012 Jun 8. PMID: 22681259.
44. Santos MP, Lemos F, Gomes J, Romão JM, Veiga D. Topical capsaicin 8% patch in peripheral neuropathic pain: Efficacy and quality of life. Br J Pain. 2024 Feb;18(1):42-56. doi: 10.1177/20494637231201502. Epub 2023 Sep 12. PMID: 38344267; PMCID: PMC10851892.
45. Mavrommatis CI, Argyra E, Vadalouka A, Vasilakos DG. Acupuncture as an adjunctive therapy to pharmacological treatment in patients with chronic pain due to osteoarthritis of the knee: a 3-armed, randomized, placebo-controlled trial. Pain. 2012 Aug;153(8):1720-1726. doi: 10.1016/j.pain.2012.05.005. Epub 2012 Jun 21. PMID: 22727499.

***Corresponding author**: Assoc. Prof. Schawanya K. Rattanapitoon, MD. E-mail: schawanya.ratt@gmail.com*

International Journal of Biomedicine 15(3) (2025) 583-589
http://dx.doi.org/10.21103/Article15(3)_OA20

ORIGINAL ARTICLE

Experimental Biology

INTERNATIONAL JOURNAL OF BIOMEDICINE

Synergistic Effects of Amino Acid Combination in Streptozotocin-Induced Diabetic Rats: Amelioration of Hyperglycemia, Hematological Aberrations, and Pancreatic Damage

Nune V. Kocharyan[1], Narine V. Tumasyan[1*], Silva S. Abrahamyan[1], Ani B. Suqiasyan[1], Alla S. Hovsepyan[2], Hasmik A. Stepanyan[1], Lusine S. Grigoryan[1], Zoya Kh. Paronyan[1], Inesa S. Sahakyan[1]

[1]*H. Buniatian Institute of Biochemistry of NAS RA, Yerevan, Armenia*
[2]*Blood Laboratory, «Avan» Health Center, Yerevan, Armenia*

Abstract

Background: This study aimed to investigate the therapeutic potential of an amino acid combination (AAC) comprising gamma-aminobutyric acid, β-alanine, glutamine, and ethanolamine-O-sulfate for synergistic effects in type 1 diabetes mellitus (T1DM).
Methods and Results: The experiments were conducted on albino male rats, divided into three groups: control rats, streptozotocin (STZ)-induced diabetic rats, and diabetic rats treated with AAC. Fasting blood glucose levels and hematological parameters were monitored. Morphological analysis of blood smears and histopathological examination of the pancreas were performed using histological (Hematoxylin and Eosin, Giemsa staining) methods. AAC treatment significantly reduced fasting blood glucose levels and improved hematological parameters, including red and white blood cell counts, which were initially decreased due to STZ-induced diabetes. AAC treatment mitigated the erythrocyte abnormalities observed in diabetic rats. Histopathological examination of the pancreas revealed that AAC partially restored the structural integrity of its tissue, resulting in a slight increase in the size and number of shrunken islets of Langerhans.
Conclusions: AAC exerts a synergistic effect, improving glycemic control, ameliorating hematological aberrations, and promoting partial regeneration of pancreatic islets in T1DM rats. This study highlights the potential of AAC as a therapeutic agent for managing T1DM and its associated complications.(**International Journal of Biomedicine. 2025;15(3):583-589.**)

Keywords: glycemic control • blood cell count • blood cell morphology • pancreas

For citation: Kocharyan N, Tumasyan N, Abrahamyan S, Suqiasyan A, Hovsepyan A, Stepanyan H, Grigoryan L, Paronyan Z, Sahakyan I. Synergistic Effects of Amino Acid Combination in Streptozotocin-Induced Diabetic Rats: Amelioration of Hyperglycemia, Hematological Aberrations, and Pancreatic Damage. International Journal of Biomedicine. 2025;15(3):583-589. doi:10.21103/Article15(3)_OA20

Abbreviations

AAC, amino acid combination; **Ala**, β-alanine; **DM**, diabetes mellitus; **DC**, differential count; **EOS**, ethanolamine-O-sulfate; **FBGL**, fasting blood glucose level; **GABA**, gamma-aminobutyric acid; **Gln**, glutamine; **RBCs**, red blood cells, **STZ**, streptozotocin; **T1DM**, type 1 diabetes mellitus; **T2DM**, type 2 diabetes mellitus; **WBCs**, white blood cells.

Introduction

Diabetes mellitus (DM) is a common chronic metabolic disorder characterized by a deficiency of insulin, resulting in hyperglycemia of a defined degree, with or without glucosuria, and hyperlipidemia. In addition to the metabolic dysregulation itself, this leads to numerous long-term secondary complications, including stroke,[1] neuropathy,[2] nephropathy,[3] retinopathy,[4] ulcers,[5] and gangrene in the extremities,[6] as well as an increased risk of cardiovascular disease leading to mortality.[7] It is known that DM weakens the body's antioxidant defenses,[8] which, together with hyperglycemia

and lipid exchange, causes a decrease in transparency of the phospholipid membrane of peripheral tissue cells and, consequently, damage to β-cells of the islets of Langerhans in the pancreas.

It is known that, due to chronic decompression of carbohydrate metabolism in patients with DM, a complex of metabolic disorders develops, pathologically affecting the morpho-functional state of peripheral blood cells. Therefore, nonenzymatic glycosylation of hemoglobin and the erythrocyte membrane proteins leads to the appearance of abnormal cell forms in the peripheral blood. Enhanced concentration of free radicals and undirected proteolysis products in the patient's organism with DM destabilizes erythrocyte cell membranes. Ultimately, the severity of metabolic stress in diabetes, complicated by angiopathy, leads to a decrease in the number of erythrocytes circulating in the blood, an increase in platelet activity, and the development of cell-depressive immunodeficiency.[9]

There are two types of DM. Type 1 diabetes mellitus (T1DM) is characterized by autoimmune destruction of insulin-producing β cells in the pancreas by CD4+ and CD8+ T cells and macrophages infiltrating the islets.[10] Type 2 diabetes mellitus (T2DM) is a non-insulin-dependent disease caused by a metabolic disorder that develops as a result of the tissue cells' decreased sensitivity to insulin. The prevalence of DM tends to increase. The rising incidence of diabetes underscores the urgent need for effective therapy with multifaceted mechanisms of lowering blood glucose levels and correcting compromised physiological oxidative mechanisms.[11]

Physicians currently have two main strategies for managing patients with T1DM: the first involves preventing the onset of autoimmunity, while the second focuses on reversing the effects of existing autoimmunity and promoting β-cell regeneration. The detection of β-cells in individuals with long-standing T1DM, despite ongoing autoimmune activity, suggests that there may be ongoing β-cell formation.[12] Substantial evidence indicates that an increase in β-cell mass during normal growth and following injury is driven by the division of existing β-cells and the formation of new β-cells from ductal or pancreatic progenitor cells.[13] This insight has opened avenues for developing innovative techniques to enhance β-cell regeneration.

Emerging evidence suggests that amino acids may play an important role in preventing diabetes and its associated complications. Gamma-aminobutyric acid (GABA) has been studied for its potential therapeutic effects in both T1DM and T2DM. GABA is known for its role in the central nervous system. Studies have shown that GABA can inhibit the autoimmune response, thereby preserving insulin production and potentially reducing the onset of diabetes.[14,15] Noteworthy, the recent publications in the field of experimental diabetes give evidence about the protective and regenerative effects of GABA on pancreatic beta cells and demonstrate its potential in reversing diabetes in diabetic mouse models.[16]

Another amino acid, β-alanine (Ala), a dietary supplement primarily known for its role in muscle performance, has not been extensively studied concerning T1DM. However, there is limited evidence suggesting that Ala could influence metabolic pathways that are relevant to diabetes. Its role in synthesizing carnosine is not directly related to T1DM but could indirectly affect metabolic health, a significant aspect of managing diabetes. The benefits of β-alanine administration in combination with increased physical activity in patients with T2DM led to a reduction in glycemia and a simultaneous improvement in physical capacity.[17]

It has been shown that glutamine (Gln) significantly affects glucose metabolism and insulin sensitivity, including nitrogen transport, immune function, and gut health. Research has demonstrated that Gln can improve insulin sensitivity and reduce hyperglycemia in T1DM and T2DM models.[18,19] Its ability to reduce oxidative stress and support immune function is also beneficial in managing DM, particularly in reducing complications associated with the disease.

It is known that ethanolamine-O-sulfate (EOS) increases GABA levels by inhibiting GABA transaminase. While EOS is not widely studied in the context of diabetes, the resulting increase in GABA levels could have protective effects similar to those observed with direct GABA supplementation. This could contribute to β-cell preservation and reduced autoimmune activity in T1DM, though specific studies on EOS in diabetes are limited. This suggests potential therapeutic uses for EOS in managing diabetes, particularly through the modulation of GABAergic pathways.[20] Studies have shown that administering both EOS and Gln produced a protective effect on the amino acids in the brain and the pancreas of rats with experimental STZ diabetes.[21] We also revealed the effect of the combined administration of the above-mentioned 3 neuroactive amino acid mixture in T1DM.[22] In particular, to create an antidiabetic preparation, Prof. Kamalyan compiled a mixture that included GABA, Gln, Ala, and EOS. The study showed the promising therapeutic effects of this mixture on the function of the pancreas in alloxan-induced diabetic rats [23]

Our study explored how combining investigating compounds (GABA, Ala, Gln, and EOS) might impact T1DM. We have attempted to use them in combination for their probable synergistic effect, which can enhance therapeutic efficacy by acting through multiple mechanisms. We hope the amino acid combination (AAC) is a synergistic pharmacological agent that acts simultaneously and dynamically.

This study aimed to investigate the therapeutic potential of AAC comprising gamma-aminobutyric acid, β-alanine, glutamine, and ethanolamine-O-sulfate for synergistic effects in T1DM.

Materials and Methods

Animals

The experiments were conducted on 18 albino male rats weighing 180-240 g. Animals were maintained at a controlled temperature of 23 ± 4 °C with a humidity of 55 ± 5% and a 12-hr dark-light cycle. The rats were fed a standard rat chow and tap water *ad libitum*. Animal care, regular monitoring for general health conditions and weight, and all-animal study experiments were performed based on the IACUC policies and animal care standards, regulations adopted by the Armenian Ethical Committee of the Institute of Biochemistry

named after H. Buniatian, National Academy of Science of the Republic of Armenia (IRB0001621 - IORG0009782).

Induction of Experimental Diabetes

Streptozotocin (STZ) is a cytotoxic alkylating agent that induces swift and irreversible necrosis in pancreatic β-cell islets.[24] It is primarily used to induce T1DM in experimental models, especially rodents.

Rats were induced to be diabetic by a single intraperitoneal injection of 60 mg/kg STZ (Sigma-Aldrich Co., USA) dissolved in 50 mM sodium citrate buffer, pH 4.5 (2.0 ml/kg body weight).[25] The induction of DM was confirmed after STZ treatment by estimating elevated fasting blood glucose level (FBGL). Only those rats with FBGL ≥ 13 mmol/L were included in the study.

Experimental Design

In the experiment, 18 normal healthy rats were used. The animals were weighed and divided into three groups consisting of 6 rats: Group 1 (Control): normal healthy rats; Group 2 (STZ): STZ-induced diabetic rats; and Group 3 (STZ+AAC): STZ-induced diabetic rats treated with AAC.

The diabetes model was induced in 12 animals (Groups 2 and 3) by i/p injection of STZ at a dose of 60 mg/kg. The animals of the control group were injected with an appropriate amount of citrate buffer instead of STZ. The level of peripheral blood glucose (mmol/L) was measured daily in the morning after overnight fasting by taking a drop of blood from the proximal ventral tail vein and using a glucometer (Accu-Chek Active, Roche, Germany). Rats with blood glucose concentrations over 13 mmol/L were considered to have T1DM and were used for further experiments. The control group was selected among intact animals, which had glucose concentrations in the range of 5.0–5.8 mmol/L.

Treatment of Diabetic Rats with AAC

Pharmacological evaluation of the antidiabetic activity of the combination of GABA, Ala, Gln, and EOS was carried out using the STZ-induced diabetes model in rats.

Five days after the injection of STZ (receiving well-established diabetes) to improve the animals' health, Group 3 rats were weighed and given i/p injections of AAC solution (100 mg GABA, 50 mg Glu, 100 mg Ala, 300 mg EOS/2.0 ml/kg) daily for 10 days. An appropriate amount of normal saline was injected into Group 1 and Group 2 animals for all consecutive days. Blood glucose was determined each day during the treatment period.

Histopathological Study

At the end of the treatment, the animals were fasted overnight, anesthetized by i/p injection of 40-50 mg/kg Nembutal, and subjected to instant euthanasia, after which the pancreas of all animal groups and the blood samples were collected to perform morphological investigations.

The blood samples were collected into EDTA-containing vacutainer tubes and used immediately to determine hematological values—white blood cell count (WBCs), red blood cell count (RBCs), and differential count (DC), including lymphocytes, monocytes, basophils, neutrophils, and eosinophils—using an automated hematology analyzer Uritmedical BH-40.

Standard methods were used to prepare blood smears using Giemsa histological staining.[26] Pancreas of all animal groups were isolated; samples were fixed in 10% buffered formalin and embedded in paraffin; 5-10 μm sections were prepared and stained with Hematoxylin-Eosin (H&E).[27] Blood smears and the pancreatic tissue specimens were examined/photographed with a light microscope (Optica B-1000FL-HBO; Camera- C-P20).

Statistical Analysis

Data were statistically analyzed using SigmaStat software. All values are presented as mean ± standard error of the mean (SEM). The statistically reliable comparison was performed by using the Student's t-test. Statistical significance was considered at $P<0.05$.

Results

After a single i/p injection of STZ at a dose of 60 mg/kg, stable hyperglycemia was observed after 5 days. A nearly 7-fold increase in the fasting blood glucose level in experimental rats was observed compared to the control. The animals exhibited the following symptoms: increased water consumption (more than 120 mL), frequent urination, sudden weight loss, hair loss, and depression. In Group 3 animals, the daily treatment of AAC reduced the FBGL by 80%, reaching the norm on Day 3 ($P<0.001$), persisting for several days, and then gradually increased in the following days, to 14% vs. untreated STZ rats (Fig. 1).

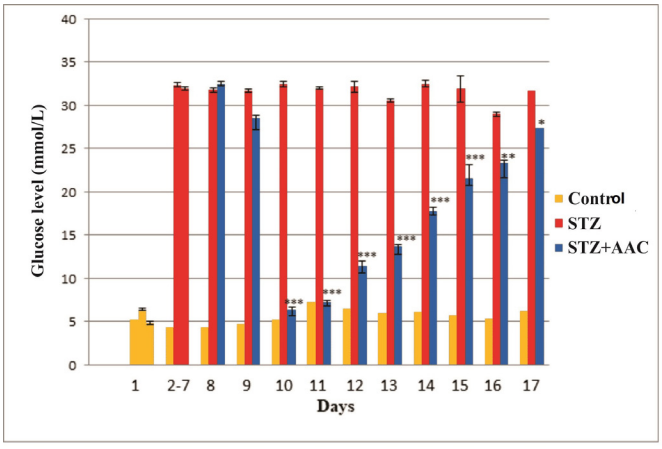

Fig.1. *Results of daily FBGL measurements in the male albino rats of the study groups. Data are shown as mean ± SEM. *P<0.05, ** P<0.01, and *** P<0.001 compared to the STZ group.*

Examination of the total number of RBCs, WBCs, DC of leukocytes of all groups of animals was performed to determine the percentage of each type of white blood cell present in the blood. Diabetic rats showed a significant decrease in the total number of RBCs and WBCs than the normal control

group rats. Differential count showed that neutrophils and lymphocytes levels were significantly decreased. An increased number of monocytes was observed in diabetic rats (Table 1). Changes in DC eosinophils and basophils were within normal limits. After 10 days of treatment by AAC, these indicators gradually return to normal. Blood cell counts appeared to recover from the STZ-induced decrease observed in the treatment group, reaching baseline levels like those observed in the control group. These findings correlate with the positive effect of AAC on blood glucose levels.

Table 1.

Total number of RBCs, WBCs, and DC of leukocytes of the studied rat groups.

Parameter	Control (n=6)	STZ (n=6)	STZ+AAC (n=6)	RR*
RBC ($\times10^{12}$/L)	8.445±0.164	6.395±0.086	8.868±0.111	7.8-10.2
WBC ($\times10^{9}$/L)	10.731±0.107	7.370±0.070	11.267±0.117	9.7-12.9
Neutrophils, %	21.083±0.49	13.067±0.088	16.817±0.111	13-36
Lymphocytes, %	75.000±0.577	58.250±0.167	66.167±0.358	61-86
Monocytes, %	1.233±0.084	6.017±0.060	3.95±0.070	1-4
Eosinophyls, %	0.730±0.042	0.853±0.015	0.812±0.023	0-2
Basophils, %	0.455±0.0226	0.168±0.012	0.352±0.005	0.3-0.5

**RR, reference range. Intergroup comparison of all animal groups showed significant P-values (P<0.05).*

Blood cell morphology is a key tool in laboratory hematology. Deviations from the norm in size, shape, color, distribution, or presence of inclusion bodies suggest possible pathological processes. Data from the morpho-functional study demonstrated that the leukocytes, platelets, and erythrocytes of the control rats' blood were normal (Fig. 2A). Erythrocytes were discoid (biconcave), about 7–8 μm in diameter, which corresponds to the size of the nucleus of a small lymphocyte and with a central area of pallor, which occupies a third of the diameter of erythrocytes and well hemoglobinized on the outer two-thirds of the diameter of the cells without any inclusions.

Of particular interest was the study of the blood smears of the diabetic untreated rats, which demonstrated morphological aberrations, shape abnormalities (poikilocytes), rouleaux formations or agglutinations, partial destruction (hemolysis) of the erythrocytes under the influence of STZ (Fig. 2B,C). We observed codocytes, also known as target cells (with a dark central hemoglobinized area, surrounded by a white ring, an area of relative pallor, followed by a dark outer, peripheral second ring containing a band of hemoglobin;[28] echinocytes or burr cells (reversible condition, referred to a form of red blood cell that have an abnormal cell membrane characterized by many small, evenly spaced thorny projections);[29] spherocytes (smaller than normal red blood cells with a lack central pallor, occurring in the setting of immune-mediated hemolysis or red cell membrane defect resulting from plasma membrane protein deficiency).[30] We also found disruption of the leukocytes' membrane integrity and morphological abnormalities (Fig. 2C,D), such as neutrophils with hypersegmented nuclei.

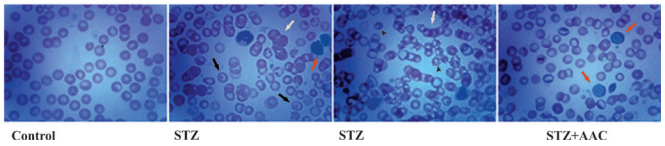

Fig. 2. *Blood cell morphology of the studied rat groups. Codocytes or target cells (black arrows), rouleaux formations or agglutinations (white arrows), leucocytes with impaired membrane integrity and morphological abnormalities (red arrows), echinocytes or burr cells (black arrowhead). Staining with Giemsa. Magnification: 1000x.*

The observation of the blood smears of the AAC-treated group showed that RBCs were generally morphologically normal compared to the blood of the diabetic untreated rats. An increased number of WBCs, such as small and large lymphocytes, was also detected.

Histopathological evaluations were carried out through H&E staining to determine the amount of pancreatic damage in each experimental group of animals.

Morphological investigation of the specimens showed that in the normal healthy rats from the control group, the endocrine part occupied a much smaller area of pancreatic tissue (Fig. 3A). It was represented by dispersed islets of Langerhans - clusters of endocrinocytes penetrated by a dense network of blood capillaries. The islets were predominantly round and oval and were separated from the acini by a thin connective tissue layer. Microscopic examination of pancreatic sections from the untreated diabetic rats revealed degenerative and necrotic changes, as well as shrinkage of the pancreatic islets of Langerhans, decreased islet cell density, marked vacuolization, and a severe reduction in the number of islet cells, which is typical of T1DM (Fig. 3B). However, the pancreatic acinar tissues mostly appeared normal. Treatment with AAC partially restores the morphological structure of pancreatic tissue and contributes to a slight increase in the size of wrinkled islets and the number of endocrinocytes (Fig. 3C). The results of this study show that the use of AAC in diabetes partially induces the regeneration of the islets, thereby restoring the functional activity of the pancreas.

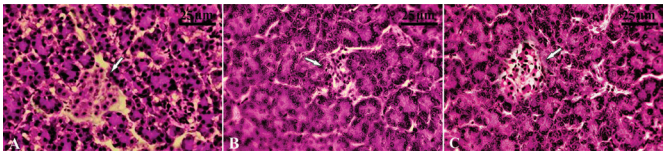

Fig. 3. *Histological image of the pancreas of the studied rat groups. (A) Control group: well-defined acini structures and normal islets of Langerhans, (B) STZ-induced diabetic group: numerous degenerative and necrotic changes in endocrine parts, (C) AAC-treated group: mild improvement of islets of Langerhans area. White arrows show islets of Langerhans. Staining with H&E. Magnification: 400x.*

Discussion

Researchers are actively exploring methods to restore functional β-cell mass as a strategy for diabetes management. These approaches aim to stimulate their replication and regeneration and prevent their damage and death. Potential strategies include promoting the proliferation of residual β-cells, encouraging the differentiation of their progenitors, and inducing the transdifferentiation of non-β-cells into insulin-producing cells, both within and beyond the pancreas.

Persistent hyperglycemia during DM can induce many chemical alterations, which are responsible for most of the clinical complications observed in diabetic patients.

Oxidative stress has been implicated as a primary factor in the progression of diabetes mellitus.[31] Hyperglycemia increases the generation of free radicals by glucose auto-oxidation, damaging vital organs.[32] This necessitates a therapy with multifaceted mechanisms of lowering blood glucose levels and correcting compromised physiological oxidative mechanisms.

As confirmed by our current study, the diabetic group showed an increase in FBGL, suggesting that STZ significantly destroyed the pancreatic β-cells. The combined use of the four investigating compounds included in AAC, based on synergism, has a strongly significant effect on the FBGL. The latter is because GABA, combined with GABA-ergic amino acids and EOS, is involved in carbon and protein metabolism in pancreatic β-cells, partially prevents the destruction of these cells, and, improving its condition, participates in the regulation of hormone secretion and the homeostasis of the islets of Langerhans. However, this effect did not last long, which is explained by the irreversible effects caused by STZ. The use of AAC may cause the release of insulin synthesized by the pancreas. The obtained results correspond with the literature data. It was shown that GABA induced a significant increase in insulin secretion from the pancreas of normal rats. In a diabetic pancreas, GABA evoked an increased insulin secretion, but the increase was statistically insignificant. These findings showed that the number of GABA-like immunoreactive (GABA-LIR) cells is reduced significantly in diabetes. Moreover, GABA is a strong secretagogue of insulin from the pancreas of a normal rat.[33]

Our study showed that in diabetic rats, RBCs and WBCs counts, DC of neutrophils and lymphocytes were found to be significantly decreased, while monocytes, on the contrary, increased. The DC of basophils and neutrophils remained within normal limits. Several studies support this finding. A possible explanation would be cell-specific autoantibodies.[34] Alteration of neutrophil migration may be another reason. The rate of neutrophil migration is lower in T1DM than in T2DM and healthy controls.[35] Moreover, neutropenia can be developed due to neutrophil sequestration in pancreatic tissue or neutrophil infiltration of the islets of Langerhans.[36] Low neutrophil counts are linked with a shortened half-life, increased turnover, and enhanced clearance by macrophages during chronic autoimmune inflammation and islet autoimmunity. Decreased lymphocytes suggest an increase in apoptosis.[37] Additionally, T1DM is characterized by cell-mediated autoimmune destruction of β-cells in the pancreas. This aberrant T-cell activation can destroy immune cells.[38] Activated phagocytosis may be another explanation for affecting neutrophils.[39] Our study revealed an increased monocyte count in the STZ-induced diabetic group. The possible reason may be the severity of diabetic ketoacidosis and evidence of infection. On the other hand, monocytosis may be a leukemoid reaction rather than a systemic inflammatory response. Imbalances in hormones, cytokines, and mediators may also increase monocyte counts.[40]

RBC mass also significantly decreased in diabetic rats compared with non-diabetic controls. Hyperglycemia may have long-term effects that result in the production of ROS, which could lead to irreversible glycation of Hb and RBC membranes.[41] Moreover, elevated levels of chronic hyperglycemia-induced proinflammatory cytokines contribute significantly to insulin resistance and cause anemia. The increase in interleukin-6 in hyperglycemic individuals has an anti-erythropoietic effect that may promote the death of immature RBCs.[42]

In addition to quantitative changes in blood cells, we also found morphological changes in diabetic rats compared to controls. In particular, a high prevalence of changes in erythrocyte morphology was observed. It is known that nonenzymatic glycosylation of proteins in the body induced by diabetic hyperglycemia is another pathway for implementing glucose toxicity.[43] It leads to irreversible structural and functional modifications of the peripheral blood cells, reduces the stability of cells, increases their fragility and deformability (the ability of red blood cells to undergo reversible changes in size and shape), and also changes their aggregation.[44]

Increased lipid peroxides may also lead to RBC membrane damage, hemolysis, and anemia.[45] It has been established that erythrocyte disorders developed as a result of absolute or relative insulin insufficiency significantly impede their functioning. Thus, disorders of erythrocyte morphofunctional state under prolonged hyperglycemia are more pronounced in the development of its decompensation, subsequently leading to quantitative and qualitative disorders of the peripheral link of erythron.

The present study investigated the hematological effects of AAC in STZ-induced diabetic rats. Blood smears from the AAC treatment group showed a nearly normal pattern compared to the blood of diabetic control rats. However, single morphologically changed RBCs and WBCs were still seen.

Our investigations show that after 10 days of treatment by AAC, the blood cell count, DC, and morphological changes gradually return to normal, which is significantly modulated with the regulation of glycemic control. Blood cell counts appeared to recover from the streptozotocin-induced decrease observed in the treated group, reaching baseline levels like those observed in the control group. These findings also correlate with the positive effect of the test substances on blood glucose levels.

The results of H&E staining of pancreatic tissue samples in all groups of rats were evaluated, especially considering the morphology of the islets of Langerhans.

Microscopic examination of the pancreas in healthy rats demonstrated well-defined acini structures with normal islets of Langerhans. In diabetic animals, degenerative and necrotic changes were observed in the endocrine part, such as a decrease in the number and marked destruction and atrophy of the persisted islets of Langerhans, which is why they appear shrunken.[46] Damage to pancreatic β-cells causes the body not to produce insulin, causing hyperglycemia. On the other hand, hyperglycemic conditions can result in the formation of reactive oxygen species (ROS). An increase in ROS that is not balanced with an increase in endogenous antioxidant enzymes, for example, SOD, as a body defense mechanism, can cause oxidative stress and can exacerbate damage to pancreatic β-cells. In the AAC-treated group, the pattern and percentage distribution of the islets of Langerhans were similar to that of diabetic ones. The morphology of the islets of Langerhans, which are slightly enlarged, indicates a moderate increase in the regeneration of the islet β-cells.

Our study shows that in DM, administration of a combined AAC mixture in a relatively short period somewhat regenerates the islets, but cannot significantly slow down pancreatic damage. With long-term use, better results can be expected, which we have planned for the future. It is known that pancreatic Langerhans β-cells are a group of stable cells that can proliferate throughout their life to synthesize insulin again.[47]

In conclusion, the combined action of substances included in AAC in our experiments had a hypoglycemic effect. More importantly, the present results were consistent with the histopathological findings. Interestingly, this study demonstrated significantly improved hematological changes in AAC-treated diabetic animals. This study highlights the potential of AAC as a therapeutic agent for managing T1DM and its associated complications.

Competing Interests

The authors declare that they have no competing interests.

References

1. Lee M, Saver JL, Hong KS, Song S, Chang KH, Ovbiagele B. Effect of pre-diabetes on future risk of stroke: meta-analysis. BMJ. 2012 Jun 7;344:e3564. doi: 10.1136/bmj.e3564.
2. Galiero R, Caturano A, Vetrano E, Beccia D, Brin C, Alfano M, et al. Peripheral Neuropathy in Diabetes Mellitus: Pathogenetic Mechanisms and Diagnostic Options. Int J Mol Sci. 2023 Feb 10;24(4):3554. doi: 10.3390/ijms24043554.
3. Lim AKh. Diabetic nephropathy - complications and treatment. Int J Nephrol Renovasc Dis. 2014 Oct 15;7:361-81. doi: 10.2147/IJNRD.S40172.
4. Nentwich MM, Ulbig MW. Diabetic retinopathy - ocular complications of diabetes mellitus. World J Diabetes. 2015 Apr 15;6(3):489-99. doi: 10.4239/wjd.v6.i3.489.
5. Vileikyte L. Diabetic foot ulcers: a quality of life issue. Diabetes Metab Res Rev. 2001 Jul-Aug;17(4):246-9. doi: 10.1002/dmrr.216.
6. Pitt DF. Management of gangrene in diabetic extremities. Can J Surg. 1984 Jul;27(4):386-9.
7. Leon BM, Maddox TM. Diabetes and cardiovascular disease: Epidemiology, biological mechanisms, treatment recommendations and future research. World J Diabetes. 2015 Oct 10;6(13):1246-58. doi: 10.4239/wjd.v6.i13.1246.
8. Lopes-Virella MF, Klein RL, Lyons TJ, Stevenson HC, Witztum JL. Glycosylation of low-density lipoprotein enhances cholesteryl ester synthesis in human monocyte-derived macrophages. Diabetes. 1988 May;37(5):550-7. doi: 10.2337/diab.37.5.550.
9. Ciepiela O. Old and new insights into the diagnosis of hereditary spherocytosis. Ann Transl Med. 2018 Sep;6(17):339. doi: 10.21037/atm.2018.07.35.
10. Foulis AK, McGill M, Farquharson MA. Insulitis in type 1 (insulin-dependent) diabetes mellitus in man--macrophages, lymphocytes, and interferon-gamma containing cells. J Pathol. 1991 Oct;165(2):97-103. doi: 10.1002/path.1711650203.
11. Danaei G, Finucane MM, Lu Y, Singh GM, Cowan MJ, Paciorek CJ, et al.; Global Burden of Metabolic Risk Factors of Chronic Diseases Collaborating Group (Blood Glucose). National, regional, and global trends in fasting plasma glucose and diabetes prevalence since 1980: systematic analysis of health examination surveys and epidemiological studies with 370 country-years and 2·7 million participants. Lancet. 2011 Jul 2;378(9785):31-40. doi: 10.1016/S0140-6736(11)60679-X.
12. Meier JJ, Bhushan A, Butler AE, Rizza RA, Butler PC. Sustained beta cell apoptosis in patients with long-standing type 1 diabetes: indirect evidence for islet regeneration? Diabetologia. 2005 Nov;48(11):2221-8. doi: 10.1007/s00125-005-1949-2.
13. Bonner-Weir S, Sharma A. Are there pancreatic progenitor cells from which new islets form after birth? Nat Clin Pract Endocrinol Metab. 2006 May;2(5):240-1. doi: 10.1038/ncpendmet0186.
14. Tian J, Dang HN, Yong J, Chui WS, Dizon MP, Yaw CK, Kaufman DL. Oral treatment with γ-aminobutyric acid improves glucose tolerance and insulin sensitivity by inhibiting inflammation in high fat diet-fed mice. PLoS One. 2011;6(9):e25338. doi: 10.1371/journal.pone.0025338.
15. Tian J, Lu Y, Zhang H, Chau CH, Dang HN, Kaufman DL. Gamma-aminobutyric acid inhibits T cell autoimmunity and the development of inflammatory responses in a mouse type 1 diabetes model. J Immunol. 2004 Oct 15;173(8):5298-304. doi: 10.4049/jimmunol.173.8.5298.
16. Soltani N, Qiu H, Aleksic M, Glinka Y, Zhao F, Liu R, Li Y, Zhang N, Chakrabarti R, Ng T, Jin T, Zhang H, Lu WY, Feng ZP, Prud'homme GJ, Wang Q. GABA exerts protective and regenerative effects on islet beta cells and reverses diabetes. Proc Natl Acad Sci U S A. 2011 Jul 12;108(28):11692-7. doi: 10.1073/pnas.1102715108.
17. Nealon RS, Sukala WR. The Effect of 28 Days of Beta-alanine Supplementation on Exercise Capacity and Insulin Sensitivity in Individuals with Type 2 Diabetes Mellitus: A Randomised, Double-blind and Placebo-controlled Pilot Trial. Sport Nutr Ther. 2016;1:1-7. doi: 10.4172/2473-6449.1000111.
18. Torres-Santiago L, Mauras N, Hossain J, Weltman AL, Darmaun D. Does oral glutamine improve insulin sensitivity in adolescents with type 1 diabetes? Nutrition. 2017 Feb;34:1-6. doi: 10.1016/j.nut.2016.09.003.
19. Samocha-Bonet D, Wong O, Synnott EL, Piyaratna N,

Douglas A, Gribble FM, Holst JJ, Chisholm DJ, Greenfield JR. Glutamine reduces postprandial glycemia and augments the glucagon-like peptide-1 response in type 2 diabetes patients. J Nutr. 2011 Jul;141(7):1233-8. doi: 10.3945/jn.111.139824.
20. Qume M, Fowler LJ. Effect of chronic treatment with the GABA transaminase inhibitors gamma-vinyl GABA and ethanolamine O-sulphate on the in vitro GABA release from rat hippocampus. Br J Pharmacol. 1997 Oct;122(3):539-45. doi: 10.1038/sj.bjp.0701383.
21. Kamalyan RG, Khachatryan NKh, Vardanyan AG, Taroyan SQ, Eritsyan IN. The influence of glutamine and ethanolamine-o-sulphate on neuroactive amino acids content in the rat organs in norm and with experimental streptozotocine diabetes. Biological Journal of Armenia. 2015;3(67):61-6.
22. Khachatryan HS, Sahakyan IK, Tumasyan NV, Kocharyan NV. Effects of ethanol and the amino acids mixture on pathophysiological processes in rats with alloxan-induced diabetes. Biological Journal of Armenia. 2021;3(73):102-8.
23. Khachatryan RS, Khachatryan NKh, Kamalyan RG. Antidiabetic effect of a complex of neuroactive amino acids in an alloxan diabetes model. Biological Journal of Armenia. 2019;4(71):66-9.
24. Arora S, Ojha S, Vohora D. Characterisation of streptozotocin induced diabetes mellitus in swiss albino mice. Global Journal of Pharmacology. 2009;3:81-4.
25. Furman BL. Streptozotocin-Induced Diabetic Models in Mice and Rats. Curr Protoc. 2021 Apr;1(4):e78. doi: 10.1002/cpz1.78. PMID: 33905609.
26. Hewitt R. GIEMSA PREPARATION FOR STAINING BLOOD FILMS. Science. 1937 Dec 10;86(2241):548. doi: 10.1126/science.86.2241.548. PMID: 17794484.
27. Spector DL, Goldman RD. In: Basic Methods in Microscopy. Protocols and Concepts from Cells: A Laboratory Manual Cold Spring Harbor Laboratory Press, Cold Spring Harbor, NY: USA; 2006.
28. Bau-Gaudreault L, Grimes C. Evaluation of erythrocyte morphology and prevalence of poikilocytes in peripheral blood of sick domestic ferrets (*Mustela putorius furo*). Journal of Exotic Pet Medicine. 2019;31:86-90. doi: 10.1053/j.jepm.2019.07.014.
29. Owen JS, Brown DJ, Harry DS, McIntyre N, Beaven GH, Isenberg H, Gratzer WB. Erythrocyte echinocytosis in liver disease. Role of abnormal plasma high density lipoproteins. J Clin Invest. 1985 Dec;76(6):2275-85. doi: 10.1172/JCI112237.
30. Ciepiela O. Old and new insights into the diagnosis of hereditary spherocytosis. Ann Transl Med. 2018 Sep;6(17):339. doi: 10.21037/atm.2018.07.35.
31. Kumaran A, Karunakaran R. In Vitro Antioxidant Activities of Methanol Extracts of Five Phyllanthus Species from India. LWT-Food Science and Technology. 2007;40:344-52. doi: 10.1016/j.lwt.2005.09.011.
32. Kim JS, Ju JB, Choi CW, Kim SC. Hypoglycemic and Antihyperglycemic Effect of Four Korean Medicinal Plants in Alloxan Induced Diabetic Rats. American Journal of Biochemistry and Biotechnology. 2006;2(4):154-60. doi:10.3844/ajbbsp.2006.154.160.
33. Adeghate E, Ponery AS. GABA in the endocrine pancreas: cellular localization and function in normal and diabetic rats. Tissue Cell. 2002 Feb;34(1):1-6. doi: 10.1054/tice.2002.0217.
34. Harsunen MH, Puff R, D'Orlando O, Giannopoulou E, Lachmann L, Beyerlein A, von Meyer A, Ziegler AG. Reduced blood leukocyte and neutrophil numbers in the pathogenesis of type 1 diabetes. Horm Metab Res. 2013 Jun;45(6):467-70. doi: 10.1055/s-0032-1331226.
35. Huang J, Xiao Y, Zheng P, Zhou W, Wang Y, Huang G, Xu A, Zhou Z. Distinct neutrophil counts and functions in newly diagnosed type 1 diabetes, latent autoimmune diabetes in adults, and type 2 diabetes. Diabetes Metab Res Rev. 2019 Jan;35(1):e3064. doi: 10.1002/dmrr.3064.
36. Berezin A. Neutrophil extracellular traps: The core player in vascular complications of diabetes mellitus. Diabetes Metab Syndr. 2019 Sep-Oct;13(5):3017-3023. doi: 10.1016/j.dsx.2018.07.010.
37. Ibrahim MSM, Khalil AA, Ali A-SAA. Neutrophils-to-lymphocytes ratio in children with acute heart failure. Egyptian Journal of Hospital Medicine. 2020;81:1878-83. doi: 10.21608/ejhm.2020.121015.
38. Singh S, Usha, Singh G, Agrawal NK, Singh RG, Kumar SB. Prevalence of Autoantibodies and HLA DR, DQ in Type 1 Diabetes Mellitus. J Clin Diagn Res. 2016 Jul;10(7):EC09-13. doi: 10.7860/JCDR/2016/18657.8163.
39. Costantini C, Micheletti A, Calzetti F, Perbellini O, Pizzolo G, Cassatella MA. Neutrophil activation and survival are modulated by interaction with NK cells. Int Immunol. 2010 Oct;22(10):827-38. doi: 10.1093/intimm/dxq434.
40. Gonzalez LK, Malhotra S, Levine M, Jacobson-Dickman E. Leukemoid Reaction in a Pediatric Patient With Diabetic Ketoacidosis. Pediatr Emerg Care. 2017 Aug;33(8):e27-e29. doi: 10.1097/PEC.0000000000000558.
41. Abdel N, Hamed M. Alterations in hematological parameters: could it be a marker in diabetes mellitus? BAOJ Diabetes. 2016;2:1-9.
42. Angelousi A, Larger E. Anaemia, a common but often unrecognized risk in diabetic patients: a review. Diabetes Metab. 2015 Feb;41(1):18-27. doi: 10.1016/j.diabet.2014.06.001.
43. Kennedy L, Baynes JW. Non-enzymatic glycosylation and the chronic complications of diabetes: an overview. Diabetologia. 1984 Feb;26(2):93-8. doi: 10.1007/BF00281113.
44. Koga T, Moro K, Terao J. Protective effect of a vitamin E analog, phosphatidylchromanol, against oxidative hemolysis of human erythrocytes. Lipids. 1998 Jun;33(6):589-95. doi: 10.1007/s11745-998-0244-4.
45. Wang T, Wen XJ, Mei XB, Wang QQ, He Q, Zheng JM, Zhao J, Xiao L, Zhang LM. Lipid peroxidation is another potential mechanism besides pore-formation underlying hemolysis of tentacle extract from the jellyfish Cyanea capillata. Mar Drugs. 2013 Jan 9;11(1):67-80. doi: 10.3390/md11010067.
46. Szkudelski T. The mechanism of alloxan and streptozotocin action in B cells of the rat pancreas. Physiol Res. 2001;50(6):537-46. PMID: 11829314.
47. McGavin MD, Zachary JF. Basis of Veterinary Disease. 4th ed. St. Louis: Mosby-Elsevier; 2007.

***Corresponding author**: Narine Tumasyan, PhD. Group of Histochemistry and Functional Morphology, H. Buniatian Institute of Biochemistry, NAS RA, Yerevan, Armenia. E-mail: tumasyannarine@gmail.com*

International Journal of Biomedicine 15(3) (2025) 590-593
http://dx.doi.org/10.21103/Article15(3)_CR1

CASE REPORT

INTERNATIONAL JOURNAL OF BIOMEDICINE

Pediatric Tumefactive Multiple Sclerosis Case Report and Literature Review: A Saudi Experience

Muhannad Alanazi[1*], Raed AlRuwaili[2]

[1]*Department of Internal Medicine, Division of Radiology, College of Medicine, Jouf University, Sakaka, Saudi Arabia*
[2]*Department of Internal Medicine, College of Medicine, Northern Border University, Arar, Saudi Arabia*

Abstract

Tumefactive demyelinating lesions (TDLs) are rare, mass-like lesions that present a significant diagnostic challenge, often mimicking brain tumors on magnetic resonance imaging (MRI). This case report describes a 9-year-old male who presented with progressive neurological symptoms, including persistent headaches, ataxia, and dysarthria. MRI findings raised concerns for both demyelinating and neoplastic processes, but a biopsy confirmed the diagnosis of tumefactive multiple sclerosis (TMS). The patient was successfully treated with high-dose corticosteroids, resulting in marked clinical improvement. This case emphasizes the importance of differentiating TDLs from neoplasms, particularly in pediatric patients, and highlights the role of biopsy and advanced imaging techniques in achieving an accurate diagnosis. Long-term follow-up with disease-modifying therapies is crucial to prevent relapse and progression.(**International Journal of Biomedicine. 2025;15(3):590-593.**)

Keywords: tumefactive demyelinating lesions • multiple sclerosis • corticosteroid therapy • brain tumor

For citation: Alanazi M, Raed AlRuwaili R. Pediatric Tumefactive Multiple Sclerosis Case Report and Literatures Review: A Saudi Experience. International Journal of Biomedicine. 2025;15(3):590-593. doi:10.21103/Article15(3)_CR1

Abbreviations

CNS, central nervous system; **DWI**, diffusion-weighted imaging; **FLAIR**, fluid-attenuated inversion recovery; **MS**, multiple sclerosis; **PWI**, perfusion-weighted imaging; **PLEX**, plasma exchange; **RRMS**, relapsing-remitting multiple sclerosis; **TDLs**, tumefactive demyelinating lesions; **TMS**, tumefactive multiple sclerosis.

Introduction

Tumefactive demyelinating lesions (TDLs) are a distinct and diagnostically challenging variant of demyelinating diseases within the multiple sclerosis (MS) spectrum. Tumefactive demyelinating lesions typically present as large, mass-like lesions that mimic neoplasms on magnetic resonance imaging (MRI) due to their size, ring enhancement, and associated edema.[1,2] These lesions are relatively uncommon, with an estimated prevalence of 1–3 per 1,000 MS patients. Still, they pose significant diagnostic challenges due to their resemblance to brain tumors such as gliomas and central nervous system (CNS) lymphomas.[3,4]

Tumefactive demyelinating lesions are often mistaken for tumors because of their radiological appearance and mass effect, making it essential to differentiate them from neoplasms to avoid inappropriate treatments.[5] Although more common in adults, pediatric cases of TDLs are particularly rare, with limited literature available on their clinical presentation and management.[1]

This case report aims to provide insights into the diagnostic process, treatment, and follow-up of a child with tumefactive multiple sclerosis.

***Corresponding author**: Muhannad Faleh Alanazi, Department of Internal Medicine, Division of Radiology, College of Medicine, Jouf University, Sakaka, Saudi Arabia. E-mail: mfra642@hotmail.com*

Advanced imaging techniques, such as diffusion-weighted imaging (DWI) and perfusion-weighted imaging (PWI), have been increasingly employed to distinguish TDLs from neoplasms. Yet, biopsy remains the gold standard for definitive diagnosis.[6] Treatment typically involves high-dose corticosteroids, and in cases refractory to corticosteroids, immunosuppressive therapies such as plasma exchange (PLEX) or rituximab may be considered.[7,8]

This case report presents a 9-year-old male diagnosed with a TDL, highlighting the clinical and radiological complexities involved in distinguishing it from neoplastic lesions and discussing the role of biopsy and tailored therapy in ensuring a favorable outcome.

Case Presentation

A 9-year-old male with no significant medical history presented to the neurology outpatient clinic with a two-month history of progressively worsening neurological symptoms. The patient's symptoms included persistent headaches, ataxia, and dysarthria. His parents reported that the headaches had increased in intensity over the past few weeks, becoming debilitating. There was no history of trauma, infection, or systemic illness. His family history was negative for neurological or autoimmune diseases, including multiple sclerosis or hereditary conditions.

Clinical Findings and Investigations

On neurological examination, the patient exhibited: 1) Ataxia: A wide-based, unsteady gait consistent with cerebellar dysfunction, 2) Dysarthria: Speech was slow and slurred, indicating impaired control of speech muscles, 3) Cranial Nerves: The cranial nerve examination was normal, with no evidence of optic neuritis, diplopia, or facial asymmetry, 4) Motor and Sensory Systems: Muscle strength was normal in all four limbs, and no sensory deficits were noted, and 5) Reflexes: Deep tendon reflexes were brisk but symmetrical, with no clonus or abnormal plantar responses. No signs of meningeal irritation were observed. The initial blood workup, including a complete blood count, metabolic panel, and inflammatory markers (C-reactive protein, erythrocyte sedimentation rate), was within normal limits.

Neuroimaging was pursued due to the progressive nature of the patient's symptoms and the absence of systemic signs of infection or other causes. Magnetic resonance imaging (MRI) of the brain revealed two large intra-axial lesions in the left cerebral hemisphere, primarily affecting the white matter. T2-weighted imaging (T2WI) showed that the lesions are hyperintense, suggesting the presence of edema or demyelination. Fluid-attenuated inversion recovery (FLAIR) imaging revealed that the lesions exhibit partial central suppression, indicative of active inflammation and demyelination. Gadolinium-enhanced T1-weighted imaging showed that faint, incomplete marginal enhancement was observed, a pattern characteristic of demyelinating processes where there is a partial breakdown of the blood-brain barrier. Diffusion-weighted imaging (DWI) revealed that the lesions exhibit areas of mild diffusion restriction, which can suggest tumefactive demyelination or, less likely, a neoplastic process. As a mass effect, the lesions caused a mild rightward shift of the midline structures, contributing to the patient's headaches and increased intracranial pressure (Figure 1).

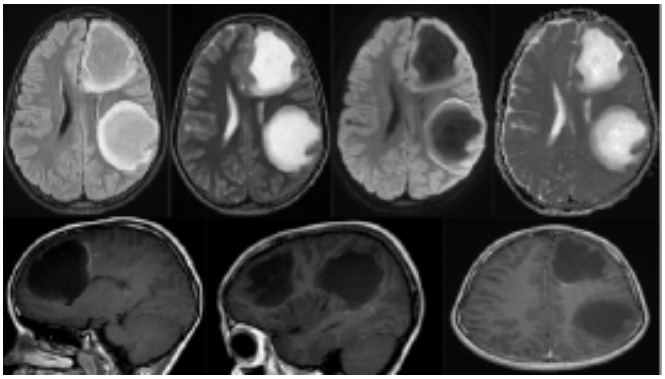

Figure 1. *A 9-year-old boy presented with headache, ataxia, and dysarthria for 2 months. Two large intra-axial, mildly expansile mass-like abnormalities centered within the left cerebral hemisphere white matter regions, with relative preservation of the overlying cortex. Imaging: T2WI hyperintensity with partial central FLAIR suppression, faint incomplete marginal enhancement, and marginal curvilinear areas of mild diffusion restriction causing mild rightward midline shift, mild effacement of left lateral ventricle, and left hemispheric sulcal effacement. The degree of mass effect is disproportionate to the lesion's size. No optic nerves or spinal cord lesions. The conclusive diagnosis is tumefactive demyelination lesions.*

Differential Diagnosis

Given the patient's clinical presentation and imaging findings, the differential diagnosis included: 1) Tumefactive Demyelinating Lesions (TDLs): These are large demyelinating plaques often mistaken for neoplasms due to their size and mass effect, 2) Pediatric Low-Grade Gliomas: Gliomas are more common in children but typically show more robust and homogeneous enhancement on imaging, and 3) Primary CNS Lymphoma: Although rare in children, lymphoma can present with ring-enhancing lesions, but these lesions tend to have more pronounced diffusion restriction. Given the uncertainty of the imaging findings and the potential for serious outcomes, a stereotactic biopsy of the larger lesion was performed to establish a definitive diagnosis.

Histopathological Findings

Histopathological analysis confirmed extensive demyelination with prominent loss of myelin and relative preservation of axons. Perivascular lymphocytic infiltration was observed, consistent with an inflammatory demyelinating process. There was no evidence of neoplastic cells or infection, ruling out both neoplastic and infectious etiologies. The final pathology report confirmed the diagnosis of a tumefactive demyelinating lesion consistent with tumefactive multiple sclerosis.

Treatment and Clinical Course

Following the confirmed diagnosis of TDL, the patient was treated with high-dose intravenous methylprednisolone (1,000 mg/day) for five days. This was followed by a tapering

course of oral corticosteroids over the next several weeks. The patient showed significant clinical improvement, with a marked reduction in headache severity and gradual resolution of ataxia and dysarthria.

The patient was discharged with a plan for close neurological follow-up and regular MRI scans to monitor for lesion progression or the formation of new lesions. Long-term management will likely include disease-modifying therapies to prevent future relapses, and the family was counseled on the importance of recognizing early signs of relapse.

Discussion

The exact pathophysiology of TDLs remains under investigation, though they are generally considered part of the MS spectrum. Studies have demonstrated a shared underlying autoimmune mechanism between TDLs and other demyelinating disorders, such as RRMS and neuromyelitis optica spectrum disorder (NMOSD).[2,9] Demyelination in TDLs is accompanied by perivascular lymphocytic infiltration and axonal preservation, as seen in this case. This suggests that the immune system selectively targets myelin sheaths without extensive neuronal damage, a hallmark of inflammatory demyelinating diseases.[8] There is growing evidence that environmental factors, including viral infections such as Epstein-Barr virus (EBV), and genetic predisposition may contribute to the development of TDLs. The association of TDLs with certain human leukocyte antigen (HLA) class II alleles, such as HLA-DRB1*15, supports the role of genetic susceptibility in the pathogenesis of these lesions.[10,11]

Tumefactive demyelinating lesions are a rare but important consideration in pediatric patients with mass-like brain lesions. The radiological appearance of TDLs, particularly their large size, ring enhancement, and mass effect, often leads to diagnostic confusion with neoplastic processes such as gliomas or CNS lymphomas.[4,6] This case highlights the importance of a thorough diagnostic workup, including advanced imaging techniques and, when necessary, histopathological confirmation through biopsy.

While advanced MRI techniques such as DWI and perfusion-weighted imaging (PWI) can help differentiate TDLs from tumors, the overlap in imaging characteristics often necessitates a biopsy for definitive diagnosis. In this case, the biopsy findings of demyelination and lymphocytic infiltration confirmed the diagnosis of a tumefactive demyelinating lesion, effectively ruling out malignancy and guiding appropriate treatment.[2,12-14]

Tumefactive demyelinating lesions are thought to be part of the MS spectrum, with their pathophysiology involving acute inflammatory demyelination. The presence of perivascular lymphocytic infiltration on histopathology suggests an autoimmune process similar to that seen in relapsing-remitting MS (RRMS).[9] Corticosteroid therapy is the mainstay of treatment for TDLs, with most patients responding well to high-dose steroids, as seen in this case.[8] For patients who do not respond to corticosteroids, additional immunosuppressive therapies such as plasma exchange (PLEX) or rituximab may be necessary.[7]

The prognosis for patients with TDLs varies, with many experiencing a monophasic course and complete resolution of symptoms following treatment. However, some patients may go on to develop relapsing-remitting multiple sclerosis (RRMS) or experience recurrent episodes of tumefactive lesions.[15,16] Studies suggest that up to 30% of patients with tumefactive demyelinating lesions may progress to RRMS, emphasizing the importance of long-term follow-up and early intervention with disease-modifying therapies.[5,15] In this case, the patient responded well to corticosteroid therapy, with resolution of his acute neurological symptoms. However, continued monitoring and preventive measures, such as immunomodulatory treatments, will be crucial to prevent future relapses and long-term neurological decline.

While conventional MRI remains the primary diagnostic tool for detecting CNS demyelination, additional advanced imaging modalities can be used to further differentiate TDLs from other lesions. Dynamic susceptibility contrast (DSC) MRI can help differentiate demyelinating lesions from high-grade gliomas by evaluating the relative cerebral blood volume (rCBV). Tumefactive demyelinating lesions typically have lower rCBV compared to high-grade tumors.[6] Similarly, diffusion tensor imaging (DTI) can provide information about white matter tract disruption, which is more pronounced in tumors than in demyelinating lesions.[14,17]

Magnetic resonance spectroscopy is another useful tool for distinguishing TDLs from neoplasms by analyzing the biochemical composition of the lesion. A lower choline/creatine ratio is more commonly seen in demyelinating lesions, whereas a higher ratio is characteristic of neoplastic processes. [12-14,18] Despite these advancements, histopathological examination remains the gold standard for confirming the diagnosis, particularly when the imaging findings are ambiguous.

Corticosteroids remain the first-line treatment for TDLs, as they reduce inflammation and accelerate lesion resolution. This patient's favorable response to intravenous methylprednisolone aligns with the literature, where corticosteroid therapy has been shown to improve clinical outcomes in most cases.[13-16] However, in cases where corticosteroids are insufficient, plasma exchange (PLEX) and other immunosuppressive therapies, such as rituximab or cyclophosphamide, have been successfully used.[7,19] Using disease-modifying therapies, such as interferon-beta or glatiramer acetate, may also reduce the likelihood of future relapses.[12-16]

The long-term prognosis for TDLs is generally favorable, especially in patients with a monophasic disease course. However, in patients who transition to RRMS or experience recurrent tumefactive episodes, the risk of accumulating disability increases.[5,14] This highlights the importance of early diagnosis, appropriate treatment, and long-term follow-up to monitor potential relapses and initiate preventive therapies when necessary.[14,15]

Conclusion

Our case demonstrates the diagnostic challenges of differentiating tumefactive demyelinating lesions from brain tumors, especially in pediatric patients. Advanced imaging

techniques and histopathological confirmation are essential for accurate diagnosis. Early and aggressive treatment with corticosteroids can lead to significant clinical improvement, as seen in this case. Long-term follow-up with regular MRI scans and the use of disease-modifying therapies will be crucial in preventing future relapses and maintaining the patient's neurological health.

Ethical Considerations

The patient's legal guardians gave informed consent for publishing the case report, including images and other clinical information, except individual details identifying the patient.

Competing Interests

The authors declare that they have no competing interests.

References

1. Algahtani H, Shirah B, Alassiri A. Tumefactive demyelinating lesions: A comprehensive review. Mult Scler Relat Disord. 2017 May;14:72-79. doi: 10.1016/j.msard.2017.04.003. Epub 2017 Apr 9. PMID: 28619436.
2. Lucchinetti CF, Gavrilova RH, Metz I, Parisi JE, Scheithauer BW, Weigand S, Thomsen K, Mandrekar J, Altintas A, Erickson BJ, König F, Giannini C, Lassmann H, Linbo L, Pittock SJ, Brück W. Clinical and radiographic spectrum of pathologically confirmed tumefactive multiple sclerosis. Brain. 2008 Jul;131(Pt 7):1759-75. doi: 10.1093/brain/awn098.
3. Höftberger R, Lassmann H. Tumefactive demyelination in multiple sclerosis and other demyelinating diseases. Handbook of Clinical Neurology. 2017;145:417-432. doi: 10.1016/B978-0-12-802395-2.00037-5
4. Suh CH, Kim HS, Jung SC, Choi CG. Tumefactive demyelinating lesions: The usefulness of conventional MRI features in differentiating from glioma and primary central nervous system lymphoma. European Radiology. 2018;28(4):1396–1405. doi: 10.1007/s00330-017-5094-1
5. Tremblay MÉ, Lecours C, Samson L, Sánchez-Sánchez SM, Matarazzo V. Tumefactive demyelinating lesions: Review of pathophysiological mechanisms and role of glial cells. Progress in Neurobiology. 2017;153:153-172. doi: 10.1016/j.pneurobio.2017.06.007
6. Hiremath SB, Saisooraj S, Mahadevan A, Yadav R, Narayan S. Tumefactive demyelination versus glioma: Can MR perfusion help differentiate? Journal of Neuroradiology. 2017;44(6):387-394. doi: 10.1016/j.neurad.2017.03.001
7. Magaña SM, Keegan BM, Weinshenker BG, Erickson BJ, Pittock SJ, Lennon VA, Rodriguez M, Thomsen K, Weigand S, Mandrekar J, Linbo L, Lucchinetti CF. Beneficial plasma exchange response in central nervous system inflammatory demyelination. Arch Neurol. 2011 Jul;68(7):870-8. doi: 10.1001/archneurol.2011.34. Epub 2011 Mar 14. PMID: 21403003; PMCID: PMC3134547.
8. Brod SA, Brod MA, Weinstein R. Diagnosis and treatment of tumefactive multiple sclerosis. Journal of Clinical Neuroscience. 2019;66:90-96. doi:10.1016/j.jocn.2019.03.006
9. van Langelaar J, Rijvers L, Smolders J, van Luijn MM. B and T Cells Driving Multiple Sclerosis: Identity, Mechanisms and Potential Triggers. Front Immunol. 2020 May 8;11:760. doi: 10.3389/fimmu.2020.00760. PMID: 32457742; PMCID: PMC7225320.
10. Parnell GP, Booth DR. The genetics of multiple sclerosis. Multiple Sclerosis and Related Disorders. 2017;13:18-25. doi: 10.1016/j.msard.2017.01.013
11. De Silvestri A, Capittini C, Mallucci G, Bergamaschi R, Rebuffi C, Pasi A, Martinetti M, Tinelli C. The Involvement of HLA Class II Alleles in Multiple Sclerosis: A Systematic Review with Meta-analysis. Dis Markers. 2019 Nov 6;2019:1409069. doi: 10.1155/2019/1409069. PMID: 31781296; PMCID: PMC6875418.
12. Villarreal JV, Abraham MJ, Acevedo JAG, Rai PK, Thottempudi N, Fang X, Gogia B. Tumefactive multiple sclerosis (TMS): A case series of this challenging variant of MS. Mult Scler Relat Disord. 2021 Feb;48:102699. doi: 10.1016/j.msard.2020.102699. Epub 2020 Dec 26. PMID: 33373797.
13. Fereidan-Esfahani M, Decker PA, Weigand SD, Lopez Chiriboga AS, Flanagan EP, Tillema JM, Lucchinetti CF, Eckel-Passow JE, Tobin WO. Defining the natural history of tumefactive demyelination: A retrospective cohort of 257 patients. Ann Clin Transl Neurol. 2023 Sep;10(9):1544-1555. doi: 10.1002/acn3.51844. Epub 2023 Jul 13. PMID: 37443413; PMCID: PMC10502639.
14. Ongphichetmetha T, Aungsumart S, Siritho S, Apiwattanakul M, Tanboon J, Rattanathamsakul N, Prayoonwiwat N, Jitprapaikulsan J. Tumefactive demyelinating lesions: a retrospective cohort study in Thailand. Sci Rep. 2024 Jan 16;14(1):1426. doi: 10.1038/s41598-024-52048-w. Erratum in: Sci Rep. 2024 Mar 4;14(1):5332. doi: 10.1038/s41598-024-56016-2. PMID: 38228919; PMCID: PMC10791607.
15. Codjia P, Zivadinov R, Gandhi S, Durfee J, Weinstock-Guttman B. Tumefactive MS and risk of conversion to relapsing multiple sclerosis. Journal of Neuroimmunology.2019;332:132-138. doi:10.1016/j.jneuroim.2019.04.004
16. Altintas A, Petek B, Isik N, Terzi M, Bolukbasi F, Tavsanli M, Saip S, Boz C, Aydin T, Arici-Duz O, Ozer F, Siva A. Clinical and radiological characteristics of tumefactive demyelinating lesions: follow-up study. Mult Scler. 2012 Oct;18(10):1448-53. doi: 10.1177/1352458512438237. Epub 2012 Mar 14. PMID: 22419670.
17. Giussani C, Falini A, Cadioli M, Marotta G. Diffusion tensor MRI for primary brain tumor characterization. Neurosurgical Review. 2010;33(3):251-259. doi:10.1007/s10143-010-0267-1
18. Palanichamy A, Chakravarti A. Metabolic and diffusion MRI features in tumor vs. non-tumor lesions: Evaluation of diagnostic tools. Neuroradiology. 2017;59(5):487-493. doi: 10.1007/s00234-017-1824-3
19. Sato DK, Nakashima I, Takahashi T. Rebound syndrome following discontinuation of fingolimod therapy in patients with multiple sclerosis. Neurology. 2018;90(3):e157-e163. doi: 10.1212/WNL.0000000000004853

International Journal of Biomedicine 15(3) (2025) 594-597
http://dx.doi.org/10.21103/Article15(3)_CR2

CASE REPORT

INTERNATIONAL JOURNAL OF BIOMEDICINE

Unwinding the Spine: Advanced Diagnostic and Surgical Strategies for Lumbar Dumbbell Schwannoma

Flaka Pasha[1,2], Lavdim Ymeri[2,3*], Berat Elshani[3], Blana Krasniqi[4], Art Uka[5]

[1]*Department of Pharmacology and Toxicology and Clinical Pharmacology, Faculty of Medicine, University of Prishtina "Hasan Prishtina," Prishtina, Kosovo*
[2]*Clinic of Radiology, University Clinical Center of Kosovo, Prishtina, Kosovo*
[3]*Alma Mater Europaea Campus College "Rezonanca," Prishtina, Kosovo*
[4]*Department of General Medicine, Tirana University of Medicine, Tirana, Albania*
[5]*Faculty of Medicine, University of Prishtina "Hasan Prishtina," Prishtina, Kosovo*

Abstract

We present a rare case of a lumbar dumbbell-shaped schwannoma in a 36-year-old male with persistent lumbar pain and paresthesia. MRI revealed a contrast-enhancing mass at L3–L4 compressing the right L3 nerve root. A combined posterior and retroperitoneal approach enabled complete resection. Histopathology confirmed schwannoma with Antoni A/B areas and S-100 positivity. Postoperatively, the patient had full symptom resolution and no recurrence at three months. This case highlights the importance of timely diagnosis, imaging, and surgical resection for symptom relief and definitive diagnosis in managing lumbar dumbbell schwannomas, with adjunct therapies considered for incomplete or inoperable cases. (**International Journal of Biomedicine. 2025;15(3):594-597.**)

Keywords: lumbar dumbbell schwannoma • spinal tumor • MRI • surgical resection • postoperative management

For citation: Pasha F, Ymeri L, Elshani B, Krasniqi B, Uka A. Unwinding the Spine: Advanced Diagnostic and Surgical Strategies for Lumbar Dumbbell Schwannoma. International Journal of Biomedicine. 2025;15(3):594-597. doi:10.21103/Article15(3)_CR2

Introduction

Schwannomas are nerve sheath tumors,[1] accounting for 25–30% of all primary spinal tumors,[2] with a predilection for the cervical and thoracic regions. Lumbar schwannomas are relatively rare, especially those presented in a "dumbbell" shape, extending through intervertebral foramen, with both intraspinal and paraspinal components.[3] Depending on the etiology, schwannomas can be either sporadic or congenital, as a manifestation of neurofibromatosis.[4]

Due to their anatomical location and neurologic symptoms, lumbar dumbbell schwannomas pose significant diagnostic and therapeutic challenges.[5] Lumbar dumbbell schwannomas may compress adjacent neural structures, causing radiculopathy, motor impairment, and low back pain, depending on the level of the lesion.[6] Back pain, numbness in the lower extremities, weakness, tingling, clumsiness, difficulty walking, or even urinary incontinence are the main symptoms of lumbar dumbbell schwannoma.[7] Advances in imaging have greatly improved diagnostic accuracy. Surgical resection remains the cornerstone of treatment for schwannomas.[8] However, this surgery is highly challenging due to the tumor's proximity to critical neural and vascular structures, requiring laminectomy to access the tumor and spinal fusion to maintain spinal stability.[9]

We present a rare case of a lumbar dumbbell schwannoma, its diagnostic approach, surgical management, and clinical outcomes, underscoring the importance of multidisciplinary collaboration in the proper management of lumbar spinal tumors. Clinical manifestations were assessed by a comprehensive neurological examination. Particular attention was paid to identifying signs indicating compression of nerve roots or spinal cord damage. Preoperative magnetic resonance imaging (MRI)

***Corresponding author**: Dr. Lavdim Ymeri: lavdimymeri1@gmail.com*

with detailed visualization and definition of the boundaries of the intradural and extraforaminal components was performed to assess the size, location, and extent of the schwannoma. Computed tomography was used to assess bone involvement and the relationship of the tumor to adjacent structures.

Surgical resection was performed using a microsurgical approach, including posterior laminectomy for intradural access and extraforaminal decompression for the paraspinal component. Intraoperative monitoring ensured the safety of both neural and vascular functions. In the postoperative period, the patient was closely monitored for neurological changes and underwent a course of pain relief and rehabilitation. Control MRI was performed after 3, 6, and 12 months to assess relapses or complications. Clinical outcomes were evaluated through neurological exams, and patient pain, mobility, and quality of life were measured using the Visual Analog Scale (VAS) and Japanese Orthopedic Association (JOA) score for neurological function.

Case Presentation

A 36-year-old male, weighing 84 kg with a height of 176 cm (BMI=27.1 kg/m²), presented with a six-month moderate right lumbar pain. The patient reported an increase in pain intensity over the past month, reaching a severity of 8/10 on the visual analog scale (VAS). The pain was persistent and resistant to non-steroidal anti-inflammatory therapy. The patient presented with right lumbar paresthesia, which significantly affected his daily activities and quality of life. There was no medical history of surgical interventions. No other significant comorbidities or family history of similar diseases were identified. However, the patient was a heavy smoker, smoking more than 20 cigarettes per day for more than 15 years.

Initial clinical examination, including a detailed neurological examination, revealed decreased sensation in the right lumbar region without motor impairment, while reflexes were preserved bilaterally. To further clarify the source of pain, an abdominal ultrasound was performed. The ultrasound revealed a hypoechoic lesion in the area of the right kidney, which raised concerns about a possible retroperitoneal lesion. Subsequently, a contrast-enhanced MRI of the lumbar spine was performed to more accurately characterize the lesion and its anatomical location. Subsequently, a contrast-enhanced lumbar MRI was performed to characterize the lesion and its anatomical localization.

The MRI results revealed a well-defined, heterogeneously contrast-enhanced mass located at the L3-L4 level on the right. The lesion had a classic dumbbell shape, extending through the intervertebral foramen, with intraspinal and paraspinal components. The intraspinal portion of the tumor caused significant compression of the right L3 nerve root and displacement of adjacent neural structures. The paraspinal component was encapsulated and showed no evidence of infiltration into surrounding tissues. These imaging features were highly suggestive of a schwannoma (Figure 1).

We further performed a computed tomography scan to evaluate bone remodeling, erosion, or widening of the intervertebral foramen, particularly where the tumor exerts pressure. Computed tomography findings are presented in Figure 2.

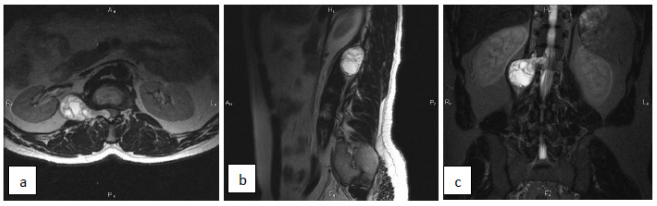

Fig. 1. *On the T1 post-contrast axial (a), sagittal (b), and coronal (c) MRI sequences, we notice a well-demarcated intraspinal mass, with mixed hyperintense contrast enhancement and visible hypointense septations, close to the right neural root, measuring 64x40 mm, suggestive of a lumbar dumbbell schwannoma. The coronal view demonstrates its proximity to the spinal canal, highlighting its spatial relationship to surrounding structures.*

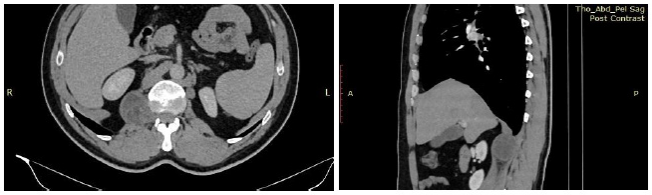

Fig. 2. *A CT scan reveals an isodense circumscribed mass with smooth, well-defined margins that extends through the intervertebral foramen, with both intraspinal and extraforaminal components, displacing right nerve roots. There were no bone erosions or remodeling detected.*

Surgical intervention was considered necessary to alleviate the patient's symptoms while relieving neural compression and achieving the definitive histological diagnosis. The patient was informed regarding the risks and benefits of surgery and agreed to a combined posterior and retroperitoneal surgical approach to ensure complete resection of both intraspinal and paraspinal components of the tumor. The postoperative course was successful. Histopathological examination of the excised area confirmed the diagnosis of schwannoma, characterized by the presence of Antoni A and Antoni B zones, as well as immunohistochemical positivity for S-100 protein. The neoplasm consisted of intertwined bundles of spindle-shaped cells with oval nuclei, eosinophilic cytoplasm, unclear cytoplasmic borders, and intranuclear vacuoles. In the postoperative period, the patient noted significant pain relief and complete disappearance of paresthesia within two weeks following surgery. A follow-up MRI performed three months postoperatively (Figure 3) showed no residual tumor, and the patient returned to work without any neurological deficits.

Fig. 3. *The post-contrast T1-weighted MRI axial, sagittal, and coronal images demonstrate complete resection of a spinal schwannoma. There is no enhancement at the resection site indicating successful tumor removal, with no signs of recurrence. The surrounding tissues, including the nerve roots and spinal cord, appear intact, with no evidence of pathological enhancement.*

This case highlights the importance of a multidisciplinary approach in diagnosing and managing lumbar dumbbell schwannomas. Early and accurate diagnosis of clinical and imaging features, combined with timely surgical intervention, can lead to favorable outcomes, even in complex cases like this one.

Discussion

Schwannomas are often asymptomatic and are discovered incidentally; in such cases, a conservative approach, including observation and regular monitoring, may be appropriate.[10] This strategy includes serial imaging, especially MRI, to detect any progression in tumor size or the emergence of symptoms that would necessitate intervention. This approach is particularly suited for patients with minimal symptoms, or at high surgical risk.[11]

Contrary, the most frequent treatment of lumbar dumbbell schwannomas is surgical resection, which remains the cornerstone for both symptomatic relief and definitive histological diagnosis.[5] Surgical intervention is typically indicated when the tumor exerts significant compression on adjacent neural structures, leading to symptoms such as pain, paresthesia, or neurological deficits. The surgical approach involves posterior laminectomy to access the spinal canal, complemented by anterior decompression if the tumor extends through the intervertebral foramen.[12] In cases with extensive involvement, a combined anterior-posterior approach may be necessary to achieve complete tumor excision. Recently, minimally invasive procedures like microsurgical resection with laminectomy, endoscopic-assisted and robotic-assisted surgeries, offer significant advantages by minimizing muscle dissection, reducing blood loss, and lowering the risk of postoperative complications, due to smaller incisions, reduced tissue trauma, and faster recovery times. Yet, open resection, on the other hand, allows superior visualization and complete tumor removal. Therefore, the choice between a minimally invasive procedure and open surgery depends on the tumor's size, its complexity in relation to the surrounding tissues, and location.

Additionally, radiation therapy plays an adjunctive role, especially in cases where complete surgical resection is not feasible or residual tumor remains postoperatively. Schwannomas are generally radiosensitive, and modalities such as stereotactic radiosurgery offer targeted treatment with minimal impact on surrounding tissues. Radiation therapy is also employed as a primary treatment for inoperable cases or when surgery poses significant risks due to comorbidities.[13]

Lumbar dumbbell schwannomas generally have a favorable prognosis, particularly following complete surgical excision. Recurrence rates are low when resection is complete, underscoring the importance of meticulous surgical planning and execution.[14] The recurrence risk of spinal dumbbell schwannomas is generally low following complete resection, but factors such as incomplete excision, tumor size, and location can influence this risk. Incomplete resection, often due to the tumor's proximity to critical neural or vascular structures, significantly increases the likelihood of recurrence. Larger tumors, particularly those in difficult-to-access areas, also have a higher recurrence rate. To monitor for recurrence, long-term MRI surveillance is essential, with follow-up imaging typically starting at three months' post-surgery, and continuing at six, 12, and 24 months. Annual MRI may be performed thereafter if no recurrence is found. Magnetic resonance imaging (MRI) is preferred for its sensitivity in detecting soft tissue changes. Regular imaging during the first two years is crucial, as this is when the risk of recurrence is highest. Early detection through imaging ensures timely intervention if necessary.

When diagnosing a retroperitoneal mass located in close proximity to the spinal cord, it is essential to carefully consider the differential diagnosis with dumbbell schwannoma of the lumbar spine. The differential diagnoses for a lumbar dumbbell schwannoma include a range of neoplastic, infectious, and inflammatory conditions that can mimic its presentation in clinical and imaging findings, including neurofibromas, meningiomas, metastatic lesions, ependymomas, paragangliomas, abscess or infectious lesions, lipoma or hemangiomas.[15] Schwannomas, neurofibromas, and metastatic tumors can be distinguished based on their MRI characteristics. Schwannomas typically present as well-defined, oval or round masses, often with a "dumbbell" shape due to extension through the intervertebral foramen. They are usually hypo- to isointense on T1 and hyperintense on T2, with homogeneous or heterogeneous contrast enhancement. Schwannomas are generally encapsulated and cause minimal peritumoral edema. In contrast, neurofibromas are more ill-defined and infiltrative, often following the course of the nerve from which they originate, with heterogeneous signal intensity on both T1- and T2-weighted images. On post-contrast images, neurofibromas exhibit less uniform enhancement and may show an infiltrative pattern along the nerve roots. While metastatic tumors are typically irregular, heterogeneous, and infiltrative, often involving bone, soft tissue, and epidural space, with central necrosis in larger masses. Thus, while schwannomas tend to be more localized and well-defined, neurofibromas and metastatic tumors present with more aggressive, infiltrative patterns and greater variability in signal intensity and enhancement.

Therefore, accurate lumbar schwannomas' diagnosis relies on correlating clinical presentation with imaging features, supplemented by histopathological confirmation in surgical cases. Recognizing these differential diagnoses is crucial for guiding appropriate management and optimizing patient outcomes.

The management of these tumors benefits from a multidisciplinary approach, involving neurosurgeons, radiologists, and oncologists to tailor treatment strategies to individual patient needs. Advances in minimally invasive surgical techniques and precision radiotherapy have significantly enhanced the therapeutic landscape, reducing morbidity and improving quality of life.[16]

In conclusion, the successful management of lumbar dumbbell schwannomas relies on timely diagnosis, individualized surgical treatment planning, and a comprehensive follow-up strategy. Surgical resection remains

the definitive treatment, augmented by radiation therapy in select cases. A collaborative, patient-centered approach ensures optimal results by combining therapeutic efficacy with preservation of neurological function and overall quality of life.

Competing Interests

The authors declare that they have no competing interests.

References

1. Louis DN, Perry A, Reifenberger G, von Deimling A, Figarella-Branger D, Cavenee WK, Ohgaki H, Wiestler OD, Kleihues P, Ellison DW. The 2016 World Health Organization Classification of Tumors of the Central Nervous System: a summary. Acta Neuropathol. 2016 Jun;131(6):803-20. doi: 10.1007/s00401-016-1545-1. Epub 2016 May 9. PMID: 27157931.
2. Budiman Gondowardojo YR, Ompusunggu SE, Dahlan RH. Giant invasive lumbosacral spinal schwannoma. Neurol Spinal Med Chirurg. 2022;5(2):106. doi:10.4103/nsmc.nsmc_6_22.
3. Rong HT, Fan YS, Li SP, Zhang ZS, Liu H, Liu T, Zhu T, Zhang JN. Management of Dumbbell and Paraspinal Tumors of the Thoracic Spine Using a Single-stage Posterolateral Approach: Case Series. Orthop Surg. 2018 Nov;10(4):343-349. doi: 10.1111/os.12405. Epub 2018 Nov 8. PMID: 30406971; PMCID: PMC6594492.
4. Cleveland Clinic. Schwannoma: what it is, causes, symptoms & treatment [Internet]. [cited 2025 Jan 5]. Available from: https://my.clevelandclinic.org/health/diseases/17877-schwannoma
5. Lenzi J, Anichini G, Landi A, Piciocchi A, Passacantilli E, Pedace F, Delfini R, Santoro A. Spinal Nerves Schwannomas: Experience on 367 Cases-Historic Overview on How Clinical, Radiological, and Surgical Practices Have Changed over a Course of 60 Years. Neurol Res Int. 2017;2017:3568359. doi: 10.1155/2017/3568359. Epub 2017 Sep 18. PMID: 29075532; PMCID: PMC5624174.
6. Chu EC, Trager RJ, Yee WJ, Ng KK. Lumbar Schwannoma as a Rare Cause of Radiculopathy in the Chiropractic Office: A Case Report. Cureus. 2022 Nov 21;14(11):e31758. doi: 10.7759/cureus.31758. PMID: 36569702; PMCID: PMC9771692.
7. Yang JJ, Landier W, Yang W, Liu C, Hageman L, Cheng C, Pei D, Chen Y, Crews KR, Kornegay N, Wong FL, Evans WE, Pui CH, Bhatia S, Relling MV. Inherited NUDT15 variant is a genetic determinant of mercaptopurine intolerance in children with acute lymphoblastic leukemia. J Clin Oncol. 2015 Apr 10;33(11):1235-42. doi: 10.1200/JCO.2014.59.4671. Epub 2015 Jan 26. PMID: 25624441; PMCID: PMC4375304.
8. Strong MJ, Yee TJ, Khalsa SSS, Saadeh YS, Muhlestein WE, North RY, Szerlip NJ. Resection of a Lumbar Intradural Extramedullary Schwannoma: 2-Dimensional Operative Video. Oper Neurosurg (Hagerstown). 2021 Jun 15;21(1):E38. doi: 10.1093/ons/opab097. PMID: 33825885.
9. Conti P, Pansini G, Mouchaty H, Capuano C, Conti R. Spinal neurinomas: retrospective analysis and long-term outcome of 179 consecutively operated cases and review of the literature. Surg Neurol. 2004 Jan;61(1):34-43; discussion 44. doi: 10.1016/s0090-3019(03)00537-8. PMID: 14706374.
10. Columbia Neurosurgery. Spinal schwannoma diagnosis & treatment—NYC [Internet]. 2021 Apr 8 [cited 2025 Jan 5]. Available from: https://www.neurosurgery.columbia.edu/patient-care/conditions/spinal-schwannoma
11. Gui C, Canthiya L, Zadeh G, Suppiah S. Current state of spinal nerve sheath tumor management and future advances. Neurooncol Adv. 2024 Jul 17;6(Suppl 3):iii83-iii93. doi: 10.1093/noajnl/vdae067. PMID: 39430389; PMCID: PMC11485951.
12. D'Andrea G, Sessa G, Picotti V, Raco A. One-Step Posterior and Anterior Combined Approach for L5 Retroperitoneal Schwannoma Eroding a Lumbar Vertebra. Case Rep Surg. 2016;2016:1876765. doi: 10.1155/2016/1876765. Epub 2016 Sep 27. PMID: 27766176; PMCID: PMC5059541.
13. Hwang L, Okoye CC, Patel RB, Sahgal A, Foote M, Redmond KJ, Hofstetter C, Saigal R, Mossa-Basha M, Yuh W, Mayr NA, Chao ST, Chang EL, Lo SS. Stereotactic body radiotherapy for benign spinal tumors: Meningiomas, schwannomas, and neurofibromas. J Radiosurg SBRT. 2019;6(3):167-177. PMID: 31998537; PMCID: PMC6774487.
14. Senapati SB, Mishra SS, Dhir MK, Patnaik A, Panigrahi S. Recurrence of spinal schwannoma: Is it preventable? Asian J Neurosurg. 2016 Oct-Dec;11(4):451. doi: 10.4103/1793-5482.145060. PMID: 27695564; PMCID: PMC4974985.
15. Takashima H, Takebayashi T, Yoshimoto M, Onodera M, Terashima Y, Iesato N, Tanimoto K, Ogon I, Morita T, Yamashita T. Differentiating spinal intradural-extramedullary schwannoma from meningioma using MRI T_2 weighted images. Br J Radiol. 2018 Dec;91(1092):20180262. doi: 10.1259/bjr.20180262. Epub 2018 Aug 7. PMID: 30052467; PMCID: PMC6319836.
16. Argiti K, Watzlawick R, Hohenhaus M, Vasilikos I, Volz F, Roelz R, Scholz C, Hubbe U, Beck J, Neef M, Klingler JH. Minimally invasive tubular removal of spinal schwannoma and neurofibroma - a case series of 49 patients and review of the literature. Neurosurg Rev. 2024 Aug 10;47(1):418. doi: 10.1007/s10143-024-02656-x. PMID: 39123090; PMCID: PMC11315786.

International Journal of Biomedicine 15(3) (2025) 598-600
http://dx.doi.org/10.21103/Article15(3)_CR3

CASE REPORT

INTERNATIONAL JOURNAL OF BIOMEDICINE

Antiphospholipid Syndrome Associated with Systemic Lupus Erythematosus: A Case Report

Ina Toska[1*], Ervin Rapushi[2], Rexhep Shkurti[1], Anila Mitre[3]

[1]*Department of Biotechnology, Faculty of Natural Sciences, University of Tirana, Tirana, Albania*
[2]*University of Medicine, Tirana, Albania*
[3]*Department of Biology, Faculty of Natural Sciences, University of Tirana, Tirana, Albania*

Abstract

Antiphospholipid syndrome (APS) is an autoimmune disorder characterized by venous or arterial thrombosis and/or pregnancy outcomes in the presence of persistent antiphospholipid antibodies like lupus anticoagulant (LAC), anti-cardiolipin (aCL), and anti-β2glucoprotein. Antiphospholipid syndrome may occur as a primary disorder or in association with other autoimmune diseases, especially with systemic lupus erythematosus (SLE). This case reports a 28-year-old woman diagnosed with SLE and APS after her first thrombotic event, a deep vein thrombosis in the right leg. All SLE patients must be screened for antiphospholipid antibodies, even when thrombotic events have not occurred, to determine the antiphospholipid antibody profile, which is important for future thrombotic risk events. (**International Journal of Biomedicine. 2025;15(3):598-600.**)

Keywords: antiphospholipid syndrome • antiphospholipid antibodies • systemic lupus erythematosus

For citation: Toska I, Rapushi E, Shkurti R, Mitre A. Antiphospholipid Syndrome Associated with Systemic Lupus Erythematosus: A Case Report. International Journal of Biomedicine. 2025;15(3):598-600. doi:10.21103/Article15(3)_CR3

Abbreviations

aCL, anti-cardiolipin; **APS**, antiphospholipid syndrome; **ANA**, antinuclear antibody; **CT**, computed tomography; **DVT,** deep vein thrombosis; **ENA**, extractable nuclear antigen; **IVC**, inferior vein cava; **INR**, international normalized ratio; **LAC**, lupus anticoagulant; **PE**, pulmonary embolism; **SLE**, systemic lupus erythematosus.

Introduction

Antiphospholipid syndrome (APS) is an autoimmune disorder characterized by venous or arterial thrombosis and/or pregnancy outcomes in the presence of persistent antiphospholipid antibodies like lupus anticoagulant (LAC), anti-cardiolipin (aCL), and anti-β2glucoprotein.[1] Classification criteria for APS have changed over the years. Sapporo criteria were first published in 1999 and updated in 2006 (Sydney criteria). Diagnosis for APS, based on revised Sapporo criteria, requires at least one clinical and one laboratory manifestation.[2] Clinical criteria comprise arterial/vascular thrombosis or pregnancy morbidity, while laboratory ones include the presence of medium or high titers of IgG and/or IgM anti-cardiolipin (aCL) antibodies, IgG/IgM anti-beta 2 glycoprotein I antibodies (anti-β2GPI), and/or LAC positive on two or more occasions at least 12 weeks apart.[3]

Antiphospholipid syndrome may occur as a primary disorder, but when it is associated with other autoimmune diseases, most commonly with systemic lupus erythematosus (SLE), it is defined as a secondary APS.[4,5]

Systemic lupus erythematosus is an autoimmune disease that affects connective tissues, leading to chronic inflammatory illness of skin, joints, kidneys, lymph nodes, and the lining layers of the blood vessels with increased risk of arterial and venous thrombotic events.[6] When SLE was associated with antiphospholipid antibodies, an increased number of thrombotic events was observed. The presence of antiphospholipid antibodies has been described in around 50% of SLE patients, while around 20% of APS patients have SLE.[7]

***Corresponding author:** Ina Toska, E-mail: ina.toska@yahoo.com*

This case reports a 28-year-old woman diagnosed with SLE and APS after her first thrombotic event, a deep vein thrombosis (DVT) in the right leg.

Case Presentation

A 28-year-old female patient experienced her first thrombotic event at the age of 14: DVT in the right leg, in the absence of varicose veins or other coagulation disorders, and did not report using oral contraceptives. She was hospitalized at Shkodra hospital and was stabilized after treatment with nadroparin calcium. After leaving the hospital, she was treated with acenocoumarol with dosing adjusted according to the INR level.

One year later (January 2012), this patient underwent several examinations due to her poor health condition. CT was also performed, resulting in normal findings. Six months later, this young lady was hospitalized at the University Hospital Center "Mother Tereza," (Tirana, Albania) for an accurate diagnosis. She reported experiencing several symptoms like fatigue, physical weakness, pain in the hands and feet, stains in the skin of the abdomen, hair loss, numbness of hands and feet, and even mouth ulcers. Upon general examination, the patient was alert and oriented. The skin of the face had a butterfly-shaped rash over the cheeks and nose. Respiratory effort appeared slightly labored.

An abdominal ultrasound was performed and resulted in normal findings, while bone and joint pathology was revealed by hand x-ray. A series of laboratory examinations, including cell blood count, biochemical balance, coagulation, and immunological profiles, were performed (Table 1).

Comparison of laboratory results from January to June revealed transient thrombocytopenia, reduced hemoglobin levels, and decreased complement C3 and C4 levels. Antinuclear antibodies (ANA), extractable nuclear antigen (ENA) screening, and anti-cardiolipin IgM/IgG were all positive.

Based on clinical and laboratory evaluation, the diagnosis was SLE and APS with anti-cardiolipin IgM/IgG positive and thrombotic events.

The medical treatment started immediately and included acenocoumarol, according to the level of INR, plaquenil (400 mg/d), medrol (8 mg/d), and vitamin D (2000 IU/d). The clinical situation appeared to be stabilized upon the receipt of the medical protocol.

In 2014, this patient interrupted the treatment with acenocoumarol, and a clinical complication occurred. She was admitted to the hospital with difficulty breathing, and according to laboratory examinations (Table 1) and CT, she was diagnosed with bilateral pulmonary thromboembolism. The treatment protocol remained the same, on the condition that therapy with acenocoumarol, not be interrupted.

In recent years, this patient has reported increased leg pain and varicose veins. The last CT showed blockage of the inferior vein cava (IVC), suggesting a post-thrombotic event occurring there and suggesting the necessity of surgical intervention. The latest laboratory examination data are also presented in Table 1.

Table 1.

Summary of laboratory examinations.

Laboratory tests	01.2012	06.2012	2014	2025	Reference values
RBC	4.73	4.36	5.1	5.55	4-5×10^6/µL
WBC	4.9	4.85	12	5.71	5-10×10^3/uL
Hb	12.3	10.7	8.8	15.4	12-16 g/dL
PLT	17	292	498	263	140-400×10^3/uL
ALT	92.8	23.6	21	22.4	< 35 U/L
AST	76.8	23.9	42	27.4	<31 U/L
TPU 24H		271.5	Negative		< 150 mg/24h
Ca	9.96		8.8		9.2-11 md/dL
CRP		5.1	14	1.05	<5 mg/L
CK		35	107		<170 U/L
LDH	301	205	289		< 480 U/L
RF	2.7	3.9	21	7.1	<14 IU/mL
FIB	439.1		397		200-400 mg/dL
APTT	79.7		47.3	36.9	25-35 sec
D-DI	1.8		1.66		< 0.5 ug/mL
C3		73	134	100	90-180 mg/dL
C4		7	11.7	14	10-40 mg/dL
LAC			107.1	94.5	31.4-43.4 sec
ANA	Positive	Positive	Positive	1:160	<1:80 Negative
DsDNA			Positive		Negative
ENA SCREEN		Positive	Positive		< 20 Negative
aCL IgM	Positive		Positive	Negative	<12 U/mL
aCL IgG	Positive			Positive	>12 U/mL
anti-ß2GPI IgG				Positive	>20 RU/ml

RBC, red blood cells; WBC, white blood cells; Hb, hemoglobin; PLT, platelets; ALT, alanine transaminase; AST, aspartate transaminase; TPU 24H: proteinuria; Ca, calcium; CRP, C-reactive protein; CK, creatin kinase; LDH, lactate dehydrogenase; RF, rheumatoid factor; FIB, fibrinogen; APTT, activated partial thromboplastin time; D-DI, d-Dimer; C3, C3 complement; C4, C4 complement; LAC, lupus anticoagulant; ANA, antinuclear antibodies; DsDNA, anti-double stranded DNA antibodies; ENA Screen, extractable antigen test; aCL IgM, anti-cardiolipin IgM; aCL IgG, anti-cardiolipin IgG; anti -ß2GPI, antiß2-glycoprotein.

Discussion

Antiphospholipid syndrome and systemic lupus erythematosus are two diseases related to each other due to the similarities that they have in terms of thrombotic events and clinical manifestations, including the presence of antiphospholipid antibodies. When SLE is associated with APS, it significantly increases the risk of thrombotic events in comparison with the general population. In SLE patients, approximately 50% are aPL positive, compared to those with SLE alone.[8]

According to recent data and meta-analysis of venous thromboembolism in SLE, patients with lupus erythematosus have a 4.38-fold higher relative risk of venous thromboembolism than the general population. When SLE coexists with APS, the absolute venous thromboembolism

risk increases to 63%. For DVT and PE, the risk rises from 1% to ~26% and 22%, respectively, when SLE is associated with APS.[9]

All laboratory findings in this patient, including positive ANA, ENA screen, anti-cardiolipin IgM/IgG, and proteinuria, confirmed the diagnosis of SLE with APS according to their respective classification protocols. SLE patients should be screened for antiphospholipid antibodies to determine their aPL profile. It is reported that in new SLE patients, double or triple aPL-positivity increases the risk for future vascular events.[10]

This case is an example of the coexistence of SLE and APS, which highlights the increased probability of thrombotic events. A young girl experienced DVT in the right leg at the age of 14, followed by bilateral pulmonary thromboembolism and, recently, an obstruction of the IVC, suggesting a post-thrombotic event occurring there. Although it is a very rare complication, particularly when the anticoagulation therapy is insufficient without immunosuppression, some cases of IVC have been reported in the literature. It is important to emphasize that our patient was not treated with immunosuppressants, a fact that could be a possible cause of the current situation.

Currently, in a review of several publications regarding immunosuppression in APS-positive patients with recurrent thrombotic events, anticoagulant therapy, hydroxychloroquine, and rituximab are recommended to reduce the titer of circulating antiphospholipid antibodies.

One of the cases reports a 14-year-old patient with active SLE, Evans syndrome, and secondary APS with acute abdominal pain, resulting in mesenteric vasculitis and thrombosis of the IVC.[11] Initial medical therapy with fraxiparin, followed by acenocumarol according to INR levels, showed that it was effective until its discontinuation, which led to PE, emphasizing the importance of continuing therapy in patients with SLE/APS with prior thrombotic events. Immunosuppressive therapy is also recommended, especially when thromboses persist despite anticoagulation therapy.

Thus, patients with SLE and APS have an increased risk for thrombotic events. All SLE patients must be screened for antiphospholipid antibodies, even when thrombotic events have not occurred, to determine the antiphospholipid antibody profile, which is important for future thrombotic risk events.

Acknowledgments

The authors are grateful to the patient for kindly allowing us to publish her case.

Competing Interests

The authors declare that they have no competing interests.

References

1. Musiał J. New classification criteria for antiphospholipid syndrome —2023. Journal of Transfusion Medicine [Internet]. 2023 [cited 2023 Nov 24];16(3):103–9. Available from: https://journals.viamedica.pl/journal_of_transfusion_medicine/article/view/97795/74984

2. Miyakis S, Lockshin MD, Atsumi T, Branch DW, Brey RL, Cervera R, Derksen RH, DE Groot PG, Koike T, Meroni PL, Reber G, Shoenfeld Y, Tincani A, Vlachoyiannopoulos PG, Krilis SA. International consensus statement on an update of the classification criteria for definite antiphospholipid syndrome (APS). J Thromb Haemost. 2006 Feb;4(2):295-306. doi: 10.1111/j.1538-7836.2006.01753.x. PMID: 16420554.

3. Dabit JY, Valenzuela-Almada MO, Vallejo-Ramos S, Duarte-García A. Epidemiology of Antiphospholipid Syndrome in the General Population. Curr Rheumatol Rep. 2022 Jan 5;23(12):85. doi: 10.1007/s11926-021-01038-2. PMID: 34985614; PMCID: PMC8727975.

4. Bahar Keleşoğlu Dinçer A, Erkan D. The ABCs of antiphospholipid syndrome. Archives of rheumatology [Internet]. 2023 May;38(2):163–73. Available from: https://pubmed.ncbi.nlm.nih.gov/37680521/

5. Branch DW. What's new in obstetric antiphospholipid syndrome. Hematology Am Soc Hematol Educ Program. 2019 Dec 6;2019(1):421-425. doi: 10.1182/hematology.2019000043. PMID: 31808896; PMCID: PMC6913435.

6. Ibrahim AAG, Shadi HWE, Elamin AAY, Draz HE. Retrospective cohort study of thromboembolic events in systemic lupus erythematosus with or without secondary antiphospholipid syndrome and their correlation to lupus activity and dyslipidemia. Egyptian Rheumatology and Rehabilitation. 2023 Feb 16;50(1).

7. Bazzan M, Vaccarino A, Marletto F. Systemic lupus erythematosus and thrombosis. Thromb J. 2015 Apr 23;13:16. doi: 10.1186/s12959-015-0043-3. PMID: 25908929; PMCID: PMC4407320.

8. Nakashima M, Kobayashi M. Preceding Antiphospholipid Syndrome before the Onset of Systemic Lupus Erythematosus Presenting with Iliocaval Deep Vein Thrombosis: A Case Report and Literature Review. Annals of Vascular Diseases [Internet]. 2024 [cited 2025 Jul 13];17(4):409–12. Available from: https://pmc.ncbi.nlm.nih.gov/articles/PMC11669031/

9. Bello N, Meyers KJ, Workman J, Marcano Belisario J, Cervera R. Systematic Literature Review and Meta-analysis of Venous Thromboembolism Events in Systemic Lupus Erythematosus. Rheumatol Ther. 2023 Feb;10(1):7-34. doi: 10.1007/s40744-022-00513-1. Epub 2022 Dec 6. PMID: 36471199; PMCID: PMC9931974.

10. Pericleous C, D'Souza A, McDonnell T, Ripoll VM, Leach O, Isenberg D, Giles I, Rahman A. Antiphospholipid antibody levels in early systemic lupus erythematosus: are they associated with subsequent mortality and vascular events? Rheumatology (Oxford). 2020 Jan 1;59(1):146-152. doi: 10.1093/rheumatology/kez239. PMID: 31257438; PMCID: PMC6909892.

11. Wang G, Li B, Luo Y, Li J, Wen Z. Mesenteric vasculitis with inferior vena cava thrombosis associated with systemic lupus erythematosus. Arch Med Sci. 2023 Feb 17;19(2):544-545. doi: 10.5114/aoms/158532. PMID: 37034506; PMCID: PMC10074299.

International Journal of Biomedicine 15(3) (2025) 601-604
http://dx.doi.org/10.21103/Article15(3)_CR4

CASE REPORT

INTERNATIONAL JOURNAL OF BIOMEDICINE

Diagnostic Imaging of Chronic Prepatellar Bursitis (Housemaid's Knee): An Elderly Patient Case Report

Meaad Elbashir[1], Dafalla Bashier[2], Awatif M. Omer[3], Mogahid M.A Zidan[4], Abdu M. Khormi[1], Sara Ali[1*]

[1]*Diagnostic Radiography Technology Department, College of Nursing &Health Sciences, Jazan University, Jazan, Saudi Arabia*
[2]*Tiaba Hospital, Omdurman, Sudan*
[3]*Department of Diagnostic Radiology Technology, College of Applied Medical Sciences, Taibah University, Madina, 41477, Saudi Arabia*
[4]*Diagnostic Radiology Department, Faculty of Radiology and Nuclear Medicine Sciences, The National Ribat University, Khartoum, 11111, Sudan*

Abstract

Prepatellar bursitis, often referred to as "Housemaid's Knee," is an inflammation of the prepatellar bursa, usually caused by repeated trauma or extended periods of kneeling. Diagnosing chronic cases can be particularly challenging, especially in older individuals and when advanced imaging techniques are not advisable. This case report details a 70-year-old man who experienced swelling in the right front of his knee, difficulty walking, and pain when kneeling for six months. A musculoskeletal (MSK) ultrasound showed a clearly defined cystic mass measuring 4.8×2.1 cm located in front of the patella, with internal lobulations and cloudy fluid, indicative of chronic prepatellar bursal effusion. There was no evidence of internal blood flow or solid masses. Additional observations included irregularities and calcifications at the insertion of the suprapatellar tendon, suggesting chronic degenerative changes. The bursal sac was surgically removed, and histopathological analysis confirmed chronic prepatellar bursitis. The patient gradually showed improvement in symptoms and functional recovery after the surgery.

Our case highlights the value of MSK ultrasound in diagnosing chronic prepatellar bursitis, particularly when other imaging methods are not feasible. Surgical intervention remains an effective treatment for chronic, stubborn cases. Accurate diagnosis depends on a thorough assessment that combines clinical symptoms, ultrasound findings, and histopathological evidence. (**International Journal of Biomedicine. 2025;15(3):601-604.**)

Keywords: housemaid's knee • inflammation • MSK ultrasound • prepatellar bursitis

For citation: Elbashir M, Bashier D, Omer AM, Zidan MMA, Khormi AM, Ali S. Diagnostic Imaging of Chronic Prepatellar Bursitis (Housemaid's Knee): An Elderly Patient Case Report . International Journal of Biomedicine. 2025;15(3):601-604. doi:10.21103/Article15(3)_CR4

Introduction

Housemaid's knee is the name given to inflammation of the prepatellar bursa, hence, prepatellar bursitis. Housemaid's knee is a condition of prepatellar bursitis, which is caused by inflammation of the bursa (a fluid-filled sac) that is in front of the patella.[1] It commonly occurs in people who spend long periods of time kneeling, and the bursa between the skin and the kneecap (the prepatellar bursa) is most commonly affected.[2,3]

Musculoskeletal (MSK) ultrasound demonstrates the tendons, ligaments, bursa, and muscles, thereby enhancing its diagnostic accuracy. Its advantages include the ability to apply compression, perform dynamic assessments, and easily compare with the contralateral side.[4] The normal appearance of the prepatellar bursa is visualized as a fluid-filled anechoic structure lined by a hyperechoic wall.[5] In this article, I will present a case study on Housemaid's knee, using MSK ultrasound for diagnosis. The case will explore the patient's symptoms, clinical evaluation, and the role of MSK ultrasound in assessing the knee joint, synovial thickening, and other pathological changes, and treatment.

***Corresponding author:** Sara Ali, sarraali@jazanu.edu.sa*

Case Presentation

A 70-year-old male presented to the Tiba Hospital (Omdurman, Sudan) with complaints of swelling over the right knee for six months, with a gradual increase in the size of the swelling and difficulty in walking for six months. The patient had no history of trauma. The swelling was mildly compressible and associated with minimal pain or tenderness; however, he noted increased tenderness during kneeling, particularly during prayer.

Clinical examination of the right knee revealed globular swelling in the anterior region. The swelling had a variegated consistency, described as firm, hard, and cystic in different locations, and was nonmobile. Due to persistent swelling, the unusual consistency of the swelling, and the patient's reported symptoms, the physician ordered an ultrasound of the right knee.

Ultrasound revealed a well-defined cystic lesion measuring 4.8×2.1 cm in the anterior knee, exhibiting internal lobulations and a turbid collection, consistent with a chronic prepatellar bursal effusion. No internal vascularity or solid component was observed. Quadriceps muscle and tendons were normal. Suprapatellar tendon insertion showed irregularity with calcifications, suggestive of chronic degenerative changes. The synovium, patella, patellar tendon, anterior cruciate ligament (ACL), and medial collateral ligament (MCL) were all normal. The medial and lateral menisci were normal, without adjacent osteophytes. Baker's cysts were absent in the posterior knee region, and the popliteal artery and vein were normal. The ultrasound impression was prepatellar bursitis (Housemaid's knee) and suprapatellar calcific tendinopathy.

Further imaging with CT or MRI was considered but was contraindicated due to the patient's renal impairment, which precluded the use of contrast media. Given the persistent symptoms and ultrasound findings, a decision was made to proceed with surgical intervention.

Surgical exploration and excision of the bursal sac were then performed. Histopathological examination of the excised tissue confirmed a diagnosis of chronic prepatellar bursitis. Postoperatively, the patient experienced a gradual improvement in symptoms and a reduction in knee swelling. Follow-up evaluations revealed satisfactory wound healing and improved knee function.

Discussion

Prepatellar bursitis, commonly referred to as "Housemaid's knee," is a prevalent inflammatory condition affecting the bursa anterior to the kneecap.[8] This condition is primarily attributed to trauma, infection, or chronic irritation and is particularly common among cleaners, plumbers, floor layers, wrestlers, and other professionals who frequently engage in kneeling activities.

In this case, a 70-year-old patient presented with swelling of the right knee, difficulty walking, and mild tenderness localized to the anterior knee, which is consistent with the classical manifestations of prepatellar bursitis.

The diagnosis was confirmed based on clinical examination with MSK ultrasound imaging. Ultrasound is regarded as the first-line imaging modality for assessing superficial bursae because it enables dynamic assessment, image-guided aspiration, accessibility, and cost-effectiveness. In the current case, high-resolution ultrasonography scan identified a well-defined, anechoic cystic lesion measuring 4.8×2.1 cm in the front of the knee, featuring internal lobulations and a cloudy collection, which is indicative of a chronic prepatellar bursal effusion (Figure 1).

Figure 1. *Long-axis ultrasound of the anterior knee joint presented a well-defined cystic lesion measuring 4.8×2.1 cm in the anterior knee, exhibiting internal lobulations and a turbid collection.*

There was no evidence of internal vascularity or solid components (Figure 2). Quadriceps muscles and tendons were normal. Insertion of the suprapatellar tendon showed irregularities with calcifications, suggesting chronic degenerative changes. The synovium, patella, patellar tendon, anterior cruciate ligament (ACL), and medial collateral ligament (MCL) were normal. The medial and lateral menisci were normal, and no adjacent osteophytes were present. The posterior knee area showed no signs of Baker's cyst, and the popliteal artery and vein were normal. Ultrasound findings were consistent with prepatellar bursitis and suprapatellar calcific tendinopathy.

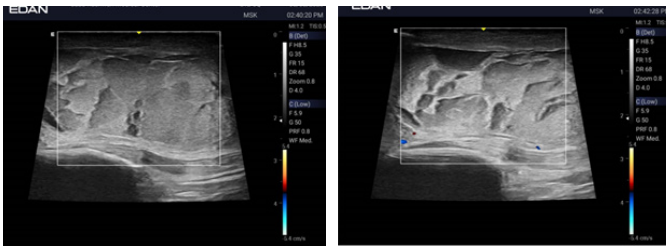

Figure 2. *Long-axis Doppler ultrasound of the anterior knee joint presented a well-defined cystic lesion, exhibiting internal lobulations and a turbid collection. No internal vascularity or solid components were identified.*

These findings are consistent with a study conducted by Ivanoski and Vasilevska, which pointed out that a significant ultrasound sign of bursitis is the swelling of the bursa, characterized by an increased volume of fluid, which may sometimes appear anechoic. In other cases, increased echogenicity is apparent due to debris, blood in acute trauma,

or puss if an infection appears. Other signs include thickening of the hyperechoic synovial wall, which can be uniform or irregular. The latter sign is more often observed in cases of chronic bursitis.[9]

To the best of our knowledge, while other imaging modalities, particularly plain radiography, play a significant role in ruling out bony involvement or foreign bodies, they are not sensitive to soft tissue changes (Figure 3).[10] However, MRI offers superior soft tissue resolution (Figures 4 and 5) and may be particularly useful in chronic or complicated cases, such as when deep-seated infection or mass-forming lesions.[11]

Figure 3. *Superficial infrapatellar bursitis. An 80-year-old female presented with an anterior knee swelling. AP (A) and lateral knee x-ray (B) images show swelling in front of the patella with constant pain, especially in the sitting position.*[6]

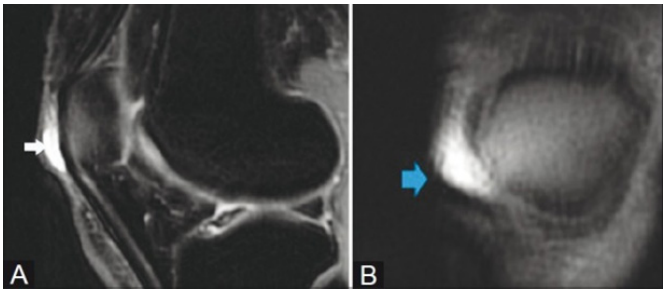

Figure 4. *Prepatellar bursitis. A 44-year-old female presented with anterior knee pain. Axial (A) and coronal (B) T2W fat-saturated images showing a distended prepatellar bursa (arrows).*[7]

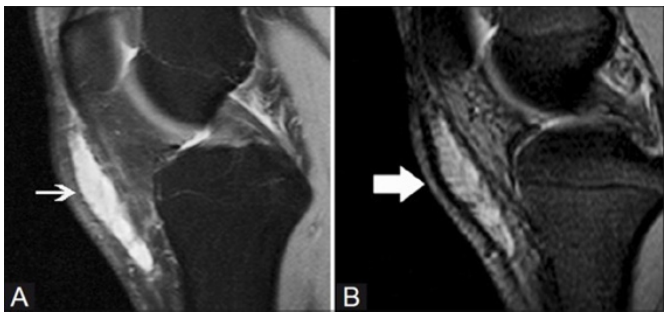

Figure 5. *Superficial infrapatellar bursitis. A 42-year-old female presented with an anterior knee swelling. Sagittal proton-density fat-saturated (A) and sagittal gradient-echo T2W (B) images show a distended superficial infrapatellar bursa (arrows).*[7]

In typical cases, such as ours, the use of MRI is not necessary, as ultrasound effectively serves both diagnostic and interventional purposes because ultrasound can be used for dynamic assessment, allowing real-time evaluation of movement-related pain and swelling, and is cost-effective and easily accessible, especially compared to MRI.[12]

On the other side, bursitis can clinically be misdiagnosed as joint-, tendon-, or muscle-related pain. Pathological processes often result from inflammation secondary to excessive local friction, infection, arthritis, or direct trauma. In this regard, knowledge of the normal anatomy, pathology, and imaging characteristics of the bursae is essential. Differentiation of bursitis from other causes of joint, tendon, and muscle pain allows for adequate treatment.[5]

Conclusion

This case underscores the necessity of including prepatellar bursitis in the differential diagnosis of anterior knee swelling, particularly in older patients with non-traumatic causes. Ultrasound remains an invaluable diagnostic tool, especially when other imaging modalities are restricted owing to patient comorbidities.

Surgical treatment, confirmed by histopathological evidence, proved effective in managing chronic, stubborn cases. A thorough understanding of clinical, imaging, and pathological characteristics is vital for prompt diagnosis and suitable management.

Acknowledgments

We thank the patients who agreed to participate in this study. In addition, we extend our thanks to the Tiba Hospital staff.

Ethical Considerations

Written informed consent was obtained from all participants.

Competing Interests

The authors declare that they have no competing interests.

References

1. Sato M, Watari T. Housemaid's Knee (Prepatellar Septic Bursitis). Cureus. 2020 Sep 11;12(9):e10398. doi: 10.7759/cureus.10398. PMID: 33062518; PMCID: PMC7549991.
2. McAfee JH, Smith DL. Olecranon and prepatellar bursitis. Diagnosis and treatment. West J Med. 1988 Nov;149(5):607-10. PMID: 3074561; PMCID: PMC1026560.
3. Mercadante JR, Marappa-Ganeshan R. Anatomy, Skin Bursa. 2022 Oct 8. In: StatPearls [Internet]. Treasure Island (FL): StatPearls Publishing; 2025 Jan–. PMID: 32119325.

4. Friedman L, Finlay K, Jurriaans E. Ultrasound of the knee. Skeletal Radiol. 2001 Jul;30(7):361-77. doi: 10.1007/s002560100380. PMID: 11499776.
5. Hirji Z, Hunjun JS, Choudur HN. Imaging of the bursae. J Clin Imaging Sci. 2011;1:22. doi: 10.4103/2156-7514.80374. Epub 2011 May 2. PMID: 21966619; PMCID: PMC3177464.
6. D'Imporzano M, Peretti G , Zeni S. Orthopedics and Rheumatology Archives. Special Volume. Springer Verlag, 2003.
7. Chatra PS. Bursae around the knee joints. Indian J Radiol Imaging. 2012 Jan;22(1):27-30. doi: 10.4103/0971-3026.95400. PMID: 22623812; PMCID: PMC3354353.
8. Aaron DL, Patel A, Kayiaros S, Calfee R. Four common types of bursitis: diagnosis and management. J Am Acad Orthop Surg. 2011 Jun;19(6):359-67. doi: 10.5435/00124635-201106000-00006. PMID: 21628647.
9. Ivanoski S, Nikodinovska VV. Sonographic assessment of the anatomy and common pathologies of clinically important bursae. J Ultrason. 2019 Nov;19(78):212-221. doi: 10.15557/JoU.2019.0032. Epub 2019 Sep 30. PMID: 31807327; PMCID: PMC6856779.
10. Maguire A, Lawrence C, Nicolai P, Rosenbloom C. Massive Bilateral Haemorrhagic Prepatellar Bursitis: A Case Report. Cureus. 2024 Nov 24;16(11):e74351. doi: 10.7759/cureus.74351. PMID: 39720372; PMCID: PMC11668264.
11. Bellon EM, Sacco DC, Steiger DA, Coleman PE. Magnetic resonance imaging in "housemaid's knee" (prepatellar bursitis). Magn Reson Imaging. 1987;5(3):175-7. doi: 10.1016/0730-725x(87)90018-x. PMID: 3626787.
12. Demirturk Kocasarac H, Angelopoulos C. Ultrasound in Dentistry: Toward a Future of Radiation-Free Imaging. Dent Clin North Am. 2018 Jul;62(3):481-489. doi: 10.1016/j.cden.2018.03.007. PMID: 29903563.

International Journal of Biomedicine 15(3) (2025) 605-607
http://dx.doi.org/10.21103/Article15(3)_CR5

CASE REPORT

INTERNATIONAL JOURNAL OF BIOMEDICINE

Bone Ring Technique: A Case Report

Sinan Arllati[1*], Kreshnik Syka[1]

[1]*Dental Laser Center, Dental Clinic, Kosovo, Prishtina*

Abstract

Tooth extraction is accompanied by vertical reduction of the alveolar ridge as a result of the bone atrophy. In cases involving the upper jaw, changes in alveolar bone dimensions can also be accompanied by pneumatization of the maxillary sinus. These changes are even more common after the extraction of the maxillary first and second molars, and especially after the extraction of two or more teeth in a row in the distal maxillary region. Different techniques and materials are used to provide adequate bone support for dental implants in these cases. In the presented case, the autogenous bone ring (bone ring technique) transplantation technique, combined with the immediate placement of the implant during the same surgical session, was applied. (**International Journal of Biomedicine. 2025;15(3):605-607.**)

Keywords: tooth extraction • bone resorption • implant • autogenous bone rings

For citation: Arllati S, Syka K. Bone Ring Technique: A Case Report. International Journal of Biomedicine. 2025;15(3):605-607. doi:10.21103/Article15(3)_CR5

Introduction

Early extraction of the teeth of the distal region of the maxilla is often accompanied by a large bone loss, and as a result, it leads to the reduction of the vertical dimension of the alveolar ridge. In cases involving the upper jaw, changes in the dimensions of the alveolar bone can also be associated with the pneumatization of the maxillary sinus.[1,2] These changes are more pronounced after the extraction of the first or second maxillary molar, and especially in cases of the extraction of two or more teeth in a row in the distal region. The replacement of an extracted natural tooth with an osseointegrated implant represents one of the most important advances in contemporary dentistry.

Various procedures and materials are in use to provide adequate bone support for dental implants.[3-5] In cases with advanced bone resorption and maxillary sinus pneumatization,[6] the autogenous bone ring transplantation technique, combined with immediate implant placement in the same session, is an advanced method that significantly reduces the time compared to other methods.[7-11] For the application of this technique, the specific indication is the thickness of the remaining bone, which must be under 2 mm. Through this technique, vertical regeneration is achieved through the autogenous bone.

***Corresponding author:** Sinan Arllati. Email: sinanarllati@gmail.com*

The peculiarity of this technique lies in the immediate placement of the dental implant alongside the bone ring. The bone ring in this case serves as the primary stabilizer of the implant, simultaneously acting as a bone deposit to increase the level of deficient bone.

Case Presentation

During an intraoral examination of a 46-year-old male patient, it was discovered that tooth #16 was absent, having been extracted 10 years prior. In the 3D CBCT digital radiological examination, a low level of the alveolar ridge in that region with pronounced pneumatization of the maxillary sinus was found (Figure 1).

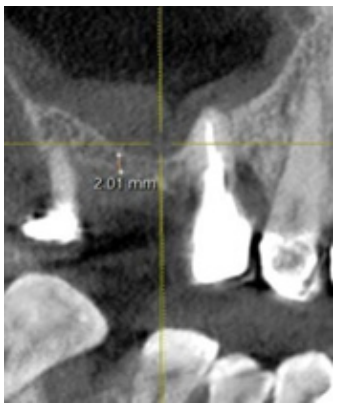

Fig. 1. *Photo 1. 3D CBVT digital radiography, analysis of the bone in the distal part of the maxilla, in the region of tooth #16, marked bone insufficiency is observed in the alveolar ridge (>2 mm).*

From the anamnestic data, there is no evidence of any health condition that would contraindicate surgical intervention. He does not smoke, and biochemical laboratory tests show normal values. Bone augmentation after raising the maxillary sinus is performed using an autogenous bone ring taken from the patient, bone particles in the form of Xenograft artificial granules, and a self-absorbing collagen membrane fixed in place with titanium screws, each with a length of 4-6 mm. The surgical technique with an autogenous bone ring enables the immediate placement of the dental implant by facilitating vertical augmentation of the alveolar ridge in the distal region of the upper jaw.

Surgical Intervention

In the lower jaw, in the retromandibular region, a bone ring is taken, which is pulled through special trephines to collect the bone, which remains in physiological digestion in order not to lose organic matter until the moment of augmentation. After the bone osteotomy in the region of tooth #16, the window for lateral access to the maxillary sinus was opened, the membrane (Schneiderian) was carefully raised, and sufficient space was created for vertical augmentation with autogenous bone rings. The dental implant was immediately placed and fixed through the autogenous bone ring. Augmentation was done with xenograft and autograft in a 50/50% ratio. To secure the augmenting material, a self-absorbing collagen membrane was applied (Figures 2-4).

Fig. 2. *Bone ring.*

Fig. 3. *Immediate placement of the dental implant and its fixation through the autogenous bone ring.*

Fig. 4. *Augmentation with xenograft (Geistlich Bio-Oss) and autograft (Bone ring), as well as placement of a collagen membrane (self-absorbing), to provide the augmenting material.*

Four months after the surgical intervention, a digital radiological check-up was performed, which revealed that the bone augmentation and osseointegration of the dental implant were complete. The bone ring showed very low rates of resorption, as well as high rates of integration into the xenograft artificial bone (Figure 5). The physical parameters of the measurements indicate that the length of the bone ring was 9.3 mm, and the total length was 17.4 mm. The autogenous bone ring also did not undergo internal resorption during the time of osseointegration of the implant. From 10 mm at the time of placement, it was rooted to 9.3 mm of bone height, which proves a satisfactory regenerative result.

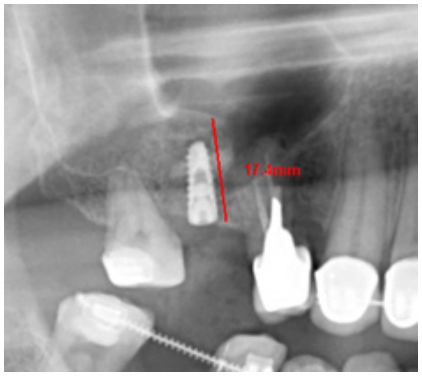

Fig. 5. *The vertical level of the alveolar ridge marks a significant increase from 2.1 mm to 17.4 mm bone height.*

Discussion

Alveolar bone augmentation is often necessary when planning the placement of dental implants. Invasive augmentation procedures frequently require staged implant placement, which increases the overall treatment duration.

The innovative approach, which combines ring-shaped autogenous bone grafts with dental implant placement in a

single session, has been demonstrated to be efficient and safe for alveolar ridge augmentation. Autogenous bone ring grafts are safely stabilized through dental implants. Their dimensions were determined by the diameter of the dental implant and the degree of bone atrophy, ensuring adequate stability of the implant and good biocompatibility with both the alveolar bone and the implant. The application of this technique results in less bone resorption compared to other bone regeneration techniques.

In conclusion, scientific sources demonstrate the advantages of the autogenous bone ring augmentation technique for regenerating vertical bone defects in the distal region of the upper jaw,[10-14] particularly in cases where the pneumatization of the maxillary sinus is pronounced. This technique significantly reduces the waiting time for the patient's final prosthesis, eliminates the need for multiple surgical interventions, and utilizes autogenous bone to compensate for the resorbed vertical dimension over time.

Competing Interests

The authors declare that they have no competing interests.

References

1. Couso-Queiruga E, Stuhr S, Tattan M, Chambrone L, Avila-Ortiz G. Post-extraction dimensional changes: A systematic review and meta-analysis. J Clin Periodontol. 2021 Jan;48(1):126-144. doi: 10.1111/jcpe.13390. Epub 2020 Nov 4. PMID: 33067890.

2. Tan WL, Wong TL, Wong MC, Lang NP. A systematic review of post-extractional alveolar hard and soft tissue dimensional changes in humans. Clin Oral Implants Res. 2012 Feb;23 Suppl 5:1-21. doi: 10.1111/j.1600-0501.2011.02375.x. PMID: 22211303.

3. Tolstunov L, Hamrick JFE, Broumand V, Shilo D, Rachmiel A. Bone Augmentation Techniques for Horizontal and Vertical Alveolar Ridge Deficiency in Oral Implantology. Oral Maxillofac Surg Clin North Am. 2019 May;31(2):163-191. doi: 10.1016/j.coms.2019.01.005. PMID: 30947846.

4. Urban I. Guided bone regeneration: vertical growth. In: Sonick M, Hwang D, eds. Implant Site Development. 2015. doi: 10.1002/9781119136194.ch12.

5. Schropp L, Wenzel A, Kostopoulos L, Karring T. Bone healing and soft tissue contour changes following single-tooth extraction: a clinical and radiographic 12-month prospective study. Int J Periodontics Restorative Dent. 2003 Aug;23(4):313-23. PMID: 12956475.

6. Sharan A, Madjar D. Maxillary sinus pneumatization following extractions: a radiographic study. Int J Oral Maxillofac Implants. 2008 Jan-Feb;23(1):48-56. PMID: 18416412.

7. Paolantonio M, Dolci M, Scarano A, d'Archivio D, di Placido G, Tumini V, Piattelli A. Immediate implantation in fresh extraction sockets. A controlled clinical and histological study in man. J Periodontol. 2001 Nov;72(11):1560-71. doi: 10.1902/jop.2001.72.11.1560. PMID: 11759868.

8. Giraddi GB, Saifi AM. Bone Ring Augmentation Around Immediate Implants: A Clinical and Radiographic Study. Ann Maxillofac Surg. 2017 Jan-Jun;7(1):92-97. doi: 10.4103/ams.ams_58_17. PMID: 28713743; PMCID: PMC5502523.

9. Nakahara K, Haga-Tsujimura M, Igarashi K, Kobayashi E, Schaller B, Lang NP, Saulacic N. Single-staged implant placement using the bone ring technique with and without membrane placement: Micro-CT analysis in a preclinical in vivo study. Clin Oral Implants Res. 2020 Jan;31(1):29-36. doi: 10.1111/clr.13543. Epub 2019 Oct 1. PMID: 31541500.

10. Omara M, Abdelwahed N, Ahmed M, Hindy M. Simultaneous implant placement with ridge augmentation using an autogenous bone ring transplant. Int J Oral Maxillofac Surg. 2016 Apr;45(4):535-44. doi: 10.1016/j.ijom.2015.11.001. Epub 2015 Nov 28. PMID: 26644216.

11. Buser D, editor. 2nd ed. 20 Years of Guided Bone Regeneration in Implant Dentistry. Chicago: Quintessence Pub Co.; 2009.

12. Bauer TW, Muschler GF. Bone graft materials. An overview of the basic science. Clin Orthop Relat Res. 2000 Feb;(371):10-27. PMID: 10693546.

13. Nunes MP, Nunes LFP, Filho DPN, Pinho RCM, Cimões R. Bone Ring Technique for the Treatment of Vertical and Horizontal Bone Defects with Immediate Implants: A Report of Two Cases. Int J Periodontics Restorative Dent. 2021 May-Jun;41(3):413-421. doi: 10.11607/prd.4401. PMID: 34076639.

14. Fukuda M, Takahashi T, Yamaguchi T. Bone grafting technique to increase interdental alveolar bone height for placement of an implant. Br J Oral Maxillofac Surg. 2000 Feb;38(1):16-8. doi: 10.1054/bjom.1999.0134. PMID: 10783441.

IJBM

INTERNATIONAL JOURNAL OF BIOMEDICINE

Instructions for Authors

International Journal of Biomedicine (IJBM) publishes peer-reviewed articles on the topics of basic, applied, and translational research on biology and medicine. International Journal of Biomedicine welcomes submissions of the following types of paper: Original articles, Reviews, Perspectives, Viewpoints, and Case Reports.

All research studies involving animals must have been conducted following animal welfare guidelines such as *the National Institutes of Health (NIH) Guide for the Care and Use of Laboratory Animals*, or equivalent documents. Studies involving human subjects or tissues must adhere to the *Declaration of Helsinki and Title 45, US Code of Federal Regulations, Part 46, Protection of Human Subjects*, and must have received approval of the appropriate institutional committee charged with oversight of human studies. Informed consent must be obtained.

Pre-submissions

Authors are welcome to send an abstract or draft manuscript to obtain a view from the Editor about the suitability of their paper. Our Editors will do a quick review of your paper and advise if they believe it is appropriate for submission to our journal. It will not be a full review of your manuscript.

Manuscript Submission

Manuscript submissions should conform to the guidelines set forth in the Recommendations for the Conduct, Reporting, Editing and Publication of Scholarly Work in Medical Journals (ICMJE Recommendations), available from www.ICMJE.org.

Original works will be accepted with the understanding that they are contributed solely to the Journal, are not under review by another publication, and have not previously been published except in abstract form.

All manuscripts must be submitted through the International Journal of Biomedicine`s online submission system (www.ijbm.org/submission.php). Manuscripts must be typed, double-spaced using a 14-point font, including references, figure legends, and tables. Leave 1-inch margins on all sides. Assemble the manuscript in this order: Title Page, Abstract, Key Words, Text (Introduction, Methods, Results, and Discussion), Acknowledgments, Sources of Funding, Disclosures, References, Tables, Figures, and Figure Legends. References, figures, and tables should be cited in numerical order according to first mention in the text.

The preferred order for uploading files is as follows: Cover letter, Full Manuscript PDF (PDF containing all parts of the manuscript including references, legends, figures and tables), Manuscript Text File (MS Word), Figures (each figure and its corresponding legend should be presented together), and Tables. Files should be labeled with appropriate and descriptive file names (e.g., SmithText.doc, Fig1.eps, Table3.doc). Text, Tables, and Figures should be uploaded as separate files. (Multiple figure files can be compressed into a Zip file and uploaded in one step; the system will then unpack the files and prompt the naming of each figure. See www.WinZip.com for a free trial.)

Authors who are unable to provide an electronic version or have other circumstances that prevent online submission must contact the Editorial Office prior to submission to discuss alternate options (editor@ijbm.org).

Cover Letter

The cover letter should be saved as a separate file for upload. In it, the authors should (1) state that the manuscript, or parts of it, have not been and will not be submitted elsewhere for publication; (2) state that all authors have read and approved the manuscript; and (3) disclose any financial or other relations that could lead to a conflict of interest. If a potential conflict exists, its nature should be stated for each author. When there is a stated potential conflict of interest a footnote will be added indicating the author's equity interest in or other affiliation with the identified commercial firms.

The corresponding author should be specified in the cover letter. All editorial communications will be sent to this author. A short paragraph telling the editors why the authors think their paper merits publication priority may be included in the cover letter.

Types of articles

Original articles

Original articles present the results of original research. These manuscripts should present well-rounded studies reporting innovative advances that further knowledge about a topic of importance to the fields of biology or medicine. These can be submitted as either a full-length article (no more than 6,000 words, 4 figures, 4 tables) or a Short Communication (no more than 2,500 words, 2 figures, 2 tables). An original

article may be Randomized Control Trial, Controlled Clinical Trial, Experiment, Survey, and Case-control or Cohort study.

Case Reports

Case reports describe an unusual disease presentation, a new treatment, a new diagnostic method, or a difficult diagnosis. The author must make it clear what the case adds to the field of medicine and include an up-to-date review of all previous cases in the field. These articles should be no more than 5,000 words with no more than 6 figures and 3 tables. Case Reports should consist of the following headings: Abstract (no more than 100 words), Introduction, Case Presentation (clinical presentation, observations, test results, and accompanying figures), Discussion, and Conclusions.

Reviews

Reviews analyze the current state of understanding on a particular subject of research in biology or medicine, the limitations of current knowledge, future directions to be pursued in research, and the overall importance of the topic. Reviews could be non-systematic (narrative) or systematic. Reviews can be submitted as a Mini-Review (no more than 2,500 words, 3 figures, and 1 table) or a long review (no more than 6,000 words, 6 figures, and 3 tables). Reviews should contain four sections: Abstract, Introduction, Topics (with headings and subheadings, and Conclusions and Outlook.

Perspectives

Perspectives are brief, evidenced-based and formally structured essays covering a wide variety of timely topics of relevance to biomedicine. Perspective articles are limited to 2,500 words and usually include ≤10 references, one figure or table. Perspectives contain four sections: Abstract, Introduction, Topics (with headings and subheadings), Conclusions and Outlook.

Viewpoints

Viewpoint articles include academic papers, which address any important topic in biomedicine from a personal perspective than standard academic writing. Maximum length is 1,200 words, ≤70 references, and 1 small table or figure.

Manuscript Preparation

Title Page

The first page of the manuscript (title page) should include (1) a full title of the article, (2) a short title of less than 60 characters with spaces, (3) the authors' names, academic degrees, and affiliations, (4) the total word count of the manuscript (including Abstract, Text, References, Tables, Figure Legends), (5) the number of figures and tables, and (6) the name, email address, and complete address of corresponding author.

Disclaimers. An example of a disclaimer is an author's statement that the views expressed in the submitted article are his or her own and not an official position of the institution or funder.

Abstract

The article should include a brief abstract of no more than 200 words. Limit use of acronyms and abbreviations. Define at first use with acronym or abbreviation in parentheses. The abstract should be structured with the following headings: Background, Methods and Results, and Conclusions. The Background section should describe the rationale for the study. Methods and Results should briefly describe the methods and present the significant results. Conclusions should succinctly state the interpretation of the data. Authors should supply a list of up to four key words not appearing in the title, which will be used for indexing. The key words should be listed immediately after the Abstract. Use terms from the Medical Subject Headings (MeSH) list of Index Medicus when possible.

Main text in the IMRaD format

Introduction should describe the purpose of the study and its relation to previous work in the field; it should not include an extensive literature review.

Methods should be concise but sufficiently detailed to permit repetition by other investigators. Previously published methods and modifications should be cited by reference. A subsection on statistics should be included in the Methods section.

Results should present positive and relevant negative findings of the study, supported when necessary by reference to Tables and Figures.

Discussion should interpret the results of the study, with emphasis on their relation to the original hypotheses and to previous studies. The importance of the study and its limitations should also be discussed.

The IMRaD format does not include a separate Conclusion section. The conclusion is built into the Discussion. More information on the structure and content of these sections can be found in the Recommendations for the Conduct, Reporting, Editing and Publication of Scholarly Work in Medical Journals (ICMJE Recommendations), available from www.ICMJE.org.

Acknowledgments, Sources of Funding, and Disclosures

Acknowledgments : All contributors who do not meet the criteria for authorship should be listed in an acknowledgments section. Examples of those who might be acknowledged include a person who provided purely technical help, writing assistance, or a department chairperson who provided only general support. Authors should declare whether they had assistance with study design, data collection, data analysis, or manuscript preparation. If such assistance was available, the authors should disclose the identity of the individuals who provided this assistance and the entity that supported it in the published article.

Sources of Funding: All sources of financial support for the study should be cited on the title page, including federal or state agencies, nonprofit organizations, and pharmaceutical or other commercial sources.

Disclosure and conflicts of interest: All authors must disclose any financial or other relations that could lead to a conflict of interest. If a potential conflict exists, its nature should be stated for each author. All sources of financial support for the study should be cited, including federal or state agencies, nonprofit organizations, and pharmaceutical or other commercial sources. Please use ICMJE Form for Disclosure of Potential Conflicts of Interest (http://www.icmje.org/conflicts-of-interest/).

References

References should follow the standards summarized in the NLM's International Committee of Medical Journal Editors (ICMJE) Recommendations for the Conduct,

Reporting, Editing and Publication of Scholarly Work in Medical Journals: Sample References webpage (www.nlm.nih.gov/bsd/uniform_requirements.html) and detailed in the NLM's Citing Medicine, available from www.ncbi.nlm.nih.gov/books/NBK7256/. MEDLINE abbreviations for journal titles (www.ncbi.nlm.nih.gov/nlmcatalog/journals) should be used.

References should be presented in the Vancouver style. The first six authors should be listed in each reference citation (if there are more than six authors, "et al" should be used following the sixth). Periods are not used in authors' initials or journal abbreviations. Examples of journal reference style:

Journal Article: Serruys PW, Ormiston J, van Geuns RJ, de Bruyne B, Dudek D, Christiansen E, et al. A Polylactide Bioresorbable Scaffold Eluting Everolimus for Treatment of Coronary Stenosis: 5-Year Follow-Up. J Am Coll Cardiol. 2016;67(7):766-76. doi: 10.1016/j.jacc.2015.11.060.

Book: Murray PR, Rosenthal KS, Kobayashi GS, Pfaller MA. Medical Microbiology. 4th ed. St. Louis: Mosby; 2002.

Chapter in Edited Book: Meltzer PS, Kallioniemi A, Trent JM. Chromosome alterations in human solid tumors. In: Vogelstein B, Kinzler KW, editors. The Genetic Basis of Human Cancer. New York: McGraw-Hill; 2002:93–113.

References should be numbered consecutively in the order in which they are first mentioned in the text. Identify references in text, tables, and legends by Arabic numerals in parentheses and listed at the end of the article in citation order.

Tables

Tables should be comprehensible without reference to the text and should not be repetitive of descriptions in the text. Every table should consist of two or more columns; tables with only one column will be treated as lists and incorporated into the text. All tables must be cited in the text and numbered in order of appearance. Tables should include a short title. Place explanatory matter in footnotes, not in the heading. Explain all nonstandard abbreviations in footnotes, and use symbols to explain information if needed. Each table submitted should be double-spaced, each on its own page. Each table should be saved as its own file as a Word Document. Explanatory matter and source notations for borrowed tables should be placed in the table footnote.

Figures and Legends

All illustrations (line drawings and photographs) are classified as figures. All figures should be cited in the text and numbered in order of appearance. Figures should be provided in .tiff, .jpeg or .eps formats. Color images must be at least 300 dpi. Gray scale images should be at least 300 dpi. Line art (black and white or color) and combinations of gray scale images and line art should be at least 1,000 dpi. The optimal size of lettering is 12 points. Symbols should be of a similar size. Figures should be sized to fit within the column (86 mm) or the full text width (180 mm). Line figures must be sharp, black and white graphs or diagrams, drawn professionally or with a computer graphics package. Legends should be supplied for each figure and should be brief and not repetitive of the text. Any source notation for borrowed figures should appear at the end of the legend. Figures should be uploaded as individual files.

Units of Measurement

Measurements of length, height, weight, and volume should be reported in metric units (meter, kilogram, or liter) or their decimal multiples. Temperatures should be in degrees Celsius. Blood pressures should be in millimeters of mercury. All measurements must be given in SI or SI-derived units. Drug concentrations may be reported in either SI or mass units, but the alternative should be provided in parentheses where appropriate.

Style and Language

The journal accepts manuscripts written in English. Spelling should be US English only. The language of the manuscript must meet the requirements of academic publishing. Reviewers may advise rejection of a manuscript compromised by grammatical errors. Non-native speakers of English may choose to use a copyediting service.

Abbreviations and Symbols

Use only standard abbreviations; use of nonstandard abbreviations can be confusing to readers. Avoid abbreviations in the title of the manuscript. The spelled-out abbreviation followed by the abbreviation in parenthesis should be used on first mention unless the abbreviation is a standard unit of measurement.

Drugs should be referred to by their generic names. If proprietary drugs have been used in the study, refer to these by their generic name, mentioning the proprietary name, and the name and location of the manufacturer, in parentheses.

Permissions

To use tables or figures borrowed from another source, permission must be obtained from the copyright holder, usually the publisher. Authors are responsible for applying for permission for both print and electronic rights for all borrowed materials and are responsible for paying any fees related to the applications of these permissions. This is necessary even if you are an author of the borrowed material. It is essential to begin the process of obtaining permission early, as a delay may require removing the copyrighted material from the article. The source of a borrowed table should be noted in a footnote and of a borrowed figure in the legend. It is essential to use the exact wording required by the copyright holder. A copy of the letter granting permission, identified by table or figure number, should be sent along with the manuscript. A permission request form is provided for the authors use in requesting permission from copyright holders.

Page Proofs

Page proofs are sent from the Publisher electronically and must be returned within 72 hours to avoid delay of publication. Generally, peer review is completed within 4-5 weeks.

It is important to note that when citing an article from IJBM, the correct citation format is **International Journal of Biomedicine.**

IJBM

INTERNATIONAL JOURNAL OF BIOMEDICINE

International Journal of Biomedicine (IJBM) is an open access journal. IJBM publishes peer-reviewed articles on aspects of basic, applied, and translational research in biology and medicine. The main purpose of IJBM is to establish a scientific platform for targeted promotion of new scientific ideas and biomedical technologies focused on the applied aspects of biomedicine.

The journal publishes articles on:

Internal Medicine
Cardiology
Pulmonology
Endocrinology
Neurology
Hepatology
Gastroenterology
Nephrology
Ophthalmology
Otorhinolaryngology
Radiology
Surgery
Obstetrics and Gynecology
Pediatrics
Dermatology and STD
Clinical Immunology
Oncology
Genomics and Proteomics
Population Genetics
Epidemiology and Population Health
Reproductive Health
Adolescent Health
Cell Biology
Experimental Biology
Biotechnology
Dentistry
Infectious Diseases
Sports Medicine

Authors are invited to submit:

Original articles
Review articles
Case reports
Perspectives
Viewpoints